PROCEEDINGS

DEPARTMENT OF VETERINARY PATHOLOGY
WEDNESDAY SLIDE CONFERENCE
2009-2010

ARMED FORCES INSTITUTE OF PATHOLOGY
WASHINGTON, D.C. 20306-6000
2010

ML2010

Armed Forces Institute of Pathology
Department of Veterinary Pathology

WEDNESDAY SLIDE CONFERENCE
2009-2010

100 Cases
100 Histopathology Slides
1 Electron Photomicrograph
295 Images

PROCEEDINGS PREPARED BY:
Shannon H. Lacy, DVM, MPH, Diplomate ACVPM

Chief Editor:
Edward L. Stevens, DVM, Diplomate ACVP

Copy Editor:
Sean Hahn

Layout and Copy Editor:
Fran Card

WSC Online Management and Design
Scott Shaffer

ARMED FORCES INSTITUTE OF PATHOLOGY
Washington, D.C. 20306-6000
2009

ML2010

PREFACE

The Armed Forces Institute of Pathology, Department of Veterinary Pathology has conducted a weekly slide conference during the resident training year since 12 November 1953. This ever-changing educational endeavor has evolved into the annual Wednesday Slide Conference program in which cases are presented on 25 Wednesdays throughout the academic year and distributed to approximately 135 contributing military and civilian institutions from around the world. Many of these institutions provide structured veterinary pathology resident training programs. During the course of the training year, histopathology slides, digital images, and histories from selected cases are distributed to the participating institutions and to the Department of Veterinary Pathology at the AFIP. Following the conferences, the case diagnoses, comments, and reference listings are posted online to all participants.

This study set, composed of 100 cases, 100 histopathology slides, 1 electron photomicrograph, and 295 digital images, was assembled from the cases studied during the 2009-2010 conference series. This set has been assembled in an effort to make Wednesday Slide Conference materials available to a wider circle of interested pathologists and scientists, and to further the education of veterinary pathologists and residents-in-training. The number of histopathology slides that can be reproduced from smaller lesions requires us to limit the number of participating institutions. Gross images and photomicrographs were submitted by contributing institutions where indicated. Additional digital photomicrographs were captured by Jeremy Bearss and Leonora Dickson.

For their participation and permission to use their cases in this study set, we wish to thank each institution, and especially the individuals who prepared and submitted the selected cases. We also give special thanks to the American Veterinary Medical Association and the American College of Veterinary Pathologists, who are co-sponsors of the Registry of Veterinary Pathology. The C.L. Davis Foundation also provides substantial support for the Registry.

A special note of appreciation is extended to the associate editors who helped review this year's individual case summaries: Edward Stevens, William Culp, Christine Christensen, and Dr. Michelle Fleetwood. Additionally, we thank Dr. Chris Gardiner for his expert review of cases involving parasitic entities. We also wish to thank Todd Johnson, Dr. Bruce Williams, Dr. Tom Lipscomb, and Dr. Yvonne Schulman for reviewing selected cases. For copy edit and layout, we extend our gratitude to Sean Hahn and Fran Card.

A final note of thanks goes to the moderators, who selflessly gave of their time and expertise to make each conference both enjoyable and educational.

Armed Forces Institute of Pathology, Department of Veterinary Pathology
WEDNESDAY SLIDE CONFERENCE 2009-2010
Table of Contents

Case	AFIP No.	Slide No.	Species	Etiology/ Condition	Tissue	Page
Conference 20	**07 Apr 2010**			**Moderator: Dr. Donald Schlafer**		
1	3066307	AFIP Case2	Horse	*Bipolaris* sp.	Placenta	251
2	3139936	09-30175	Horse	Teratoma	Testis	253
3	3134193	W9332754	Dog	Dysgerminoma	Ovary	256
4	3134304	09030 WFUHS	Rhesus macaque	Cervical adenocarcinoma (rhesus papillomavirus type D)	Cervicovaginal junction	258
Conference 21	**14 Apr 2010**			**Moderator: Dr. F. Yvonne Schulman**		
1	3134335	59688	Long-tailed finch	*Acuaria skrjabini*; *Macrorhabdus ornithogaster*; *Cryptosporidium* sp.	Ventriculous; proventriculus	261
2	3138207	13738-09	Dog	Mucinous adenocarcinoma	Small intestine	264
3	3134626	12303-08	Cat	*Listeria monocytogenes*	Brain	267
4	3152276	07-21444	Dog	Granular cell tumor	Brain	269
Conference 22	**28 Apr 2010**			**Moderator: Dr. Steven Weisbrode**		
1	3147900	3147900	Horse	Ossifying fibroma	Bone	271
2	2988004	04-2259	Cat	Osteogenesis imperfecta (suspected)	Bone	274
3	3122074	0801631	Mouse	Osteosarcoma	Bone	277
4	3148218	AFIP 08001	Rat	Corticosteroid induced osteosclerosis	Bone	279

Case	AFIP No.	Slide No.	Species	Etiology/ Condition	Tissue	Page
Conference 23	**05 May 2010**			**Moderator: Dr. Thomas Lipscomb**		
1	3136277	09021035	Ox	Biliary atresia	Liver	283
2	3149858	6860-09; 8358-08	Herring gull	Avian circovirus; *Ichthyocotylurus platycephalus*	Bursa of Fabricius	286
3	3036133	N06-358-9	Baboon	Neuroendocrine carcinoma (carcinoid)	Liver	288
4	3149417	D0810008	Ox	Microcystin LR toxicosis	Liver	290
Conference 24	**12 May 2010**			**Moderator: Dr. Thomas Lipscomb**		
1	3153650	072188-03	Cynomolgus macaque	*Anatrichosoma* sp.	Nasal vestibule	293
2	2948651	R04-43	Crocodile	*Aspergillus* sp. (suspected)	Lung	296
3	2940154	0408061	Boa constrictor	Boid inclusion body disease (retrovirus suspected)	Liver	298
4	3134333	60848	Octopus	*Ichthyobodo* sp.	Gill	299

Case	AFIP No.	Slide No.	Species	Etiology/ Condition	Tissue	Page
Conference 25	**19 May 2010**		**Moderator:**	**Jo Lynne Raymond**		
1	3134358	089-65832	Skunk	*Filaria taxideae*; canine distemper virus (morbillivirus)	Skin	303
2	3134511	SP-08-8399	Dog	Complex adenocarcinoma of the gland of the third eyelid	Eye	306
3	3149836	D-09-7312(18)	Chicken	Highly-pathogenic avian influenza (influenza A virus, orthomyxovirus)	Brain	311
4	3149913	C9775-08	Dog	*Leptospira* sp.	Kidney	314

The Armed Forces Institute of Pathology
Department of Veterinary Pathology

Conference Coordinator:
Shannon Lacv. DVM. MPH

WEDNESDAY SLIDE CONFERENCE 2009-2010

Conference 1

9 September 2009

Conference Moderator:

Todd Johnson, DVM, Diplomate ACVP

CASE I: H03-0754A 03-0782 (AFIP 2935567).

Signalment: 4-year-old castrated, male Australian terrier (*Canis familiaris*).

History: The dog presented with a history of a mass in the right axilla occurring approximately one year prior to presentation. The mass had recurred after drainage and biopsy. Antibiotics, including clavulanic acid/amoxicillin, chloramphenicol, and doxycycline, had been prescribed over several months without significant response. Physical examination indicated extensive pyogranulomatous skin disease extending cranial, ventral and caudal to the right axilla with involvement of the prescapular lymph node. The owners were unable to afford the biopsy and culture procedures suggested for diagnosis, and based on previous histopathology results showing a pyogranulomatous deep dermatitis with filamentous Gram-positive organisms, the dog was placed on a trial of potentiated sulphonamides for suspected *Actinomyces* infection. After one month, the lesions showed significant improvement, but five months later there had been recurrence and the owners asked for the animal to be euthanized.

Gross Pathology: A castrated male Australian terrier. There was focally extensive alopecia and ulcerated multinodular swelling of the right axillary region extending over the right forelimb (**fig. 1-1**). Subcutaneous dissection revealed multinodular to coalescing, focally extensive accumulations of light brown semifluid purulent material with black flecks throughout (**fig. 1-2**). This extended 10-15 mm deep into the subcutis, passing over the lateral aspect of the thorax, medial to the scapula almost to its dorsal limit, and cranially to the level of the thoracic inlet, plus distally to the level of the right elbow. The right retropharyngeal lymph node was enlarged to 2 cm in length and appeared soft and edematous. The right prescapular and axillary nodes were unable to be located amongst the purulent pockets. There were no other significant findings.

Laboratory Results: Bacterial culture of both fresh tissue and a deep tissue swab from the affected area yielded a scanty to light growth of a Gram-positive filamentous bacterium. The isolate formed pearl-colored, shiny, waxy, adherent colonies, with Gram stain showing Gram-positive long filaments. There was pure growth on the agar and a molar tooth appearance to the colonies on aging. Partial

*Sponsored by the American Veterinary Medical Association, the American College of Veterinary Pathologists, and the C. L. Davis Foundation.

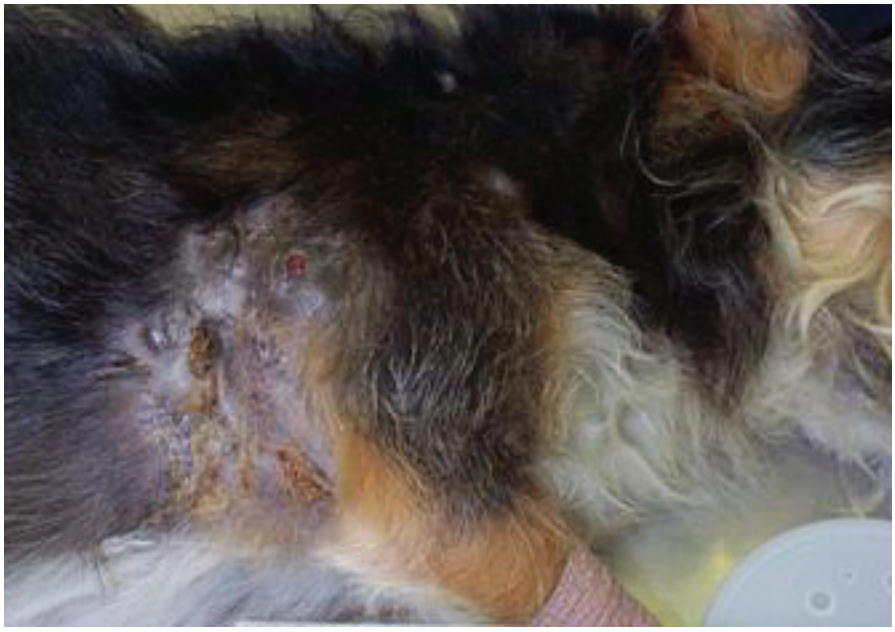

1-1, 1-2. Skin, right axillary region, dog. Focally extensive area of alopecia and ulceration overlying a multinodular cutaneous swelling. There are accumulations of light brown purulent material admixed with black flecks within the ulcerated areas. Photographs courtesy of Division of Health Sciences, Murdoch University, South Street, Murdoch, WA6150 Australia, aohara@central.murdoch.edu.au.

DNA sequencing of the isolate was undertaken. A total of 404 bases were sequenced and there was a 100% match with the *Streptomyces cyaneus* 16s ribosomal RNA gene (partial sequence-Locus AY232254) held on the NCBI nucleotide database (http://www.ncbi.nlm.nih.gov/entrez).

Contributor's Morphologic Diagnosis: Right axilla and forelimb: Focally extensive, severe, chronic pyogranulomatous dermatitis and cellulitis, with numerous intralesional filamentous pigmented bacteria (*Streptomyces cyaneus*).

Contributor's Comment: The section provided was taken from the right lateral thoracic wall. Beneath focally parakeratotic, focally ulcerated, and acanthotic epidermis, there is a severe, focally extensive infiltrate of neutrophils and macrophages, the latter often containing light brown pigment, with numerous intralesional club colonies. The colonies have an eosinophilic centre and a black pigmented periphery (**fig. 1-3**). Filamentous organisms can be seen within the colonies. The infiltrate extends through deep dermis and hypodermis, down to underlying fascia and

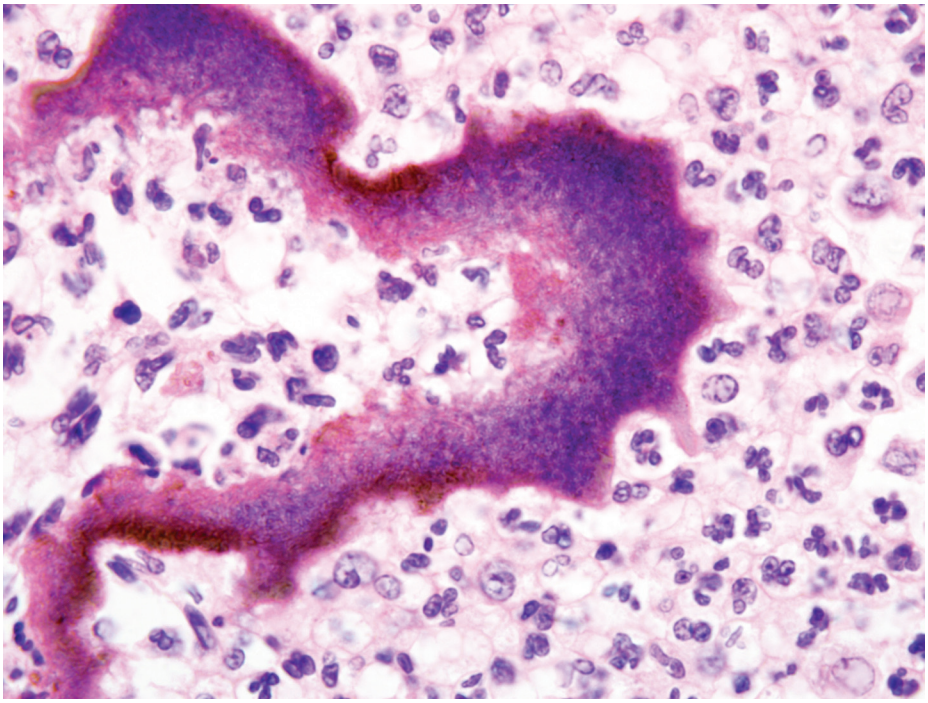

1-3. Skin and subcutis, dog. Multifocally, pyogranulomatous inflammation is centered on large colonies of 1x5 um filamentous bacteria which are surrounded by abundant golden brown pigment. (HE 1000X)

muscle. The organisms are negative for Ziehl-Neelsen staining, positive with Gram staining, and negative for the Periodic Acid Schiff reaction. Steiner's silver stain demonstrated the organisms clearly. The organism's long filamentous morphology and Gram-positive reaction were well-demonstrated on smears made from the isolated colonies.

Streptomyces are of the family Streptomycetaceae, within the order Actinomycetales. Other bacteria within this order are *Nocardia, Mycobacteria,* and *Actinomyces*. *Streptomyces* are aerobic (unlike *Actinomyces*) and non acid-fast organisms (unlike *Nocardia* and *Mycobacteria*) comprising several hundred species. Most are found in the soil and most produce pigments. Many antibiotics, such as the aminoglycosides, tetracyclines and macrolides, are derived from these species. The bacteria are regarded as pathogenic in humans but rarely pathogenic for animals [11], and are a common laboratory contaminant. The genus, however, is clearly pathogenic, as indicated by various reports in the human [9,10] and veterinary [4,7,8,12] literature. Invasive *Streptomyces* infections of humans are uncommon and have been reviewed recently.[3]

The isolation of this organism on two separate occasions, each time from two different sites plated onto different plates, makes contamination most unlikely. The bacteriology samples collected at necropsy were taken through shaved and ethanol scrubbed skin with sterile instruments to minimize contamination. Additionally, the presence of filamentous bacteria on the histology section clearly demonstrates a genuine intralesional organism. The original source of the infection is not clear in this case, although at this site a perforating and contaminated traumatic injury is a possible inciting cause. These organisms are associated with lesions that are reported to have a low cure rate, often requiring protracted antibiotic treatment.[10] The case reported here indicates that the isolation of *Streptomyces* from veterinary cases should not necessarily be considered a contamination.

AFIP Diagnosis: Haired skin and subcutis: Dermatitis and cellulitis, pyogranulomatous, diffuse, severe, with large colonies of pigmented, filamentous bacteria.

Conference Comment: Considerable discussion surrounded the brown intracytoplasmic pigment within macrophages in this case. Ultimately, conference participants concluded that this was bacterial pigment; however, many considered hemosiderin a possibility. Some participants' sections contained an area of epidermal ulceration overlain by a serocellular crust, and some sections had small amounts of intralesional Splendore-Hoeppli material.

Conference attendees discussed the differential diagnosis for the presence of intralesional colonies of filamentous bacteria, and the contributor provided a very good rubric for refining the differential diagnosis based on atmospheric oxygen requirements and the presence or absence of acid-

fast staining. Importantly, most *Nocardia* sp. only stain acid-fast positive with a modified acid-fast stain (e.g. Fite-Faraco method), which may be useful in differentiating *Nocardia* sp. from opportunistic *Mycobacteria* sp., which are strongly positive with routine acid-fast stain.[5] However, not all species of *Nocardia* are acid-fast positive; in such cases, culture is necessary for differentiation from *Actinomyces* sp.[5] Other notable members of order Actinomycetales include *Dermatophilus congolensis* and *Streptobacillus moniliformis*.[2] Most members of the order are Gram positive; however, *Mycobacteria* sp. possess a complex cell wall that precludes Gram staining, while *Nocardia* sp. are only weakly Gram-positive.[11]

Compared with *Actinomyces* sp. and *Nocardia* sp., *Streptomyces* sp. and *Actinomadura* sp. are infrequent causes of disease.[5] Clinically, the lesions caused by these four actinomycetes are indistinguishable, with the classic lesion being an actinomycotic mycetoma.[5] By definition, a mycetoma is a destructive lesion of the skin, subcutis, fascia, and sometimes bone characterized by the triad of tumefaction, draining tracts, and tissue grains (i.e. "sulphur granules") of various colors (e.g. white, black, yellow, red, or brown) corresponding to the etiologic agent.[1] Actinomycetic and eumycotic mycetomas are caused by the aforementioned actinomycetes and opportunistic fungi, respectively.[6] *Nocardia* sp. produces tissue grains less frequently than does *Actinomyces* sp.[5, 6] *Scedosporium apiospermum* (*Pseudoallesheria boydii*) and *Acremonium hyalinum* cause white-grain eumycotic mycetomas, while *Curvularia geniculata, Madurella grisea*, and *Phaeococcus* sp. cause black-grain eumycotic mycetomas.[5, 6]

Pseudomycetomas are characterized by the same triad of clinical signs as mycetomas, but lack a cement substance unique to true mycetomas.[6] Dermatophytic pseudomycetomas are caused by dermatophytic fungi, most classically in Persian cats.[6] The reader is referred to WSC 2008-2009, Conference 9, case III for an example of dermatophytic pseudomycetoma. Bacterial pseudomycetoma results when non-branching bacteria (e.g. *Staphylococcus* sp., *Streptococcus* sp., *Pseudomonas* sp., or *Proteus* sp.) cause the Splendore-Hoeppli reaction in tissue, resulting in nodules composed of pyogranulomatous inflammation with or without fistulous tracts.[6]

Contributor: School of Veterinary and Biomedical Sciences, Division of Health Sciences, Murdoch University, Murdoch WA 6150, Australia
http://www.murdoch.edu.au

References:

1. Anderson DM: Dorland's Illustrated Medical Dictionary, 28th ed., p. 1086. WB Saunders, Philadelphia, PA, 1994
2. Biberstein EL, Hirsh DC: Filamentous bacteria: *Actinomyces, Nocardia, Dermatophilus*, and *Streptobacillus. In:* Veterinary Microbiology, eds. Hirsh DC, MacLachlan NJ, Walker RL, 2nd ed., pp. 215-222. Blackwell Publishing, Ames, IA, 2004
3. Carey J, Motyl M, Perlman DG: Catheter-related bacteremia due to *Streptomyces* in a patient receiving holistic infusions. Emer Infect Dis **7(**6):1043-1045, 2001
4. Elzein S, Hamid ME, Quintana E, Mahjoub A, Goodfellow M: *Streptomyces* sp., a cause of fistulous withers in donkeys. Dtsch Tierarztl Wochenschr **109**(10):442-443, 2002
5. Ginn PE, Mansell JEKL, Rakich PM: Skin and appendages. *In:* Jubb, Kennedy, and Palmer's Pathology of Domestic Animals, ed. Maxie MG, 5th ed., vol. 1, pp. 686-702. Elsevier Saunders, Philadelphia, PA, 2007
6. Gross TL, Ihrke PJ, Walder EJ, Affolter VK: Skin Diseases of the Dog and Cat: Clinical and Histopathologic Diagnosis, 2nd ed., pp. 272-309. Blackwell Publishing, Ames, IA, 2005
7. Lewis GE, Filder JW, Crumrine MH: Mycetoma in a cat. J Am Vet Med Assoc **161**(5):500-503, 1972
8. Moore CP, Heller N, Majors LJ, Whtley RD, Burgess EC, Weber J: Prevalence of ocular microorganisms in hospitalized and stabled horses. Am J Vet Res **49**(6):773-777, 1989
9. Mossad SB, Tomford JW, Stewart R, Railiff NB, Hall GS: Case report of *Streptomyces* endocarditis of a prosthetic aortic valve. J Clin Microbiol **33**(12):3335-3337, 1995
10. Moss WJ, Sager JA, Dick JD, Ruff A: *Streptomyces bikiniensis* bacteriemia. Emerg Infect Dis **9**(2):273-274, 2003
11. Quinn PS, Carter ME, Markey BK, Carter GR: The Actinomycetes. *In:* Clinical Veterinary Microbiology,. pp. 44-145. Wolfe Medical Publications Ltd., London, England, 1995
12. Reinke SI, lhrke PJ, Reinke JD, Stannard AA, Jang SS, Gillette DM, Hallock KW: Actinomycotic mycetoma in a cat. J Am Vet Med Assoc **9**(4):446-449, 1986

CASE II: N090-010 (AFIP 2938315).

Signalment: 26-week-old male Tg.AC hemizygous mouse (*Mus musculus*).

History: Mouse had a steadily enlarging mandibular mass.

Gross Pathology: Firm pale 1 centimeter mass adjacent to the incisors.

Contributor's Morphologic Diagnosis: Mandible: Odontogenic tumor, ameloblastic, tooth.

Contributor's Comment: The mandibular bone contains an invasive neoplasm that is composed of thin irregular anastomosing cords of cuboidal to low columnar palisading epithelial cells separated by a loose undifferentiated spindle cell stroma resembling ameloblastoma (**figs. 2-1 and 2-2**). The stroma contains cells with oval nuclei with finely stippled chromatin and indistinct cytoplasmic borders, consistent with ameloblasts.

Odontogenic neoplasms are the most common spontaneous neoplasms in Tg.AC mice, occurring at an incidence of approximately 13% in males and 17% in females.[2] Grossly, they occur as firm masses in the maxilla or mandible. Microscopically, 3 morphologic types occur, the most frequent of which is the ameloblastic type as in the present case submission.[2,3] The second type, which appears to arise from the periodontal ligament, is the mesenchymal type which is composed of mesenchymal cells embedded in a dense eosinophilic matrix. The third morphologic type resembles odontomas and is composed largely of irregular abortive tooth structures formed by enamel, dentin and well-differentiated ameloblasts and odontoblasts.

Other common neoplasms of Tg.AC transgenic mice include squamous papillomas of the forestomach, skin papillomas, alveolar/bronchiolar adenoma, salivary gland duct carcinoma and erythroleukemia seen primarily in the liver with involvement of the spleen, bone marrow and lymph nodes.

AFIP Diagnosis: Mandible: Odontogenic tumor, ameloblastic.

Conference Comment: Conference participants discussed odontogenesis and the distinguishing characteristics of odontogenic epithelium: 1) peripheral palisading of epithelial cells, 2) location of the nucleus at the apical pole in the palisaded cells, 3) cytoplasmic clearing at the basilar pole in the palisaded cells, and 4) prominent intercellular bridging among the internal epithelial cells.[1]

All participants' slides contained a pre-existing tooth at the periphery of the neoplasm. In addition, some participants' slides contained a smaller tooth-like structure within the neoplasm. Considerable discussion centered on the origin of this structure, with some participants interpreting it as tooth recapitulation by neoplastic cells,

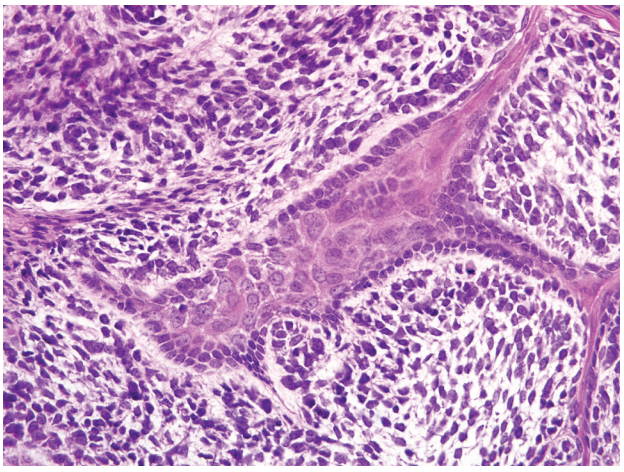

2-1. Odontogenic tumor, ameloblastic, mandible, mouse. The neoplasm is composed of thin anastomosing cords of odontogenic epithelium, separated by abundant stroma composed of undifferentiated mesenchymal cells. (HE 400X)

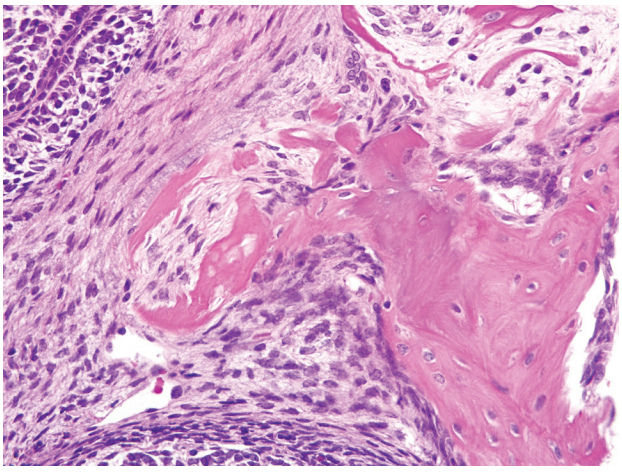

2-2. Odontogenic tumor, ameloblastic, mandible, mouse. Multifocally the neoplasm invades adjacent alveolar bone, separating and surrounding fragments of osteolytic and necrotic bone. (HE 400X)

while other participants favored a pre-existing structure. The classification of odontogenic tumors in transgenic mice, as summarized by the contributor, is convenient and avoids the problem of interpreting this tooth-like structure. However, participants noted that classification using the World Health Organization (WHO) scheme for domestic animals would hinge on interpretation of this structure. If this structure is interpreted as recapitulation by the neoplasm, the diagnosis would be ameloblastic fibro-odontoma, while the absence of this feature would make the tumor consistent with an ameloblastic fibroma using the WHO scheme.[1]

While in domestic species most odontogenic tumors have similar biological behavior (i.e. local destruction by expansion, amenability to surgical excision), there are two notable exceptions. Canine acanthomatous ameloblastoma is aggressive, locally infiltrative, and prone to recurrence; fibromatous epulis of periodontal ligament origin is benign, and a surgical cure is often achieved despite incomplete surgical margins.[1]

The high incidence of odontogenic tumors in Tg.AC transgenic mice is attributed to the expression of the *ras* oncogene. Odontogenic tumors appear in up to 100% of dual transgenic mice expressing both *ras* and *myc* oncogenes, and occur as early as 4 weeks of age.[3] Oncogenes are constitutively active genes that promote autonomous cell growth in cancer cells in the absence of normal growth-promoting signals. Oncogenes result from mutations in proto-oncogenes, and their products are called oncoproteins. Normal *ras* proteins are bound to the cytoplasmic aspect of the plasma membrane, and are activated only upon growth factor binding to plasma membrane receptors. Activated *ras* stimulates the mitogen-activated protein kinase cascade, resulting in signals to the nucleus for cell proliferation. Mutated *ras* proteins are continually activated, usually due to point mutations that impair guanosine trhiphosphate (GTP) hydrolysis, resulting in continuous stimulation of downstream proliferation signals. The mechanisms by which *myc* oncogene expression influences cell proliferation are less clear. *Myc* modulates myriad cellular activities, and is thought to be involved in carcinogenesis via some of its many targets, including ornithine decarboxylase and cyclin D2.[5]

Contributor: National Institute of Environmental Health Sciences, P.O. Box 12233, Research Triangle Park, NC 27709
http://ntp-server.niehs.nih.gov

References:

1. Head KW, Cullen JM, Dubielzig RR, Else RW, Misdorp W, Patnaik AK, Tateyama S, van der Gaag I: Histological Classification of Tumors of the Alimentary System of Domestic Animals, 2nd series, vol. X, ed. Schulman FY, pp. 47-54. Armed Forces Institute of Pathology (in cooperation with the ARP and the WHO Collaborating Center for Worldwide Reference on Comparative Oncology), Washington, DC, 2003
2. Mahler JF, Flagler ND, Malarkey DE, Mann PE, Haseman JK, Eastin W. Spontaneous and chemically induced proliferative lesions in Tg.AC transgenic and p53-heterozygous mice. Toxicologic Pathology **26**(4):501-511, 1998
3. Mahler M, Rozell, Mahler JF, Merlino G, Devor-Hennemn D, Ward JM, Sundberg JP. Pathology of the gastrointestinal tract of genetically engineered and spontaneous mutant mice. *In:* Pathology of Genetically Engineered Mice, eds. Ward JM, Mahler JF, Maronpot RR, Sundberg JP, Fredrickson RM, pp. 269-298. Iowa State University Press, Ames, IA, 2000
4. National Toxicology Program CD-Rom, Laboratory of Experimental Pathology. Lesions of Genetically Altered Mice, 2001 (http://dir.niehs.nih.gov/dirlep/genmice2/open_me.htm)
5. Stricker TP, Kumar V: Neoplasia. *In:* Robbins and Cotran Pathologic Basis of Disease, eds. Kumar V, Abbas AK, Fausto N, Aster JC, 8th ed., pp. 279-286. Saunders Elsevier, Philadelphia, PA, 2010

CASE III: D03-33535 (AFIP 2944782).

Signalment: 14-week-old male Toggenburg goat (*Capra hircus*).

History: This goat kid presented to the veterinarian with hind limb paresis of 6 weeks duration with progression to ataxia, recumbency, facial tremors, and strabismus. The goat kid was euthanized.

Gross Pathology: The goat was in good postmortem and nutritional condition. **Musculoskeletal:** There was redness and swelling of the tendons and muscles of the caudal aspect of the right rear leg extending from the hoof to the distal femur. There were two areas of hemorrhage and dark friable muscle along the left lateral thorax and focally in the left cervical muscles. **Respiratory:** There was a mild amount of green purulent fluid in the frontal sinuses. There was redness, wetness and consolidation

of 50% of the left cranial, left middle and accessory lung lobes. **Nervous:**The lateral ventricles were slightly dilated. The meninges were multifocally congested and wet. **Integumentary, cardiovascular, alimentary, hemolymphatic, endocrine, urinary and reproductive systems** had no lesions.

Laboratory Results: **Bacteriology:** There was no significant growth from aerobic cultures of the brain, joint, lung, liver, meninges, skeletal muscle or sinuses. There was no *Salmonella* spp. isolated. **Molecular Diagnostics:** A PCR test for pestivirus (border disease virus) on the tissue homogenate was negative. **Toxicology:** A liver mineral analysis was performed. The liver copper concentration of 8.4 ppm was interpreted as deficient. The liver selenium concentration of 1.43 was interpreted as adequate. **Immunohistochemistry:** The CAEV IHC on the lung and spinal cord was positive.

Contributor's Morphologic Diagnosis: Severe, focally extensive leukomyelitis, perivascular, lymphoplasmacytic and histiocytic, caprine arthritis-encephalitis virus.

Contributor's Comment: Caprine arthritis encephalitis virus (CAEV) is a retrovirus in the subfamily *Lentivirinae*.[2] Phylogenetic analyses demonstrate similarity to maedi/visna virus (MVV) of sheep, one of the first lentiviruses to be discovered.[2] Both MVV and CAEV are characterized clinically by slow progressive and debilitating illnesses of sheep and goats.[3] Subclinical infections with CAEV occur commonly in goats and subclinically infected animals can be sources of virus transmission to others in the herd.[5] Infection with CAEV results in persistent infection of macrophage-monocyte cells, and virus is expressed and then shed upon transition of the precursor monocyte to its mature macrophage type.[4]

Several clinical entities of CAEV infection are recognized: progressive arthritis in adults, progressive weight loss in adults, indurative mastitis or hard bag in adult does, interstitial pneumonia and a leukoencephalomyelitis in kids 2 to 6 months of age.[3,4,6] The pathological feature of each is lymphocytic/lymphoproliferative inflammation due to a host immune response with the expressed viral proteins.[4]

The goat kid in this case, in addition to having leukomyelitis, had focal area of lymphoplasmacytic and histiocytic inflammation of the cerebral white matter; moderate, multifocal, interstitial pneumonia with lymphoplasmacytic and histiocytic thickening of the alveolar septa, perivasculitis and peribronchitis; and mild multifocal lymphoplasmacytic and histiocytic synovitis. Postmortem diagnosis can be confirmed through detection of virus, with immunohistochemistry and polymerase chain reaction tests being more rewarding than virus isolation.[4]

Antemortem diagnosis is commonly achieved by detecting antibodies using agar gel immunodiffusion (AGID) or ELISA [4,6] and much of the disease control efforts are focused on isolation or culling of seropositive animals.[4,5]

AFIP Diagnosis: Spinal cord, white matter: Meningomyelitis, necrotizing and lymphohistiocytic, focally extensive, severe, with spheroids and gliosis.

Conference Comment: There is significant slide variation, with the distribution ranging from unilateral and confined primarily to the white matter to bilateral and nearly diffuse. Predominantly within the white matter, but also extending into the adjacent gray matter and overlying leptomeninges, a perivascular infiltrate composed of numerous lymphocytes and fewer histiocytes and plasma cells expands Virchow-Robin space and extends variably into the adjacent neuropil. Affected blood vessels are lined by hypertrophied reactive endothelium. Affected white matter is often lost and replaced by myriad macrophages with abundant foamy cytoplasm (gitter cells), astrocytes that often contain phagocytic debris, and fewer lymphocytes and reactive microglia (**fig. 3-1**). Remaining myelin sheaths are frequently dilated, occasionally mineralized, and either empty or expanded by swollen axons (spheroids) (**fig. 3-2**). There is mild gliosis and rare neuronal necrosis within the gray matter. Numerous lymphocytes and fewer histiocytes and plasma cells multifocally expand the leptomeninges.

Conference participants discussed the differential diagnosis for neurologic disease in goats [1,4]:

– Copper deficiency (enzootic ataxia, "swayback")
– Neuronal vacuolar degeneration of Angora goats
– Cerebrospinal nematodiasis
– Polioencephalomalacia
– Spinal abscess
– Listeriosis
– Rabies
– CAEV

The contributor provided a concise overview of the pathogenesis and clinical manifestations of CAEV. Small ruminant lentiviruses are enveloped, single-stranded RNA viruses that are more homologous to the feline immunodeficiency virus (FIV) than to other retroviruses, but differ from feline and primate lentiviruses in that they are not immunosuppressive.[1] Like other retroviruses, CAEV expresses the following viral genes [1]:

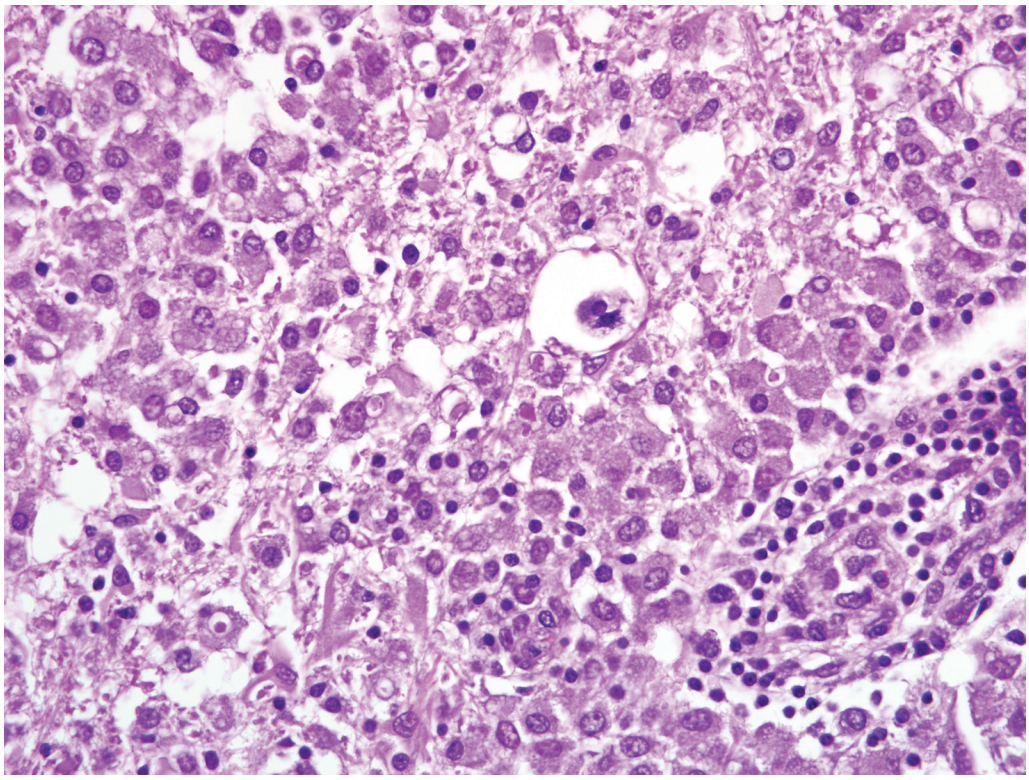

3-1. Spinal cord, cervical, goat. White matter is replaced by many foamy macrophages (gitter cells) and necrotic debris, and dilated axon sheaths which are either devoid of axons or occasionally contain gitter cells. Virchow-Robin's spaces are filled with a lymphoplasmacytic infiltrate and endothelium is hypertrophied. (HE 400X)

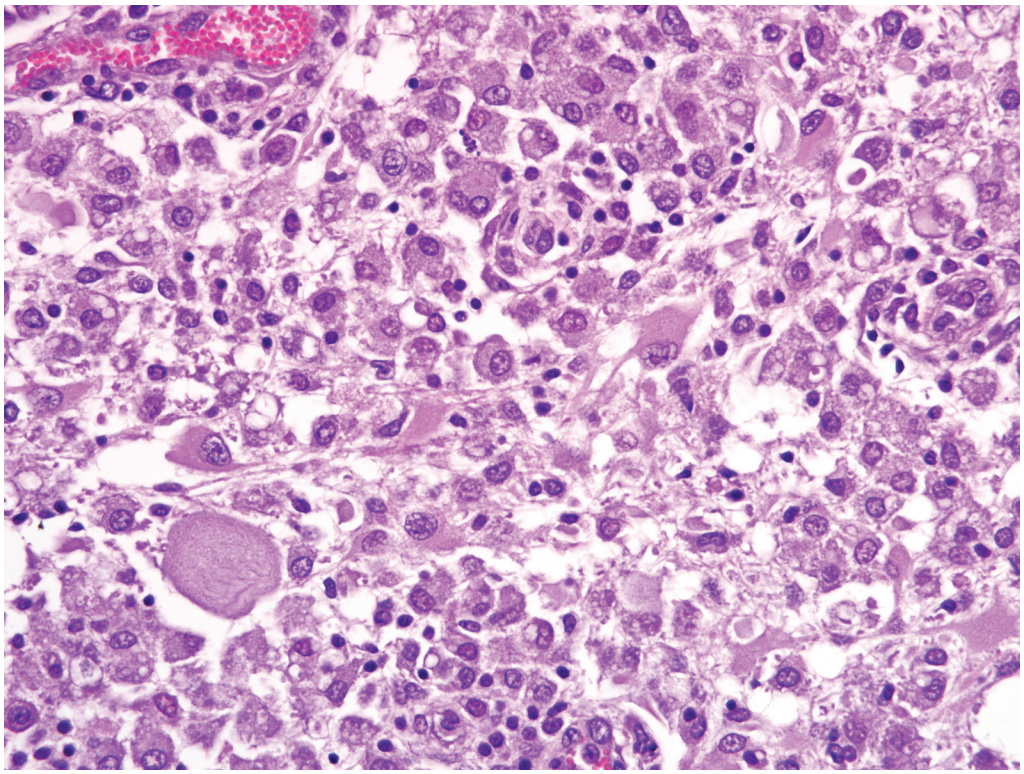

3-2. Spinal cord, cervical, goat. Multifocally within the white matter, there are spheroids and gemistocytic astrocytes. (HE 400X)

– *gag*: encodes nucleocapsid and matrix glycoproteins that are detected by antibody-based diagnostic tests
– *pol*: encodes a variety of viral enzymes, including reverse transcriptase
– *env*: encodes surface glycoprotein that mediates binding to cell receptors and entry into cells

Contributor: Minnesota Veterinary Diagnostic Laboratory, Department of Veterinary Population Medicine, College of Veterinary Medicine, University of Minnesota, 1333 Gortner Ave., St. Paul, MN 55108 http://www.vdl.umn.edu

References:

1. Caswell JL, Williams KJ: Respiratory system. *In:* Jubb, Kennedy, and Palmer's Pathology of Domestic Animals, ed. Maxie MG, 5th ed., vol. 2, pp. 618-620. Elsevier Saunders, Philadelphia, PA, 2007
2. Desrosiers, RC: Nonhuman lentiviruses. *In:* Fields Virology, eds. Knipe DM, Howley, PM, 4th ed., vol. 2, pp. 2095-2122. Lippincott, Williams & Wilkins, Philadelphia, PA, 2001
3. Maxie MG, Youssef S: Nervous system. *In:* Jubb, Kennedy, and Palmer's Pathology of Domestic Animals, ed. Maxie MG, 5th ed., vol. 1, pp. 426-428. Elsevier Saunders, Philadelphia, PA, 2007
4. Radostits OM, Gay CC, Hinchcliff KW, Constable PD: Veterinary Medicine, A Textbook of the Diseases of Cattle, Horses, Sheep, and Goats, 10th ed., pp. 1410-1413. Saunders Elsevier, Philadelphia, PA, 2007
5. Rowe, JD, East, NE: Risk factors for transmission and methods for control of caprine arthritis-encephalitis virus Infection. Vet Clin North Amer: Food An Prac **13**(1):35-53, 1997
6. Wolf, CB: The difficult diseases of CAEV, Johne's disease, and caseous lymphadenitis. Proc. 141st AVMA Ann Mtg, 2003

CASE IV: TVDML A1 (AFIP 3134285).

Signalment: 6-year-old Angus cow (*Bos taurus*).

History: The herd has been out at pasture with no significant abnormalities described. The owner noticed excessive hair loss on this animal several days prior to its acute death.

Gross Pathology: A 1050 pound adult female cow is presented for necropsy and most of the carcass is noted to be alopecic. In multifocal to coalescing foci the cardiac muscle is tan to pale yellow and slightly raised on cut section.

Laboratory Results: Only postmortem contaminants were isolated via bacterial culture of the myocardium.

Histopathologic Description: In multifocal to coalescing foci there is extensive replacement of the epicardium and myocardium by predominately a granulomatous and lymphocytic infiltrate with fewer eosinophils and plasma cells. Multinucleated giant cells containing up to 30 nuclei (both foreign body type and Langhan's type) are common (**fig. 4-1**). Degenerative changes in adjacent myofibers include hypereosinophilia, loss of cytoplasmic detail (cross striations) and mineralization. A similar type of inflammatory infiltrate was found histologically in the kidney, liver, adrenal gland, and skin. PAS, Grams stain, and Acid-Fast staining failed to illustrate etiologic agents.

Contributor's Morphologic Diagnosis:
Myocarditis, granulomatous and lymphocytic, multifocal to coalescing, chronic, severe.

Contributor's Comment: The multiorgan distribution of a granulomatous infiltrate described in this case and the failure to identify causative etiologic agents is consistent with hairy vetch (*Vicia villosa*) toxicosis. Hairy vetch is a forage legume and can be commonly found in pastures in the United States and other temperate regions of the world. It is widely cultivated and used as pasturage, harvested as hay and silage, and utilized as a cover crop although it has been associated with a systemic granulomatous disease in some cattle. The specific etiologic factors and pathogenic mechanisms involved in the development of this syndrome remain unknown. It is unusual that hairy vetch is commonly ingested by cattle without the development of clinical signs and it is difficult to routinely induce the disease experimentally. It has been proposed that a plant

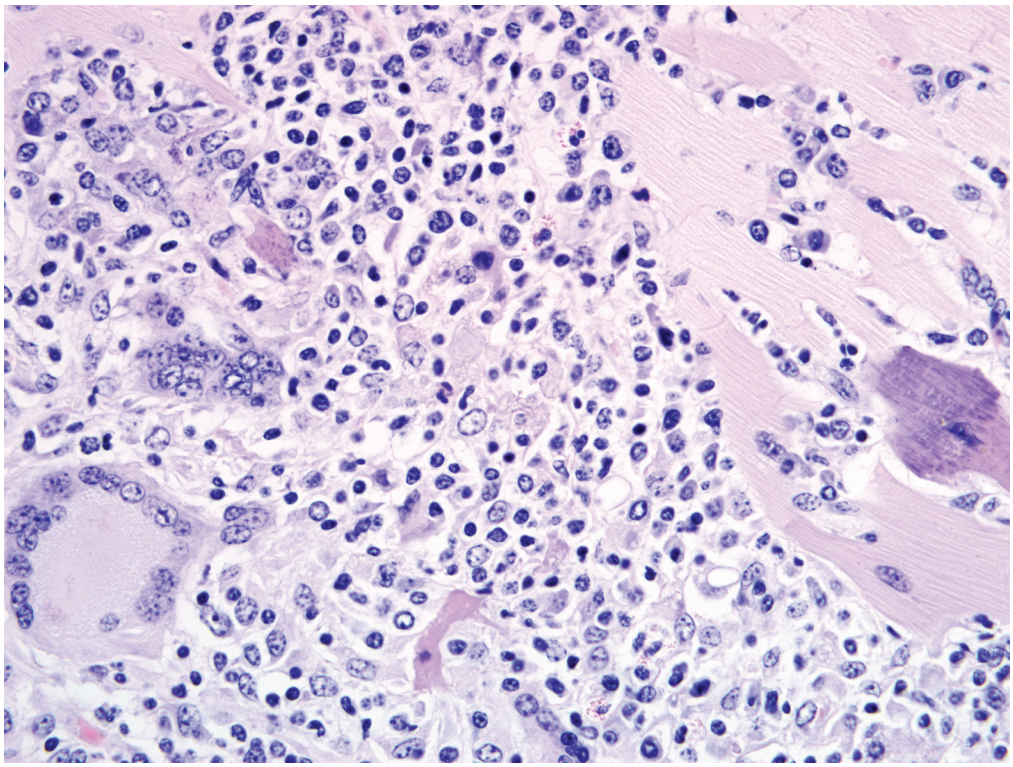

4-1. Myocardium, ox. Multifocally cardiac myocytes are surrounded and separated by many histiocytes admixed with fewer lymphocytes, eosinophils, and multinucleated giant cells of the foreign body and Langhans type. Occasionally, individual myocytes are degenerate, necrotic or mineralized. (HE 400X)

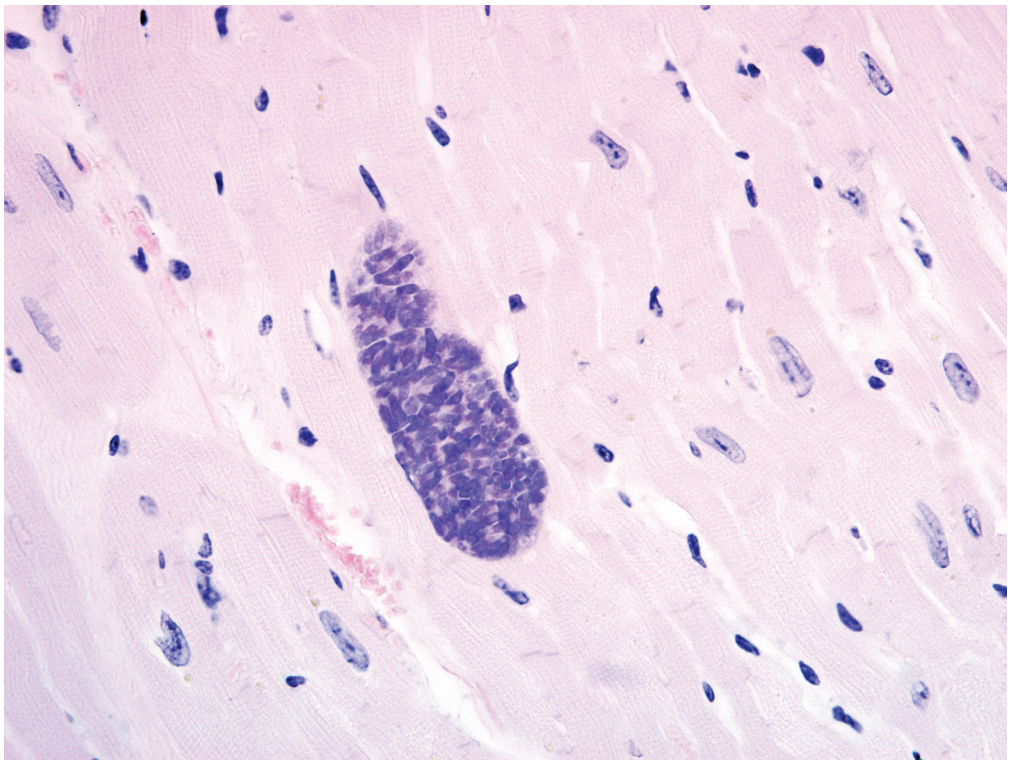

4-2. Myocardium, ox. Multifocally individual myocytes are expanded up to 150 um in diameter by protozoal cysts which contain numerous 5x7 um bradyzoites. (HE 400X)

constituent (lectins) induces a type IV, or cell mediated hypersensitivity reaction or potentially directly activates T lymphocytes initiating the systemic granulomatous reaction described with the syndrome. Furthermore, the low incidence of disease and disease occurrence when availability of vetch is limited suggest duration of exposure or repeated exposure to the plant help support a hypersensitivity theory. As the syndrome mainly occurs in Holstein and Angus cattle a genetic predisposition has also been suggested.[2,3]

Cattle that develop clinical disease usually have been grazing a pasture that contains a mixture of hairy vetch and small grains, including rye, wheat, and oats and outbreaks typically occur during the season of maximal vetch growth.[2] Additionally, development of the disease occurs after grazing an affected pasture for at least 2-6 weeks. Vetch associated disease is typically more severe in adult cattle greater than 3 years old.

The clinical syndrome associated with Vetch toxicosis varies and three different clinical manifestations have been described. One syndrome involves acute neurological signs and death consistent with cyanogenic glycosides contained in the seeds. A second syndrome involves subcutaneous swellings of the head, neck, and body with ulcers of the oral mucous membranes, purulent nasal discharge, rales, cough and congestion. The third syndrome involves the systemic granulomatous response and presents clinically as a dermatitis and conjunctivitis with diarrhea and weight loss.[3] With the systemic granulomatous syndrome gross lesions include a multifocal to coalescing, soft, and gray to yellow infiltrate disrupting the normal architecture of the involved tissues (liver, kidney, spleen, heart, adrenal gland, skin). Histologically, the salient feature is a multifocal to coalescing granulomatous infiltrate disrupting the affected tissue architecture. The infiltrate is typically characterized by epitheloid macrophages, multinucleated giant cells, lymphocytes, plasma cells and typically eosinophils.

AFIP Diagnosis: 1. Heart: Myocarditis, granulomatous and eosinophilic, multifocal to coalescing, severe, with myocyte degeneration and necrosis.
2. Heart, myocardium: Sarcocysts, few.

Conference Comment: The contributor provided an excellent overview of hairy vetch toxicosis. As the contributor noted, the pathogenesis of hairy vetch toxicosis remains somewhat unclear, and cattle exposed to the plant do not consistently develop disease. Therefore, hairy vetch toxicosis remains a diagnosis of exclusion. Conference participants discussed the importance of ruling out other causes of granulomatous inflammation, even when affected cattle are known to be exposed to hairy vetch. Special stains for bacterial and fungal etiologies were performed by the contributor, and repeated at AFIP, with no causative organisms seen. Some slides contained low numbers of sarcocysts that were not associated with inflammation, and were considered incidental (**fig. 4-2**).

Other compounds that may induce the production of lesions indistinguishable from vetch toxicosis include di-ureido-isobutane (DUIB) and citrus pulp.[1] In horses, vetch toxicosis causes lesions similar to those in cattle, with the notable exceptions being the relative lack of eosinophils in the infiltrate and the lack of heart involvement.[1]

Contributor: Texas Veterinary Medical Diagnostic Laboratory, P.O. Box 3200, Amarillo, TX 79116
http://tvmdlweb.tamu.edu

References:

1. Ginn PE, Mansell JEKL, Rakich PM: Skin and appendages. *In:* Jubb, Kennedy, and Palmer's Pathology of Domestic Animals, ed. Maxie MG, 5th ed., vol. 1, pp. 686-702. Elsevier Saunders, Philadelphia, PA, 2007
2. Johnson B, Moore J, Woods LW, Galey FD: Systemic granulomatous disease in cattle in California associated with grazing hairy vetch (*Vicia villosa*). J Vet Diagn Invest **4:**360-362, 1992
3. Panciera RJ, Mosier DA, Ritchey JW: Hairy vetch (*Vicia villosa Roth*) poisoning in cattle: Update and experimental induction of disease: J Vet Diagn Invest **4:**318-325, 1992

The Armed Forces Institute of Pathology
Department of Veterinary Pathology

Conference Coordinator:
Shannon Lacy, DVM, MPH

WEDNESDAY SLIDE CONFERENCE 2009-2010

Conference 2

16 September 2009

Conference Moderator:

Sarah Hale, DVM, Diplomate ACVP

CASE I: A07-194 (AFIP 3133675).

Signalment: 12-year-old, male, intact Rhesus macaque (*Macaca mulatta*).

History: This monkey was inoculated with SIVmac251 and had undergone routine phlebotomies. Several months after inoculation, the animal developed diarrhea and loss of appetite. The animal was treated with Baytril®, with partial resolution of the animal's diarrhea and improvement in appetite. Following discontinuation of Baytril®, the overall condition of the animal continued to decline with increased respiratory effort at rest and mucoid nasal discharge. Complete blood count and blood chemistry were within normal limits. A weight loss of 5 kilograms (from 21 to 16 kilograms) was recorded over a three month period. At the end of this period, the animal still had marked diarrhea and pneumonia. A cardiac ultrasound at this time revealed a thrombus attached to the right atrioventricular valve. The animal was placed on amoxicillin treatment; however, due to failure to respond to treatment, the animal was euthanized.

Gross Pathology: The animal was markedly obese. The axillary and inguinal lymph nodes were mildly enlarged. The lungs were mottled with cranioventral consolidation. There was an approximately 2 cm diameter thrombus attached to the right atrioventricular valve. The small and large intestines were filled with fluid digesta and gas. The gallbladder contained a pasty white fluid. There were no gross lesions noted on examination of the brain or spinal cord.

Laboratory Results: CBC and blood chemistry were within normal limits.

Histopathologic Description: Brain (telencephalic/diencephalic junction- including thalamus, lateral ventricle, and substantia nigra; some sections are composed of mesencephalon): Replacing extensive regions of the white matter and multifocally spreading into the adjacent gray matter are variably sized foci of liquefactive necrosis. These foci contain large numbers of macrophages that contain abundant, intracytoplasmic, degenerate myelin (gitter cells) and are admixed with fewer lymphocytes and reactive astrocytes (some of which are multinucleate). The adjacent neuroparenchyma is loosened (edema) and contains large numbers of reactive astrocytes (gemistocytes) and rod-shaped microglia. Both within the foci of liquefactive necrosis and in the adjacent neuroparenchyma are large numbers of astrocytes that are characterized by large, swollen nuclei that contain a

***Sponsored by the American Veterinary Medical Association, the American College of Veterinary Pathologists, and the C. L. Davis Foundation.**

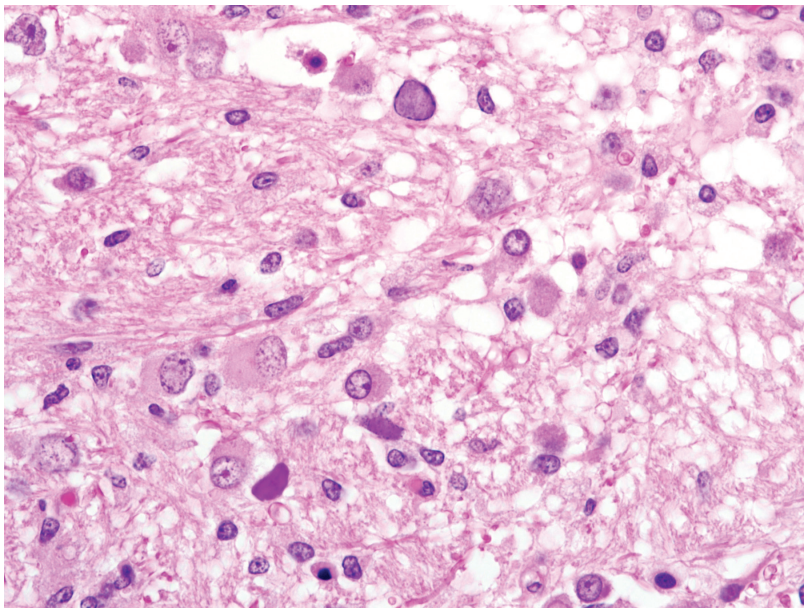

1-1. Cerebrum, rhesus macaque. Within areas of liquefactive necrosis are numerous gemistocytic astrocytes which occasionally contain large, pale basophilic 15 um intranuclear inclusion bodies which peripheralize the chromatin. Photomicrograph courtesy of New England Primate Research Center, Harvard Medical School, One Pine Hill Drive, Southborough, MA 01772, Andrew_miller@hms.harvard.edu.

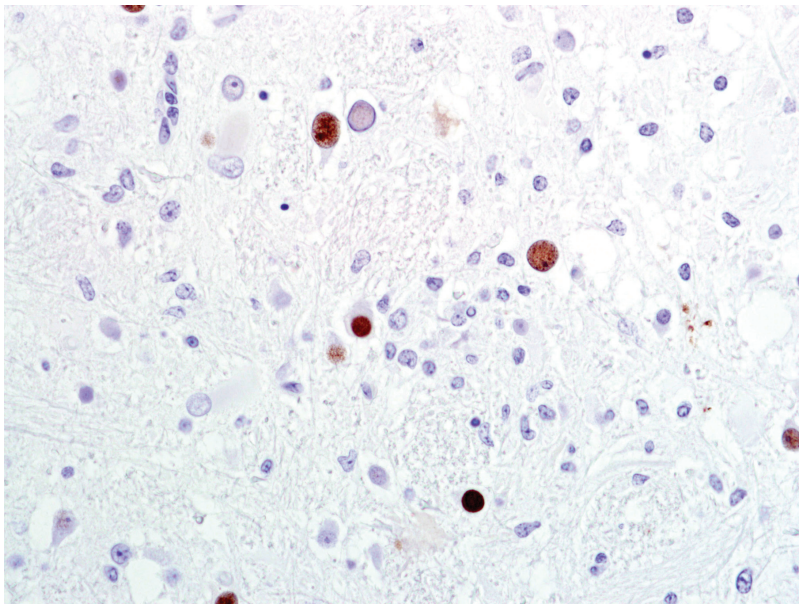

1-2. Cerebrum, rhesus macaque. Intranuclear inclusion bodies are strongly immunohistochemically positive for SV40 antigen. Photomicrograph courtesy of New England Primate Research Center, Harvard Medical School, One Pine Hill Drive, Southborough, MA 01772, Andrew_miller@hms.harvard.edu.

single, round, 10-20µm, amphophilic, glassy inclusion body (**fig. 1-1**). There are multiple foci of gliosis in the adjacent neuropil and occasional perivascular cuffs of lymphocytes are present within the gray matter. A small section of lateral ventricle is present in this section and the ependyma lining the lateral ventricle is irregular, proliferative, and broken in multiple sites. The ependymal cells have abundant cytoplasm and large, reactive nuclei and there are small numbers of lymphocytes within the ependyma. Blood vessels throughout the lesions are reactive and branched and typically are lined by reactive, hypertrophied endothelium. Immunohistochemistry for SV40 confirmed CNS infection (**fig. 1-2**).

Contributor's Morphologic Diagnosis: Brain (thalamus/substantia nigra): Severe, multifocal, chronic necrotizing encephalitis with intranuclear polyomaviral inclusions, marked astrocytosis and gliosis.

Contributor's Comment: Simian virus 40 (SV40) is a non-enveloped, oncogenic, double-stranded, DNA virus belonging to the Papovaviridae family and the

Polyomavirinae subfamily. The viral genome consists of early- and late-coding regions and a non-coding regulatory region. The early region encodes DNA binding proteins, known as large or small T (tumor) antigens, which bind to the regulatory region of the genome to facilitate replication of late region viral DNA, which encodes three capsid proteins (VP1, VP2, VP3) that display genus-specific antigenic determinants. Polyomaviruses cause tumors when inoculated into species (e.g. hamsters) unrelated to their natural host.[1,2] Other primate polyomaviruses are: JC virus and BK virus, which infect humans; SA12 isolated from a South African vervet monkey kidney culture; B-lymphotrophic polyomavirus (LPV) isolated from an African green monkey lymphoblast cell line; baboon polyomavirus isolated from baboon kidney cell culture; and cynomolgus polyomavirus (CPV) isolated from immunosuppressed cynomolgus monkeys. Other non-primate mammalian polyomaviruses include Murine polyomavirus (MPyV), Hamster polyomavirus (HaPyV), Bovine polyomavirus (BPyV), Rabbit kidney vacuolating virus (RKV), Murine pneumotropic virus, and finally various avian polyomaviruses including budgerigar fledgling disease virus (BFDV).[2]

Polyomaviruses are virtually ubiquitous and harmless in healthy hosts, but can cause severe disease in immunocompromised individuals. In immunocompetent natural hosts, polyomaviruses remain latent within renal tissue and likely the central nervous system, with periodic asymptomatic reactivation of latent virus during pregnancy, diabetes, or old age. In immunocompromised SIV-infected macaques with simian AIDS, primary infection or reactivation of a latent infection results in interstitial nephritis, interstitial pneumonia, and either meningoencephalitis (ME) or progressive multifocal leukoencephalopathy (PML). In human AIDS patients, PML occurs in up to 5% of affected individuals and is considered an AIDS-defining lesion. It is characterized by multifocal demyelination primarily of the white matter due to infection of oligodendrocytes. The ME variant is diffuse and distinct from PML, affecting cerebral gray matter without demyelination.[1,3] PML is characterized by variably sized foci of necrosis that start in the white matter and merge into the adjacent gray matter. Reactive astrocytosis is a common finding around the lesions. Inclusion bodies are typically numerous and are most often found in astrocytes.

Cases of PML and ME are rare in the primate literature. The ME manifestation is typically seen in animals with concurrent nephritis, as tubular nephritis has been reported to be a feature of primary SV40 infection but not SV40 reactivation in SIV infected macaques. The current animal had mild interstitial nephritis; however, no SV40 antigen could be found by immunohistochemistry. In addition to polyomavirus, this Rhesus macaque had several other AIDS defining opportunistic infections, including biliary, pancreatic and tracheal cryptosporidiosis and adenoviral enteritis. Other AIDS defining lesions that were not present in this animal include *Pneumocystis* sp. pneumonia and Cytomegalovirus infection.

A spontaneously occurring disease with characteristics similar to PML has been described in eight macaques. This observation was published in 1975, years before the discovery of SIV, and immunological competence was not determined in the monkeys reported.[4,5] Other virally-induced CNS lesions with inclusion bodies in non-human primates include CMV-associated meningoencephalitis; poliomyelitis virus-induced poliomyelitis; and measles virus-induced encephalitis. CMV-associated meningoencephalitis is differentiated from SV40-induced PML by the characteristic feature of cytomegaly with prominent intranuclear inclusion bodies. In addition, CMV associated encephalitis is not associated with necrosis and is typically more localized to the meninges. Poliomyelitis infection in non-human primates is rare and is restricted to the gray matter. Measles virus can affect the gray and white matter; however, the inclusion bodies are found both in the nucleus and the cytoplasm and are similar to other morbillivurses.[5,6] Finally, SIV-associated encephalitis has frequently been described in literature; however, the lesions in SIV encephalitis are present in both gray and white matter and composed of multifocal glial nodules, perivascular cuffs, and perivascular/meningeal aggregates of giant cells that lack inclusion bodies.[5,7]

AFIP Diagnosis: Brain, thalamus and substantia nigra: Encephalitis, necrotizing, multifocal, marked, with gliosis and amphophilic intranuclear inclusion bodies.

Conference Comment: The contributor provided a comprehensive synopsis of this entity and the differential diagnosis for CNS lesions with viral inclusion bodies in nonhuman primates. Conference participants discussed the importance of recognizing that the severity of lesions in this case suggests underlying immunocompromise and raises the index of suspicion for concomitant infection with other opportunistic pathogens. This case provided conference participants with excellent examples of classic polyomaviral inclusions, gemistocytic astrocytes, and gitter cells.

Contributor: New England Primate Research Center, Harvard Medical School, One Pine Hill Dr., Southborough, MA 01772
http://www.hms.harvard.edu/nerprc/

References:

1. Horvath CJ, Simon MA, Bergsagel DJ, Pauley DR, King NW, Garcea RL, Ringler DJ: Simian virus 40-induced disease in rhesus monkeys with simian acquired immunodeficiency syndrome. Am J Pathol **140**(6):1431-40, 1992
2. Imperiale MJ, Major EO: Polyomaviruses. *In*: Fields Virology, eds. Knipe DM, Howley PM, Griffin DE, Lamb RA, Martin MA, Roizman B, and Straus SE, 5th ed., vol. 2, pp. 2263-98. Lippincott Williams & Wilkins, Philadelphia, PA, 2007
3. Simon MA, Ilyinskii PO, Baskin GB, Knight HY, Pauley DR, Lackner AA: Association of simian virus 40 with a central nervous system lesion distinct from progressive multifocal leukoencephalopathy in macaques with AIDS. Am J Pathol **154**(2):437-46, 1999
4. Gribble DH, Haden CC, Schwartz LW, Henrickson RV: Spontaneous progressive multifocal leukoencephalopathy (PML) in macaques. Nature **254**(5501):602-4, 1975
5. Cusick PK, Morgan SJ: Nervous System. *In:* Nonhuman Primates in Biomedical Research: Diseases, eds. Bennett BT, Abee CR, Hedrickson R, 1st ed., pp. 461-83. Academic Press, 1998
6. Steele MD, Giddens WE Jr, Valerio M, Sumi SM, Stetzer ER: Spontaneous paramyxoviral encephalitis in nonhuman primates (*Macaca mulatta* and *M. nemestrina*). Vet Pathol **19**(2):132-9, 1982
7. Sharer LR, Baskin GB, Cho ES, Murphey-Corb M, Blumberg BM, Epstein LG: Comparison of simian immunodeficiency virus and human immunodeficiency virus encephalitides in the immature host. Ann Neurol **23** Suppl:S108-12, 1988

CASE II: 09-456, 09-457 (AFIP 3133950).

Signalment: Adult, mixed breed, beef cow (*Bos taurus*).

History: This is a 25-cow herd of adult mixed breed beef cows in late gestation. Several animals developed a staggering gait over weeks and were euthanized.

Gross Pathology: No gross lesions.

Histopathologic Description: Scattered neurons in the brain stem around the cerebral aqueduct and in the pons contain green-brown granular material in the cytoplasm. Many neurons contain golden pigment consistent with lipofuscin. Occasional neuronal necrosis is seen. Some sections have axonal degeneration of nerves along the ventral surface of the brain stem.

Contributor's Morphologic Diagnosis: Neuronal pigmentation, brain stem, mild, with axonal degeneration and neuronal necrosis.

Contributor's Comment: The pigment in neurons is consistent with that seen in poisoning by plants of the genus *Phalaris*. Ultrastructurally, the granules within the neuronal cytoplasm are membrane-bound and composed of concentric membranous lamellae that may be intermingled with fine granular material. They are considered to be lysosomal in nature.[1] The toxic principle is a mix of methyl tryptamine and beta carboline indoleamines that are related to the neurotransmitter serotonin. The experimental administration of these alkaloids to sheep has induced the acute syndrome, presumably by interfering with the function or metabolism of serotonin.

Phalaris toxicosis is typically a disease of sheep causing staggers. Onset of staggers may be rapid following ingestion of the plant or delayed by several months. Most animals recover from the staggering syndrome but some do not. Cattle are occasionally poisoned by *Phalaris* and develop staggers from which they usually do not recover. Sudden death is another less common manifestation of *Phalaris* poisoning seen in sheep and occasionally horses.[3]

The *Phalaris* species likely involved in the poisoning of these cattle is *Phalaris arundinacea* or reed canarygrass. This plant was found in the pasture grazed by the affected cattle.

AFIP Diagnosis: Brainstem: Neuronal pigmentation, multifocal, with mild gliosis.

Conference Comment: Conference participants discussed the tinctorial and morphologic differences between lipofuscin and the pigment imparted by *Phalaris* toxicosis. The distinction is important, because although the "wear and tear" pigment of lipofuscin indicates free radical and lipid peroxidation of polyunsaturated lipids of subcellular membranes, it is does not generally cause injury to the cell.[2] In *Trachyandra* intoxication, lipofuscinosis may be intense in central and peripheral neurons; however, the relationship between this storage process and clinical signs is uncertain. The pigment in many of the "ceroid lipofuscinoses" is not lipofuscin, but rather protein subunit c of mitochondrial ATP synthase.[3]

In this case, tan, globular lipofuscin is predominantly concentrated in the axon hillock of motor nuclei. The

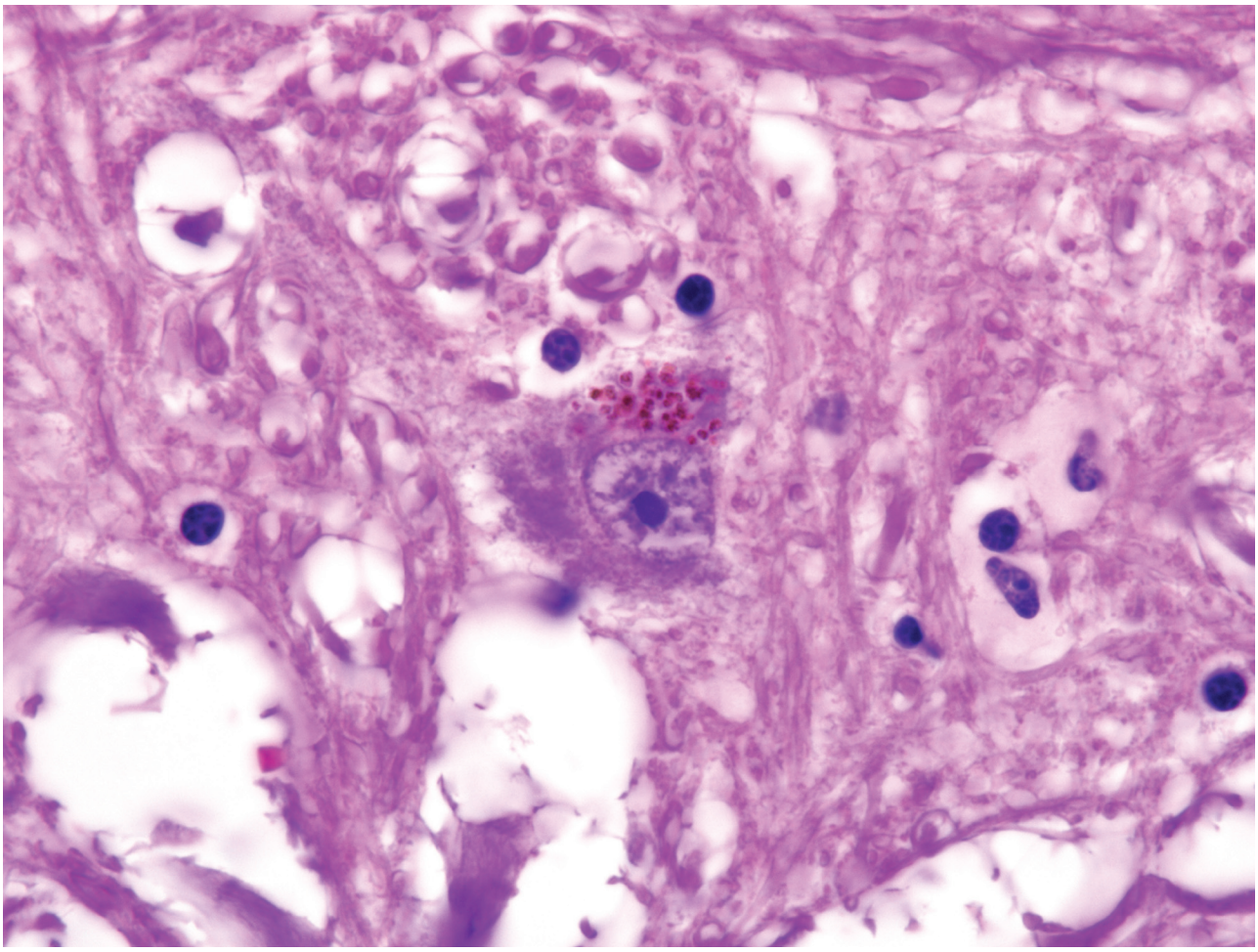

2-1. Mesencephalon, ox. Multifocally neurons contain small amounts of brown granular cytoplmasic pigment. (HE 1000X)

storage granules resulting from *Phalaris* toxicosis are more granular, brown to green, and have a predominantly perinuclear distribution (**fig. 2-1**). Similar granules may occur in the renal tubular epithelium of affected animals, and in severe cases the granules impart a grossly visible green discoloration to kidneys and gray matter.[3]

Phalaris toxicosis is one of several induced storage diseases caused by plants. Others include the aforementioned lipofuscinosis associated with *Trachyandra* toxicosis; *Solanum*-induced cerebellar neuronal degeneration and loss; Gomen disease, a suspected toxicosis of horses in New Caledonia; and alpha-mannosidosis induced by the indolizadine alkaloid swainsonine, found in a variety of plants, including locoweed (*Astragalus* sp., *Oxytropis* sp.), poison pea (*Swainsona* sp.), and the shrubby morning glory (*Ipomoea* sp.).[3]

The term "staggers," as applied to the clinical manifestation of *Phalaris* toxicosis, should not be confused with "staggering disease," caused by Borna disease virus, or "ryegrass staggers," which includes both perennial and annual ryegrass staggers. Annual ryegrass staggers is caused by a corynetoxin produced by the bacterium *Corynebacterium rathayi* in nematode-induced seed head galls; host plants include annual ryegrass (*Lolium rigidum*), annual beardgrass (*Polypogon monsppeliensis*), chewings fescue (*Festuca nigrescens*), and Pacific bent grass (*Agrostis avenacea*). The corynetoxin inhibits lipid-linked N-glycosylation of glycoproteins, compromising membrane integrity, and causing increased vascular permeability in multiple organs, including the brain.[3] Perennial ryegrass staggers is caused by tremorgenic mycotoxins (lolitrems) produced by the endophytic fungus *Neotyphodium lolii* in perennial ryegrass (*Lolium perenne*); disease is milder than in annual ryegrass staggers and is often reversible.[4]

Contributor: Virginia-Maryland Regional College of Veterinary Medicine, Virginia Tech, Duck Pond Drive, Blacksburg, VA 24061
http://www.vetmed.vt.edu/

References:

1. East NE, Higgins RJ: Canary grass (*Phalaris* sp) toxicosis in sheep in California. J Am Vet Med Assoc **192:**667-669, 1989
2. Kumar V, Abbas AK, Fausto N, Aster JC: Robbins and Cotran Pathologic Basis of Disease, 8th ed., pp. 36-37. Saunders Elsevier, Philadelphia, PA, 2010
3. Maxie MG, Youssef S: Nervous system. *In*: Jubb, Kennedy, and Palmer's Pathology of Domestic Animals, ed. Maxie MG, 5th ed., vol. 1, p. 331. Elsevier Saunders, Philadelphia, PA, 2007
4. Radostits OM, Gay CC, Hinchcliff KW, Constable PD: Veterinary Medicine, A Textbook of the Diseases of Cattle, Horses, Sheep, and Goats, 10th ed., pp. 1410-1413. Saunders Elsevier, Philadelphia, PA, 2007

CASE III: TP0950 CASE 1 (AFIP 3134515).

Signalment: 10- to11-month-old, male and female, Beagle dogs (*Canis familiaris*).

History: These dogs were part of the high dose group involved in a 7-day study with an orally administered experimental drug. Dogs were dosed once daily and euthanized on day 8. The animal care and experimental procedures of this study were conducted in compliance with the U.S. Animal Welfare Act and were performed in accordance with the standards of the Institute of Laboratory Animal Resources (ILAR) Guide (1996). The Association for Assessment and Accreditation of Laboratory Animal Care (AAALAC) International accredited the facility in which this study was conducted.

Gross Pathology: In the heart of a few animals in the high dose group, there were multifocal areas of red or pale discoloration.

Laboratory Results: Hematologic alterations in the high dose group included decreased red blood cell count, hemoglobin, and hematocrit with an increased white blood cell count due to elevated neutrophils and monocytes. Clinical chemistry perturbations in the high dose group included increases in troponin and total bilirubin.

Histopathologic Description: The tunica media of multiple small- to medium-sized arteries in the epicardium and myocardium is segmentally to circumferentially replaced by brightly eosinophilic, homogenous material (fibrinoid necrosis), with small to moderate numbers of degenerate neutrophils and histiocytes, scattered karyorrhectic debris, and occasionally hemorrhage (**figs. 3-1 and 3-2**). Smooth muscle fibers of the tunica media in some arteries contain plump, vesicular nuclei. There is moderate expansion of the tunica adventitia by edema and inflammatory cells. Multifocally in the myocardium,

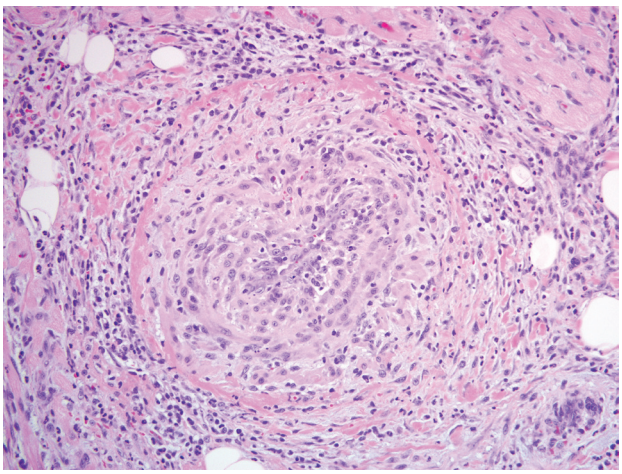

3-1. Heart, dog. The tunica media and adventitia of numerous coronary vessels is markedly expanded by numerous myofibroblasts, histiocytes, and fewer neutrophils, occasionally occluding vascular lumina. (HE 200X)

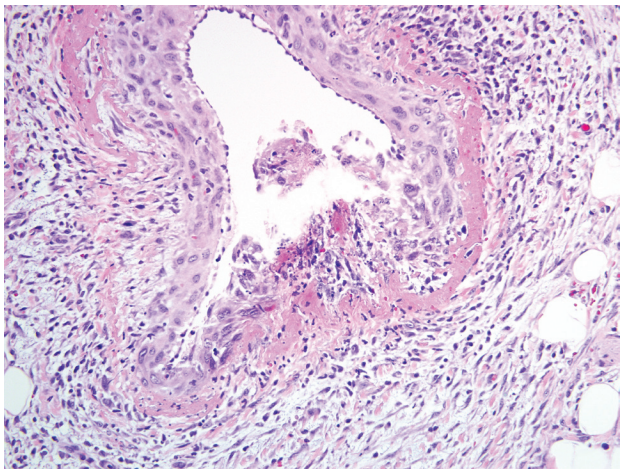

3-2. Heart, dog. Multifocally tunics of coronary arteries are disrupted by eosinophilic cellular and karyorhectic debris admixed with viable and degenerate neutrophils (necrotizing vasculitis). Endothelium lining these vessels is often hypertrophied and protrudes into the vascular lumen. (HE 200X)

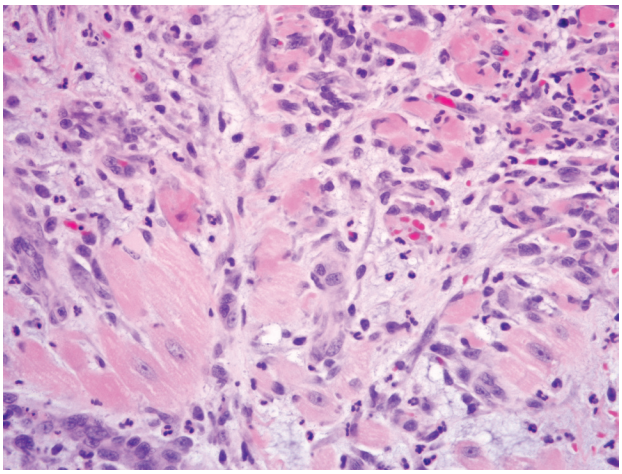

3-3. Heart, dog. Multifocally cardiac myocytes surrounding affected vessels are necrotic, and the interstitium is expanded by a moderate amount of edema and low numbers of neutrophils, lymphocytes, and histiocytes. (HE 400X)

particularly the atria, there are foci of interstitial expansion by edema with loose infiltration by small numbers of neutrophils, histiocytes and lymphocytes. Scattered cardiomyofibers in affected areas are shrunken and hypereosinophilic, and often surrounded by cells with large, vesicular nuclei (**fig. 3-3**). Capillaries in affected areas are lined by plump endothelial cells. In some sections, there is multifocal subendocardial and/or subepicardial hemorrhage.

Contributor's Morphologic Diagnosis: Heart: 1) Severe, multifocal, subacute, necrotizing arteritis with myocardial degeneration and necrosis.
2) Minimal, multifocal, subendocardial and subepicardial hemorrhage (some sections).

Contributor's Comment: This case represents an example of drug-induced vascular injury (DIVI) due to administration of a phosphodiesterase inhibitor in the dog. DIVI is currently a topic of debate in regulatory circles, as several drugs are associated with vascular injury in laboratory animals without concordant vascular injury in humans. In laboratory beagles, compounds that cause DIVI often have a predilection for the coronary vascular bed. This vascular bed is also a common area for spontaneous arterial lesions; therefore, care must be taken when interpreting vascular changes.[1,5] Manifestations of DIVI in laboratory beagles include vasoactive arteriopathy (produced by some vasodilator/positive inotropic and vasoconstrictor compounds), toxic vasculitis, and hypersensitivity vasculitis.[1]

Vasodilator and/or positive inotropic drugs (e.g. minoxidil, phosphodiesterase inhibitors, theobromine, others) produce distinctive, time-dependent, arterial changes affecting primarily extramural and intramural, small to medium-sized arteries. Gross changes include epicardial and possibly myocardial petechial and ecchymotic hemorrhages. At 7 days of treatment or less, microscopic changes include necrosis of the tunica media and hemorrhage, with inflammation and perivascular edema. Intimal and adventitial proliferative changes are observed with more chronic treatment.[1,4] Distinct changes associated with administration of phosphodiesterase III inhibitors to dogs include coronary arteriopathy generally restricted to extramural coronary arteries, myocardial necrosis with endocardial hemorrhage, and atrial hemorrhage with formation of granulation tissue.[1,3]

Vasoconstrictive agents (e.g. endothelin-1, digoxin, others) induce arterial changes consisting of medial thickening and necrosis, with hyalinization after longer-term treatment, and tend to affect small caliber arteries in a variety of organs. Some compounds (e.g. allylamine, systemic administration of monocrotaline and mitomycin C) may act directly on the arterial wall (endothelium and/or smooth muscle) causing toxic necrotizing vasculitis characterized by changes varying from acute necrosis of the tunica media with infiltration by neutrophils to medial scarring and intimal/adventitial fibrosis. Some drugs have been reported to cause immune-mediated disease due to Type III and, more commonly, Type IV hypersensitivities. Arterial changes associated with the Type IV hypersensitivity are not confined to coronary vascular beds, and are characterized by infiltration with mononuclear cells, possibly mixed with eosinophils, without medial necrosis.[1,4,5]

The pathogenesis of DIVI due to vasoactive compounds is still not clear. Vasodilator/positive inotropic agents produce their pharmacologic effects via a variety of mechanisms, including: direct relaxation of arterial smooth muscle, opening of potassium channels, inhibition of vascular smooth muscle phosphodiesterase, or blockage of endothelin receptors. The most frequently cited mechanism for the pathologic changes incurred by vasodilator/positive inotropic agents is vasodilation -> increased blood flow -> turbulence, altered shear stress -> homeostatic imbalance of endothelial cells -> injury.[2] Arterial changes due to vasoconstrictor agents are attributable to local and/or systemic hypertension produced by these compounds.[5]

AFIP Diagnosis: Heart, epicardial and myocardial arteries: Arteritis, proliferative and necrotizing, multifocal, marked, with multifocal myocardial degeneration and necrosis.

Conference Comment: Because the submitted slides

are from multiple dogs, there is some section variation. Some slides feature reactive mesothelium overlying the epicardial surface and/or serous atrophy of pericardial fat.

The contributor provides an excellent synopsis of this entity. Of immense practical concern is the differentiation of drug-induced from spontaneous vascular injury in general, and idiopathic polyarteritis of beagle dogs in particular. While many features overlap, there are some diagnostically useful differences between DIVI and idiopathic polyarteritis. The clinical signs in DIVI are variable and likely unrelated to vascular effects, while in idiopathic canine polyarteritis there is generally fever, weight loss, cervical neck pain (thus the clinical term, "beagle pain syndrome"), and neutrophilic leukocytosis. In DIVI, vascular lesions are generally restricted to coronary arteries, while in idiopathic canine polyarteritis multiple organs are affected. While the histologic lesions of the vasculature may be similar in these entities, idiopathic canine polyarteritis generally exhibits mononuclear periarterial to transmural inflammation, a feature which is absent or only mild in DIVI. Finally, atrial hemorrhage is characteristic of DIVI, but not idiopathic canine polyarteritis.[1]

Contributor: Pfizer Inc. Global Research and Development, Eastern Point Rd., Groton, CT 06340 http://www.Pfizer.com

References:

1. Clemo FAS, Evering W, Snyder PW, Albassam MA: Differentiating spontaneous from drug-induced vascular injury in the dog. Toxicol Pathol **31**(Suppl.):25-31, 2003
2. Enerson BE, Lin A, Lu B, Zhao H, Lawton M, Floyd E: Acute drug-induced vascular injury in beagle dogs: pathology and correlating genomic expression. Toxicol Pathol **34:**27-32, 2006
3. Joseph EC: Arterial lesions induced by phosphodiesterase III (PDE III) inhibitors and DA1 agonists. Toxicol Lett **112-113**:537-546, 2000
4. Louden C, Brott D, Katein A, Kelly T, Gould S, Jones H, Betton G, Valetin J, Richardson R: Biomarkers and mechanisms of drug-induced vascular injury in non-rodents. Toxicol Pathol **34:**19-26, 2006
5. Louden C, Morgan DG. Pathology and pathophysiology of drug-induced arterial injury in laboratory animals and its implications on the evaluation of novel chemical entities for human clinical trials. Pharmacol Toxicol **89:**158-170, 2001

CASE IV: 47888 (AFIP 3135957).

Signalment: 7-year-old, castrated male domestic shorthair cat (*Felis catus*).

History: The cat presented for decreased activity, inappetance, dyspnea and tachypnea of 10 days duration. A markedly enlarged tracheobronchial lymph node, which was compressing the trachea, was noted on thoracic radiographs. Sternal lymph nodes were also enlarged. The patient returned after 4 days with progressive lethargy and inappetance. Neurological exam revealed signs consistent with a left supratentorial lesion (circling to the left, right conscious proprioceptive deficits, absent menace on the right side, and decreased facial sensation on the right side). The patient was euthanized 5 days after initial presentation, and a complete necropsy performed.

Gross Pathology: A 5.5 X 5.0 X 2.6 cm, soft, multinodular, mottled tan to pale tan mass (presumed tracheobronchial lymph node) is present at the tracheal carina. Adjacent epicardium and lung lobes are adhered to the mass. The sternal lymph nodes are soft, mottled pale tan to red and enlarged (up to 1.4 X 1 X 0.7 cm). The apex of the heart is mildly rounded. There are two, 0.3 cm diameter, well-demarcated, coalescent nodules in the myocardium at the apex. The left lung lobes are ~85% dark red, non-collapsing and slightly rubbery. The right lung lobes contain multifocal, tan to dark red, slightly rubbery foci predominantly at the periphery of the lobes. Both sides exude a moderate amount of blood when sectioned. There are multifocal, up to 0.5 cm diameter, well-demarcated, pale tan, soft nodules protruding from the endothelial surface of multiple pulmonary veins, partially or completely occluding the vascular lumina. In the left frontal gyrus, there is a poorly demarcated, 0.9 X 0.5X 0.5 cm, tan mass, with multifocal pinpoint red foci, that is slightly more firm than surrounding cerebral parenchyma.

Laboratory Results: **Relevant serum chemistry:** Total protein 10.1 g/dL (5.9-8.5); Albumin 3.4 g/dL (2.5-3.9); Globulin 6.7 g/dL (2.4-5.3). **Protein electrophoresis:** Total protein 9.8 g/dL (5.9-8.5); Albumin 4.09 g/dL (2.1-3.3); Alpha 1 globulins 0.06 g/dL (0.2-1.1); Alpha 2 globulins 0.82 g/dL (0.4-0.9); Beta globulins 1.72 g/dL (0.9-1.9); Gamma globulins 3.11 g/dL (1.7-4.3); A/G ratio 0.72. **Electrophoresis interpretation:** Consistent with polyclonal gammopathy, most often due to nonspecific chronic inflammation or infection. FeLV and FIV ELISA: negative. **Hematology:** No significant findings. PCR (via Washington Animal Disease Diagnostic Lab): A portion

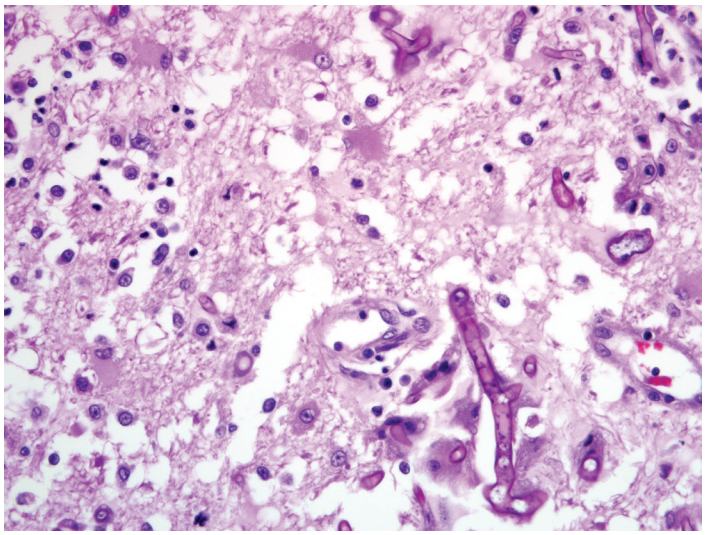

4-1. Cerebrum, cat. Within areas of liquefactive necrosis are numerous gemistocytic astrocytes, macrophages, and fewer neutrophils and multinucleated giant cells centered on fungal hyphae. Hyphae have 10-20um diameter non-parallel walls, are rarely septate, exhibit non-dichotomous right angle and acute angle branching, and frequently have bulbous dilatations. (HE 400X)

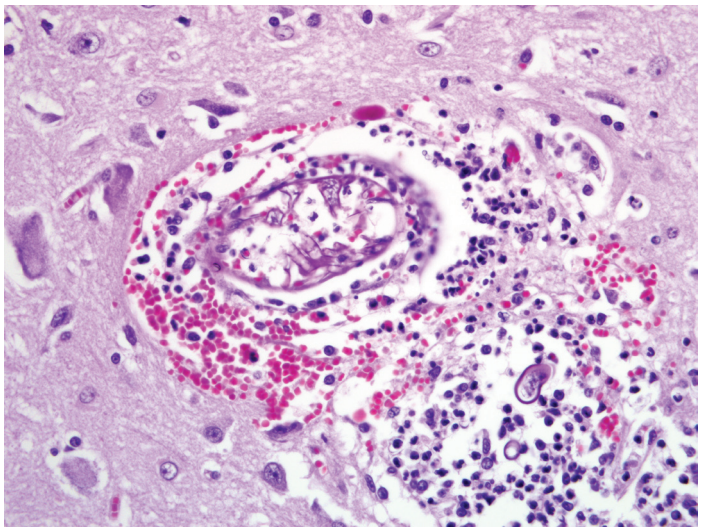

4-2. Cerebrum, cat. Multifocally vessels within the cerebral white matter are cuffed by many neutrophils, macrophages, lymphocytes, and hemorrhage. There is multifocal necrotizing vasculitis, and vessel lumens contain numerous previously described fungal hyphae. (HE 400X)

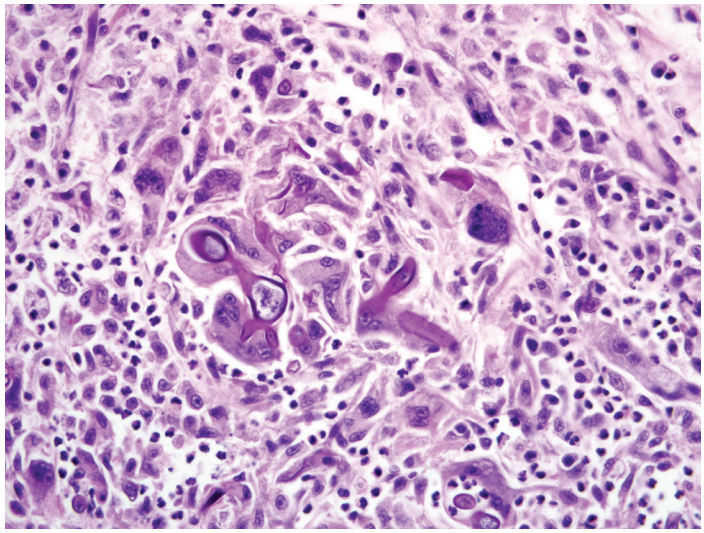

4-3. Heart, cat. Within areas of lytic necrosis are many neutrophils and macrophages and fewer multinucleated giant cells and eosinophils which surround the previously described fungal hyphae. Occasionally hyphae are found in the cytoplasm of multinucleated giant cells. (HE 400X)

of 28S ribosomal RNA gene was amplified and sequenced. The sequence most closely matched *Alternaria alternata* or *Alternaria tenuissimi* (>99% sequence identity) when compared with sequences in GenBank. These two species are synonymous.

Histopathologic Description: Brain: Sections of left frontal (rostral cerebral) cortex reveal multifocal infiltration and effacement of both gray and white matter by numerous fungal organisms and inflammatory cells. Fungal hyphae range from 7-15 micron in width, with nonparallel walls and frequent bulbous swellings (up to 30 microns in diameter). The hyphae contain infrequent septae, with irregular, dichotomous and non-dichotomous, acute angle to right angle branching (**fig. 4-1**). Occasionally, granular eosinophilic or basophilic material is present within hyphae. The hyphae are present on a background of rarified and often hypereosinophilic neuroparenchyma, which is multifocally infiltrated by moderate to large numbers of neutrophils, histiocytes and multinucleated giant cells with fewer lymphocytes and plasma cells. Occasionally, fragments of fungal hyphae are present within the cytoplasm of multinucleated giant cells (**fig. 4-3**). Moderate populations of gitter cells, microglia and astroglia are scattered throughout the affected areas along with mild hemorrhage. Large astroglial cells with abundant eosinophilic cytoplasm (gemistocytic astrocytes) are multifocally observed. Multifocally, small to moderate populations of lymphocytes, plasma cells and neutrophils are present within Virchow Robin spaces (perivascular cuffs) of the adjacent unaffected cortex. There is fibrinoid degeneration of vessel walls, with fibrin exudation, necrosis, leukocytoclasia, and vascular infiltration by neutrophils and fungal hyphae (**fig. 4-2**). Small numbers of similar inflammatory cells are multifocally present within the meninges.

Heart: A section of the heart reveals multifocal to coalescing nodules within the myocardium composed of fungal hyphae and inflammatory populations similar to those described above. Inflammatory populations include numerous histiocytes and neutrophils with fewer multinucleated giant cells, and lymphocytes and plasma cells on a background of loose connective tissue stroma. Histiocytes multifocally contain abundant, granular, brown cytoplasmic pigment (hemosiderin). Entrapped myofibers are often hypereosinophilic and shrunken with loss of cross striations, rarely vacuolated sarcoplasm and pyknotic nuclei (degenerative change). There is mild interstitial edema and few Anitschkow cells characterized by elongated, undulating nuclei. Multifocally, there are few foci of interstitial fibrosis in the remaining, unaffected myocardium.

Tracheobronchial lymph node (tissue not included): The tracheobronchial lymph node is diffusely effaced by pyogranulomatous inflammation containing fungal hyphae similar to those described above. This inflammation is often partially surrounded by fibrous connective tissue. Inflammatory cells extend to the adjacent pulmonary parenchyma and vessels, which are partially to completely occluded by the granulomas. Vascular changes, including fibrinoid degeneration and inflammation similar to that described in the brain, is also multifocally present.

Contributor's Morphologic Diagnosis: 1. Brain, cerebral cortex: Severe, multifocal to coalescing, chronic ongoing pyogranulomatous encephalitis with intralesional fungal hyphae and multifocal fibrinonecrotizing vasculitis.
2. Heart: Severe, multifocal to coalescing, chronic ongoing, pyogranulomatous myocarditis with intralesional fungal hyphae, myocardiocyte degeneration and loss.
3. Tracheobronchial lymph node (tissue not included): Severe, diffuse, chronic-ongoing pyogranulomatous lymphadenitis with invasion into adjacent pulmonary parenchyma, multifocal fibrinonecrotizing vasculitis and intralesional fungal hyphae.

Contributor's Comment: Prior to PCR identification, other fungi, namely zygomycetes such as *Rhizopus, Absidia, Mucor* or *Mortierella* spp. were considered, especially in light of the fungal morphology and lack of visible melanin on H&E.

Alternaria alternata is a dematiaceous (pigmented), saprophytic fungus that is ubiquitous in the environment (indoors and outdoors) and can be isolated from the skin or fur of healthy humans and animals.[4,13] It is an uncommon cause of phaeohyphomycosis in humans with reports of cases in cats, dogs, goats, horses and deer.[4] In humans, lesions are mainly cutaneous with cases of osteomyelitis, sinusitis, keratitis, onychomycosis and pulmonary granulomas.[3,4,13] In veterinary species, lesions are usually confined to the skin and subcutis with few reports of nasal involvement in cats and keratitis in a horse.[4,5,9,11] Human cases are associated with hypersensitivity syndromes such as "woodworker's lung," asthma and eosinophilic pneumonia.[9,11,13] Because of the ubiquitous nature of the fungus, immunosuppression is often suspected, if not proven, in clinical cases.[11-13]

Phaeohyphomycoses are usually opportunistic infections in which fungi generally gain entry via skin wounds.[5,7] Systemic or visceral phaeohyphomycoses are rare, but seem to have a predisposition for the central nervous system (CNS).[1,3,6,10] In these cases, the route of infection is thought to be inhalation with subsequent hematogenous

spread to the brain.[3,6,10] CNS phaeohyphomycoses are almost always attributed to *Cladophialophora bantiana* (previously known as *Torula bantiana, Cladosporium bantianum, Xylohypha bantiana, Cladosporium trichoides* and *Xylohypha emmonsii*).[1,10] This species exhibits marked neurotropism, which is related to the presence of introns at the 18S rDNA subunit.[1] There is a single report of fatal systemic illness in a cat due to *Cladophialophora bantiana* without CNS involvement.[6] Other species implicated in phaeohyphomycoses in cats include *A. infectoria, Exophiala jeanselmai, Dreschlera spicifera, Exophiala spinifer, Fonsecaea pedrosoi, Moniliella suaveolens, Scolecobasidium humicola, Staphylotrichum coccosporum,* and *Ochronic gallopavum*.[1,11,12]

Systemic illness in cats due to *Alternaria* species has not been reported. It is interesting that this cat also had CNS involvement, although the clinical progression suggests a tracheobronchial lymphadenitis that disseminated to the brain rather than primary brain lesion. No cutaneous lesions were noted in this case, and it is suspected that inhalation may be the route of infection. *Alternaria* spp. have small spores that may allow it to gain entry to lower airways and subsequently to draining lymph nodes.[5]

Identification of dematiaceous fungi requires culture and examination of fungal morphology or molecular techniques such as PCR. *Alternaria* spp. in culture are pigmented, with tapering of one end of the conidia to form a characteristic beak. The shape of the beak can help differentiate between different species. The conidia form long chains, which may or may not branch depending on the species.[13]

Dematiaceous fungi always form pigment in culture; however, pigment may not be readily visible in H&E tissue sections.[3] Often, melanin stains, such as Fontana-Masson, are recommended to highlight the presence of melanin in hyphae.[3,5,12] In this case, Fontana-Masson was performed on the tissue sections from the affected cat, as well as in a control case of non-pigmented fungus (morphology consistent with *Aspergillus* sp.), and revealed staining of the hyphae of both types of fungi. Fontana-Masson staining of fungal hyphae should be interpreted with caution, as there may be nonspecific uptake of silver stain in fungal hyphae as demonstrated in this case. A copper-sulfide-silver method [2] described for fungal cultures was modified for use in fixed tissue to try to find a more discriminatory staining technique. This method resulted in inconsistent staining of all fungal hyphae examined (presumed melanized as well as non-melanized).

AFIP Diagnosis: 1. Brain, cerebrum: Encephalitis, necrotizing and pyogranulomatous, multifocal to coalescing, severe, with vasculitis and fungal hyphae.
2. Heart: Myocarditis, pyogranulomatous, multifocal coalescing, marked, with myocardial degeneration, necrosis and loss, and fungal hyphae.

Conference Comment: There is some slide variation with respect to lesion distribution, particularly in the heart, where the lesion ranges from intramural to transmural and from focal to multifocal coalescing.

The contributor provided an excellent review of phaeohyphomycosis in general, and alternariosis in particular. Most conference participants considered disseminated zygomycosis to be the most likely etiologic diagnosis, which is not surprising in light of the lack of pigmentation in this particular case. Zygomycosis refers to infection by fungi of the orders Entomophthorales (*Basidiobolus* sp. and *Conidiobolus* sp.) and Mucorales (*Mucor* sp., *Rhizopus* sp., *Rhizomucor* sp., and *Absidia* sp.). In both, hyphae are broad and poorly septate; however, in entomophthoromycosis they are characteristically bounded by brightly eosinophilic sleeves, which are lacking in this case.[8] For many participants, the differential diagnosis also included hyalohyphomycosis caused by nondematiaceous opportunistic fungi that also form hyphae in tissue. These differ from the hyphae in phaeohyphomycosis in that they generally have thinner walls and are not pigmented.[8] This case highlights the utility of molecular diagnostics in practice.

The incidence of phaeohyphomycosis is increasing, resulting in a dramatic increase in importance in human medicine in recent years.[13] As noted by the contributor, it is important to recall that while the production of pigment is characteristic of dematiaceous fungi in culture, it may not be visible on H&E sections. *Alternaria infectoria* is the most common clinically important species in human cases of alternariosis, but its lack of pigmentation and poor ability to sporulate in routine media make it difficult to diagnose. As a result, numerous cases have been erroneously attributed to *A. alternata* or *A. tenuissima*, when *A. infectoria* was the true etiology.[13]

In contrast to localized phaeohyphomycosis, which is only rarely associated with immunosuppression in dogs and cats, disseminated disease is usually associated with immunosuppression. The polyclonal gammopathy present in this case is common with this disease, indicating a persistent, but ineffective humoral immune response.[8]

Contributor: The Animal Medical Center, Department of Pathology, 510 East 62nd St., New York, NY 10065
http://www.amcny.org/

References:

1. Abramo F, Bastelli F, Nardoni S, Mancianti F: Feline cutaneous phaeohyphomycosis due to *Cladophyalophora bantiana*. J Fel Med Surg **4:**157-163, 2002
2. Butler MJ, Gardiner RB, Day AW: Fungal melanin detection by the use of copper sulfide-silver. Mycologia **97**(2):312-319, 2005
3. Chandler FW, Kaplan W, Ajello L: Color Atlas and Text of the Histopathology of Mycotic Diseases, pp. 10, 92-95. Year Book Medical Publishers, Inc. Chicago, IL, 1980
4. Dhein CR, Leathers CW, Padhye AA, Ajello L: Phaeohyphomycosis caused by *Alternaria alternata* in a cat. J Am Vet Med Assoc **193:**1101-1103, 1988
5. Dye C, Johnson EM, Gruffyd-Jones TJ: Short communication: *Alternaria* species infection in nine domestic cats. J Fel Med Surg **11:**332-336, 2009
6. Elies L, Balandraud V, Boulouha L, Crespeau F, Guillot J: Fatal systemic phaeohyphomycosis in a cat due to *Cladophialophora bantiana*. J Vet Med A Physiol Pathol Clin Med **50:**50-53, 2003
7. Genovese LM, Whitbread TJ, Campbell CK: Cutaneous nodular phaeohyphomycosis in five horses associated with *Alternaria alternata* infection. Vet Rec **148:**55-56, 2001
8. Grooters AM, Foil CS: Miscellaneous fungal diseases. *In:* Infectious Diseases of the Dog and Cat, ed. Greene CE, 3rd ed., pp. 637-650. Saunders Elsevier, St. Louis, MO, 2006
9. Kalina WV, Anderson ML, Gershwin LJ: *Alternaria* aerosol during a bovine respiratory syncytial virus infection alters the severity of subsequent re-infection and enhances IgE production. Comp Immunol Microbiol Infect Dis **29:**138-156, 2006
10. Mariani CL, Platt SR, Scase TJ, Howerth EW, Chrisman CL, Clemmons RM: Cerebral phaeohyphomycosis caused by *Cladosporium* spp. in two domestic shorthaired cats. j Am Anim Hosp Assoc **38:**225-230, 2002
11. McKay JS, Cox CL, Foster AP: Cutaneous alternariosis in a cat. J Small Anim Pract **42:**75-78, 2001
12. Outerbridge CA, Myers SL, Summerbell RC: Phaeohyphomycosis in a cat. Can Vet J **36:**629-630, 1995
13. Pastor FJ, Guarro J: *Alternaria* infections: laboratory diagnosis and relevant clinical features. Clin Microbiol Infect **14:**734-746, 2008

The Armed Forces Institute of Pathology
Department of Veterinary Pathology

Conference Coordinator:
Shannon Lacv. DVM. MPH

WEDNESDAY SLIDE CONFERENCE 2009-2010

Conference 3

23 September 2009

Conference Moderator:

Marc E. Mattix, DVM, MSS, Diplomate ACVP

CASE I: 3383-08 (AFIP 3103744).

Signalment: Placenta from an aborted meat goat fetus (*Capra hircus*).

History: Increased late-term abortions were reported in the herd. We received a placenta only on the first submission and 2 fetuses with placentas later.

Gross Pathology: The fetal tissues were unremarkable and the placentas had diffuse rough thickening of the cotyledons and multifocal to coalescing pale, slightly raised foci and plaques on the intercotyledonary membranes (**fig. 1-1**).

Laboratory Results: **Culture**: No *Brucella* sp. or other significant bacteria from the placenta or fetus (4+ alpha *Streptococcus* sp. and 4+ *E. coli* in the abomasal fluid and placenta). ***Leptospira* F.A.:** Negative on fetal kidneys. ***Chlamydia* (*Chlamydophila*) PCR:** Negative. ***Coxiella burnetii* immunohistochemistry:** Positive (done at UC Davis).

Histopathologic Description: There is diffuse cotyledonary necrosis with intralesional, intracellular (intratrophoblastic) minute, basophilic organisms and multifocal intercotyledonary necrotizing placentitis (**fig. 1-2**). Intact trophoblasts laden with the numerous intracytoplasmic bacteria are somewhat more evident on the intercotyledonary placenta (**fig. 1-3**).

Contributor's Morphologic Diagnosis: Necrotizing placentitis, due to *Coxiella burnetii* (Q Fever).

Contributor's Comment: Myriad intracellular minute bacteria are in the surface trophoblasts of the cotyledons and on the intercotyledonary chorion with essentially diffuse necrosis that spares only limited sections of the intercotyledonary chorion. Ruminants, especially sheep and goats, are susceptible to *Coxiella burnetti* placentitis and abortion, and humans are very susceptible to infection. The organisms are acid-fast,[8] as were ours, with a diffuse granular red staining of the infected trophoblast cytoplasm (**fig. 1-4**). They also stain with Gimenez as intracellular clusters of coccobacilli or thin rods, whereas *Chlamydophila* are uniformly round.[7,8] Our Giemsa stain also demonstrated that the swollen trophoblasts were filled with granular organisms. Toxoplasmosis was ruled out by the minute size of the organisms and lack of involvement

***Sponsored by the American Veterinary Medical Association, the American College of Veterinary Pathologists, and the C. L. Davis Foundation.**

1-1. Placenta, goat. The cotyledons are diffusely thickened and rough, and there are multifocal to coalescing pale raised foci and plaques on the intercotyledonary membranes. Photograph courtesy of Livestock and Poultry Commission, P.O. Box 8505, Little Rock, AR 72215, jbritt@alpc.ar.gov

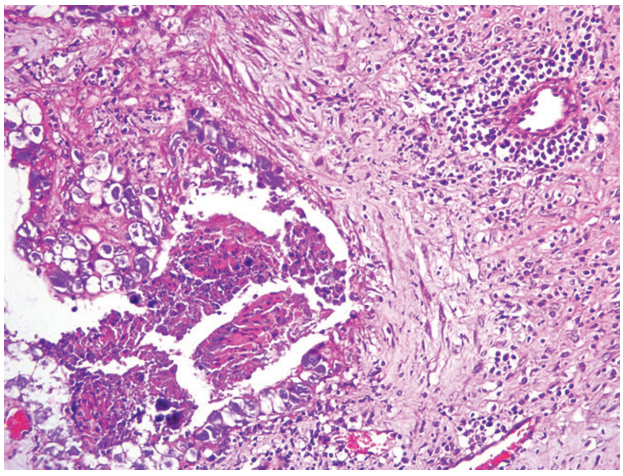

1-2. Placenta, goat. The placenta is diffusely edematous, with multifocal necrosis of the cytotrophoblasts and perivascular infiltrates of lymphocytes and plasma cells. (HE 200X)

of the brain and other internal fetal tissues and lack of reaction with PAS. Fetal lesions are generally lacking with Q fever, although the agent can be found in the fetal tissues by PCR [10] and about 10% of the fetuses may have multifocal subacute or histiocytic inflammation.[7] *Chlamydophila* would be the main consideration, and our PCR for it was negative. The causative agent for that has been renamed from *Chlamydia psittaci* serotype 1 to *Chlamydophila abortus*.

Coxiella, Brucella, and *Chlamydophila* infections in sheep and goats cause both cotyledonary and intercotyledonary necrosis [3,4,8] and all 3 agents target the intracellular fetal trophoblast cells.[10] *Campylobacter* infection causes similar lesions with necrotic inflammation also being in the fetal tissues.[4,5] Campylobacteriosis only affects the cotyledons in cows.[3]

One survey in France [8] found that infected or carrier cows and goats generally shed Coxiella in their milk and sheep mostly in vaginal secretions and feces. Since human infection is generally by aerosol, this might explain why humans are at greater risk from contact with sheep. This study did not find a correlation between recent parturition and shedding of organisms.

A PCR survey [5] of milk goat abortions on the island of Sardinia found 82.7% negative for an infectious agent and 16.3% positive with the results as below from 23 caprine fetuses and 8 placentas:

- *Toxoplasma*: 13% / 25% (fetus / placenta)
- *Salmonella abortusovis*: 0% / 0%
- *C. burnetti*: 0% / 12.5%
- *Chlamydophila abortus*: 0% / 12.5%
- *Neospora caninum*: 8.6% / 0%

Goats may abort with *Coxiella* infection in 2 consecutive pregnancies although they have antibodies, so there may not be protective immunity after the first infection and a carrier state is possible.[1] Another survey found 9% of the goat abortions being due to Coxiella infection, but lesions were usually limited to the placenta and many submissions did not have the placenta.[7]

AFIP Diagnosis: Chorioallantois: Placentitis, necrotizing and suppurative, subacute, multifocal, marked, with vasculitis and intratrophoblastic coccobacilli.

Conference Comment: The contributor provides a succinct review of this entity and the differential diagnosis. Conference participants noted the foamy appearance of cells containing the *Coxiella burnetti* organism in this case, which is characteristic. Both *Coxiella burnetti* and *Chlamydophila abortus* stain positively with the modified acid fast stain or by the Gimenez method, which differentiates them from *Brucella abortus* and *Campylobacter* species. *Coxiella burnetti* and *Chlamydophila abortus* are morphologically distinct; the former are thin, pleomorphic, rod-shaped structures, while the elementary bodies in *Chlamydophila abortus* infection are round and smaller.[4] The pleomorphism of the *Coxiella* organism is attributed to the fact that when it replicates by binary fission, three distinct developmental forms result: spore, small cell variant, and large cell variant.[2]

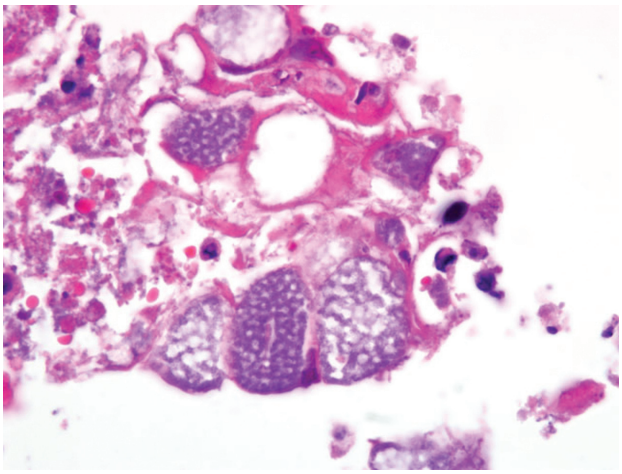

1-3. Placenta, goat. Multifocally intercotyledonary cytotrophoblasts are swollen with numerous intracytoplasmic basophilic organisms. (HE 1000X)

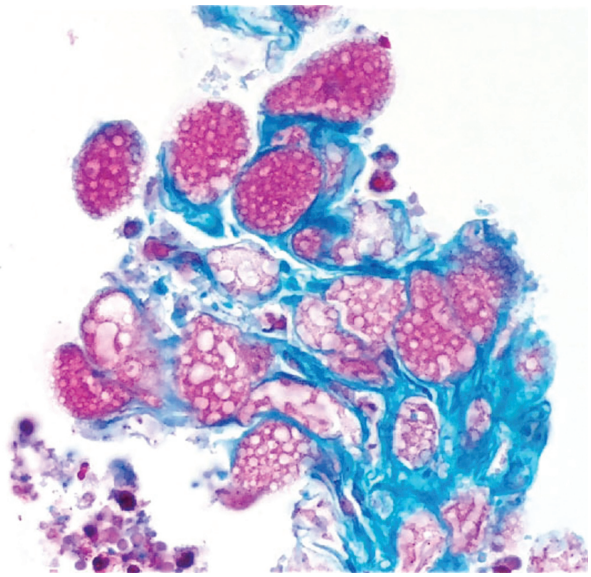

1-4. Placenta, goat. Diffusely, intratrophoblastic organisms are acid-fast. Modified acid-fast photomicrograph courtesy of Livestock and Poultry Commission, P.O. Box 8505, Little Rock, AR 72215, jbritt@alpc.ar.gov

While both organisms can cause both cotyledonary and intercotyledonary necrosis, the gross lesions of *Chlamydophila* infection affect the cotlyledons and intercotyledonary regions in roughly equal proportions, while the placental lesions in *Coxiella burnetti* infection are most prominent in the intercotyledonary region. Both organisms can cause vasculitis in the placenta, although it is characteristically more marked in *Chlamydophila* abortion.[4]

Contributor: Arkansas Livestock and Poultry Commission, 1 Natural Resources Dr., Little Rock, AR 72205 http://www.arlpc.org/

References:

1. Berri M, Rousset E, Champion JL, Russo P, Rodolakis, A: Goats may experience reproductive failures and shed Coxiella burnetii at two successive parturitions after a Q fever infection. Res Vet Sci **83:**47-52, 2007
2. Brogden KA: Cytopathology of pathogenic prokaryotes. *In:* Ultrastructural pathology: the comparative cellular basis of disease, ed. Cheville NF, 2nd ed., p. 476, Wiley-Blackwell, Ames, IA, 2009
3. Buergelt CL: Color Atlas of Reproductive Pathology of Domestic Animals. Mosby, St. Louis, MO, pp. 179-187, 1997
4. Kennedy PC, Miller RB: The female genital system. *In:* Pathology of Domestic Animals, eds. Jubb KVF, Kennedy PC, Palmer N, 4th ed., vol. 3, pp. 396-419, Academic Press, San Diego, CA, 1993
5. Ladds PW, We F-M, Chang W-F, Shyu J-J: A Color Atlas of Veterinary Reproductive Pathology. Pig Research Institute, Taiwan, pp. 292-294, 297-298, 1997
6. Masala G, Porcu R, Daga C, Denti S: Detection of pathogens in ovine and caprine samples from Sardinia, Italy, by PCR. J Vet Diagn Invest **19:**96-98, 2007
7. Moeller RB: Causes of caprine abortion: diagnostic assessment of 211 cases (1991-2998), J Vet Diag Invest 13:265-270, 2001
8. Moore JD, Barr BC, Daft BM, O'Connor MT: Pathology and diagnosis of Coxiella burnetii infection in a goat herd. Vet Pathol **28:**81-84, 1991
9. Rodolakis A, Berri M, Héchard C, Caudron C, et al: Comparison of *Coxiella burnetii* infection in milk of dairy bovine, caprine, and ovine herds. J Dairy Sci **90:**5352-5360, 2007
10. Sánchez J, Souriau A, Buendía AJ, Arricau-Bouvery N, Martínez CM, Salinas J, Rodolakis A, Navarro JA: Experimental *Coxiella burnetii* infection in pregnant goats: a histo-pathological and immunohistochemical study. J Comp Pathol **135:**108-115, 2006

CASE II: 976/08 (AFIP 3134294).

Signalment: Adult, female banded mongoose (*Mungos mungo*).

History: The whole population of 8 banded mongooses (*Mungos mungo*) of a zoological park was affected and died within 11 days. Animals were housed in an outdoor enclosure. Some animals showed anorexia, lethargy and staggering gait. Severe dyspnea and swelling of the intermandibular region were regularly observed. Therapy with prednisolone and antibiotics was unsuccessful. There was no previous animal transfer in the population. Similar fatalities in other animal species did not occur. The animal keepers were healthy and free of any skin lesion. Mongooses died about two days after onset of disease. Four mongooses were submitted to our institute for pathomorphological examination.

Gross Pathology: Animals were in good nutritional condition. There were multiple inconspicuous skin lesions predominately at the head and ventral trunk, measuring up to 0.5 cm in diameter. Some lesions appeared as small papules or vesicles, others as pustules. Single skin lesions were covered by crusts. There was a small ulcer on the tongue in one animal. Retropharyngeal tissue (including lymph nodes) was replaced by a firm whitish mass compressing the larynx. Within liver and spleen there were miliary white foci of necrosis and multiple petechiae.

Laboratory Results: Orthopoxvirus was detected virologically and identified as cowpoxvirus (negative staining, transmission electron microscopy, cell culture, PCR, sequencing).

Histopathologic Description: Liver: Multifocally to coalescing there are randomly distributed foci of hepatocellular degeneration and necrosis, characterized by hypereosinophilia, loss of cellular detail, cellular debris, and pyknotic as well as karyorrhectic nuclei (coagulative necrosis). Foci vary in size from 40 to 200 µm; in some locations only single hepatocytes are affected. In less affected areas, hepatocytes are swollen, have pale eosinophilic cytoplasm and swollen nuclei (degeneration). Centrally in the necrotic zone there is extravasation of blood cells (acute hemorrhage) admixed with fibrin and degenerated inflammatory cells. Within the cytoplasm of necrotic cells, degenerating cells and unaltered hepatocytes there are up to five, oval or round, bright eosinophilic inclusion bodies ranging in 5-10 µm in size (**figs. 2-1 and 2-2**). Additionally, there is mild portal fibrosis and bile duct proliferation. There is a mild portal infiltration of lymphocytes and plasma cells. Single hepatocytes show cytoplasmic vacuolization (fatty change) and there is a mild intracanalicular cholestasis. **Spleen and lymph node** lesions (slides not submitted) were characterized by necrotizing inflammation, and cytoplasmic inclusion bodies were detectable occasionally. **Skin** lesions (slides not submitted) showed hyperplasia and degeneration of epithelial cells (ballooning degeneration) with acantholysis. Within the subcutaneous tissue of the neck there was marked edema and necrosuppurative cellulitis and necrotizing lymphadenitis of retropharyngeal lymph nodes.

Contributor's Morphologic Diagnosis: Liver: Hepatitis, necrotizing, multifocal to coalescing, random, subacute, severe, with intralesional hemorrhage and numerous intracytoplasmic inclusion bodies, banded mongoose, *Mungos mungo*. Etiology: Consistent with systemic cowpoxvirus infection.

Contributor's Comment: Poxvirus infections in nonnative hosts are a focus of epidemiological studies and there is an obvious zoonotic potential.[7,11,13,14] The most common sources of human infection are infected cats.[1] Recently, cases of cowpoxvirus infection in humans have been described in France and Germany after transmission from pet rats.[2,9] Wild rodents are suspected as reservoir hosts.[3] There are several reports on cowpox virus infection in zoo animals. Reports of lethal poxvirus infections in elephants [4] and fatal cases in felids [1,8] can be found in the literature. Felids usually develop a mild dermal or a fatal pulmonary course of the disease. Necrotizing hepatitis due to cowpox virus is rare in felids; however, cases have been described in lions and cheetahs.[8]

In the banded mongooses the most severe lesions were necrotizing hepatitis, splenitis and lymphadenitis with occurrence of characteristic eosinophilic cytoplasmic inclusion bodies. In contrast to cases of cowpox virus in other members of the suborder Feliformia, the lungs were unaltered. The etiologic diagnosis was confirmed by cell culture, electron microscopy, PCR and sequencing. Wild rodents may have served as reservoir and vector in our cases. This hypothesis was supported by observation of poxvirus lesions in a captured rat in the surrounding of the outdoor enclosure.

AFIP Diagnosis: Liver: Hepatitis, necrotizing, multifocal to coalescing, random, severe, with numerous intracytoplasmic eosinophilic inclusion bodies.

Conference Comment: Despite its name, cowpox virus infection is neither endemic nor common in cattle.[2,14]

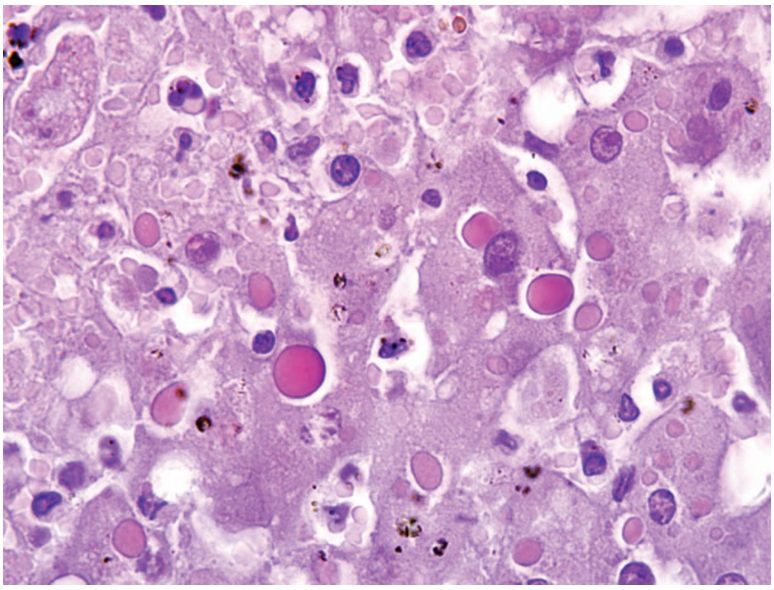

2-1. Liver, mongoose. Multifocal random areas of hepatocellular lytic necrosis, with degenerate hepatocytes containing one to five, round to oval, brightly eosinophilic, cytoplasmic inclusion bodies. (HE 1000X)

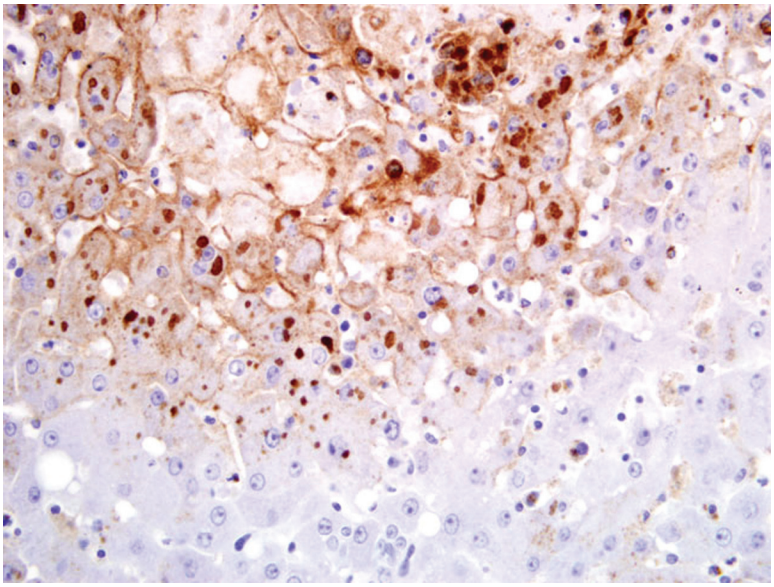

2-2. Liver, mongoose. Affected hepatocytes, have positive strong cytoplasmic immunoreactivity for cowpox viral antibody. (400X)

The contributor's review provides due emphasis on the role of cats in zoonotic cowpox virus infection. Many attribute an apparent increase in human infections with cowpox virus to waning immunity to orthopoxviruses in general, associated with the cessation of immunization with Vaccinia virus for smallpox.[2,14]

While many members of the Poxviridae family cause only localized cutaneous disease, the following characteristically produce systemic disease, which may be severe: Sheeppox virus, Ectromelia virus, Monkeypox virus, and Variola virus.[5] Conference participants discussed these and other poxviruses of veterinary importance, which are summarized by genus as follows:

- Avipoxvirus: 10 species, including Fowlpox virus
- Capripoxvirus: Goatpox virus, Lumpy skin disease virus, Sheeppox virus
- Cervidpoxvirus: Deerpox virus W-848-83
- Leporipoxvirus: Myxoma virus, Rabbit (Shope) fibroma virus, Squirrel fibroma virus
- Molluscipoxvirus: Molluscum contagiosum virus
- Orthopoxvirus: Camelpox virus; Cowpox virus; Ectromelia virus; Monkeypox virus; Vaccinia virus (buffalopox virus, rabbit pox virus); Variola virus
- Parapoxvirus: Bovine papular stomatitis virus; Orf virus; Parapoxvirus of red deer in New Zealand; Pseudocowpox virus
- Suipoxvirus: Swinepox virus

- Yatapoxvirus: Tanapox virus; Yaba monkey tumor virus
- Unassigned: Squirrel poxvirus [5,6]

Typical poxviral lesions are both proliferative and necrotizing. As poxviruses are epitheliotropic, replication within cells causes degeneration (i.e. "ballooning degeneration") and necrosis, which is further exacerbated by ischemia when the virus replicates in endothelial cells and causes vascular damage. Several virulence factors may account for the ability of poxviruses to induce proliferation, including a gene whose product resembles epidermal growth factor.[5]

Unlike other DNA viruses, poxviruses produce intracytoplasmic, rather than intranuclear inclusion bodies. All poxviruses produce small, basophilic, intracytoplasmic inclusion bodies, designated *type B* or Guarnieri's bodies, early in the replication cycle. These represent the actual sites of virus replication. The numerous, large, prominent, eosinophilic, intracytoplasmic inclusion bodies noted in this case are designated *type A* or acidophilic-type inclusions (ATI), and they are produced later in the replication cycle. In humans, type A inclusions are diagnostically useful, because they are only associated with certain poxviruses (e.g. Cowpox and Ectromelia virus, but not Monkeypox, Variola, or Vaccinia virus). Capripoxviruses generally produce *type A* inclusions; the large inclusions in Avipoxvirus infections are known as Bollinger bodies and they contain smaller Borrel bodies representing virus particles.[12]

Contributor: Institut für Veterinaer-Pathologie, Universitaet Giessen, Frankfurter Str. 96, 35392 Giessen, Germany
http://www.uni-giessen.de/cms/fbz/fb10/institute_klinikum/institute/pathologie/

References:

1. Baxby D, Bennett M, Getty B: Human cowpox 1969-93: a review based on 54 cases. Br J Dermatol **131:**598-607, 1994
2. Campe H, Zimmermann P, Glos K, Bayer M, Bergemann H, Dreweck C, Graf P, Weber BK, Meyer H, Büttner M, Busch U, Sing A: Cowpox virus transmission from pet rats to humans, Germany. Emerg Infect Dis **15**(5):777-80, 2009
3. Chantrey J, Meyer H, Baxby D, Begon M, Bown KJ, Hazel SM, Jones T, Montgomery WI, Bennett M: Cowpox: reservoir hosts and geographic range. Epidemiol Infect **122**(3):455-460, 1999
4. Essbauer S, Meyer H, Kaaden OR, Pfeffer M: Recent cases in the German poxvirus consulting laboratory. Revue Med Vet **153:**635-642, 2002
5. Ginn PE, Mansell JEKL, Rakich PM: Skin and appendages. *In:* Jubb, Kennedy, and Palmer's Pathology of Domestic Animals, ed. Maxie MG, 5th ed., vol. 1, pp. 664-674. Elsevier Saunders, Philadelphia, PA, 2007
6. International Committee on Taxonomy of Viruses (Internet): Virus taxonomy. Available from: http://www.ictvonline.org, 2008
7. Kurth A, Wibbelt G, Gerber HP, Petschaelis A, Pauli G, Nitsche A: Rat-to-elephant-to-human transmission of Cowpox virus. Emerg Infect Dis **14**(4):670-671, 2008
8. Marennikova SS, Maltseva NN, Korneeva VI, Garanina N: Outbreak of pox disease among carnivora (felidae) and edentata. J Infect Dis **135:**358-366, 1977
9. Ninove L, Domart Y, Vervel C, Voinot C, Salez N, Raoult D, Meyer H, Capek I, Zandotti C, Charrel RN: Cowpox virus transmission from pet rats to humans, France. Emerg Infect Dis **15**(5):781-784, 2009
10. Nitsche A, Kurth A, Pauli G: Viremia in human Cowpox virus infection. J Clin Virol **40**(2):160-162, 2007
11. Pahlitzsch R, Hammarin AL, Widell A: A case of facial cellulitis and necrotizing lymphadenitis due to cowpox virus infection. Clin Infect Dis **43**(6):737-742, 2006
12. Pfeffer M, Meyer H: Poxvirus diagnostics. *In:* Poxviruses, eds. Mercer AA, Schmidt A, Weber O, p. 359. Birkhäuser Verlag, Basel, Switzerland, 2007
13. Schulze C, Alex M, Schirrmeier H, Hlinak A, Engelhardt A, Koschinski B, Beyreiss B, Hoffmann M, Czerny CP: Generalized fatal Cowpox virus infection in a cat with transmission to a human contact case. Zoonoses Public Health **54**(1):31-37, 2007
14. Wolfs TF, Wagenaar JA, Niesters HG, Osterhaus AD: Rat-to-human transmission of Cowpox infection. Emerg Infect Dis **8**(12):1495-1496, 2002

CASE III: 0418271 (AFIP 2991560).

Signalment: 7-year-old, spayed female, domestic shorthair cat (*Felis catus*).

History: This cat was presented with general lethargy and responded initially to anti-inflammatory therapy (Rimadyl) for 24 hours. Marked swelling of the left cervical lymph node and tongue occurred after hospitalization. The animal's condition worsened, with respiratory signs (rales, rapid and open mouth breathing, dyspnea). The animal eventually was unable to stand, and was euthanized.

Gross Pathology: This cat had enlarged cervical lymph nodes with a draining lesion of the left cervical

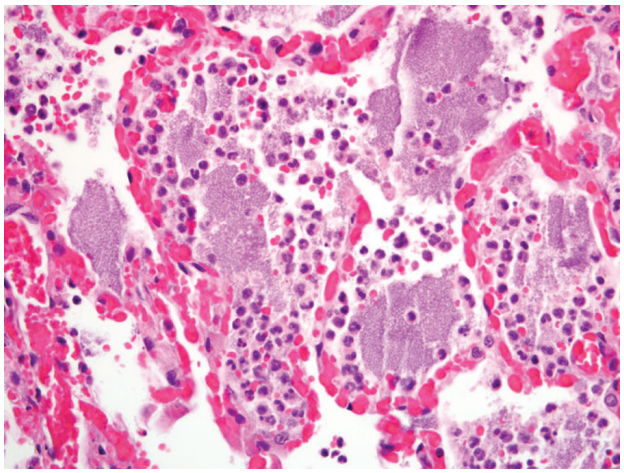

3-1. Lung, cat. Multifocally flooding alveoli are many viable and degenerate neutrophils and fewer alveolar macrophages centered upon large colonies of 1x3um bacilli. (HE 1000X)

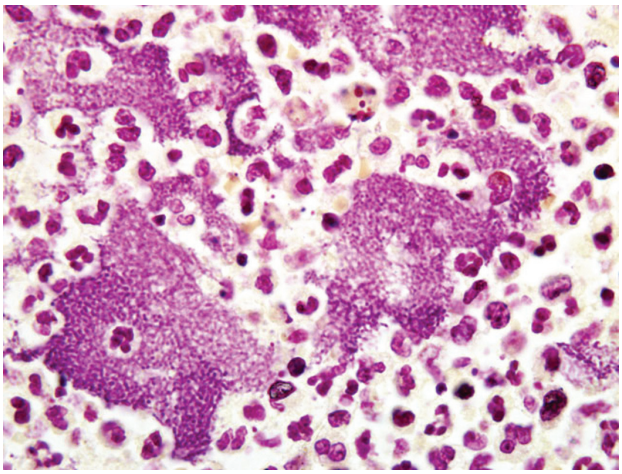

3-2. Lung, cat. Intraalveolar organisms are diffusely gram negative. (Brown and Hopps 1000X)

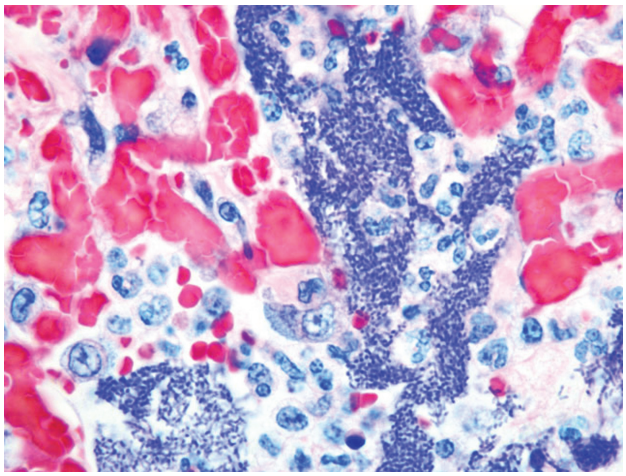

3-3. Lung, cat. Intraalveolar organisms are diffusely Giemsa positive, occasionally exhibiting bipolar staining. (1000X)

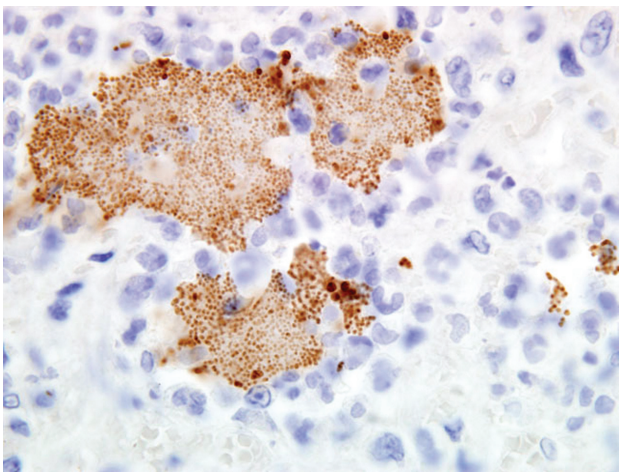

3-4. Lung, cat. Intraalveolar organisms have strong immunoreactivity for Yersinia antibody. (1000X)

node. The left tonsil was enlarged, and there was a large area of swelling and reddening under the tongue. A pseudomembrane was over a portion of this area. All lobes of lung were markedly congested, deep reddish-purple, and just barely floated in formalin.

Laboratory Results: Bacteriology: *Yersinia pestis* was isolated from lung. Lung was also positive on FA testing of lung swab smears for *Y. pestis*.

Histopathologic Description: In the lung, there are multifocal to coalescing areas of necrosis that obliterate the normal architecture. In the affected areas, the bronchioles and alveoli are filled with numerous bacteria, intact and degenerate neutrophils, fewer macrophages, fibrin, and edema fluid (**fig. 3-1**). Alveolar macrophages sometimes contain phagocytosed erythrocytes, necrotic cellular debris, and bacteria. The alveolar capillaries are engorged with RBCs and the necrotic foci occasionally contain fibrin thrombi.

Contributor's Morphologic Diagnosis: Lung: Pneumonia, necrotizing, suppurative, acute, multifocal to coalescing, moderate with intralesional bacteria colonies of *Yersinia pestis.*

Contributor's Comment: Plague is a zoonotic infection caused by *Yersinia pestis* affecting rats, mice,

ground squirrels, prairie dogs, kangaroo rats, bobcats, cats, rabbits, and chipmunks. The disease has also been described in ferrets, llamas, camels, mule deer, and goats. In New Mexico, it is occasionally also seen in dogs, although most of the literature cites that dogs are resistant. In our experience, we would modify that statement to "most dogs are resistant". *Yersinia pestis* is a pleomorphic, non-motile, non-spore forming, facultative anaerobe, gram negative, bipolar staining coccobacillus of the family *Enterobacteriaceae* (**figs. 3-2, 3-3 and 3-4**). The organism is now more accurately classified as a subspecies of *Y. pseudotuberculosis* based upon DNA-DNA pairing. It is a disease of antiquity, decimating human populations at various stages in history. Plague continues to be a problem today in many parts of the world, particularly in the western United States. In the Southwest, it is seen primarily in northern New Mexico and northeastern Arizona. In New Mexico, plague is most commonly found at elevations where piñon and juniper trees flourish. The main reservoirs are rock squirrels and prairie dogs, as well as deer mice and kangaroo rats. The principal mode of transmission of *Y. pestis* in mammals is via flea bite. A less common mode of transmission is ingestion of, or exposure to another animal infected with *Y. pestis*. Inhalation of aerosolized bacteria from animal with pneumonic plaque is a rare but effective mode of transmission also.

Cats (and dogs) acquire the disease most commonly following predation on infected rodents and lagomorphs or by bites from the prey's plague-infected fleas. The "season" for plague in New Mexico begins in mid-May, and peaks in August, tailing off in October. However, cases occur at any time with proper conditions. In New Mexico, plague cases increase after unusually wet winter and spring weather; these conditions are conducive to increase in the rodent (and subsequently, flea) population.

The lesions seen in *Y. pestis*-infected animals vary according to the mode of transmission of the organism and susceptibility of the host. The three classic clinical manifestations of *Y. pestis* infection include bubonic, pneumonic and septicemic plague and are seen primarily in susceptible non-rodent species. Cats submitted to our laboratory typically have some type of enlargement of tonsils, cervical lymph nodes, or both. These may or may not present as draining lesions. Exudate produced is typically mucoid, grey, and contains large numbers of bacteria. When the disease has progressed to the lungs, all lobes of both lungs will typically be deep reddish-purple, very congested, and often will sink (or just barely float) in formalin. When presented with a suspect plague case (either clinically or in the laboratory), it is important to take proper precautions with the animal. Intense and immediate flea control is paramount with these cases; in our laboratory, suspect cases are routinely sprayed liberally with an appropriate pyrethrin based insecticide prior to any examination or handling.

Clinically, these animals usually present with some type of oral lesion, salivating, gagging, respiratory difficulty or distress, and lymph node enlargement accompanied by a high temperature. There may be a draining lesion from the cervical lymph node region or tonsils. When diagnosed early, these animals respond readily to appropriate antibiotic therapy. The disease is so common in Santa Fe County in the summer months as to commonly be one of the differentials in ADR (i.e. "ain't doing right") cats. This disease is of importance as a public health risk, and as one of the select agents of bioterrorism.

AFIP Diagnosis: Lung: Pneumonia, necrosuppurative, multifocal to coalescing, severe, with myriad extracellular coccobacilli.

Conference Comment: Pneumonic plague has killed more people than any other bacterial pathogen in recorded history[1], and the contributor appropriately emphasized the importance of 1) having a high index of suspicion for plague based on geographical location and clinical and gross findings, and 2) using appropriate personal protective equipment when handling suspect cases in a clinical or diagnostic setting.

The virulence of *Yersinia* sp. depends on its ability to invade the host and evade host immune responses. This begins in the gut of the infected flea, where *Y. pestis* forms a biofilm that obstructs the gut; the flea then must regurgitate before feeding, and thus infects the host that it bites. Via an elaborate gene complex, the Yop virulon, *Yersinia* spp. form proteins that assemble into a type III secretion system, a hollow tube that projects from the bacterial surface, binds to host cells, and injects the bacterial toxins, known as *Yersinia* outercoat proteins (Yops). YopE, YopH, and YopT interfere with actin polymerization inside the host cell, thus blocking phagocytosis of the bacterium. YopJ inhibits the production of inflammatory cytokines by inhibiting the signaling pathways that are activated by lipopolysaccharide.[9]

While natural *Y. pestis* infections still occur in humans, large outbreaks have been prevented by improved sanitation and prompt, successful antibiotic treatment of patients with the bubonic form of the disease. However, it is now apparent that that *Y. pestis* can acquire multidrug resistance via plasmids that are readily horizontally transmitted, and in 1995, two fatal cases of bubonic plague were caused by multidrug resistant *Y. pestis*. As a result, the threat of

Y. pestis emergence as a deadly, multidrug resistant epidemic has prompted renewed interest in vaccination as a best line of defense against resurgent plague.[1]

Because whole cell vaccines are considered potentially unsafe and unreliable, vaccine research has focused on two antigens, F1 and LcrV. The F1 protein is a bacterial surface antigen that aids *Y. pestis* in evading recognition by the innate immune system; it is not essential for virulence, however, and is therefore not considered sufficient as a sole vaccine antigen. The LcrV protein is essential for virulence, and mediates insertion of a translocation pore, assembled via the type III secretion system, in the host cell membrane. Vaccines which combine both LcrV and F1 show promise against bubonic and pneumonic plague in animal models. The Brown Norway rat has emerged as a model for both human bubonic and pneumonic plague.[1]

Contributor: NMDA-Veterinary Diagnostic Services, 700 Camino de Salud NE, Albuquerque, NM 87106-4700 http://128.123.206.6/animal-and-plant-protection/veterinary-diagnostic-services

References:

1. Anderson DM, Ciletti NA, Lee-Lewis H, Elli D, Segal J, DeBord KL, Overheim KA, Tretiakova M, Brubaker RR, Schneewind O: Pneumonic plague pathogenesis and immunity in Brown Norway rats. Am J Pathol **174**(3):910-21, 2009
2. Behr M: Clarification about plague and its diagnosis. J Am Vet Med Assoc **211**(6):698, 1997
3. Cleri DJ, Vernaleo JR, Lombardi LJ, Rabbat MS, Mathew A, Marton R, Reyelt MC: Plague pneumonia disease caused by Yersinia pestis. Semin Respir Infect **12**(1):12-23, 1997
4. Eidson M, Thilsted JP, Rollag OJ: Clinical, clinicopathologic and pathologic features of plague in cats: 119 cases (1977-1988). J Amer Vet Med Assoc **199:**1191-1196, 1991
5. Ettestad, PE: Veterinary Epidemiologist, NM Dept Health, Personal Communication, July, 2005
6. Lappin MR: Feline zoonotic diseases. Vet Clin North Am Small Anim Pract **23**(1):57-78,1993
7. Lopez T: Plague. Finding ways to stop a killer. J Am Vet Med Assoc **211**(3):280-281, 1997
8. Macy DW: Plague. *In:* Infectious Diseases of the Dog and Cat, ed. Greene CE, 2nd ed., pp. 295-300. WB Saunders Co., Philadelphia, PA, 1998
9. McAdam AJ, Sharpe AH: Infectious diseases. *In:* Robbins and Cotran Pathologic Basis of Disease, eds. Kumar V, Abbas AK, Fausto N, Aster JC, 8th ed., p. 365. Saunders Elsevier, Philadelphia, PA, 2010
10. Rosser WW: Bubonic plague. J Am Vet Med Assoc **191**(4):406-9, 1987
11. Watson RP, Blanchard TW, Mense MG, Gasper PW: Histopathology of experimental plague in cats. Vet Pathol **38:**165-172, 2001

CASE IV: 1484/03 (AFIP 2940307).

Signalment: 12-week-old, male castrated pig (*Sus scrofa*), body weight 27 kg.

History: Died after anorexia, depression and weight loss with multiple hemorrhagic and necrotic skin lesions.

Gross Pathology: Irregular, red to purple macules and papules, which tend to coalesce, located mainly on the hind limbs and perineal area; moderately enlarged lymph nodes all over the body; kidneys enlarged, edematous, and pale with petechial cortical hemorrhages.

Laboratory Results: Porcine circovirus 2 positive.

Contributor's Morphologic Diagnosis: Severe, diffuse, segmental fibrinous glomerulonephritis with infiltration of neutrophilic leukocytes; sporadic glomerular sclerosis; interstitial nonsuppurative nephritis; proteinaceous casts and necrotizing vasculitis.

Contributor's Comment: Porcine Dermatitis and Neprhopathy Syndrome (PDNS) mainly affects growing pigs between 12 and 16 weeks of age, and less commonly older animals. The syndrome has been observed in herds of various genetic origin and health status.

The most striking clinical signs of PDNS are necrotizing skin lesions due to necrotizing vasculitis. At necropsy, other frequent findings are enlarged and pale kidneys with cortical petechiae. Microscopically, these renal lesions vary from acute necrotizing glomerulitis to chronic glomerular sclerosis. Besides the skin lesions, systemic necrotizing vasculitis in a variety of organs has been observed.[7] As a possible pathogenetic mechanism for this disease a type III hypersensitivity reaction due to microscopic features has been suggested.[7]

The etiology still remains unknown, but porcine circovirus 2 (PCV2) and porcine reproductive and respiratory syndrome virus (PRRSV) and *Pasteurella multocida* are discussed in the literature as possible contributing etiological agents.[8]

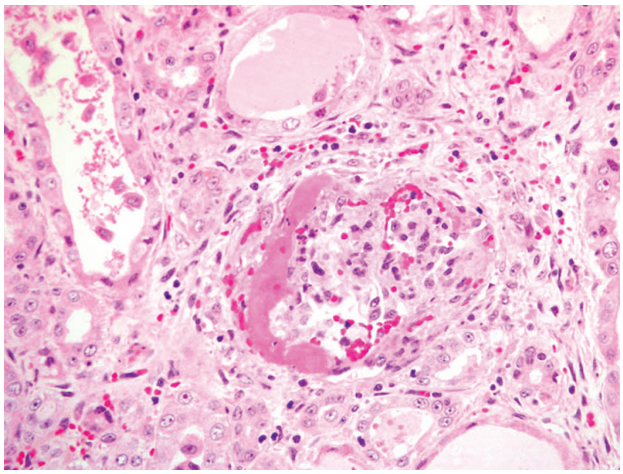

4-1. Kidney, pig. In the cortex, glomeruli are necrotic and expanded by abundant of fibrin, hemorrhage, and occasional macrophages. Multifocally tubules are degenerative or necrotic, and contain pink proteinaceous material and sloughed cellular debris. (HE 400X)

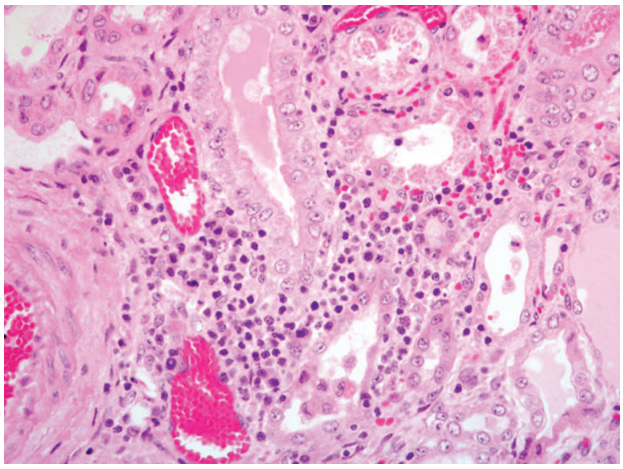

4-2. Kidney, pig. Multifocally the cortical interstitium is moderately expanded by many macrophages, lymphocytes, plasma cells, and edema. (HE 400X)

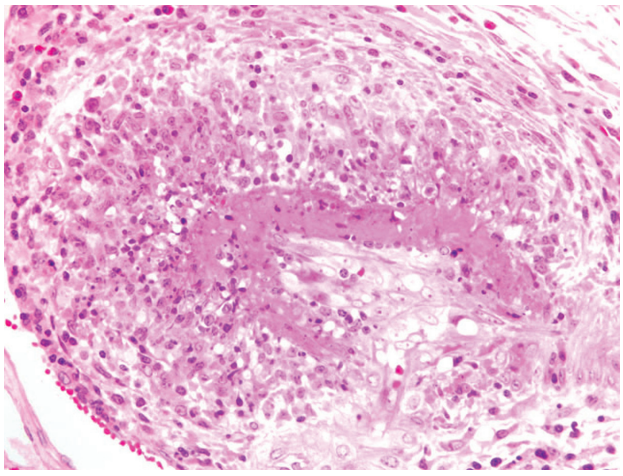

4-3. Kidney, pig. Within the renal pelvis, there is multifocal necrotizing vasculitis. (HE 400X)

PDNS was first described in the United Kingdom in 1993. Since then, several cases in Europe, North and South America and Africa have been described, suggesting a worldwide distribution.[7] This syndrome sometimes, but not always, occurs in commercial pig farms simultaneously with Postweaning Multisystemic Wasting Syndrome (PMWS). The relationship between the two syndromes is unclear.[7]

Differential diagnosis includes classical swine fever, African swine fever, swine erysipelas, and porcine stress syndrome. Bacterial diseases causing reddish discoloration of skin, petechiae, or cyanosis include infections by *Actinobacillus suis*, *Actinobacillus pleuropneumoniae*, *Streptococcus suis*, *Haemophilus parasuis*, and salmonellosis.

AFIP Diagnosis: 1. Kidney: Glomerulonephritis, exudative and membranoproliferative, diffuse, severe, with multifocal glomerular thrombosis and necrosis.
2. Kidney, arcuate arteries and branches: Arteritis, necrotizing and proliferative, diffuse, moderate to severe.
3. Kidney, pelvis: Epithelial hyperplasia and hypertrophy, diffuse, moderate, with marked cytoplasmic vacuolation.

Conference Comment: In the submitted sections of kidney, all levels of the nephron are affected. Diffusely, glomeruli exhibit one or more of the following changes (**fig. 4-1**): markedly dilated uriniferous space containing abundant fibrin with varying hemorrhage and necrotic debris; increased glomerular tuft cellularity with increased numbers of mesangial cells and thickened capillary basement membranes (membranoproliferative glomerulopathy); glomerular tuft thrombosis and necrosis; hypertrophy and hyperplasia of the parietal epithelium; attachment of the glomerular tuft to Bowman's capsule (synechia); and periglomerular fibrosis. Cortical tubules are ectatic and contain intraluminal hemorrhage, hematoidin, or hyaline casts. Multifocally, tubular epithelium is degenerate, necrotic, regenerative, or attenuated. Throughout the cortical interstitium, there are moderate numbers of histiocytes, lymphocytes, plasma cells, and rare hypertrophied fibroblasts (**fig. 4-2**). Multifocally, arcuate arteries and their branches at the corticomedullary junction are transmurally disrupted by neutrophils, macrophages, lymphocytes, plasma cells, and necrotic debris (**fig. 4-3**). The transitional epithelium

lining the renal pelvis is moderately hyperplastic and hypertrophied, and often contains one or more large, clear, intracytoplasmic vacuoles.

In the United States, the incidence of PCV2-associated disease (PCVAD) is increasing. Clinically, PCVAD is characterized by one or more of the following manifestations: PMWS, PDNS, respiratory disease, enteritis, reproductive disease, myocarditis, vasculitis, and exudative dermatitis.[2,5] The preponderance of evidence suggests that PCV2 is essential, but not sufficient, for PCVAD development. Therefore, PCVAD can best be thought of as multifactorial, with such factors as the virus, host, cofactors, and immune modulation playing important roles in disease pathogenesis.

Circoviridae are small, single-stranded, circular DNA viruses. The Circoviridae family consists of the following genera: Gyrovirus, which contains chicken anemia virus as its sole member the recently-discovered Anellovirus; and Circovirus. Along with PCV1 and PCV2, the Circovirus genus includes several avian circoviruses: beak and feather disease virus (BFDV), canary circovirus, goose circovirus, pigeon circovirus, duck circovirus, finch circovirus, and gull circovirus.[5,6] PCV1, which was initially discovered in tissue culture, is distributed worldwide and is nonpathogenic. PCV2 is very stable in the environment and has been found in wild boar in Germany and Spain, suggesting that they may be a reservoir.[6] PCV2 persists in dendritic cells, which are thought to serve as a vehicle for transport throughout the host.[5]

This case was submitted in 2004, and while there has been much work in the interim to further elucidate the cause and pathogenesis of PDNS, the role of PCV2 in the disease remains enigmatic and controversial. Numerous other etiologies, including PRRSV and a variety of bacteria have been proposed.[5] In one study, a high anti-PCV2 antibody titer was significantly associated with the development of PDNS, and PCV2 DNA was present in all PDNS cases; PPV and PRRSV nucleic acids were absent in many of the cases.[10] However, PDNS has not been experimentally reproduced in using PCV2, and PCV2 proteins are not detected in the vascular and glomerular lesions of PDNS.[4]

In a recent study, inoculation of gnotobiotic 2- and 3-day-old pigs with either of the following produced PDNS: 1) pooled plasma from healthy feeder pigs in a herd that was in the initial phases of a respiratory disease outbreak, and 2) a combination of PRRSV and tissue homogenate containing genogroup 1 torque teno virus (g1-TTV). All pigs seroconverted to PRRSV and were PCR-negative for PCV2; this was the first report of experimental induction of PDNS renal and cutaneous lesions in swine, and the authors concluded that PDNS is a manifestation of disseminated intravascular coagulation.[4] Interestingly, g1-TTV was also shown to potentiate PMWS in gnotobiotic pigs when inoculated together with PCV2. Disease was not produced by g1-TTV or PCV2 alone, or when PCV2-infected pigs were later challenged with g1-TTV.[3]

In addition to those listed by the contributor, other diseases that may mimic the skin lesions of PDNS include exudative epidermitis and swine pox. For the described gross renal lesions, i.e. "turkey egg kidney", the differential diagnosis includes salmonellosis, African swine fever, and classical swine fever.[2] The cause and significance of the marked vacuolation of the epithelium lining the renal pelvis in this case is unclear.

Contributor: Institute of Veterinary Pathology, Ludwig-Maximmians-University of Munich, Veterinaerstrasse 13, 80539 Munich, Germany
http://www.patho.vetmed.uni-muenchen.de/

References:

1. Allan GM, McNeilly E, Kennedy S, Meehan B, Moffett D, Malone F, Ellis J, Krakowka S: PCV-2-associated PDNS in Northern Ireland in 1990. Vet Rec **146:**711-712, 2000
2. Chae C: A review of porcine circovirus 2-associated syndromes and diseases. Vet J **169:**326-336, 2005
3. Ellis JA, Allan G, Krakowka S: Effect of coinfection with genogroup 1 porcine torque teno virus on porcine circovirus type 2–associated postweaning multisystemic wasting syndrome in gnotobiotic pigs. Am J Vet Res **69**(12):1608-1614, 2008
4. Krakowka S, Hartunian C, Hamberg A, Shoup D, Rings M, Zhang Y, Allan G, Ellis JA: Evaluation of induction of porcine dermatitis and nephropathy syndrome in gnotobiotic pigs with negative results for porcine circovirus type 2. Am J Vet Res **69**(12):1615-1622, 2008
5. Opriessnig T, Meng XJ, Halbur PG: Porcine Circovirus Type 2 associated disease: Update on current terminology, clinical manifestations, pathogenesis, diagnosis, and intervention strategies. J Vet Diagn Invest **19:**591-615, 2007
6. Radostits OM, Gay CC, Hinchcliff KW, Constable PD: Veterinary Medicine, A Textbook of the Diseases of Cattle, Horses, Sheep, and Goats, 10th ed., pp. 1185-1193. Saunders Elsevier, Philadelphia, PA, 2007
7. Rosell C, Segalés J, Ramos-Vara JA, Folch JM, Rodríguez-Arrioja GM, Duran CO, Balasch M, Plana-Durán J, Domingo M: Identification of porcine circovirus in tissues of pigs with porcine dermatitis and nephropathy syndrome. Vet Rec **146**:40-43, 2000

8. Segalés J, Rosell C, Domingo M: Pathological findings associated with naturally acquired porcine circovirus type 2 associated disease. Vet Microbiol **98:**137-149, 2004
9. Smith WJ, Thomson JR, Done S: Dermatitis nephropathy syndrome of pigs. Vet Rec **132:**47, 1993
10. Wellenberg GJ, Stockhofe-Zurwieden N, de Jong MF, Boersma WJ, Elbers AR: Excessive porcine circovirus type 2 antibody titres may trigger the development of porcine dermatitis and nephropathy syndrome: a case-control study. Vet Microbiol **99:**203-214, 2004

The Armed Forces Institute of Pathology
Department of Veterinary Pathology

Conference Coordinator:
Shannon Lacy, DVM, MPH

WEDNESDAY SLIDE CONFERENCE 2009-2010

Conference 4

30 September 2009

Conference Moderator:

Taylor B. Chance, DVM, Diplomate ACVP

CASE I: Case II (AFIP 2936428).

Signalment: 7-year-old gelding quarter horse (*Equus caballus*).

History: Examined by a local veterinarian for skin lesions on the back, which were then biopsied.

Gross Pathology: Firm mass present on the back of the saddle region of horse.

Histopathologic Description: Microscopically, collagen degeneration with multifocal regions of dystrophic mineralization is observed in regions of the deep dermis with degranulating and degenerative eosinophils (**fig. 1-1**). Superficial and deep perivascular dermatitis with marked eosinophilia and smaller numbers of macrophages, lymphocytes and plasma cells are noted (**fig. 1-2**). Endothelial reactions (i.e. hyperplastic and hypertrophic endothelial cells) are present with infiltrates of eosinophils and severe edema. Thrombus (not present in all submitted slides) with chronic infiltrates of eosinophils, lymphocytes, macrophages, and marked fibroplasia is observed.

Contributor's Morphologic Diagnosis: Skin: Dermatitis, moderate, eosinophilic granulomatous with collagenolysis and mineralization, Quarter Horse (*Equus caballus*), equine.

Contributor's Comment: This lesion, frequently encountered in skin biopsies from asymptomatic horses, is known as nodular necrobiosis, nodular collagenolytic granuloma, acute collagen necrosis, or eosinophilic granuloma.[5] There is no apparent breed, age, or sex predisposition for this disease.[4,5] The etiology of this lesion is unknown, but a hypersensitivity reaction to an arthropod injury is suspected because the lesion occurs more commonly in warmer months.[5,7] Due to lesions commonly occurring in the saddle region, it also has been suggested that trauma may be a contributing factor.[4,5] Furthermore, atopy has been suggested as a predisposing factor based on positive skin test results in a horse with collagenolytic granulomas.[4] More than one causal agent is likely responsible for a seemingly identical clinicopathologic entity.[5]

With eosinophilic granulomas, single or multiple lesions, ranging from 0.5 to 10 cm in diameter, are most commonly found on the withers and back, but can also be seen in the girth area, the mane, the rump, and the face. The lesions are often round, firm, and well-circumscribed with no

*Sponsored by the American Veterinary Medical Association, the American College of Veterinary Pathologists, and the C. L. Davis Foundation.

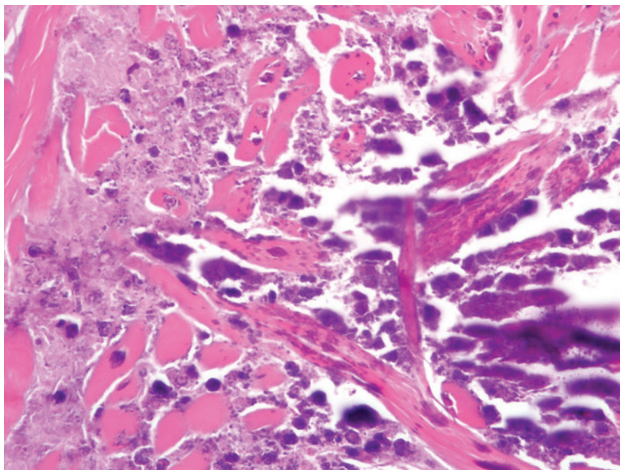

1-1. Dermis, horse. Multifocally dermal collagen fibers are degenerate or mineralized, and surrounded by numerous degenerate eosinophils and collagenolytic debris. (HE 400X)

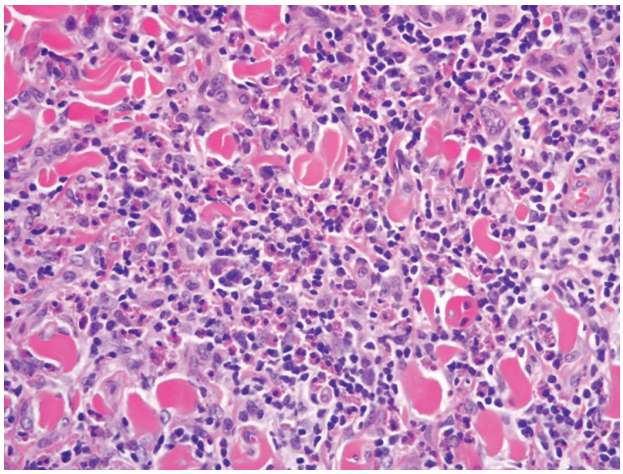

1-2. Dermis, horse. Multifocally surrounding and separating dermal collagen are nodular cellular infiltrates of high numbers of eosinophils and fewer macrophages, lymphocytes, and plasma cells. (HE 400X)

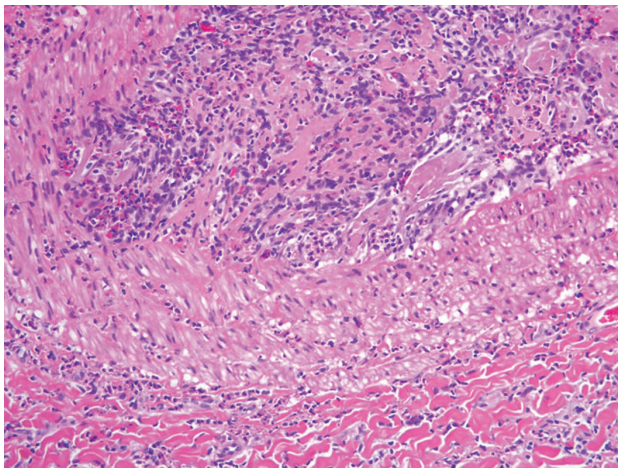

1-3. Dermis, horse. Multifocally occluding arteries are organizing fibrin thrombi which are composed of lamellations of collagen, eosinophils, and fibroblasts. The tunica intima and tunica media of affected vessels is disrupted by transmigrating eosinophils; myocytes within the tunica media are often degenerate. (HE 200X)

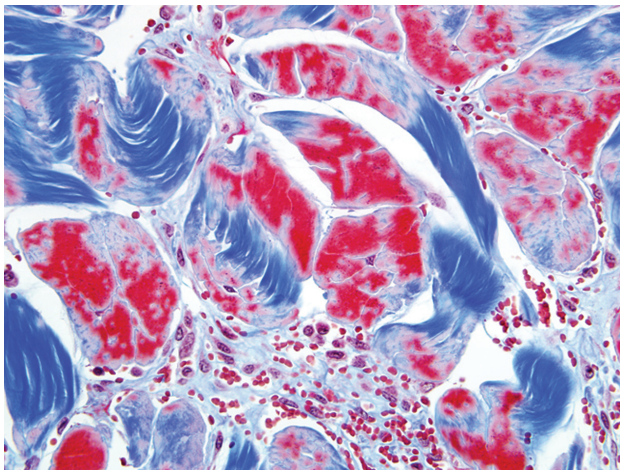

1-4. Dermis, horse. Masson's trichrome staining revealed abnormal, red-staining collagen cores in over 90% of the dermal collagen bundles. (Masson's 400X)

ulceration or alopecia. Pain and pruritus are not present. Some lesions can be cystic or plaque-like with a central caseous core.[4,5]

Massive central necrosis consisting of degranulating, degenerative eosinophils is a key element of this lesion.[6] The amount of collagenolysis varies among lesions. To date, the reason for the absence of collagenolysis in some lesions is not known. Collagen degeneration has been hypothesized to be the result of toxic products derived from degranulating eosinophils, such as major basic protein.[6] Some more chronic lesions can present with dystrophic mineralization and thus be misdiagnosed as calcinosis circumscripta or tumoral calcinosis.[5]

Histologically, the lesions of nodular collagenolytic granulomas (eosinophilic granulomas) need to be differentiated from those of habronemiasis and hypoderma nodules.[7] Cutaneous habronemiasis (summer sores) is caused by the larval activity of three nematodes that inhabit

the horse's stomach, especially *Draschia megastoma*, during the summer months. The larvae are deposited on the skin by flies, which are attracted to a pre-existing wound. Lesions are particularly common in the skin of the pectoral region, between the forelegs. The larvae penetrate deeply into the dermis and elicit an eosinophilic and granulomatous response. The alopecic ulcerated skin becomes encrusted by a serous exudate that oozes from the surface.[3] In hypodermiasis, by contrast, there is the presence of a breathing pore for the parasite. Cutaneous habronemiasis was considered as the primary differential diagnosis; however, due to the absence of larvae in the sections, the lack of skin ulceration and alopecia, and the presence of degenerate collagen, eosinophilic granuloma (nodular collagenolytic granulomas) was diagnosed.

AFIP Diagnosis: Haired skin and subcutis: Dermatitis, eosinophilic and granulomatous, multifocal to coalescing, moderate, with collagenolysis, mineralization, and eosinophilic arteritis.

Conference Comment: Conference participants discussed the diagnostic approach to dermatitis in domestic animals, beginning with a brief review of pattern analysis and its diagnostic utility in dermatopathology. Participants discussed the following ten non-neoplastic reaction patterns:[1]

1. Perivascular dermatitis
2. Interface dermatitis
3. Vasculitis
4. Nodular and diffuse dermatitis
5. Intraepidermal vesicular and pustular dermatitis
6. Subepidermal vesicular and pustular dermatitis
7. Perifolliculitis, folliculitis, and furunculosis
8. Fibrosing dermatitis
9. Panniculitis
10. Atrophic dermatitis

In addition to the entities well-described by the contributor (i.e. eosinophilic granuloma, habronemiasis, and hypodermiasis), the differential diagnosis for eosinophilic dermatitis in horses includes mast cell tumor, cutaneous pythiosis, multisystemic eosinophilic epitheliotropic disease, sterile eosinophilic folliculitis and furunculosis, unilateral papular dermatosis, and axillary nodular necrosis. For most of these, differentiation from eosinophilic granuloma is relatively straightforward; however, axillary nodular necrosis and unilateral papular dermatosis bear many histomorphologic similarities to eosinophilic granuloma, often creating a diagnostic challenge. These conditions were discussed at length, and their key features are summarized in the table below:[1,5]

Condition	Clinical and Gross Findings	Histomorphology
Eosinophilic granuloma (nodular necrobiosis, collagenolytic granuloma)	Most common equine cutaneous eosinophilic nodular disease; 0.5-10 cm diameter nodules anywhere on the body (often withers and back); trauma or hypersensitivity to insect bites or silicone coating on needles suspected	Dermal collagen flame figures surrounded by eosinophilic granulomatous inflammation; +/- eosinophilic folliculitis or furunculosis; +/- dystrophic mineralization; +/- lymphoid follicles; true collagen degeneration is rare
Axillary nodular necrosis	Usually unilateral; few (3-10) cutaneous and subcutaneous, 1-10 cm diameter nodules; truncal, caudal to axilla ("girth galls")	Eosinophilic coagulative necrosis surrounded by eosinophilic granulomatous dermatitis and panniculitis; dermal collagen flame figures; dystrophic mineralization of collagen; lymphoid nodules; eosinophilic or necrotizing vasculitis with endothelial cell hypertrophy, vessel lumen occlusion, and intimal mucinosis
Unilateral papular dermatosis	More common in spring and summer; Quarter Horses over-represented; numerous (30 to 300) unilateral, truncal, 2-10 mm diameter cutaneous nodules and papules; ectoparasite hypersensitivity suspected	Eosinophilic folliculitis and furunculosis; eosinophilic dermal inflammation; +/- dermal collagen flame figures

While the anatomic location is most consistent with eosinophilic granuloma, the vascular lesions observed by several conference participants in this case are strongly suggestive of axillary nodular necrosis (**fig. 1-3**). Throughout the deep dermis, all arterioles contain abundant, pale, basophilic, finely-granular subendothelial material (intimal mucinosis). Additional histologic findings present in some sections include hair shafts embedded in the deep dermis, recanalization of the thrombus in a large arteriole, few lymphocytes and plasma cells in the superficial dermis and periadnexally, and mild acanthosis, spongiosis, and orthokeratotic hyperkeratosis of the overlying epidermis.

Finally, conference participants discussed the terms "collagenolysis" and "flame figure". Collagenolysis or collagen necrobiosis, which implies true collagen degeneration, is the term classically used for the characteristic intense, acellular, eosinophilic material centered on collagen fibers in a variety of eosinophilic dermatoses. However, in many of these conditions Masson's trichrome staining and ultrastrucutural examination are inconsistent in demonstrating true collagen degeneration. Often, abnormal (i.e. red) staining of collagen fibers with Masson's trichrome is as likely to be present in areas of eosinophil degranulation as it is in other, apparently unaffected areas of the tissue section; therefore, many prefer the term "flame figure" to describe the histologic features, particularly when true collagen degeneration cannot be definitively demonstrated. In this case, Masson's trichrome staining revealed abnormal, red-staining collagen cores in over 90% of the dermal collagen bundles, but not areas containing flame figures (**fig. 1-4**). Major basic protein from degranulating eosinophils is now thought to be the source of the intense eosinophilic material seen in flame figures.[2]

Contributor: Wyeth Research, Department of Pathology, 641 Ridge Road, Chazy, New York 12921
http://www.wyeth.com

References:

1. Ginn PE, Mansell JEKL, Rakich PM: Skin and appendages. In: Jubb, Kennedy, and Palmer's Pathology of Domestic Animals, ed. Maxie MG, 5th ed., vol. 1, pp. 569-575, 739-741. Elsevier Saunders, Philadelphia, PA, 2007
2. Gross TL, Ihrke PJ, Walder EJ, Affolter VK: Skin Diseases of the Dog and Cat: Clinical and Histopathologic Diagnosis, 2nd ed., pp. 356-357. Blackwell Publishing, Ames, IA, 2005
3. Jones TC, Hunt RD, King NW: Veterinary Pathology, 6th ed., pp. 639. Williams and Wilkins, Baltimore, MD, 1997
4. Mathison PT: Eosinophilic nodular dermatoses. Vet Clin North Am Equine Pract **11:**75-89, 1995
5. Scott DW, Miller WH: Equine Dermatology, pp. 647-667. Saunders Elsevier, St. Louis, MO, 2003
6. Slovis NM, Watson JL, Affolter VK, Stannard AA: Injection site eosinophilic granulomas and collagenolysis in 3 horses. J Vet Intern Med **13:**606-612, 1999
7. Yager JA, Scott DW: The skin and appendages. *In:* Pathology of Domestic Animals, eds. Jubb KVF, Kennedy PC, Palmer N, 4th ed., vol. 1, pp. 700-701. Academic Press, San Diego, CA, 1993

CASE II: HN2108 (AFIP 2943303).

Signalment: 6-year-old, male Siberian husky (*Canis familiaris*).

History: This dog was presented to the veterinary teaching hospital initially with hind limb paraparesis. Mild atrophy of hind limb muscles was also observed. Abdominal radiographs revealed severe calcification in the abdominal aorta. Despite treatment with levothyroxine, the rear legs became paralyzed. Gangrene of the extremities appeared and worsened. The dog was euthanized due to poor prognosis and necropsied. This animal had not been given a high-cholesterol diet.

Gross Pathology: 1. Systemic arteriosclerosis showing marked calcification in the arterial wall and luminal narrowing.
2. Thrombosis of the internal iliac, femoral, popliteal, and right superficial branchial arteries.
3. Atrophy of the pituitary and thyroid glands.
4. Dry gangrene in the tail, bilateral hind limbs and right forelimb.

Laboratory Results: Serum biochemical profile before starting levothyroxine treatment revealed elevated cholesterol, triglyceride, alkaline phosphatase and creatine kinase (total cholesterol, 1560 mg/dL; triglyceride, 596 m/dL; ALKP, 8434 U/L; CK, 1178 U/L) and subnormal levels of thyroid hormones (T3, 0.3 ng/mL; T4, 0.2 ng/mL; free T4, 0.3 ng/mL).

Histopathologic Description: Grossly, epicardial coronary arteries were prominently thickened, firm, yellow-white, and appeared as cord-like structures. Multiple whitish foci were recognized within the ventricular walls by incisions after formalin fixation. Histologically, massive deposition of cholesterol clefts and

calcification with infiltration of foamy macrophages was noted in the thickened wall of epicardial arteries (**figs. 2-1 and 2-2**). Staining for elastin demonstrated the structural disorganization, such as the destruction of internal and external elastic membranes, intimal thickening, and the disappearance of the medial smooth muscle layer. Small foci of granulation tissue were scattered in the ventricular wall (**fig. 2-3**). Atherosclerotic lesions were also found in many organs, including aorta, spleen, kidney, lung, prostate, and brain. Both elastic arteries and large to middle-sized muscular arteries were involved.

Contributor's Morphologic Diagnosis: Heart (left ventricle): Coronary atherosclerosis, with small multifocal myocardial infarcts, Siberian husky, canine.

Contributor's Comment: Atherosclerosis occurs only infrequently in animals and rarely leads to clinical diseases, such as infarction of heart or brain.[6] Naturally occurring atherosclerosis has been reported in aged pigs and birds, and in dogs with hypothyroidism that develop an accompanying hypercholesterolemia.[6] Hypothyroidism in most dogs results from progressive loss of functional thyroid tissues due to primary dysfunction of the gland.[2] Histological changes in the thyroid gland of this dog were replacement of parenchyma by adipose tissue with the absence of inflammatory cell infiltrates. Acute degeneration and necrosis of secretory cells, including TSH immunoreactive cells, were observed in the adenohypophysis; however, the cause and relationship of this lesion with the thyroid atrophy were unclear.

AFIP Diagnosis: Heart: Coronary arterial atherosclerosis, transmural and circumferential, diffuse, marked, with mineralization and multifocal chronic myocardial infarcts.

Conference Comment: Conference participants engaged in a lively discussion regarding the areas of myocardial infarction in the submitted sections. Specifically, opinions on the age of the lesions varied widely, with participants who felt the lesions consisted of immature granulation tissue favoring a subacute process, while those who felt there was increased collagen deposition favored a chronic process. We consulted with the AFIP Department of Cardiovascular Pathology and estimate the infarcts to be over one month old. The evolution of the histomorphologic changes in myocardial infarction in humans is well-characterized, and is summarized below:[5]

Time	Light Microscopic Findings
0 to 0.5 hr	None
0.5 to 4 hrs	None, or myofiber waviness at the border of the lesion
4 to 12 hrs	Early coagulation necrosis with hemorrhage and edema
12 to 24 hrs	Coagulation necrosis; myocyte hypereosinophilia and pyknosis, contraction band necrosis; early neutrophilic infiltrate
1 to 3 days	Coagulation necrosis; loss of cross striations and loss of nuclei; increased neutrophilic infiltrate
3 to 7 days	Early myofibers disintrigration; necrosis of neutrophils; macrophages at the border of the lesion
7 to 10 days	Increased macrophage infiltrate with phagocytosis of necrotic cells; early granulation tissue at infarct margins
10 to 14 days	Well-developed granulation tissue
2 to 8 weeks	Increased collagen deposition; decreased cellularity; regression of granulation tissue capillaries
>2 months	Dense collagenous scar

In addition to hypothyroidism-induced hypercholesterolemia, diabetes mellitus is often associated with atherosclerosis in dogs. In one study, dogs with atherosclerosis were over 53 times more likely than dogs without atherosclerosis to have diabetes mellitus, and over 51 times more likely to have hypothyroidism than dogs without atherosclerosis, but were not more likely to have hyperadrenocorticism than dogs without athoersclerosis.[1] Dogs are otherwise considered relatively atheroresistant, as are cats, cattle, goats, and rats. While this condition is only rarely clinically significant in domestic animals, nonhuman primates and pigs are the most popular animal

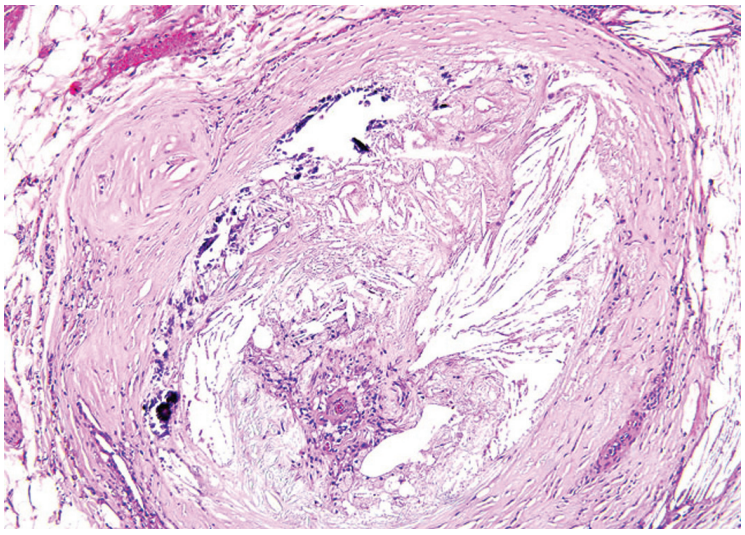

2-1. Heart, dog. Within extramural coronary arteries, the tunic media is markedly expanded and the vessel lumens are nearly or completely occluded. The tunica media is disrupted by acicular clefts and mineralization. (HE 100X)

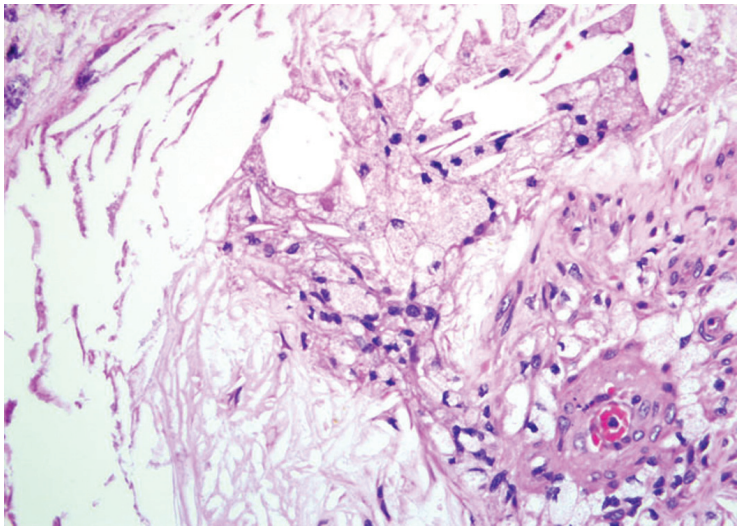

2-2. Heart, dog. The tunica media of affected vessels is expanded by many lipid-laden macrophages (foam cells), myofibroblasts, and large, clear, acicular clefts (cholesterol). (HE 400X)

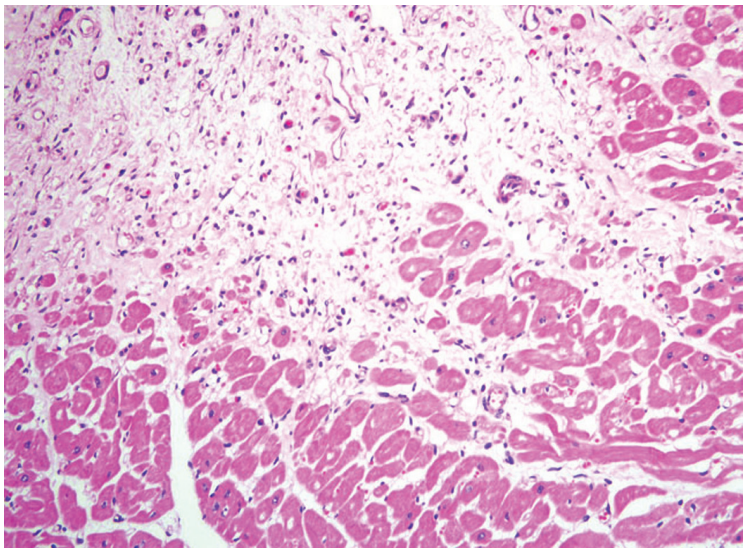

2-3. Heart, dog. Multifocally within the surrounding myocardium are large zones of regressing mature granulation tissue and chronic fibrosis rimmed by occasional degenerate and necrotic myocytes (chronic infarct). (HE 200X)

models of human disease. As atherosclerosis is a significant cause of human mortality, it merits considerable research interest. Pigs, rabbits, and chickens are atherosensitive, and develop the disease in response to high dietary cholesterol intake, particularly when the proportion of very low density lipoproteins (VLDL) is increased.[3]

The pathogenesis of atherosclerosis in humans is well-studied, and the currently-accepted model, the response-to-injury hypothesis, characterizes atherosclerosis as a chronic response of the arterial wall to endothelial injury. An exhaustive review of the pathogenesis is beyond the scope of this report. Briefly, hypothyroidism or diabetes mellitus results in dyslipoproteinemia (i.e. increased low density lipoprotein (LDL) cholesterol, decreased high density lipoprotein (HDL) cholesterol, and/or increased levels of abnormal lipoprotein (a)). This causes endothelial damage by a variety of mechanisms, including oxygen free radical production that speeds the decay of nitric oxide and decreases its vasodilator activity. The damaged endothelium allows lipoproteins to accumulate in the intima, where they are oxidized by free radicals generated by macrophages and endothelial cells. Oxidized LDLs, which are directly toxic to endothelium and smooth muscle cells, are ingested by macrophages and smooth muscle cells, which become characteristic so-called "foam cells". Damaged endothelium also allows the adhesion of platelets and expresses vascular cell adhesion molecule 1 (VCAM-1), which binds monocytes and T lymphocytes. Platelets and migrating leukocytes elaborate platelet-derived growth factor, interleukin-1, and interferon-gamma, which promote smooth muscle proliferation and extracellular matrix synthesis.[4] The resulting characteristic histologic lesion is the deposition of lipid in the vessel wall (i.e. "atheroma"), which is overlain by fibrosis and mineralization. The lesion in dogs differs from that of humans with respect to the location of lipid, which is primarily within the tunica media and adventitia in dogs, but primarily within the tunica intima in humans. With chronicity, atheromas may cause luminal narrowing and/or ulceration, leading to thrombosis, hemorrhage, or aneurysm.[3]

Most affected are the aorta, iliac, carotid, coronary, and femoral arteries. Grossly, affected vessels are enlarged and firm, with prominent yellow-brown nodules that project into the lumen. Other degenerative arterial diseases in domestic species include arteriosclerosis, and medial calcification, summarized in the table below.[6]

Name	**Clinical and Gross Findings**	**Histomorphology**
Atherosclerosis	Pigs, rabbits, chickens are atherosensitive; dogs, cats, cattle, goats, and rats are atheroresistant; affects large elastic and large and medium muscular arteries; seen most commonly in dogs with hypothyroidism or diabetes mellitus; gross = vessel wall thickened and firm with yellow-brown nodules projecting into the lumen	Fibrofatty plaque or atheroma in the vessel wall (tunica intima and media) and lipid-laden macrophages and/or smooth muscle cells (i.e. "foam cells") in the media and intima
Arteriosclerosis	Occurs in many species but rarely clinically significant; age-related, degenerative change; means "arterial hardening"; results in loss of elasticity; abdominal aorta most frequently affected; also occurs at arterial branching sites (turbulent blood flow); gross = raised, firm, white plaques	Intimal thickening by mucopoly-saccharides (early) or medial thickening by proliferating smooth muscle cells and fibrosis that infiltrates into the intima (later); splitting of the internal elastic lamina
Arterial medial calcification	Common; affects elastic and muscular arteries; caused by certain plant toxins (e.g. *Cestrum diurnum, Solanum malacoxylon, Trisetum flavescens*), vitamin D toxicosis, renal disease (aged guinea pigs and rats), and paratuberculosis; spontaneous in rabbits; gross = solid, pipe-like vessels with white, solid, raised intimal plaques	Prominent, granular, basophilic material on medial elastic fibers; form a circumferential ring of mineralization in muscular arteries

In horses, intimal bodies in small arteries and arterioles, and siderocalcinosis of cerebral vessels are usually incidental findings of no clinical significance.(3,6)

Contributor: Laboratory of Comparative Pathology, Department of Veterinary Clinical Sciences, Graduate School of Veterinary Medicine, Hokkaido University, North 18 West 9, Kita-ku, Sapporo 060-0818, Japan

References:

1. Hess RS, Kass PH, Van Winkle TJ: Association between diabetes mellitus, hypothyroidism or hyperadrenocorticism, and atherosclerosis in dogs. J Vet Intern Med **17**:489-94, 2003
2. Kemppainen RJ, Clark TP: Etiopathogenesis of canine hypothyroidism. Vet Clin North Am Small Anim Pract **24**:467-476, 1994
3. Maxie MG, Robinson WF: Cardiovascular system. *In:* Jubb, Kennedy, and Palmer's Pathology of Domestic Animals, ed. Maxie MG, 5th ed., vol. 2, pp. 56-62. Elsevier Saunders, Philadelphia, PA, 2007
4. Mitchell RN, Schoen FJ: Blood vessels. *In:* Robbins and Cotran Pathologic Basis of Disease, eds. Kumar V, Abbas AK, Fausto N, Aster JC, 8th ed., pp. 496-504. Saunders Elsevier, Philadelphia, PA, 2010
5. Schoen FJ, Mitchell RN: The heart. *In:* Robbins and Cotran Pathologic Basis of Disease, eds. Kumar V, Abbas AK, Fausto N, Aster JC, 8th ed., pp. 547-559. Saunders Elsevier, Philadelphia, PA, 2010
6. Van Vleet JF, Ferrans VJ: Cardiovascular system. *In:* Pathologic Basis of Veterinary Disease, eds. McGavin MD, Zachary JF, 4th ed., pp. 599-602. Mosby Elsevier, St. Louis, MO, 2007

CASE III: V07-00718 (AFIP 3067153).

Signalment: 9-year-old, male castrated domestic shorthair cat (*Felis catus*).

History: The cat had a history of anorexia, weight loss, mild anemia and dyspnea. The animal had been treated with antibiotics without improvement.

Gross Pathology: The cat was in poor body condition. Multifocally in the lung and spleen, there were numerous, 3-6 mm diameter, firm, white nodules.

Laboratory Results: Aerobic culture from the lung and spleen was negative. Fluorescent antibody test (FA) for plague was negative.

Histopathologic Description: There are multifocal to coalescing foci where alveoli are filled with numerous epithelioid macrophages and smaller numbers of neutrophils, lymphocytes, and a few plasma cells. Many of the macrophages contain small numbers of cytoplasmic 2-5 micron diameter yeast that have a 1-3 micron diameter central basophilic body surrounded by clear halo (capsule) (**fig. 3-1**). The interstitium of the lung is variably infiltrated by mixed leukocytes.

Contributor's Morphologic Diagnosis: Lung: Pneumonia, granulomatous / pyogranulomatous, multifocal to coalescing, moderate with intrahistiocytic yeast, domestic shorthair, feline (*Felis catus*), etiology consistent with *Histoplasma capsulatum.*

Contributor's Comment: Histoplasmosis is caused by *Histoplasma capsulatum*, which is an intracellular parasite of the monocyte and macrophage system and involves the reticuloendothelial system.[7] The organism is a soil-borne dimorphic fungus, and in the environment it exists as a mycelial form that produces small spores (2-3 um in size, microconidia) and large, thick-walled chlamydospore with surface projections (8-12 um, macroconidia). In the parasitic phase inside the body it transforms to a yeast-like form. In the soil, the organism appears as white-brown mold.[3] The organism prefers warm and humid areas, and proliferates best in nitrogen-rich soil.[2] A relationship has been established between bird and bat excrement and occurrence of the disease.[3,7]

The disease affects a wide variety of mammals.[3] In North America, histoplasmosis is often diagnosed in the Mississippi, Ohio, and Missouri River areas. The disease is mostly non-contagious in humans, dogs, cats, swine, horse, wild animals, and cattle. In companion animals, it is most often found in dogs and less frequently in cats.[7] True rate in companion animals is difficult to measure due to subclinical infections.[2] The infection is initiated by inhalation or ingestion of dust from soil. The majority of infections occur without signs and lesions, whereas when infection becomes clinically apparent, it is disseminated, and always fatal.[7] It is known now that in humans and lower animals, an acute, nonfatal form is more prevalent than the disseminated, fatal, rare form. The infection is connected to common environmental source rather than contagion from host to host.[3]

The genus *Histoplasma*, besides the three conventionally accepted species (*capsulatum*, *duboisii*, and *farciminosum*), was reported to have eight clades from different geographic

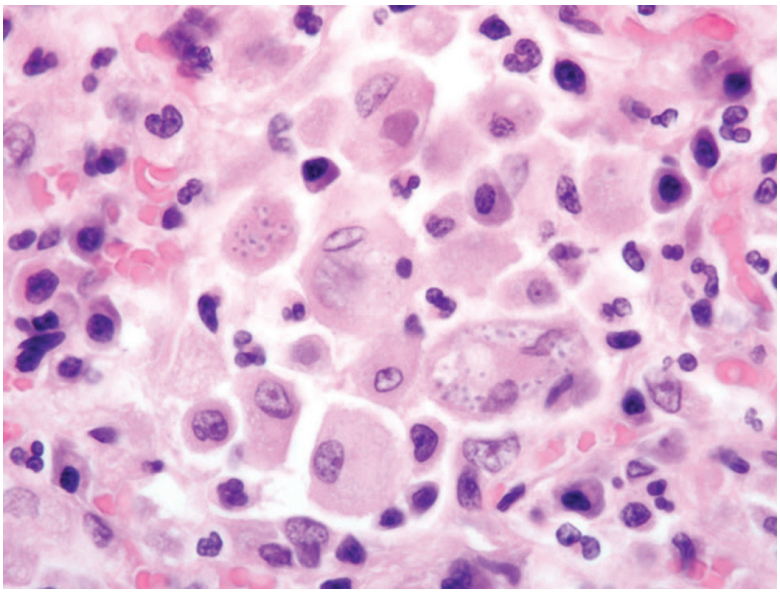

3-1. Lung, cat. Multifocally within alveoli are large numbers of alveolar macrophages which contain up to 20 circular yeasts which are 3-4um in diameter with a 1um basophilic central nucleus and a 1um thick clear halo. (HE 1000X)

regions, suggesting that genetically distinct geographical populations exist.[1,4] Genetic polymorphisms in the same areas were 100% similar.[6] *Histoplasma capsulatum* is the cause of classic histoplasmosis worldwide. *H. duboisii* is the cause of African histoplasmosis and *H. farciminosum* is the cause of epizootic lymphangitis in horses. This is characterized by chronic indurative ulceration of the skin with enlargement of regional lymph nodes.[3]

When inhaled, the microconidia are able to reach the lower respiratory tract. The incubation period is usually 12-16 days, during which the microconidia transform into yeast phase and reproduce by budding. The yeast is phagocytosed by mononuclear phagocytes and replicates further inside the cell.[2] This route accounts for the infection in the cervical and bronchial lymph nodes, but the usual intestinal lesions were also suggested to occur directly via ingestion, or by secondary infections like in the case of many other organs. The latent infections might persist without causing illness for months to years in different species. The signs of advanced disease include diarrhea, pyrexia, emaciation, hepatomegaly, splenomegaly, a lymphadenopathy, and a nonregenerative, normochromic, normocytic anemia. In later stages the leukocyte counts are low, and toxic changes occur, such as the appearance of Doehle bodies. The disease usually causes lymphopenia and eosinopenia. Diagnosis can be made from fine-needle aspirations of liver, spleen, enlarged lymph nodes, bone marrow, or skin with microscopic examination. Cytologically, the organism can be detected in the cytosol of macrophages.[7]

If the spore dose is high or the host's immune system is compromised, the infection can cause severe disease. The host's cellular immune system, mainly involving cytokine-mediated macrophage killing, can control the infection. In some instances, the infection is not completely cleared and if immune suppression takes place, a reactivation can occur. The yeast form is more resistant to host defense due to its more invasive nature as it can severely impair phagocyte function. Moreover, the fungus can induce nonspecific anergy by overproducing interleukin-4, thus interfering with cellular immune response.[2]

In dogs, the primary disease in the lung appears as classic granulomas containing epithelioid and multinucleated giant cells carrying the organisms. After recovery, these regress to fibrocalcareous nodules present in the lungs for many years. Sometimes, similar lesions may be found in other organs.[3] Pathologically, the pulmonary lesions are 1-2 cm grayish nodules.

In the intestines, the lesions most frequently occur in the lower part of the small intestine as nodular thickenings of the mucosa in the lamina propria and submucosa that are the result of infiltration of lymphocytes, plasma cells and macrophages. In rare instances, ischemic ulcerations might occur when the thickening is extreme.[7] In the intestine the lymph nodules and adjacent lymph nodes are greatly enlarged.[3]

Lymph nodes are firm and dry and greatly enlarged. In histological preparations, coalescing granulomas that replace portions of the cortex can be seen.[7] In lymph nodes, the predominant infiltrating cell type is histiocytic, with a less frequent plasma and lymphoid cell presence.[3] The spleen is also enlarged, grey, and firm, characterized by sinus expansion and colonization with macrophages

containing the organism.

The liver becomes enlarged, and diffuse grey discoloration, due to capsular thickening without focal lesions, occurs.[7] Liver enlargement is caused by diffuse interlobular and intralobular proliferation of mononuclear phagocytes, leading to displacement of liver parenchyma, and causing liver dysfunction.[3]

The disease often involves the adrenal gland's cortex, medulla, or both.[7] The involvement of adrenal glands in fatal cases is very striking, characterized by the replacement of the gland by macrophages. This phenomenon is most likely connected to the terminal stage of the disease, as it is not seen in animals sacrificed earlier.[3]

The organ enlargements are caused by intense infiltration of extensively proliferating monocytes and epitheloid macrophages carrying the organisms in their cytoplasm. The 2-4 um yeast bodies appear as basophilic dots surrounded by a halo (part of the cell wall) on sections stained with eosin and hematoxylin. The halo can be stained for bound glycogen, appearing as a ring, that helps distinguish the organism from cellular debris.[7] The cell wall can be stained selectively by PAS, Bauer, GMS or Gridley fungus method, resulting in a red or black ring appearance.[3]

When the organism is present in abundance, the staining is not necessary. However, in case of occult infection, isolation of organism from tissues must be done for diagnosis. Care must be taken during isolation to prevent inhalation of chlamydospores. The organism can only be held responsible for focal, nonprogressive lesions if it can be histologically demonstrated from tissue sections. For biopsy, enlarged lymph nodes or aspiration biopsy of bone marrow can be used.[7] Also, biopsies of tonsils and liver, which are places of extensive mononuclear phagocyte proliferation, or in certain cases, smears of circulating blood, can be used. Serologic tests are not reliable.[3]

Differential diagnosis is necessary from *H. farciminosum* by culturing the organism, as in tissue sections they appear the same, though the geographic and anatomical locations of the two diseases can reduce this difficulty. Differentiating from other protozoan and mycotic organisms can be done by immunologic staining techniques or can be based on morphological differences. *Leishmania donovani* contains a bar-shaped kinetoplast that is not present in histoplasmosis. *Toxoplasma gondii* is smaller and does not have rings when stained for bound glycogen. *Blastomyces dermatitidis* yeasts are larger and the budding base is different. Differentiating from *Sporothrix schenckii* requires immunologic staining. Some malignant neoplasms such as lymphoma can lead to uptake of tissue debris by macrophages; however, in these cases the absence of organism can differentiate from histoplasmosis.[3]

Public Health considerations: Animals and people traveling through endemic areas might be at risk. Direct host-to-host transmissions have not been reported. Also, transplanting kidneys of infected donor can carry the disease to the host.[2] In humans, the disease can affect people with AIDS or on immunosuppressive therapy. The disease can be the result of reactivation from a latent infection in both humans [8] and dogs.[1,5]

AFIP Diagnosis: Lung: Pneumonia, pyogranulomatous, multifocal to coalescing, moderate to marked, with numerous intrahistiocytic yeasts, etiology consistent with *Histoplasma* species.

Conference Comment: In some sections there is pyogranulomatous pleuritis and/or reactive pleural mesothelium. The contributor provided a thorough overview of this entity and the differential diagnosis. Currently, the accepted nomenclature for the organisms described above is *Histoplasma capsulatum* var. *capsulatum, H. capsulatum* var. *farciminosum*, and *H. capsulatum* var. *duboisii*.[2,7]

Contributor: NMDA-Veterinary Diagnostic Services, 700 Camino de Salud NE, Albuquerque, NM 87106-4700 http://128.123.206.6/animal-and-plant-protection/veterinary-diagnostic-services

References:

1. Bromel C, Sykes JE: Histoplasmosis in dogs and cats. Clin Tech Small Anim Pract, **20:**227-32. 2005
2. Green CE: Histoplasmosis. *In:* Infectious Diseases of the Dog and Cat, ed. Greene CE, 3rd ed., pp. 577-584. Saunders Elsevier, St. Louis, MO, 2006
3. Jones TC, Hunt RD, King NW: Veterinary Pathology, 6th ed., pp. 519 - 522. Lippincott Williams and Wilkins, Baltimore, MD, 1997
4. Kasuga T, White TJ, Koenig G, McEwen J, Restrepo A, Castañeda E, Lacaz CDS, Heins-Vaccari EM, De Freitas RS, Zancopé-Oliveira RM, Qun Z, Negroni R, Carter DA, Mikami Y, Tamura M, Taylor ML, Miller GF, Poonwan N, Taylor J: Phylogeography of the fungal pathogen *Histoplasma capsulatum*. Mol Ecol **12:**3383-401, 2003
5. Mackie JT, Kaufman L, Ellis D: Confirmed histoplasmosis in an Australian dog. Aust Vet J **75:**362-3, 1997
6. Muniz MM, Pizzini CV, Peralta JM, Reiss E, Zancopé-Oliveira RM: Genetic diversity of Histoplasma capsulatum strains isolated from soil, animals, and clinical specimens in Rio de Janeiro State, Brazil, by a PCR-based random amplified polymorphic DNA assay. J Clin Microbiol **39:**4487-94, 2001

7. Valli VEO: Hematopoietic system. *In:* Jubb, Kennedy, and Palmer's Pathology of Domestic Animals, ed. Maxie MG, 5th ed., vol. 2, pp. 299-302. Elsevier Saunders, Philadelphia, PA, 2007
8. Wheat LJ, Kauffman CA: Histoplasmosis. Infect Dis Clin North Am **17:**1-19, vii, 2003

CASE IV: CASE I (AFIP 3134286).

Signalment: 1-year and 11-month-old female Springer spaniel (*Canis familiaris*).

History: The dog collapsed and died after having shown declining exercise tolerance over 5 weeks and tachypnea, dyspnea, inappetence and pyrexia of several days duration.

Gross Pathology: The thoracic cavity contained approximately 100 mL of hemorrhagic turbid fluid. The mediastinum and parietal pleura were markedly thickened with velvety proliferations, dull and reddish discolored. Multiple small yellow soft granules, which measured up to 0.3 cm in diameter, were present within the pleural tissue (interpreted as sulfur granules). The lungs were decreased in size and the overlying visceral pleura was wrinkled (interpreted as compression atelectasis) (**figs. 4-1 and 4-2**). Tracheobronchial lymph nodes were enlarged, measuring up to 6 x 3 x 3 cm.

Laboratory Results: Pleural tissue and a sterile swab obtained from the pleural effusion were submitted for bacteriology. A heavy mixed growth of *Actinomyces viscosus* and a *Bacteroides* sp. was isolated from the pleural fluid. Bacteriology on the pleural tissue revealed a moderate mixed growth of *Actinomyces viscosus* and a *Bacteroides* sp.

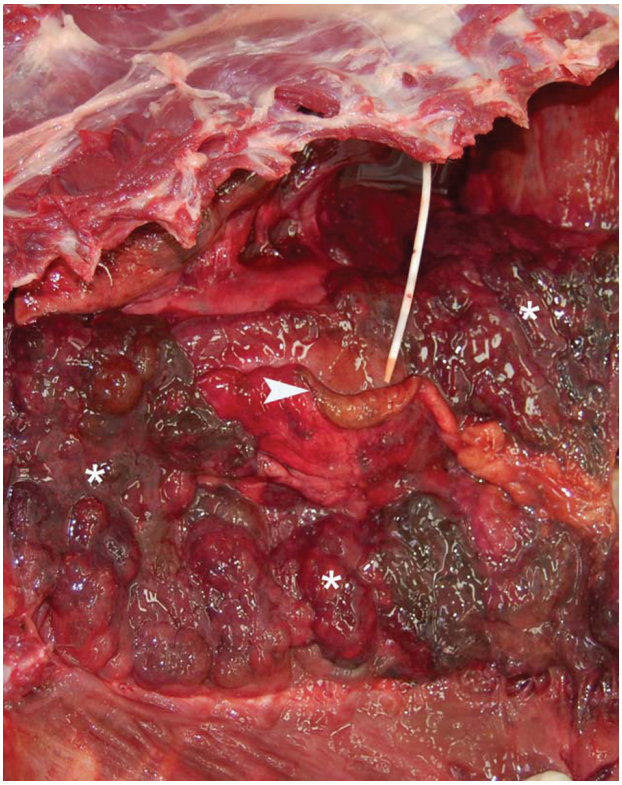

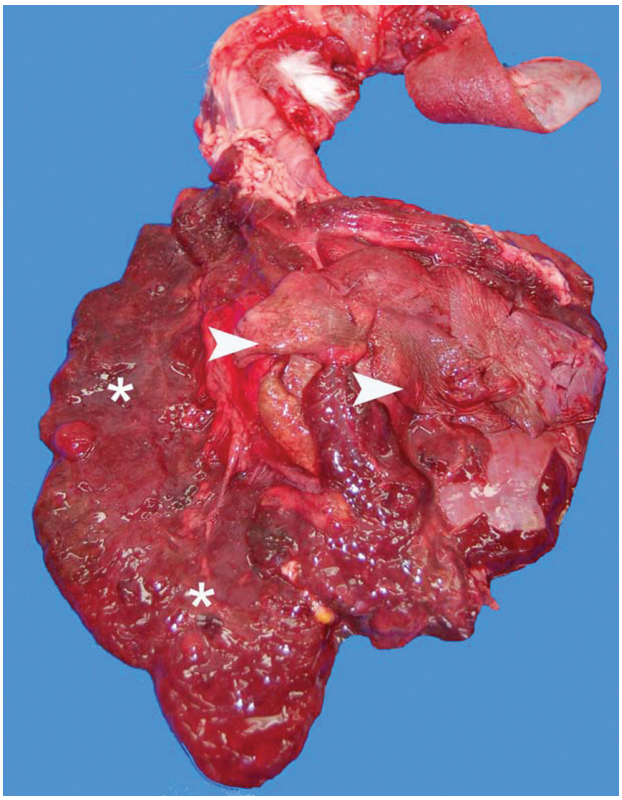

4-1, 4-2. Thorax and thoracic pluck, dog. The mediastinum and parietal pleura are dull red and markedly thickened with velvety proliferations (asterisk). There are multiple yellow soft granules which measure up to 0.3 cm in diameter within the pleural tissue, and lungs are decreased in size with thickened and wrinkled pleura (arrowhead). Photograph courtesy of The Royal Veterinary College, Department of Pathology and Infectious Diseases, Hawkshead Lane, North Mymms, Hatfield, Herts AL97TA, United Kingdom, sschoeniger@rvc.ac.uk

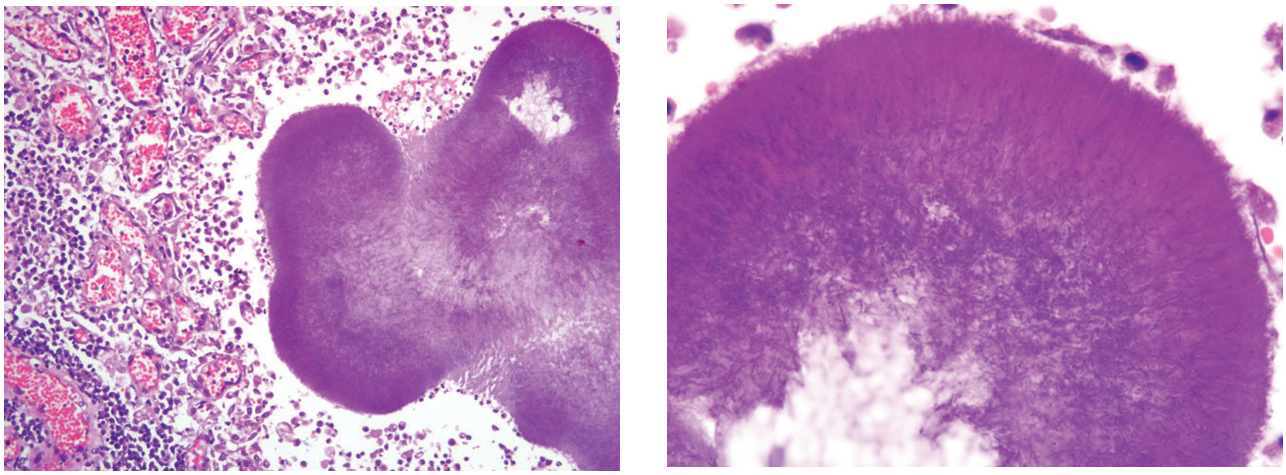

4-3, 4-4. Pleura, dog. Pleura are markedly expanded by abundant granulation tissue and pyogranulomatous inflammation, often centered on large colonies of filamentous bacteria which are embedded in a brightly eosinophilic proteinaceous material. (HE 400X, HE 1000X)

Histopathologic Description: **Parietal pleura:** The pleura was diffusely expanded by infiltration with numerous histiocytes and neutrophils (pyogranulomatous inflammation), which surrounded intralesional large bacterial colonies composed of radiating filamentous bacteria. In addition, the pleura contained numerous small-sized congested vessels, mild fibroblast proliferation and multifocal infiltration with lymphocytes and plasma cells (**figs. 4-3 and 4-4**).

Lungs: The visceral pleura was expanded by infiltration with numerous lymphocytes, plasma cells, epithelioid macrophages and scattered neutrophils, and contained numerous small-sized congested vessels and mild fibroblast proliferation. In the subpleural parenchyma, alveoli were lined by cuboidal cells (hyperplasia of type II pneumocytes). Scattered alveoli contained intraluminal macrophages and/or a few erythrocytes. Numerous alveolar spaces were decreased in size (atelectasis). There was mild anthracosis. Some pulmonary capillaries contained intraluminal megakaryocytes.

Contributor's Morphologic Diagnosis: 1. Parietal pleura: Proliferative and pyogranulomatous pleuritis with intralesional large colonies of filamentous bacteria.
2. Lungs: Pyogranulomatous pleuritis and pulmonary atelectasis.

Contributor's Comment: The main pathological finding was proliferative and pyogranulomatous pleuritis with intralesional large colonies of radiating filamentous bacteria. Intralesional large colonies of filamentous bacteria can be observed in Actinomycosis and Nocardiosis. In the present case, a mixed growth of *Actinomyces viscosus* and a *Bacteroides* sp. was cultured from the pleura and the thoracic effusion.

Infection with either *Actinomyces* or *Nocardia* is associated with similar clinical signs and macroscopic and microscopic pathological findings.[10] Accurate ante mortem diagnosis of the agent involved by bacterial culture and/or molecular methods is important, since *Actinomyces* and *Nocardia* spp. require different antibiotic treatments.[3]

Actinomyces spp. are anaerobic or facultative anaerobic, Gram-positive filamentous bacteria, which are non-acid-fast.[3,7,13] They are commensal bacteria of the mucosa of the oral cavity, urogenital-, upper respiratory- and gastrointestinal tracts. Certain *Actinomyces* spp., e.g. *A. hordeovulneris*, are saprophytes, which are mostly attached to plant material such as grass awns.[3,7,10,12,13] Actinomycosis is caused by either endogenous or exogenous infection.[3,13] Endogenous infections are initiated by mucosal injury, through which *Actinomyces* spp. gain access to the underlying soft tissues. Exogenous infections result from contaminated bite wounds and inhaled or ingested grass awns with attached bacteria. The grass awns can migrate in tissues causing infections at distant sites.[3,7,13] Within infected tissues, *Actinomyces* usually spreads by direct extension; hematogenous dissemination is rare.[7] Bacterial spread is facilitated by proteolytic enzymes released from neutrophils and macrophages.[7] Actinomycosis in dogs usually causes (sub)cutaneous and intracavitary infections.

Subcutaneous lesions are often located in the cervico-

facial or interdigital areas. Regional lymphadenopathy may be present. Intracavitary infections are mostly located in the thoracic cavity; infections of the abdominal cavity and the retroperitoneal space are uncommon.[4,7,10,12] In dogs, *Actinomyces* has also been reported as a rare cause of meningoencephalitis and endophthalmitis.[6,2] *Actinomyces*-induced pyogranulomatous meningo–encephalitis has been reported in a 1-year-old German Shepherd dog without history of trauma or involvement of other organs by *Actinomyces* infection.[6] A migrating foxtail was considered as a possible cause for the meningoencephalitis.[6] Concurrent endophthalmitis and pneumonia due to Actinomyces infection have been described in a Rottweiler dog.[2] *Actinomyces* spp. were also isolated from canine corneas with ulcerative keratitis.[11]

Diseases caused by infection with *Actinomyces* spp. in other species include osteomyelitis of the mandible and maxilla in cattle (lumpy jaw; *A. bovis* and *A. israelii*), supra-atlantal ("poll evil") and supraspinal ("fistulous withers") bursitis of horses (*A. viscosus* and *A. bovis* together with *Brucella suis* or *Brucella abortus*), mastitis, abortion, pneumonia, cystitis and pyelonephritis in pigs (*A. bovis, A. suis*) and abscesses in brain and temporal bone in a goat.[1,3,8,13]

Actinomyces spp. are often isolated together with other commensal bacteria [7], particularly *Bacteroides* spp., *Escherichia coli* and *Fusobacterium* spp. The presence of additional bacteria results in an increased pathogenicity, since it facilitates the formation of bacterial aggregates, which are relatively resistant against phagocytosis and bactericidal enzymes released by inflammatory cells. Bacterial aggregates are formed by the attachment of fimbriae present on the surface of *Actinomyces* spp. to surface receptors of other bacteria.[7]

In comparison to *Actinomyces* spp., *Nocardia* spp. are aerobic and partially acid-fast Gram-positive bacteria, which exist in coccobacillary (resting phase) to filamentous (active growing phase) forms.[3] Infection with *Nocardia* is always exogenous; *Nocardia* spp. are present as saprophytes in the environment, where they are attached to soil, dust and plant material. Infection can be acquired by ingestion, inhalation and wound contamination.[3,7,13] In cattle, mastitis is usually caused by infection through the teat canal.[13] The primary localized infection may be followed by hematogenous dissemination.[3,7,13] The most common agent for nocardiosis in dogs is *N. asteroides*.[7] *Nocardia* infection causes three main disease manifestations: (sub)cutaneous, thoracic, and disseminated.[13] The (sub)cutaneous form is usually associated with lymphadenopathy of regional lymph nodes.[10] The thoracic form is characterized by the pleuritis and/or pneumonia.[3,13] Disseminated nocardiosis develops often secondary to the pulmonary disease.[7] Nocardial infections in other species include mastitis and abortion in cattle; pneumonia, lymphadenitis and abortion in pigs; and wound infection, mastitis and pneumonia in sheep, cattle and horses.[3,13]

The pathogenicity of *Nocardia* spp. is dependent on bacterial factors (strain and growth phase) and host immunity. Certain strains of *Nocardia* are more virulent due to an ability to survive in phagocytic vacuoles of neutrophils and macrophages.[3,7] Disease caused by *Nocardia* spp. is often associated with immune suppression or heavy bacterial exposure.[3,7]

Since infections with *Actinomyces* and *Nocardia* spp. cause similar lesions, the distinction between actinomycosis and nocardiosis is not possible based on macroscopic and microscopic pathological findings.[3,7,10] Macroscopically, (sub)cutaneous actinomycosis and nocardiosis are characterized by the presence of skin edema and inflammation. Ulceration and draining tracts are common.[10] In the thoracic form, the parietal and visceral pleura are inflamed and thickened by velvety proliferations. Similar lesions may be present within the mediastinum or pericardial sac. The thoracic cavity often contains a reddish-brown turbid effusion due to accumulation of sanguinopurulent fluid, which can cause compression atelectasis of the lungs.[3,5,13] Grossly, infected tissues might contain yellowish granules measuring about 0.1 cm in diameter ("sulfur granules", tissue grains). Sulfur granules are common in actinomycosis, but rare in nocardiosis.[3,9,10] Occasionally sulfur granules might be observed in infection with *N. caviae* and *N. braziliensis*, whereas they are usually absent in infection caused by *N. asteroides*.[10]

The microscopic hallmark of nocardiosis and actinomycosis is pyogranulomatous inflammation with intralesional large colonies of filamentous bacteria.[5] If the infection exists over a longer time, granulation tissue formation, fibrosis and/or infiltration with lymphocytes and plasma cells is usually present. A modified acid-fast stain (e.g. Fite-Faraco modification) will stain *Nocardia* spp., but not *Actinomyces* spp.[3] On cytological and histopathological examination, the sulfur granules are composed of large bacterial colonies surrounded by eosinophilic clubbed material. The eosinophilic clubbed material is considered to be caused by an antigen-antibody reaction (Splendore-Hoeppli reaction).[6,9,10]

Proliferative pleuritis with reddish-brown turbid thoracic effusion is diagnostic for actinomycosis and nocardiosis. Skin lesions of actinomycosis and nocardiosis have to be

differentiated from bacterial pseudomycetoma, which is also characterized by skin edema and pyogranulomatous inflammation. Ulceration, draining tracts and tissue grains might be present as well. In contrast to actinomycosis and nocardiosis, the intralesional bacterial colonies in pseudomycetoma are composed of non-filamentous Gram-positive or Gram-negative bacteria surrounded by Splendore-Hoeppli reaction. Possible causes of bacterial pseudomycetoma are *Staphylococcus, Streptococcus, Proteus* spp. and *Pseudomonas* spp.[10]

An incidental finding in this case, unrelated to the actinomycosis, was the presence of megakaryocytes in some pulmonary capillaries. Megakaryocytes can occasionally be observed within pulmonary capillaries of different animal species. It has been shown that megakaryocytes can exit the intact bone marrow and arrest in pulmonary capillaries, where they can release platelets in the circulation.[14]

AFIP Diagnosis: Lung: Pleuritis, proliferative and pyogranulomatous, diffuse, chronic, severe, with granulation tissue, atelectasis, and large colonies of filamentous bacteria.

Conference Comment: There is slide variation with respect to the number of bacterial colonies present intralesionally. The contributor provided a complete review of this entity, with due emphasis on the key differences between nocardiosis and actinomycosis, which were reviewed during the conference. For more information on the differential diagnosis for intralesional filamentous bacteria, sulphur granules, mycetomas, and pseudomycetomas, the reader is referred to WSC 2009-2010, Conference 1, case I.

Contributor: Royal Veterinary College, Department of Pathology and Infectious Diseases, Hawkshead Lane, Hatfield, Hertfordshire, United Kingdom AL97TA
http://www.rvc.ac.uk

References:

1. Aalbaek B, Christensen H, Bisgaard M, Lijegren CH, Nielsen OL, Jensen HE: *Actinomyces hyovaginalis* associated with disseminated necrotic lung lesions in slaughter pigs. J Comp Pathol **129:**70-77, 2003
2. Barnes LD, Grahn BH: Actinomyces endophthalmitis and pneumonia in a dog. Can Vet J **48**:1155-1158, 2007
3. Biberstein EL, Hirsh DC: Filamentous bacteria: *Actinomyces, Nocardia, Dermatophilus*, and *Strepto–bacillus*. *In:* Veterinary Microbiology, eds. Hirsh DC, MacLachlan NJ, Walker RL, 2nd ed., pp. 215-222. Blackwell Publishing, Oxford, UK, 2004
4. Brown CC, Baker DC, Barker IK: Alimentary system. *In*: Jubb, Kennedy and Palmer's Pathology of Domestic Animals, ed. Maxie MG, 5th ed., vol. 2, pp. 1-296. Saunders, Elsevier, Philadelphia, PA, 2007
5. Caswell JL, Williams KJ: Respiratory system. *In*: Jubb, Kennedy and Palmer's Pathology of Domestic Animals, ed. Maxie MG, 5th ed., vol. 2, pp. 523-653. Saunders, Elsevier, Philadelphia, PA, 2007
6. Couto SS, Dickinson PJ, Jang S, Munson L: Pyogranulomatous meningoencephalitis due to *Actinomyces sp*. in a dog. Vet Pathol **37**:650-652, 2000
7. Edwards, DF: Actinomycosis and Nocardiosis. *In*: Infectious Diseases of the Dog and Cat, ed. Greene CE, 2nd ed., pp. 303-313. W.B. Saunders Company, Philadelphia, PA, 1998
8. Hirai T, Nunoya T, Azuma R: Actinomycosis of the brain and temporal bone in a goat. J Vet Med Sci **69**:641-643, 2007
9. Ginn PE, Mansell JEKL, Rakich PM: Skin and appendages. *In:* Jubb, Kennedy and Palmer's Pathology of Domestic Animals, ed. Maxie MG, 5th ed., vol. 1, pp. 553-781. Saunders, Elsevier, Philadelphia, PA, 2007
10. Gross TL, Ihrke PJ, Walder EJ, Affolter VK: Infectious nodular and diffuse granulomatous and pyogranulomatous diseases of the dermis. *In:* Skin Diseases of the Dog and Cat: Clinical and Histopathologic Diagnosis, eds. Gross TL, Ihrke PJ, Walder EJ, Affolter VK, 2nd ed., pp. 272-319. Blackwell Publishing, Oxford, UK, 2005
11. Ledbetter EC, Scarlett JM: Isolation of obligate anaerobic bacteria from ulcerative keratitis in domestic animals. Vet Ophthalmol **11**:114-122, 2008
12. Pelle G, Makrai L, Fodor L, Dobos-Kovács M: Actinomycosis of dogs caused by *Actinomyces hordeo–vulneris*. J Comp Pathol **123**:72-76, 2000
13. Quinn PJ, Markey BK, Carter ME, Donnelly WJ, Leonard FC: Pathogenic bacteria. *In:* Veterinary Microbiology and Microbial Disease, eds. Quinn PJ, Markey BK, Carter ME, Donnelly WJ, Leonard FC, pp. 43-215, Blackwell Publishing, London, UK, 2002
14. Zucker-Franklin D, Phillipp CS: Platelet production in the pulmonary capillary bed. Am J Pathol **157**:69-74, 2000

The Armed Forces Institute of Pathology
Department of Veterinary Pathology

Conference Coordinator:
Shannon Lacv. DVM. MPH

WEDNESDAY SLIDE CONFERENCE 2009-2010

Conference 5

7 October 2009

Conference Moderator:

Shannon M. Wallace, DVM, Diplomate ACVP

CASE I: 1096/02 (AFIP 2948705).

Signalment: 4-year-old, male beagle (*Canis familiaris*).

History: The dog presented with a two-month history of abdominal enlargement. Hepatomegaly was diagnosed. Two weeks prior to death, high fever (40.5 C), vomiting, diarrhea, weight loss, and lethargy were noticed. The dog arrived at the clinic severely weakened with bright yellow (jaundiced) mucous membranes and a tense abdomen. The patient died the next day.

Gross Pathology: Severe jaundice and extreme enlargement of the lymphocentrum mesentericum craniale were the main postmortem findings. The lymph nodes showed a light brown to yellow cut surface with extensive necrosis; a differentiation between cortex and medulla was not possible. Other lymph nodes were moderately enlarged with a light brown cut surface. In vivo diagnosis of hepatomegaly was confirmed. The liver had a coarsely humped surface with multiple, confluent, light brown, not raised foci in the parenchyma of approximately one centimeter in diameter. Other findings included splenomegaly due to pulpy hyperplasia and a mild granulomatous nephritis.

Laboratory Results: Microbiological culture of the liver and kidneys revealed mycobacteria, which were identified as *Mycobacterium avium* by PCR and reverse hybridization.

Histopathologic Description: The histopathological examination of the liver, spleen, and lymph nodes of the lymphocentrum mesentericum craniale revealed an extreme infiltration of these organs with macrophages, which were characterized by a very large, euchromatic nucleus and a foamy, basophilic, granular cytoplasm, and sporadic giant cells of the Langhans type. The liver showed a severe interlobular, periportal, and intralobular infiltration with macrophages and a small number of lymphocytes causing almost total destruction of organ specific structures (**fig. 1-1**). Pressure atrophy of the surrounding liver tissue developed as a result of the extensive cellular invasion. Aside from the macrophage infiltration, the lymph nodes of the lymphocentrum mesentericum craniale showed central necrosis with multifocal calcification. Necrosis could not be found in other lymph nodes (e.g. lymphocentrum inguinale profundum, hepatic lymph nodes, lymphocentrum axillare), which were sinusoidally infiltrated with macrophages as well. Mild, circumscribed, predominantly perivascular infiltration with macrophages was present in both kidneys, the left

***Sponsored by the American Veterinary Medical Association, the American College of Veterinary Pathologists, and the C. L. Davis Foundation.**

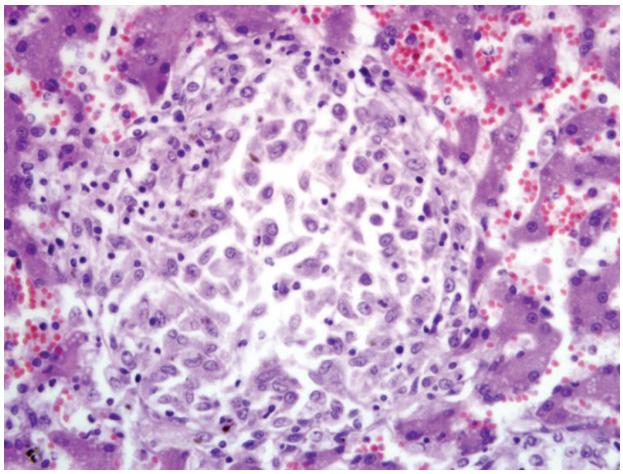

1-1. Liver, dog. Granulomas composed of epithelioid macrophages admixed with scant amounts of necrotic debris, bounded by fibroblasts and lymphocytes. (HE 400X)

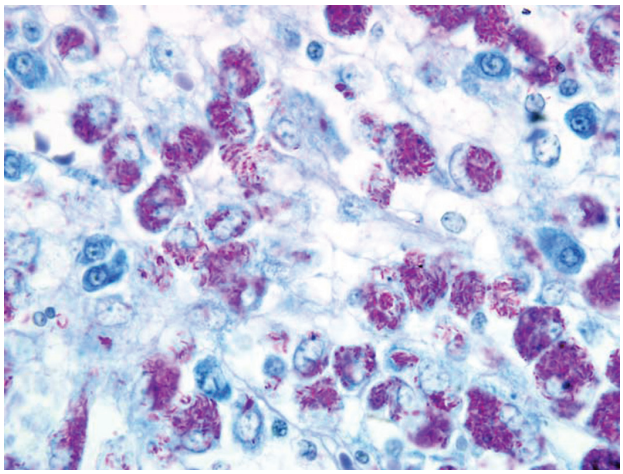

1-2. Liver, dog. Epithelioid macrophages within granulomas contain many 1x5 um acid fast-bacilli. (Ziehl-Neelsen 1000X)

ventricular myocardium and the lamina propria mucosae of the small intestine. The femoral bone marrow turned out to be myelopoetically active without any indication of osteomyelitis. The Ziehl-Neelsen stain revealed a massive presence of acid-fast rod-shaped bacilli in the macrophages infiltrating the liver, lymph nodes, spleen, kidneys, heart and intestine (**fig. 1-2**).

Contributor's Morphologic Diagnosis: Liver: Severe granulomatous hepatitis with an abundance of intrahistiocytic acid-fast rod shaped bacilli (Ziehl-Neelsen stain); etiology consistent with *Mycobacterium avium* (dog, beagle).

Contributor's Comment: Disease due to *Mycobacterium avium* occurs in mammals, especially as opportunistic infections, in the course of hereditary or acquired immune deficiencies. Generalized forms of tuberculosis as caused by *M. tuberculosis* or *M. bovis* have been rarely reported in dogs and cats in the last decades; but disseminated disease due to *M. avium* and other atypical mycobacterioses are described more often in the current literature.[1,3-5,7]

A dog with *M. avium* infection was mentioned in 1979 by Friend et al.[5] It is supposed that the infection can be caused by incorporation of infectious liver tissue of chickens or pigs. Both dogs and cats usually show a high resistance against *M. avium*.[2-4,7] Therefore, hereditary immune deficiencies are thought to be responsible for the outbreaks described in the literature. Hereditary immune deficiencies are discussed in basset hounds [3] and miniature schnauzers, [4,7] which possibly go along with a high incidence of opportunistic infections in these breeds. Such a breed associated immune deficiency is, to our knowledge, not described in beagles.

In the presented case, it was not possible to find out if the dog was fed potentially infectious material. The route of infection remains unclear. Because the bacteria are prominent in the liver, intestine, and its lymph nodes, but not in the lungs, an oral infection is presumed. The formation of a complete primary complex with a rapid lympho-hematological spreading of the bacteria in the course of an early generalization is supposed. The massive periportal, intra- and interlobular infiltration of the liver with pathogen-bearing macrophages matches the description of the typical liver tuberculosis in carnivores according to Pallaske.[8] A similar morphology was seen in disseminated *M. avium* infection in dogs.[2,4]

AFIP Diagnosis: Liver: Hepatitis, granulomatous, multifocal to coalescing, marked, with numerous intrahistiocytic acid-fast bacilli.

Conference Comment: Because of the extent to which the granulomatous infiltrate effaces normal hepatic architecture in this case, many participants considered a neoplastic or atypical histiocytic proliferation in their initial differential diagnosis. *Mycobacterium avium* and *M. intracellulare* are two separate species that result in very similar lesions, and are thus referred to as *M. avium-intracellulare* complex (MAC).[6] These nontuberculous, nonlepromatous mycobacteria are the most common etiologic agents in disseminated mycobacteriosis in dogs, although the disease remains uncommon overall.[7] Interestingly, they are also the most common opportunistic mycobacteria isolated from localized cutaneous infections

in dogs and cats.[6] The lesions in the intestine and lymph nodes in this case, as well as in previously-reported cases, bear striking resemblance to those seen in sheep and cattle with Johne's disease. This is not particularly surprising, given that the causative agent of Johne's disease is *M. avium* subsp. *paratuberculosis*. In humans, disseminated opportunistic mycobacteriosis is usually associated with immunosuppression due to AIDS, and in reported canine cases, immunosuppression has been suspected, though not unequivocally proven. An alternate hypothesis for the pathogenesis in cases where multiple littermates are affected is exposure to a common source, possibly perinatally, as occurs in Johne's disease.[7]

Contributor: Institüt für Veterinär-Pathologie, Universität Leipzig, An den Tierkliniken 33, 04103 Leipzig, Germany

References:

1. Bauer N, Burkhardt S, Kirsch A, Weiss R, Moritz A, Baumgaertner W: Lymphadeopathy and diarrhea in a miniature schnauzer. Vet Clin Pathol **31:**61-64, 2002
2. Beaumont PR, Jezyk PF, Haskins ME: *Mycobacterium avium* infection in a dog. J Small Anim Pract **22**:91-97, 1981
3. Carpenter JL, Myers AM, Conner MW, Schelling SH, Kennedy FA, Reimann KA: Tuberculosis in five basset hounds. J Am Vet Med Assoc **192:**1563-1568, 1988
4. Eggers JS, Parker GA, Braaf HA, Mense MG: Disseminated *Mycobacterium avium* infection in three miniature schnauzer litter mates. J Vet Diagn Invest **9:**424-427, 1997
5. Friend SCE, Russell EG, Hartley WJ, Everist P: Infection of a dog *with Mycobacterium avium* serotype II. Vet Pathol **16:**381-384, 1979
6. Ginn PE, Mansell JEKL, Rakich PM: Skin and appendages. *In:* Jubb, Kennedy, and Palmer's Pathology of Domestic Animals, ed. Maxie MG, 5th ed., vol. 1, pp. 689-691. Elsevier Saunders, Philadelphia, PA, 2007
7. Horn B, Forshaw D, Cousins D, Irwin PJ: Disseminated *Mycobacterium avium* infection in a dog with chronic diarrhoea. Aus Vet J **78:**320-325, 2000
8. Pallaske G: Spezifische Entzundungen der Leber. *In:* Handbuch der speziellen pathologischen Anatome der Haustiere, ed. Joest E, Band VI, Digestionsapparat 2, pp. 159-178. Verlag Paul Parey, Berlin, Hamburg, Germany, 1967

CASE II: 05-0947 (AFIP 3101430).

Signalment: 3.5-week-old, female pixie-bob kitten (*Felis catus*).

History: This kitten died after a five-day clinical course characterized by coughing and gagging. She had been treated with antibiotics and subcutaneous fluids.

Gross Pathology: The right cranial and middle lung lobes and the left cranial and caudal lung lobes were dark red, collapsed and firm. There was a small amount of clear fluid in the thorax and abdomen.

Laboratory Results: There was no bacterial growth from the lung. Viral isolation yielded feline herpesvirus-1.

Histopathologic Description: Sections of affected lung had multifocal areas in which alveolar spaces were filled with fibrin, cellular debris, edema, and hemorrhage associated with accumulations of pulmonary alveolar macrophages and neutrophils (**fig. 2-1**). Less affected alveoli were lined by plump type II pneumocytes. Alveolar septa were thickened by infiltration of mononuclear cells. Numerous sloughed epithelial cells within necrotic areas and lining alveoli had nuclei with peripheralized chromatin and containing amphophilic to eosinophilic nuclear inclusions. Other histologic lesions included erosive tracheitis, necrotizing lymphadenitis of the hilar lymph nodes and thymic atrophy. No viral inclusions were seen in any other tissues.

Contributor's Morphologic Diagnosis: Necrotizing interstitial pneumonia with epithelial intranuclear inclusions (FeHV-1).

Contributor's Comment: Feline herpesvirus 1 is an α-herpesvirus, the host range of which is generally restricted to domestic cats and wild felidae.[2] It is a double stranded DNA virus with a single serotype that is antigenically closely related to canine herpesvirus-1 and phocine herpesvirus-1. It does not persist for long periods in the environment so transmission must be by direct contact and exchange of ocular and nasal fluids. Like many herpesviruses, it grows best at low temperatures, so replication is usually restricted to the ocular and nasal tissues. Infected cats often become latent carriers that can re-shed the virus during periods of stress.[a]

The classic disease associated with infection is 'feline rhinotracheitis,' most commonly manifested as upper respiratory disease with conjunctivitis in susceptible

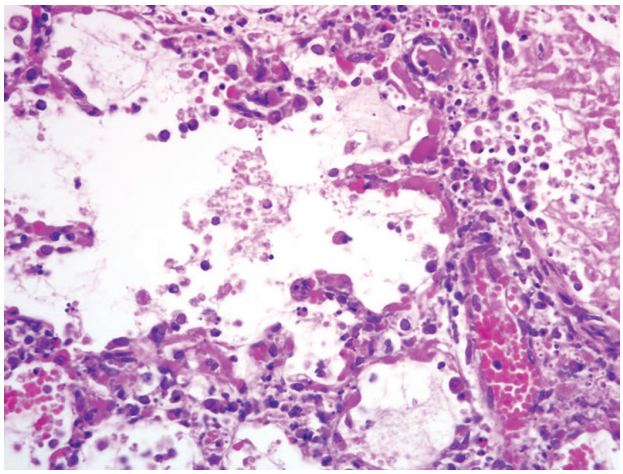

2-1. Lung, cat. Alveolar septa are necrotic and replaced by brightly eosinophilic debris, or expanded by neutrophils and histiocytes. Alveoli contain many macrophages, neutrophils, and sloughed epithelial cells admixed with fibrin and edema. (HE 400X)

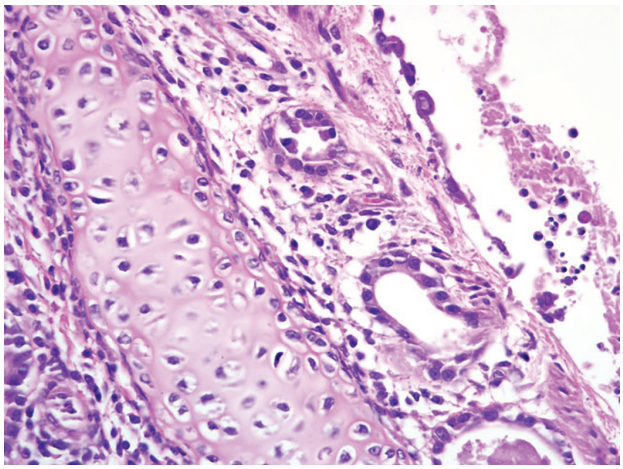

2-2. Lung, cat. Attenuated and necrotic bronchiolar epithelium overlain with fibrin and sloughed necrotic epithelium. The peribronchiolar interstitium is expanded by edema admixed with histiocytes, neutrophils, and fewer lymphocytes. (HE 400X)

kittens. More recently, the virus has been implicated in cases of chronic conjunctivitis and periocular skin disease in adult cats.[5] Although abortion has been induced experimentally in pregnant queens by intravenous inoculation, it is not thought to occur with significant frequency as a natural disease.[2] Likewise, neonatal disease can be induced by exposure of kittens within the vaginal vault, but spontaneous cases of systemic disease in cats and kittens are rare.

Definitive diagnosis of herpesviral respiratory disease is often made clinically, but viral isolation from oropharyngeal swabs is possible if needed. The advent of PCR and in situ hybridization has made possible the implication of feline herpesvirus-1 in chronic keratoconjunctivitis and dermatitis as described above.[5]

Systemic disease characterized by interstitial pneumonia has been reported in kittens, [3] and in one case a seven-month-old cat with severe glossal ulcers was reported to have died of systemic illness characterized by multifocal hepatic necrosis with typical nuclear inclusions in hepatocytes.[4] In our case, a three-week-old Pixie-bob kitten had primary respiratory signs and at necropsy had lesions restricted to the lung. The diagnosis was suspected due to the presence of typical nuclear inclusions in pneumocytes and macrophages and was confirmed by viral isolation. Systemic herpesviral infections in kittens can be the result of immunosuppression, lack of protective antibodies or high pathogen load.[2] There are no reported genetic diseases of Pixie-bob cats that might predispose to severe viral infections. A possible scenario in this

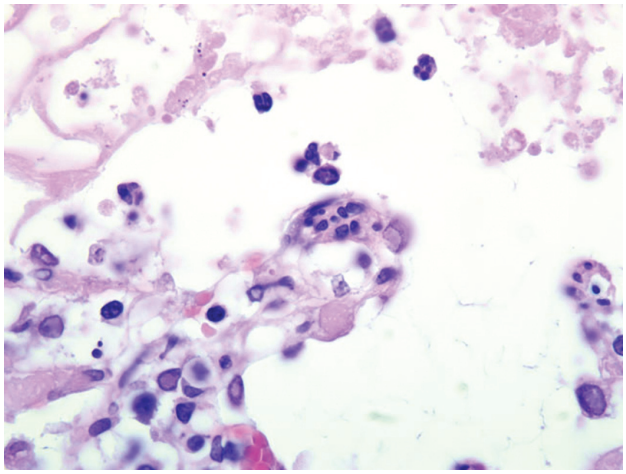

2-3. Lung, cat. Intranuclear inclusions and few syncytial cells are observed. (HE 400X)

case would be stress-related recrudescence of FeHV-1 infection in the dam with transmission to a kitten with low protective antibodies. Chilling of a neonatal kitten to below body temperature may have allowed the virus to proliferate in systemic tissues.

AFIP Diagnosis: Lung: Pneumonia, bronchointerstitial, necrotizing, subacute, multifocal to coalescing, marked, with intraepithelial intranuclear inclusion bodies and syncytia.

Conference Comment: There is significant section

variation with respect to the severity of the lesions in this case. In addition to the histopathologic changes described by the contributor, several conference participants observed necrosis of the bronchiolar epithelium and viral syncytia (**figs. 2-2 and 2-3**).

Alpha-herpesviruses specifically affecting the lung of domestic animals include feline herpesvirus 1 (feline viral rhinotracheitis), canine herpesvirus 1, gallid herpesvirus 1 (infectious laryngotracheitis), bovine herpesvirus 1 (infectious bovine rhinotracheitis), suid herpesvirus 1 (pseudorabies), caprine herpesvirus 1, equine herpesviruses 1 and 4 (abortion and rhinopneumonitis), and equine herpesvirus 5 (equine multinodular pulmonary fibrosis).[1] For a partial list of alpha-herpesviruses of veterinary importance, readers are referred to WSC 2007-2008, Conference 13, case II.

The contributor provided a succinct review of this entity. Conference participants also reviewed some less common clinical presentations of FeHV-1 infection, including ulcerative facial and nasal dermatitis, and stomatitis with eosinophilic infiltrates in cats and cheetahs.[2] For most participants, the differential diagnosis for necrotizing respiratory tract lesions in cats included feline calicivirus (FCV) infection, chlamydophilosis, and toxoplasmosis. When present, the characteristic herpesviral inclusions allow differentiation from FCV infection. However, herpesviral inclusions are only transient, and are usually absent after seven days post-infection. Herpesviruses are unique in that they elicit neutrophilic inflammation and fibrin exudation during respiratory infection, even in the absence of a secondary infection.[2] Feline calicivirus-induced pneumonia is generally interstitial in distribution, whereas FeHV-1 pneumonia is bronchointerstitial. Similarly, toxoplasmosis generally results in necrotizing multifocal to diffuse interstitial pneumonia, but the identification of intralesional protozoal cysts aids in making the diagnosis. *Chlamydophila felis* is an important cause of conjunctivitis in cats and a minor upper respiratory pathogen, but not an important cause of pulmonary disease.[1]

Contributor: Department of Veterinary Microbiology and Pathology, Washington State University, Pullman, WA 99164-7040
http://www.vetmed.wsu.edu/depts-vmp

References:

1. Caswell JL, Williams KJ: Respiratory system. *In*: Jubb, Kennedy, and Palmer's Pathology of Domestic Animals, ed. Maxie MG, 5th ed., vol. 2, pp. 594, 648-651. Elsevier Saunders, Philadelphia, PA, 2007
2. Gaskell R, Dawson S, Radford A, Thiry Etienne: Feline herpesvirus. Vet Res **38:**337-354, 2007
3. Love DN: Feline herpesvirus associated with interstitial pneumonia in a kitten. Vet Rec **89**:178-181, 1971
4. Sheilds RP, Gaskin JM: Fatal, generalized feline viral rhinotracheitis in a young adult cat. J Am Vet Med Assoc **170:**139-141, 1977
5. Suchy A, Bauder B, et al: Diagnosis of feline herpesvirus infection by immunohistochemistry, polymerase chain reaction and in situ hybridization. J Vet Diagn Invest **12:**186-191, 2000

CASE III: 09-855 (AFIP 3134523).

Signalment: 6-year and 7-month-old, female, spayed boxer dog (*Canis familiaris*).

History: No history of prior illness, current on vaccinations and preventative medicine. Found dead two hours after vigorous exercise.

Gross Pathology: There were a small number (10-15) of scattered petechial hemorrhages on the epicardial surface of the heart.

Histopathologic Description: The right ventricular wall is severely infiltrated by individual and small aggregates of well differentiated adipocytes which replace approximately 50-60% of the cardiomyocytes (**fig. 3-1**).

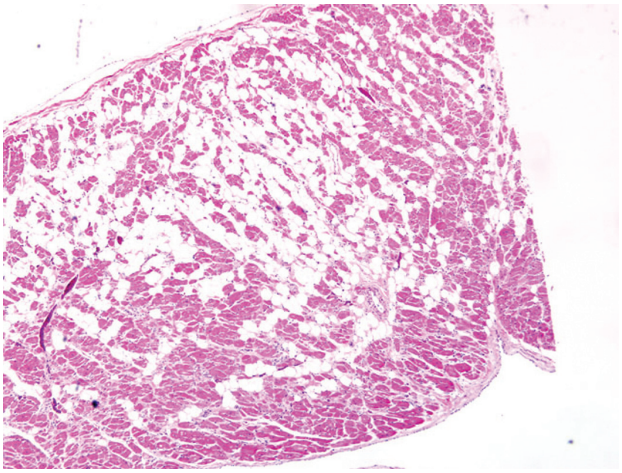

3-1. Heart, dog. Approximately 50% of cardiac myocytes in the right ventricle are replaced by adipocytes, and many of the remaining myocytes are atrophied or degenerate. (HE 400X)

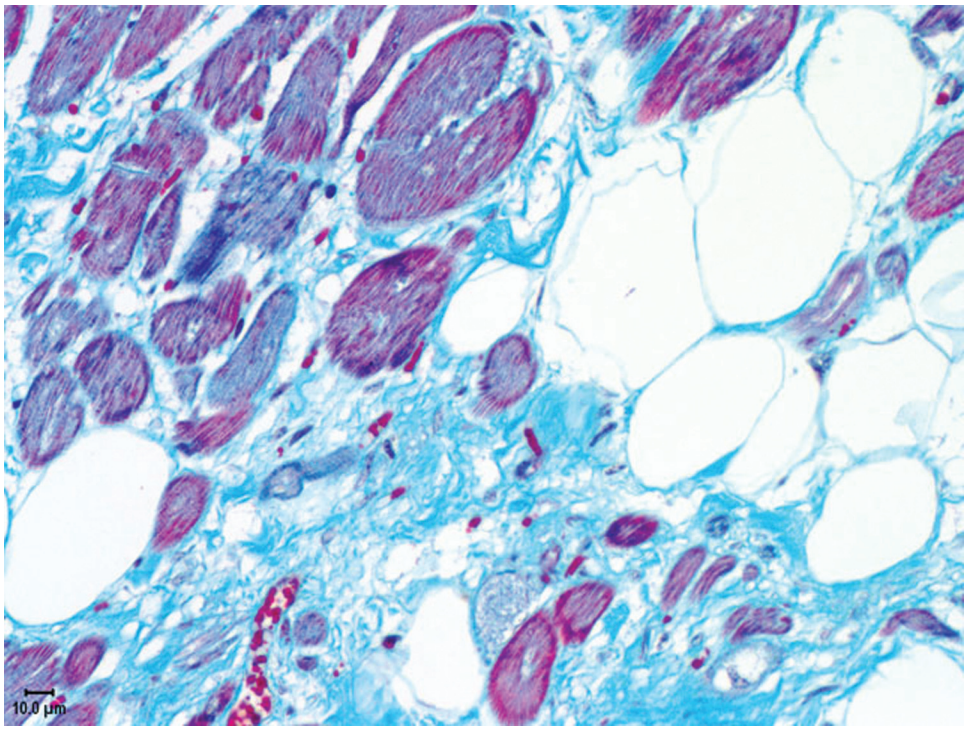

3-2. Heart, dog. Remaining cardiac myocytes are separated and surrounded by a moderate amount of fibrosis. (Masson's trichrome) Photomicrograph courtesy of Department of Population Health and Pathobiology College of Veterinary Medicine North Carolina State University 4700 Hillsborough Street Raleigh, NC 27606, sandra_horton@ncsu.edu.

There is multifocal moderate atrophy of the remaining cardiomyocytes and regionally extensive interstitial fibrosis (**fig. 3-2**). These changes are most severe in the subepicardial region of the ventricular wall. The right atrium and interventricular septum are similarly, but less severely, affected.

Contributor's Morphologic Diagnosis: Heart: Chronic moderate myocardial atrophy and interstitial fibrosis with replacement by adipocytes.

Contributor's Comment: These histologic findings are consistent with arrhythmogenic right ventricular cardiomyopathy (ARVC). ARVC is a variant of dilated cardiomyopathy (DCM), which occurs in boxer dogs, cats and humans. It is characterized histologically by severe myocyte atrophy in the right ventricular free wall and replacement by adipocytes and/or fibrous tissue. Replacement extends from the epicardial surface and extends towards the endocardium. Occasionally, the left ventricle and interventricular septum may also be involved.[1,5-7] Two variants exist: fatty and fibrofatty forms. The fatty form consists of multifocal regions of adipocyte replacement within the right ventricular wall accompanied by a mild interstitial fibrosis. The fibrofatty form is characterized by focal-diffuse regions of myocardial replacement by adipose tissue and marked fibrosis.[1] The disease in dogs closely parallels that seen in humans; loss of right ventricular myocytes with replacement by fat or fibrofatty tissue is considered the pathologic hallmark of human ARVC.[1] Clinical signs of ARVC may include ventricular arrhythmias, syncope, heart failure or sudden death. A spontaneous form of ARVC is also seen in cats, although unlike in dogs and humans, sudden death is not a feature of the disease.[3,4]

ARVC is thought to be transmitted as an autosomal dominant trait in both boxer dogs and humans, although an autosomal recessive trait has also been identified in humans. In humans, mutations in the genes coding for various intercellular adhesion proteins, components of the sarcoplasmic reticulum calcium channel and cytokines have been implicated in the pathogenesis of ARVC.[2] To date, published reports of homologous genes in the dog have failed to identify equivalent mutations.[8,10] However, a seven base pair deletion within the non-coding regulatory sequence of a calcium modulating gene on chromosome 17 has recently been identified as responsible for ARVC in boxer dogs.[9] Although precise information regarding this mutation has not yet been released into the public domain, Washington State University College of Veterinary Medicine now offers a genotyping service for canine ARVC (http://www.vetmed.wsu.edu/deptsVCGL/Boxer/test.aspx).

AFIP Diagnosis: Heart: Cardiomyocyte degeneration, necrosis, and loss, multifocal, marked, with fibrofatty infiltration.

Conference Comment: There is some variation

within the sections, with most participants' slides having a predominantly fatty infiltrate, while in a few slides, adipocytes are accompanied by a small amount of fibrosis (i.e. fibrofatty infiltrate) and rarely, a mononuclear cell infiltrate. This is interesting considering the sudden death of the dog in this case, because in one study of 23 boxer dogs with ARVC, of the nine dogs that died suddenly, all had myocarditis in the left and/or right ventricle, and six had the fibrofatty form. Of the 14 dogs with ARVC that did not die suddenly, only seven had myocarditis, and only two had a fibrofatty infiltrate. Myocarditis may lead to arrhythmias that cause sudden death. In cats, the fibrofatty form predominates, but sudden death is not a feature of ARVC in felids.[1] Dilated cardiomyopathy (DCM), of which ARVC is one variant, is the most common canine cardiomyopathy, with a number of large- and giant-breed dogs being predisposed. An infantile form in Portuguese water dogs is inherited as an autosomal recessive trait, while an X-linked recessive gene is suspected in Great Danes. Nutritional deficiencies (e.g. taurine and carnitine deficiency) and endocrinopathies (e.g. hypothyroidism) have also been associated with DCM. Less common in dogs are hypertrophic cardiomyopathy, characterized by disproportionate interventricular septal thickening and myofiber disarray, and canine X-linked muscular dystropy, a disease of golden retrievers characterized by subendocardial interstitial fibrosis.[6]

Contributor: Department of Population Health and Pathobiology, College of Veterinary Medicine, North Carolina State University, 4700 Hillsborough Street, Raleigh, NC 27606
http://cvm.ncsu.edu/dphp/index.html

References:

1. Basso C, Fox PR, Meurs KM, Towbin JA, Spier AW, Calabrese F, Maron BJ, Thiene G: Arrhythmogenic right ventricular cardiomyopathy causing sudden cardiac death in boxer dogs: A new animal model of human disease. Circulation **109:**1180-1185, 2004
2. Corrado D, Basso C, Thiene G: Arrhythmogenic right ventricular cardiomyopathy: an update. Heart **95:**766-773, 2009
3. Fox PR: Arrhythmogenic right ventricular cardio–myopathy. *In:* Consultations in Feline Internal Medicine, ed. August JR, vol. 5, pp. 319-322. Elsevier, St. Louis, Mo, 2006
4. Fox PR, Maron BJ, Basso C, Liu SK, Thiene G: Spontaneously occurring arrhythmogenic right ventricular cardiomyopathy in the domestic cat: A new animal model similar to the human disease. Circulation **102:**1863-1870, 2000
5. Harpster N: Boxer Cardiomyopathy. *In:* Current Veterinary Therapy, ed. Kirk RW, 8th ed., pp. 329-337. W. B. Saunders Co., Philadelphia, PA, 1983
6. Maxie GM, Robinson WF: Cardiovascular system. *In:* Jubb, Kennedy and Palmer's Pathology of Domestic Animals, ed. Maxie GM, 5th ed., vol. 3, pp. 48-49. Elsevier, Philadelphia, PA, 2007
7. Meurs KM: Boxer dog cardiomyopathy: an update. Vet Clin Small Anim **34:**1235-1244, 2004
8. Meurs KM, Ederer MM, Stern JA: Desmosomal gene evaluation in boxers with arrhythmogenic right ventricular cardiomyopathy. Am J Vet Res **68:**1338-1341, 2007
9. Meurs KM, Mauceli E, Acland G, Lindblad-Toh K: 2009 ACVIM forum and Canadian veterinary medical association convention, abstract #11: Genome-wide association identifies a mutation for arrhythmogenic right ventricular cardiomyopathy in the boxer dog. J Vet Intern Med **23:**687-688, 2009
10. Oyama MA, Reiken S, Lehnart SE, Chittur SV, Meurs KM, Stern J, Marks AR: Arrhythmogenic right ventricular cardiomyopathy in boxer dogs is associated with calstabin2 deficiency. J Vet Cardiol **10:**1-10, 2008

CASE IV: N2009-23-3 (AFIP 3135081).

Signalment: 13-year-old female axis deer (*Axis axis*).

History: This axis deer was found dead without any premonitory signs. The keepers had reported repeated episodes of dominant behavior and aggression from other deer in the group.

Gross Pathology: At necropsy, the abdominal cavity was filled with 1.5 to 2 gallons of frank blood with many free-floating blood clots. Several of these clots were loosely adhered to the serosal surfaces of the viscera and to the hepatic capsule. Approximately 60-75% of the liver was effaced and replaced by a soft, yellow/tan, lobulated, partially hemorrhagic, nodular mass (**fig. 4-1**). Blood clots and a portion of the omentum were loosely adhered to the central area of the mass. Randomly scattered throughout all lung lobes were numerous, up 1.5 cm diameter soft, yellow/tan, nodules that occasionally are surrounded by a rim of dark red discoloration (hemorrhage). The cranioventral lung lobes were slightly "meaty" and mottled dark red (congestion). All cut sections of the lungs floated readily in formalin except the cranioventral portions, which floated just beneath the surface. This deer was also

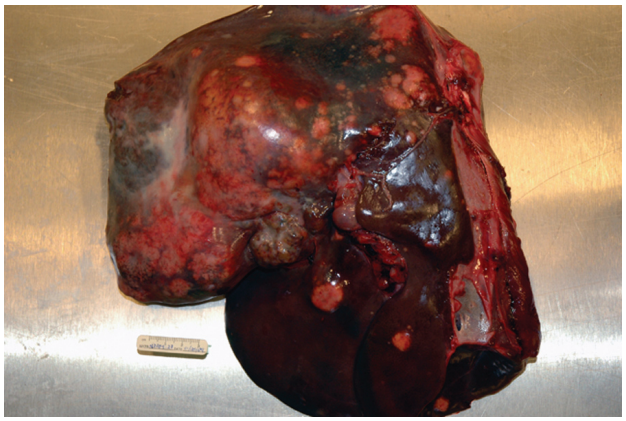

4-1. Hepatocellular carcinoma, liver, Axis deer. Approximately 60-75% of the liver is replaced by a soft, yellow/tan, lobulated, partially hemorrhagic, mass. Photograph courtesy of Wildlife Conservation Society Global Health Program – Pathology 2300 Southern Boulevard Bronx, NY 1046 crodriguez@wcs.org.

in thin body condition and there were several areas of bruising along the thoracic and abdominal body wall.

Histopathologic Description: Participants that review slide A will have a section of lung from caudal lobes and those that receive slide B will have a section of lung from the cranioventral lobe. All slides have sections of the liver.

Liver: Approximately 40% of the preexistent hepatic parenchyma is effaced, compressed and replaced by a focally extensive, unencapsulated, vagely lobulated, infiltrative nodular mass. The mass is composed of irregular cords and trabeculae of polygonal cells with discrete cytoplasmic borders, abundant finely granular cytoplasm and a single to occasionally multiple round to elongated vesicular nuclei with coarsely clumped chromatin and one to multiple prominent nucleoli (**fig. 4-2**). Neoplastic cells display marked anisocytosis and anisokaryosis, marked nuclear atypia and a low mitotic rate (1-2 mitoses per 10 40X fields). Separating the neoplastic cells into lobules and nests is a pervasive, densely cellular fibrous connective tissue stroma that occasionally contains atrophied ductular structures. Within central areas of the mass there are regions of loss of cellular detail and differential staining that are replaced with cellular and karyorrhectic debris (necrosis). Peritumoral hepatic cords are compressed and there is variable congestion and hemorrhage (not present in all slides). Single and small clusters of pigment-laden macrophages (hemosiderophages) are present throughout the section both within the sinusoids as well as associated with portal regions.

Lung: Effacing approximately 30% of the pulmonary tissue is a focally extensive, unencapsulated, vaguely lobulated, infiltrative nodular mass. The neoplastic cells display morphologic features consistent with the neoplastic cells previously described in the liver. In addition, variably prominent throughout the sections, clusters of neoplastic cells are present within the lumen of vascular structures (neoplastic emboli) and often extend into and adjacent alveolar spaces (**fig. 4-3**). In sections of lung from the cranioventral lobes (slide B) there is marked hemorrhage and edema that obscure most of the alveolar spaces accompanied by peribronchiolar, intralumenal and intraalveolar dense aggregates of viable and degenerate neutrophils and macrophages that contain ingested erythrocytes as well as coarse, golden yellow pigment granules (hemosiderin).

Contributor's Morphologic Diagnosis: 1. Liver: Hepatocellular carcinoma, pseudoglandular, regionally extensive, severe with fibrosis, intratumoral necrosis and perilesional parenchymal compression and hemorrhage.
2. Liver: Hemosiderosis, chronic, multifocal, mild to moderate.
3. Lung (all slides): Hepatocellular carcinoma, metastatic, regionally extensive, severe with intratumoral necrosis and hemorrhage and multifocal vascular tumor emboli.
4. Lung (slide B): Pneumonia, bronchointerstitial, acute to subacute, regionally extensive, moderate to severe with regionally extensive hemorrhage, edema, fibrin, erythrophagocytosis and hemosiderin deposition.

Contributor's Comment: Hepatocellular carcinomas, although relatively uncommon, have been reported in most domestic and in several wild animal species, [1-10] with some sources citing the highest incidence in ruminants, particularly sheep, [2] and others, in dogs.[1] These tumors are often massive and may involve one or more entire lobes of the liver.[1,2] The left lateral lobe is reported to be more commonly affected.[1] This tumor is characterized histologically by disorganized arrays of neoplastic hepatocytes but their morphology can vary greatly, from well differentiated hepatocytes to markedly anaplastic and bizarre cells. Based on their histologic pattern, hepato–cellular carcinomas can be classified as trabecular, adenoid (or pseudoglandular) and solid.[1,2,10] Trabecular carcinomas are composed of variably wide (up to 20 cells thick) cords of hepatocytes with minimal supportive connective tissue stroma. In these tumors, neoplastic hepatocytes may or may not exhibit features of malignancy and differentiating between a well-differentiated hepatocellular carcinoma

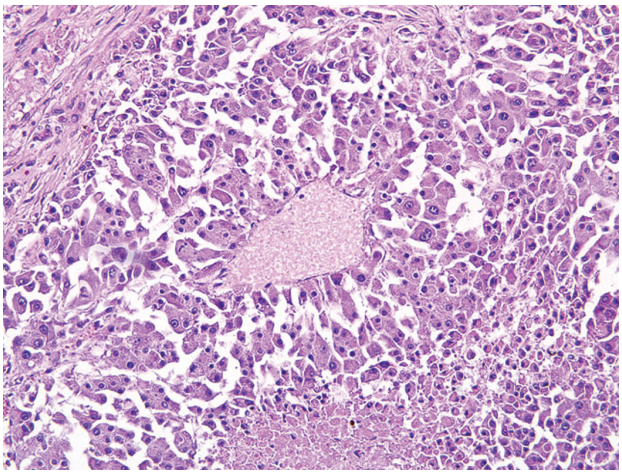

4-2. Hepatocellular carcinoma, liver, Axis deer. Effacing up to 50% of the section is a neoplasm composed of polygonal cells which occasionally recapitulate hepatic lobules. There is marked anisokaryosis and anisocytosis, and there are multifocal binucleate neoplastic cells. (HE 200X)

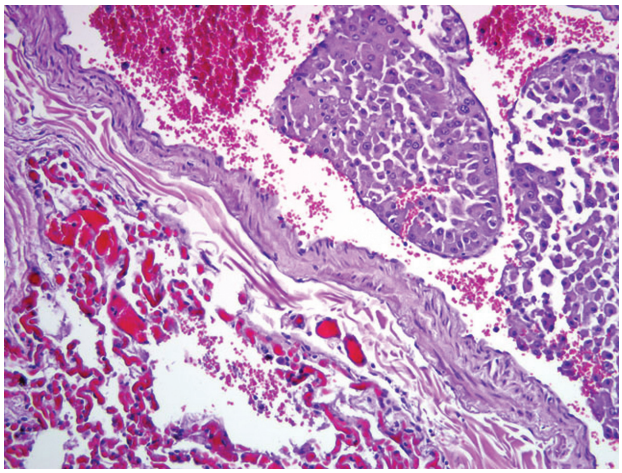

4-3. Hepatocellular carcinoma, lung, Axis deer. Multifocally, neoplastic cells are found within pulmonary vasculature. (HE 200X)

and a hepatocellular adenoma can present a daunting challenge.[1,2] Adenoid, or pseudoglandular tumors exhibit the formation of irregular acini that may develop a lumen containing proteinaceous fluid. Discriminating between a well-differentiated carcinoma with a pseudoglandular pattern and a cholangiocarcinoma may also be very challenging.[1] Solid carcinomas are often poorly-differentiated and are composed of sheets of pleomorphic neoplastic cells with no apparent pattern of distribution. In less well-differentiated neoplasms, cellular and nuclear variability can be marked and often giant cells with karyomegalic forms or multiple nuclei can be found.[1]

Intrahepatic metastases are common and vascular, rather than lymphatic invasion, is more typical in these tumors.[2,10] Metastatic spread to the lungs and to lymph nodes within the cranial abdomen is also a feature of this neoplasm, as is invasion of the hepatic capsule and seeding of the peritoneal cavity.[1,2,10] Rupture of these neoplasms can occur spontaneously [10] and, as in this case, can result in a fatal intraabdominal hemorrhage; however, rupture of the tumor in this deer may have resulted from aggressive or dominant behavior between individuals in the herd. In addition, at the time of the necropsy there was evidence of mild aspiration pneumonia (not represented in all slides) that may have also been the result of repeated harassment or trauma by other members of the herd in the hours to days prior to death.

The etiology of most hepatocellular carcinomas is unknown. Numerous chemical compounds used in industrial and/or experimental settings have been linked to the development of hepatic neoplasia in humans and laboratory animals, but significant exposure of these to domestic and wild animal species is unlikely.[1] Naturally occurring toxic compounds, such as aflatoxins, pyrrolizidines and nitrosamines, and infectious agents, such as hepatitis B viruses, woodchuck hepatitis virus and *Helicobacter* spp. in some strains of mice, have been implicated in hepatic carcinogenesis.[1] Dietary factors and availability of foraging substrates are also suspected of playing a role in the increased incidence of hepatocellular carcinomas within geographically distinct populations of roe deer (*Capreolus capreolus*) in Britain.[3,7]

In non-domestic species, hepatocellular carcinomas have been reported in black-tailed prairie dogs (*Cynomys ludivicianus*) and other members of the Sciuridae family, in which a viral etiology is suspected.[5] Nearly all woodchucks (*Marmota marmota*) infected with the woodchuck hepatitis virus are known to develop hepatocellular carcinoma.[1] In cervids, hepatocellular carcinomas have been reported in roe deer (*Capreolus capreolus*) and white-tailed deer (*Odocoileus virginianus*).[3,7,8] Other neoplasms reported in cervids include spontaneous abomasal and uterine adenocarcinomas in an elk (*Cervus elaphus nelsoni*)[4], cardiac rhabdomyosarcoma in a juvenile fallow deer (*Dama dama*) [6], and uterine adenocarcinoma in a sika deer (*Cervus nippon*).[9]

AFIP Diagnosis: 1. Liver: Hepatocellular carcinoma. 2. Lung: Hepatocellular carcinoma, metastatic.

Conference Comment: The contributor provides an excellent review of hepatocellular carcinoma in domestic and non-domestic species. Noteworthy, the lung and liver are the most common organs for metastasis of malignant neoplasms, and most hepatic neoplasms are not of primary liver origin, but rather represent metastases from other organs. In addition to hepatocellular carcinoma, primary hepatic neoplasms include hepatocellular adenoma, cholangiocellular adenoma and carcinoma, carcinoids, and mesenchymal neoplasms, such as fibrosarcoma, leiomyosarcoma, osteosarcoma, and hemangiosarcoma. Hepatocellular neoplasms are differentiated from hyperplastic nodules by their paucity of portal tracts, which are retained in the latter. Hepatocellular adenomas are most common in young ruminants, and are usually single masses composed of uniform plates of well-differentiated hepatocytes that compress and orient at right angles to adjacent normal hepatocytes. As noted by the contributor, hepatocellular adenomas may be difficult to distinguish from well-differentiated hepatocellular carcinomas of the trabecular type. In contrast, cholangiocellular adenomas are most common in cats, and may form large, cystic structures lined by flattened epithelium. Cholangiocellular carcinomas may be well- or poorly-differentiated, and often appear umbilicated on gross examination. They are usually firm as a result of a robust scirrhous response, and the metastatic rate to the lungs and/or abdominal lymph nodes is high. Carcinoids arise from neuroendocrine cells of the biliary epithelium, may be intrahepatic or extrahepatic, and may stain positively with neuroendocrine markers, such as chromogranin A.[1,2]

Contributor: Wildlife Conservation Society, Global Health Program-Pathology, 2300 Southern Boulevard, Bronx, NY 10464
http://www.wcs.org

References:

1. Cullen JM, Popp JA: Tumors of the liver and gall bladder. *In*: Tumors in Domestic Animals, ed. Meuten DJ, 4th ed., pp. 486-492, 2002
2. Cullen JM: Liver, biliary system, and exocrine pancreas. *In*: Pathologic Basis of Veterinary Diseases, ed. McGavin MD, Zachary JF, 4th ed., pp. 450-451, 2007
3. De Jong CB, Van Wieren SE, Gill RMA, Munro R: Relationship between diet and liver carcinomas in row deer in Kielder Forest and Galloway Forest. Vet Rec **155**(7):197-200, 2004
4. Duncan C, Powers J, Davis T, Spraker T: Abomasal and uterine adenocarcinomas in a captive elk (*Cervus elaphus nelsoni*). J Vet Diagn Invest **19**(5):560-563, 2007
5. Garner MM, Raymond JT, Toshkov I, Tennant BC: Hepatocellular carcinoma in Black-tailed prairie dogs (*Cynomys ludivicianus*): Tumor morphology and immunohistochemistry for hepadenavirus core and surface antigens. Vet Pathol **41:**353-361, 2004
6. Kolly C, Bidaut A, Robert N: Cardiacrhabdomyosarcoma in a juvenile fallow deer (*Dama dama*). J Wildl Dis **40**(3):603-606, 2004
7. Munro R, Youngon RW: Hepatocellular tumours in roe deer in Britain. Vet Rec **138:**542-546, 1996
8. Placke ME, Roscoe DE, Wyand DS, Nielsen SW: Hepatocellular adenocarcinoma in a white-tailed deer (*Odocoileus virginianus*). Can J Comp Med **46**(2):198-200, 1982
9. Robert N, Pothaus H: Uterine adenocarcinoma in a captive sika deer. J Wildl Dis **35**(1):141-144, 1999
10. Stalker MJ, Hayes MA: Liver and biliary system. *In*: Jubb, Kennedy, and Palmer's Pathology of Domestic Animals, ed. Maxie MG, 5th ed., vol. 2, p. 384. Elsevier Saunders, Philadelphia, PA, 2007

The Armed Forces Institute of Pathology
Department of Veterinary Pathology

Conference Coordinator:
Shannon Lacy, DVM, MPH

WEDNESDAY SLIDE CONFERENCE 2009-2010

Conference 6

21 October 2009

Conference Moderator:

Dale G. Dunn, DVM, Diplomate ACVP

CASE I: 08N2533 (AFIP 3134342).

Signalment: 7-month-old spayed, female Maltese mix dog (*Canis familiaris*).

History: This dog presented with a 5-day history of lethargy and 2-day history of anorexia and vomiting. She was up to date on vaccines and had no prior medical problems. On physical exam the dog was obtunded and laterally recumbent. Mucous membranes were pale and tacky with prolonged capillary refill time. She had moderate tachycardia with synchronous, weak femoral pulses. She was hypothermic with a rectal temperature of 96.8 degrees Fahrenheit. Dehydration was assessed as 8-10%. Following rehydration, the dog developed watery melena and vomited frank blood.

Gross Pathology: The duodenum was thickened (3 mm) and mottled dark red and tan on the serosal surface. Gastric and intestinal contents were dark red and mucoid. Scattered throughout the gastrointestinal tract, but noted most prominently in the gastric cardia and fundus, duodenum, and colon, were numerous (>100) 1 mm diameter, raised, pale, tan nodules with pinpoint central depressions (**fig. 1-1**). The splenic surface was irregular with shallow 2-3 mm pits over the entire surface. There was petechiation on the capsular surface of an enlarged mesenteric lymph node (approximately twice normal size). On cut surface, the medulla and part of the cortex was dark red (hemorrhage); the remaining cortex was pale pink (**fig. 1-2**).

Laboratory Results: **Bloodwork** revealed elevated packed cell volume, increased blood urea nitrogen, and mild hyponatremia, hypokalemia, and hypochloremia. **Abdominal radiographs** showed increased soft tissue density in the ileocecocolic region, but were otherwise unremarkable. **Parvovirus fecal antigen test:** negative. **Fecal flotation:** *Nanophyetus salmincola* eggs isolated.

Histopathologic Description: **Mesenteric lymph node:** In this lymph node, follicles are absent and subcapsular and medullary sinuses are filled with numerous macrophages that have abundant eosinophilic cytoplasm and frequently contain numerous basophilic, less than 1 um diameter, coccoid to coccobacillary organisms surrounded by a thin clear space or occasionally forming clusters within vacuoles (**figs. 1-3 and 1-4**). Smaller numbers of macrophages are scattered through the cortex, where there are multifocal to coalescing areas of necrosis. Increased numbers of plasma cells are present throughout the cortex and medullary cords.

***Sponsored by the American Veterinary Medical Association, the American College of Veterinary Pathologists, and the C. L. Davis Foundation.**

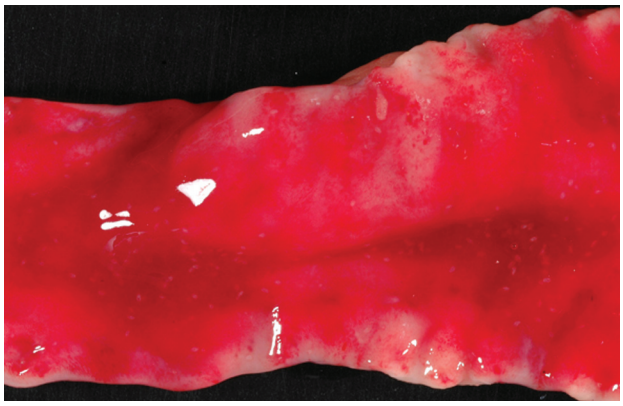

1-1. Duodenum, dog. The duodenum is thickened and mottled dark red and tan with scattered 1 mm diameter raised pale nodules with pinpoint central depressions. Photographs courtesy of University of California, Davis, Veterinary Medical Teaching Hospital, One Shields Ave, Davis, CA 95616, *rmgriffey@ucdavis.edu.*

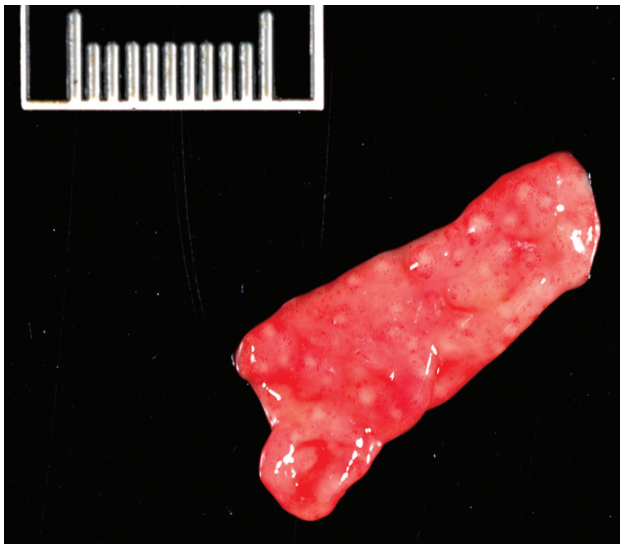

1-2. Lymph node, dog. On cut surface, the medulla and part of the cortex are hemorrhagic. Photographs courtesy of University of California, Davis, Veterinary Medical Teaching Hospital, One Shields Ave, Davis, CA 95616, rmgriffey@ucdavis.edu.

Duodenum: In this section of duodenum, there is generalized villous blunting with multifocal, epithelial necrosis and accumulation of sloughed cells within crypts (crypt abscesses). Embedded within the mucosa as well as within the intestinal lumen are multiple profiles of acoelomic parasites with a spiny cuticle, suckers, and operculated eggs (**fig. 1-5**). Some sections of individual parasites have both spermatids and ova (hermaphroditic). Moderate numbers of lymphocytes and plasma cells with fewer macrophages infiltrate the lamina propria and form a nearly circumferential band between the muscularis mucosa and the base of villi. Macrophages containing clusters of the same intracellular organisms observed in the lymph node (described above) are occasionally noted within the muscularis mucosa and submucosa. Mucosal epithelium is alternately attenuated to regenerative with some cells exhibiting large, vesicular nuclei. There are scattered regions of submucosal hemorrhage.

Special stains: The organisms seen within macrophages on H&E stained red (gram-negative) with Brown and Brenn and purple-blue with Giemsa stains. Machiavello's stain was inconclusive.

Contributor's Morphologic Diagnosis: 1. Mesenteric lymph node: Severe, multifocal to coalescing granulomatous and necrotizing lymphadenitis with intracellular rickettsiae (*Neorickettsia helmintheoca*, presumptive).
2. Duodenum: Moderate, multifocal, chronic, granulo–matous enteritis with intracellular rickettsiae.
3. Duodenum: Trematodiasis (*Nanophyetus salmincola*).
4. Duodenum: Moderate, diffuse, chronic, lympho–plasmacytic enteritis.

Contributor's Comment: This case presents some of the classical clinical signs and gross and histopathologic lesions of salmon poisoning disease caused by *Neorickettsia helminthoeca*, a 0.3 um coccoid to coccobacillary, gram-negative, obligate intracellular bacteria, which occasionally forms rods up to 2 um long.[3] *N. helminthoeca* is transmitted via the helminth *Nanophyetus salmincola*, a trematode whose life cycle requires two intermediate hosts and one definitive host. Development from miracidia to cercariae occurs within the first intermediate host, a snail (*Oxytrema silicula)*. Cercariae are then released into the water where they infect a secondary intermediate host via skin penetration. Salmonid fish are the typical secondary host, but infection of some non-salmonid fish and the Pacific giant salamander does occur.[3] Cercariae develop to metacercariae and localize mainly in the kidneys and skeletal muscle, although they may be found in any organ.[1] Transmission to the definitive host follows ingestion of an infected fish. Adult trematodes then develop within the intestine where they attach to the mucosa and ova are released to the environment in feces, generally in 5-7 days post-infection.[3] *N. helminthoeca* is transmitted transovarially within the trematode and is present in all life cycle stages.[7] It is inoculated by unknown means into the intestines of definitive hosts, where replication

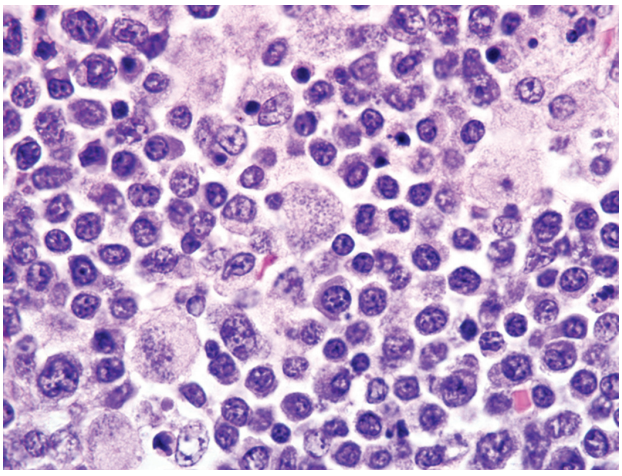

1-3. Lymph node, dog. Multifocally within medullary sinuses are high numbers of histiocytes with abundant eosinophilic cytoplasm and frequently containing numerous basophilic, <1 um rickettsiae surrounded by a thin clear vacuole. (HE 1000X)

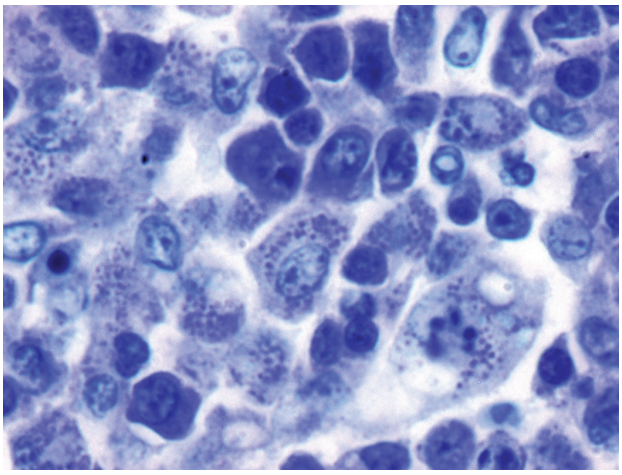

1-4. Lymph node, dog. Intrahistiocytic rickettsiae stain purple-blue with Giemsa stain. Photomicrograph courtesy of University of California, Davis, Veterinary Medical Teaching Hospital, One Shields Ave, Davis, CA 95616, rmgriffey@ucdavis.edu.

initially occurs in either intestinal epithelium or lymphoid follicles.[3] Definitive hosts of the trematode may be any fish-eating bird or mammal. There are a number of known natural avian and mammalian definitive hosts; however, primarily canid species, including domestic dogs, coyotes, and foxes, are susceptible to *N. helminthoeca* infection.[3] In addition, several species of captive bears have been reported that developed clinical signs of salmon poisoning disease following ingestion of raw or improperly stored fish from the endemic area and were passing *N. salmincola* eggs.[2,7]

Salmon poisoning disease generally has an incubation period of 5-7 days and common clinical signs are fever, anorexia, vomiting, diarrhea, and lymphadenopathy.[3] Bloody diarrhea and hypothermia may develop in the late stages of the disease, as was the case in this dog. The presence of the fluke is generally of little clinical significance.[3] If left untreated, the disease has a high mortality rate; the specific cause of death is unknown. *Neorickettsia* are able to evade the immune system by inhibition of lysosomal fusion with its parasitophorous vacuole, a process which has been shown to be reversed by oxytetracycline treatment.[9] Accordingly, appropriate treatment of the disease warrants an excellent prognosis. In one study, 91% of naturally infected dogs treated with tetracycline made a full recovery.[8] Recovered animals generally develop immunity.[3]

Antemortem diagnosis is based on history and typical clinical signs along with presence of *N. salmincola* ova on

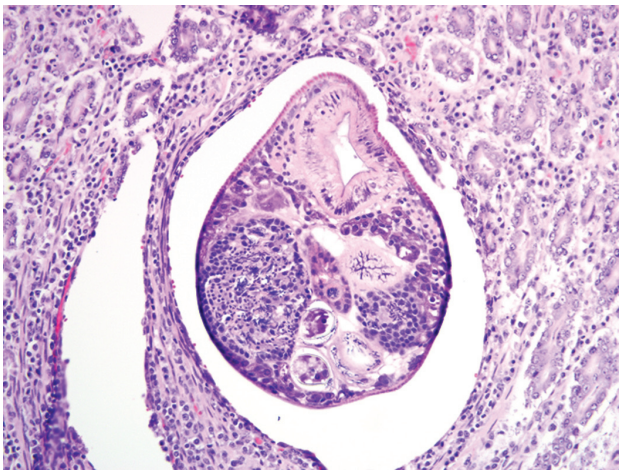

1-5. Small intestine, dog. Embedded deep within an intestinal crypt is a cross section of an adult trematode. (HE 200X)

fecal flotation.[8] Further confirmation is provided by lymph node aspirates showing macrophages with rickettsia-like cytoplasmic inclusions. The organisms stain purple with Giemsa, red with Macchiavello's, black or dark brown with Levaditi's method, and pale blue with hematoxylin and eosin. Peripheral lymphadenopathy was not present in this case. On necropsy, gross lesions typically involve the lymphoid tissues, spleen, and gastrointestinal tract. These include lymphoid tissue enlargement, lymph node petechiation, splenomegaly, and petechiation and ulceration in the gastrointestinal tract.[3] Similar gross findings were noted in the present case, with the addition of gross thickening of the duodenum and pinpoint raised

mucosal nodules in the stomach, duodenum, and colon, which corresponded histologically to lymphoid follicles and inflammatory nodules in which there were macrophages with intracellular rickettsiae. The presence of the rickettsiae in macrophages within the stomach wall has not been reported. Given that *N. helminthoeca* is presumed to be inoculated into the intestinal mucosa, its presence in the stomach suggests either inoculation in gastric mucosa as well, or a particular affinity for this tissue during systemic distribution. Diagnosis in this case was facilitated by the finding of classic microscopic lesions. In the lymphoid tissues, these are depletion of mature lymphocytes, foci of necrosis, and hyperplasia of mononuclear phagocytes with intracytoplasmic rickettsia-like organisms. Trematodes are found embedded in the intestinal mucosa, primarily in the duodenum, as was the case here. Nonsuppurative meningitis or meningoencephalitis has been reported experimentally, but neither was observed in this case.[4]

The endemic area of *O. silicula*, the first intermediate host of the trematode, ranges from southern Vancouver Island as far south as Lake Tahoe along the western slopes of the Cascade and Sierra mountains.[7] The natural habitat of the snail used to define the affected area, but stocking of sport fisheries and other public waters with infected fish from both state and private hatcheries, as well as natural movement of salmonid fish to new areas, has expanded the range of infected fish, thereby expanding the range of potential cases of salmon poisoning disease.[7] In the present case, further questioning of the owner revealed that the family had eaten trout from a region in the Sierra foothills southwest of Lake Tahoe, which could represent the source of exposure for this dog. Interestingly, salmon poisoning or a similar disease could be emerging in an entirely separate region. There are reports from southern Brazil of a disease in dogs with gross and histopathologic lesions similar to salmon poisoning disease.[6] In these cases, intracytoplasmic organisms were observed, and trematodes were present in the large intestine of one dog that were considered consistent with *Ascocotyle arnaldoi*, a trematode that also requires both a snail and fish intermediate host. Preliminary PCR studies have isolated gene fragments with close homology to *N. helmintheoca* from tissues of two such affected dogs.[5]

AFIP Diagnosis: 1. Duodenum: Enteritis, lympho–histiocytic and plasmacytic, diffuse, moderate, with villar blunting and fusion, crypt hyperplasia and abscesses, fibrinous vasculitis, hemorrhage, and numerous intra–histiocytic rickettsiae.
2. Duodenum: Intramucosal adult trematode.
3. Lymph node, mesenteric (per contributor): Lymphadenitis, necrotizing and histiocytic, multifocal to coalescing, moderate, with plasmacytosis, and numerous intrahistiocytic rickettsiae.

Conference Comment: This case is an excellent example of a classic entity, and the contributor provides a thorough review of the disease pathogenesis, clinical signs, gross and microscopic lesions, and epidemiology. In most conference participants' slides there are multifocal areas of hemorrhage within the submucosa and serosal adventitia of the duodenum. Vessels in these areas are frequently characterized by fibrinoid necrosis and mild vasculitis, as indicated in the AFIP morphologic diagnosis. Participants also noted moderate amounts of erythrophagocytosis by sinus histiocytes in the submitted lymph node. This is a common incidental finding in canine mesenteric lymph nodes.

Contributor: Anatomic Pathology Service, Veterinary Medical Teaching Hospital and Department of Pathology, Microbiology and Immunology, School of Veterinary Medicine, University of California, Davis, One Shields Avenue, Davis, CA 95616
http://www.vmth.ucdavis.edu
http://www.vetmed.ucdavis.edu/PMI

References:
1. Baldwin NL, Millemann RE, Knapp SE: Salmon poisoning disease. III. Effect of experimental *Nanophyetus salmincola* infection the fish host. J Parasitol **53**(3):556-564, 1967
2. Gai JJ, Marks SL: Salmon poisoning disease in two Malayan sun bears. J Am Vet Med Assoc **232**(4):586-588, 2008
3. Gorham JR, Foreyt WJ: Salmon poisoning disease. In: Infectious Diseases of the Dog and Cat, ed. Greene CE, 3rd ed. pp. 198-203. WB Saunders, Philadelphia, PA, 2006
4. Hadlow WJ: Neuropathology of experimental salmon poisoning of dogs. Am J Vet Res 18(69):898-908, 1957
5. Headley SA, Scorpio D, Barat N, Vidotto O, Dumler JS: Neorickettsia helminthoeca in dog, Brazil. Emerg Infect Dis 12(8):1303-1305, 2006
6. Headley SA, Vidotto O, Scorpio D, Dumler JS, Mankowski J: Suspected cases of Neorickettsia-like organisms in Brazilian dogs. Ann NY Acad Sci 1026:79-83, 2004
7. Hedrick RP, Amandi A, Manzer D: Nanophyetus salmincola: the trematode vector of Neorickettsia helminthoeca. Calif Vet 44:18-22, 1990
8. Mack RE, Bercovitch MG, Ling GV, Lobingier RT, Melli AC: Salmon poisoning disease complex in dogs – a review of 45 cases. Calif Vet 44:42-45,1990
9. Rikihisa Y: Mechanisms to create a safe haven by members of the family Anaplasmataceae. Ann NY Acad Sci **990:**548-55, 2003

CASE II: 089-43900 (AFIP 3134372).

Signalment: 6-year-old castrated, male domestic shorthair cat (*Felis catus*).

History: Anorexia, soft tissue abdominal mass, no response to medical treatment.

Gross Pathology: Jejunum: Marked transmural expansion by a firm, homogenous tan mass with mucosal ulceration (**fig. 2-1**).

Laboratory Results: Moderate leukocytosis and eosinophilia.

Histopathologic Description: Jejunum: Expanding and infiltrating the ulcerated mucosa, submucosa, tunica muscularis, and extending to the serosa is a poorly demarcated and unencapsulated mass. Neoplastic cells are arranged in a trabecular pattern separated, surrounded, and dissected by variably dense bands of stromal collagen (sclerosis). Neoplastic cell morphology varies from round to polygonal to spindled with variably distinct cell borders and a moderate amount of eosinophilic cytoplasm that very rarely contains basophilic granules. Nuclei range from round to oval to elongate with dispersed chromatin and one to two prominent nucleoli. Mitoses are infrequent, ranging from zero to one per 400X field. There is moderate to marked anisocytosis and anisokaryosis with occasional karyomegalic cells. Admixed throughout the neoplastic population are moderate to marked infiltrates of eosinophils.

Contributor's Morphologic Diagnosis: Jejunum: Sclerosing mast cell tumor.

Contributor's Comment: This case was selected from a series of a unique and unreported sclerosing variant of feline intestinal mast cell tumor (MCT) recognized at the Colorado State University Veterinary Diagnostic Laboratory. Visceral forms of MCT are relatively common in the cat, with intestinal MCT being the third most common primary intestinal tumor following lymphoma and adenocarcinoma.[10] Furthermore, visceral forms (splenic and intestinal) of mast cell tumor are more often reported in the cat compared to the dog.[5] While these tumors typically display similar microscopic features regardless of anatomical location[7,8], a sub-group of intestinal MCT in the cat is presented here which is morphologically and biologically distinct from other mast cell tumors in this species, characterized by a significant stromal component. Masson's trichrome stain was pursued to confirm the stromal collagen composition of the sclerosing component, which is characterized by intense blue staining. Poorly discernible intracytoplasmic granules, which demonstrated metachromasia and enhanced visibility with giemsa and toluidine blue stains, suggest mast cell origin. Immunohistochemical staining for mast cell-specific tryptase further supported mast cell origin.[3]

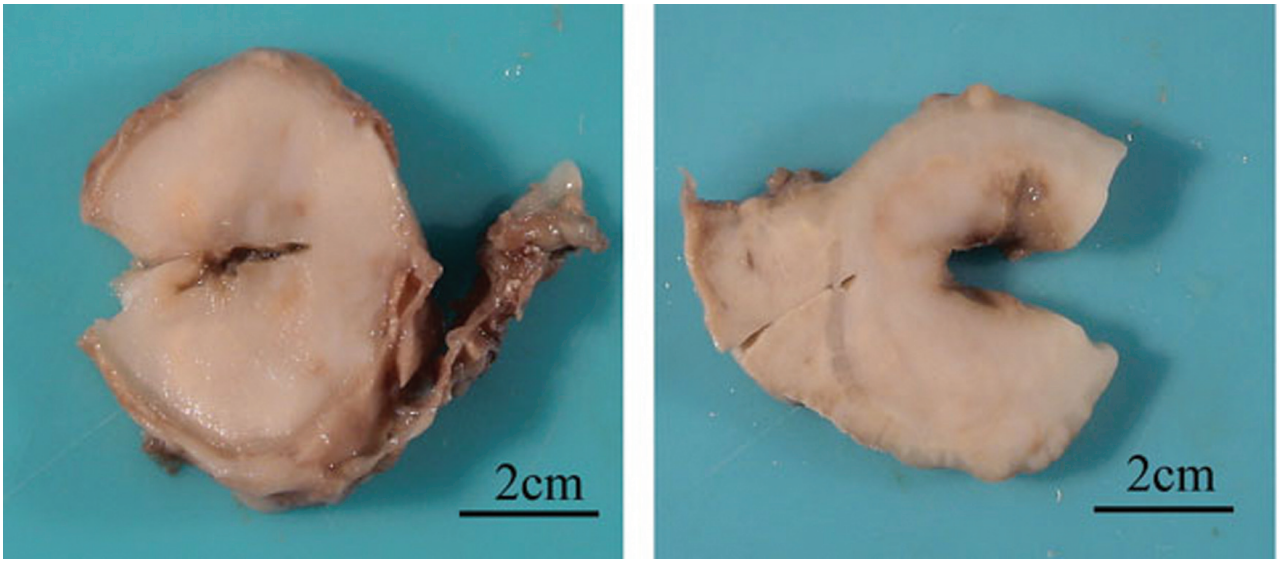

2-1. Jejunum, cat. There is marked transmural expansion by a firm, homogenous tan mass with mucosal ulceration. Photograph courtesy of Colorado State University, Department of Microbiology, Immunology, Pathology, 1619 Campus Delivery, Fort Collins, CO 80523, Karen.Fox@colostate.edu.

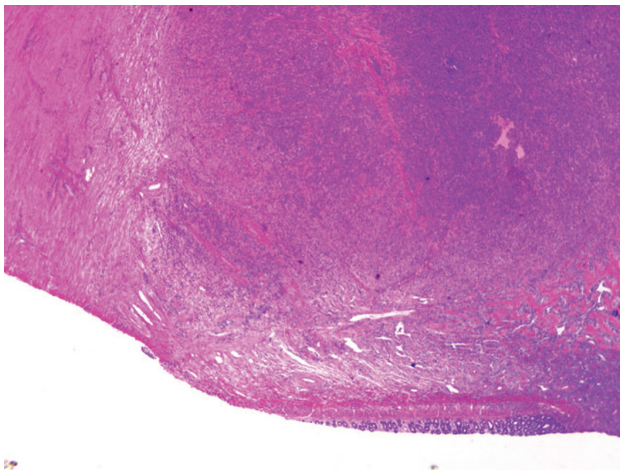

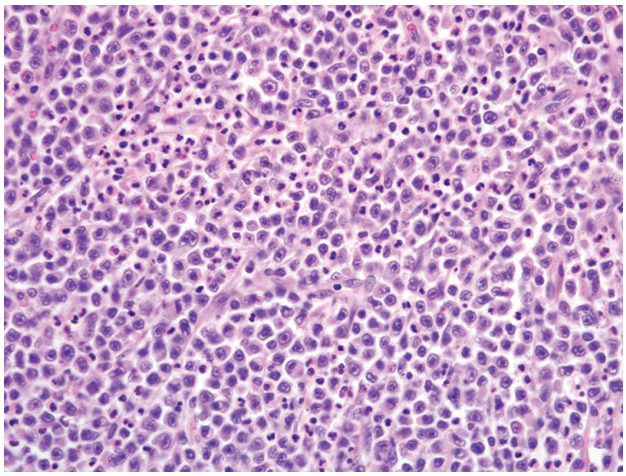

2-2, 2-3. Jejunum, cat. Infiltrating a focally extensive area of the submucosa and extending to the tunica muscularis is a moderately cellular, nodular proliferation of neoplastic round cells characterized by central nuclei, prominent nucleoli, moderate anisokaryosis, and a high mitotic rate. Fewer eosinophils are admixed with neoplastic cells. (HE 20X, HE 400X)

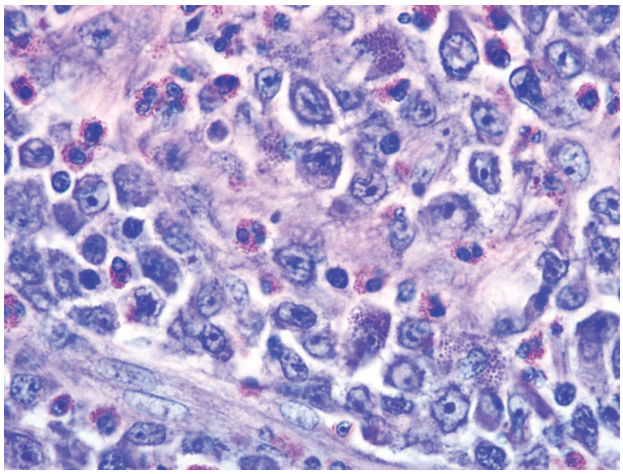

2-4. Jejunum, cat. Numerous non-neoplastic mast cells with metachromatic cytoplasmic granules are present within the nodular cellular proliferation. (Giemsa 1000X)

Howl and Petersen (1995) described a single case report of an intestinal mast cell tumor in a cat that presented with eosinophilic enteritis. In addition to the marked eosinophilic infiltrate, this case was characterized by a marked scirrhous response surrounding the neoplastic population similar to the case presented here.[6] This demonstrates the diagnostic challenge the eosinophilic infiltrate may introduce. Thus, when confronted with a significant eosinophilic intestinal population, close attention to all histological features is necessary in order to differentiate feline intestinal sclerosing mast cell tumors from other lesions such as eosinophilic granulomatous disease[6] and feline gastrointestinal eosinophilic sclerosing fibroplasia.[2] While the marked eosinophilic infiltrate in these tumors may pose a diagnostic challenge, the presence of eosinophils is not uncommon with mast cell disease. Mast cells promote eosinophilic inflammation by producing eosinophil-directed cytokines, such as IL-4 and IL-5. These cytokines subsequently induce chemokines that specifically attract eosinophils, such as eotaxin-1 and 2.[9] In addition, the mucosal ulceration may be due, in part, to local vasoconstriction in response to the release of vasoactive substances from the mast cells, such as histamine, and subsequent devitalization of the overlying mucosal epithelium as well as by direct infiltration and mucosal effacement by the neoplastic cells.

The sclerotic component was a unique feature in all cases evaluated. There is increasing evidence that mast cells play a central role in tissue remodeling in chronic inflammatory reactions. Among the numerous substances released by mast cell tumors are the fibrogenic cytokines fibroblast growth factor and transforming growth factor β1.[1,4] These cytokines promote activation, proliferation, and migration of fibroblasts with subsequent collagen production and contraction. In addition to mast cells, eosinophils have also been shown to play a role in fibrosis. Eosinophils are similarly involved in tissue remodeling and fibrosis in allergic reactions via the release of fibrogenic cytokines such as TGF-β and IL-1β.[2,4] The release of these fibrogenic cytokines by mast cells and/or eosinophils suggests a possible mechanism of mast cell-induced sclerosis in this tumor.

AFIP Diagnosis: 1. Jejunum: Malignant round cell neoplasm.

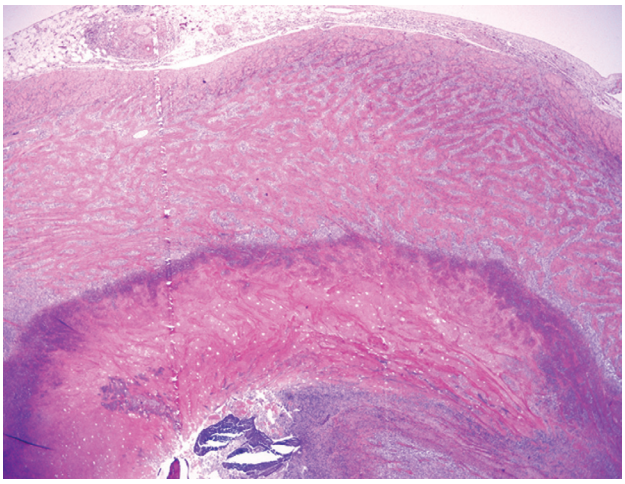

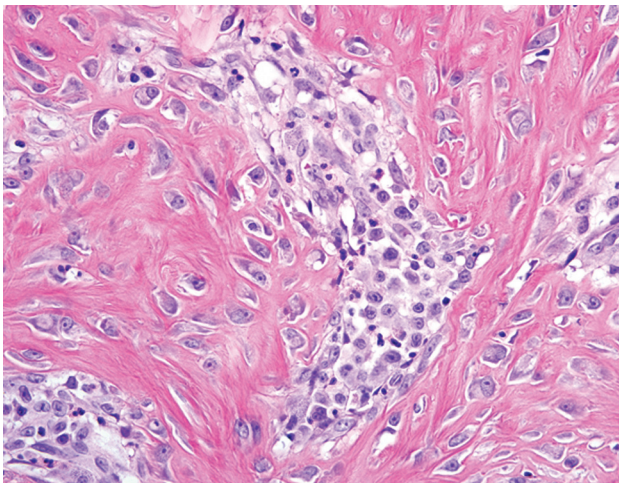

2-5, 2-6. Jejunum, cat. Multifocally within the submucosa and tunica muscularis are numerous evenly-spaced, anastomosing trabeculae of dense fibrous connective tissue interspersed with a moderate cellular infiltrate. Trabeculae of fibrous connective tissue are surrounded by reactive fibroblasts. The cellular infiltrate is composed of numerous non-neoplastic mast cells, macrophages, and fewer eosinophils. (HE 20X, HE 400X)

2. Jejunum: Enteritis, ulcerative, eosinophilic and mastocytic, sclerosing, transmural, severe, with mixed bacteria and anisotropic foreign material.

Conference Comment: This very intriguing case stimulated a vibrant discussion during the conference. While conference participants carefully considered the contributor's diagnosis of mast cell tumor, most participants favored the less specific diagnosis of malignant round cell neoplasm (**figs. 2-2 and 2-3**). Further, most participants considered the malignant neoplasm to be a separate, albeit possibly related, lesion from the eosinophilic and sclerosing fibroplasia. At the AFIP, additional histochemical and immunohistochemical stains did not further elucidate the histogenesis of the neoplasm. The Giemsa and toluidine blue histochemical stains demonstrated numerous metachromatic cytoplasmic granules within many mast cells throughout the areas of sclerosis in the section (**fig. 2-4**); the mast cells were interpreted as non-neoplastic, as they lack features of malignancy and are relatively evenly spaced within bands of collagen and fibroblasts (**figs. 2-5, 2-6, and 2-7**). Furthermore, metachromatic granules were not demonstrable in the population interpreted as neoplastic cells, i.e. the sheets of monomorphic round cells with atypia and increased mitotic rate. Immunohistochemical staining with CD117a (c-kit) was noncontributory. While poorly-differentiated mast cell tumor with lack of typical cytoplasmic granules remains a possibility, many participants considered lymphoma in the differential diagnosis and attributed the prominent eosinophilic infiltrate secondary to cytokines released by neoplastic lymphocytes. Immunohistochemical staining with CD3 and CD79a revealed moderate numbers of intralesional T- and B-lymphocytes, respectively; however, the overtly neoplastic cells were negative for these markers. Based on histomorphology, and histochemical and immunohistochemical findings, participants ultimately favored the histologic diagnoses indicated above. This case demonstrates the diagnostic difficulties sometimes encountered when attempting to determine the histogenesis of poorly differentiated tumors.

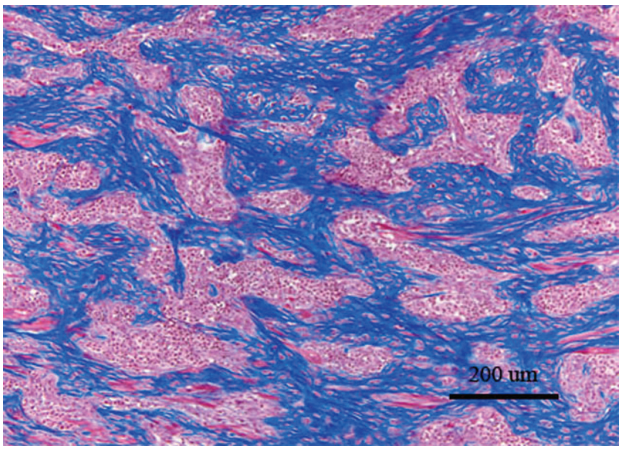

2-7. Jejunum, cat. Masson's trichrome is staining stromal collagen (sclerosis) blue and cytoplasm red. Photomicrograph courtesy of Colorado State University, Department of Microbiology, Immunology, Pathology, 1619 Campus Delivery, Fort Collins, CO 80523, Karen.Fox@

The eosinophilic and sclerotic lesion in this case is remarkable, and the contributor offers a sound hypothesis

for its pathogenesis. In a recent case series involving 25 cats, Craig and co-authors[2] proposed the term "feline gastrointestinal eosinophilic sclerosing fibroplasia" for a distinctive gastrointestinal lesion characterized by the mural presence of thick trabeculae of collagen separated by dense aggregates spindled cells. As in the present case, eosinophils and mast cells were numerous, and evenly scattered throughout the lesion. Immunohistochemical positivity for vimentin and smooth muscle actin was consistent with myofibroblastic differentiation and the authors speculated that bacteria were important in the pathogenesis of this condition. Additionally, the authors hypothesized that some cats may have a genetic predisposition to the development of this lesion, as has been proposed for other feline eosinophilic inflammatory conditions, in response to a variety of antigens. As a result, eosinophilic sclerosing fibroplasia may be thought of as a nonspecific reaction pattern to foreign antigen in genetically susceptible cats. In this case, the round cell neoplasm may have incited eosinophilic sclerosing fibroplasia by a number of mechanisms. Neoplastic cells, regardless of origin, may have directly recruited eosinophils and fibroblasts through cytokine production as hypothesized by the contributor. Alternatively, the neoplasm may have rendered the intestine vulnerable to antigen exposure by causing ulceration, partial obstruction, or altered peristalsis, allowing bacteria and digesta to penetrate the mucosa. This is supported by the presence of ulceration, numerous mixed bacteria, and embedded anisotropic foreign material (i.e. hair and food material) in many of the sections. We thank the contributor for this interesting submission.

Contributor: Colorado State University, College of Veterinary Medicine and Biomedical Sciences, Department of Microbiology, Immunology, Pathology, 1619 Campus Delivery, Fort Collins, CO 80523
http://www.cvmbs.colostate.edu/mip/

References:

1. Batlle M, Pérez-Villa F, Lázaro A, Garcia-Pras E, Ramirez J, Ortiz J, Orús J, Roqué M, Heras M, Roig E: Correlation between mast cell density and myocardial fibrosis in congestive heart failure patients. Transplantation Proc **39:**2347-2349, 2007
2. Craig LE, Hardam EE, Hertzke DM, Flatland B, Rohrbach BW, Moore RR: Feline gastrointestinal eosinophilic sclerosing fibroplasia. Vet Pathol **46:**63-70, 2009
3. Fernandez NJ, West KH, Jackson ML, Kidney BA: Immunohistochemical and histochemical stains for differentiating canine cutaneous round cell tumors. Vet Pathol **42:**437-435, 2005
4. Gomes I, Mathur SK, Espenshade BM, Mori Y, Varga J, Ackerman SJ: Eosinophil-fibroblast interactions induce fibroblast IL-6 secretion and extracellular matrix gene expression: implications in fibrogenesis. J Allergy Clin Immuno **116:**796-804, 2005
5. Gross TL, Ihrke PJ, Walder EJ, Affolter VK: Feline mast cell tumors. *In:* Skin Diseases of the Dog and Cat, 2nd ed., pp. 858-861. Blackwell PublishingAmes, IA, 2005
6. Howl JH, Petersen MG: Intestinal mast cell tumor in a cat: presentation as eosinophilic enteritis. J Am Anim Hosp Assoc **31:**457-461, 1995
7. Johnson TO, Schulman FY, Lipscomb TP, Yantis LD: Histopathology and biological behavior of pleomorphic cutaneous mast cell tumors in fifteen cats. Vet Pathol **39:**452-457, 2002
8. Litster AL, Sorenmo KU: Characterisation of the signalment, clinical and survival characteristics of 41 cats with mast cell neoplasia. J Fel Med Surg **8:**177-183, 2006
9. Shakoory B, Fitzgerald SM, Lee SA, Chi DS, Krishnaswamy G: The role of human mast cell-derived cytokines in eosinophil biology. J Inter Cyto Res **24:**271-281, 2004
10. Thamm DH, Vail DM: Mast cell tumors. *In:* Withrow and MacEwan's Small Animal Clinical Oncology, eds. Withrow SJ, Vait DM, 4th ed., pp. 402-424. Saunders Elsevier, St. Louis,MO, 2007

CASE III: 09RD990 (AFIP 3134608).

Signalment: 3-year-old spayed, female domestic shorthair cat (*Felis catus*).

History: The cat presented to a veterinary ophthalmologist 4 months prior to enucleation with an intraocular mass that involved approximately 25% of the ventral iris, extending from 4 o'clock to 7 o'clock. At the time of enucleation, the mass filled approximately 85% of the anterior chamber. There was no history of glaucoma.

Gross Pathology: Grossly, approximately 75% of the iris and anterior chamber are obliterated by a multinodular mass (**fig. 3-1**). On cut section, a solid white to tan mass bulges into the anterior chamber, fills the posterior chamber, and protrudes into the anterior vitreal space (**fig. 3-2**). The lens is displaced peripherally by the mass. Part of the retina is wrinkled and separated from the choroid with a translucent, gelatinous exudate in the subretinal space.

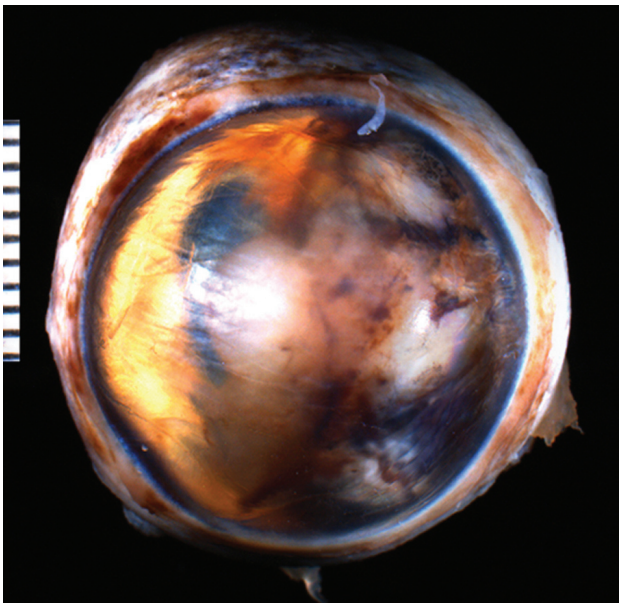

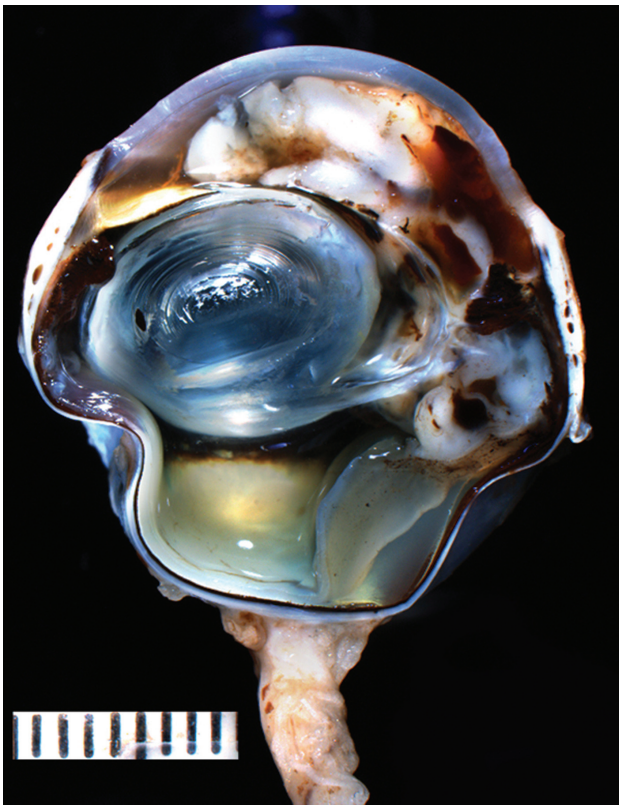

3-1, 3-2. Eye, cat, iridociliary adenoma. Photographs courtesy of Department of Pathobiological Sciences, School of Veterinary Medicine, University of Wisconsin-Madison, 2015 Linden Drive, Madison, WI 53701-1102, dubielzr@svm.vetmed.wisc.edu.

Histopathologic Description: Microscopically, there is a cross-section of globe with a mass that is broadly adherent to and continuous with the nonpigmented ciliary body epithelium and effaces the stroma of the iris leaflet and fills the iridocorneal angle (**fig. 3-3**). The mass is composed of tightly packed sheets or compressed cords of uniform polygonal cells with indistinct borders and scant cytoplasm, supported by a very fine vascular stroma. Neoplastic cells occasionally form rosettes and pseudorosettes (**figs. 3-4 and 3-5**). Nuclei are round to oval with a granular chromatin pattern and occasional single central nucleolus. There is moderate anisokaryosis and mitotic figures are rare (1 seen in ten 400x fields). There are several variably-sized cavitated spaces throughout the mass that contain blood and/or serum protein. At the periphery of the mass adjacent to the ciliary body, there is a rim of homogenous eosinophilic material that histologically resembles osteoid. The superior iridocorneal angle shows an open cleft and intact corneoscleral trabecular meshwork. The non-pigment ciliary body epithelium of the pars plana is expanded by multiple variably sized cysts. At the lens equator nearest to and presumed to have been in contact with the mass, there is degeneration and dissolution of the lens cortex characterized by spherical to irregularly-shaped eosinophilic aggregates of lens protein (Morgagnian globules), some of which contain a nucleus (bladder cells). The lens epithelium extends across the posterior aspect of the lens (subcapsular cataract). On the ventral aspect of the cornea, the mass abuts Descemet's membrane, the endothelium is unapparent and there is mild neovascularization of the superficial corneal stroma. Segmentally within the inferior retina, there is hypertrophy of the retinal pigment epithelium and retinal detachment with serum protein in the subretinal space. Ganglion cells are present in adequate numbers throughout the retina. Equivocally, there are increased numbers of glial cells within the substance of the optic nerve immediately posterior to the lamina cribrosa. An alcian blue periodic acid-Schiff (PAS) stain reveals a complex network of delicate PAS positive basement membranes surrounding individual or groups of neoplastic cells (**fig. 3-6**). Multifocally, both near and distant from the tumor, there is strandy to glassy Alcian blue positive material coating the inner aspect of the nonpigmented ciliary body epithelium (acid mucopolysaccharide secretion).

Contributor's Morphologic Diagnosis: 1. Feline iridociliary adenoma
2. Equatorial cortical cataract
3. Segmental retinal detachment
4. Epithelial cysts of the pars plana

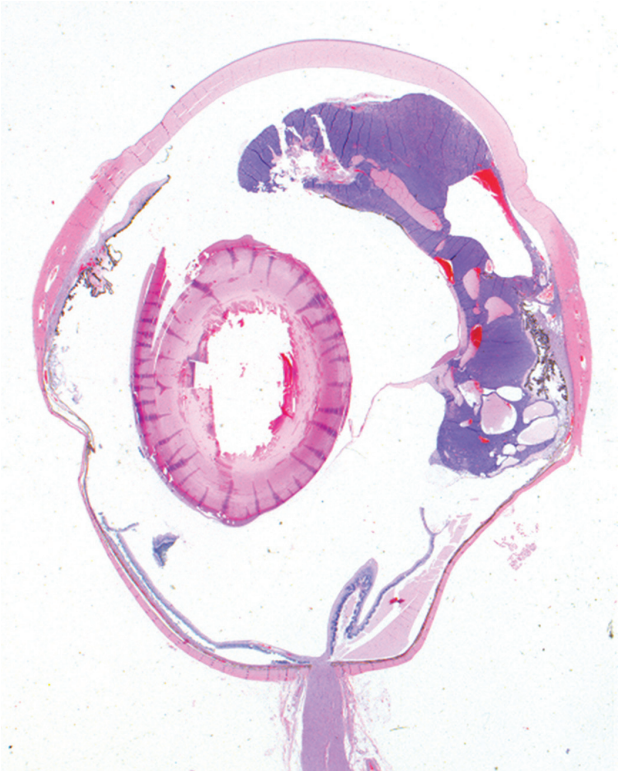

3-3. Eye, cat, iridociliary adenoma. A highly cellular mass effaces a portion of the anterior uveal tract and is composed of sheets of small, uniform epithelial cells with several cavitated spaces variably filled with blood or serum protein. There is a focal area of retinal detachment with a protein exudate in the subretinal space. Photomicrograph courtesy of Department of Pathobiological Sciences, School of veterinary medicine, University of Wisconsin-Madison, 2015 Linden Drive, Madison, WI 53701-1102, dubielzr@svm.vetmed.wisc.edu.

Contributor's Comment: In the slides submitted, the lens was removed for processing. This case was chosen because it represents the classic features of feline iridociliary adenoma.

The epithelium of the iris and ciliary body is derived from the neuroectoderm by expanding forward from the margins of the optic cup.[2] Neoplasia of the neuroectoderm of animals is considered uncommon (iridociliary adenomas and carcinomas) or rare (medulloepitheliomas, retinoblastomas, astrocytomas and gliomas).[3,4] With the exception of ciliary adenocarcinomas, these neoplasms are considered benign.[3] Iridociliary epithelial tumors are the second and third most common primary intraocular tumor in the dog and cat, respectively.[1] They arise from the pigmented or non-pigmented epithelial cells, usually from the *pars plicata* of the ciliary body.[1]

Clinically, these tumors usually present as white to brown or black, fairly well delineated, sometimes pedunculated, slow growing masses, that usually grow into the vitreous behind the lens.[4] They are usually visible through the pupil in the posterior chamber. Invasion through the iris or protrusion through the pupil can lead to a localized mass visible in the anterior chamber.[3] Clinical signs usually include a retro-iridal mass that may displace the iris or lens by expansive growth, and if the tumor is large, secondary glaucoma, ocular pain and/or intraocular hemorrhage may be noted.[4] Hyphema and aqueous flare may be present due to the common formation of preiridal fibrovascular membranes.[3] In cases where the intraocular hemorrhage and flare impair the direct observation of the tumor, ultrasonographic imaging may prove helpful in delineating a mass lesion in the posterior chamber.[1]

Histologic features of feline iridociliary adenomas include a solid non-pigmented epithelial tumor with packets of cells surrounded by thin PAS positive basement membrane structures.[2] The defining feature of adenocarcinoma, versus adenoma, is invasion into the sclera by the neoplastic population rather than features of cellular atypia.[2] Thus, most iridociliary adenocarcinomas in both cats and dogs have relatively benign cellular features.

A retrospective study of 101 cases of feline iridociliary tumors conducted in the Comparative Ocular Pathology Laboratory of Wisconsin (COPLOW) (unpublished data) identified other common features of these tumors. Of the 101 cases, 84 (83.1%) of the tumors were classified as adenomas. Seventeen (16.9%) presented scleral or choroidal invasion and were classified as adenocarcinomas. Adenomas presented a solid pattern in 97.6% (82/84) of the cases. They were either classified as uveoinvasive (52.3%) and non-uveoinvasive (47.7%). The most common histological features of adenomas were PAS positive basement membranes (present in 82.3% of the cases), cavitated spaces filled with blood and/or proteinaceous material (77.3%), presence of osteoid matrix (42.8%), osseous metaplasia (12%), and formation of pseudo-rosettes (26.2%). Mitotic figures were rare in both adenomas and adenocarcinomas. Two cases of iridociliary adenomas presented atypical patterns, one papillary and the other a mucoid variant that presents PAS positive basement membrane and positivity for vimentin and cytokeratin. Most tumors were positive for vimentin and only carcinomas presented variable positivity for cytokeratin. A previous study demonstrated that 50% of feline and canine iridociliary adenomas were positive for S-100, 1/3 of the feline cases were positive for glial fibrillary acidic protein (GFAP) and all canine cases were positive for neuron-specific enolase (NSE).[2]

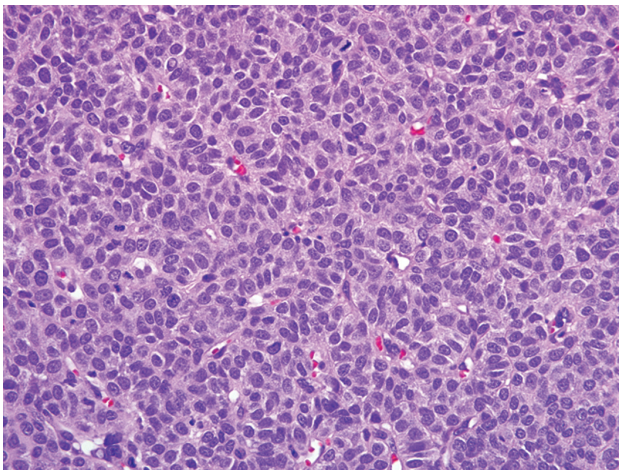

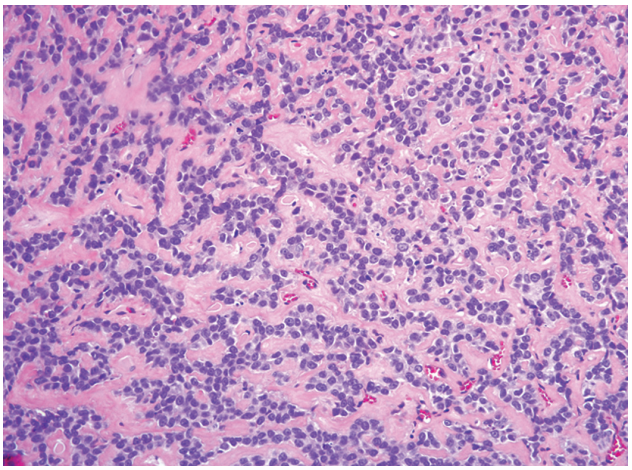

3-4, 3-5. Eye, cat, iridociliary adenoma. Markedly expanding the iris and ciliary body is a densely cellular neoplasm arranged in pseudorosettes, cords and tubules. (HE 400X)

In the recent unpublished study, the age of the animals ranged from 2 to 18 years (average 9.1). The most common secondary abnormalities detected were glaucoma, preiridal fibrovascular membrane, hyphema and retinal detachment. Presence of an intraocular mass was the main reason for presentation to the veterinarian and enucleation. Glaucoma is a common secondary condition associated with iridociliary tumors, in part because these tumors are associated with the formation of fibrovascular membranes that can lead to peripheral anterior synechia and obstruction of the iridocorneal angle.[1]

In the case presented, the evidence of glaucoma is equivocal. The most reliable microscopic evidence of glaucoma is absence or reduced numbers of retinal ganglion cells. In cats, even cases of chronic glaucoma can show an otherwise robust retina that lacks ganglion cells. In contrast, the glaucomatous canine globe frequently shows atrophy of the inner retinal layers to full-thickness atrophy in chronic cases. Gliosis of the optic nerve is also reliable evidence of glaucoma. Atrophy of the optic nerve with cupping of the optic nerve head is also common, particularly in dogs. Finally, a feature of glaucoma seen characteristically in dogs with primary glaucoma (goniodysgenesis) is "tapetal sparing" in which the tapetal (superior) retina is less profoundly atrophied than the non-tapetal (inferior) retina. Presence of epithelial cysts of the pars plana is a common finding in older cats and presumed to be a degenerative condition not related to the tumor in this case.

In sum, solid nonpigmented tumors arising from the ciliary body or iris epithelium with small epithelial cells packed by thin PAS-positive membranes and staining positive for vimentin are significant features defining iridociliary tumors in cats.

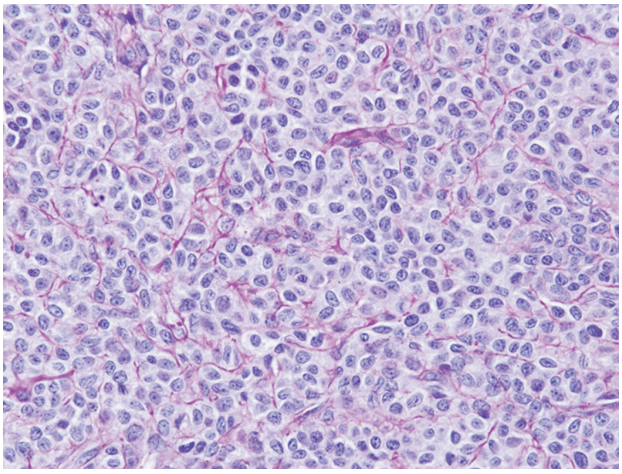

3-6. Eye, cat, iridociliary adenoma. PAS-positive basement membranes surround individual or clusters of neoplastic epithelial cells. (Alcian blue-PAS 200X) Photomicrograph courtesy of Department of Pathobiological Sciences, School of veterinary medicine, University of Wisconsin-Madison, 2015 Linden Drive, Madison, WI 53701-1102, dubielzr@svm.vetmed.wisc.edu.

AFIP Diagnosis: 1. Eye: Iridociliary adenoma.
2. Eye, retina: Detachment, segmental.

Conference Comment: We thank the contributor for providing this excellent example and thorough analysis of the entity. Conference participants discussed the microscopic features that distinguish iridociliary adenoma from adenocarcinoma, with emphasis on scleral invasion as an important feature of the latter, as the contributor

noted. While metastasis of iridociliary adenocarcinoma is extremely rare, it has been reported in dogs.[5] Normal iridociliary epithelium and adenomas express vimentin, but not cytokeratin, while adenocarcinomas may express both vimentin and cytokeratin AE1/AE3.[2,5]

Contributor: Department of Pathobiological Sciences, School of Veterinary Medicine, University of Wisconsin-Madison, 2015 Linden Drive, Madison, WI 53701 http://www.vetmed.wisc.edu/home

References:

1. Dubielzig RR: Tumors of the eye. *In:* Tumors in Domestic Animals, ed. Meuten DJ, 4th ed., pp. 739-754. Iowa State Press, Ames, IA, 2002
2. Dubielzig RR, Steinberg H, Garvin H, Deehr AJ, Fisher B: Iridociliary epithelial tumors in 100 dogs and 17 cats: a morphological study. Vet Ophthalmol **1:**223-231, 1998
3. Grahn BH, Peiffer RL: Fundamentals of veterinary ophthalmic pathology. *In:* Veterinary Ophthalmology, ed. Gellat KN, 4th ed., pp. 355-437. Blackwell Publishing, Ames, IA, 2007
4. Miller PE, Dubielzig RR: Ocular tumors. *In:* Withrow and McEwen's Small Animal Clinical Oncology, ed. Withrow SJ, Vail, DM, 4th ed., pp. 686-698. Elsevier, St. Louis, MO, 2007
5. Zarfoss MK, Dubielzig RR: Metastatic iridociliary adenocarcinoma in a Labrador retriever. Vet Pathol **44**:672-676, 2007

CASE IV: 09H2862 (AFIP 3134618).

Signalment: 7-year-old castrated, male paint horse (*Equus caballus*).

History: Small, non-visual left eye for the past one year; clinically suspected chronic uveitis. The right eye was normal.

Gross Pathology: Globe was somewhat small with a cloudy cornea.

Histopathologic Description: Eyeball (a-d): The cornea contains a modest amount of neovasculature within the superficial third of the stroma. The anterior chamber is filled with eosinophilic flocculent material (serous exudate). The iris is greatly thickened and distorted; it contains a marked perivascular to diffuse infiltrate of plasma cells and lymphocytes (**fig. 4-1**). In addition, the anterior and posterior surfaces are covered with a layer of fibrovascular tissue (preiridial fibrovascular membrane) and adherent plasma cells and lymphocytes, which spans the pupil and is adhered to the anterior lens capsule (posterior synechia). The filtration angle is variably collapsed and the ciliary cleft contains a moderate accumulation of lymphocytes, plasma cells, and melanophages. The ciliary body is distorted and contains an infiltrate similar to the iris; in addition, it contains scattered follicular aggregates of lymphocytes and plasma cells. Also, the neuroepithelium of the ciliary body is covered by a thick layer of homogeneous eosinophilic, congophilic material that has a somewhat ragged surface; this material has green birefringence with polarized light (**figs. 4-2 and 4-3**). There is a layer of fibrillar fibrous material extending from the surface of the ciliary body along the surface of the posterior lens capsule (cyclitic membrane). The choroid is diffusely congested and contains a few scattered aggregates of lymphocytes and plasma cells. The retina is detached in several places and the subretinal space contains eosinophilic flocculent material and a few melanophages. The retinal pigment epithelium is hypertrophied in the corresponding detached areas. The nontapetal retina is thin due to a thinned nerve fiber layer, thinned inner and outer plexiform layers, a diminished number of ganglion cells, and a hypocellular inner nuclear layer, which somewhat blends into the outer nuclear layer. Ganglion cells that are present have central chromatolysis. The photoreceptors are evident but blunted. There are a few folds in the retina. The tapetal retina is more nearly normal. The lens capsule is ruptured in several foci, especially on the anterior surface adjacent

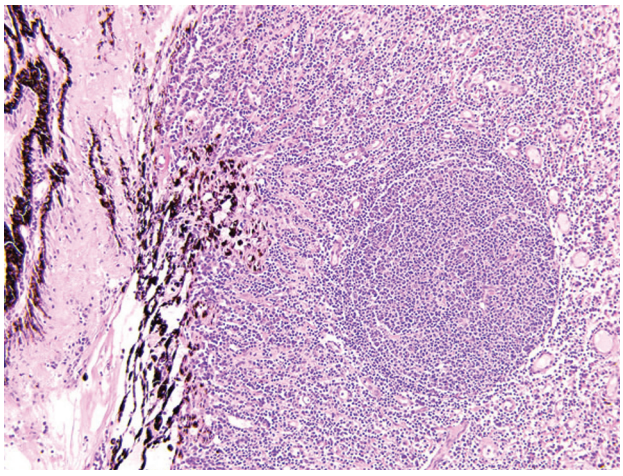

4-1. Eye, horse. Multifocally expanding the iris are nodular cellular infiltrates composed of lymphocytes and plasma cells. (HE 100X)

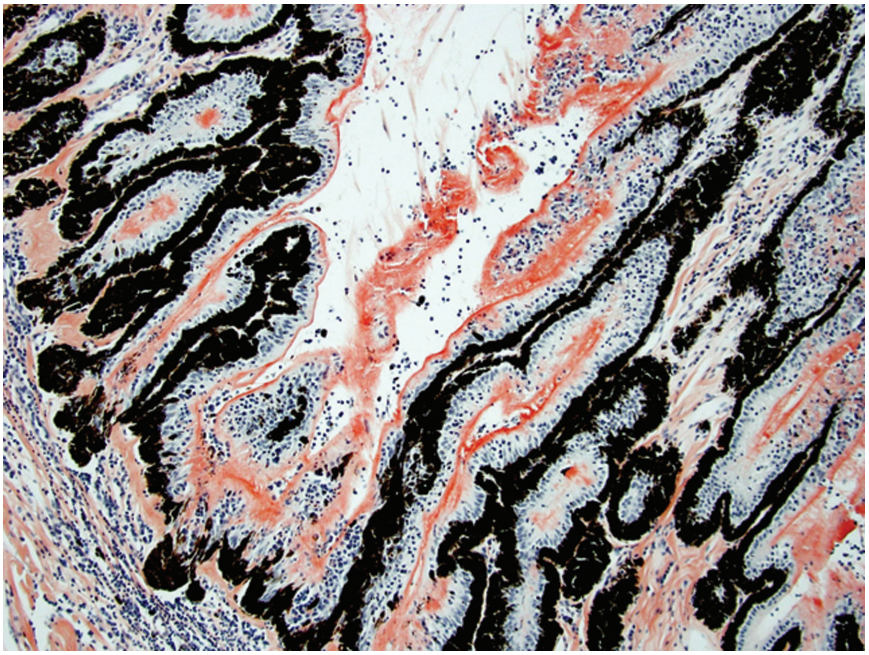

4-2. Eye, horse. Neuroepithelium of the ciliary body is covered by a thick layer of homogeneous eosinophilic amyloid-like material. (Congo red 100X) Photomicrograph courtesy of Department of Veterinary Pathology, Iowa State University, Ames, IA 50011, rkmyers@iastate.edu

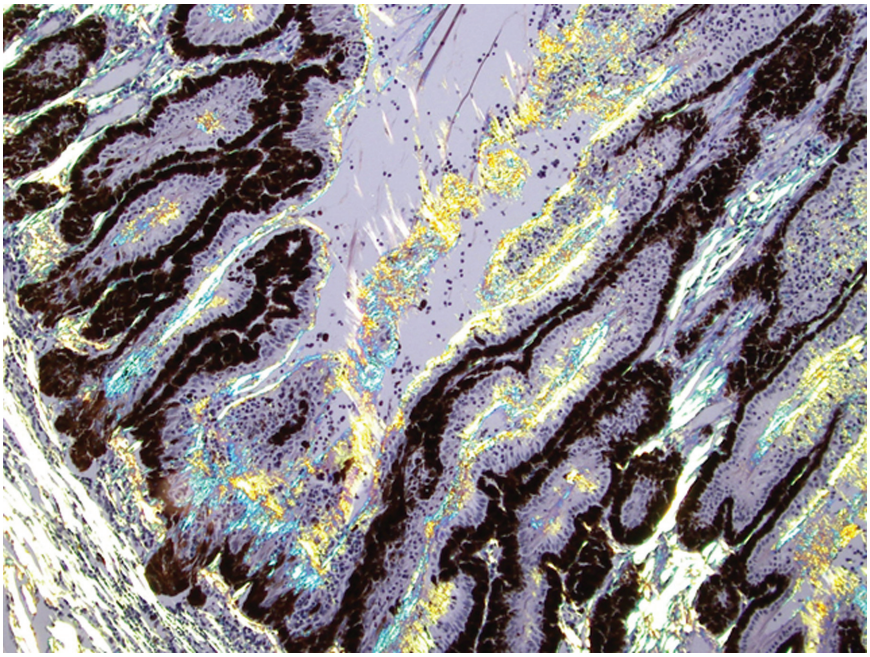

4-3. Eye, horse. Homogeneous eosinophilic amyloid-like material, congo red positive material has green birefringence with polarized light. (Congo red, polarized, 100X) Photomicrograph courtesy of Department of Veterinary Pathology, Iowa State University, Ames, IA 50011, rkmyers@iastate.edu

to the posterior synechiae. In these areas, the anterior cortical lens fibers are swollen, fragmented and some have undergone fibrous metaplasia, which has produced a thick fibrous layer that covers the inner surface of the anterior lens capsule. The vitreous body has deteriorated and the vitreous chamber is filled with eosinophilic flocculent material (plasmoid vitreous). The bulbar conjunctiva at the limbus contains a marked follicular infiltrate of lymphocytes and plasma cells.

Contributor's Morphologic Diagnosis: Eyeball: Chronic lymphoplasmacytic uveitis (especially anterior uveitis) with posterior synechiae, partial filtration angle closure, cortical cataract with capsule rupture and fibrous metaplasia, retinal detachment and retinal degeneration, non-tapetal retina.

Contributor's Comment: This eye has chronic lymphoplasmacytic uveitis (especially anterior uveitis)

with many secondary changes that include posterior synechiae, partial filtration angle closure, cortical cataract, retinal detachment and retinal degeneration. The pattern of the uveitis with the accumulation of congophilic material (amyloid) on the ciliary body is typical of equine recurrent uveitis (ERU). ERU is a fairly common form of uveitis in horses; apparently there is breed predisposition, with Appaloosas being very susceptible and, when affected, having bilateral involvement about 80% of the time. Some aspects of the cause and pathogenesis are not clear, but the consensus seems to be that the uveitis develops due to an autoimmune reaction. The prevailing theory is that certain bacterial antigens, most notably those on certain serovars of *Leptospira interrogans* (especially *L. pomona*) are similar to intrinsic antigens in the uvea, and that the immune response generated against the bacterial antigens cross-reacts with the uveal antigens resulting in autoimmune mediated inflammation.[1] The retinal degeneration has a pattern that is consistent with secondary glaucoma (non-tapetal involvement) but also could have been caused by ocular hypertension, a condition that often accompanies ERU.[1]

AFIP Diagnosis: Eye: Endophthalmitis, lympho–plasmacytic, chronic, diffuse, mild to moderate, with posterior synechia, pre-iridial fibrovascular membrane, post-iridial amyloid-like material, retinal detachment and atrophy, peripheral corneal neovascularization, and cataractous change.

Conference Comment: Equine recurrent uveitis (ERU) is one of several immune-mediated endophthalmitides of veterinary importance; others include canine uveodermatologic syndrome, canine lymphocytic uveitis, feline idiopathic lymphonodular uveitis, and lens-induced uveitis. Because ERU is a progressive disease, a wide range of potential microscopic findings, from uveitis to endophthalmitis to phthisis bulbi, exists.[2] This case nicely illustrates several of the characteristic features of ERU, including the hallmark lesion, deposition of hyalinized congophilic (i.e. amyloid-like) material in the apical cytoplasm of the posterior iridociliary epithelium.[2] The presence of numerous additional pathologic findings makes for a very descriptively challenging slide. The retinal lesions, as suggested by the contributor, may be the result of secondary glaucoma; however, glaucoma is a rare complication of ERU, and it is thought that the trabecular meshwork is less important than uveoscleral resorption for aqueous drainage in horses, in contrast to the mechanism of aqueous outflow in dogs and cats.[1,2] Some researchers suggest that a retinopathy may be the primary immunological event in equine uveitis and that interphotoreceptor retinoid-binding protein (IRBP) is the major autoantigen in ERU. This autoantigen, along with others, may be unmasked by a variety of intraocular inflammatory events leading to a common final pathway that is characteristic of ERU. Alternatively, as alluded to by the contributor, the mimicry of autoantigens by infectious agents is a popular hypothesis; a 90-kd protein common to several serovars of *Leptospira interrogans* shares epitopes with an equine corneal peptide, lending credence to this hypothesis.[1]

The pathogenesis of immune-mediated endophthalmitis is complex and its discussion is enhanced by a rudimentary understanding of a recently-discovered, carefully-regulated system of ocular immunity called anterior chamber-associated immune deviation (ACAID). Briefly, ACAID is a series of responses to intraocular antigen that ultimately results in impaired delayed-type hypersensitivity (DTH) expression and suppressed complement-fixing antibody production without suppressing antigen-specific cytotoxic T cell activity. As a result, "innocent bystander" intraocular tissues are spared collateral damage from T cell-driven inflammation.[1] More specifically, a number of cytokines, e.g. TGF-β2, TNF-α, vasoactive intestinal peptide, and substance P, alter intraocular antigens, which are then processed by resident antigen presenting cells (APCs), i.e. macrophages and dendritic cells, within the uvea. The APCs travel to the spleen where they promote the development of specific suppressor T-cells, which then return to the uvea and suppress DTH and complement-fixing antibody production, but not cytotoxic T cell activity. When this system is overwhelmed or impaired by uncontrolled introduction of antigen into the globe, perivascular aggregates of lymphocytes develop in the iris, ciliary body, choroid, and retina, and may eventually form vague lymphoid follicles. Amplification results in decreased specificity for the initial inciting antigen among the acquired lymphoid population and a stereotyped response to circulating antigens that enter the eye through a now-damaged blood-eye barrier.[2]

Taken together, the evidence suggests that ERU is multifactorial, as is the predisposition to its development. The contributor mentioned that Appaloosas are predisposed, with 80% of cases being bilateral. In contrast, only 20% of non-Appaloosas with ERU develop bilateral disease, and Appaloosas with light coats and many spots are more likely to develop ERU than are Appaloosas with dark coats and few spots, suggesting that melanin may be protective. In German Warmblood horses, the MHC I haplotype ELA-A9 is strongly associated with ERU, further supporting the hypothesis of a genetic predisposition.[1]

Contributor: Department of Veterinary Pathology, Iowa State University, Ames, IA 50011
http://vetmed.iastate.edu/

References:

1. Brooks DE, Matthews AG: Equine ophthalmology. *In:* Veterinary Ophthalmology, ed. Gellat KN, 4th ed., pp. 1239, 1244-1248. Blackwell Publishing, Ames, IA, 2007
2. Wilcock BP: Eye and ear. *In:* Jubb, Kennedy, and Palmer's Pathology of Domestic Animals, ed. Maxie MG, 5th ed., vol. 1, pp. 505-509. Elsevier Saunders, Philadelphia, PA, 2007

The Armed Forces Institute of Pathology
Department of Veterinary Pathology

Conference Coordinator:
Shannon Lacy, DVM, MPH

WEDNESDAY SLIDE CONFERENCE 2009-2010

Conference 7

28 October 2009

Conference Moderator:

Mark A. Bryant, DVM, Diplomate ACVP

CASE I: RAT (AFIP 3139909).

Signalment: Young, adult, female Sprague-Dawley rats (*Rattus norvegicus*).

History: At necropsy, multiple asymmetrical nodules were present in the uterine body of young adult female control rats.

Gross Pathology: Multiple asymmetrical nodules were present in the uterine body of several control rats. Nodules were submitted for microscopic examination as incidental lesions.

Histopathologic Description: In the mesometrial side of the uterus, there is an expansile, partially encapsulated nodular mass composed of three poorly defined zones or layers of pleomorphic cells asymmetrically centered on a dilated endometrial gland lumen (not visible in all sections). From the periphery of the nodule, just deep to capsule, the mesometrial zone is composed of an irregular, thin, poorly demarcated band of small spindle-shaped cells with poorly defined cell borders, finely vacuolated basophilic to amphophilic cytoplasm and small oval nuclei ("spiny" cells). Deep to the mesometrial zone, also on the mesometrial aspect of the uterine horn, there are clusters and nests of variably sized (approximately 30 to 50 um diameter) cells composing the transition zone characterized by more abundant coarse clear cytoplasmic vacuoles, round, finely vesicular nuclei and abundant basophilic to amphophilic cytoplasm ("glycogenic" area). Intermixed with the cells in this mesometrial zone, there are numerous larger cells containing coarse, deeply eosinophilic cytoplasmic granules (PAS not available). Deep to this zone, approaching the uterine lumen and partially surrounding the endometrial gland lumen, there are clusters of large (approximately 120 to 150 um), pleomorphic, coarsely vacuolated epithelioid giant cells containing coarsely vesicular chromatin in large oval nuclei with one to four variably shaped nucleoli and abundant coarsely granular amphophilic to basophilic cytoplasm (decidual cells). Deep to and partially surrounding these cells, there is an irregular layer of nests and clusters of small, occasionally multinucleate or binucleate cells with small, central, oval nuclei containing finely vesicular chromatin and a single small eccentric nucleolus (antimesometrial basal zone). The cells of the nodule are supported on a fine fibrovascular stroma (compressed endometrial stroma) with numerous small congested blood vessel profiles. There is erosion

***Sponsored by the American Veterinary Medical Association, the American College of Veterinary Pathologists, and the C. L. Davis Foundation.**

of the overlying endometrial surface, focally, with small numbers of degenerate neutrophils perivascularly and at the endometrial surface (not present in all sections).

Contributor's Morphologic Diagnosis: Uterus: Decidual alteration (deciduoma).

Contributor's Comment: Decidual alteration or reaction, also referred to as a deciduoma, is an infrequent, self-limiting, proliferative but not neoplastic entity in young adult female rats. Decidual alteration has been observed in the guinea pig, rabbit, mouse, dog, hamster and monkey.[4] The incidence of decidual alteration in this control group was unusual in our experience. Although slides and sections varied in submitted material, decidual alteration comprises a fairly structured architecture/organization, as described above. Elcock and co-authors, in *Monographs on Pathology of Laboratory Animals: Genital System* provide detailed histologic and ultrastructural descriptions of deciduoma/decidual alteration.[4]

Decidual alteration was referred to as deciduoma in earlier lab exploratory pathology literature because the lesion was originally regarded as neoplastic.[5] Instead, this is a proliferative, well organized structure that generally follows a predictable time-course. The alteration can be induced between days 3 and 4 of pseudopregnancy, and requires priming or sensitization of the uterus by progesterone for at least 48 hours, followed by minute amounts of estrogen.[4] Most often, this sequence of events is linked to the late luteal phase of the estrus cycle.[5,6] Decidual alteration in the rat has also been reported following various forms of mechanical irritation or trauma, electrical stimulation, intrauterine instillation of agents such as sesame oil, Hank's balanced salt solution, histamine, air, or prostaglandins, as well as administration of progestin, such as 19-norpregnane.[4,5] The alteration will generally undergo regression between days 12-16 (nodular form) and 21 (diffuse form) of pseudopregnancy, with necrosis and cleavage of the capsule from the underlying uterine wall.[4]

Decidual alteration occurs spontaneously in rats, usually at a low incidence (<1% over a 10 year period in one study).[4] The incidence in this group of young adult control rats was unusual in our experience. According to Elcock et al., vitamin E deficiency may be a contributing factor to increased spontaneous incidence of deciduoma, with 60% of rats fed vitamin E deficient diets developing spontaneous deciduoma compared with 4% on natural food.[4]

AFIP Diagnosis: Uterus: Exuberant myometrial and stromal decidualization with maternal and embryofetal placental structures.

Conference Comment: This edifying case elicited a vivacious discussion during the conference, and was therefore subsequently reviewed in consultation with several veterinary pathologists with special expertise in laboratory animal and/or reproductive pathology. While a unified consensus on the histogenesis of this incidental finding was not achieved, several possibilities were raised, with many suspecting a placental disk consistent with normal pregnancy. Deciduoma and pregnancy are mutually exclusive diagnoses; deciduoma accompanies pseudopregnancy as noted by the contributor, while myometrial and stromal decidualization is an expected physiologic response to normal pregnancy, and is accompanied by placental tissues of embryofetal origin. In many slides, a large proportion of the nodule consists of placental tissues not of maternal origin.

Although participants recognized exuberant decidualization in the mesometrial aspect of the uterus, characterized by the ubiquitous presence of large, pale, glycogen-rich decidual cells in the myometrium and stroma, many could not discern the six components of a classic deciduoma, i.e. metrial gland in the myometrium on the mesometrial side of the uterus, basal zone separating the deciduoma from the myometrium, a capsule just luminal to the basal zone, mesometrial and antimesometrial regions, and a "glycogenic" transitional area.[6] Rather, participants noted five distinct layers in the mesometrial aspect of the uterus that, collectively, are interpreted as structures of a placental disk (**fig. 1-1**). Notably, the characteristic layers are not described as part of a deciduoma. From adluminal to luminal, they are:

1. Decidualized myometrium: The mesometrial myometrium is composed of large decidual cells with abundant, slightly basophilic, vacuolated cytoplasm that often contains PAS-positive granules, round nuclei and one or two distinct nucleoli. Larger vessels within the decidualized myometrium are surrounded by numerous metrial cells, and the endothelium is often covered by large cytotrophoblasts (**fig. 1-2**).
2. Decidualized stromal layer: Separated from the decidualized myometrium by a discontinuous, indistinct, thin band of myometrial smooth muscle cells is a completely decidualized stromal layer; this layer is composed of decidual cells as described in the myometrium, with clear cytoplasmic vacuoles that become progressively prominent toward the luminal surface.
3. Giant cell layer: A layer of giant trophoblasts separates maternal-origin tissue (decidua) from embryofetal-origin tissue. Giant trophoblasts are

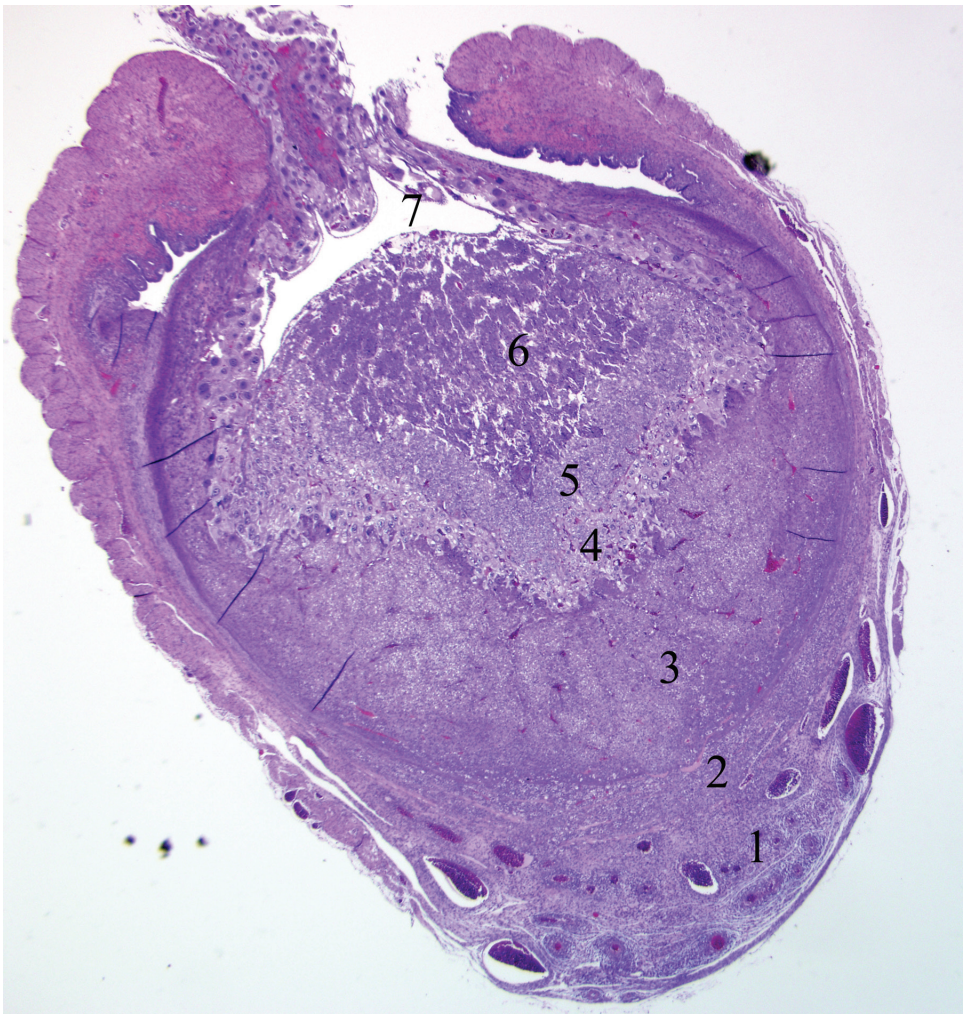

1-1. Uterus, rat. Distinct areas within the affected segment of uterus are evident. From anti-mesometrial to mesometrial, these are: Metrial gland (1), decidualized myometrium (2), stromal layer (3), layer of giant trophoblasts (4), trophospongium (5), labyrinth (6), and yolk sac (7). (HE 12.5X)

up to 150 um in diameter and have abundant, finely-granular, microvacuolated, pale basophilic cytoplasm that often contains distinct PAS-positive droplets. Nuclei are large and round to oval with finely-stippled or coarsely-clumped chromatin and contain one to ten distinct, variably-sized, irregularly-shaped nucleoli (**fig. 1-3**).

4. Trophospongium: Interposed between the giant cell layer and the labyrinth is a band of 20-40 um diameter polygonal cells with moderate amounts of basophilic, vacuolated cytoplasm containing numerous small, PAS-positive granules; these cells are often bi-nucleate with frequent mitoses. Groups of cells comprising this population are separated by fewer large (60-80 um diameter) syncytiotrophoblasts and small vascular lacunae containing mature erythrocytes.
5. Labyrinth: The luminal-most layer of the mesometrial side of the uterus is composed of trophoblasts arranged in trabeculae that separate large and small blood-filled lacunae. Trophoblasts contain moderate amounts of basophilic, microvacuolated cytoplasm, and are mitotically active. Larger lacunae contain mature erythrocytes (maternal circulation), while smaller lacunae contain only large, immature, nucleated erythrocytes with pale eosinophilic to basophilic cytoplasm (fetal circulation). Generally, maternal and fetal lacunae are separated by three layers of trophoblasts (hemotrichorial placentation) (**fig. 1-4**).

In the affected rats of this case the yolk sac placenta is present in the uterine lumen in most histologic sections, which consists of a single layer of plump, cuboidal, luminally-oriented cells resting on a 2-5 um thick, glassy, hyaline basement membrane (Reichert's membrane) (**fig. 1-5**). Employing the morphologic reference data set provided by de Rijk and colleagues[2] as a guide, the placental features described above are interpreted as consistent with a placenta at approximately day 12-14 of pregnancy. However, not all of these features are present on every section, and most slides have two sections,

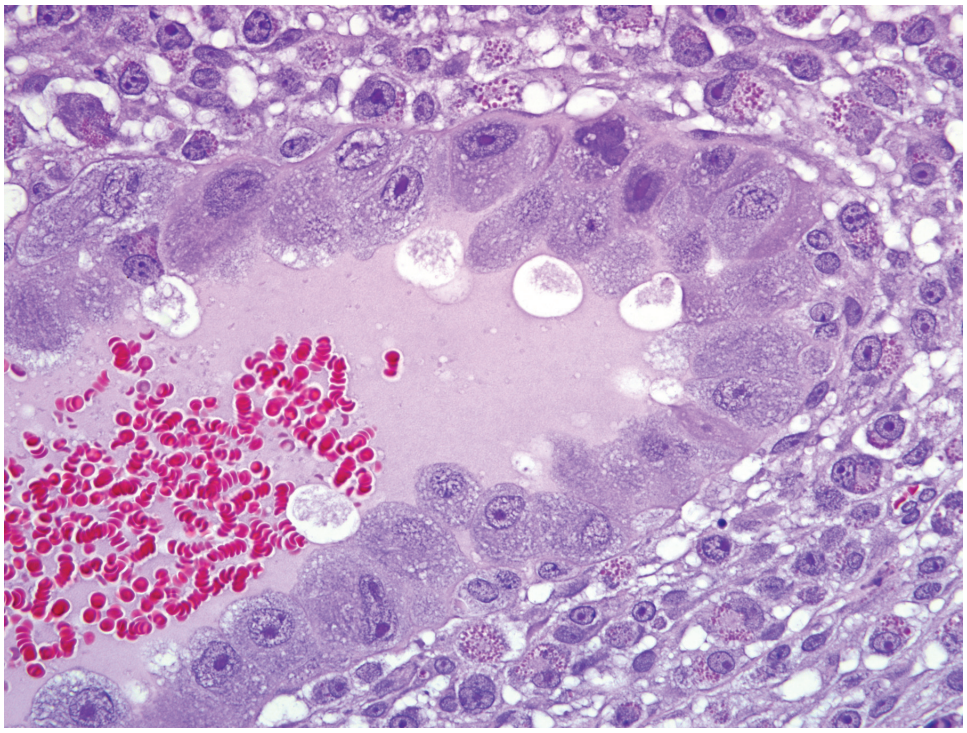

1-2. Uterus, rat. The endothelial cells of vessels within the myometrium are invested by trophoblasts. (HE 400X)

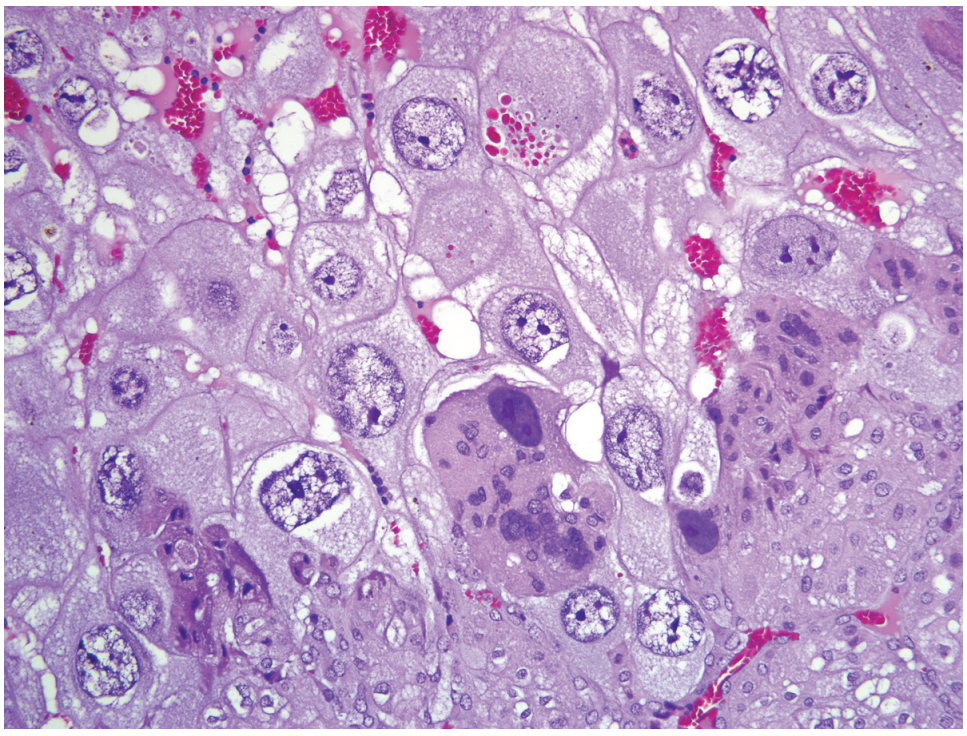

1-3. Uterus, rat. The layer of giant trophoblasts invades the decidualized stroma. (HE 400X)

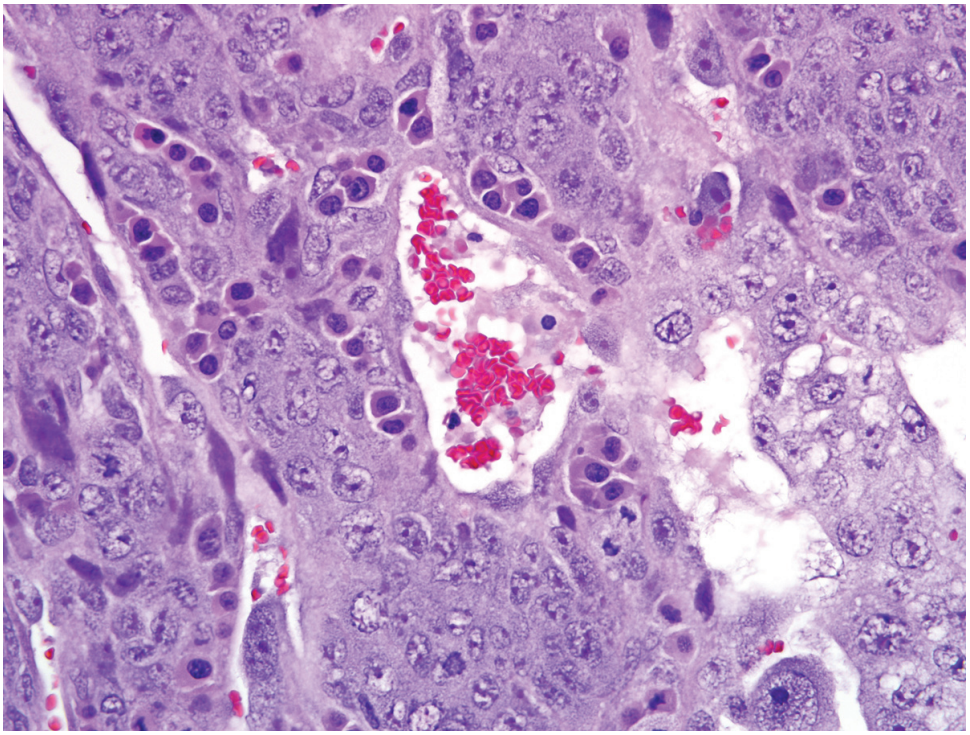

1-4. Uterus, rat. Within the labyrinth, there are large lacunae containing mature anucleate maternal erythrocytes that are separated from smaller lacunae by up to three layers of syncytiotrophoblasts; smaller lacunae contain more basophilic nucleated fetal erythrocytes. (HE 400X)

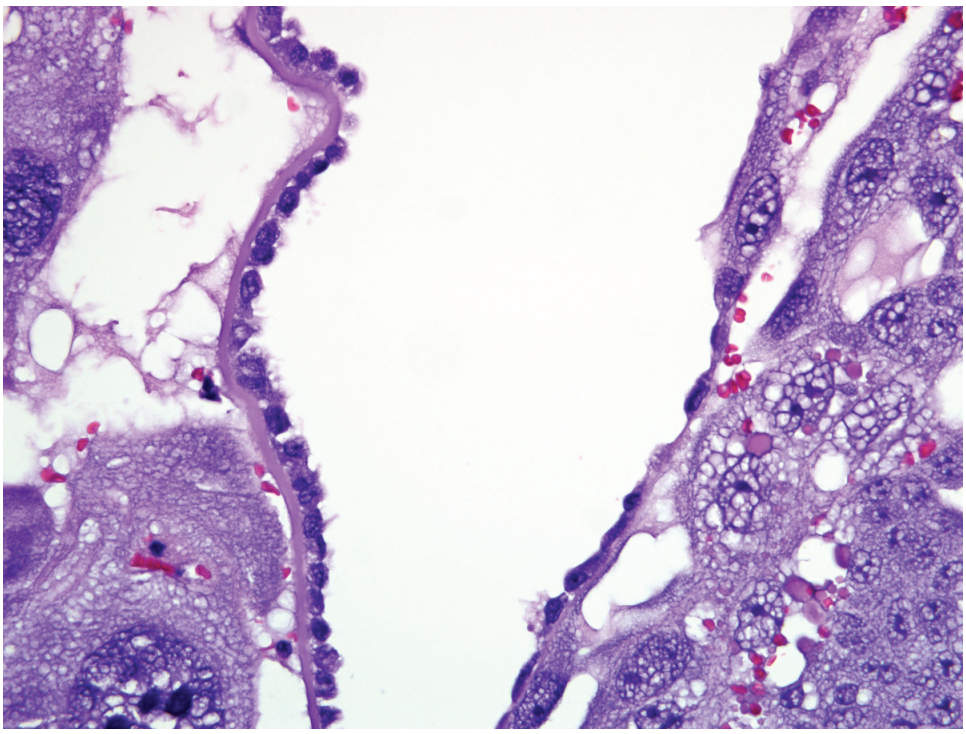

1-5. Uterus, rat. The yolk sac is lined by plump yolk sac epithelium which rests on a glassy, hyalinized membrane (Reichert's membrane). (HE 400X)

one of which lacks the giant cell layer, trophospongium, labyrinth, and yolk sac altogether. Additionally, other features of a normal rat pregnancy, i.e. a conceptus and fetal umbilical vessels, are conspicuously absent. One possible explanation for the presence of both maternal and embryofetal placental structures in the absence of a conceptus is embryonic death. For example, embryonic death attributed to an intercurrent infection with Sendai virus and *Pasteurella pneumotropica* resulted in the formation of deciduomas with trophoblastic giant cells in rats[1]; admittedly, this unlikely scenario does little to account for the clinical history in this case, and would likely result in significantly more placental pathology than is present in the examined sections.

In light of the lively discussions elicited by this case, the contributor was contacted to confirm the case history and ensure the possibility of pregnancy was excluded. Indeed, the submitted specimens were sampled from several female control rats that were pair-housed in a long-term study, and pregnancy would have been self-evident given the length of the study. Anecdotally, some experienced pathologists have noted extremely well-organized decidual reactions like this in rats that were certainly not pregnant; unfortunately, such examples are not reported in the literature, and we are unable to explain the presence of placental components of apparent fetal origin. A parthenogenetic process was also considered as a possible cause, but deemed exceedingly unlikely in this case given the signalment and clinical history provided by the contributor. Thus, we conclude that the histologic findings are most compatible with pregnancy and very recent embryonic loss. However, these histologic features in a known unmated animal are unique in our experience, and the pathogenesis remains unclear. We extend our sincere thanks to the contributor for submitting this very interesting case, and to the veterinary pathologists who graciously shared their opinions and expertise.

Contributor: Wyeth Research, Department of Pathology, 641 Ridge Road, Chazy, New York 12921
http://www.wyeth.com

References:

1. Carthew P, Aldred P: Embryonic death in pregnant rats owing to intercurrent infection with Sendai virus and *Pasteurella pneumotropica*. Lab Anim **22:**92-97, 1988
2. de Rijk EPCT, van Esch E, Flik G: Pregnancy dating in the rat: placental morphology and maternal blood parameters. Toxicol Pathol **30:**271-282, 2002
3. Elcock LH, Stuart BP, Mueller RE, Hoss HE: Deciduoma, uterus, rat. *In:* Monographs on Pathology of Laboratory Animals: Genital System, eds. Jones TC, Mohr U, Hunt RD, pp. 140-145. Springer-Verlag, Berlin Heidelberg, 1987
4. Greaves P: Female genital tract. *In:* Histopathology of Preclinical Toxicity Studies: Interpretation and Relevance in Drug Safety Evaluation, 3rd ed., pp 728-29. Elsevier, London, UK, 2007
5. Leininger JR and Jokinen MP: Oviduct, uterus and vagina. *In:* Pathology of the Fischer Rat: Reference and Atlas, eds. Boorman GA, Eustis SL, Elwell MR, Montgomery Jr. CA, MacKenzie WF, pp. 450-452. Academic Press, Inc., London, UK, 1990

CASE II: 34 (AFIP 2936324).

Signalment: 1.5-year-old, male knockout mouse (specific mutation not provided) (*Mus musculus*).

Gross Pathology: In mice older than 8 months, the stomach was contracted and contained scant ingesta. The wall of the glandular stomach was pale, markedly thickened, and formed prominent folds apparent from the serosal and mucosal aspects (**fig. 2-1**).

Histopathologic Description: Stomach: The normal glandular mucosa is completely replaced by hyperplastic mucosa. Chief cells and parietal cells are virtually absent and the distinction between the cardiac, fundic, and pyloric regions is lost. The abnormal mucosa is very tall and measures approximately 900-1800 um in thickness. By comparison, in wild-type (WT) controls, the fundic mucosa is approximately 450 um (300-700 um) thick and the pyloric mucosa is 250 um (200-350 um) thick. There is pronounced elongation of the gastric pits and glands, which are lined by two (or three, see below) epithelial cellular types (**fig. 2-2**). In the basal mucosa, the lining cells are cuboidal to columnar with pale, wispy cytoplasm and resemble lining cells of the normal mucous glands in the antral/pyloric mucosa. In the adlumenal region, two intimately admixed cell types are seen: one population is cuboidal to columnar with amphophilic to eosinophilic cytoplasm and is similar to normal surface epithelial cells/pit cells. The second population, which apparently arises from the latter and is very common in this specimen, is tall columnar with homogenous brightly eosinophilic cytoplasm, so-called hyaline change,[1] hyalinosis, or eosinophilic cytoplasmic change.[2] The hypereosinophilic

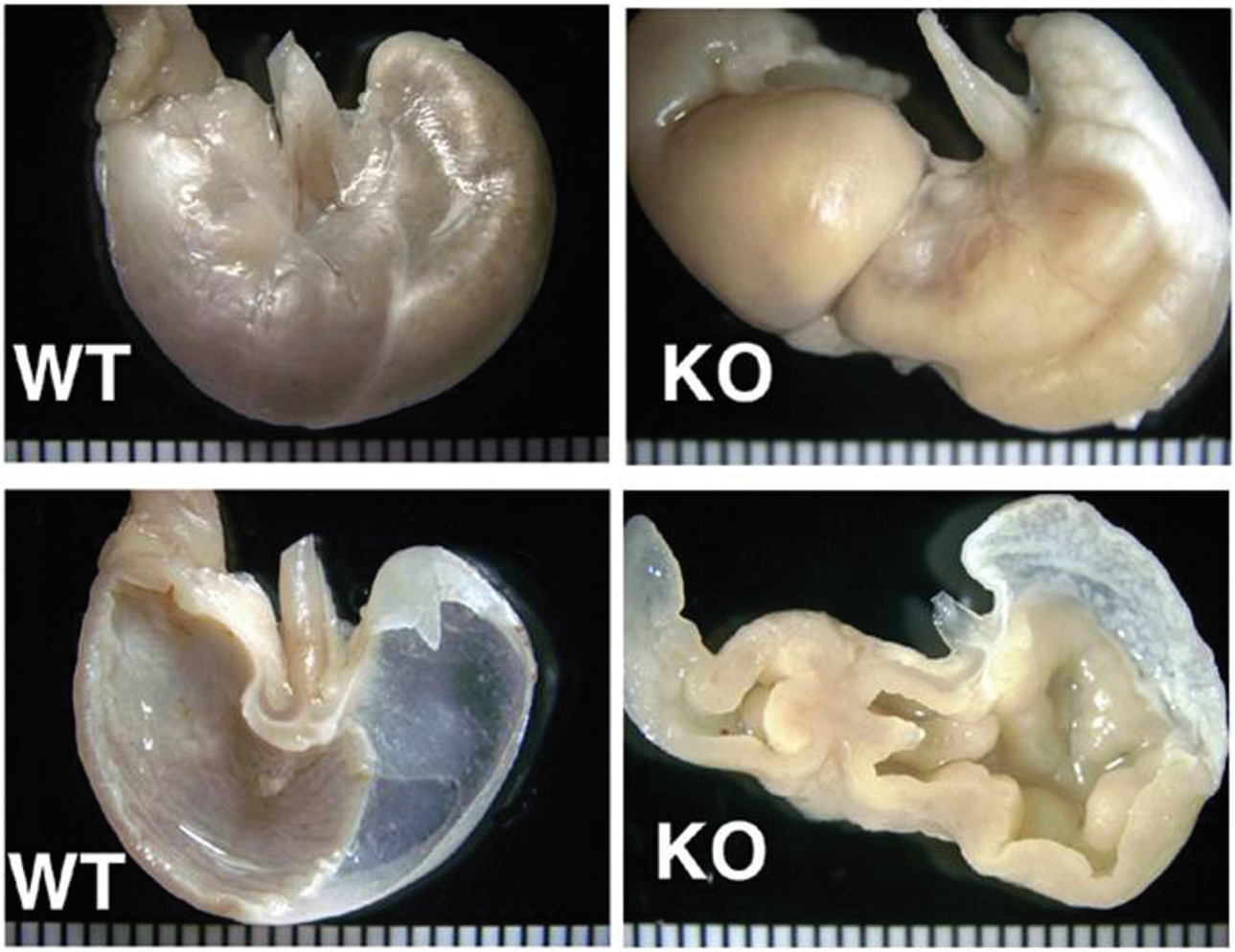

2-1. Stomach, mouse. The wall of the glandular stomach was pale, markedly thickened, and formed prominent folds apparent from the serosal and mucosal aspect (affected mouse on right, normal on left). Photograph courtesy of Weizmann Institute of Science, Department of Veterinary Resources, Rehovot 76100, Israel, www.weizmann.ac.il

material either forms a discrete globular accumulation within the cytoplasm or fills it entirely. There is scattered cytoplasmic vacuolation in the hyperplastic and often hypertrophic pit cells. Large aggregates of rectangular acicular and globular hypereosinophilic crystalline material are commonly seen within distended lumena of hyperplastic pits, at times with a small amount of cellular debris (**fig. 2-3**). There is multifocal cystic dilation predominantly of the glands, with multifocal 'herniation' into subjacent layers up to, but not through, the serosa. There is mild multifocal lymphoplasmacytic and eosinophilic lamina proprial and submucosal infiltration with occasional accumulation of granular yellow-brown pigment-laden macrophages. In some areas there is epithelial erosion with neutrophilic infiltration and bacterial colonies. There is mild to moderate multifocal fibrosis of the lamina propria. Mitotic figures are commonly seen. Dysplastic foci are occasionally recognized and exhibit atypia in the form of nuclear pleomorphism, nuclear stratification, loss of nuclear polarity, increased nuclear to cytoplasmic ratio and hyperchromasia. In some sections, polypoid mucosal masses are present and exhibit pronounced dysplasia, marked mixed inflammatory infiltration and advanced fibrosis. The pylorus (not present on all slides) is dilated and hyperplastic mucosa bulges into and distends the duodenal lumen. The villi in this region are nearly completely effaced. The mucosa overlying Brunner's gland is abnormal and similar to the hyperplastic gastric mucosa (metaplasia). More distally, there is marked infiltration of the lamina propria by lymphocytes, plasma cells, eosinophils and granular yellow-brown pigment-laden macrophages. Mucosal architecture is distorted with

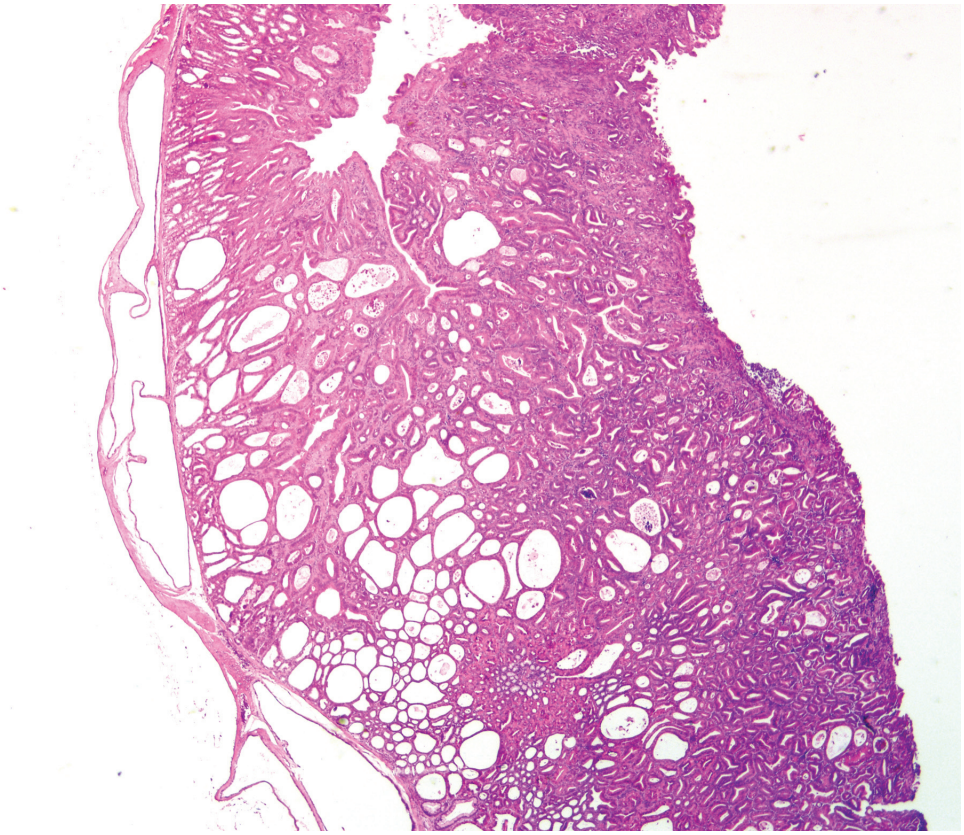

2-2. Stomach, mouse. Diffusely, the mucosa is markedly hyperplastic, forming tubular and cystic spaces which often extend through the muscularis mucosa and occasionally through the tunica muscularis. (HE 20X)

prominent villous blunting and fusion, crypt elongation and goblet cell hyperplasia. There are scattered crypt abscesses. In the forestomach, there is diffuse moderate thickening of the keratin layer and minimal multifocal mononuclear and eosinophilic infiltration.

Contributor's Morphologic Diagnosis:
1. Stomach (glandular portion): Severe diffuse adenomatous hyperplasia with hyalinosis, mild to moderate multifocal mononuclear, eosinophilic and erosive gastritis.
2. Stomach (squamous portion): Moderate diffuse orthokeratotic hyperkeratosis.
3. Proximal duodenum: Mucosal metaplasia with hyalinosis, moderate to marked diffuse chronic-active lymphoplasmacytic and eosinophilic enteritis.

Contributor's Comment: In mice, hyperplasia of the glandular mucosa with variable degrees of inflammatory infiltration is a heterogeneous condition known by several alternative designations: adenomatous hyperplasia, gastric hyperplasia, fundic mucosal hyperplasia, giant hypertrophic gastritis, hypertrophic gastropathy, chronic gastritis and proliferative gastritis.[1,4,7] Conditions in which this lesion is encountered include the following:

i. As a spontaneous lesion in several mouse strains including Han:NMRI,[14] strain I,[1] aging C57BL/6x129 and 129/Sv mice[2] and CD-1 mice.[3]
ii. In experimental infection with *Helicobacter felis* of WT C57BL/6 mice[5] and several mutant strains (e.g. IL-10-/-).
iii. With long-term treatment of mice with H_2 blocking drugs [13] and other antisecretory compounds.[1]
iv. In experimental infection of immunodeficient mice with *Taenia taeniaformis*.[8]
v. In several knockout and transgenic mice.[10]
vi. In densely housed mice.[7]
vii. In association with colitis in mutant mice.[4,5]

The gastric hyperplasia observed in the above conditions may have distinguishing gross and/or histologic features depending on the specific etiology. Common to these is mucosal hyperplasia with loss of specialized cells, also referred to as mucous metaplasia. The degree of inflammatory infiltration is variable. In the gastric lesion

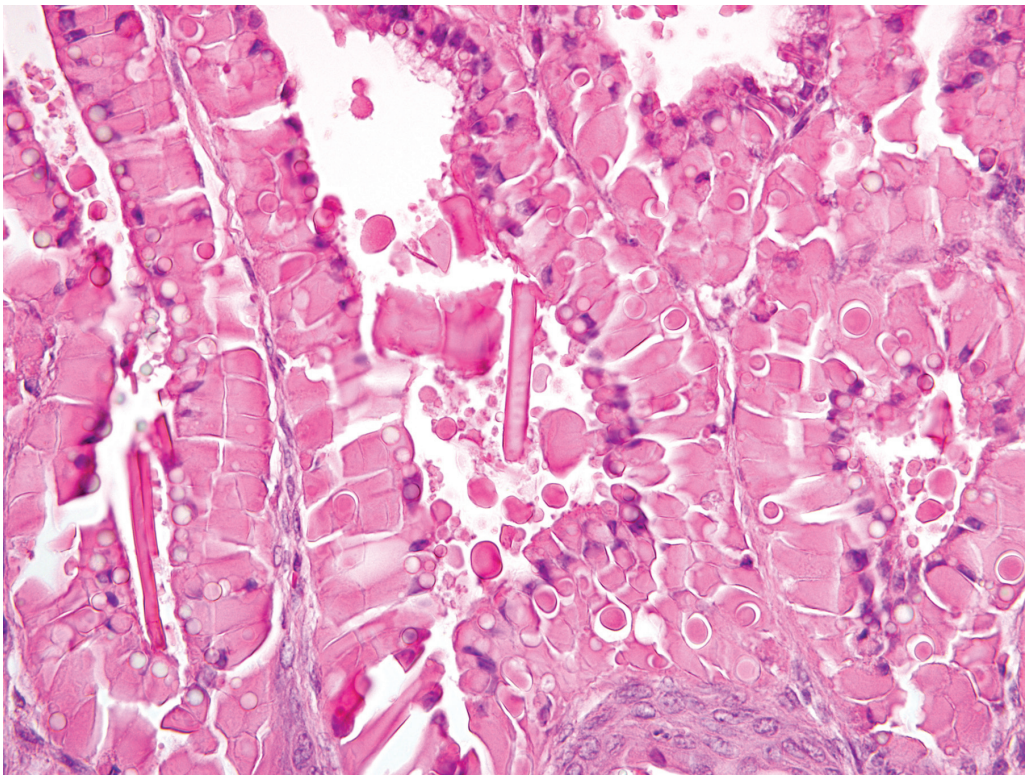

2-3. Stomach, mouse. Multifocally, dilated crypts in the hyperplastic mucosa contain brightly eosinophilic crystalline material. Epithelial cells often contain intracytoplasmic, 10-15 um spherical globules of pale to brightly eosinophilic material. (HE 400X)

from this knockout, the degree of hyperplasia clearly outstrips inflammation. Alcian blue and periodic acid Schiff stains demonstrate altered mucin production, as expected.[7] The extent of hyalinosis in this case is striking. The globular hypereosinophilic material was strongly immunoreactive with a polyclonal antibody raised against Ym1/T-lymphocyte-derived eosinophil chemotactic factor (immunohistochemical staining kindly provided by JM Ward, NCI). Proteins in this family are believed to play a role in mucosal defense against parasites.[15]

The cause of the lesion in this knockout, as in many of the above, remains undetermined. In some cases it may be due to hormonal imbalance, e.g. hypergastrinemia. The hyperkeratosis in the forestomach is consistent with insufficient mechanical abrasion of keratin due to reduced food intake.[3] The proliferative enteritis in the proximal duodenum is always encountered in conjunction with the gastric lesion, to which it is assumed to be secondary. While in man metaplasia of the gastric mucosa is associated with an increased risk of carcinoma, the murine condition is often not associated with increased incidence of gastric malignancy.[3,14]

In domestic animals, conditions which bear some resemblance to this lesion include giant hypertrophic gastritis (Menetrier's disease) in dogs and chronic abomasitis with mucous metaplasia in ruminants caused by infestation with *Ostertagia* sp. ("Morocco leather").

AFIP Diagnosis: 1. Stomach, glandular: Hyperplasia, adenomatous, diffuse, marked, with cystic mural herniation, chief and parietal cell loss, epithelial hyalinosis, mucous metaplasia, acicular eosinophilic crystalline material, and mild multifocal eosinophilic and neutrophilic gastritis.
2. Stomach, squamous: Hyperkeratosis, orthokeratotic, diffuse, moderate.

Conference Comment: In addition to the gastric lesions described above, participants' slides contained an array of duodenal changes, ranging from proliferative lesions to diffuse blunting and fusion of villi with chronic-active and eosinophilic inflammation. The contributor provides a concise summary of potential causes for gastric hyperplasia in mice. This case was submitted in 2004; more recently, long-term infection with *Helicobacter heilmannii* has been reported to cause mucosal nodular hyperplasia due to gastric epithelial proliferation in C57BL/6 mice. In contrast to the present case, affected mice developed mucosal and submucosal lymphoid follicles composed predominantly of CD45R+ cells.[12] Silver stains using the Warthin-Starry and Steiner's methods did not reveal an etiologic agent in this case.
During the conference, participants compared the slide

for this case with a section of normal mouse stomach to emphasize the striking mucous metaplasia and hyalinosis present herein. Hyalinosis has been described in a variety of tissues and a variety of mouse strains. In the glandular stomach of affected 129S4/SvJae and B6,129 mice, the extracellular and eosinophilic crystals were determined to be composed of Ym2 protein, a chitinase-related protein. Other sites reportedly affected by hyalinosis in mice include biliary and pancreatic duct epithelium, and the respiratory epithelium lining the nasal cavity and respiratory tract.[15]

In addition to the examples cited by the contributor, conference participants discussed other instances of proliferative gastric lesions in domestic animals, including equine hypertrophic gastritis associated with *Habronema* spp. and *Trichostrongylus axei*, hypertrophic gastritis in nonhuman primates caused by *Nochtia nocti*, gastritis in pigs caused by *Hyostrongylus rubidus*, and gastritis in cats caused by *Ollulanus tricuspis*.[6] In addition to ostertagiosis, *Cryptosporidium andersoni* has been recognized as a cause of proliferative abomasitis in cattle.[11]

Contributor: Weizmann Institute of Science, Department of Veterinary Resources, Rehovot 76100, Israel
http://www.weizmann.ac.il/

References:

1. Betton GR, Whiteley LO, Anver MR, Brown R, Deschl U, Elwell M, Germann PG, Hartig F, Kuttler K, Mori H, Nolte T, Puscher H, Tuch K: Gastrointestinal tract. *In:* International Classification of Rodent Tumors, the Mouse, ed. Mohr U, p. 38. Springer-Verlag, Berlin, 2001
2. Ennulat D, Kawabe M, Kudo G, Peters JM, Kimura S, Morishima H, Gonzalez FJ, Ward JM: Hyperplastic gastric mucosal lesions with eosinophilic cytoplasmic inclusions in aging C57BL/6N x 129 and Sv/129 mice. Abstract Vet Pathol **35:**456, 1998
3. Faccini JM, Abbott DP, Paulus GJJ: Mouse Histopathology: a Glossary for Use in Toxicity and Carcinogenicity Studies, pp. 98-102. Elsevier, New York, NY, 1990
4. Fernandez-Salgureo PM, Ward JM, Sundberg JP, Gonzalez FJ: Lesions of aryl-hydrocarbon receptor-deficient mice. Vet Pathol **34:**605-614, 1997
5. Fox JG, Dangler CA, Schauer DB: Inflammatory bowel disease in mouse models: role of microintestinal microbiota as proinflammatory modulators. *In:* Pathology of Genetically Engineered Mice, eds. Ward JM, Mahler JF, Maronpot RR, Sundberg JP, pp. 302-303. Iowa State University Press, Ames, IA, 2000
6. Gelberg HB: Alimentary system. *In:* Pathologic Basis of Veterinary Disease, eds. McGavin MD, Zachary JF, 4th ed., pp. 339-341. Mosby Elsevier, St. Louis, MO, 2007
7. Greaves P, Boiziau JL: Altered patterns of mucin secretion in gastric hyperplasia in mice. Vet Pathol **21:**224-228, 1984
8. Lagapa JT, Konno K, Oku Y, Nonka N, Ito M, Kamiya M: Gastric hyperplasia and parietal cell loss in *Taenia taeniaformis* inoculated immunodeficient mice. Parasito Int **51:**81-89, 2002
9. Leininger JR, Jokinen MP, Dangler CA, Whiteley LO: Oral cavity, esophagus and stomach. *In:* Pathology of the mouse, eds. Maronpot RR, Boorman GA, Gaul BW, 1st ed., pp. 36-37. Cache River Press, Vienna, IL, 1999
10. Maehler M, Rozell B, Mahler JF, Merlino G, Devor-Henneman DE, Ward JM, Sundberg JP: Pathology of the gastrointestinal tract of genetically engineered and spontaneous mutant mice. *In:* Pathology of Genetically Engineered Mice, eds. Ward JM, Mahler JF, Maronpot RR, Sundberg JP, pp. 269-298. Iowa State University Press, Ames, IA, 2000
11. Masuno K, Yanai T, Hirata A, Yonemaru K, Sakai H, Satoh M, Masegi T, Nakai Y: Morphological and immunohistochemical features of *Cryptosporidium andersoni* in cattle. Vet Pathol **43:**202-207, 2006
12. Park JH, Seok SH, Baek MW, Lee HY, Kim DJ, Park JH: Gastric lesions and immune responses caused by long-term infection with *Helicobacter heilmannii* in C57BL/6 mice. J Comp Pathol **139:**208-217, 2008
13. Poytner D, Selway SAM, Papworth SA, Riches SR: Changes in the gastric mucosa of the mouse associated with long lasting unsurmountable histamine H_2 blockade. Gut **27:**1338-1346, 1986
14. Rehm S, Sommer R, Derberg F: Spontaneous nonneoplastic gastric lesion in female Han:NMRI mice and influence of food restriction throughout life. Vet Pathol **24:**216-225, 1987
15. Ward, JM, Yoon M, Anver M, Haines DC, Kudo G, Gonzalez FJ, Kimura S: Hyalinosis in Ym1/Ym2 gene expression in the stomach and respiratory tract of 129S4/SvJae and wild-type and CYP1A2-null B6,129 mice. Am J Pathol **158:**323-332, 2001

CASE III: Novartis case #2 (AFIP 3134885).

Signalment: Male, spontaneously hypertensive (SH) rat (*Rattus norvegicus*).

History: The rat was found to be dorsally recumbent, with head tilting to the right and nystagmus of the left eye.

Gross Pathology: Pale, finely pitted kidneys.

Histopathologic Description: Kidney: The renal capsular surface is diffusely undulant, with multiple shallow cortical indentations and multifocal tubular ectasia. Cortical indentations are often associated with perivascular cortical interstitial expansion and basophilia that correlate to an inflammatory cellular infiltrate comprised of small to moderate numbers of lymphocytes and macrophages, and a few light yellow brown pigment-laden macrophages (presumed hemosiderophages). The leukocytic infiltrate is multifocally accompanied by enhanced prominence of blood vessels, occasional hemorrhage, minimal to mild fibrosis, and separation/compression/loss of renal tubules. Renal proximal tubules and collecting ducts are multifocally ectatic with proteinaceous casts. In lesser affected tubules, the epithelium contains modest numbers of hyaline droplets. Other tubules exhibit sloughing of renal tubular epithelium (degeneration), presence of cellular and karyorrhectic debris (necrosis) and cellular and granular casts. Many scattered renal tubules exhibit tubular basophilia (regeneration). A few tubules also have thickened basement membranes. Glomeruli in markedly affected areas are often closely arranged due to tubular drop out. Multifocally, basement membranes of glomerular tufts and capsules are thickened and fibrotic (glomerulosclerosis) (**figs. 3-1 and 3-2**). Multiple arcuate and/or interlobular arteries in the renal cortex exhibit reduction of vascular lumen, intimal deposits and medial smooth muscle hyperplasia with occasional degeneration of medial smooth muscle (**fig. 3-3**). The pelvic lamina propria has multifocal infiltrates of lymphocytes.

Contributor's Morphologic Diagnosis: Nephro–pathy, chronic, marked, with multifocal lymphohistiocytic interstitial nephritis, glomerular and tubular basement membrane thickening, glomerulosclerosis, tubular degeneration/necrosis/regeneration, tubular ectasia, casts and hyaline droplets, and arterial smooth muscle hyperplasia and degeneration.

Contributor's Comment: The case represents chronic progressive nephropathy (CPN) in rats, which is common in old, male, Sprague-Dawley or Fischer 344 rats fed high protein diets.[4] CPN is a combination of both degenerative and proliferative lesions, and basophilic tubules are considered to be an early lesion in this nephropathy.[2,3] In chronic studies, the proliferative components of CPN may need to be discriminated from pre-neoplastic proliferative changes.[2] Degenerative lesions similar to those observed in this case could result from infections, degenerative nephrosis or toxic insults. However, the inciting factor is often difficult to discern by histologic evaluation. The vascular changes observed in this case may be related to the rat being spontaneously hypertensive and may have

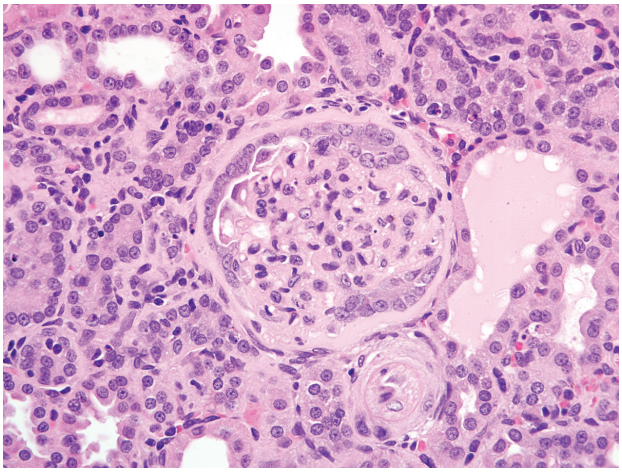

3-1. Kidney, rat. Glomeruli within the cortex often have thickened capillary loops, increased mesangium within the glomerular tuft, and hyperplastic parietal epithelium with multifocal synechiae. (HE 400X)

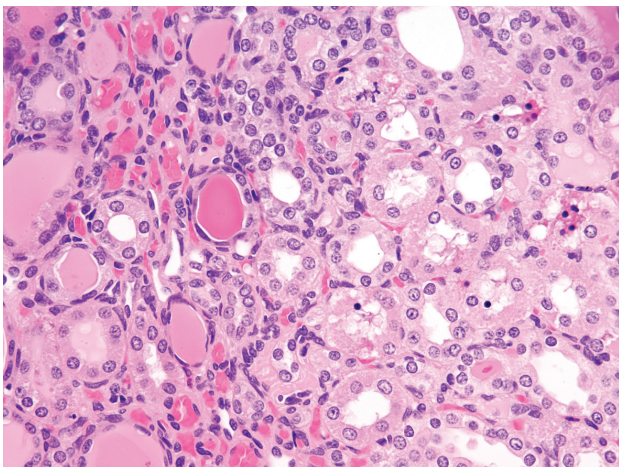

3-2. Kidney, rat. Multifocally, cortical tubular epithelium is attenuated, necrotic, or regenerative, and tubular lumina often contain abundant brightly eosinophilic proteinaceous material. (HE 400X)

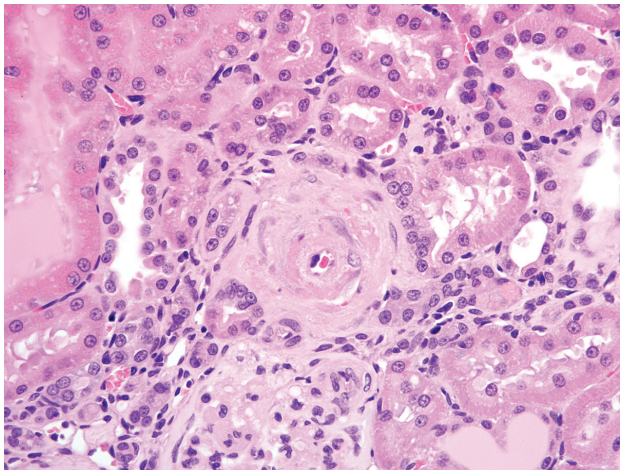

3-3. Kidney, rat. Arterioles within the cortex are often surrounded by concentric layers of fibrosis; the tunica media of these vessels is expanded by eosinophilic material, and the endothelium is hypertrophied. (HE 400X)

contributed to the development of the renal lesions.[1,2] Vascular lesions are typically not described in cases of CPN. Hence, in other strains, polyarteritis nodosa would be a good differential.

AFIP Diagnosis: 1. Kidney: Glomerulonephropathy, diffuse, chronic, marked, characterized by glomerular sclerosis and synechia, tubular atrophy, degeneration, necrosis, regeneration, ectasia, and proteinosis, and interstitial fibrosis and nephritis.

2. Kidney, cortex: Arteriolosclerosis, proliferative, multifocal, moderate, with medial degeneration and necrosis, and smooth muscle hyperplasia.

Conference Comment: In addition to the lesions described above, several conference participants' slides contained fibrinoid necrosis in multiple affected vessels. As mentioned by the contributor, vascular lesions are not typical of CPN, so their presence should raise the index of suspicion for another cause, such as strain phenotype. Recognized risk factors for the development of CPN in rats include the following:[3]

1. Age: greater than 12 months
2. Sex: male
3. Strain: Sprague-Dawley or Fischer 344
4. Diet: high protein and/or total caloric intake
5. Mesangial IgM deposition
6. Elevated prolactin levels

Conference participants discussed the importance of CPN as a potential confounder in laboratory investigations in general, and in two-year carcinogenicity assessments in particular, as alluded to by the contributor. The earliest changes, i.e. basophilic tubules with thickened basement membranes, may be present in kidneys of rats as young as two months of age. In advanced stages, the proliferative lesions of CPN may be difficult to distinguish from preneoplastic hyperplastic lesions, termed atypical tubule hyperplasia (ATH). Specific criteria to make this important distinction have been proposed, and are summarized in the table below:[2]

	Simple Tubule Hyperplasia	Atypical Tubule Hyperplasia
Significance	Compensatory regenerative response to cellular injury and loss	Preneoplastic developmental stage in a continuum with renal tubule adenoma/carcinoma
Cytoplasm	Basophilic	Mostly basophilic "glassy" cytoplasm; eosinophilic, clear, chromophobic, and oncocytic forms also described
Histomorphology	Thickened basement membrane; increased number of epithelial cells; extends laterally but not generally inward beyond the single layer of tubule lining	Proliferation beyond a single layer of tubular epithelium to form a solid tubule profile; expands into surrounding matrix and partially surrounded by rim of connective tissue cells; transition to early adenoma when proliferation extends beyond the nephron integrity

Contributor: Novartis Institutes for BioMedical Research, One Health Plaza, East Hanover, New Jersey 07836
http://www.nibr.com/

References:

1. Feld LG, Van Liew JB, Galaske RG, Boylan JW: Selectivity of renal injury and proteinuria in the spontaneously hypertensive rat. Kidney Int **12:**332-343, 1977
2. Hard GC, Seely JC: Recommendations for the interpretation of renal tubule proliferative lesions occurring in rat kidneys with advanced chronic progressive nephropathy (CPN). Toxicol Pathol **33:**641-649, 2005
3. Hill GS: Hypertensive nephrosclerosis. Curr Opin Nephrol Hypertens **17:**266-270, 2008
4. Percy DH, Barthold SW: Pathology of Laboratory Rodents and Rabbits, 3rd ed., pp. 161-162. Blackwell Publishing, Ames, IA, 2007

CASE IV: 09-468 (AFIP 3138312).

Signalment: Approximately 12-week-old, male, acid sphingomyelinase knockout (asmase$^{-/-}$) mouse (*Mus musculus*) on C57BL/6 background.

History: Recent onset of weakness, twitching, and shaking.

Gross Pathology: This mouse presented in thin body condition. The liver was mildly enlarged and mottled pale tan and yellow. No adipose tissue was present in the abdominal cavity.

Laboratory Results:

Hematology:

Manual Differential:

- Manual Neutrophil %: 46 (3-22.5)
- Band %: 3
- Manual Lymphocyte %: 29 (69-93.5)
- Manual Monocyte %: 4 (0-8)
- Others %: 18
- WBC Morphology (reported by technician): Atypical cells that are classified as others are variable in size ranging from 5 to 20 um. The nucleus of these cells is irregular in shape. Some are angular, others indented, and some are folded. The nuclear chromatin material is clumped in some of the cells and smooth in others.
- Cytoplasm varies from being scant to moderate. In some of the cells the cytoplasm resembles that of a monocyte.
- RBC Morphology: RBC morphology is within normal limits.
- Platelet Morphology: No abnormality noted.

CBC with automatic differential:

- Red Blood Cells: 9.04 (8.2-10.4)
- Hemoglobin: 14.6 (14.5-16.2)
- Hematocrit: 41.7% (38.5-46.0)
- MCV: 46.1 fL (42-48)
- MCH: 16.1 pg (14.5-16.2)
- MCHC: 35.0 g/dL (31.4-36.8)
- RDW: 19.8% (13.8-17.0)
- Platelets: 445 K/uL (799-1,300)

Chemistry (liver panel):

- ALP: 83 IU/L (23-181)
- ALT (SGPT): 110 IU/L (16-58)
- AST (SGOT): 1551 IU/L (36-102)
- GGT: 0.0 IU/L (0-2)
- Total Bilirubin: 0.3 mg/dl (0.0-0.3)
- Total Protein: 5.1 g/dl (4.1-6.4)
- Albumin: 3.2 g/dl (2.5-3.9)
- Blood Urea Nitrogen: 27 mg/dl (14-32)
- Creatinine: 0.3 mg/dl (0.1-0.6)
- B/C Ratio: 90.0 (21-127)

Histopathologic Description: **Brain**: There is a moderate to marked loss of Purkinje cells that is most severe in the anterior lobes of the cerebellum. Some remaining Purkinje cells are undergoing degeneration and necrosis, with shrinkage, hypereosinophilia, and nuclear pyknosis (**fig. 4-1**). Most of the remaining Purkinje cells and many other neurons throughout the brain contain well-delineated, small, lipid-containing vacuoles. There is mild to moderate multifocal gliosis, with an infiltrate of lipid-laden gitter cells. Many choroid plexus cells also contain lipid-laden vacuoles within their cytoplasm (**fig. 4-2**).

Lung: There is a moderate to marked diffuse intraalveolar infiltrate of macrophages, the cytoplasm of which is moderately to markedly distended with foamy vacuolation (lipid). Many macrophages also contain eosinophilic crystalline material within their cytoplasm, and similar material is present extracellularly within alveolar spaces (**fig. 4-3**). Occasional multinucleated giant cells and neutrophils are present, particularly in more severely affected areas. In more severely affected areas, there is an intraalveolar infiltrate of fibrin, and in the most severely affected areas, alveoli are filled with macrophages,

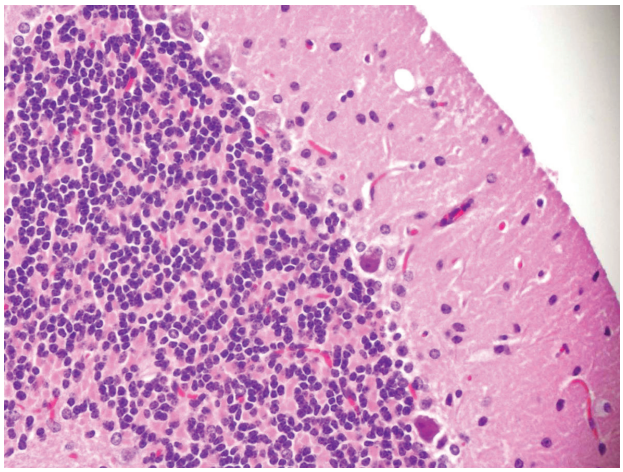

4-1. Cerebellum, mouse. There is a moderate to marked loss of Purkinje cells that is most severe in the anterior lobes of the cerebellum. Some remaining Purkinje cells are undergoing degeneration and necrosis, with shrinkage, hypereosinophilia, and nuclear pyknosis. Most of the remaining Purkinje cells and many other neurons throughout the brain contain well-delineated, small, lipid-containing vacuoles. Photomicrograph courtesy of Memorial Sloan Kettering Cancer Center, 1275 York Ave., Box 270, New York, NY 10021, monettes@mskcc.org.

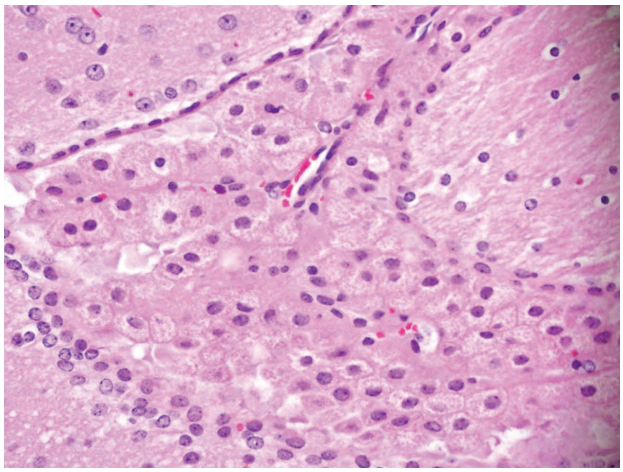

4-2. Brain, mouse. Many choroid plexus cells contain lipid-laden vacuoles within their cytoplasm. Photomicrograph courtesy of Memorial Sloan Kettering Cancer Center, 1275 York Ave., Box 270, New York, NY 10021, monettes@mskcc.org.

crystalline material, and fibrin, with loss of air spaces. Interstitial connective tissue is moderately expanded by edema.

Infiltrates of vacuolated macrophages were also present within the bone marrow, liver, adrenal gland, thymus, thyroid, epididymis, preputial gland, mesenteric lymph node, and myocardium. Vacuolation was also present within ganglion cells adjacent to the heart and neurons within the spinal cord, as well as follicular epithelial cells of the thyroid, epithelial cells of the epididymis, and renal tubular epithelial cells.

Contributor's Morphologic Diagnosis: 1. Lung: Alveolar histiocytosis, diffuse, moderate to marked, with intracytoplasmic lipid.
2. Lung: Eosinophilic crystalline pneumonia, regionally extensive, moderate, with intraalveolar fibrin.
3. Brain, cerebellum: Purkinje cell necrosis and loss, diffuse, moderate to marked.
4. Brain: Neuronal vacuolation, diffuse, moderate.
5. Brain: Gliosis, multifocal, mild to moderate, with gitter cells containing intracytoplasmic lipid.

Contributor's Comment: Sphingomyelin is the main lipid constituent of the plasma membrane and plasma-membrane-derived membranes (e.g. endosomes, lysosomes).[7] Lysosomal acid hydrolases (such as acid sphingomyelinase) play an important role in the turnover of membrane lipids from any cell. Acid sphingomyelinase (ASM) is present in endosomes and lysosomes of all cells, particularly the reticuloendothelial cells of the liver, spleen, bone marrow, lung, and macrophages. During times of cell stress, ASM is translocated from lysosomes to the outer leaflet of the cell membrane, where it functions to hydrolyze sphingomyelin into ceramide and phosphocholine.[2] Ceramide stimulates reorganization of membrane rafts (composed of sphingolipids and cholesterol) into larger, ceramide enriched 'platforms', thus bringing together signaling proteins and causing downstream changes within the cell.[2,11] Documented roles and potential roles of ceramide include phosphorylation/dephosphorylation of intracellular signaling molecules, calcium transport across membranes, cell differentiation, mitogenesis, inflammatory mediation (primarily through TNF-induced signaling), immune responses, and apoptosis.[4] Types of cell stress documented to cause ASM translocation to the cell membrane (with resulting ceramide formation) include irradiation, conjugation of cell surface receptors, heat shock, and exposure of cells to bacterial pathogens, to name a few.[11] The roles of ASM and ceramide in cell responses to these stressors is supported by the fact that ASM knockout (ASMKO) mice are resistant to cell death induced by irradiation and ischemia, and are resistant

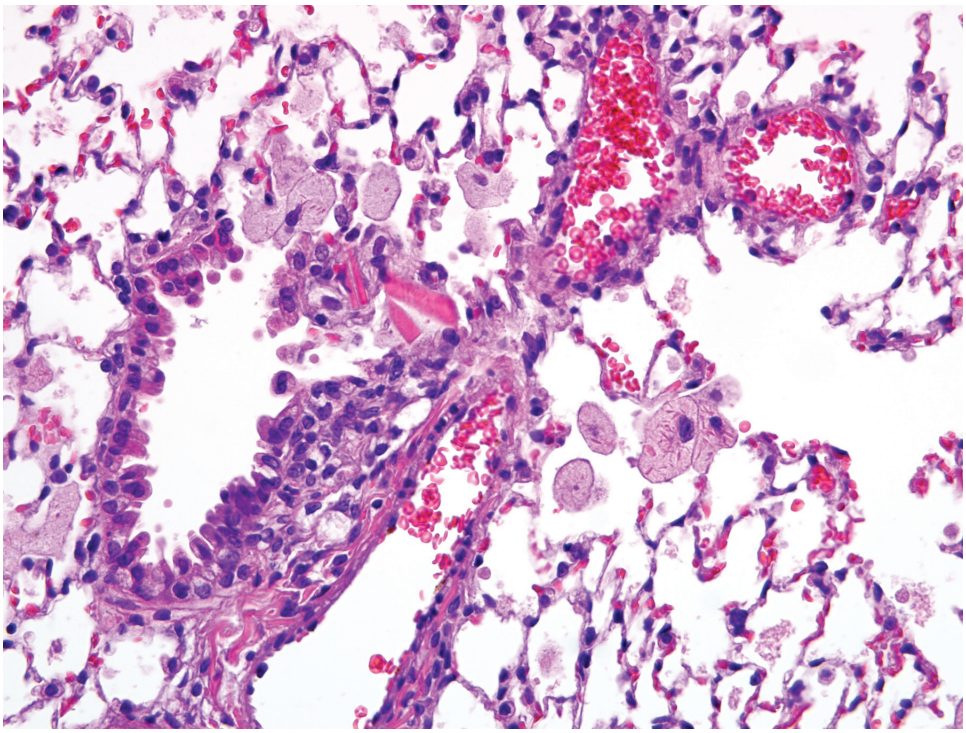

4-3. Lung, mouse. Within alveolar lumina there are numerous large, lipid-laden alveolar macrophages. Multifocally within terminal bronchioles and alveoli there are brightly eosinophilic rectangular crystals; similar eosinophilic crystalline material is occasionally found within the cytoplasm of macrophages. (HE 400X)

to infection by various pathogens (often because the organisms are unable to cross the cell membrane).

In humans, an inherited (autosomal recessive) deficiency of ASM activity results in A and B forms of Niemann-Pick disease (NPD).[4,7] Over a dozen mutations cause defects in the ASM enzyme leading to NPD types A and B. Type A NPD is a severe neurodegenerative disorder leading to death by 3 years of age. Individuals with this form of the disease have very little (<5%) ASM activity. In type B NPD, there is little to no neurological involvement, and individuals often survive into adulthood. The decreased severity of clinical signs in these patients is thought to be due to variable amounts (>5%) of ASM activity.[7] A third form of NPD, type C, is also a lipid storage disease, but is due to mutation in unrelated genes (called NPC-1 or NPC-2).

In ASMKO mice, the disease is also autosomal recessive, and the phenotype of affected mice is essentially identical to humans with type A NPD.[4] Mice are normal at birth, with ataxia and tremors beginning at approximately 8 weeks of age. There is rapid disease progression, with lethargy, decreased responses to stimuli, and difficulty eating by 12-16 weeks of age. Severe ataxia is also generally present by 16 weeks of age. Death usually occurs by 6-8 months of age. Biochemical analysis of homozygous ASMKO mice reveals no detectable ASM activity in any tissues tested (i.e. liver, lung, spleen, kidney, heart, brain). Lipid analysis of liver and brain showed approximately 15 and 5-fold increases, respectively in sphingomyelin. Total blood cholesterol levels are elevated approximately 80% in these mice, and nearly all of this is associated with the high density lipoprotein (HDL) fraction. Heterozygotes have approximately 50% ASM activity and present with no clinical disease.

Reported gross pathology findings in ASMKO mice at the time of naturally-occurring death included a hunched appearance, 50% loss in body and brain weight, and hepatosplenomegaly. Histopathologically, lipid-laden foam cells (so-called NPD cells) were present in most major organs. Electron microscopic evaluation revealed multilamellar cytoplasmic inclusions in all tissues, especially the brain. Additionally, Purkinje cell loss and atrophy of the cerebellum and midbrain were present. The neuronal activity of Purkinje cells far exceeds most other cell types in the CNS, and they form excitatory and inhibitory synapses and relay sensory information from all parts of the body.[7] This high activity level leads to rapid membrane turnover, and this has been hypothesized to account for their increased rate of death in comparison with other neurons in the CNS. This hypothesis is supported by the observation that Purkinje cell loss occurs in the anterior lobules of the cerebellum first, with preservation of the posterior lobular neurons until late in the course

of the disease. Posterior lobular Purkinje cells contain high levels of sphingosine kinase, which may serve as an alternate mechanism for sphingolipid breakdown.

In addition to neuronal disease, both humans with types A and B NPD and ASMKO mice are reported to develop lung pathology. In human type A NPD, neurodegeneration usually causes death before pulmonary disease becomes advanced. However, individuals with the type B form may show progressive pulmonary dysfunction and respiratory infections that can be fatal.[5] Pulmonary disease is primarily related to alterations of surfactant, which contains increased saturated phosphatidylcholine and sphingomyelin compared to normal individuals. This leads to decreased catabolism by alveolar macrophages (a process that requires lysosomal activity), and subsequent decreased clearance from the lungs. In addition to elevated levels of surfactant, the increased sphingomyelin contributes to abnormal surfactant function. Pulmonary macrophage dysfunction is also thought to play a role in lung disease.[1] Decreased superoxide production by pulmonary macrophages has been documented in ASMKO mice and the addition of ASM *in vitro* increased superoxide production, further supporting the role of ASM in macrophage function. Additionally, ASMKO mice had elevated levels of macrophage inflammatory proteins (MIP), specifically MIP1α (a monocyte chemoattractant) and MIP2 (a neutrophil chemoattractant). These chemokines are normally produced by macrophages and bronchial epithelial cells, leading to increased inflammatory cell recruitment. Histopathologically, alveolar macrophages were most affected by the accumulation of intracellular lipids, but ciliated cells of airways, type I pneumocytes, and endothelial cells were also affected. Interestingly, there was no evidence of fibrosis within affected lungs of ASMKO mice, indicating preservation of normal architecture and potential for normal function if ASM activity is restored.

Eosinophilic crystalline pneumonia commonly occurs in strains on a C57BL/6 background.[3] It may occur spontaneously or in concert with other pulmonary lesions, such as pulmonary adenomas, lymphoproliferative disease, allergic pulmonary disease, and parasitic or fungal infection. The crystals in eosinophilic crystalline pneumonia are composed predominately of Ym1 protein, a chitinase-like protein associated with neutrophil granule products and secreted by activated macrophages. The function of Ym1 protein is not fully understood but is believed to be involved in host immune defense, eosinophil recruitment, and cell-cell and cell-matrix interactions consistent with tissue repair. The mechanism of induction of eosinophilic crystalline pneumonia is unknown.

AFIP Diagnosis: 1. Lung: Alveolar histiocytosis, multifocal, moderate, with intrabronchiolar and intrahistiocytic eosinophilic crystalline material and histiocytic lipid-type cytoplasmic vacuolation.
2. Brain, cerebellum: Purkinje cell degeneration, necrosis, and loss, diffuse, moderate, with gliosis, and neuronal and glial lipid-type cytoplasmic vacuolation.
3. Brain, cerebrum: Neuronal degeneration, necrosis, and loss, diffuse, marked, with gliosis, and neuronal and glial lipid-type cytoplasmic vacuolation.

Conference Comment: The contributor provides an excellent example of the ASMKO phenotype, a concise review of sphingomyelin in plasma membrane physiology, and a complete summary of this knockout and its relevance as a model for NPD in humans. Type A NPD has also been reported in cats and a miniature poodle dog[6], and findings in a Hereford calf with sphingomyelinase deficiency were most consistent with type A NPD.[10] In general, lysosomal storage diseases are characterized by the intracellular accumulation of substrates that cannot be degraded by lysosomes, ultimately resulting in cell death. Several mechanisms explain dysfunction of lysosome-mediated degradation of substrate: 1) mutation resulting in reduced synthesis of lysosomal enzymes; 2) synthesis of dysfunctional or inactive proteins that resemble lysosomal enzymes; 3) misdirection of enzymes to sites other than lysosomes due to defective post-translational processing; 4) lack of enzyme activators or protector proteins; 5) lack of substrate activator proteins; and 6) lack of transport protein to eliminate digested material from lysosomes.[12] While most cell types are susceptible to the accumulation of substrates, neurons and cardiomyocytes are particularly affected due to their long post-mitotic lifespan. Lysosomal storage diseases are classified as inherited or acquired, and subdivided by the class of macromolecule whose degradation is defective. Clinically, a common theme among the inherited storage diseases is juvenile-onset progressive neurologic dysfunction. The following table summarizes a small selection of the growing list of inherited lysosomal storage diseases described in animals:[8,12]

Macromolecule Class	Lysosomal Storage Disease
Sphingolipidoses	GM_1 gangliosidosis (generalized gangliosidosis) GM_2 gangliosidosis Glucocerebrosidosis (Gaucher disease) Sphingomyelinosis (NPD Types A, B, and C) Galactosialidosis Galactocerebrosidosis (globoid cell leukodystrophy, Krabbe disease)
Glycoproteinoses	α-Mannosidosis β-Mannosidosis α -L-fucosidosis
Mucopolysaccharidoses	Mucopolysaccharidosis types I, III, VI, VII, and others
Glycogenoses	Glycogenosis type II (Pompe disease) Glycogenosis type III (Cori disease) Glycogenosis type IV (Polyglucosan body disease)
Mucolipidoses	Inclusion-cell disease (mucolipidosis II)
Ceroid lipofuscinoses	Neuronal ceroid-lipofuscinosis (Batten disease) (see WSC 2008-2009, Conference 24, Case III)
Miscellaneous	Lafora disease Motor neuron disease of English Pointers

In addition to the C57BL/6 strain, other laboratory mice commonly affected by eosinophilic crystalline pneumonia include 129SvJae and its derivatives, severe combined immunodeficiency (SCID) mice, and knockout mice targeting specific components of the immune system.[3] An example of eosinophilic crystalline pneumonia is available in WSC 2007-2008, Conference 8, case I.

Focally affecting some sections of lung in this case, alveoli contain small amounts of necrotic cellular debris admixed with low numbers of viable and degenerate neutrophils and macrophages, and the adjacent pleura and alveolar septa are infiltrated by lymphocytes, macrophages, and neutrophils.

Contributor: Memorial Sloan Kettering Cancer Center, New York, NY 10021 http://www.mskcc.org

References:

1. Dhami R, He X, Gordon RE, Schuchman EH: Analysis of the lung pathology and alveolar macrophage function in the acid sphingomyelinase-deficient mouse model of Niemann-Pick disease. Lab Invest **81:**987-999, 2001
2. Gulbins E, Dreschers S, Wilker B, Grassme H: Ceramide, membrane rafts, and infections. J Mol Med **82:**357-363, 2004
3. Hoenerhoff MJ, Starost MF, Ward JM: Eosinophilic crystalline pneumonia as a major cause of death in 129S4/SvJae mice. Vet Pathol **43:**682-688, 2006
4. Horinouchi K, Erlich S, Perl DP, Ferlinz K, Bisgaier CL, Sandhoff K, Desnick RJ, Stewart CL, Schuchman EH: Acid sphingomyelinase deficient mice: a model of types A and B Niemann-Pick disease. Nat Genet **10:**288-293, 1995
5. Ikegami M, Rajwinder D, Schuchman E: Alveolar lipoproteinosis in an acid sphingomyelinase-deficient mouse model of Niemann-Pick disease. Am J Physiol Lung Cell Mol Physiol **284:**L518-L525, 2003
6. Jolly, RD, Walkley SU: Lysosomal storage diseases of animals: an essay in comparative pathology. Vet Pathol **34:**527-548, 1997
7. Macauley SL, Sidman RL, Schuchman EH, Taksir T, Stewart GR: Neuropathology of the acid sphingomyelinase knockout mouse model of Niemann-Pick: A disease including structure-function studies associated with cerebellar Purkinje cell degeneration. Exp Neurol **214:**181-192, 2008
8. Maxie MG, Youssef S: Nervous system. *In*: Jubb, Kennedy, and Palmer's Pathology of Domestic Animals, ed. Maxie MG, 5th ed., vol. 1, pp. 322-330. Elsevier Saunders, Philadelphia, PA, 2007
9. Otterbach B, Stoffel W: Acid sphingomyelinase-deficient mice mimic the neurovisceral form of human lysosomal storage disease (Niemann-Pick disease). Cell

81:1053-1061, 1995
10. Saunders GK, Wegner DA: Sphingomyelinase deficiency (Niemann-Pick disease) in a Hereford calf. Vet Pathol **45:**201-202, 2008
11. Schuchman EH: The pathogenesis and treatment of acid sphingomyelinase-deficient Niemann-Pick disease. J Inherit Metab Dis **30:**654-663, 2007
12. Zachary JF: Nervous system. *In:* Pathologic Basis of Veterinary Disease, eds. McGavin MD, Zachary JF, 4th ed., pp. 928-930. Mosby Elsevier, St. Louis, MO, 2007

The Armed Forces Institute of Pathology
Department of Veterinary Pathology

Conference Coordinator:
Shannon Lacv. DVM. MPH

WEDNESDAY SLIDE CONFERENCE 2009-2010

Conference 8

19 November 2009

Conference Moderator:

Gary D. Coleman, DVM, PhD, Diplomate ACVP, Diplomate ACVPM

CASE I: A08-352 (AFIP 3133678).

Signalment: 5-year-old, male, intact Rhesus macaque (*Macaca mulatta*).

History: This macaque presented for necropsy at the end of an experiment investigating vaccine candidates for Simian Immunodeficiency Virus (SIV). The animal had been losing weight for the previous four months but was clinically unremarkable. Experimental manipulation included biweekly phlebotomy. Two years prior to necropsy, the animal had been vaccinated with an experimental vaccine and seven months prior to necropsy had been inoculated with SIVmac251.

Gross Pathology: The animal was thin with few fat reserves and the right atrium was moderately dilated. There was a moderate amount of serous pericardial effusion. The lungs were firm and failed to deflate upon opening the chest cavity.

Laboratory Results: Serial chemistry profiles were unremarkable.

Histopathologic Description: Labial mucosa: Multifocally submucosal nerves and hair follicles are partially to completely effaced by large aggregates of degenerate and non-degenerate neutrophils admixed with fewer histiocytes, lymphocytes and necrotic cellular debris (**fig. 1-1**). Frequently, histiocytes within the inflammatory infiltrate are enlarged and contain large, eosinophilic, intranuclear, round to ovoid, 10-20 µm diameter inclusion bodies and smaller eosinophilic intracytoplasmic inclusion bodies (**figs. 1-2 and 1-3**). Nerve fibers are completely effaced by the infiltrate and there is a dual loss of the myelin sheath and the axon. Inflammatory cells frequently infiltrate into the surrounding musculature. In these areas myofibers are variably swollen, hypereosinophilic and degenerate with sarcoplasmic vacuolation and loss of cross striations. Several large hair follicles are surrounded by a moderate amount of fibrosis and a similar neutrophilic and histiocytic infiltrate with frequent intracytoplasmic and rare intranuclear inclusion bodies. The inflammatory cells are especially abundant in the perifollicular tissue, but also are present through all layers of the hair follicle and are associated with moderate perifollicular hemorrhage and congestion.

*Sponsored by the American Veterinary Medical Association, the American College of Veterinary Pathologists, and the C. L. Davis Foundation.

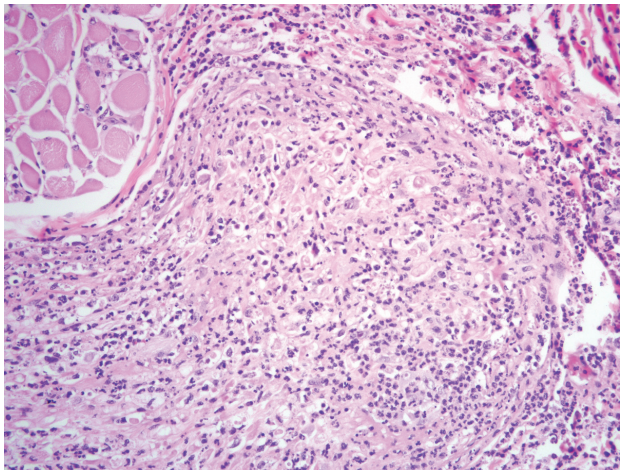

1-1. Lip, peripheral nerve, rhesus macaque. Separating and surrounding axons, expanding the perineurium, and infiltrating adjacent collagen and myocytes are high numbers of neutrophils and fewer histiocytes admixed with necrotic debris. Multifocally axon sheaths are swollen and degenerate. (HE 200X)

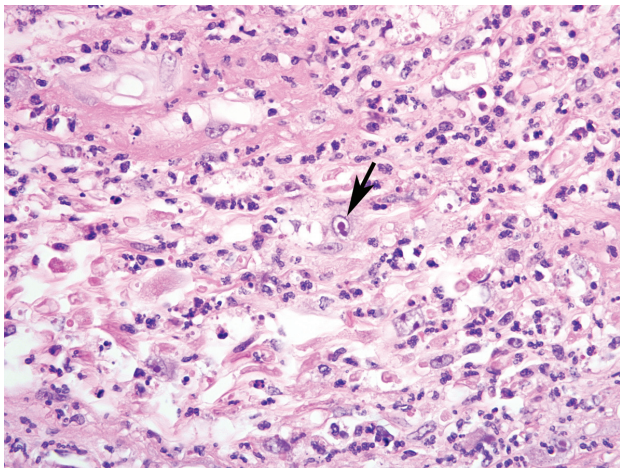

1-2. Lip, peripheral nerve, rhesus macaque. Multifocally, cells contain large lightly basophilic intranuclear inclusions that marginalize the chromatin (arrow). Multifocally there is axonal degeneration and abundant necrotic debris admixed with many neutrophils and histiocytes. (HE 400X)

Contributor's Morphologic Diagnosis: 1. Labial mucosa and haired skin: Severe, multifocal, subacute neutrophilic neuritis with cytomegaly and intrahistiocytic, intranuclear and intracytoplasmic herpetic inclusions (Cowdry type A).
2. Labial mucosa and haired skin: Severe, multifocal, subacute to chronic neutrophilic folliculitis with perifollicular fibrosis, cytomegaly, and intrahistiocytic, intranuclear and intracytoplasmic herpetic inclusions (Cowdry type A).

Contributor's Comment: Simian immunodeficiency virus (SIV) was first isolated in rhesus macaques at the New England Primate Research Center in 1985 and since then numerous strains of SIV which are endemic to different species of African monkeys have been identified. When these viruses are transmitted to Asian species they induce a disease similar to human AIDS, making the rhesus macaque model of SIV infection uniquely suited to studying HIV/AIDS pathogenesis.[2]

Common clinical and pathologic findings in SIV infected rhesus macaques include lymphadenopathy/lymphoma, chronic diarrhea and wasting, giant cell disease, pulmonary arteriopathy, viral associated dermatitis, and a wide spectrum of opportunistic infections. The most common opportunistic infectious agents in rhesus macaques progressing to AIDS include *Pneumocystis carinii, Mycobacterium avium* complex, *Trichomonas* sp., cytomegalovirus, adenovirus, *Cryptosporidium*, SV-40, *Candida* sp., and rhesus lymphocryptovirus.[10] Additionally, infections with *Enterocytozoon bienusi*, *Entamoeba, Giardia* and various alphaherpes viruses are also seen regularly.

Cytomegaloviruses (CMV) are host-specific beta-herpesviruses that frequently establish latent infections in both rhesus macaques and humans. In rhesus macaques, CMV seroprevalence approaches 100% by one year of age but there are generally no clinical or pathologic findings associated with infection in otherwise healthy individuals.[3,11] Transmission is thought to be through contact with virus shed in urine, saliva, and genital secretions which is similar to findings in humans. Unlike in humans, vertical transmission has not been documented, most likely due to near 100% seroprevalence with resultant high maternal antibodies and fetal protection.

With immune suppression, as occurs with AIDS, latent CMV becomes reactivated. It is the most common viral opportunistic infection identified and among the most common opportunistic infections overall in both rhesus macaques and man with isolation from the retina, gastrointestinal tract, lungs, and adrenal gland common in humans and gastrointestinal tract, lungs, central nervous system, liver and lymph nodes in macaques.[4,5]

Common gross pathologic features of cytomegalovirus infection depend on the organ involved. A common finding at the NEPRC is gastrointestinal pseudotumors which present as raised, red lesions multifocally throughout the small intestine.[7] Less common gross findings include multifocal interstitial pneumonia, necrotizing orchitis, and gastrointestinal ulceration. Histologically, lesions are

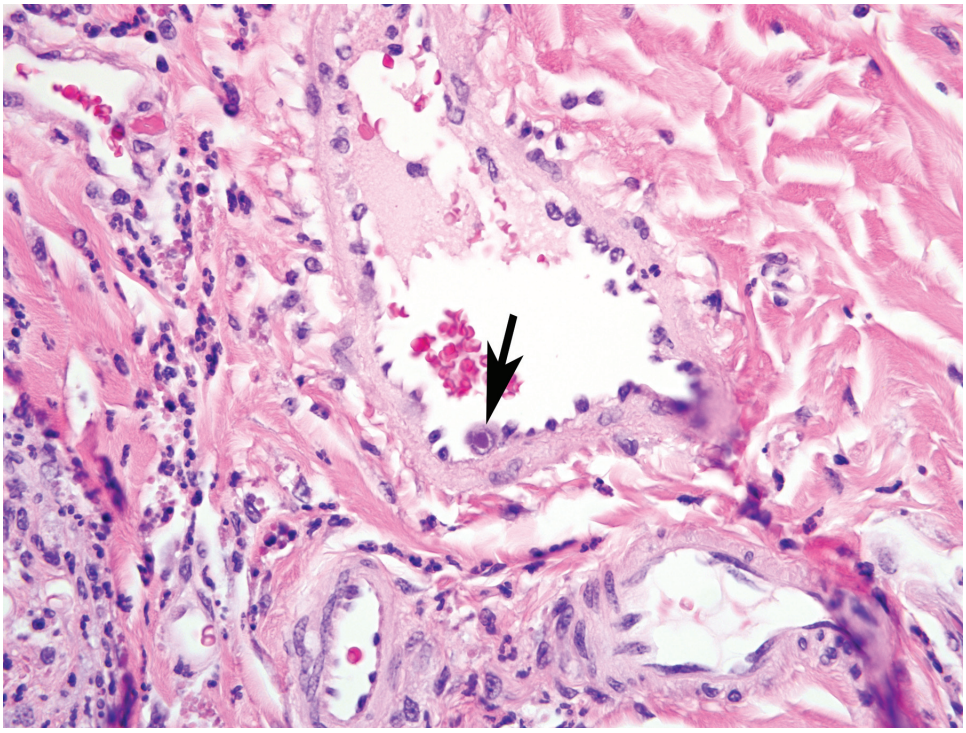

1-3. Lip, rhesus macaque. Rarely endothelial cells contain large lightly basophilic intranuclear inclusions which are surrounded by a clear halo and peripheralize the chromatin (arrow). (HE 400X)

frequently characterized by intense neutrophilic infiltrates admixed with fewer lymphocytes and plasma cells. Scattered throughout these areas there are frequently large intranuclear inclusion bodies, so-called "owl's eye cells" and also smaller intracytoplasmic inclusion bodies.

Unfortunately, these cells are not always present and as many as one half of infected animals may show varying degrees of pathology without characteristic inclusion bodies making immunohistochemistry important for definitive diagnosis of suspected cases. In fact, immunohistochemistry has shown that some animals with no underlying pathology have viral reactivation in multiple organs.[5]

In this case, the CMV-associated neuritis and folliculitis of the labial mucosa is quite striking. While not a common finding with CMV reactivation, neuritis is seen occasionally in rhesus macaques at the NEPRC and is most commonly seen in the labial and buccal mucosa. In humans, CMV optic neuritis and retinitis is a common finding. We have not previously identified folliculitis and this is an uncommon finding in humans as well.

AFIP Diagnosis: 1. Haired skin and mucocutaneous junction, lip: Polyneuritis, suppurative, acute, moderate, with axonal degeneration and intranuclear and intracytoplasmic eosinophilic and amphophilic inclusion bodies.
2. Haired skin and mucocutaneous junction, lip: Epidermal hyperplasia, focally extensive, moderate, with hyperkeratosis.

Conference Comment: The contributor provides an excellent synopsis of a unique presentation of CMV infection in this case, and conference participants used the discussion as a starting point to review the concepts of latency and recrudescence in herpesviral infection. Immunocompetent, asymptomatically-infected rhesus macaques expend substantial immunological resources to maintain a stable virus-host relationship, and possess high numbers of circulating CD4+ and CD8+ rhesus CMV-specific T cells in peripheral blood.[11] Like other herpesviruses, human CMV evades the immune system by downregulating MHC class I and II molecules, and producing homologues of MHC class I molecules, IL-10, and tumor necrosis factor (TNF) receptor.[6] Rhesus CMV has also been shown to encode inhibitors of natural killer cell function and class I MHC assembly and transportation, and homologues of cellular IL-10, a viral inhibitor of caspase activation, and a viral inhibitor of apoptosis.[11]

Participants briefly reviewed other cytomegaloviruses of importance in veterinary medicine, which are summarized in the table below:[1,8,9]

Cytomegaloviruses in Veterinary Species

Name	Virus Subfamily	Species Affected	Summary
Simian CMV (includes Rhesus CMV)	Betaherpesvirus	Rhesus macaque; other NHP have host-specific CMV	Seroprevalence nearly 100% in rhesus macaques; clinical disease occurs only with immunosuppression (SIV) or experimental manipulation
Caviid herpesvirus	Betaherpesvirus	Guinea pig	Subclinical infection is common; useful model of human CMV; typical "owl's eye" inclusions; targets are salivary gland, kidney, and liver
Murine CMV (Murid herpesvirus 1)	Betaherpesvirus	Mouse	BALB/c and A strain mice are susceptible; B6, B10, CBA, and C3H mice are resistant; disease occurs in immunocompromised mice; typical lesions are in salivary glands; persistent infections may cause immune complex glomerulitis
Rat CMV	Betaherpesvirus	Rat	Common in wild rats; nonexistent in laboratory rats; typical lesions in salivary and lacrimal glands with intranuclear and intracytoplasmic inclusions in ductal epithelium
Bovine herpesvirus 4	Gammaherpesvirus	Ox	Associated with "epivag" (i.e. vaginitis, salpingitis, oophoritis, or epidiymitis), pneumonia, enteritis, metritis, mammillitis, and abortion
Suid herpesvirus 2	Betaherpesvirus	Pig	Causes inclusion body rhinitis in neonates; infection in pregnant sows results in small litters, mummification, stillborith, or weak, premature offspring; typical cytomegaloviral inclusions in nasal mucosa, lung, or kidney, but not seen in the placenta
Equid herpesvirus 2	Gammaherpesvirus	Horse	Clinical significance unknown; has been identified in few cases of bronchointerstitial pneumonia in foals

The contributor's observation of inflammation involving the hair follicles was also discussed. Most conference participants interpreted the folliculitis as a secondary extension of the neurocentric inflammation into the sinus hairs, rather than primary folliculitis due to viral infection of hair follicles. When present, inflammation of the hair follicles was generally confined to well-innervated sinus hairs, and in less severely affected follicles, the inflammatory cells appeared to extend from the peripheral nerve into the stroma surrounding the adnexa.

Contributor: New England Primate Research Center, Harvard Medical School, One Pine Hill Dr., Southborough, MA 01772
http://www.hms.harvard.edu/nerprc/

References:

1. Caswell JL, Williams KJ: Respiratory system. *In:* Jubb, Kennedy, and Palmer's Pathology of Domestic Animals, ed. Maxie MG, 5th ed., vol. 2, p. 569. Elsevier Saunders, Philadelphia, PA, 2007

2. Geretti AM: Simian immunodeficiency virus as a model of human HIV disease. Rev Med Virol **9:**57-67, 1999
3. Ho M: The history of cytomegalovirus and its diseases. Med Microbiol Immunol **197:**65-73, 2008
4. Jellinger KA, Setinek U, Drlicek M, Bohm G, Steurer A, Lintner F: Neuropathology and general autopsy findings in AIDS during the last 15 years. Acta Neuropathol **100:**213-220, 2000
5. Kuhn EM, Stolte N, Matz-Rensing K, Mach M, Stahl-Henning C, Hunsmann G, Kaup FJ: Immunohistochemical studies of productive rhesus cytomegalovirus infection in rhesus monkeys (Macaca mulatta) infected with simian immunodeficiency virus. Vet Pathol **36:**51-56, 1999
6. McAdam AJ, Sharpe AH: Infectious diseases. *In:* Robbins and Cotran Pathologic Basis of Disease, eds. Kumar V, Abbas AK, Fausto N, Aster JC, 8th ed., pp. 353-355. Saunders Elsevier, Philadelphia, PA, 2010
7. Mohan H, Bal A, Garg S, Dalal U: Cytomegalovirus-associated pseudotumor simulating gastric malignancy in acquired immunodeficiency syndrome: a case report with review of literature. Jpn J Infect Dis **60:**134-136, 2007
8. Percy DH, Barthold SW: Pathology of Laboratory Rodents and Rabbits, 3rd ed., pp. 19-21, 127, 221-222. Blackwell Publishing, Ames, IA, 2007
9. Schlafer DH, Miller RB: Female genital system. *In:* Jubb, Kennedy, and Palmer's Pathology of Domestic Animals, ed. Maxie MG, 5th ed., vol. 3, pp. 528-529, 531-532. Elsevier Saunders, Philadelphia, PA, 2007
10. Simon MA, Chalifoux LV, Ringler DJ: Pathologic features of SIV-induced disease and the association of macrophage infection with disease evolution. AIDS Res Hum Retroviruses **8:**327-337, 1992
11. Yue Y, Barry PA: Rhesus cytomegalovirus a nonhuman primate model for the study of human cytomegalovirus. Adv Virus Res **72:**207-226, 2008

CASE II: T292/09 (AFIP 3134307).

Signalment: 4-year-old female German shorthaired pointer dog (*Canis familiaris*).

History: The dog was regularly used for hunting purposes. In January 2009 the owner noticed single coughing attacks after trailing a wounded animal. The next morning the dog showed apathy, inappetence and recurrent coughing attacks. Clinical observations revealed no other symptoms. Body temperature was normal. There were no abnormal auscultation findings of thorax and abdomen. Antibiotic therapy was initiated and the owner gave a cough syrup. In the evening the animal showed regurgitation of reddish-brown fluid, salivation and progressive deterioration with dyspnea. The dog was referred to a veterinary clinic immediately. There were no specific radiographic findings and bronchoscopy was inconclusive. The animal suddenly died 30 hours after the first attack of coughing. The clinicians suspected intoxication. Pseudorabies was discussed differentially but ruled out due to the lack of itch and other central nervous signs.

Gross Pathology: Unfortunately, the owner did not permit a full necropsy. However, the clinician collected samples of stomach and intestine and removed the brain for histology and/or toxicology 48 hours post mortem.

Histopathologic Description: Due to the suboptimal brain sampling, slides contain an angular section of cerebellum and brainstem. In the brain stem there is a moderate perivascular infiltration and cuffing composed of mononuclear cells (lymphocytes and macrophages) (**fig. 2-1**). Focally there are acute perivascular hemorrhages. Multifocally in the brainstem there are single degenerating neurons (dark neurons) and within the neuropil there are multifocal accumulations of activated microglial cells (rod cells, microgliosis) admixed with few infiltrating neutrophils (**fig. 2-2**). Single neurons and glial cells show intranuclear round eosinophilic inclusion bodies with chromatin margination. The cerebellum is unaltered. Immunohistochemically, porcine herpesvirus 1 antigen was detected within neurons and glial cells using the PAP method (**fig. 2-3**). Initially, using fresh material from intestine and brain, herpesvirus DNA was not detectable with PCR or in cell culture. In paraffin embedded material, using the gB-region in a nested PCR, porcine herpesvirus DNA was detectable.

Contributor's Morphologic Diagnosis: Cerebellum and brain stem: encephalitis, nonsuppurative, multifocal,

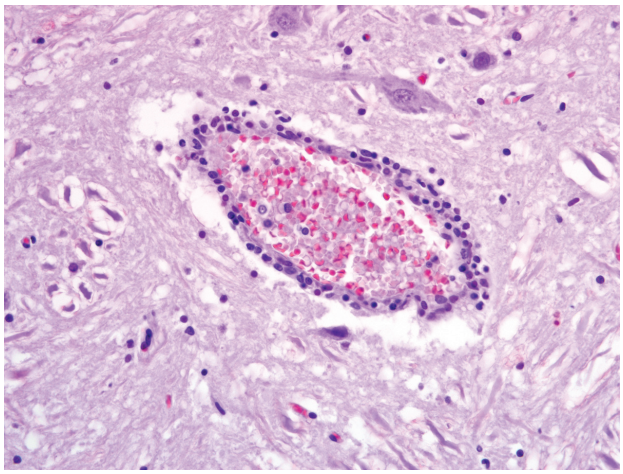

2-1. Brainstem, dog. Multifocally within the gray matter, Virchow-Robbins spaces contain moderate numbers of lymphocytes and fewer macrophages. (HE 400X)

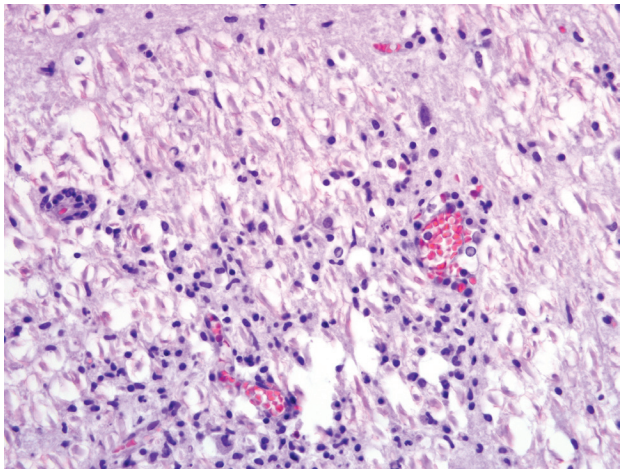

2-2. Brainstem, dog. Multifocally there are glial nodules, composed of reactive astrocytes and microglia and fewer lymphocytes. (HE 400X)

moderate with perivascular lymphohistiocytic cuffing, neuronal degeneration, microgliosis and perivascular hemorrhages; Aujeszky´s disease, pseudorabies; German shorthaired pointer dog (*Canis familiaris*).

Contributor's Comment: Pseudorabies, also known as Aujeszky´s disease, infectious bulbar paralysis or mad itch, is caused by suid herpesvirus 1, an alphaherpesvirus of the genus varicellovirus.[4] The disease was first described and its infectious cause identified by Aladár Aujesky (1896-1933), a Hungarian veterinary pathologist, in 1902. An interesting historical essay was published in 2003 by Köhler and Köhler.[3] Farm animals in many countries in Europe are free of the disease. But the increasing population of wild pigs in some areas (especially in Germany) serves as a reservoir and there is a general risk of transmission to livestock.[8] Suid herpesvirus was the object of intensive virological research in the past and the virus serves as model for other alphaherpesvirus infections and for developing marker vaccines and DNA vaccines.[2,5,7,9] The typical clinical symptom in animals other than pigs is intense pruritus at the locus of inoculation and the outcome is lethal in nonnative hosts. Dogs can be infected by ingestion of raw meat from infected pigs (farm or wild pigs) or percutaneously (bites, trauma). The virus spreads centripetally after inoculation along nerves to the spinal ganglia and the central nervous system.[4] Symptoms in dogs are similar to rabies but the clinical course is much shorter. Gross lesions are limited to self trauma due to severe itching.[4] Histologically, nonsuppurative encephalitis with gliosis and ganglioneuritis (e.g. trigeminal or spinal ganglia) can be found. Typical herpesvirus inclusion bodies can be found in neurons and glial cells. Virus antigen can be detected immunohistochemically on paraffin-embedded formalin-fixed material.[4]

The clinical course in the present case was very rapid (only 30 hours) with early lethal outcome. Contact of the dog with a wild pig or blood and/or carcasses of hunted wild pigs can be presumed. Due to the coughing attacks as the predominant symptoms, inhalation as possible route of infection can be discussed. Unfortunately, lung material was not submitted for examination. Stomach and intestine were unaltered. Virus antigen could not be detected immunohistochemically within tissues other than the brain.

AFIP Diagnosis: Brainstem: Encephalitis, non-suppurative, multifocal, mild to moderate, with gliosis.

Conference Comment: Participants readily attributed the striking nonsuppurative encephalitis in this case to a viral etiology; however, nonsuppurative inflammation in the central nervous system (CNS) is not entirely specific for viral infections, with salmonellosis in pigs and neorickettsial infection (i.e. "salmon poisoning") in dogs being notable examples of non-viral causes of nonsuppurative CNS inflammation.[4] There was variation with respect to the presence of intranuclear inclusion bodies and scattered neuronophagia, and most participants developed a differential diagnosis that included several viral etiologies. Many conference participants suspected canine morbillivirus as the etiology; however, this case lacks the characteristic morbilliviral intracytoplasmic and intranuclear viral inclusions, which are generally detectable in astrocytes, and occasionally ependymal

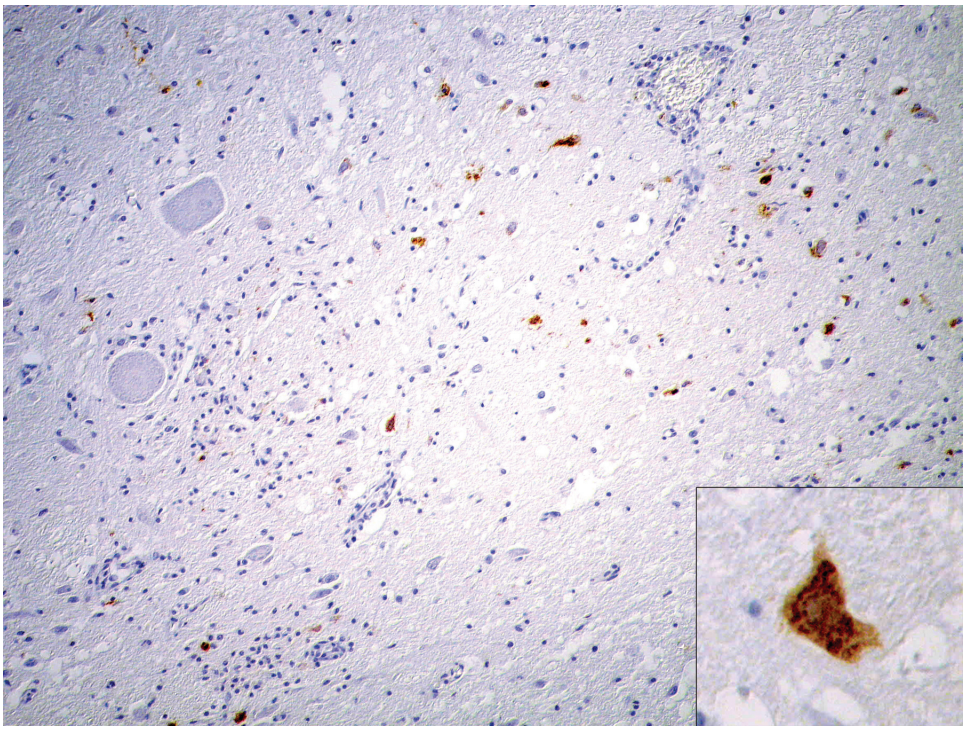

2-3. Brainstem, dog. Neurons and glial cells are immunohistochemically positive for porcine herpesvirus 1 antigen. Photomicrograph courtesy of Institute for Veterinary Pathology, University of Giessen, Frankfurter Str. 96, 35392 Giessen, Germany, kernt.koehler@vetmed.uni-giessen.de

cells and neurons, in dogs with canine distemper virus infection. In early canine distemper, lesions include demyelination, status spongiosus, astrocytic hypertrophy and hyperplasia, and variable syncytial cell formation, all of which are lacking in this case. In late-stage canine distemper, lesions include nonsuppurative perivascular cuffing, leptomeningitis, and choroiditis, with occasional gitter cells, and most participants who favored a diagnosis of distemper specifically favored "old dog encephalitis" associated with distemper.[4] Other viral etiologies considered by conference participants included rabies and the arboviruses.

Pseudorabies is an unusual alphaherpesvirus in that it is proficient in interspecies transmission. Conference participants briefly discussed two other closely-related alphaherpesviruses that share this capability: human herpesvirus-1 (HHV-1, herpes simplex virus) and cercopithecine herpesvirus-1 (herpes B virus, BV). Humans are the primary hosts of HHV-1, with a seroprevalence of approximately 80%. Infection in humans is generally mild, characterized by labial, oral, and ocular lesions, with encephalitis being a rare consequence of centripetal infection through the olfactory, optical, or trigeminal nerves. However, rabbits are exquisitely sensitive to HHV-1, where the virus is exclusively neurotropic and almost invariably fatal. Less susceptible species include rats, mice, and chinchillas.[6] An analogous situation exists with BV, which is endemic in macaques and a seroprevalence of 80-100% in most populations. Following initial replication in mucosal epithelial cells, the virus is transmitted by axonal transport to dorsal root ganglia, where it establishes latency characterized by a lack of viral replication and a limited pattern of transcription. Episodes of recrudescence are generally asymptomatic, or less frequently cause oral herpetic lesions. Humans, by contrast, are exquisitely sensitive to BV, with infection being almost uniformly fatal in the absence of early treatment with antiviral therapy.[1] Other alphaherpesviruses of veterinary importance were briefly reviewed in WSC 2009-2010, Conference 5, case II.

Contributor: Institut für Veterinaer-Pathologie, Universitaet Giessen, Frankfurter Str. 96, 35392 Giessen, Germany
http://www.uni-giessen.de/cms/fbz/fb10/institute klinikum/institute/pathologie

References:

1. Barry P, Marthas M, Lerche N, McChesney MB, Miller CJ: Virology research. *In:* The Handbook of Experimental Animals: The Laboratory Primate, eds. Wolfe-Coote S, Bullock G, Petrusz P, pp. 572-573, Elsevier Academic Press, San Diego, CA, 2005
2. Ekstrand MI, Enquist LW, Pomeranz LE: The alpha-

herpesviruses: molecular pathfinders in nervous system circuits. Trends Mol Med. **14:**134-40, 2008
3. Köhler M, Köhler W: Zentralblatt für Bakteriologie--100 years ago Aladár Aujeszky detects a 'new' disease--or: it was the cow and not the sow. Int J Med Microbiol **292:**423-427, 2003
4. Maxie MG, Youssef S: Nervous system. *In:* Jubb, Kennedy, and Palmer's Pathology of Domestic Animals, ed. Maxie MG, 5th ed., vol. 1, pp. 411, 416-417, 432-433. Elsevier Saunders, Philadelphia, PA, 2007
5. Mettenleiter TC: Aujeszky's disease (pseudorabies) virus: the virus and molecular pathogenesis--state of the art. Vet Res **31:**99-115, 2000
6. Müller K, Fuchs W, Heblinski N, Teifke JP, Brunnberg L, Gruber AD, Knopfleisch R: Encephalitis in a rabbit caused by human herpesvirus-1. J Am Vet Med Assoc **235:**66-69, 2009
7. Pomeranz LE, Reynolds AE, Hengartner CJ: Molecular biology of pseudorabies virus: impact on neurovirology and veterinary medicine. Microbiol Mol Biol Rev **69:**462-500, 2005
8. Ruiz-Fons F, Vidal D, Höfle U, Vicente J, Gortázar C: Aujeszky's disease virus infection patterns in European wild boar. Vet Microbiol **120:**241-50, 2007
9. Zuckermann FA: Aujeszky's disease virus: opportunities and challenges. Vet Res **31:**121-31, 2000

CASE III: 08N592 (AFIP 3134541).

Signalment: Four 5-week-old, cross-bred pigs (*Sus scrofa*).

History: The pigs were weaned two weeks previously, and treated with ivermectin at weaning. About 20 pigs died in a herd of 200 animals.

Gross Pathology: All four pigs had a generalized, greasy, moist appearance on the skin with multifocal crusting (**fig. 3-1**). Multifocally, there were multiple, raised, circular, crusty lesions (0.5-2.0 cm in diameter) around the eyes, and on the snout, chin, thorax, abdomen and legs (**figs. 3-2 and 3-3**). Exudate matted the eyes of one pig closed. There was mild separation of the hooves and erosions were present on the coronary bands.

Laboratory Results: **Bacteriology:** *Staphylococcus hyicus* was cultured from multiple skin samples. **Virology:** Swinepox virus was identified with electron microscopy from the circular, raised lesions.

Histopathologic Description: Multifocally, the epidermis is ulcerated with an overlying serocellular crust composed of neutrophils, fibrin, and serous proteinaceous material admixed with numerous colonies of bacterial cocci; additionally, there are frequent intracorneal pustules composed of degenerate neutrophils that expand the stratum corneum (**figs. 3-4, 3-5, and 3-6**). The epidermis in intact areas is multifocally, moderately hyperplastic with prominent rete pegs, and there are frequent neutrophils noted in exocytosis across the epithelial surface. Multiple follicular lumina are also filled with numerous degenerate neutrophils with occasional eosinophils. Multifocally, epithelial cells exhibit ballooning degeneration or hydropic change and contain occasional 5-7 µm diameter, eosinophilic, intracytoplasmic inclusion bodies (poxviral inclusions) (**fig. 3-7**). There are occasional apoptotic cells scattered throughout the epidermis and follicular epithelium characterized by shrunken, hypereosinophilic cells with pyknotic or karyorrhectic nuclei. The dermis subjacent to the ulcerated areas is heavily infiltrated by lymphocytes, plasma cells, histiocytes, and scattered neutrophils with frequent fibroblasts and small capillaries (granulation tissue).

Contributor's Morphologic Diagnosis: 1. Skin: dermatitis, proliferative and ulcerative, multifocal severe, with ballooning degeneration, granulation tissue, and intracytoplasmic eosinophilic inclusion bodies, porcine (*Sus scrofa*).
2. Skin: epidermitis and folliculitis, suppurative (exudative), multifocal to coalescing, severe, with numerous bacterial cocci colonies, porcine (*Sus scrofa*).

Contributor's Comment: Greasy pig disease, or exudative epidermitis, is caused by *Staphylococcus hyicus*, a gram positive bacterium. The disease occurs most commonly following introduction of carrier animals into a naïve herd.[12] The pathogenesis of exudative epidermitis is not completely known; however, trauma from fighting, unclipped teeth, rough bedding, or other factors leading to exposure of the dermis may allow the bacteria to establish the infection.[6,12] Initially, there is reddening of the skin with multiplication of bacteria on skin surface and growth between keratinocytes. In infected skin, there is generally marked inflammation with hyperplasia of the stratum corneum and neutrophilic infiltration followed by epidermal erosion.[12] The most important factor in pathogenesis of infection is the production of exfoliative toxins. The exfoliative toxins are known as: ExhA, ExhB, ExhC, ExhD, SHETA and SHETB.[3,10] Exudative epidermitis is regarded as a porcine homologue of Staphylococcal Scalded Skin Syndrome (SSSS) or bullous impetigo in

3-1. Haired skin, pig. There is generalized, greasy, moist skin with multifocal crusting. Photograph courtesy of Louisiana State University, School of Veterinary Medicine, Dept. of Pathobiological Sciences, Baton Rouge, LA 70803, dcho@vetmed.lsu.edu

humans. SSSS results in loss of keratinocyte cell-to-cell adhesion and leads to blister formation.[9] The virulent strains of *S. aureus* produce exfoliative toxins, namely ETA, ETB and ETD.(1) It has been reported that these toxins are glutamate specific serine proteases that cleave a single peptide bond in the extracellular region of human and mouse desmoglein (Dsg) 1.[2] In human epidermis, Dsg1 and Dsg3 are present predominantly in stratified squamous epithelium.[11] Recent studies have suggested that pathophysiological mechanisms of intraepidermal splitting in exudative epidermitis are similar to human SSSS by cleavage of Dsg1.[5,8,9] The detailed differential list for exudative epidermitis has already been described in WSC 2008-2009, Conference 9, case I.

Swine pox is a typical poxvirus primarily affecting young pigs and lesions are usually confined to the ventrolateral abdomen.[3] Transmission is typically through direct contact, although lice (*Haematopinus suis*) and other blood-sucking insects can be an important means of transmission in swine herds as well.[3] Lesions follow the typical pox progression: erythematous macules becoming papules, then vesicles progressing to pustules, leading to rupture and crust formation.[3] Differentials for swine pox must include other vesicular diseases, sarcoptic mange, and erysipelas.[3] Swinepox virus is the sole member of the *suipoxvirus* genus and is morphologically similar to vaccinia virus; it has a double-stranded DNA genome of 146 kilobase pairs and 150 predicted genes.[4] Following an abrasion to the skin, swinepox may enter the host and preferentially replicates in epidermal keratinocytes of the stratum spinosum; replication occurs exclusively in the cytoplasm, as indicated by the intracytoplasmic inclusion bodies.[4]

In this case, the swine pox infection was likely the predisposing factor leading to the staphylococcal infection. In addition to the skin lesions in these cases, there was evidence of embolic showering of bacteria within the lungs and lymph nodes with suppurative inflammation in all pigs examined (evidence for systemic infection). Therefore, the cause of death in these pigs appears to be sepsis secondary to epidermal infection with *Staphylococcus hyicus*, made possible by the ulcerative lesions caused by the poxviral infection.

AFIP Diagnosis: Haired skin: Dermatitis, proliferative and necrosuppurative, chronic, diffuse, marked, with epidermitis, folliculitis, and many cocci.

Conference Comment: During the conference, the moderator highlighted that the presence of many

3-2, 3-3. Haired skin, pig. Multifocally there are multiple raised, circular, crusty lesions on the snout, chin, thorax, abdomen, and legs. Photograph courtesy of Louisiana State University, School of Veterinary Medicine, Dept. of Pathobiological Sciences, Baton Rouge, LA 70803, dcho@vetmed.lsu.edu

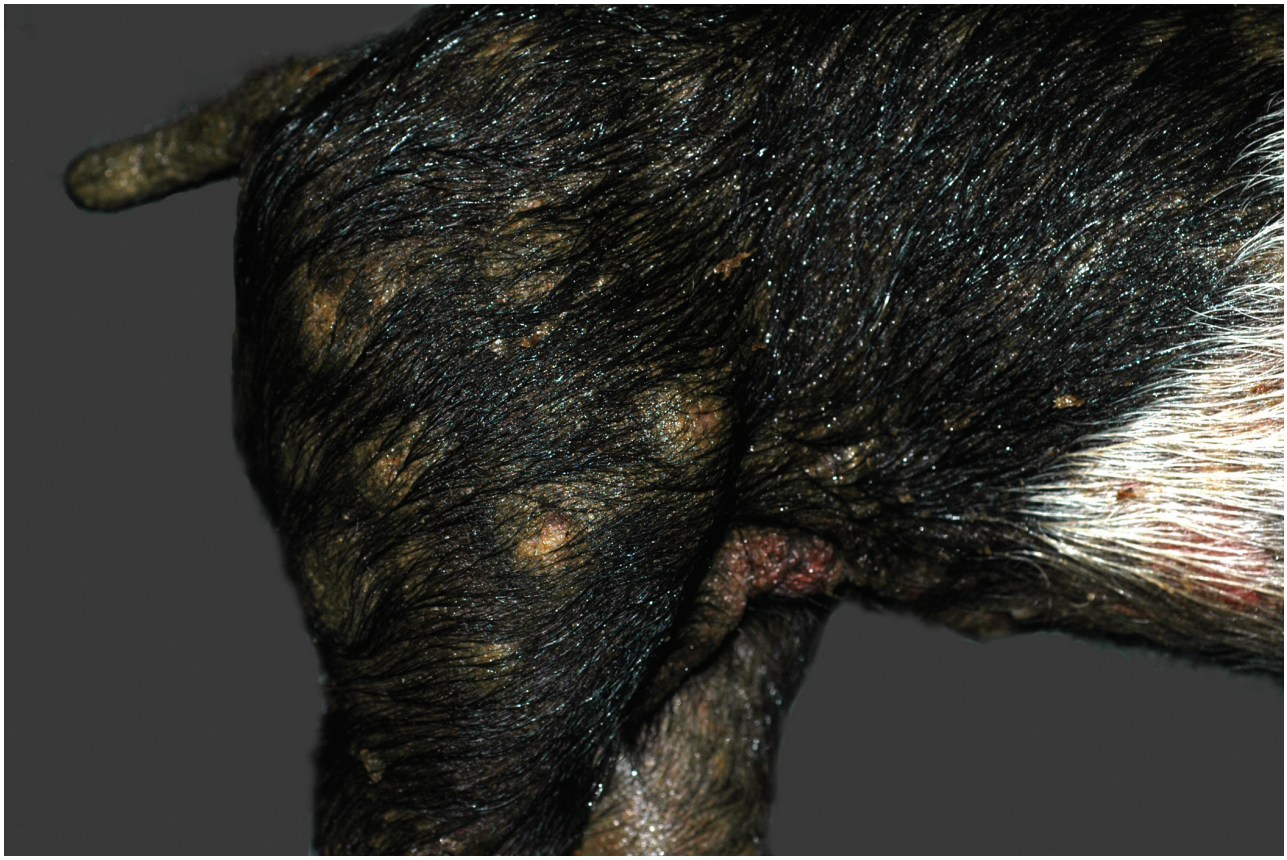

acantholytic keratinocytes in this case is reminiscent of the autoimmune condition of pemphigus foliaceus. This observation is meaningful in light of the contributor's comments concerning the pathogenesis of staphylococcal cutaneous infections, and this case provides an exquisite example of two diseases sharing a common molecular link, i.e. desmogleins as the target of bacterial toxins and autoantibodies, resulting in histomorphological similarities. As noted by the contributor, Dsg1 and Dsg3 are both components of desmosomes, but differ with respect to their histologic distributions within the epidermis and anatomic locations. The Dsg1 protein, the target of autoantibodies in pemphigus foliaceus, is most abundant in the superficial layers of the epidermis and is scarce in oral

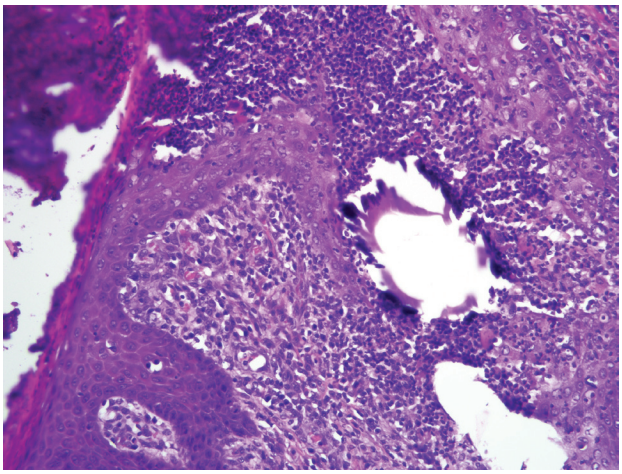

3-4. Haired skin, pig. Within the epidermis, dermis, and hair follicle epithelium are numerous pustules containing many degenerate neutrophils, with overlying parakeratotic and orthokeratotic hyperkeratosis. (HE 400X)

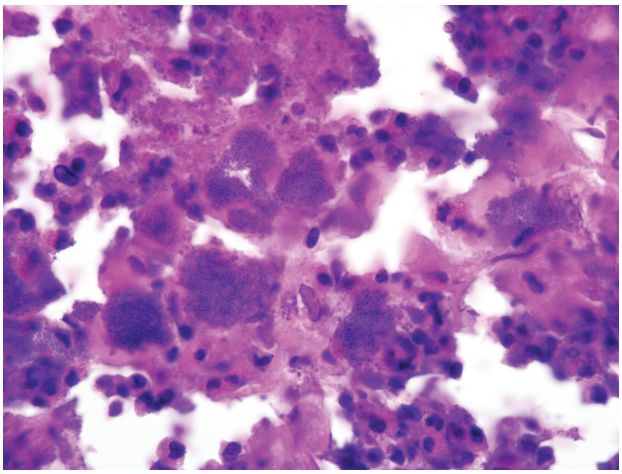

3-5. Haired skin, pig. Within the degenerate hair follicle are numerous aggregates of neutrophilic inflammation and necrotic cellular debris which center upon large colonies of 2um diameter basophilic cocci. (HE 1000X)

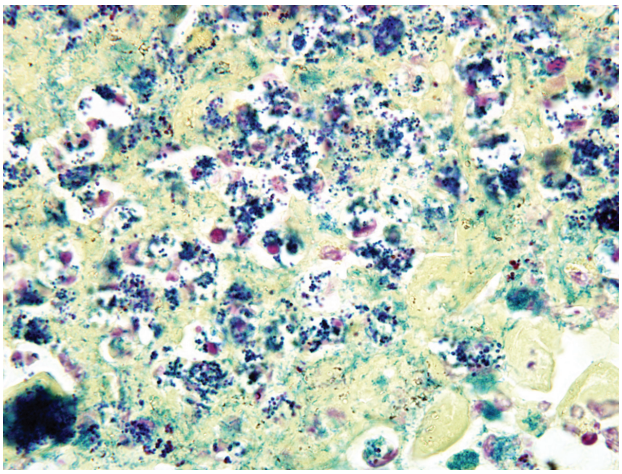

3-6. Haired skin, pig. Large colonies of cocci are gram positive. (B&B 1000X)

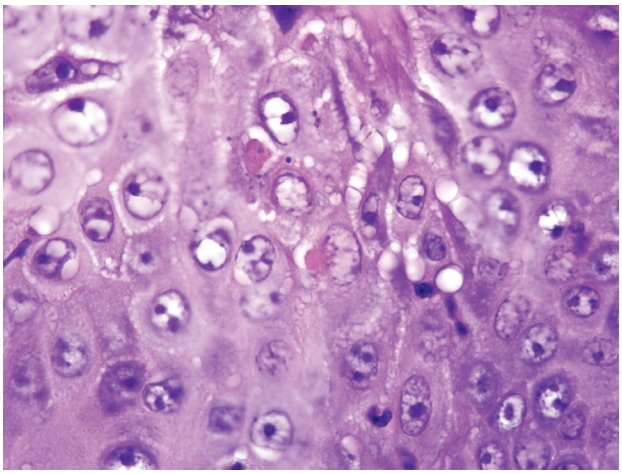

3-7. Haired skin, pig. Rarely epithelial cells contain large eosinophilic cytoplasmic viral inclusions and nuclear chromatin of affected cells is peripheralized. (HE 1000X)

mucosa, which accounts for the characteristic histologic pattern of acantholytic subcorneal and intragranular pustular dermatitis and an absence of oral lesions in the disease. The Dsg3 protein is more abundant in the basal layers of the epidermis and oral mucosa and, along with Dsg1, is targeted by autoantibodies in pemphigus vulgaris thus explaining the characteristic suprabasilar clefting in the epidermis and lesions found in the oral mucosa.[7]

There is substantial slide variation with respect to the ballooning degeneration and poxviral inclusions described by the contributor. Most conference participants' slides lacked this feature or had only rare examples. This variation is not surprising given that the submission consisted of samples from multiple animals. The contributor provided a succinct review of swinepox, and readers are referred to WSC 2009-2010, Conference 5, case II for additional discussion regarding poxviruses.

Contributor: Louisiana State University, School of Veterinary Medicine, Baton Rouge, LA 70803
http://www.vetmed.lsu.edu/pbs

References:

1. Amagai M, Matsuyoshi N, Wang ZH, Andl C, Stanley JR: Toxin in bullous impetigo and staphylococcal scalded-skin syndrome targets desmoglein 1. Nat Med **6:**1275-1277, 2000

Sugai M, Stanley JR: Staphylococcal exfoliative toxin B specifically cleaves desmoglein 1. J Invest Dermatol **118:**845-850, 2002
3. Andresen L, Bille-Hansen V, Wegener H: *Staphylococcus hyicus* exfoliative toxin: purification and demonstration of antigenic diversity among toxins from virulent strains. Microb Pathog 2**2:**113-122, 1998
4. Cameron R: Diseases of the skin. *In:* Diseases of Swine, eds. Straw BE, Zimmerman J, D'Allaire S, Taylor D, 9th ed., pp. 179-198. Blackwell Publishing, Ames, IA, 2006
5. Delhon G, Tulman E, Afonso C, Rook DL: Swine pox. *In:* Diseases of Swine, eds. Straw BE, Zimmerman J, D'Allaire S, Taylor D, 9th ed., pp. 483-487. Blackwell Publishing, Ames, IA, 2006
6. Fudaba Y, Nishifuji K, Andresen LO, Yamaguchi T, Komatsuzawa H, Amagai M, Sugai M: *Staphylococcus hyicus* exfoliative toxins selectively digest porcine desmoglein 1. Microb Pathog **39:**171-176, 2005
7. Ginn PE, Mansell JEKL, Rakich PM: Skin and appendages. *In:* Jubb, Kennedy, and Palmer's Pathology of Domestic Animals, ed. Maxie MG, 5th ed., vol. 1, pp. 647-650. Elsevier Saunders, Philadelphia, PA, 2007
8. Nishifuji K, Fudaba Y, Yamaguchi T, Iwasaki T, Sugai M, Amagai M: Cloning of swine desmoglein 1 and its direct proteolysis by *Staphylococcus hyicus* exfoliative toxins isolated from pigs with exudative epidermitis. Vet Dermatol **16:**315-323, 2005
9. Nishifuji K, Sugai M, Amagai M: Staphylococcal exfoliative toxins: "molecular scissors" of bacteria that attack the cutaneous defense barrier in mammals. J Dermatol Sci **49:**21-31, 2008
10. Sato H, Watanabe T, Higuchi K, Teruya K, Ohtake A, Murata Y, Saito H, Aizawa C, Danbara H, Maehara N: Chromosomal and extrachromosomal synthesis of exfoliative toxin from *Staphylococcus hyicus*. J Bacteriol **182:**4096-4100, 2000
11. Shirakata Y, Amagai M, Hanakawa Y, Nishikawa T, Hashimoto K: Lack of mucosal involvement in pemphigus foliaceus may be due to low expression of desmoglein 1. J Invest Dermatol **110:**76-78, 1998
12. Wegener H, Skov-Jensen E: Exudative epidermitis. *In:* Diseases of swine, eds. Straw B, Zimmerman J, D'Allaire S, Taylor D, 9th ed., pp. 675-679. Blackwell Publishing, Ames, IA, 2006

CASE IV: 07-684-5 (AFIP 3136053).

Signalment: 5-year-old spayed female golden retriever dog (*Canis familiaris*) weighing 30.9 kg.

History: The dog, who lived in the northeastern United States, initially presented to the referring veterinarian for a two-week history of vomiting, decreased appetite, polydipsia, and lethargy.

Gross Pathology: Both kidneys were reniform in shape with smooth capsular surfaces and diffusely pale tan cortices; medullae were diffusely bulging on cut section. There was marked perirenal edema and subcutaneous tissues were severely edematous. Hematomas were present in the right retroperitoneal space and ventral abdominal midline. Parathyroid glands were enlarged bilaterally (5 x 3 x 0.5 mm and 6 x 3 x 1 mm).

Laboratory Results: **Hematocrit:** 17.4 (37-55%). **Reticulocyte count:** 15,750 (>60,000 indicates regeneration). **Serum biochemistry**: BUN 70 (7-27 mg/dl), creatinine 4.9 (0.4-1.8 mg/dl), phosphorous 16.1 (2.1-6.3), total protein 4.1 (5.1-7.8 g/dl), albumin 1.0 (2.3-4.0 g/dl). **Urinalysis:** urine protein 1,253 (10-50 mg/dl), creatinine 76.8 (100-500 mg/dl), protein/creatinine ratio 16.3 (<0.5). Urine culture: no growth. **Coagulation profile:** normal PT 7.5 (6.8-10.2 s), slightly prolonged PTT 16.9 (10.7-16.4 s), increased d-dimers 0.28 (<0.2 ug/ml), and decreased platelets 49 (177-398 x 10^3/ul), consistent with disseminated intravascular coagulation. **Serology:** negative for *Rickettsia rickettsii, Bartonella* spp., *Ehrlichia canis, Anaplasma* spp., *Dirofilaria immitis*, and *Leptospira* spp.; positive for *Borrelia burgdorferi* (Idexx SNAP® 4Dx® test).

Histopathologic Description: Kidney: Diffusely throughout the cortex, glomerular tufts and capillary walls are thickened by hyaline, eosinophilic material, with increased cells in the glomeruli. The parietal epithelium is hypertrophied; often there are synechiae between glomerular tufts and Bowman's capsule (**fig. 4-1**). Occasional glomerular capillaries contain fibrin thrombi. The urinary space occasionally contains cellular and rarely mineralized debris and hyaline to globular proteinaceous material. Bowman's capsule is moderately thickened by hyaline to fibrillar eosinophilic material and surrounded by fibrosis (**fig. 4-2**). Tubules throughout the cortex and medulla are moderately ectatic and contain eosinophilic stippled proteinaceous material, protein casts, occasional sloughed epithelial cells, and rare crystals.

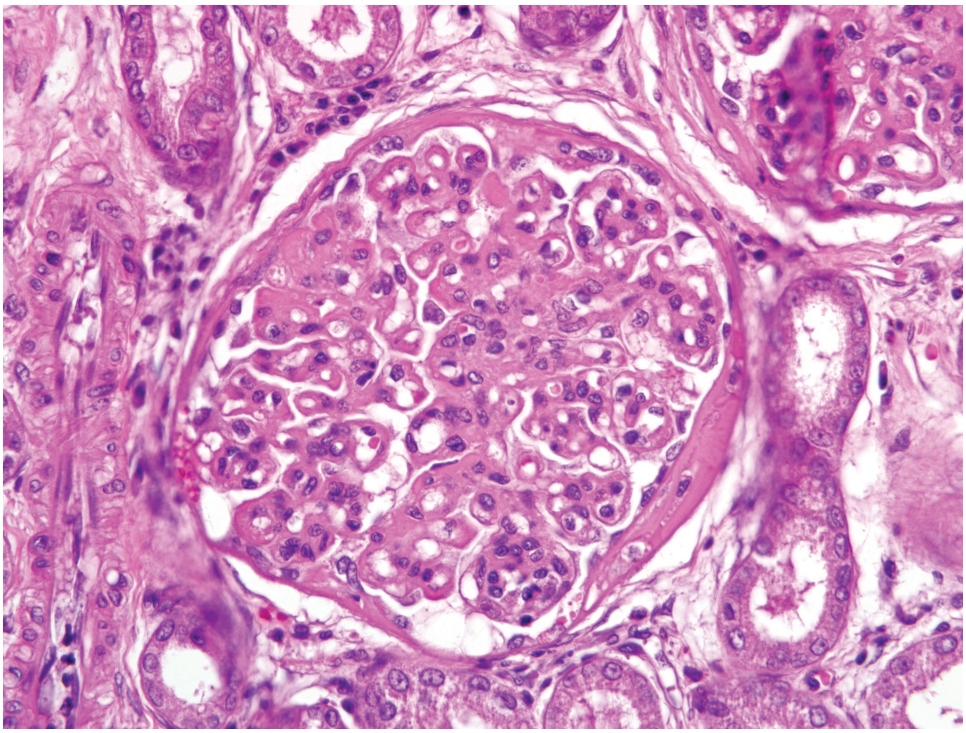

4-1. Kidney, dog. Diffusely and globally, glomeruli have increased cellularity, increased thickness of mesangium, thickened capillary loops, periglomerular fibrosis, hyperplasia of the parietal epithelium with multifocal synechia, and occasional necrotic cells within the glomerular tuft. (HE 400X)

Tubules multifocally contain individual cells with brightly eosinophilic cytoplasm and pyknotic nuclei (necrosis), and are lined by thin, attenuated epithelium, cuboidal epithelial cells with swollen, vacuolated cytoplasm, or by epithelial cells with basophilic cytoplasm, increased nuclear to cytoplasmic ratio and rare mitoses (regeneration) (**fig. 4-3**). Occasional tubules are mineralized. Multifocally, tubular epithelial cells contain small amounts of brown globular cytoplasmic pigment. The interstitium is multifocally infiltrated by small numbers of plasma cells, lymphocytes, and fewer macrophages and neutrophils. Occasional hilar arterioles have walls expanded by acellular hyaline eosinophilic material with narrowing of the arteriole lumen. Occasionally there is proliferation of small arterioles within the cortical interstitium.

Contributor's Morphologic Diagnosis: Kidneys: Moderate diffuse global membranoproliferative glomerulonephritis with tubular necrosis, regeneration, luminal protein casts, tubular mineralization, multifocal chronic lymphoplasmacytic tubulointerstitial nephritis, and glomerular fibrin thrombi.

Contributor's Comment: The glomerular, tubular, and interstitial changes are consistent with a histologically and clinically unique renal syndrome in dogs associated with infection by the spirochete, *Borrelia burgdorferi*. Golden and Labrador retriever dogs are more likely to develop Lyme nephritis than the general canine population.[2] This syndrome is characterized clinically by a protein-losing nephropathy, the presence of serum antibodies to *B. burgdorferi*, and rapidly progressive fatal renal failure in dogs in Lyme endemic areas.

Diagnosis of infection can be determined by a commercially available enzyme-linked immunosorbent assay (ELISA) that does not react to commercially available Lyme borreliosis vaccines.[8] This ELISA detects the C_6 peptide derived from a conserved immunodominant region (IR_6) of a segment of a *B. burgdorferi* surface protein named VlsE (Vmp-like sequence, expressed).[8] Alternatively, Western blot may be used to distinguish between natural and vaccine exposure in dogs by detecting antibodies to OspA or OspB.[3] Minimal evidence exists to support the presence of *B. burgdorferi* or other bacterial organisms in the kidneys of affected dogs; rare spirochetes have been seen in silver stains.[4] *B. burgdorferi* DNA is rarely amplified by PCR in renal tissue from affected dogs, and often *B. burdorferi* antigen is not detected by immunohistochemical staining.[1] It is thought that the lesions seen in Lyme nephritis are due to a sterile immune complex disease.

The most common glomerular lesion in Lyme nephritis is membranoproliferative glomerulonephritis, with adhesions of glomerular tufts to Bowman's capsule, and often periglomerular fibrosis of Bowman's capsule. The membranous component is the result of immune mediated glomerulonephritis with subendothelial deposits, IgG, IgM,

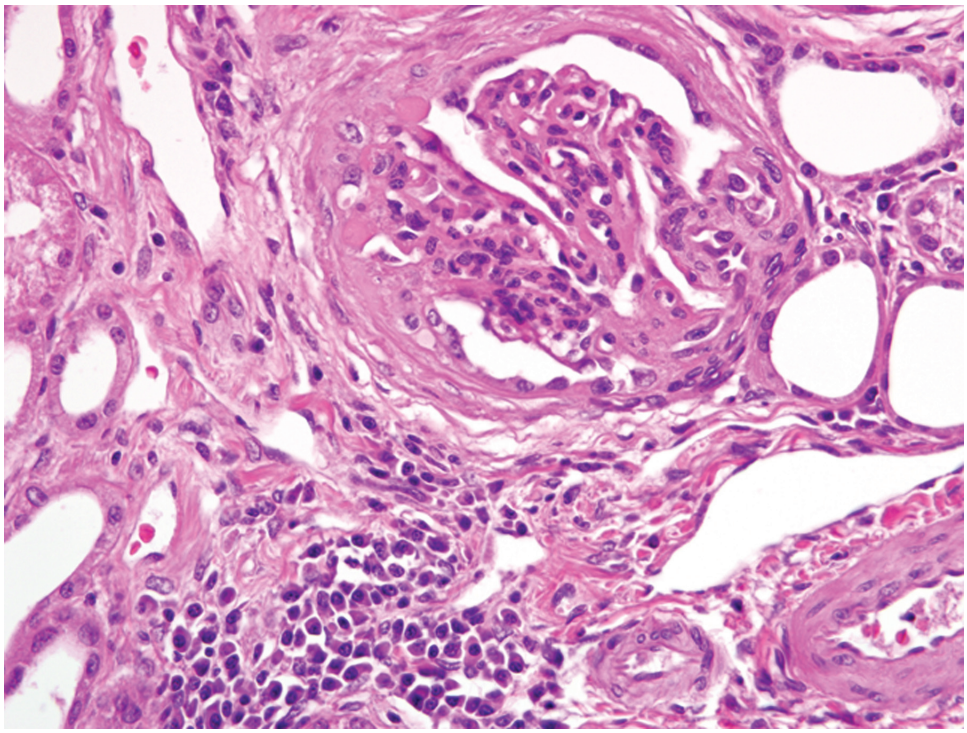

4-2. Kidney, dog. Multifocally the cortical interstitium is mildly expanded by low numbers of lymphocytes and plasma cells. Occasional glomeruli are sclerotic. (HE 400X)

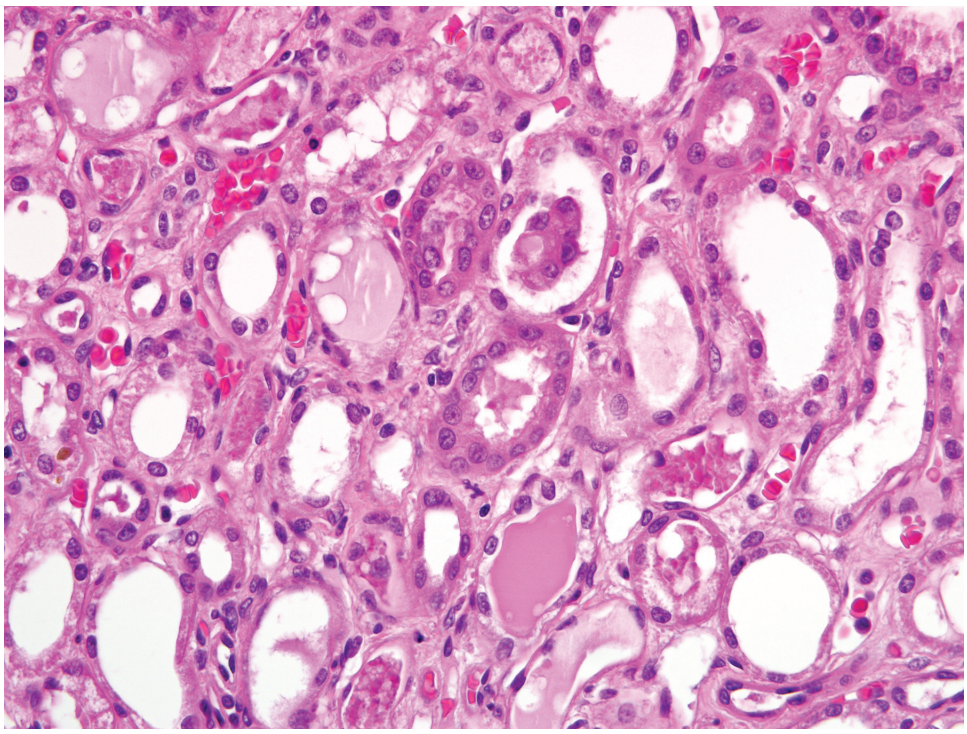

4-3. Kidney, dog. Multifocally tubular epithelium is degenerate, necrotic, or regenerative, and there is often an eosinophilic proteinaceous material within tubular lumina. (HE 400X)

and C3 present along glomerular basement membranes. The proliferative component is due to increased mesangial cell number and influx of inflammatory cells (macrophages and neutrophils). The severe, diffuse glomerular lesions are likely the primary lesion and responsible for subsequent tubular changes including multifocal dilation with necrosis and regeneration. Tubular damage most likely results from cellular hypoxia and/or nephrotoxin exposure due to

profound proteinuria; damaged tubules express vimentin. Interstitial fibrosis is often present to some degree, and mild to moderate lymphoplasmacytic inflammation is present throughout the cortex. Arteriolar changes are occasionally noted and include fibrinoid necrosis of small to medium arterioles or deposition of PAS-positive hyaline material in hilar arteriolar walls, lesions commonly associated with renal disease-induced hypertension.[2]

B. burgdorferi is transmitted by *Ixodes* spp. ticks, which may feed on and cause disease in several species including dogs, horses, cattle, cats and people. The most common manifestation of disease in dogs is polyarthritis, with fewer cases of nephritis, and one case report of myocarditis.[5,9] In addition to arthritis, horses may also develop ocular disease and probably encephalitis, and abortions may be seen in cattle. The tick vector for *B. burgdorferi* has a two-year life cycle. Larvae and nymphs primarily feed on birds and small mammals; the main mammalian host is the white footed mouse and deer mouse (*Peromyscus* spp.). Adults primarily feed on white-tailed deer (*Odocoileus virginianus*), which are asymptomatic carriers. Adult ticks must attach to the host for a minimum of 24 hours in order to transmit the bacterium. Deer flies and horse flies may act as mechanical vectors in areas where infection is well maintained in the wildlife population by tick vectors.[9]

AFIP Diagnosis: Kidney: Glomerulonephritis, membranoproliferative and fibrinous, global, diffuse, marked, with synechiae, tubular degeneration, necrosis, regeneration, and proteinosis, and mild multifocal lymphoplasmacytic cortical interstitial nephritis.

Conference Comment: The clinical history of relatively acute onset of renal failure, laboratory evidence of Borrelia burgdorferi infection, and the distinctive histologic feature of extensive tubular necrosis with concurrent membranoproliferative glomerulonephritis and interstitial nephritis are consistent with canine Lyme nephritis in this dog. The contributor provides an outstanding description of this renal syndrome of suspected sterile immune complex disease. A partial list of the numerous other diseases associated with immune-complex glomerulonephritis in the dog follows:[6,7]

- Adenoviral hepatitis (infectious canine hepatitis caused by canine adenovirus-1)
- Borreliosis (Lyme nephritis caused by *B. burgdorferi*)
- Chronic disease (pancreatitis, hepatitis, pyoderma, neoplasia)
- Dirofilariasis (heartworm disease caused by *Dirofilaria immitis*)
- Hereditary C3 deficiency
- Immune-mediated disease (hemolytic anemia, polyarthritis, systemic lupus erythematosis)
- Polyarteritis
- Prostatitis
- Pyometra

This case also stimulated conference participants to review the proposed pathogenesis of immune-complex glomerulonephritis. Classically, immune-complex glomerulonephritis is thought to result from prolonged antigenemia, with circulating antigen equivalent to or in slight excess of circulating antibody; this results in the formation of soluble antigen-antibody complexes that deposit in glomerular capillaries within or on either side of the glomerular basement membrane (GBM), where they initiate complement fixation and cause elaboration of neutrophil chemotaxins (e.g. C3a, C5a, and C567). Neutrophils release proteinases, arachidonic acid metabolites, oxygen-derived free radicals, and hydrogen peroxide, damaging the GBM and inciting monocyte infiltration.[7] There is some controversy concerning the significance and importance of soluble immune complexes in the pathogenesis of glomerulonephritis; several investigators suggest the presence of immune complexes within and around the GBM may be secondary to the damage on the glomerulus rather than the inciting stimulus for the glomerular lesions.[6]

Contributor: University of Pennsylvania, School of Veterinary Medicine, Laboratory of Pathology and Toxicology, 3950 Spruce Street, Philadelphia, PA 19104
http://www.vet.upenn.edu/FacultyandDepartments/Pathobiology/PathologyandToxicology/tabid/412/Default.aspx

References:

1. Chou J, Wünschmann A, Hodzic, Borjesson DL: Detection of *Borrelia burgdoreri* DNA in tissues from dogs with presumptive Lyme borreliosis. J Am Vet Med Assoc **229:**1260-1265, 2006
2. Dambach DM, Smith CA, Lewis RM, Van Winkle TJ: Morphologic, immunohistochemical, and ultrastructural characterization of a distinctive renal lesion in dogs putatively associated with *Borrelia burgdorferi* infection: 49 cases (1987-1992). Vet Pathol **34:**85-96, 1997
3. Gauthier DT, Mansfield LS: Western immunoblot analysis for distinguishing vaccination and infection status with *Borrelia burgdorferi* (Lyme disease) in dogs. J Vet Diagn Invest **11:**259-265, 1999
4. Hutton TA, Goldstein RE, Njaa BL, Atwater DZ, Chang Y, Simpson KW: Search for *Borrelia burgdorferi* in kidneys of dogs with suspected "Lyme nephritis." J Vet Intern Med **22:**860-865, 2008
5. Levy SA, Duray PH: Complete heart block in a dog

seropositive for *Borrelia burgdorferi*. Similarity to human Lyme carditis. J Vet Intern Med **2:**138-144, 1988
6. Maxie MG, Newman SJ: Urinary system. *In:* Jubb, Kennedy, and Palmer's Pathology of Domestic Animals, ed. Maxie MG, 5th ed., vol. 2, pp. 451-462. Elsevier Saunders, Philadelphia, PA, 2007
7. Newman SJ, Confer AW, Panciera RJ: Urinary system. *In:* Pathologic Basis of Veterinary Disease, ed. McGavin MD, Zachary JF, 4th ed., pp. 628-641. Mosby Elsevier, St. Louis, MO, 2007
8. O'Connor TP, Esty KJ, Hanscom JL, Shields P, Philipp MT: Dogs vaccinated with the common Lyme disease vaccines do not respond to IR6, the conserved immunodominant region of the VlsE surface protein of *Borrelia burgdorferi*. Clin Diagn Lab Immunol **11:**458-462, 2004
9. Thompson K. Inflammatory diseases of joints. *In:* Jubb, Kennedy, and Palmer's Pathology of Domestic Animals, ed. Maxie MG, 5th ed., vol. 1, pp. 166-167. Elsevier Saunders, Philadelphia, PA,2007

The Armed Forces Institute of Pathology
Department of Veterinary Pathology

Conference Coordinator:
Shannon Lacv. DVM. MPH

WEDNESDAY SLIDE CONFERENCE 2009-2010

Conference 9

2 December 2009

Conference Moderator:

Tim Walsh, DVM, Diplomate ACVP

CASE I: BA42/09 (AFIP 3134367).

Signalment: 5-year-old male nyala (*Tragelaphus angasii*).

History: This animal was reported to be quiet and lethargic for several hours before being found dead by zoo staff. A clear brown, watery fluid was aspirated from the cardiac region by the referring veterinarian while attempting to take a post mortem blood sample.

Gross Pathology: The carcass was in good nutritional condition. The pericardium contained approximately 40ml of red tinged watery fluid, and a cream to red, soft, smooth 8 x 0.5 x 0.2 cm clot of coagulated protein. The epicardium was multifocally mildly roughened to granular. The right atrium and atrial appendage were dilated and thin walled, and the right atrial appendage contained multifocal intramural nodules measuring 2-5mm in diameter which were firm and often had a mottled red to brown appearance, with a pale yellow / brown, firm to gritty central area (**fig. 1-1**). The right atrial wall at the atrioventricular junction was mildly thickened and spongy. The heart weighed 560g, 0.66% of body weight (maximum normal for cow and goat is 0.66%).[6] The trachea and bronchi contained a moderate amount of white frothy fluid. The dorsal aspects of both lungs contained multifocal to coalescing regions of dark red discoloration (hemorrhage), which did not extend into the parenchyma. The liver had rounded borders, and oozed moderate amounts of blood from the cut surface. Skeletal muscles were macroscopically unremarkable.

Laboratory Results: Liver: vitamin E 34.22 µmol/kg FT (ref. range bovine = 3-18 µmol/kg); selenium 1.37 mg/kg DM (ref. range bovine: >23 mg/kg).

Histopathologic Description: Right atrium, one section is examined. Regionally extensive and coalescing areas of the myocardium are replaced by loosely organized knots and whorls of plump spindloid cells (fibroblasts) (**fig. 1-2**). There are also numerous clusters of small blood vessels in these areas (neovascularization). They are lined by plump endothelial cells, and the spindle cells tend to form circumferential rings around them. Occasional eosinophilic hyaline droplets are closely associated with the small vessels, interpreted to be plasma. The surrounding stroma and myocardium is infiltrated by large numbers of foamy macrophages, moderate numbers of pyknotic eosinophils, and smaller numbers of lymphocytes and neutrophils. There are also moderate to large numbers of extravasated red blood cells (hemorrhage). These regions are often surrounded by mature dense collagen bundles and moderate to large numbers of macrophages, which contain coarsely granular, brown pigment (hemosiderophages).

*Sponsored by the American Veterinary Medical Association, the American College of Veterinary Pathologists, and the C. L. Davis Foundation.

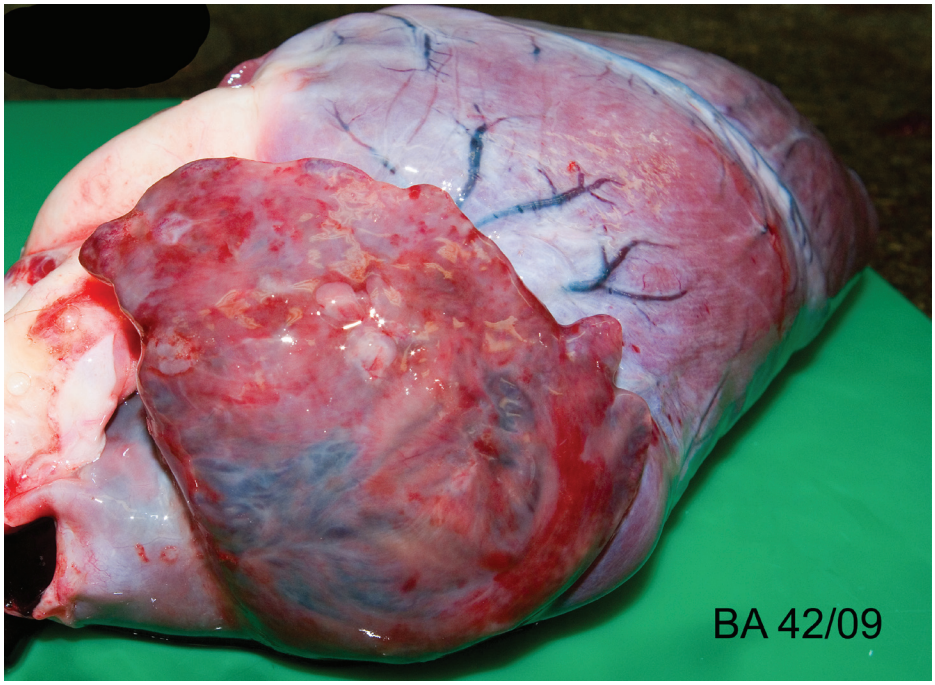

1-1. Heart, Nyala. The right atrium and atrial appendage are dilated and thin walled, with multifocal intramural, firm, mottled red to brown nodules measuring 2-5 mm in diameter which occasionally have gritty centers. Photograph courtesy of Veterinary Pathology Unit, Royal (Dick) School of Veterinary Studies, Easter Bush Veterinary Centre, Roslin, Midlothian, EH25 9RG, Scotland, sionagh.smith@ed.ac.uk.

Some blood vessels contain smudged eosinophilic material (fibrin thrombi). Occasional larger blood vessels contain moderate amounts of intramural smudged eosinophilic material (fibrin), creating a "starburst" appearance. These vessels are surrounded by a layer of foamy macrophages and fibroblasts, hemorrhage, pyknotic granulocytes, and lymphocytes (vascular fibrinoid necrosis) (**fig. 1-3**). Myofibers in the remaining myocardium are occasionally shrunken, hypereosinophilic, and fragmented (myodegeneration). Moderate numbers of plasma cells and lymphocytes are scattered throughout the myocardium, together with moderate numbers of fibroblasts. Multifocal to coalescing regions of the myocardium are replaced or separated by finely granular, palely eosinophilic material (fibrosis). Multifocal areas contain irregular fragments of trabecular bone, and one fragment of bone has a paler central core which contains numerous large, pale blue grey cells within lacunae (chondrocytes, cartilage) (**fig. 1-4**).

Contributor's Morphologic Diagnosis: Myocardial degeneration and loss, severe, multifocal to coalescing, with fibrinoid vasculitis, neovascularization, thrombosis, hemorrhage and osseous metaplasia - right atrial appendage, Nyala (*Tragelaphus angasi*).

Contributor's Comment: Given the signalment, history, gross and histological findings, a diagnosis of nutritional myopathy due to vitamin E and/or selenium deficiency was considered to be most likely. Liu et al (1985) described histopathological features of nutritional myopathy in captive nyala, in particular noting coronary arteriolar fibrinoid necrosis in affected young animals.[4] An additional feature of this case is the striking neovascularization with small blood vessels surrounded by whorls of spindle cells. This is considered most likely to be a form of granulation tissue produced as part of the reparative process.

Vitamin E (as tocopherol) and enzymes containing selenium (glutathione peroxidase / glutathione reductase system) act as antagonists to free radicals and highly reactive unstable compounds produced either during normal cell function or as a result of disease or tissue injury.[8] Damage by free radicals is primarily caused by peroxidation of cellular and subcellular lipid membranes, resulting in loss of the ability to maintain essential differential ion gradients across the membrane. Free radicals may also cause damage to proteins of various cellular components, including mitochondria and endoplasmic reticulum.[1,2,4,8] Vitamin E and the selenium-containing glutathione enzymes act synergistically. However, they may remove different free radicals; therefore, a deficiency in either can lead to disease, with deficiencies in both leading to severe disease.[1,8] In this case hepatic vitamin E levels appeared to be adequate, whilst selenium levels were considered to be low.

Oxidative damage is commonly seen in actively contracting muscle fibers where damage to the cellular membrane allows influx of calcium ions, which are actively moved away from the calcium sensitive myofibers and stored within mitochondria. This results in a

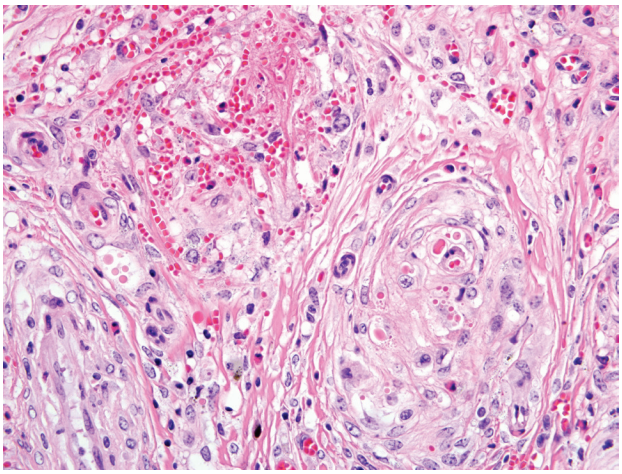

1-2. Heart, Nyala. Areas of the myocardium are replaced by streams and whorls of plump reactive fibroblasts which often center on small caliber blood vessels. Reactive fibroblasts are admixed with low numbers of lymphocytes, eosinophils, and neutrophils. (HE 400X)

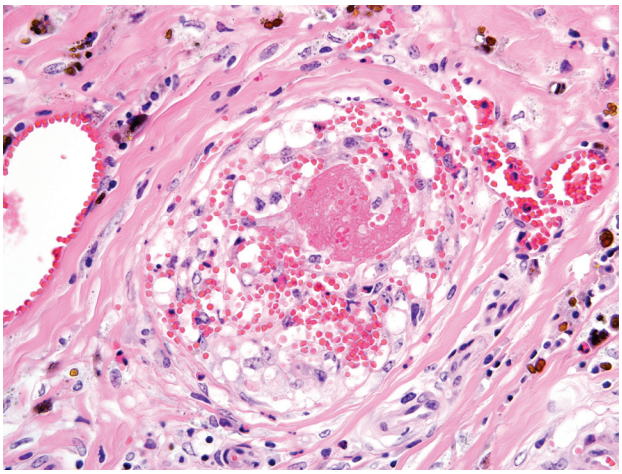

1-3. Heart, Nyala. Vessel walls are replaced by brightly eosinophilic proteinaceous material, infiltrating inflammatory cells, and hemorrhage; the endothelium of affected vessels is markedly reactive. (HE 400X)

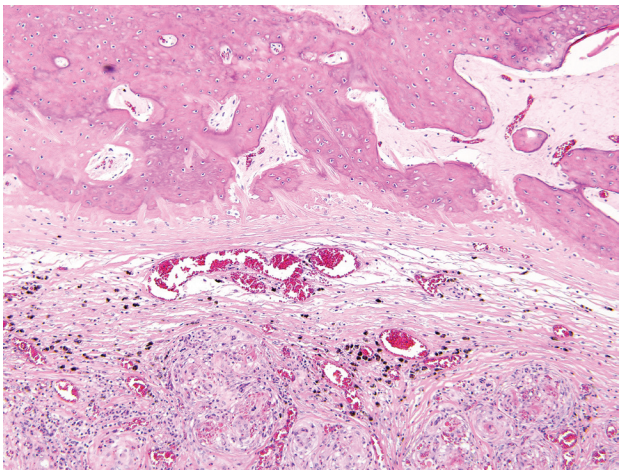

1-4. Heart, Nyala. Multifocally within the myocardium are areas of reactive fibrous connective tissue and bone. (HE 100X)

reduction in mitochondrial function and decreased energy production.[8] Calcium overload eventually causes a state of myofiber hypercontraction, causing degeneration of the myofilaments and coagulation of the contractile proteins.[8]

Nutritional myopathy (syn. white muscle disease, mulberry heart disease, nutritional myodegeneration, nutritional muscular dystrophy, stiff lamb disease) is recognized in many domestic and exotic species, most frequently associated with hypovitaminosis E and selenium deficiency. Reports in the nyala are common and it is considered to be a particularly susceptible species.[3-5,8] In domestic animals, nutritional myopathy is usually a disease of young animals, calves, lambs, swine and foals, with sporadic disease in adults. Affected young animals are usually well grown and thrifty, and affected adults are often those in good nutritional condition.[8] Factors related to vitamin E and selenium deficiencies may be rapid postnatal growth, poor quality feed, lush forage in heavily fertilized and watered pasture, selenium antagonists (e.g. copper, silver, zinc, sulphur), and grazing on dry pastures.[8]

AFIP Diagnosis: Heart, atrial appendage: Fibrinoid vascular necrosis and nodular proliferation, chronic-active, multifocal to coalescing, marked, with cardiomyocyte degeneration and loss, hemorrhage, fibrin thrombi, and fibro-osseous metaplasia.

Conference Comment: Conference participants interpreted the striking vascular changes in this case as the primary lesion, with the myocardial changes occurring secondarily as reflected in the preferred morphologic diagnosis. However, an alternative view is that the myocardial degeneration and necrosis is unrelated to the vascular changes, as is supposed in pigs with mulberry heart disease. In the latter, arterioles of the heart, kidneys, liver, stomach, intestine, mesentery, skeletal muscle, and skin exhibit changes ranging from endothelial swelling, with increased permeability, to fibrinoid change with thrombosis and smooth muscle cell necrosis. A deficiency in vitamin E, rather than selenium, is now thought pivotal in the development of mulberry heart disease.[6] While tissues from other organs were not submitted for histopathologic evaluation in this case, finding a similar distribution of

vascular lesions would be noteworthy. A list of selected diseases associated with vitamin E/selenium deficiency or imbalance in various animal species is available in WSC 2008-2009, Conference 14, case III.

Conference participants considered a number of potential etiologies, including plant toxins (i.e. cardiac glycosides), an endotheliotropic virus, encephalomyocarditis virus, and malignant catarrhal fever. This case illustrates the importance of ancillary testing in a diagnostic setting, and conference participants discussed practical approaches to making the correct etiologic diagnosis in the field. While reserving fresh frozen tissues is ideal for analysis in cases of suspected toxicity or dietary deficiency, the conference moderator reminded participants it is feasible to quantify many minerals from formalin-fixed tissues. For cases of suspected selenium deficiency, when tissue samples are unavailable from the affected animal, viable alternatives include testing samples from herdmates (i.e. animal tissues, blood, and milk), soil, or forages and grains for selenium levels. In cases where animals have been administered parenteral or enteral supplemental selenium in response to a clinical suspicion of deficiency, blood and milk levels of selenium rise rapidly, obscuring the deficiency and precluding a diagnosis. Alternatively, measuring whole blood glutathione peroxidase (GSH-PX) is still useful because its enzymatic activity depends on incorporation of selenium into erythrocytes during erythropoiesis, which requires four to six weeks for enzyme levels to rise following selenium supplementation. By contrast, plasma GSH-PX activity, which does not rely on incorporation into erythrocytes, rises more quickly following supplementation.[7]

Contributor: Division of Veterinary Clinical Sciences, Royal (Dick) School of Veterinary Studies, The University of Edinburgh, Easter Bush Veterinary Centre, Roslin, Midlothian, EH25 9RG, United Kingdom
http://www.vet.ed.ac.uk/cliniclaserv/VPU/VPU.htm

References:

1. Hill K, Motley A, Li X, May J, Burk R: Combined selenium and vitamin E deficiency causes fatal myopathy in guinea pigs. J Nutr **131:**1798-1802, 2001
2., Kumar V, Abbas A, Fausto N: Cellular adaptations, cell injury, and cell death. *In:* Robbins and Cotran Pathological Basis of Disease, eds. Kumar V, Abbas A, Fausto N, 7th ed, pp. 16-18. Elsevier Saunders, Philadelphia, PA, 2005
3. Liu SK, Dolensek EP, Herron AJ, Stover J, Doherty JG: Myopathy in the nyala. J Am Vet Med Assoc **181:**1232-1236, 1982
4. Liu SK, Dolensek EP, Tappe JP: Cardiomyopathy and vitamin E deficiency in zoo animals and birds. Heart Vessels Suppl **1:**288-293, 1985
5. Liu SK, Dolensek EP, Tappe JP, Stover J, Adams CR: Cardiomyopathy associated with vitamin E deficiency in seven gelada baboons. J Am Vet Med Assoc **185:**1347-1350, 1984
6. Maxie MG, Robinson WF: Cardiovascular system. *In:* Jubb, Kennedy, and Palmer's Pathology of Domestic Animals, ed. Maxie MG, 5th ed., vol. 3, pp. 37-41. Elsevier Saunders, Philadelphia, PA, 2007
7. Radostits OM, Gay CC, Hinchcliff KW, Constable PD: Veterinary Medicine, A Textbook of the Diseases of Cattle, Horses, Sheep, and Goats, 10th ed., pp. 1746-1747. Saunders Elsevier, Philadelphia, PA, 2007
8. Van Vleet JF, Valentine BA: Muscle and tendon. *In:* Jubb, Kennedy, and Palmer's Pathology of Domestic Animals, ed. Maxie MG, 5th ed., vol. 1., pp. 198-200, 236-242. Elsevier Saunders, Philadelphia, PA, 2007

CASE II: N08-420 (AFIP 3134650).

Signalment: 6-year-old male green iguana (*Iguana iguana*).

History: Presented to the UF VMC as an emergency. It had been profoundly and progressively lethargic for approximately 10 days. It was reported that the animal was anorexic and not drinking for at least 7 days. The animal was housed in an outdoor glass screened enclosure with access to sunlight. Diet consisted of a commercial iguana pelleted diet and lettuce. On physical exam, this iguana was cachectic, critically dehydrated (estimated 12% dehydrated) and unresponsive. The animal exhibited muscle stiffness and fasciculations. Therapy (fluids, calcium gluconate) was initiated, but this animal spontaneously died approximately 10 hours post-admission.

Gross Pathology: The iguana is in poor nutritional condition, with depleted fat bodies. The kidneys are pale tan with numerous pin-point white foci visible beneath the capsule and on cut section within the parenchyma (**fig. 2-1**). There is a thin, tan-white streak immediately subtending the epicardium of the ventricle (**fig 2-2**). The aorta is expanded by white-yellow, hard, gritty plaques which elevate the intima. There are small fragments of wood in the stomach.

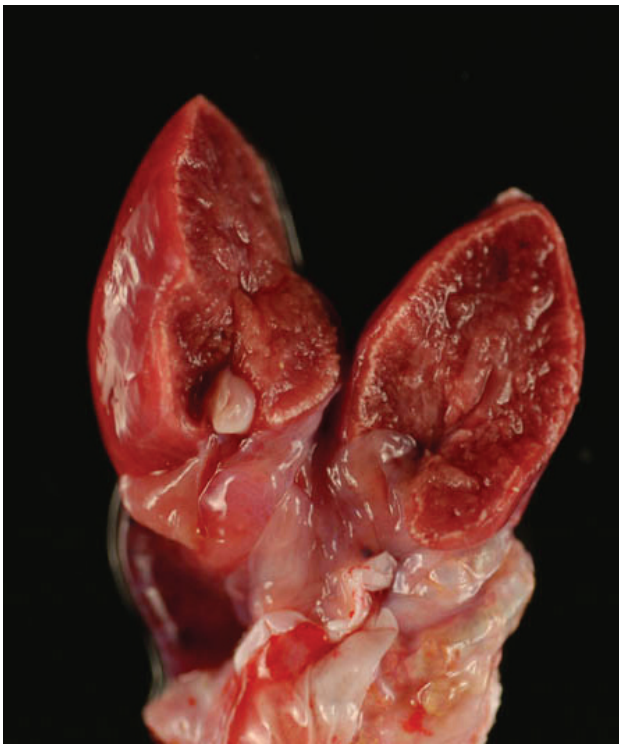

2-1. Heart, Iguana. There is a thin, tan-white streak immediately subtending the epicardium of the ventricle. Photograph courtesy of Department of Infectious Diseases and Pathology, University of Florida, 2015 SW 16th Ave, Room V3-156, Gainesville, FL 32610, farina@vetmed.ufl.edu.

Laboratory Results: Calcium 9.8 mg/dL; Ionized calcium 0.68 mmol/L (normal 1.22-1.62 mmol/L); Blood pH 6.8; Phosphorus 30.4 mg/dL; CK 133,460 U/L; Uric acid 258 mg/dL; AST 788 U/L; GGT 125 U/L; Potassium 7.6 mEq/L; WBC 21,200/µL; Heterophils 17,384/µL with mild degranulation and +2 toxicity.

Histopathologic Description: Multifocally, there is extensive mineralization of the basement membranes, mesangium and visceral and parietal epithelium of glomeruli. Diffusely, there is marked mineralization of the tubular basement membranes. Multifocally, the mineralized basement membranes are markedly expanded, and the tubular epithelium is also multifocally mineralized. Multifocally, there is mild to moderate degeneration and necrosis of tubular epithelial cells, and occasional tubular regeneration. Tubules sometimes contain small amounts of amorphous eosinophilic material and sloughed necrotic cellular debris, and occasionally, tubules are expanded by basophilic, radiating, acicular material (urate tophi) (**fig. 2-3**). The epithelial cells surrounding the urate tophi are often partially effaced and/or appear necrotic. Tubules also occasionally contain amorphous, basophilic, mineralized debris. There is multifocal mineralization of arteries and veins which expands the intima, elevating the endothelium, and extensively extends into the media. There are often aggregates of mineralized material luminally within vessels; this material sometimes has a radiating appearance.

Multifocally, there is often extensive mineralization of the gastric mucosa (**fig. 2-4**). The mineralization affects all levels of the mucosa including the luminal and crypt epithelium and the connective tissue of the lamina propria. In more severely mineralized foci, there is often fibrosis in the lamina propria and loss of glands. There is multifocal moderate mineralization of vessels in the submucosa and lamina propria. There is mild mineralization of the outer aspects of the tunica mucosa and the serosa.

Multifocally and extensively, there is mineralization of cardiac myofibers. The mineralization is evident as a linear band in the outer myocardium and also as scattered myofibers throughout the myocardium. There is extensive mineralization of the vessels in the myocardium and epicardium. There are moderate amounts of fibrous connective tissue associated with the mineralized myofibers in the linear band region (**fig. 2-5**). Surrounding myofibers are frequently markedly vacuolated and occasionally necrotic and infiltrated with moderate numbers of macrophages.

Contributor's Morphologic Diagnosis:

1. Metastatic mineralization, multifocal, chronic, moderate-severe, with:
   a. Glomerular, tubular, and vascular mineralization, chronic, multifocal, severe, kidneys.
   b. Myocardial and vascular mineralization, chronic, multifocal, marked, with mild myofiber degeneration and necrosis and mild myocardial fibrosis, heart.
   c. Gastric mucosal and vascular mineralization, chronic, multifocal, moderate, with fibrosis and loss of glands.
   d. Mineralization and fibrosis, chronic, multifocal, severe, aorta (not included in slide set).
2. Renal tubular urate tophus deposition, acute, multifocal, minimal to mild, with tubular necrosis.

Contributor's Comment: On microscopic examination, there was extensive mineralization of the tunica intima and tunica media of vessels in nearly all of the tissues examined as well as extensive mineralization of the renal tubules (predominantly basement membranes), glomeruli, myocardium, pulmonary interstitium, and other tissues. The mineralized tissue largely appeared relatively normal, consistent with metastatic mineralization.

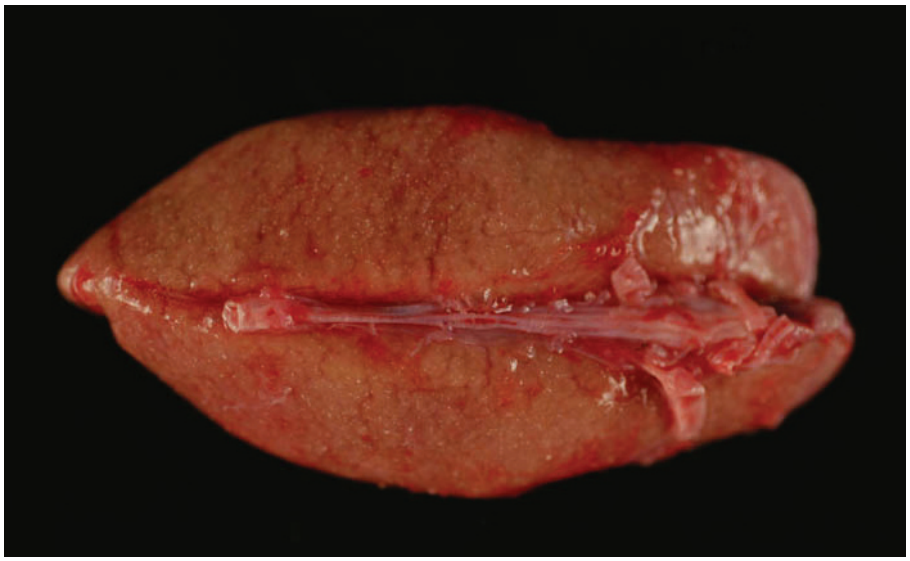

2-2. Kidney, Iguana. The kidneys are pale tan with numerous pin-point white foci visible beneath the capsule and on cut section within the parenchyma. Photograph courtesy of Department of Infectious Diseases and Pathology, University of Florida, 2015 SW 16th Ave, Room V3-156, Gainesville, FL 32610, farina@vetmed.ufl.edu.

Causes of metastatic soft tissue mineralization include hypervitaminosis D (due to excess supplementation or ingestion of vitamin D-containing rodenticides or plants [*Cestrum* spp. and *Solanum* spp.]) and elevated calcium and/or phosphorus (nutritional or renal secondary hyperparathyroidism, primary hyperparathyroidism, hypercalcemia of malignancy).[4] Specifically, animals are considered at risk for soft tissue mineralization when the calcium-phosphorus product is greater than 60-70.[4]

Green iguanas require UV-B light to convert provitamin D3 to active vitamin D3, and oral supplementation of vitamin D3 (instead of a UV-B source) has been determined to be ineffectual.[7] A study on iguanas at the National Zoological Park presenting for necropsy revealed widespread mineralization of soft tissues, especially of vessels and basement membranes, cardiac and skeletal muscle degeneration and necrosis with mineralization, and occasional mild fibrous osteodystrophy. In these animals, circulating levels of vitamin D3 were 7-36 ng/ml (normal is >400ng/ml).[7,8]

Possible causes for paradoxical soft tissue mineralization in these animals which were proposed were chronically low vitamin D levels leading to hypocalcemia, resulting in an exaggerated PTH response and excessive calcium mobilization from bone with resultant mineral deposition in soft tissues; or metabolic derangements altering the calcium-phosphorus ratio, which could result in an elevated calcium-phosphorus product which could predispose to mineralization.[7,8]

In this case, [Ca] = 9.8 mg/dL (normal 10.9-14.4), [P] = 30.4 mg/dL (normal 2.8-7.8), and [Ca] x [P] = 297.92. Therefore, in this case, we may have an explanation for mineralization based on elevated [Ca] x [P] product. Vitamin D3 levels were not determined. Given the sub-optimal husbandry reported by the clinician in this case, calcium and phosphorus abnormalities could have been nutritional and/or related to lack of adequate vitamin D3. Renal dysfunction was likely secondary to mineralization. While a few tophi were identified in renal tubules, these were acute lesions without associated inflammatory response, and likely developed terminally, possibly secondary to dehydration.

This animal did not have any evidence of fibrous osteodystrophy.

AFIP Diagnosis: 1. Kidney: Glomerular, vascular, and tubular basement membrane mineralization, diffuse, with tubular epithelial necrosis, interstitial fibrosis and few gout tophi.
2. Stomach: Mucosal and vascular mineralization, multifocal, with epithelial degeneration and necrosis and interstitial fibrosis.
3. Heart, ventricle: Myocardial and vascular degeneration, necrosis, and mineralization, multifocally extensive, moderate, with fibrosis.

Conference Comment: Conference participants reviewed several unique reptilian anatomical structures that were demonstrated in this case. Because lizards and snakes have a sexually dimorphic kidney, participants could surmise that this was a male iguana. Males possess a sexual segment of the nephron located between the distal segment and the collecting tubules, characterized by prominent hypereosinophilic intracytoplasmic granules.

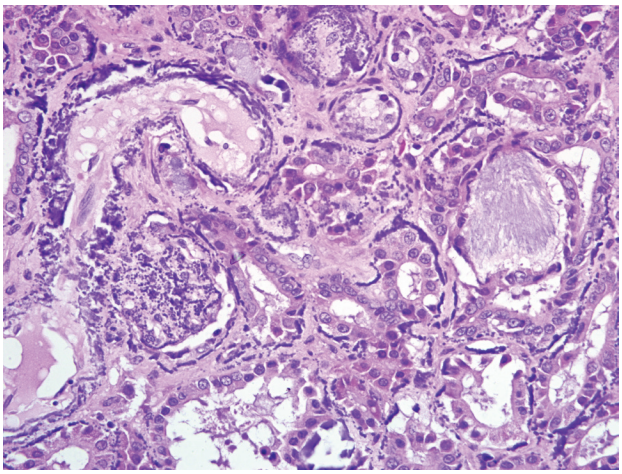

2-3. Kidney, Iguana. Multifocally displacing cortical parenchyma are large, up to 100 um diameter radiating acicular crystals (gouty tophi). Diffusely, the basement membranes of tubules, glomeruli, and blood vessels are expanded by mineral. (HE 200X)

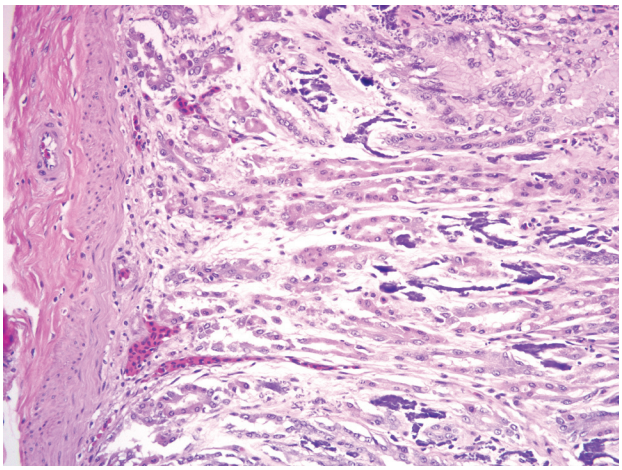

2-4. Stomach, Iguana. Multifocally the mucosa is necrotic and the epithelial basement membranes and the lamina propria are expanded by accumulations of mineral. (HE 200X)

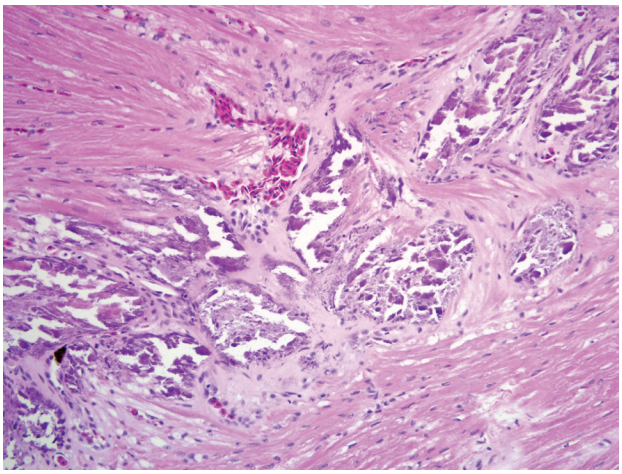

2-5. Heart, Iguana. Diffusely at the junction of the stratum compactum and the stratum spongiosum is an approximately 500 um thick band of mineralized myocardial tissue admixed with fibrosis. (HE 400X)

The secretory product that the sexual segment produces is incorporated into the seminal fluid.[2] With regard to the histologic anatomy of the heart, the ventricular myocardium consists of an outer stratum compactum and an inner stratum spongiosum. In most slides myocardial mineralization centered at the junction between the two muscular strata, and participants theorized the finding might be due to the abrupt change in myofiber orientation at this location, resulting in greater susceptibility to injury during contraction.

This case is an excellent example of metastatic mineralization of soft tissues, and the contributor provides a succinct review of the pathophysiology of the condition, including hypovitaminosis D in iguanas. Conference participants briefly reviewed the following causes of metastatic mineralization in animals:[1,3,5]

1. Kidney failure → phosphate retention → renal secondary hyperparathyroidism
2. Hypervitaminosis D (e.g. ingestion of calcinogenic plants [*Solanum malacoxylon, Cestrum diurnum*, *Trisetum flavescens*] or cholecalciferol-containing rodenticides) → secondary hyperparathyroidism
3. Hyperparathyroidism (primary or secondary) or pseudohyperparathyroidism (due to PTH-related protein production associated with canine lymphoma or adenocarcinoma of the anal sac)
4. Granulomatous disease (e.g. canine blastomycosis, bovine paratuberculosis)
5. Osteolytic bone lesions (e.g. primary or metastatic neoplasia)

In general, tissues predisposed to metastatic mineralization include the gastric mucosa, renal tubules, alveolar septa, and subpleural intercostal connective tissue.[5,6] In cattle with Johne's disease, intimal mineralization may occur in the thoracic aorta.[3] In dogs with blastomycosis, mineralization is thought to be caused by 1,25-dihydroxycholecalciferol production by activated macrophages.[1]

Contributor: University of Florida, College of Veterinary Medicine, Department of Infectious Disease

and Pathology, Gainesville, Florida 32610
http://www.vetmed.ufl.edu/college/departments/patho/

References:

1. Ferguson DC, Hoenig M: Endocrine system. *In:* Duncan & Prasse's Veterinary Laboratory Medicine Clinical Pathology, eds. Latimer KS, Mahaffey EA and Prasse KW, 4th ed., pp. 278-280. Blackwell, Ames, IA, 2003
2. Jacobsen ER: Overview of reptile biology, anatomy, and histology. *In:* Infectious Diseases and Pathology of Reptiles, ed. Jacobsen ER, pp. 13-19, CRC Press, Boca Raton, FL, 2007
3. Maxie MG, Robinson WF: Cardiovascular system. *In:* Jubb, Kennedy, and Palmer's Pathology of Domestic Animals, ed. Maxie MG, 5th ed., vol. 3, p. 61. Elsevier Saunders, Philadelphia, PA, 2007
4. Morrow CK, Volmer PA: Hypercalcemia, hyperphosphatemia and soft tissue mineralization. Comp Cont Ed Pract Vet **24:**380-387, 2002
5. Myers RK, McGavin MD: Cellular and tissue responses to injury. *In:* Pathologic Basis of Veterinary Disease, ed. McGavin MD, Zachary JF, 4th ed., pp. 48-49. Mosby Elsevier, St. Louis, MO, 2007
6. Newman SJ, Confer AW, Panciera RJ: Urinary system. In: Pathologic Basis of Veterinary Disease, ed. McGavin MD, Zachary JF, 4th ed., pp. 641-644. Mosby Elsevier, St. Louis, MO, 2007
7. Richman LK, Montali RJ, Allen ME, Oftedal, OT: Paradoxical pathologic changes in vitamin D deficient green iguanas (*Iguana iguana*). *In:* Proceedings of the American Association of Zoo Veterinarians, pp. 203-204. East Lansing, MI, 1995
8. Richman L, Montali R, Allen M, Oftedal, O: Widespread metastatic soft tissue mineralization in vitamin D deficient green iguanas (*Iguana iguana*). *In:* Proceedings of the Conference of the American College of Veterinary Pathology, p. 57. Atlanta, GA, 1995

CASE III: S16/08A, S17/08B (AFIP 3133958).

Signalment: 8-month-old, male (S 16/08) and female (S 17/08), Bearded Dragons (*Pogona vitticeps*), reptile.

History: The animals derived from a collection of several animals (the exact number is unknown), from which four animals did not gain weight, even though they were force-fed with crickets from the beginning. The rest of the collection developed normally. A scat sample tested for parasites was without diagnostic findings. The animals were treated with vitamin B and calcium, and fed with a "critical care" diet and crickets. They did not respond to treatment and were humanely killed.

Gross Pathology: At necropsy, the lizards were in a poor body condition and up to 200-300 µl of a translucent transudate was found inside the coelomic cavities. There were no other gross lesions detected.

Laboratory Results: DNA was extracted from liver tissue and cell cultured material. According to two published protocols,[1,13] PCR amplification resulted in products of about 430 bp and 520 to 550 bp, respectively. The obtained sequences of the adenoviral polymerase gene of the eight-month-old bearded dragons were compared to published sequences of reptilian adenoviruses in the GenBank by use of the Basic Local Alignment Search Tool, (BLAST) which showed a close relationship between the sequence of these animals and another agamid atadenovirus.

Histopathologic Description: The architecture of the liver is disordered and contains multiple foci of necrosis accompanied by moderate multifocal infiltration of lymphocytes and histiocytes. Numerous hepatocytes as well as epithelial cells of the bile ducts contain large amphophilic intranuclear inclusion bodies, which distend the nuclei 2 to 5-fold, partly with margination of chromatin (**fig. 3-1**). A mild proliferation of bile ducts is present.

Contributor's Morphologic Diagnosis: Liver: Hepatitis, lympho-histiocytic, multifocal, moderate, with hepatocellular degeneration and amphophilic intranuclear inclusion bodies, bearded dragon (*Pogona vitticeps*), reptile.

Contributor's Comment: The Adenoviridae family comprises four genera: the Mastadenoviruses, which infect mammalian species; the Aviadenoviruses, which infect birds; and the two recently established genera

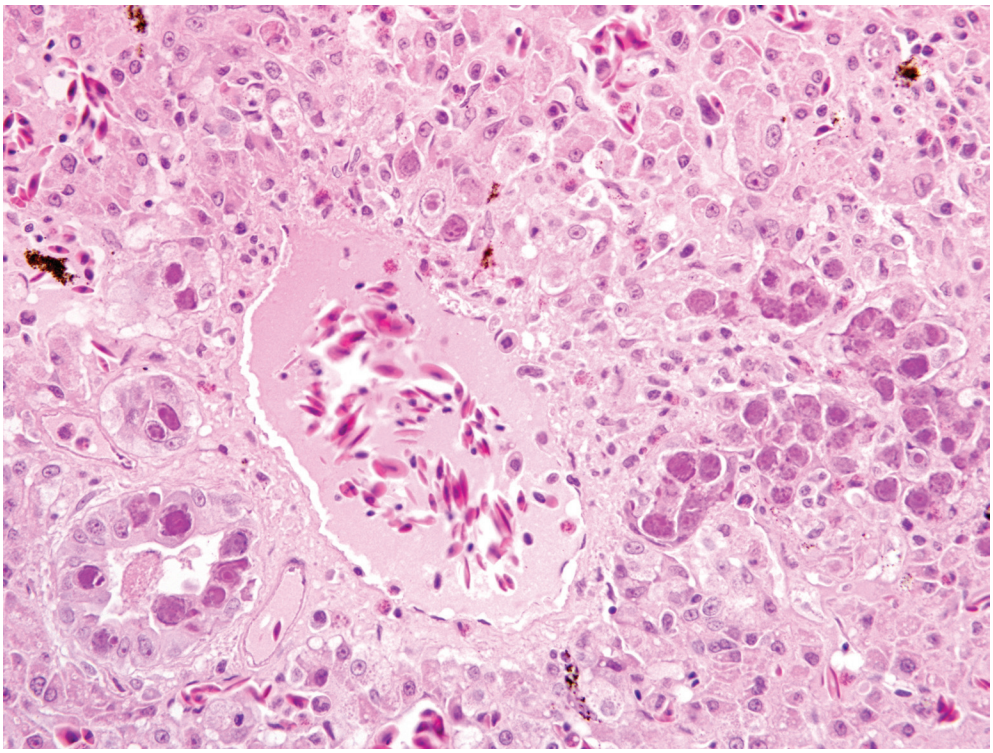

3-1. Liver, Bearded Dragon. There is hepatocellular necrosis, and degenerate hepatocytes and biliary epithelium contain large amphophilic intranuclear viral inclusion bodies that measure up to 20 um diameter. (HE 400X)

Siadenovirus (frog, poultry) and *Atadenovirus* (ruminants, birds, snakes, lizards, and a marsupial).[3,6] A fifth genus is proposed for a sturgeon adenovirus.[1,6]

Generally, adenoviruses are host specific and are transmitted by the fecal-oral route or by direct contact via oro-nasal secretions. Adenoviral infection in reptiles is reported with and without concurrent disease and in the majority of communications only individual animals are afflicted. The most common changes observed in association with an adenoviral infection include nonspecific clinical signs like wasting and anorexia, accompanied by necrosis and inflammatory changes in the gastrointestinal tract and the liver.[5,7-9,11,12] Others observed nephritis [7] or neurological signs like head tilt and circling,[8] but there are also cases of sudden death without prior signs of illness described.[9]

Additionally, the two animals investigated showed intranuclear inclusions in the tubular epithelial cells of the kidney identical to those seen in the liver associated with a moderate, multifocal, lympho-histiocytic interstitial nephritis. Furthermore, a moderate, multifocal, lympho-histiocytic, interstitial pancreatitis with numerous intranuclear inclusion bodies in epithelial cells of the pancreatic duct was detected. The microscopically visible intranuclear inclusion bodies are formed during the replication phase inside the nuclei of affected host cells. Using routine H&E stain, they are typically basophilic to amphophilic.[5,8,9,11,12] The virions form paracrystalline arrays, often causing severe condensation and margination of the host cell chromatin. Finally, they are released by cell lysis.[6] In order to substantiate the diagnosis, the products of the PCR were sequenced and compared to published sequences of reptilian adenoviruses in the GenBank by use of BLAST.[10]

AFIP Diagnosis: Liver: Hepatitis, portal and random, necrotizing and lymphohistiocytic, multifocal to coalescing, moderate, with mild biliary hyperplasia and many hepatocellular and biliary epithelial intranuclear amphophilic inclusion bodies.

Conference Comment: In addition to the degenerative hepatocellular changes reflected in the contributor's morphologic diagnosis, conference participants considered the necrosis a sufficiently prominent feature to merit incorporation in the morphologic diagnosis. Histochemical staining with reticulin highlighted the severity of disorganization in hepatic cords.

The contributor provides a useful synopsis of the pathogenesis of adenoviral infections in animals. In general, adenoviruses interact with host cells in one of three characteristic ways:[2]

1. Lytic infection: involves complete viral replication and host cell lysis, as described by the contributor

2. Latent or chronic infection: lymphoid tissue is often the site of latency
3. Oncogenic transformation (e.g., production of sarcomas in hamsters by simian and human adenoviruses): viral DNA is integrated into host cell DNA and T antigens are produced, but no infectious virions are produced

Recently, a fifth genus has been added to the Adenoviridae family: the *Ichtadenovirus* genus, containing *Sturgeon adenovirus A* as its sole species.[4] An example of canine adenovirus is available in WSC 2008-2009, Conference 3, case I, and an example of falcon adenovirus is available in WSC 2007-2008, Conference 23, case III.

Contributor: Department of Pathology, University of Veterinary Medicine Hannover, Buenteweg 17, D-30559 Hannover, Germany
http://www.tiho-hannover.de/einricht/patho/index.htm

References:

1. Benkö M, Elo P, Ursu K, Ahne W, LaPatra SE, Thomson D, Harrach B: First molecular evidence for the existence of distinct fish and snake adenoviruses. J Virol **76:** 10056-10059, 2002
2. Cheville NF, Lehmkuhl H: Cytopathology of viral diseases. *In:* Ultrastructural Pathology: The Comparative Cellular Basis of Disease, ed. Cheville NF, 2nd ed., pp. 338-343, Wiley-Blackwell, Ames, IA, 2009
3. Davison AJ, Wright KM, Harrach B: DNA sequence of frog adenovirus. J Gen Virol **81:**2431-2439, 2000
4. International Committee on Taxonomy of Viruses (Internet): Virus taxonomy. Available from: http://www.ictvonline.org, 2008
5. Jacobson ER, Kopit W, Kennedy FA, Funk RS: Coinfection of a Bearded Dragon, *Pogona vitticeps*, with adenovirus- and dependovirus-like viruses. Vet Pathol **33:**343-346, 1996
6. Jacobson ER: Viruses and viral diseases of reptiles. *In:* Infectious Diseases and Pathology of Reptiles, ed. Jacobsen ER, pp. 401-402, CRC Press, Boca Raton, FL, 2007
7. Julian AF, Durham PJ: Adenoviral hepatitis in a female bearded dragon (*Amphibolorus barbatus*). *N Z Vet* J **30**:59-60, 1982
8. Kim DY, Mitchell MA, Bauer RW, Poston R, Cho DY: An outbreak of adenoviral infection in inland bearded dragons (*Pogona vitticeps*) coinfected with dependovirus and coccidial protozoa (*Isospora* sp.). J Vet Diagn Invest **14:**332-334, 2002
9. Kübber-Heiss A, Benetka V, Filip T, Benyr G, Schilcher F, Pallan C, Möstl K: Erstmaliger Nachweis einer Adenovirus-Infektion bei einer Bartagame (*Pogona vitticeps* AHL, 1926) in Österreich. Wiener Tierärztliche Monatsschrift, **93:**68-72, 2006
10. Moormann S, Seehusen F, Reckling D, Kilwinski J, Puff C, Elhensheri M, Wohlsein P, Peters M: Systemic Adenovirus Infection in Bearded Dragons (*Pogona vitticeps*): Histological, Ultrastructural and Molecular Findings. J Comp Pathol **141:**78-83, 2009
11. Perkins LE, Campagnoli RP, Harmon BG, Gregory CR, Steffens WL, Latimer K, Clubb S, Crane M: Detection and confirmation of reptilian adenovirus infection by in situ hybridization. J Vet Diagn Invest **13:**356-368, 2001
12. Ramis A, Fernández-Bellon H, Majó N, Martínez-Silvestre A, Latimer K, Campagnoli R: Adenovirus hepatitis in a boa constrictor (*Boa constrictor*). J Vet Diagn Invest **12:**573-576, 2000
13. Wellehan JF, Johnson AJ, Harrach B, Benkö M, Pessier AP, Johnson CM, Garner MM, Childress A, Jacobson ER: Detection and analysis of six lizard adenoviruses by consensus primer PCR provides further evidence of a reptilian origin for the atadenoviruses. J Virol **78:**13366-13369, 2004

CASE IV: XN2892 (AFIP 2940472).

Signalment: Adult female goldfish (*Carassius auratus*).

History: An indoor, room temperature, 45 liter aquarium was established in July 2003 with a sparsely-planted gravel floor, fluorescent lighting and a canister filter powered by an electric pump. It was allowed to equilibrate for two weeks, then stocked with two goldfish (Carassius auratus), one orange and white and the other orange, purchased from an aquarium shop. The two goldfish remained together for six weeks and were fed on commercial goldfish pellets. In August 2003, two new goldfish, one a black moor and the other a panda moor, were purchased from a different aquarium shop and introduced to the aquarium. One week later, the original orange and white goldfish was found dead and submitted for postmortem examination.

Gross Pathology: A postmortem examination was conducted on the adult female goldfish within 15 minutes of death. The fish weighed 7 g and had a length of 90 mm from the mouth to the tail tip. Petechial hemorrhages were evident on the gills.

Laboratory Results: No parasites were detected in wet preparations of gills, skin and fins examined by light

microscopy.

Histopathologic Description: Multifocal necrosis is evident in the renal hematopoietic tissue, spleen, pancreas, and intestine of this goldfish, along with multiple eosinophilic to amphophilic intranuclear inclusion bodies (**figs. 4-1, 4-2, and 4-3**). Lymphohematopoietic hyperplasia is evident in some less severely affected areas. Mild degenerative changes are also present in renal tubules and glomeruli. There are lymphoplasmacytic inflammatory infiltrates in segments of intestinal mucosa and submucosa. Some histological sections do not include all of these affected tissues. The gills from this goldfish had lamellar fusion and chronic bronchitis, with infiltrates of eosinophilic granule cells, epithelial hyperplasia and individual epithelial necrosis. A few monogenean flukes were visible histologically in the interlamellar spaces of the gills.

Contributor's Morphologic Diagnosis: 1. Renal hematophoietic tissue: Necrosis, multifocal, locally extensive, moderate to severe, with eosinophilic intranuclear inclusion bodies, etiology consistent with herpesvirus hematopoietic necrosis, Goldfish, ornamental, *Carassius auratus*.
2. Spleen: Necrosis, multifocal, moderate, with eosinophilic intranuclear inclusion bodies.
3. Pancreas: Necrosis, multifocal, mild to moderate, with eosinophilic intranuclear inclusion bodies.
4. Intestine: Necrosis, submucosa and mucosa, segmental, multifocal, mild to severe, with eosinophilic intranuclear inclusion bodies in epithelial cells, also inflammation, lymphoplasmacytic, segmental, moderate.

Contributor's Comment: The multifocal renal hematophoietic, splenic, pancreatic, and intestinal necrosis observed histologically in this case, along with the eosinophilic intranuclear inclusion bodies, are consistent with herpesvirus hematophoietic necrosis (HVHN) of goldfish.[1,5,9,10] This disease was first observed in Japan in 1992 [9] and has subsequently been diagnosed in North America [5], Taiwan [1], and Australia [10]. It has been associated with severe outbreaks of disease and high mortality in cultured goldfish.[1,5,9] Affected fish are often lethargic and inappetent or anorexic, may exhibit increased respiratory effort and may remain at the bottom of their ponds.[1,5,9,10] Gross lesions include pallor of the gills, swelling and pallor of the spleen and kidneys, occasionally with multiple white foci, pallor of the liver and an empty intestinal tract.[5,9,10] Histological lesions are characterized by multifocal to diffuse necrosis of renal hematopoietic, splenic, pancreatic, intestinal and branchial tissue, with eosinophilic intranuclear inclusion bodies.[1,5,9,10] Gill lamellar fusion and epithelial hyperplasia have been described in affected goldfish [5,10] In addition to multifocal necrosis of the splenic parenchyma, necrosis of sheathed arterioles in the spleen has also been reported.[9] Degeneration and necrosis may occur in the oropharynx and the epidermis and dermis of the skin, but these changes are not consistent.[5] Multifocal necrosis has been described in the heart of affected goldfish [1], and diffuse necrosis has been reported in the thymus.[10]

A herpesvirus, designated goldfish hematopoietic necrosis virus (GFHNV), has been isolated from affected goldfish and shown to reproduce HVHN experimentally.[9] Herpesvirus-like particles can be detected by electron microscopy in

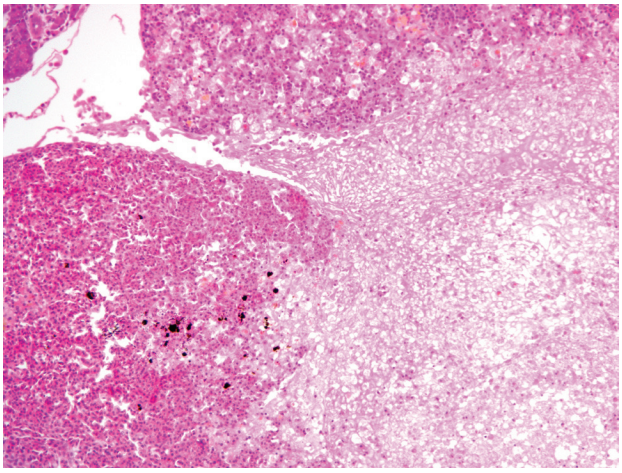

4-1. Spleen and kidney, Goldfish. Multifocally there is necrosis of lymphoid and hematopoietic tissue in the spleen and kidney. (HE 200X)

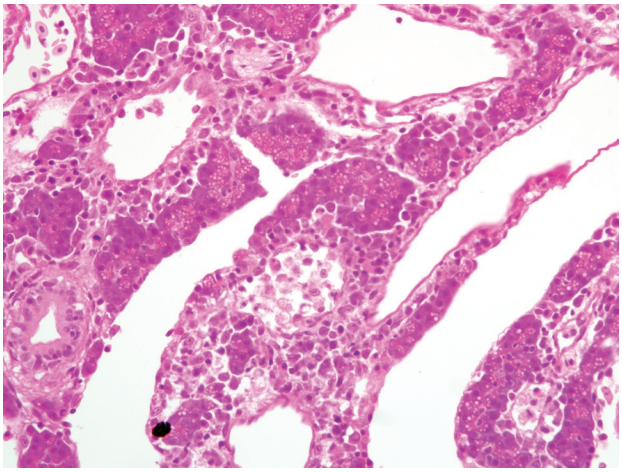

4-2. Pancreas, Goldfish. Multifocally, there is necrosis of pancreatic acini, and some inflammatory cells extend to the overlying serosal surface. (HE 400X)

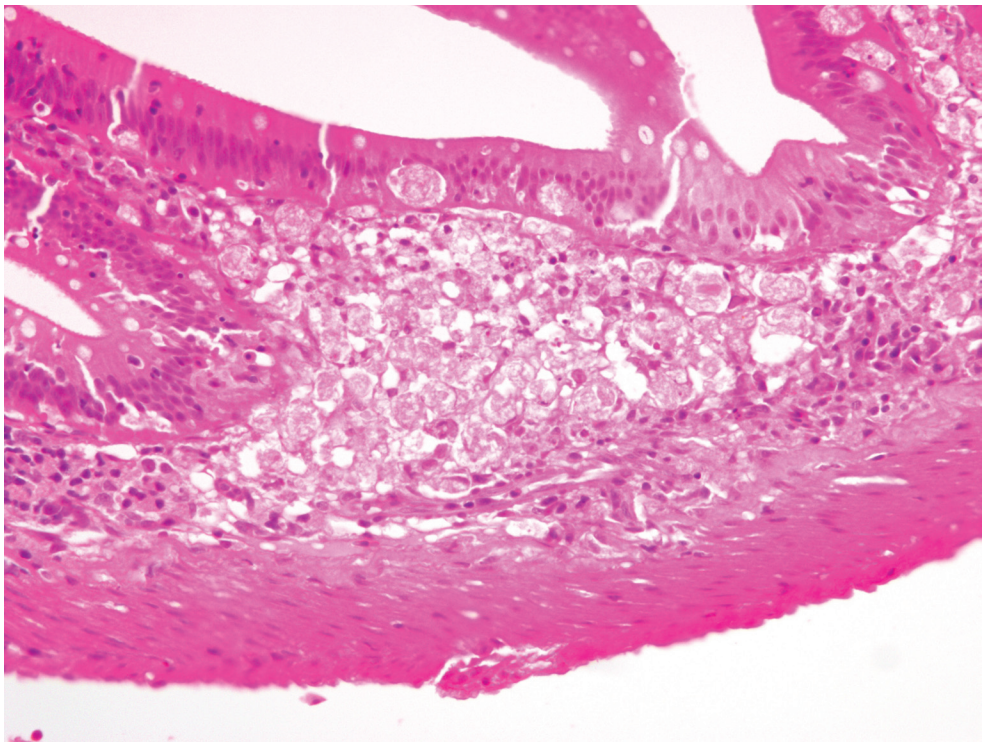

4-3. Intestine, Goldfish. Within the submucosa there are focally extensive areas of necrosis. (HE 400X)

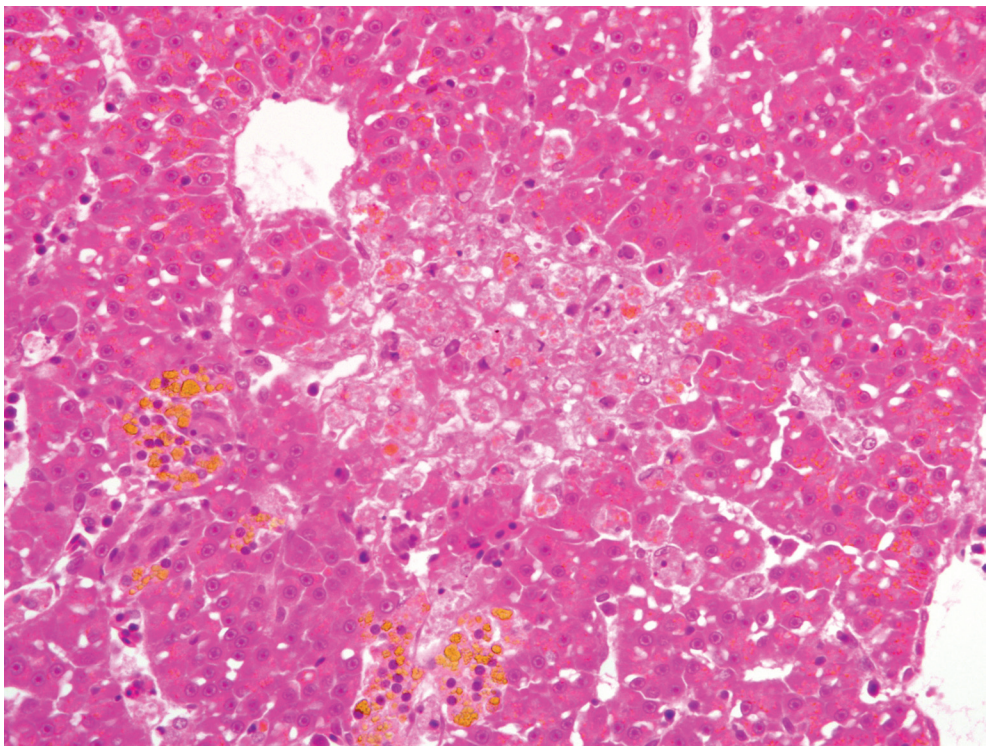

4-4. Liver, Goldfish. Multifocally within the liver there is multifocal hepatocellular necrosis. Intracellular and extracellular yellow to orange globular pigment is also present. (HE 400X)

affected tissues.[1,5,9,10] HVHN of goldfish has pathological similarities to carp nephritis and gill necrosis (CNGN), which affects koi carp (*Cyprinus carpio*) and is caused by koi herpesvirus (carp nephritis and gill necrosis virus).[6] GFHNV does not affect koi carp [1] and koi herpesvirus does not infect goldfish [6]. Outbreaks of CNGN were first observed in cultured koi carp in Israel and North America in 1998 [6] and have subsequently been reported in Japan, Indonesia and Europe, including the United Kingdom.[3,7] HVHN and CNGN are both characterized by multifocal necrosis of renal hematopoietic, splenic, pancreatic and intestinal tissue, with variable histological lesions in the gills, oropharynx and skin.[1,5,6,9,10] Necrosis, lamellar fusion and epithelial hyperplasia are observed in the gills of koi carp with CNGN, similar to gill lesions in goldfish with HVHN.[6] Koi herpesvirus can be detected in tissues from affected koi carp by electron microscopy and polymerase chain reaction.[2,4,6] Comparisons of the genomes of koi herpesvirus isolates from outbreaks of CNGN in different regions of the world by restriction fragment length polymorphism, protein gel electrophoresis and DNA hybridization have demonstrated that most isolates are nearly identical and are likely to have been derived from a common source.[2-4]

In outdoor ponds in Japan and North America, GFHNV usually causes disease in cultured goldfish in spring and autumn (fall), when the temperature of the water is in the range of 15 to 25 degrees Celsius.[5,9] Outbreaks of CNGN caused by koi herpesvirus have been reported on farms with water temperatures of 17 to 25 degrees Celsius.[6,7] Experimentally infected koi carp are susceptible to disease in water with a temperature range from 18 to 28 degrees Celsius.[3] Goldfish affected by major outbreaks of HVHN have usually been less than one year of age, with some epidemics occurring in juveniles less than two months of age, although goldfish of all ages may be affected.[1,5,9,10] Two-month-old goldfish affected by HVHN in North America were 25 to 40 mm long and weighed two to three grams.[5] A single goldfish diagnosed with HVHN in Australia weighed approximately five grams.[10] Koi carp of all ages may be affected by CNGN.[5] In the case of HVHN reported here, a single adult goldfish 90 mm long and weighing seven grams was affected. It could be speculated that this goldfish developed HVHN after first exposure to GFHNV following introduction of an infected fish. Alternatively, the goldfish may have harboured latent GFHNV that was reactivated following the stress caused by the introduction of new fish to the aquarium tank. Outbreaks of mortality due to HVHN in 20 to 25-day-old goldfish fry, as well as associated mortality in adult brood goldfish, were associated with the introduction of new fish to a hatchery in Taiwan.[1]

AFIP Diagnosis: 1. Pancreas: Pancreatitis, necrotizing, multifocal, moderate to marked, with intranuclear inclusion bodies and acute serositis.
2. Intestine, lamina propria and submucosa: Necrosis, multifocal, with intranuclear inclusion bodies.
3. Spleen; and renal hematopoietic tissue: Necrosis, multifocal, with intranuclear inclusion bodies.
4. Liver: Hepatocellular degeneration and necrosis, multifocal, mild to moderate, with few intranuclear inclusion bodies.

Conference Comment: This case was submitted in 2004; since then, the cause of this lesion has been determined as Cyprinid herpesvirus-2. There are currently three members of the genus *Cyrinivirus* within the *Alphaherpesviridae* family:[8]

- Cyprinid herpesvirus-1: carp pox herpesvirus
- Cyprinid herpesvirus-2: hematopoietic necrosis herpesvirus of goldfish
- Cyprinid herpesvirus-3: koi herpesvirus

Despite substantial variation among the slides with respect to the organs and lesions represented, participants readily recognized a systemic herpesviral infection primarily targeting hematopoietic and lymphoid tissues. During the conference, the conference moderator cautioned participants that pancreatic necrosis in fish is often very difficult to distinguish from autolysis. However, the contributor in this case provided histologic sections from particularly well-preserved tissues as a good example of this important entity, and further complimented the slides with a thorough review. Additionally, conference participants commented on finding serositis in many slides, which is not surprising given the widespread distribution of pancreatic tissue in fish (**fig. 4-2**). Furthermore, most slides contain abundant intra- and extracellular accumulations of yellow to orange, granular to globular material throughout the liver (**fig. 4-4**). Conference participants discussed various potential pigments, including hemosiderin, hematoidin, bile, melanin, and lipofuscin. In this case, an abundance of iron-containing pigment (i.e. hemosiderin) was demonstrated by the presence of intense blue staining with the Prussian blue reaction. Staining using the Hall's bile method was negative.

Contributor: Division of Pathological Sciences, Institute of Comparative Medicine, University of Glasgow Veterinary School, Glasgow G61 1QH, Scotland, United Kingdom.
http://www.gla.ac.uk/faculties/vet/

References:

1. Chang PH, Lee SH, Chiang HC, Jong MH: Epizootic of herpes-like virus infection in goldfish, *Carassius auratus*

in Taiwan. Gyobyo Kenkyu (Fish Pathol) **34:**209-210, 1999

2. Gilad O, Yun S, Andree KB, Adkison MA, Zlotkin A, Bercovier H, Eldar A, Hedrick RP: Initial characteristics of koi herpesvirus and development of a polymerase chain reaction assay to detect the virus in koi, *Cyprinus carpio koi.* Dis Aquat Organ **48:**101-108, 2002

3. Gilad O, Yun S, Adkison MA, Way K, Willits NH, Bercovier H, Hedrick RP: Molecular comparison of isolates of an emerging fish pathogen, koi herpesvirus, and the effect of water temperature on mortality of experimentally infected koi. J Gen Virol **84:**2661-2667, 2003

4. Gray WL, Mullis L, LaPatra SE, Groff JM, Goodwin A: Detection of koi herpesvirus DNA in tissues of infected fish. J Fish Dis **25:**171-178, 2008

5. Groff JM, LaPatra SE, Munn RJ, Zinkl JG: A viral epizootic in cultured populations of juvenile goldfish due to a putative herpesvirus etiology. J Vet Diagn Invest **10:**375-378, 1998

6. Hedrick RP, Gilad O, Yun S, Spangenberg JV, Marty GD, Nordhausen RW, Kebus MJ, Bercovier H, Eldar A: A herpesvirus associated with mass mortality of juvenile and audult koi, a strain of common carp. J Aquat Anim Health **12:**44-57, 2000

7. Hoole D, Bucke D, Burgess P, Wellby I: Diseases of Carp and Other Cyprinid Fishes, pp. 48-49. Fishing News Books, Blackwell Science, Oxford, UK, 2001

8. International Committee on Taxonomy of Viruses (Internet): Virus taxonomy. Available from: http://www.ictvonline.org, 2008

9. Jung SJ, Miyazaki T: Herpesviral haematopoietic necrosis of goldfish, *Carassius auratus* (L.) J Fish Dis **18:**211-220, 1995

10. Stephens FJ, Raidal SR, Jones B: Haematopoietic necrosis in a goldfish (*Carassius auratus*) associated with an agent morphologically similar to herpesvirus. Aust Vet J **82:**167-169, 2004

The Armed Forces Institute of Pathology
Department of Veterinary Pathology

Conference Coordinator:
Shannon Lacv. DVM. MPH

WEDNESDAY SLIDE CONFERENCE 2009-2010

Conference 10

16 December 2009

Conference Moderator:

Fabio Del Piero, DVM, PhD, Diplomate ACVP

CASE I: S105/07 (AFIP 3067177).

Signalment: Adult female Friesian milk sheep (*Ovis ammon aries*).

History: While being kept for educational purposes during 2004 at the University of Veterinary Medicine Hannover, Clinic for Pigs, Small Ruminants, Forensic Medicine and Ambulatory Service, the sheep tested positive for infection with maedi-visna virus (MVV) and came in 2005 for further diagnostic reasons to the Friedrich-Loeffler-Institut, Federal Research Institute for Animal Health. The animal eventually developed in 2007 severe dyspnea and coughing, and became recumbent. It was then euthanized and submitted for necropsy.

Gross Pathology: The lungs showed multifocal, subpleural and peribronchiolar nodular lesions up to 2 mm in diameter. These foci were grey and slightly elevated (**fig. 1-1**). Within the right cranial lobe there was a 3 x 2 x 2 cm sharply demarcated area of necrotizing and suppurative bronchopneumonia. The caudal mediastinal lymph nodes were enlarged and showed caseous necrosis and abscess formation.

Laboratory Results: Serological testing in 2004 by competitive ELISA revealed antibodies against MVV (more specific data not available). Bacteriological culture of lymph nodes revealed heavy growth of *Corynebacterium pseudotuberculosis* admixed with *E. coli*.

Histopathologic Description: Lung: Multifocally, there are large, up to 1 mm in diameter, aggregates and sheaths of numerous lymphocytes and fewer macrophages in a follicular pattern (BALT hyperplasia) within the parenchyma or subpleural tissue, preferentially adjacent to bronchi, bronchioles and blood vessels (**fig. 1-2**). Diffusely, alveolar septa are slightly thickened by few infiltrating lymphocytes and macrophages and rare neutrophils. Around terminal bronchioles there are prominent bundles of smooth muscle cells (hypertrophy) (**fig. 1-3**). Occasionally, in the alveolar lumina there are few detached pneumocytes.

Contributor's Morphologic Diagnosis: Lung: Pneumonia, bronchointerstitial, lymphocytic and histiocytic, multifocal, moderate, chronic with smooth muscle hypertrophy; etiology consistent with maedi-visna virus infection.

Contributor's Comment: Maedi is a persistent, chronic and progressive viral disease in sheep and

Sponsored by the American Veterinary Medical Association, the American College of Veterinary Pathologists, and the C. L. Davis Foundation.

1-1. Lung, sheep. There are multifocal, raised, grey nodular subpleural and peribronchiolar lesions up to 2 mm in diameter. Photograph courtesy of Friedrich-Loeffler-Institut, Suedufer 10, 17493 Greifswald, Germany, jens.teifke@fli.bund.de.

goats that often results in lifelong infection. Cases have been documented in numerous countries worldwide, particularly continental Europe, the United Kingdom, Canada, the United States, Peru, Kenya, South Africa, Israel, India, Myanmar, and the southern regions of the former U.S.S.R. The word, "maedi," is of Icelandic origin meaning, "shortness of breath." However, as a disease found globally, it has been called by a variety of names—Graaf-Reinet disease in South Africa, Zwoegerziekte in the Netherlands, La bouhite in France, and Montana, Marsh's, or Ovine Progressive Pneumonia (OPP) as well as Lymphoid Interstitial Pneumonia (LIP) in the United States.[4] Maedi sometimes couples with visna, another slowly progressive disease causing meningoencephalitis in sheep and goats. "Visna" is the Icelandic word for "wasting," which aptly characterizes a major clinical sign of the disease.

Maedi and visna are caused by the ovine maedi-visna virus complex (MVV). It is important to note, however, that the two diseases result from different strains of the virus.[6] MVV is a non-oncogenic retrovirus from the genus *Lentivirus* in the *Retroviridae* family. Retroviruses are spherical, enveloped virus particles with single-stranded, diploid, positive-sense RNA genomes. They possess a reverse transcriptase allowing them to integrate their genomes into the host cell DNA as a provirus. MVV is a small ruminant lentivirus (SRLV) exhibiting antigenic similarities to caprine arthritis encephalitis virus (CAEV). It can be subdivided into 5 groups (A-D) and further subtypes. MVV subtypes A1 and A2 seem to exclusively affect sheep, while A5, A7, B1, C, and D specifically affect goats. Subtypes A3, A4, A6 and B2 affect both sheep and goats.[5]

MVV is transmitted both horizontally and vertically. It can also be spread between species by direct contact. The primary mode of transmission has been via ingestion of colostrum or milk by the newborn.[5] Interestingly, there has been a higher risk of MVV infection when a newborn animal is bottle-fed colostrum from a seropositive ewe than when the newborn naturally suckles the same ewe.[3] Respiratory secretions constitute a secondary mode of transmission to ingestion of colostrum.[5]

Many sheep are seropositive for MVV, but few show clinical disease. The incubation period for the virus complex tends to be two to three years, possibly extending to eight.[6] Consequently, clinical signs will generally not appear in animals before they are two years old with the highest concentration of disease cases from five to ten years of age.[2] The primary manifestations of maedi are as follows: 1) a slow and progressively worsening dyspnea and 2) weight loss resulting in undernourishment, despite a normal appetite. With the appearance of clinical signs, maedi causes nearly 100% fatality.

On gross pathologic examination of maedi-diseased

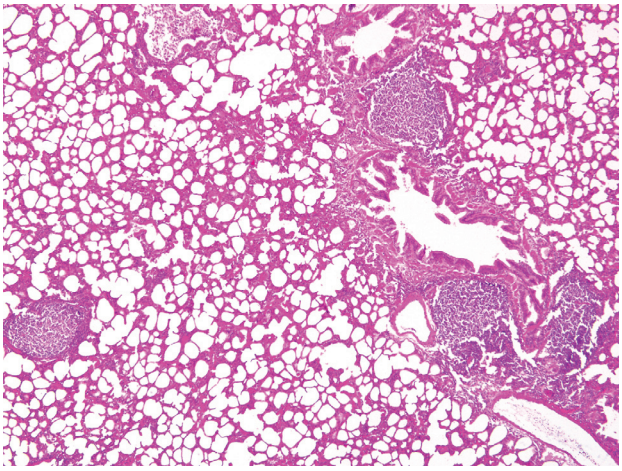

1-2. Lung, sheep. Multifocally, there is prominent nodular hyperplasia of peribronchiolar and perivascular lymphoid tissue and a diffuse cellular infiltrate within the interstitium. (HE 40X)

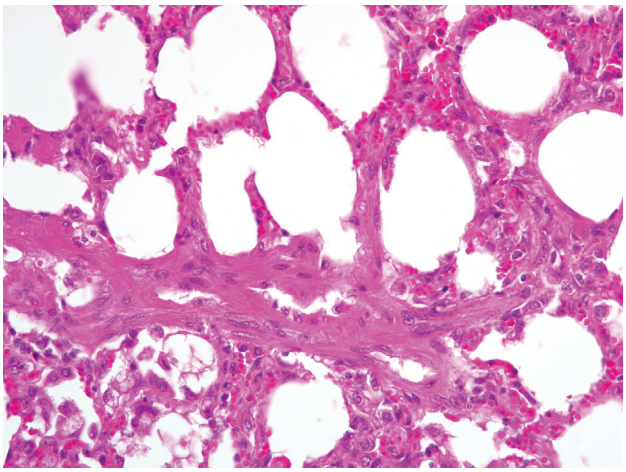

1-3. Lung, sheep. There is smooth muscle hyperplasia, lymphohistiocytic infiltration of the alveolar septa, and small amounts of fibrosis. Multifocally within alveoli there are few alveolar macrophages. (HE 400X)

animals, lungs are heavier than normal and appear expanded. Rib impressions may also be apparent. The lungs will typically be mottled and gray. The cut surface is commonly dry and exudate cannot be extruded. Regional lymph nodes—mediastinal and tracheobronchial—are often enlarged.[4]

The general pathogenesis of MVV is not fully understood. Viral RNA and proviral DNA can be detected in a broad spectrum of cells, including dendritic cells, lymphocytes, plasma cells, endothelial cells, fibroblasts, adipocytes, microglial cells, pericytes, epithelial cells of bronchi, alveoli, mammary glands, thyroid follicles, choroid plexus, small intestine, renal tubules, and third eyelid. However, viral antigen has only been found in macrophages and monocytes, suggesting these cells may be the more exclusive replication sites for the virus complex.[1] The characteristic histopathologic finding for maedi is a pulmonary lymphocytic proliferation, predominantly of T cells.[4] Opportunistic bacterial infections can also occur, making a precise diagnosis of the disease sometimes difficult.

AFIP Diagnosis: Lung: Pneumonia, interstitial, lymphohistiocytic, diffuse, mild to moderate, with peribronchiolar lymphoid hyperplasia and smooth muscle hypertrophy.

Conference Comment: The contributor provides a useful synopsis of this widespread entity. Lentiviral infections in small ruminants differ from those in felids and primates in that they do not result in immunosuppression. Progressive pneumonia is the most common manifestation of MVV infection in sheep; less frequent manifestations include encephalitis, arthritis, mastitis, and glomerulonephritis. Because it is closely related to MVV, CAEV not surprisingly produces a similar constellation of disease manifestations in goats (see WSC 2009-2010, Conference 1, case III), with several notable differences. Chief among these, arthritis in adults and neurologic disease in kids are far more common manifestations of CAEV in goats than is pneumonia. Additionally, CAEV pneumonia in goats is characterized by well-demarcated areas of type II pneumocyte hyperplasia, alveolar septal expansion by lymphocytes, and alveolar flooding with eosinophilic proteinaceous fluid. By contrast, type II pneumocyte hyperplasia is not a prominent feature of ovine progressive pneumonia, which is instead typified by interstitial pneumonia with the formation of lymphoid nodules with germinal centers, smooth muscle hypertrophy, and interstitial fibrosis.[2] In the present case, lymphoid proliferation and smooth muscle hypertrophy are the most striking lesions, although there is considerable slide variability with respect to severity, ranging from mild lymphocytic peribronchiolitis and perivasculitis to moderate lymphohistiocytic interstitial pneumonia as described above. There is infrequent type II pneumocyte hyperplasia, which participants attributed to local compression by immediately adjacent large lymphoid nodules.

Contributor: Friedrich-Loeffler-Institut, Federal Research Institute for Animal Health, Riems Island, Südufer 10, 17493 Greifswald, Germany
http://www.fli.bund.de

References:
1. Brellou GD, Angelopoulou K, Poutahidis T, Vlemmas I: Detection of maedi-visna virus in the liver and heart of naturally infected sheep. J Comp Pathol **136:**27-35, 2007
2. Caswell JL, Williams KJ: Respiratory system. *In:* Jubb, Kennedy, and Palmer's Pathology of Domestic Animals, ed. Maxie MG, 5th ed., vol. 2, pp. 618-620. Elsevier Saunders, Philadelphia, PA, 2007
3. Leginagoikoa I, Daltabuit-Test M, Alvarez V, Arranz J, Juste RA, Amorena B, de Andrés D, Luján LL, Badiola JJ, Berriatua E: Horizontal maedi-visna virus (MVV) infection in adult dairy-sheep raised under varying MVV-infection pressures investigated by ELISA and PCR. Res Vet Sci **80:**235-241, 2006
4. López A. Respiratory System. *In:* Pathologic Basis of Veterinary Diseases, ed. McGavin MD, Zachary JF, 4th ed., p. 533, Mosby Elsevier, St. Louis, MO, 2007
5. Pisoni G, Quasso A, Moroni P: Phylogenetic analysis of small-ruminant lentivirus subtype B1 in mixed flocks: evidence for natural transmission from goats to sheep. Virol **339:**147-152, 2005
6. Zachary JF. Nervous System. *In:* Pathologic Basis of Veterinary Diseases, ed. McGavin MD, Zachary JF, 4th ed., p. 936, Mosby Elsevier, St. Louis, MO, 2007

CASE II: NIAH-1 (AFIP 3133944).

Signalment: 50-day-old piglet (*Sus scrofa*).

History: The piglet was euthanized because of severe emaciation.

Gross Pathology: Consolidation with multiple microabscesses was found in the cranial-ventral portions of the lung. Multiple petechiae and microabscesses were present throughout the liver. The inguinal lymph node was swollen and edematous.

Laboratory Results: *Actinobacillus pleuropneumoniae* (*A. pleuropneumoniae*) and *Pasteurella* spp. were isolated from the lung. *Pasteurella* spp. and *Haemophilus parasuis* were isolated from the pulmonary lymph node.

Histopathologic Description: Multiple microabscesses with bacterial colonies at the center of the lesion were found in the liver, lung, spleen, lymph nodes and the serosa of the urinary bladder (**figs. 2-1 and 2-2**). The infiltrating inflammatory cells surrounding the bacterial colonies had a spindle-shaped nucleus and cytoplasm which were morphologically different from neutrophils usually seen in a typical abscess. In addition, thrombi often containing bacteria were observed in hepatic portal veins. In the lung, similar lesions of the microabscesses with bacterial colonies were formed in the alveolar space and bronchiolar lumen. Immunohistochemical examination with rabbit hyperimmune serum against *A.*

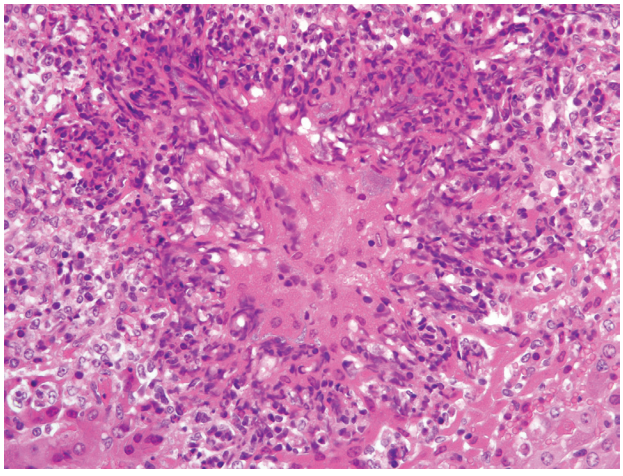

2-1. Liver, pig. There are multifocal random areas of necrosis surrounded by numerous viable and degenerate neutrophils and fewer histiocytes. Within the central areas of necrosis there are frequently large colonies of 1 x 2 um coccobacilli. (HE 400X)

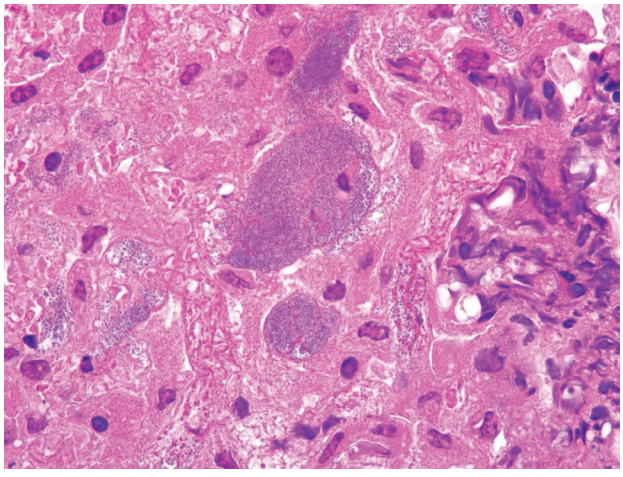

2-2. Liver, pig. Large colonies of coccobacilli within random areas of acute coagulative hepatocellular necrosis. (HE 1000X)

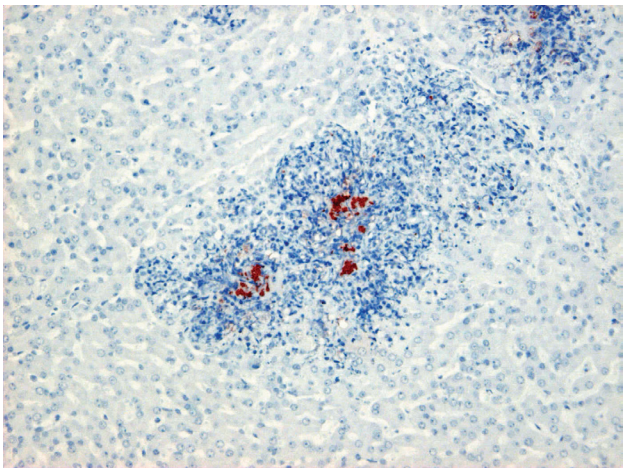

2-3. Liver, pig. Colonies of bacteria are immunohistochemically positive for Actinobacillus pleuropneumonia type-2 antigen. Photomicrograph courtesy of 3-1-5 Kannondai, Tsukuba, Ibaraki, 305-0856, Japan, yyu@affrc.go.jp.

pleuropneumoniae type 2 revealed a positive reaction of the bacteria in the liver and lung (**fig. 2-3**). Other than the lesions caused by *A. pleuropneumoniae*, lymphocytic depletion was found in the various lymphoid tissues. In the tonsil, porcine circovirus type 2 antigens were detected by immunohistochemistry. Intense plasma cell infiltration was observed in the interstitial tissue of the kidney. *Balantidium* species infected the colon. No lesions were found in the heart, stomach, duodenum, pancreas, ileum and brain.

Contributor's Morphologic Diagnosis: Liver: Multiple microabscess formation with bacterial colonies and thrombi.

Contributor's Comment: *A. pleuropneumoniae* is a pathogenic agent of the respiratory disease called porcine pleuropneumonia. In a typical case of actinobacillosis, the histopathological changes are characterized by necrosis, hemorrhage, neutrophil infiltration and widespread edema with fibrinous exudates. However, the present case is characteristic in that multiple microabscesses were observed in various organs. Ohba et al [2] reported that *A. pleuropneumoniae* produced granulomatous lesions with asteroid bodies in the liver, showing a possibility of *A. pleuropneumoniae* as a pathogenic agent affecting not only the lung but also the liver and other organs. In the present case, asteroid bodies were not observed. However, bacterial colonies positive for *A. pleuropneumoniae* type 2 were found at the center of microabscess, indicating that these microabscesses could lead to granulomatous lesions later in the course of the disease.

AFIP Diagnosis: Liver: Hepatitis, random, necrotizing and histiocytic, acute, multifocal, moderate, with fibrin thrombi and colonies of coccobacilli.

Conference Comment: This very interesting case underscores the importance of *A. pleuropneumoniae* not only as a cause of pleuropneumonia in pigs, but as a potential cause of necrotizing lesions in other organs as well. Less common lesions associated with *A. pleuropneumoniae* in pigs include meningitis, nephritis, osteomyelitis, arthritis, tenosynovitis, endocarditis, and pericarditis. In a recent case report of 11 pigs with granulomatous hepatitis caused by *A. pleuropneumoniae*, 7 had concurrent pleuropneumonia, which the authors concluded was likely the primary site of infection, with secondary dissemination to the liver; a similar pathogenesis is plausible in the present case.[2]

While conference participants generally concurred with the contributor's histopathologic description, most could not definitively identify neutrophils either within or adjacent to the lesions, and thus preferred the above morphologic diagnosis over the use of the term "microabscess." Participants interpreted the necrotic cells with streaming nuclei as predominantly Kupffer cells and hepatocytes. Despite the rather unusual anatomic location, most participants suspected *A. pleuropneumoniae* as the etiology based on 1) the characteristic nuclear streaming in foci of necrosis, 2) the presence of small to occasionally large colonies of bacilli, and 3) the abundance of fibrin within affected areas, particularly in blood vessels and sinusoids.

Nuclear streaming of leukocytes is typical in pleuropneumonia caused by *A. pleuropneumoniae*, and is attributed to secreted cytotoxins belonging to the repeats in toxin (RTX) family, namely Apx I, II, and III. These potent virulence factors are critical to the development of disease, and mutants lacking the Apx toxin have reduced virulence. Other virulence factors include a capsule that impedes phagocytosis by macrophages, lipopolysaccharide which induces macrophage activation, enzymes (e.g. superoxide dismutase, catalase, and hydroperoxide reductase) that protect against oxidative killing by leukocytes, metalloproteinase, urease, outer membrane proteins, and iron-binding proteins.[1]

Contributor: National Institute of Animal Health, 3-1-5 Kannondai, Tsukuba, Ibaraki, 305-0856 Japan
http://niah.naro.affrc.go.jp/index.html

References:

1. Caswell JL, Williams KJ: Respiratory system. *In:* Jubb, Kennedy, and Palmer's Pathology of Domestic Animals, ed. Maxie MG, 5th ed., vol. 2, pp. 587-589. Elsevier

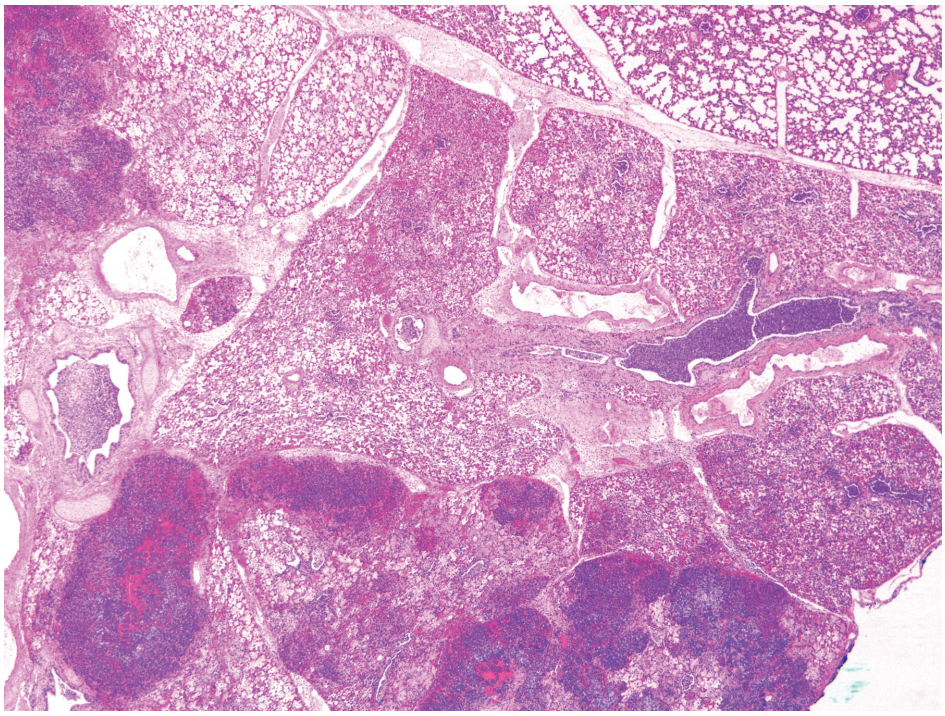

3-1. Lung, ox. Multifocally there is a lobular bronchopneumonia with marked expansion of interlobular septa by edema. (HE 20X)

Saunders, Philadelphia, PA, 2007
2. Ohba, T, Shibahara T, Kobayashi H, Takashima A, Nagoshi M, Osanai R, Kubo M: Multifocal granulomatous hepatitis caused by *Actinobacillus pleuropneumoniae* serotype 2 in slaughter pigs. J Comp Pathol **139:**61-66, 2008

CASE III: 9-35-A (AFIP 3134628).

Signalment: Two (one male and one female) 3-week-old, Holstein calves (*Bos taurus*).

History: These two calves had been housed in separate calf pens in a calf barn with 14 other calves. The calves were fed 2 liters of milk replacer twice per day and heifer calves received Deccox® in the milk daily. The calves received Calf-Guard®, Colimune® and 3 to 4 liters of colostrum at birth. These two calves became ill at 7 to 10 days of age with mildly elevated temperature, poor drinking behavior and scours and subsequently developed abnormal breathing. Despite treatment with antibiotics (Nuflor®) and tube feeding of milk and electrolytes, the calves became progressively weaker and died.

Gross Pathology: Both calves exhibited mildly sunken eyes with a moderate reduction of internal fat stores. The lungs of both calves exhibited dark red to plum purple lobular discoloration of the intermediate lobes, anteroventral aspect of the diaphragmatic lobes and ventral aspect of the anteroventral lobes. Affected lobules were depressed, firm on palpation, and on cut surface exhibited dark red to plum purple discoloration with purulent exudate in airways. The female calf also exhibited mild fibrin exudation over the pleural surface of the discolored lobes, fibrinous adhesions of these lobes to the pericardial sac and increased clear yellow fluid in the pericardial sac with fibrin strands. Intestinal content was watery.

Laboratory Results: *Mannheimia granulomatis,* 4+, in lungs of both calves; *Mannheimia granulomatis*, few, in pericardial sac of female calf; bovine respiratory syncytial virus (BRSV) positive on lung by PCR and immunohistochemistry; rotavirus and bovine coronavirus positive on intestinal contents by PCR.

Histopathologic Description: There was moderate to marked pulmonary lobular consolidation characterized by macrophages and neutrophils intermixed with edema fluid, red blood cells and fibrin strands within alveolar spaces and airway lumina. Variably sized, multifocal aggregates of highly condensed leukocytes with nuclear streaming obscured parenchymal architecture and were

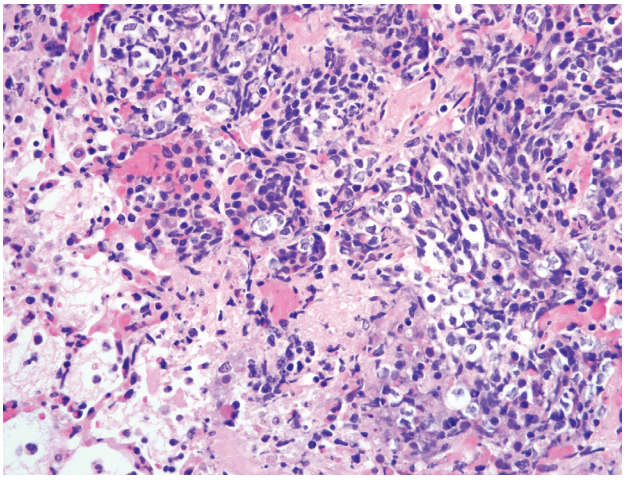

3-2. Lung, ox. There are multifocal patchy areas of coagulative necrosis which are bordered by numerous degenerate leukocytes, many of which have streaming nuclei. Rarely, there are moderate numbers of 1 x 2 um bacteria within areas of coagulative necrosis. (HE 400X)

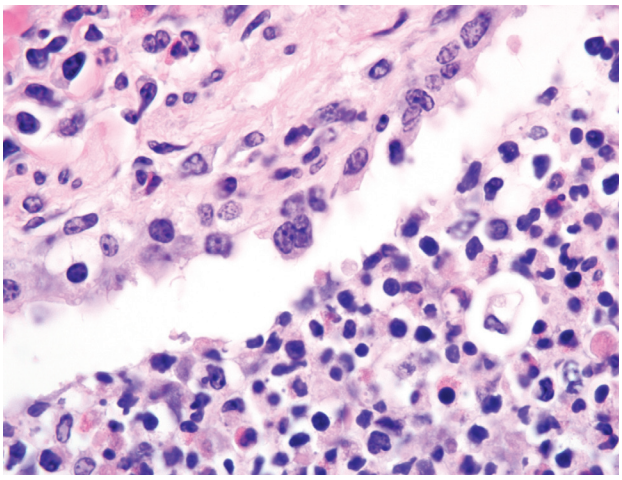

3-3. Lung, ox. Within degenerate, attenuated bronchiolar epithelium there are rare multinucleate syncytial cells. Bronchiolar lumina contain a cellular exudates composed of neutrophils, histiocytes and fewer lymphocytes admixed with low numbers of bacteria. (HE 1000X)

observed throughout the sections (**fig. 3-1**). These foci were often associated with colonies of coccobacillary bacteria, hemorrhage and fibrin (**fig. 3-2**). Depending on the section examined, foci of bronchiolar epithelial necrosis and attenuation, with and without syncytical cells, were occasionally observed (**fig. 3-3**). Interlobular interstitium and lymphatics were mildly to markedly dilated with edema fluid, fibrin strands and a mild to moderate number of neutrophils and macrophages. Fibrin was focally present on the pleural surface and there were subpleural inflammatory infiltrates similar to the interlobular interstitium. There were scattered areas of atelectasis.

Contributor's Morphologic Diagnosis: Lung, bronchopneumonia, anteroventral, marked, subacute, fibrinosuppurative with intralesional coccobacilli and focal bronchiolar necrosis with syncytial cells.

Contributor's Comment: *Pasteurella multocida* and *Mannheimia hemolytica* are the most common Pasteurellaceae bacteria isolated from bovine pneumonia.[3] These organisms are commensals of the bovine nasopharynx which, during periods of stress or viral infection, can overwhelm host defense mechanisms establishing infection in the lower respiratory tract.[3] *M. granulomatis* is one of five recognized species of the genus *Mannheimia*.[1] This bacterium has been reported in association with oral abscesses and suppurative bronchopneumonia in Australian cattle [1], purulent bronchopneumonia, pleuritis, stomatitis and abscesses in Danish Roe deer [2] , purulent bronchopneumonia and conjunctivitis in European Brown hares [5] and a fibrogranulomatous panniculitis in Brazilian cattle known as lechiguana.[6]

The bronchopneumonia in the two Holstein calves reported here was similar to pneumonia described with *M. haemolytica* infection in that there was significant leukocyte necrosis as evidenced by oat cells, widespread accumulation of edema fluid, neutrophils, macrophages, fibrin, foci of hemorrhage and bacterial aggregates within alveolar spaces and airway lumina and interlobular septae were distended with serofibrinous exudate.[3] A similar lesion to *M. haemolytica* would be anticipated as it has been shown that *M. granulomatis* has leukotoxin activity in vitro.[2,7] However, large areas of coagulation necrosis surrounded by a thick rim of leukocytes, as is frequently observed with *M. haemolytica* pneumonia [3], were lacking in the *M. granulomatis* lesion. These observations suggest that, although both *M. granulomatis* and *M. haemolytica* share virulence factors [2,7], there may be subtle differences in pathological expression. However, more cases of *M. granulomatis* pneumonia would need to be examined before any conclusions could be drawn with regard to expression of virulence.

These calves also had focal infection with BRSV which was confirmed by PCR and immunohistochemistry. Viral BRSV lesions were not present in all tissue sections submitted. Pulmonary BRSV infection likely predisposed these calves to bacterial pneumonia. While *P. multocida* and *M. haemolytica* are reported to be commensal in the bovine nasopharynx [3], it is unclear how these two calves became infected with *M. granulomatis*.

AFIP Diagnosis: Lung: Bronchopneumonia, fibrinosuppurative, multifocal to coalescing, marked, with edema, hemorrhage, and coccobacilli.

Conference Comment: The conference moderator emphasized the importance of additional diagnostic testing when assessing the histomorphology present in this case; the two most likely etiologies include *P. multocida* and *M. haemolytica*, as noted by the contributor, and definitive determination necessitates additional diagnostics, such as microbial culture, immunohistochemistry, in situ hybridization, and PCR, as employed in this case.

Leukotoxin, mentioned by the contributor, is an important virulence factor of *M. haemolytica*. A member of the repeats in toxin (RTX) family, leukotoxin is secreted during the log phase of growth, and its receptor is CD18.[3] At low concentrations, leukotoxin activates bovine platelets and leukocytes or induces their apoptosis [4], while at high concentrations it induces leukocyte lysis, resulting in the characteristic nuclear streaming noted microscopically in areas of necrosis.[3] Lipopolysaccharide, another important virulence factor, is synergistic with leukotoxin because it induces increased expression of β2-integrins on leukocytes which contain the CD18 receptor. Other important bacterial virulence factors include a polysaccharide capsule that assists in attachment and impairs phagocytosis, iron-regulated outer membrane proteins that bind transferrin and alter neutrophil function, adhesins that mediate attachment, and neuraminidase that decreases both respiratory mucus viscosity and repellant negative charge on host cells. Cytokines TNF-α, IL-1β, and IL-8 are particularly important components of the complex inflammatory milieu produced in pneumonic mannheimiosis.[8]

Bovine parainfluenza virus 3, bovine herpesvirus 1, and BRSV all increase susceptibility to *M. haemolytica*, and presumably other respiratory pathogens, by infecting ciliated epithelium and reducing mucociliary clearance; the latter two also infect and impair alveolar macrophages. Of note, bovine herpesvirus 1 is also thought to increase susceptibility to the effects of *M. haemolytica* by upregulating CD18 expression in neutrophils.[3]

As mentioned by the contributor, there is some slide variation with respect to the presence of viral syncytia. In a few sections, participants noted viral syncytia in bronchioles with multifocal bronchiolar epithelial necrosis, consistent with bronchointerstitial pneumonia due to BRSV infection. Additionally, lymphatic vessel lumina within interlobular septa are multifocally occluded by coagula of fibrin and mixed inflammatory cells. There are rare intravascular megakaryocytes in some sections, which participants speculated may be associated with terminal bone marrow hypoxia. Intravascular megakaryocytes in the human lung were first described in 1893, and it has since been demonstrated that under normal conditions, intact megakaryocytes leave the bone marrow and reach the pulmonary capillary bed, where they release platelets by fragmentation of their cytoplasm.[9]

Contributor: Animal Health Centre, BC Ministry of Agriculture and Lands, 1767 Angus Campbell Road, Abbotsford, BC, Canada V3G 2M3
http://www.al.gov.bc.ca/ahc/index.htm

References:

1. Blackall PJ, Bisgaard M, Stephens CP: Phenotypic characterization of Australian sheep and cattle isolates of *Mannheimia haemolytica, Mannheimia granulomatis* and *Mannheimia varigena*. Aust Vet J **80:**87-91, 2002
2. Bojesen AM, Larsen J, Pedersen AG, Morner T, Mattson R, Bisgaard M: Identification of a novel *Mannheimia granulomatis* lineage from lesions in roe deer (*Capreolus capreolus*). J Wildl Dis **43:**345-352, 2007
3. Caswell JL, Williams KJ: Respiratory system. *In:* Jubb, Kennedy, and Palmer's Pathology of Domestic Animals, ed. Maxie MG, 5th ed., vol. 2, pp. 601-605. Elsevier Saunders, Philadelphia, PA, 2007
4. Cudd LA, Ownby CL, Clarke CR, Sun Y, Clinkenbeard KD: Effects of *Mannheimia haemolytica* leukotoxin on apoptosis and oncosis of bovine neutrophils. Am J Vet Res **62:**136-140, 2001
5. Devriese LA, Bisgaard M, Hommez J, Uyttebroek E, Ducatelle R, Haesebrouck F: Taxon 20 (Fam. Pasteurellaceae) in European brown hares (*Lepus europaeus*). J Wildl Dis **27:**685-687, 1991
6. Riet-Correa F, Mendez MC, Schild AL, Ribeiro GA, Almeida SM: Bovine focal proliferative fibrogranulomatous panniculitis (lechiguana) associated with *Pasteurella granulomatis*. Vet Pathol **29**:93-103, 1992
7. Veit HP, Wise DJ, Carter GR, Chengappa MM: Toxin production by *Pasteurella granulomatis*. Ann NY Acad Sci **849:**479-484, 1998
8. Wollums AR, Ames TR, Baker JC: The bronchopneumonias (respiratory disease complex of cattle, sheep, and goats). *In:* Large Animal Internal Medicine, ed. Smith BP, 4th ed., pp. 613-617. Mosby Elsevier, St. Louis, MO 2009
9. Zucker-Franklin D, Philipp CS: Platelet production in the pulmonary capillary bed: new ultrastructural evidence for an old concept. Am J Pathol **157:**69-74, 2000

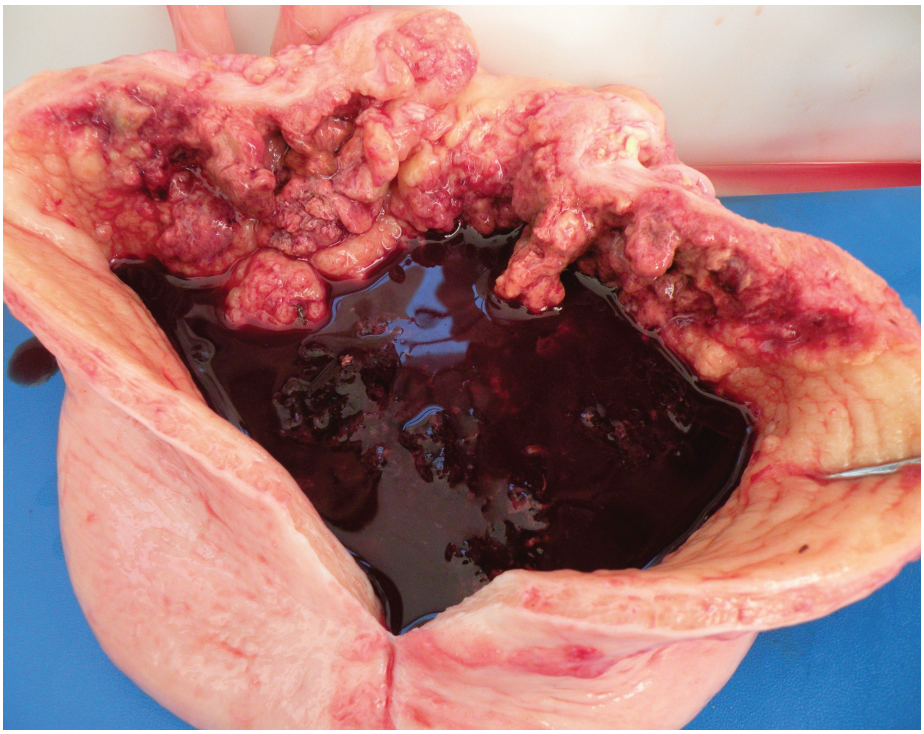

4-1. Urinary bladder, ox. The urinary bladder is distended and filled with urine admixed with blood and blood clots. The bladder wall is multifocally thickened, ulcerated, or covered with red-brown fibrin. There are several variably sized nodules which protrude into the bladder lumen which are both concentrated around areas of ulceration and randomly distributed throughout the mucosa. Photograph courtesy of Universidade Federal de Santa Maria, Departamento de Patologia, 97105-900, Santa Maria, RS, Brazil, claudioslbarros@uol.com.br.

CASE IV: UFSM-1 (AFIP 3134867).

Signalment: 7-year-old, female, mixed breed ox (*Bos taurus*).

History: This cow had chronic intermittent hematuria, anorexia, and marked weight loss over the last several weeks. During the three days before its death it assumed a lateral recumbency.

Gross Pathology: The cow was in poor body condition. There was pallor to the external mucous membranes. The urinary bladder was distended by and full with urine admixed with blood and blood clots. The bladder wall was approximately 1.5 cm in thickness and in the ostium of the ureters there was an ulcerated area of 19 x 6 cm covered with red-brown fibrin. There were also two 2.5 x 1.5 x 3 cm ulcerated areas and several 0.5 cm in diameter nodules randomly distributed throughout the vesical mucosa, but mainly localized around the ulcerated areas (**fig. 4-1**). The ureters were distended (hydroureter). The left kidney was 24 x 14 x 68 cm, had a thick and adhered capsule and multifocal irregular white-yellowish areas covered by pus and fibrin could be observed throughout the capsular surface. At cut surface pyelonephritis was evident. Hydronephrosis, pyelonephritis, and hydroureter could be observed in the contralateral kidney, where these lesions were less marked.

Histopathologic Description: There are areas of hyperplasia of the lining urothelium with clusters of transitional epithelial cells in the lamina propria (Brunn's nests). Some nests are solid and others have central empty spaces. Underneath the areas of hyperplastic urothelium there are developed acini and tubules lined by well differentiated columnar epithelial and goblet cells (glandular metaplasia = cystitis glandularis). From the lamina propria to the muscle layer there is a proliferation of neoplastic epithelial cells arranged as islands, ribbons, small clusters, or as isolated individual cells (**fig. 4-2**). There is necrosis, mainly at the center of several islands. The neoplastic cells are large, polyhedal, with eosinophilic cytoplasm and open faced and markedly pleomorphic nuclei; the nuclear chromatin is either finely loose or clumped and there are 1-2 mitoses per high power field (**fig. 4-3**). Several neoplastic emboli can be observed within lymphatic vessels and moderate desmoplasia is apparent (**fig. 4-4**).

Contributor's Morphologic Diagnosis: 1. Urinary bladder, nonpapillary and infiltrating transitional cell carcinoma; Etiology: chronic ingestion of *Pteridium aquilinum*.
2. Kidney, pyelonephritis, chronic, suppurative, severe

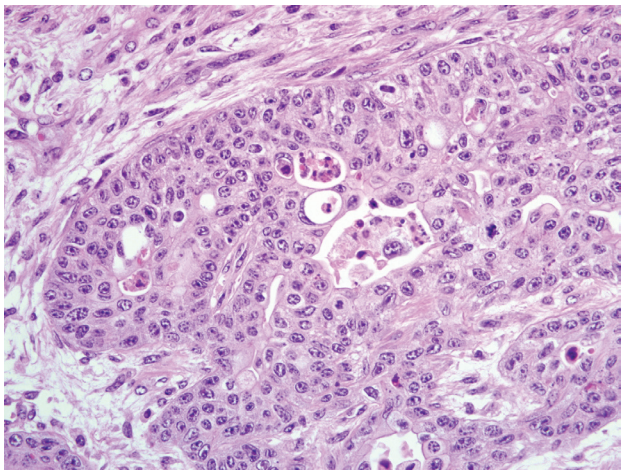

4-2. Urinary bladder, ox. Malignant neoplastic transitional epithelial cells are arranged in islands, nests, and occasional papillary projections supported by a moderate to dense fibrous stroma (desmoplasia). The mitotic rate is high, with bizarre mitoses. Multifocally there is necrosis of neoplastic cells. (HE 400X)

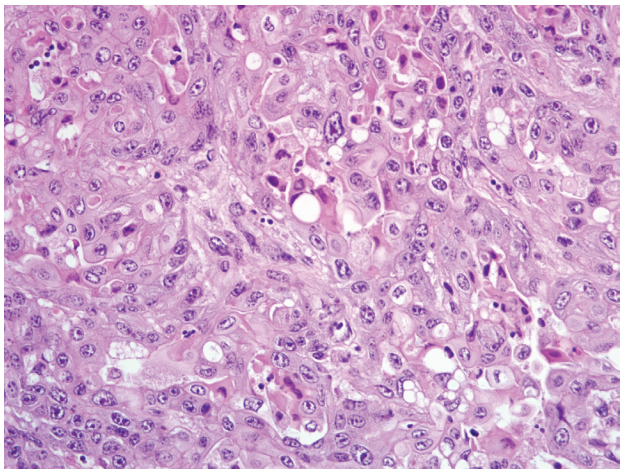

4-3. Urinary bladder, ox. Neoplastic cells have generally distinct cell borders and moderate to abundant eosinophilic cytoplasm. Multifocally neoplastic cells contain a large clear cytoplasmic vacuole which peripheralizes and compresses the nucleus (signet ring cells). (HE 400X)

(slides not included).
3. Kidney, diffuse cortical atrophy (slides not included).

Contributor's Comment: Bracken fern (*Pteridium aquilinum*) is the second most important plant poisoning in southern Brazil. It is responsible for 12% of all deaths of cattle caused by poisonous plants in this region.[13] The ingestion of bracken fern results in three forms of clinical disease in cattle, one acute and two chronic. The acute form occurs when cattle ingest amounts equal to or above 10 grams per kilogram of body weight during 2-11 weeks. Clinical signs associated with acute form of bracken fern poisoning in cattle include high fever, severe hemorrhages in various tissues, and neutropenia and thrombocytopenia due to bone marrow aplasia [1] (please see also WSC 2008-2009, Conference 19, case I).

Chronic forms of disease are characterized by development of neoplasms: 1) squamous cell carcinomas in the upper digestive tract (base of tongue, esophagus and entrance of the rumen) [15] (please see also WSC 2004-2005, Conference 12, case IV) and 2) several types of the neoplasms in the urinary bladder.[5,12] This latter condition, the one of this report, is associated with bleeding from the urinary bladder and is universally known as bovine enzootic hematuria (BEH). Ptaquiloside is reportedly the active toxic principle in bracken fern; however, as a complexing factor, bovine papillomavirus type 4 (BPV-4) is frequently associated with bracken-induced tumors of upper digestive system [4] and bovine papillomavirus type 2 (BPV-2) is frequently associated with bracken-induced tumors of the urinary bladder.[3,5]

The prevalence of BEH varies depending on the region. Morbidity rates could be up to 10% and lethality rates are 100%.[8] BEH is observed in adult cattle and the most frequent clinical signs include intermittent or continuous hematuria, weight loss, pale mucous membranes, and anemia. In lactating cows there is a severe drop in milk yield.[16] Less frequently urinary incontinency, polyuria and dysuria are seen. The amount of daily loss of blood with urine varies from 0.01 to 1.0 L [5] and results in chronic anemia; in some cases a mass or thickening of the wall can be felt in the urinary bladder by rectal palpation. Cases of BEH can go through intervals of weeks and even months in which clinical signs become inapparent, but reccurrences are the rule and death of affected animals will occur months or even up to one year after the onset of clinical signs.[7]

Due to the ureteral obstruction caused by tumors, hydronephrosis, hydroureter and pyelonephritis are common complications observed in BEH. Laboratory findings in cattle affected by BEH include lymphocytosis, neutropenia, progressive anemia, decreased albuminemia, increased globulinemia, decreased calcium and phosphorous serum levels and increased serum activities of creatinine kinase and alkaline phosphatase.[7]

Gross findings in the urinary bladder of BEH affected cattle include dilatation of the bladder, with thickening of the wall and urine admixed with blood and blood clots.

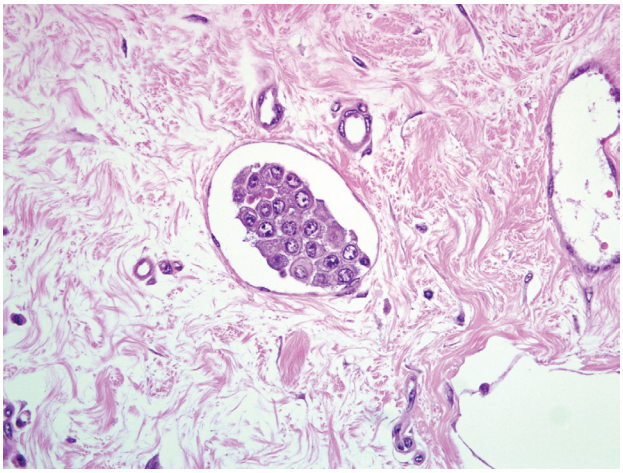

4-4. Urinary bladder, ox. Lymphatic vessels in the submucosa occasionally contain neoplastic cells. (HE 400X)

In the bladder mucosa there is congestion, markedly conspicuous vascularization, hemorrhagic foci, vascular growths, cauliflower-resembling nodules, red, white or yellow masses, pedunculated or sessile, frequently multilobulated and ulcerated and multiple translucent nodules arranged as bunches of grapes.[7,16]

Histologic examination of the bladder tumors associated with BEH reveals a large spectrum of tumor types, both of epithelial and mesencyhmal origin [7,12] and although mestastases are rare they are known to occur mainly to the lumboaortic lymph node.[5] In some cases the hematuria is not associated with the presence of neoplastic lesions, and the only lesions observed in the bladder mucosa are congestion and blood vessel ectasia.[7]

Other species, like sheep and horses, might be poisoned by *Pteridium* spp. Sheep, although much less frequently, are also affected by enzootic hematuria. In Australia the disease in sheep was attributed to the ingestion of *P. esculentum*. Changes in the bladder epithelium were metaplastic and neoplastic (carcinomas).[9] The acute hemorrhagic form of the disease, similarly to the one described in cattle, is also known to occur occasionally in sheep.[1] Three other conditions, namely intestinal tumors, the so called "bright blindness" and polioencephalomalacia are described in sheep that consume *P. aquilinum*.[10] Bright blindness is a form of retinal degeneration in which rods and cones are almost completely destroyed. Polioencephalomalacia is reportedly caused by the high thiaminase I contained in the plant.[10] Polioencephalomalacia has been reproduced in sheep by the feeding of bracken fern. A form of neurological disease due to the thiaminase action is also described in horses but the evidences for this disease are less convincing than the other forms of intoxication associated to this plant. Reportedly neurointoxication of the horse occurs more frequently in stabled horses receiving fodder contaminated with bracken fern, with clinical signs occurring 3-6 weeks after continuous exposure to the plant. Although the disease has been termed polioencephalomalacia, noteworthy pathological changes have not been described associated to presumptive bracken poisoning in horses. Horses fed for more than two months with dry bracken fern had no clinical or pathological findings in southern Brazil (unpublished data).

AFIP Diagnosis: Urinary bladder: Transitional cell carcinoma, nonpapillary and infiltrating.

Conference Comment: The contributor provides a complete review of bracken fern toxicosis, and in a well-constructed description of this neoplasm, mentions the presence of necrosis, frequently at the center of islands of neoplastic transitional epithelial cells. This histomorphologic feature, often referred to as the "comedo pattern," is frequently seen in transitional cell carcinoma (TCC). Additional features typical of TCC, including signet ring cells and desmoplasia, were also noted in several sections by conference participants.

Roperto et al [14] recently classified 400 bovine urothelial tumors in accordance with the World Health Organization morphological classification for human urothelial tumors, which is based on four distinct patterns of growth: flat, exophytic or papillary, endophytic, and invasive. In this series, urothelial tumors were usually multiple, and among flat urothelial lesions, carcinoma in situ (CIS) was the most common, accounting for 4% of the series, and occurring adjacent to papillary and invasive neoplasms in 80-90% of examined cases. The authors preferred the use of the term "urothelial CIS" to such synonyms as "non-papillary and non-infiltrating TCC"; urothelial CIS is characterized by marked local aggressive behavior, formation of von Brunn's nests, pleomorphism, and frequent microinvasion into the lamina propria.[14] In the present case, participants noted CIS adjacent to the invasive neoplasm in many sections. In the same series, low-grade papillary urothelial carcinoma, consisting of papillary fronds lined by variably orderly urothelium, was the most common urothelial tumor recorded. Invasive urothelial tumors, most of which were high-grade carcinomas as with the present case, were less common than papillary urothelial neoplasms.[14]

Ptaquiloside is the major carcinogen in bracken fern. In alkaline environments, such as the urinary bladder or ileum of cattle, ptaquiloside is activated to its unstable reactive dienone form, which induces DNA alkylation.[14] The plant also contains thiaminase, tannins, phenolic acid, and several other carcinogens (e.g. quercetin, ptaquiloside Z, aquilide A, shikimic acid, and prunasin).[2,14] Bracken

fern is also of significant public health interest in certain geographic locations due to epidemiological studies linking bracken fern consumption and cancer, either directly or indirectly through the milk of animals grazing on the plant or contaminated water.[14]

The contributor mentioned the role of BPV-2 and BPV-4 in association with bracken fern-induced tumors of the urinary bladder and upper digestive system, respectively. BPV-2 also is associated with cutaneous papillomas and fibropapillomas of the skin, esophagus, esophageal groove, and rumen.[2] The only BPVs known to infect the bladder urothelium, BPV-1 and BPV-2 are capable of infecting mesenchymal tissues and exhibiting cross-species transmission, and encode three oncoproteins (i.e. E5, E6, and E7) that initiate cellular transformation by a variety of mechanisms.[14]

Contributor: Departamento de Patologia, Universidade Federal de Santa Maria, 97105-900 Santa Maria, RS, Brazil
http://www.ufsm.br/lpv

References:

1. Anjos BL, Irigoyen LF, Fighera RA, Gomes AD, Kommers GD, Barros CSL: Acute poisoning by bracken fern (*Pteridium aquilinum*) in cattle in central Rio Grande do Sul, Brazil [Intoxicação aguda por samambaia (*Pteridium aquilinum*) em bovinos na Região Central do Rio Grande do Sul] Pesq Vet Bras **28:**501-507, 2008 (In Portuguese, Abstract in English)
2. Brown CC, Baker DC, Barker IK: Alimentary system. *In:* Jubb, Kennedy and Palmer's Pathology of Domestic Animals, ed. Maxie MG, 5th ed., vol. 2, p. 51. Saunders, Elsevier, Philadelphia, PA, 2007
3. Campo MS, Jarrett WF, Barron R, O'Neil BW, Smith KT: Association of bovine papillomavirus type 2 and bracken fern with bladder cancer in cattle. Cancer Res **52:**6898-6904, 1992
4. Campo MS: Bovine papillomavirus and cancer. Vet J **154:**175–188, 1997
5. Carvalho T, Naydan D, Nunes T, Pinto C, Peleteiro MC: Immunohistochemical evaluation of vascular urinary bladder tumors from cows with enzootic hematuria. Vet Pathol **46:**211-221, 2009
6. Dawra RK, Sharma OP, Somvanshi R: Experience with enzootic hematuria in India Bracken Fern conference. *In:* International Bracken Fern Group Conference – Bracken Fern: Toxicity, Biology and Control, ed. Taylor JA, Smith RT, Special Publication number 4, p. 150-154. International Bracken Group, Manchester, England, 2000
7. França TN, Tokarnia CH, Peixoto PV: Diseases caused by the radiomimetic principle of *Pteridium aquilinum* (Polypodiaceae): a review [Enfermidades determinadas pelo princípio radiomimético de *Pteridium aquilinum* (Polypodiaceae). Pesq Vet Bras **22:**85-96, 2002 (In Portuguese, Abstract in English)
8. Gava A, Neves DS, Saliba TM, Schild Al, Riet-Correa F. Bracken fern (*Pteridium aquilinum*) poisoning in cattle in southern Brazil. Vet Human Toxicol **44**:362-365, 2002
9. Harbutt PR & Leaver DD: Carcinoma of the bladder of sheep. Aust Vet J **45:**473-475, 1969
10. Kellerman TS, Coetzer JAW, Naudé TW, Botha CJ. Plant poisonings and mycotoxicoses of livestock in Southern Africa. 2nd ed., p 84, Oxford University Press, Oxford, 2005
11. Maxie MG, Newman SJ: Urinary system. *In:* Jubb, Kennedy, and Palmer's Pathology of Domestic Animals, ed. Maxie MG, 5th ed., vol. 2, pp. 518-521. Elsevier Saunders, Philadelphia, PA, 2007
12. Peixoto PV, França TN, Barros CSL, Tokarnia CH: Histopathological aspects of bovine enzootic hematuria in Brazil. Pesq Vet Bras **23:**65–81, 2003
13. Rissi DR, Rech RR, Pierezan F, Gabriel AL, Trost ME, Brum JS, Kommers GD, Barros CSL: Plant and plant-associated mycotoxins poisoning in cattle in Rio Grande do Sul, Brazil: 461 cases [Intoxicação por plantas e micotoxinas associadas a plantas em bovinos no Rio Grande do Sul]. Pesq Vet Bras **27:**261-268, 2007 (In Portuguese, Abstract in English)
14. Roperto S, Borzacchiello G, Brun R, Leonardi L, Maiolino P, Martano M, Paciello O, Papparella S, Restucci B, Russo V, Salvatore G, Urraro C, Roperto F: A review of bovine urothelial tumours and tumour-like lesions of the urinary bladder. J Comp Pathol (in press), 2009
15. Souto MAM, Kommers GD, Barros CSL, Piazer JVM, Rech RR, Riet-Correa F, Schild AL: Neoplasms of the upper digestive tract of cattle associated with spontaneous ingestion of bracken fern (*Pteridium aquilinum*) [Neoplasias do trato alimentar superior de bovinos associadas ao consumo espontâneo de samambaia (*Pteridium aquilinum*)]. Pesq Vet Bras **26:**112-122, 2006 (In Portuguese, Abstract in English)
16. Souto MAM, Kommers GD, Barros CSL, Rech RR, Piazer JVM: Urinary bladder neoplasms associated with bovine enzootic [Neoplasmas da bexiga associados à hematuria enzoótica bovina]. Ciência Rural **36:**1647-1650, 2006 (In Portuguese, Abstract in English)

The Armed Forces Institute of Pathology
Department of Veterinary Pathology

Conference Coordinator:
Shannon Lacy, DVM, MPH

WEDNESDAY SLIDE CONFERENCE 2009-2010

Conference 11

6 January 2010

Conference Moderator:

Cathy S. Carlson, DVM, PhD, Diplomate ACVP

CASE I: Z16753 (AFIP 3138054).

Signalment: 5-year-old, female, American Staffordshire terrier dog (*Canis familiaris*).

History: The dog presented with imbalance, a stiff gait, urinary incontinence, anorexia, inappetence and lethargy. Electromyography showed lesions at the promixal muscles of the forelimbs and the masticatory muscles. MRI revealed no abnormalities. On radiographic examination, masses were detected in the lung, multiple ribs and the dorsal processes of T2 and T5. Osteophytes were seen radiographically on the forelimb and scapulae.

Gross Pathology: Numerous flat, subperiostal, bony proliferations were detected on the diaphysis and metaphysis of humeri, scapulae, femora and tibiae. These dense proliferations varied in size from 3 mm to 2 cm in length. Multiple irregular, osseus proliferations were present on several ribs, processus dorsalis of T2 and T5 and corpus spinalis of L2. The anteroventral lung lobes showed bilaterally poorly demarcated, infiltrative growing, firm, white-tan masses.

Histopathologic Description: Rib. Two main lesions are present. The first consists of circumferential proliferation of trabecular woven bone perpendicular to the cortex (periosteal new bone formation). The cortical bone is decreased in thickness and shows a high porosity (osteopenia). Within the medullary cavity, a neoplastic mass is present (second lesion). It consists of neoplastic cells showing papillary growth in the existing bone marrow. There is an increase in fibrous tissue. Neoplastic cells are cuboidal to polygonal, 20 µm in diameter with a moderate amount of eosinophilic, poorly demarcated cytoplasm. The nucleus is round with a single prominent nucleolus and finely stippled chromatin. There is marked anisokaryosis and anisocytosis. The mitotic index is 1 per HPF. Multifocally, there are numerous islands of tumor cells with central necrosis and infiltration of neutrophils.

Contributor's Morphologic Diagnosis: Reactive periosteal new bone formation. Bone metastasis of papillary adenocarcinoma. Lesions consistent with pulmonary hypertrophic osteopathy.

Contributor's Comment: Hypertrophic osteopathy is also known as hypertrophic pulmonary disease and is characterized by new bone formation along the distal parts of the limbs. It occurs in humans and several animal species. Unlike in humans, where the condition is also called "hypertrophic osteoarthropathy," articular surfaces are not affected in animals. It is a paraneoplastic condition

*Sponsored by the American Veterinary Medical Association, the American College of Veterinary Pathologists, and the C. L. Davis Foundation.

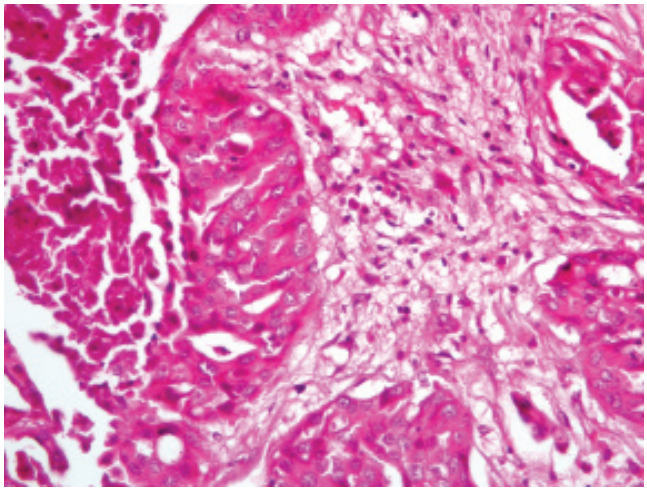

1-1. Bone, rib, dog, metastatic carcinoma. Multiple islands of neoplastic epithelial cells are surrounded by abundant reactive fibrous connective tissue (desmoplasia). (HE 400X)

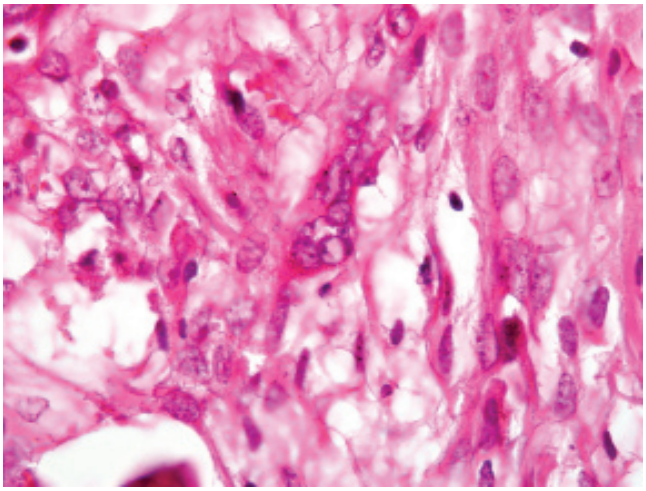

1-2. Bone, rib, dog, metastatic carcinoma. Multifocally there are multinucleated neoplastic cells with up to 6 variably sized nuclei. (HE 1000X)

generally associated with a lesion located in the thoracic cavity. In dogs it has been described in association with renal pelvis carcinoma[1,3], congenital megaesophagus[6], parasitic infection(4) and endocarditis.[2] Hypertrophic osteopathy is considered to be a reversible condition if the underlying lesion is corrected. The pathogenesis of the condition is still unclear.[2]

AFIP Diagnosis: Bone, rib: Carcinoma, metastatic.

Conference Comment: In concurrence with the contributor, conference participants identified a metastatic carcinoma, and many, including the conference moderator, favored the contributor's more specific diagnosis of metastatic adenocarcinoma based on the formation of vague tubules within the neoplasm. In the absence of a clinical history, other participants suspected a metastatic transitional cell carcinoma based on the presence of "signet ring cells" among the neoplastic population; given the history of urinary incontinence and presence of metastasis to the thoracic vertebrae, this remains a reasonable possibility. While very common in humans, metastatic bone disease is considered rare in domestic species, with carcinomas of the mammary gland, thyroid gland, prostate gland, ovary, and lung being the most common sites of origin.[5] Ultimately, we favored the less specific diagnosis of carcinoma based on the histologic features in the preponderance of slides available for evaluation, including the absence of distinct tubules in most sections. Additionally, some slides contain multinucleate neoplastic cells (**figs. 1-1 and 1-2**).

Conference attendees carefully considered the contributor's diagnosis of hypertrophic osteopathy (HO); however, most participants interpreted the florid periosteal new bone as a reactive lesion secondary to invasion by metastatic carcinoma cells, rather than the paraneoplastic condition of hypertrophic osteopathy, for the following histologic and clinical reasons: [5]

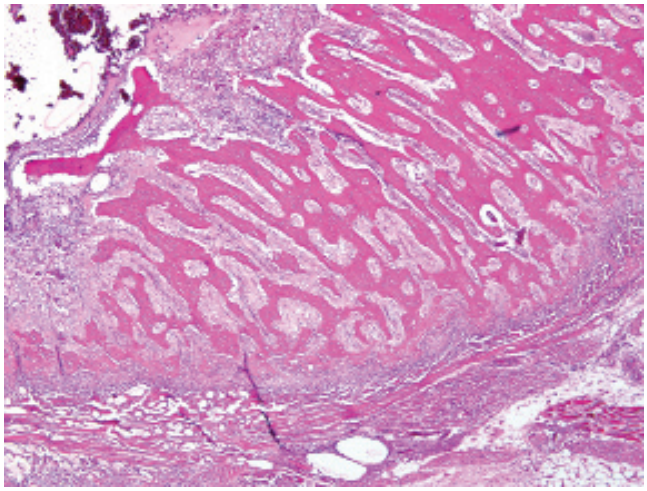

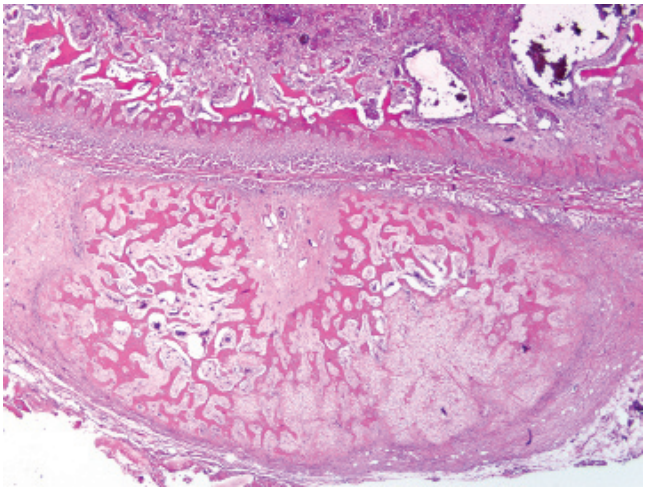

1-3, 1-4. Bone, rib, dog, metastatic carcinoma. Cortical bone is replaced by radiating spicules and trabeculae of endosteal and periosteal new bone growth. (HE 400X)

In the submitted case, the vast majority of the pre-existing cortical bone is lost and replaced by woven bone, and there are moderate numbers of osteoclasts within Howship's lacunae, indicating active bone resorption. By contrast, in HO, pre-existing lamellar cortical bone generally remains intact, with the formation of periosteal trabeculae of new woven bone oriented perpendicular to the cortex. In many of the submitted slides, there is both endosteal and periosteal new bone growth, which is best appreciated at low magnification; endosteal new bone growth is not typical of HO (**figs 1-3 and 1-4**).

The rib is not a predilection site for the development of HO lesions. Periosteal new bone formation attributed to the condition of HO is typically confined to the limbs, and preferentially affects the metacarpals, metatarsals, radius, ulna, and tibia, with sparing of the articular surfaces, upper limbs, and phalanges.

While we cannot exclude the possibility of HO at other anatomic sites in this dog, the contributor's gross description of bony proliferation exclusively affecting the bones of the upper limbs would be highly unusual, because HO classically spares the upper limbs, or affects them late in the disease process following initial and more severe lesions on the distal limbs. We thank the contributor for submitting this very interesting and edifying case.

Contributor: Laboratory of Veterinary Pathology, Faculty of Veterinary Medicine, Ghent University, Salisburylaan 133, 9820 Merelbeke, Belgium
http://www.vetpath.UGent.be/

References:

1. Chiang YC, Liu CH, Ho Sy, Lin CT, Yeh LS: Hypertrophic osteopathy associated with disseminated metastases of renal cell carcinoma in the dog: a case report. J Vet Med Sci **69**(2):209-212, 2007
2. Dunn ME, Blond L, Letard D, DiFruscia R: Hypertrophic osteopathy associated with infective endocarditis in an adult boxer dog. J Small Anim Pract **48**:99-103, 2007
3. Grillo TP, Brandao CVs, Mamprim MJ, de Jesus CMN, Santos TC, Minto BW: Hypertrophic osteopathy associated with renal pelvis transitional cell carcinoma in a dog. Can Vet J **48**:745-747, 2007
4. Mylonakis ME, Rallis T, Koutinas AF: Canine spirocercosis. Compend Contin Educ Vet **30(2)**:111-116, 2008
5. Thompson K: Bones and joints. *In:* Jubb, Kennedy, and Palmer's Pathology of Domestic Animals, ed. Maxie MG, 5th ed., vol. 1, pp. 107-108, 127-129. Elsevier Saunders, Philadelphia, PA, 2007
6. Watrous Bj, Blumenfeld B: Congenital megaesophagus with hypertrophic osteopathy in a 6-year-old dog. Vet Radiol Ultrasound **43**(6):545-549, 2002

CASE II: 07-161 (AFIP 3103929).

Signalment: Adult male Long-Evans rats (*Rattus norvegicus*).

History: As part of a cerebral aneurysm study, rats were made hypertensive by ligation of left renal artery, fed a high salt diet, and implanted with pellets of deoxycorticosterone acetate (DOCA). To further cerebral aneurysm formation, the right carotid artery was surgically occluded, and rats were fed beta-aminopropionitrile (BAPN).[3] Animals had been on study for at least two months at the time of death.

Gross Pathology: On radiographs and gross examination bilateral irregular firm white nodular masses, approximately 4 x 5 x 7 mm, were noted on the medial proximal femoral diaphyses and at the site of insertion of the pectineus and adductor longus muscles (**figs. 2-1 and 2-2**). The masses were intimately associated with these muscles. Both rats died of exsanguination due to ruptured abdominal arterial aneurysms and hemoabdomen.

Histopathologic Description: Submitted is a longitudinal section of the proximal femur including femoral head and adjacent soft tissues. Arising from the proximal medial cortex of the diaphysis and separating, surrounding and dissecting myocytes of adjacent skeletal muscle is a nodular, unencapsulated, moderately cellular mass consisting of short streaming bundles of plump spindloid cells in a coarse fibrous matrix (**figs. 2-3 and 2-4**). There is a well-differentiated proliferation of immature and mature bone adjacent to the cortex, which is multifocally absent (remodeling). These proliferations often incorporate hematopoietic elements within marrow spaces. In some sections, there are foci of hyaline cartilage, some of which transition to bone (**fig. 2-5**). At the soft tissue edges of the mass, there are numerous haphazardly arranged, variably sized, but generally small, spicules of osteoid. Spindle cells are plump with a proliferative appearance, but are cytologically relatively bland. There is minimal anisocytosis or anisokaryosis, and mitotic figures are rare (one per ten 400x HPF). There is secondary atrophy of entrapped myocytes.

Contributor's Morphologic Diagnosis: Femurs, proximal, bilateral, periosteal fibroplasia, florid, atypical, with cartilaginous and osseous differentiation and marrow formation (exostoses), chronic, moderate to severe, consistent with osteolathyrism.

Contributor's Comment: Beta-aminopropionitrile (BAPN) is a principle toxic agent of the sweet pea, *Lathyrus odoratus*, and is an irreversible inhibitor of lysyl oxidase.[5] Lysyl oxidase is required for the oxidative deamination of hydroxylysine residues in collagens and lysine residues in collagens and elastin. These deaminated aldehyde

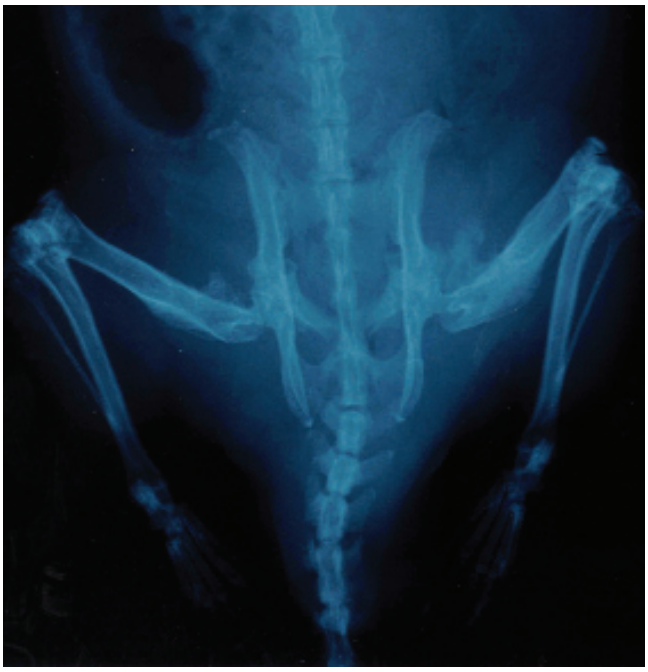

2-1, 2-2. Pelvic radiographs, rat. Bilaterally on the medial proximal femoral diaphyses at the site of insertion of the pectineus and adductor longus muscles are irregular approximately 4 x 5 x 7 mm nodular masses. Radiographs courtesy of Penn State Hershey Medical Center, Department of Comparative Medicine, H054, CG726A, 500 University Drive, PO Box 850, Hershey, PA, 17033-0850, tcooper@hmc.psu.edu.

derivatives form spontaneous intermolecular covalent bonds, cross-linking molecules and providing strength. Copper is a necessary cofactor for lysyl oxidase, and thus copper deficient diets result in functional inhibition of lysyl oxidase. BAPN intoxication and copper deficiency are phenotypically similar, although BAPN does not produce anemia.

Yeager and Hamre provide excellent descriptions of the evolution of the lesions of osteolathyrism.[7] Briefly, the exostoses develop at the site of the insertion of the tendons of the pectineus and adductor longus muscles on the periosteum of the femur through two distinct phases. In the preliminary proliferative stage, the inner layer of the periosteum becomes a highly cellular and less organized mass of tissue resembling a fibroma or fibrosarcoma. The second osteogenic stage occurs as soon as 7 to 8 days after initiation of a sweet pea diet, and consists of intra-membranous ossification at the periphery of the mass. No distant metastases were noted in any osteolathyrism studies, despite the infiltrative growth pattern, high cell density, and immature cytologic characteristics of the fibroblasts. Lesions may also develop at the deltoid ridge of the humerus, the gluteal trochanter of the femur, and the lamboidal ridge of the skull.

Although Yeager and Hamre observed no gross or histologic evidence of trauma at the site of the exostoses [7], additional studies noted that muscle tension was required for lesion development, as transected or denervated muscles failed to produce lesions, while lesions did develop at the sites of insertion of muscles that provided functional compensation for transected muscles.[1] Ponseti suggests that lifting of the periosteum is required for exostosis formation.[4]

AFIP Diagnosis: Long bone, femur, proximal epiphysis, metaphysis and diaphysis: Atypical periosteal fibroplasia, focally extensive, moderate to marked, with reactive new bone and osseous metaplasia.

Conference Comment: The contributor provides an excellent review of the effects of BAPN in adult rats. Although this is a rare condition, the case provided an excellent exercise in descriptive pathology, and conference attendees found this to be a very challenging slide. For conference attendees, the predominant differential diagnosis was osteosarcoma based on the proliferation of spindled cells and presence of osteoid. Although a reasonable consideration, especially without knowledge of the case history, the bland nature of the spindle cells, paucity of mitotic figures, and the presence of well-differentiated bone containing normal bone marrow in the nodular masses are not consistent with osteosarcoma. The bilaterally symmetric distribution, of which conference attendees were not aware prior to the conference, also is more consistent with a non-neoplastic process.

In addition to the detailed description of the lesion provided

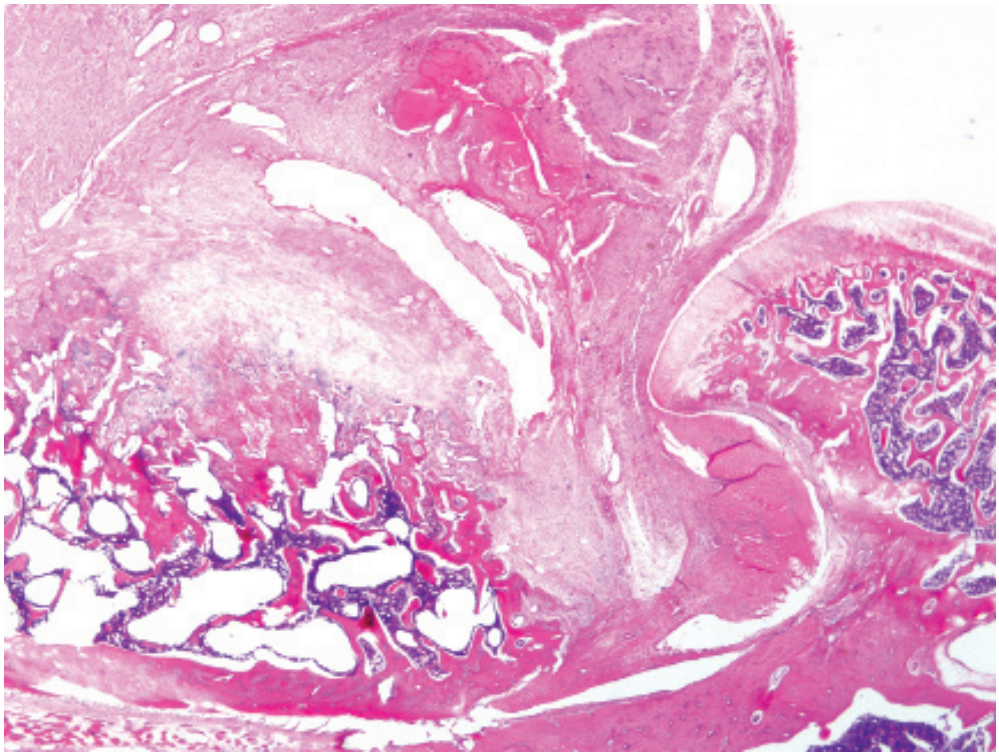

2-3. Bone, femur, rat. Extending from the cortex of the proximal diaphysis and surrounding and separating adjacent skeletal muscle fibers is a densely cellular, nodular proliferation of spindle cells. (HE 20X)

by the contributor, the moderator and attendees noted foci of new bone formation in the area of the trochanteric fossa and the lateral aspect of the proximal femur. In agreement with the contributor's description, the Armed Forces Institute of Pathology's Department of Musculoskeletal and Soft Tissue Pathology summarized the lesion as a broad-based periosteal proliferation of new bone with a poorly-formed fibrocartilagenous cap and an overlying area composed of a large cellular proliferation of fibroblastic and myofibroblastic type cells that in one area blend with tendon and muscle cells; the possibility of an exuberant myofibroblastic reaction to an avulsive injury at a tendon insertion site was considered.

Ectopic ossification is the neoformation of non-neoplastic trabecular bone at extraosseous sites, and is distinct from ectopic or heterotopic mineralization, which lacks bone formation. Most occurrences of ectopic ossification are common, clinically insignificant findings, e.g. dural ossification (ossifying pachymeningitis) in aged dogs and ectopic bone formation in the lungs of dogs and cattle; or occur in the supporting stroma of certain neoplasms, such as mammary carcinoma in dogs. Two specific diseases

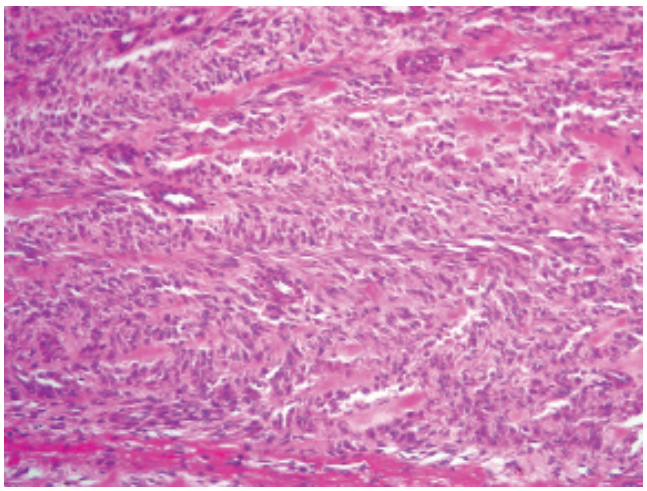

2-4. Bone, femur, rat. Spindle cells are arranged in short interlacing streams and bundles on a dense collagenous matrix. Multifocally there are spicules of brightly eosinophilic osteoid. (HE 400X)

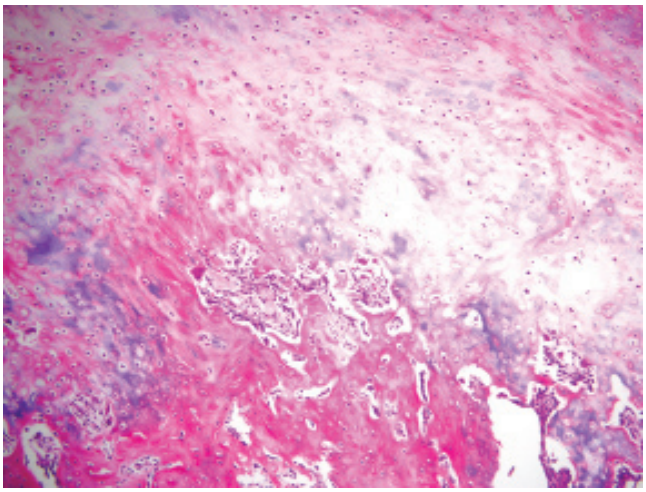

2-5. Bone, femur, rat. Foci of hyaline cartilage occasionally transition to bone. (HE 100X)

associated with ossification of soft tissues are fibrodysplasia ossificans progressiva and myositis ossificans; the former is characterized by progressive, symmetrical ossification of the subcuticular and epimysial connective tissue of the neck, dorsum, and limbs. In contrast, myositis ossificans is characterized by localized and asymmetric lesions containing a peripheral zone of orderly maturation from fibrous tissue to mineralized osteoid, which is replaced by lamellar bone.[6]

The contributor provides a useful description of the effects of BAPN on lysyl oxidase and its similarity to the pathologic effects of copper deficiency. During the conference, the effects of BAPN and similar toxins produced by members of the genus Lathyrus on domestic animals and humans were discussed. The Lathyrus genus is composed of variety of species (e.g. *Lathyrus sylvestris*, *L. sativus*); toxins produced by this genus include BAPN (*L. odoratus*), diamino-butyric acid (*L. sylvestris*), and beta-oxalyl-diamino-propionic acid (*L. sativus*). In limited amounts, Lathyrus species of legumes are a nutritious source of protein for domestic animals and humans; however, consumption of large quantities of these legumes over prolonged periods (weeks to months) results in the disease condition referred to as "lathyrism." Because of the plant's ability to survive in poor soils, flood and drought, outbreaks of lathyrism often occur in impoverished areas of the world during prolonged drought conditions.[3]

In contrast to rats, which develop skeletal deformities referred to as osteolathyrism, ingestion of *Lathyrus* spp. in humans and most domestic animals results in neurologic disorders termed neurolathyrism. Neurolathyrism is characterized by degeneration and loss of neurons in the spinal cord, resulting in gradual paralysis of the posterior limbs in cattle, horses, pigs, humans, and other species. Peripheral nerves, such as the vagus and recurrent laryngeal, are also affected. In cattle, toxicosis also leads to blindness, torticollis, and skin anesthesia. In horses, paralysis of the recurrent laryngeal nerve results in "roaring". Horses and pigs appear to be more susceptible than cattle. Death usually results from respiratory paralysis. Teratogenic effects in sheep and other species and aortic aneurysm in rats and turkeys are other pathologic effects of Lathyrus intoxication.[3]

Contributor: Department of Comparative Medicine, Penn State College of Medicine, Penn State Hershey Medical Center, Hershey, Pennsylvania 17033
http://www.hmc.psu.edu/comparativemedicine/

References:

1. Hamre CJ, Yeager VL: Influence of denervated muscles on exostoses of rats fed a sweet-pea diet. AMA Arch Pathol **65:**215-227, 1958
2. Hashimoto N, Handa H, Nagata I, Hazama F: Saccular cerebral aneurysms in rats. Am J Pathol **110:**397-399, 1983
3. Jones TC, Hunt RD, King NW: Veterinary Pathology, 6th ed., p. 757. Williams and Wilkins, Baltimore, MD 1997
4. Ponseti IV: Lesions of the skeleton and of other mesodermal tissues in rats fed sweet-pea (*Lathyrus odoratus*) seeds. J Bone Joint Surg Am **36-A:**1031-1058, 1954
5. Tinker D, Rucker RB: Role of selected nutrients in synthesis, accumulation, and chemical modification of connective tissue proteins. Physiol Rev **65:**607-657, 1985
6. Thompson K: Bones and joints. *In:* Jubb, Kennedy, and Palmer's Pathology of Domestic Animals, ed. Maxie MG, 5th ed., vol. 1, pp. 107-108, 127-129. Elsevier Saunders, Philadelphia, PA, 2007
7. Yeager VL, Hamre CJ: Histology of lathyrus-induced exostoses of rats; the initial changes at tendon-bone junction. AMA Arch Pathol **64:**171-185

CASE III: 14879-08 (AFIP 3113795).

Signalment: 9-year-old, male neutered Golden Retriever dog (*Canis familiaris*).

History: The right rear leg fractured and was pinned. One year later the leg was amputated.

Histopathologic Description: The mass has a complex histology with tumor trabecular bone, necrotic tumor and tumor bone, foci of chondro-osseous matrix, chondroid matrix, undifferentiated sarcoma, fibrosarcoma and reactive trabecular bone (**fig. 3-1**). Undifferentiated tumor cells, sometimes in bundles, form either densely cellular or moderately cellular sheets; pleomorphic nuclei have coarse chromatin and some are giant. Mitotic figures are common in some fields. Separating the nuclei in various regions is either an osseous, chondro-osseous or chondroid matrix as well as dense collagen (**fig. 3-2**). There is extensive necrosis of tumor trabecular bone and the undifferentiated cells between these trabeculae. Reactive trabecular cortical bone is at the periphery and is bordered by atrophied and fibrotic skeletal muscle.

Contributor's Morphologic Diagnosis: Bone, rear leg, telangiectatic osteogenic sarcoma.

Contributor's Comment: Medullary osteogenic sarcomas have been reported to occur at fracture sites with intramedullary pin fixation.

AFIP Diagnosis: Bone: Osteosarcoma.

Conference Comment: For many conference participants, the differential diagnosis included chondrosarcoma and reactive new bone (e.g. callous associated with fracture repair). Those favoring chrondrosarcoma based the diagnosis on the striking degree of chondroid differentiation present throughout many sections; however, careful evaluation

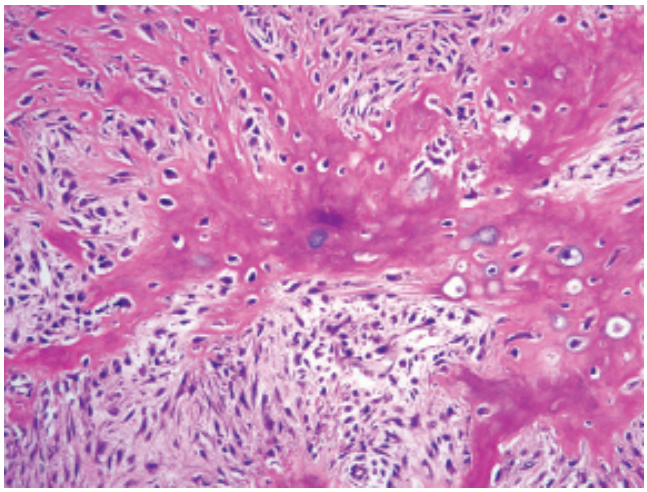

3-1. Bone, dog, osteosarcoma. The malignant neoplasm is composed of interlacing streams and bundles of spindle cells on a dense collagenous matrix which occasionally forms islands of immature bone. (HE 400X)

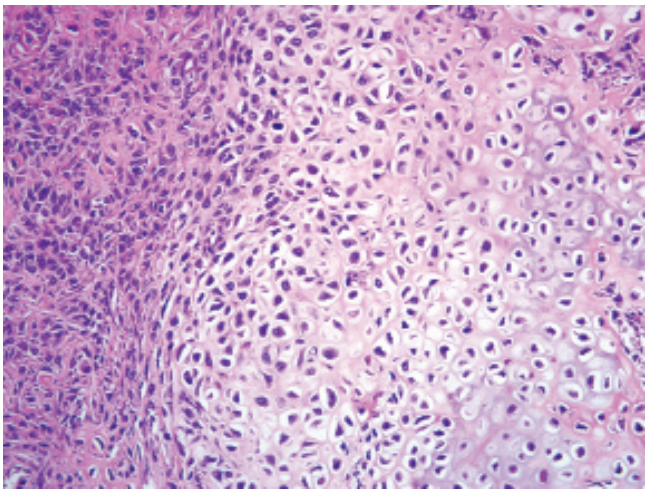

3-2. Bone, dog, osteosarcoma. There are areas of cartilage formation within the neoplasm. (HE 400X)

reveals the presence of malignant osteoblasts surrounding and investing osteoid in a disorderly orientation, most consistent with osteosarcoma (OSA). Those favoring a reactive process based the diagnosis on the proliferation of irregular trabeculae of new woven bone, a feature found not only in some cases of OSA, but also in a number of inflammatory bone lesions and in less aggressive neoplasms. Histologic differentiation can be difficult, but in reactive bone the trabeculae are interconnected and lined by a single layer of well-differentiated osteoblasts, with the intervening spaces occupied by non-neoplastic connective tissue; in the present case, spicules of neoplastic bone are lined and surrounded by haphazardly arranged pleomorphic osteoblasts.[3] Ancillary changes present in many of the slides include focally extensive skeletal muscle atrophy and fibrosis.

While the conference moderator and vast majority of conference participants concurred with the contributor's diagnosis of OSA, none of the slides evaluated by the attendees contained blood-filled spaces lined by neoplastic osteoblasts, the histologic features diagnostic for the telangiectatic subtype. The gross appearance of telangiectatic osteosarcoma is distinctive, and reflects multiple blood-filled spaces reminiscent of hemangiosarcoma; the contributor did not provide a gross description of the bone tumor in this case.

Osteosarcoma represents the single most common primary neoplasm of the appendicular skeleton in dogs and cats, where it accounts for 80% and 70% of primary bone neoplasms, respectively. In dogs, OSA is characterized by rapid progression and early metastasis to the lungs, resulting in an early and high mortality rate. The appendicular skeleton is affected far more commonly than the axial skeleton, and the forelimbs are affected more commonly than the hind limbs. The neoplasm exhibits a strong predilection for the metaphyses of the distal radius, proximal humerus, distal femur, and proximal tibia.[2,3]

Osteosarcoma can be categorized based on its site of origin, with the majority of tumors being central, i.e. arising within bones, and fewer being categorized as one of two types of peripheral OSA, i.e. arising within the periosteum. Peripheral osteosarcoma includes the periosteal subtype, which clinically behaves similar to central OSA; and parosteal OSA, which is slower-growing and more well-differentiated, with a more favorable overall prognosis. The conference moderator cautioned participants that, because of the marked intratumoral histologic variability, OSAs can be difficult to accurately classify; nevertheless, subclassification into one of six categories based on the predominant histologic pattern is well-described in veterinary pathology, and summarized below:[2,3,4]

- Poorly differentiated: undifferentiated neoplastic cells range from primitive mesenchymal to large and pleomorphic; identification as OSA depends on identifying small quantities of tumor osteoid; highly aggressive, osteolytic tumor frequently associated with pathological fractures
- Osteoblastic: anaplastic osteoblasts with angular cell borders, variable amounts of basophilic cytoplasm, and hyperchromatic, often eccentric nuclei predominate; further subclassified as nonproductive or productive based on presence or absence of tumor bone production
- Chondroblastic: neoplastic cells produce both prominent chondroid and osteoid matrices
- Fibroblastic: interlacing fascicles of spindle shaped cells, resembling those of fibrosarcoma, that produce osteoid or tumor bone
- Telangiectatic: subtype associated with the least

favorable prognosis; consists of solid areas and large blood-filled spaces lined by malignant osteoblasts that occasionally form spicules of osteoid
- Giant cell: tumor giant cells predominate in large areas of the neoplasm, which otherwise resembles nonproductive osteoblastic OSA

Based on the classification scheme above, and assuming the examined sections are representative of the entire neoplasm, the histologic features of the present case are most consistent with the chondroblastic subtype.

Contributor: Tennessee Department of Agriculture, C.E. Kord Animal Disease Laboratory, Ellington Agriculture Center, 440 Hogan Road, Nashville, Tennessee 37220
http://www.tennessee.gov/agriculture/regulatory/kord.html

References:

1. Gleiser CA, Raulston JH, Jardine RH, Carpenter RH, Gray KN: Telangiectatic osteosarcoma in the dog. Vet Pathol **18:**396-398, 1981
2. Thompson K: Bones and joints. *In:* Jubb, Kennedy, and Palmer's Pathology of Domestic Animals, ed. Maxie MG, 5th ed., vol. 1, pp. 112-118. Elsevier Saunders, Philadelphia, PA, 2007
3. Thompson KG, Pool RR: Tumors of bones. *In:* Tumors in Domestic Animals, ed. Meuten DJ, 4th ed., pp. 263-290, Iowa State Univ. Press, Ames, IA, 2002
4. Unni KK, Inwards CY, Bridge JA, Kindblom LG, Wold LE: Tumors of the Bones and Joints, AFIP Atlas of Tumor Pathology, 4th series, vol. 2, ed. pp. 119-192. American Registry of Pathology, Washington, DC, 2005

CASE IV: NCAH 2009-1 (AFIP 3134609).

Signalment: 1-year-old, male white-tailed deer (*Odocoileus virginianus*).

History: Tissues are from 1 of 20 white-tailed deer being restrained in a drop-floor chute located outside. Deer were being restrained to obtain skin biopsies of tuberculin skin test sites, as part of an on-going project. Handling and restraint began in early morning when ambient temperatures were cooler, but by the end of the exercise ambient conditions were hot and humid. This deer was the last of the 20 deer to be processed through the chute. Upon entering the chute, the deer showed markedly increased respiration (panting), frothy saliva around the mouth, and was hyperthermic to the touch, although a body temperature was not recorded. The deer was doused profusely with cool water and given several cool water enemas. Respirations slowed toward normal, but the animal remained subjectively hyperthermic. The deer was moved to an interior, cooler location. Several hours later the deer was in sternal recumbency, alert, but did not rise when approached. Eighteen hours after restraint, although alert, the animal was unable to rise and was euthanized.

Gross Pathology: The deer was in adequate nutritional status. The forestomachs contained moderate amounts of dry ingesta. Multifocal areas of both pallor and hemorrhage were present in muscles of the hindlimbs, forelimbs, epaxial and sublumbar muscles as well as the diaphragm (**figs. 4-1 and 4-2**). Lesions were bilateral but not symmetrical. Affected muscles appeared drier than normal. The heart was grossly unaffected. Bilaterally the kidneys were characterized by focally extensive black discoloration extending superficially through the cortex and involving as much as 75% of the cortical surface (**figs. 4-3 and 4-4**). The bladder contained a moderate amount of red-brown colored urine (**fig. 4-5**).

Histopathologic Description: The cross-section of skeletal muscle is characterized by focally extensive myofiber degeneration and necrosis. Slides vary with 20-60% of myofibers affected. Myofibers have lost visible cross-striations and vary greatly in size, many being large and swollen with flocculent, pale eosinophilic cytoplasm while others are smaller with hyalinized eosinophilic cytoplasm. Affected myofibers have pyknotic or karryorhectic nuclei (**fig. 4-6**). Within some myofibers there is basophilic, punctate to granular staining interpreted as mineralization. Endomysial and perimysial spaces are mildly expanded due to edema and a cellular infiltrate composed of low numbers of both neutrophils and macrophages.

Contributor's Morphologic Diagnosis: Skeletal muscle: degeneration and necrosis, focally extensive, with mineralization, white-tailed deer (*Odocoileus virginianus*).

Contributor's Comment: Capture myopathy (exertional myopathy, exertional rhabdomyolysis) is characterized by damage to skeletal muscle, and sometimes cardiac muscle, and is commonly observed after capture, immobilization (chemical or manual), and transport. It is an important cause of morbidity and mortality in captured and handled wild animals, including birds, and should always be considered in planning and designing wildlife capture and handling events.[4] All ages and sexes are susceptible and warm environmental temperatures, such as those in the present case, predispose animals to the condition.

Animals with capture myopathy may die suddenly or develop clinical signs hours, days or weeks later. Capture myopathy has been diagnosed up to a month after capture. Clinical syndromes of capture myopathy have been described based on time until onset of clinical signs as hyperacute, acute, subacute and chronic (reviewed in 4). More recently, other authors have based the classification of clinical syndromes on pathophysiology; capture shock syndrome, ataxic and myoglobinuric syndrome, ruptured muscle syndrome and a rare, poorly characterized delayed-peracute syndrome.[2] The

4-1, 4-2. Skeletal muscle, hindlimb and epaxial muscles, white-tailed deer. Multifocal areas of pallor and hemorrhage. Photograph courtesy of National Centers of Animal Health, 2300 Dayton Avenue, Ames, IA 50010, Mitchell.palmer@ars.usda.gov.

4-3, 4-4. Kidney, white-tailed deer. Focally extensive areas of black discoloration within the cortex. Photograph courtesy of National Centers of Animal Health, 2300 Dayton Avenue, Ames, IA 50010, Mitchell.palmer@ars.usda.gov.

ataxic and myoglobinuric syndrome is the most common, and is consistent with the present case.

Under normal conditions wild animals are not subjected to prolonged, maximal muscular exertion. However, during pursuit and capture such conditions may exist. Therefore, the earliest clinical signs of capture myopathy are similar to those of maximal exertion, increased respiratory and cardiac rates. Body temperature is usually elevated. Other early clinical signs may include depression, weakness, ataxia, muscle stiffness, and muscle tremors. Death may occur immediately post-capture due to marked metabolic acidosis, shock and circulatory collapse.

Animals surviving hours or even days may continue to show signs of depression, hyperthermia, tachypnea, tachycardia, weakness, and ataxia. Difficulty standing may progress to recumbency. Dark colored urine due to myoglobinuria may be seen. For weeks survivors may continue to show lameness, ataxia, muscle stiffness, and weight loss. Occasionally rupture of damaged muscle groups may occur. The gastrocnemius muscle is especially prone to rupture under such conditions.

The pathophysiology of capture myopathy is related to both shock and metabolic acidosis. The stress of pursuit and capture results in strong and prolonged sympathetic stimulation of microvasculature and eventual exhaustion of sympathetic vascular tone. Lack of vascular tone leads to: visceral pooling of blood, decreased venous return, decreased cardiac output, hypotension, and hypoxia. In spite of hypoxia, tissue metabolism continues, relying on anaerobic glycolysis and resulting in increased levels of intracellular pyruvic and lactic acid. Lactic acid diffuses into the blood at levels that overwhelm the capacity of the liver, heart and other tissues to convert lactic acid to useable energy and lactic acidosis develops.

Prolonged hypoxia and acidosis result in generalized tissue deterioration. Active transport of sodium and potassium is reduced due to low intracellular pH. Intracellular sodium and chloride levels rise as do extracellular potassium levels. Mitochondrial activity decreases, lysosomes rupture, releasing damaging enzymes. Tissue necrosis ensues,

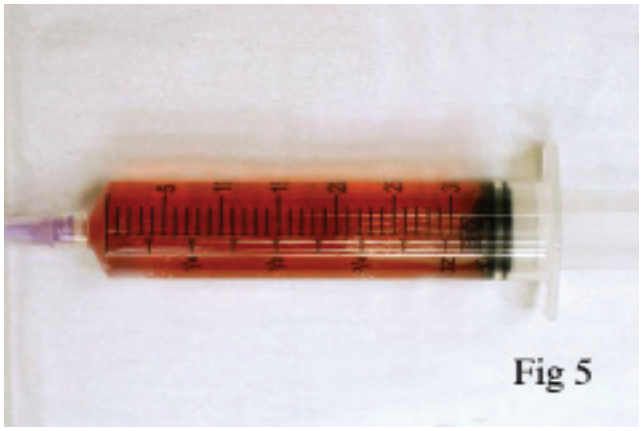

4-5. Urine, white-tailed deer. The bladder contains a moderate amount of red-brown colored urine. Photograph courtesy of National Centers of Animal Health, 2300 Dayton Avenue, Ames, IA 50010, Mitchell.palmer@ars.usda.gov.

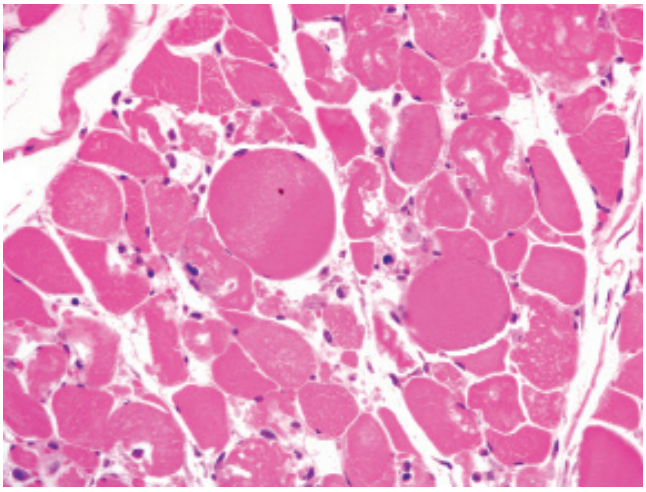

4-6. Skeletal muscle, white-tailed deer. Multifocally skeletal myocytes are swollen and degenerate or fragmented and necrotic. (HE 400X)

especially in skeletal muscle, heart, liver and lung. Renal lesions of capture myopathy are characterized by moderate to severe tubular epithelial cell degeneration and necrosis with protein (myoglobin) and cellular casts. Renal lesions are primarily the result of renal ischemia.

Hyperthermia exacerbates tissue necrosis. Heat is generated from muscle myofilament action, glycolysis, recovery heat production as metabolic processes attempt to restore muscle to a resting equilibrium, and the environment. Heat from the environment can be transferred to muscle cells during exertion.[1]

Capture myopathy is similar to march myoglobinuria or extertional rhabdomyolysis in untrained athletes or military recruits following heavy exercise at high ambient temperatures.[2]

AFIP Diagnosis: Skeletal muscle: Myocyte degeneration and necrosis, focally extensive, moderate, with mineralization and edema.

Conference Comment: The contributor provides an outstanding review of the entity. Although skeletal muscle is a remarkably plastic tissue capable of a variety of responses to injury (e.g. necrosis, degeneration, regeneration, atrophy, hypertrophy, splitting, and fiber-type conversion), segmental necrosis and regeneration is a common result of a number of causes that merit inclusion in the differential diagnosis, and definitive determination of the underlying etiology is often difficult based solely on gross and microscopic lesions.[3] Conference participants considered nutritional myopathy due to selenium and vitamin E deficiency or imbalance, toxic myopathy (e.g. ionophore toxicosis), and other types of exertional myopathies (e.g. polysaccharide storage myopathy) which could produce identical microscopic lesions, but strongly suspected capture myopathy based on the signalment. Characterizing the distribution and duration of the lesions, and in particular, classifying necrotic skeletal muscle lesions as monophasic or polyphasic, is sometimes helpful in narrowing the differential diagnosis. For instance, monophasic necrosis, as in the present case, is more consistent with an exertional or acute toxic myopathy, while polyphasic necrosis is more consistent with muscular dystrophy, selenium deficiency, or ongoing intoxication.[3]

Participants reviewed the basic stages of skeletal muscle necrosis, repair, and regeneration. Because myofibers are multinucleate, these changes can occur segmentally and are initially characterized by hyalinization of the sarcoplasm with loss of cross striations, followed by sarcoplasmic fragmentation often with mineralization. Effective skeletal muscle regeneration depends on the presence of an adequate blood supply, an intact basal lamina, and viable satellite cells. In the presence of adequate blood supply, macrophages derived from blood monocytes, with or without other leukocytes, are quickly recruited to the site of necrosis, traverse the basal lamina, and clear cytoplasmic debris. Simultaneously, satellite cells, juxtaposed between the sarcolemma and basal lamina, are activated and begin division into myoblasts in support of the regenerative effort. The remaining intact basal lamina forms a scaffold, i.e. "sarcolemmal tube," which excludes fibroblasts and guides proliferating myoblasts, which then fuse end-to-end to form myotubes that eventually produce thick and thin filaments and mature into myofibers. By contrast, if large numbers of satellite cells are killed, even with persistence of the basal lamina, healing occurs by fibrosis rather than regeneration. In cases typified by loss or disruption of the basal lamina, even with persistence of viable satellite cells, regeneration is ineffective and healing is characterized by the formation of muscle giant cells (large, bizarre multinucleated giant cells) accompanied by fibrosis.[3]

Contributor: National Centers for Animal Health, 2300 Dayton Avenue, Ames, Iowa 50010
www.nadc.ars.usda.gov/

References*:*

1. Spraker T: Pathophysiology associated with capture of wild animals. *In:* The Comparative Pathology of Zoo Animals, eds. Montali RJ, Migaki G. pp. 403-414. Smithsonian Institution Press, Washington, DC, 1980
2. Spraker T: Stress and capture myopathy in artiodactylids. *In:* Zoo and Wildlife Medicine Current Therapy 3, ed. Fowler M, pp. 481-488. W.B. Saunders, Philadelphia, PA, 1993
3. Valentine BA, McGavin MD: Skeletal muscle. *In:* Pathologic Basis of Veterinary Diseases, ed. McGavin MD, Zachary JF, 4th ed., pp. 985-989, Mosby Elsevier, St. Louis, MO, 2007
4. Williams E, Thorne E: Exertional myopathy (capture myopathy). *In:* Noninfectious Diseases of Wildlife, eds. Fairbrother A, Locke L, Hoff G, 2nd ed., pp. 181-193. Iowa State University Press, Ames, IA, 1996

The Armed Forces Institute of Pathology
Department of Veterinary Pathology

Conference Coordinator:
Shannon Lacy, DVM, MPH

WEDNESDAY SLIDE CONFERENCE 2009-2010

Conference 12

13 January 2010

Conference Moderator:

Bruce Williams, DVM, Diplomate ACVP

CASE I: X26880.08 (AFIP 3134058).

Signalment: 7-month-old, castrated male, domestic ferret (*Mustela putorius furo*).

History: A ferret that was previously vaccinated with distemper and rabies vaccines was obtained at 5 months of age. A few days after re-immunization in the right hind leg the ferret appeared lethargic and sore in that leg. Over the next few weeks the lethargy continued and the soreness of the right hind leg progressed to hind end weakness accompanied by a fever (40.1 degrees Celsius), and then the hind end weakness appeared to resolve. A complete blood count during this time revealed leukocytosis characterized by a mature neutrophilia. Despite apparent resolution of the right hind leg lameness, the ferret continued to be lethargic and unthrifty, was unkempt, failed to gain weight (appeared small for his age), and was febrile (temperature 40.7 degrees Celsius). A month after the onset of clinical signs, the ferret was humanely euthanized. Terminal blood samples were collected at the time of euthanasia for complete blood count and serum biochemistry (see below). Tissues were collected and submitted for histopathologic evaluation.

Gross Pathology: The gross postmortem examination findings reported by the submitting veterinarian indicated that the ferret was in lean body condition. Significant gross abnormalities that were recorded include: roughening and thickening of the esophagus, locally extensive pallor of the musculature of the left hind leg, focal thickening of the pericardial sac and splenomegaly.

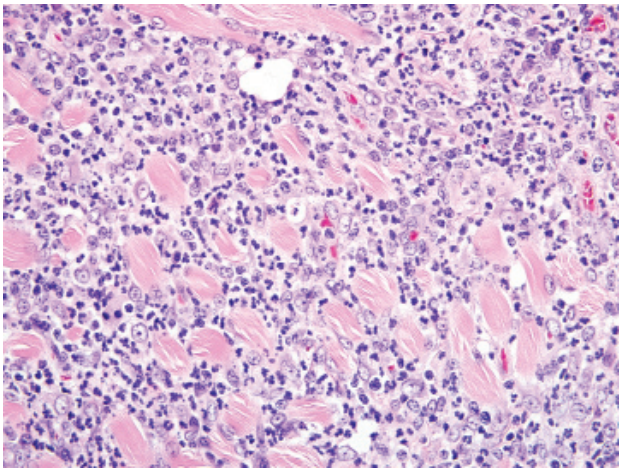

1-1. Esophagus, ferret. Myocytes in the tunica muscularis are atrophied and separated and surrounded by many neutrophils, epithelioid macrophages, and fewer lymphocytes and plasma cells. (HE 400X)

*Sponsored by the American Veterinary Medical Association, the American College of Veterinary Pathologists, and the C. L. Davis Foundation.

Laboratory Results:

Hematology	Reference ranges*	WBC Diff. (%) (x10E9/L)	Reference ranges* (%)
WBC 19.7 x10E9/L	7.7 – 15.4 x10E9/L	Segs 49% 9.653	24 – 78%
RBC 6.33 x10E12/L	7.3 – 12.18 x10E12/L	Bands 1% 0.197	0 – 2.2%
HGB 98 g/L	120 –182 g/L	Eos 7% 1.379	0 – 7%
HCT 0.266 L/L	0.36 – 0.61 L/L	Lymph 40% 7.880	28 – 69%
		Mono 3% 0.591	3.4 – 8.2%
Platelets: Clumped			
		Corr. WBC 19.7 x10E9/L	
RBC Morphology			
Anisocytosis 1+			

Biochemistry Results	Reference ranges*	Biochemistry Results	Reference ranges*
Sodium 145 mmol/L	146 – 160	Amylase 9 U/L	
Potassium 5.4 mmol/L	4.3 – 5.3	Alk.Phos. 9 U/L	30 – 120
Na:K Ratio 27		CK 110 U/L	
Chloride 117 mmol/L	102 – 121	AST [GOT] 63 U/L	
Calcium 2.12 mmol/L	2.15 – 2.62	ALT [GPT] 67 U/L	82 – 289
Phosph. 1.83 mmol/L	1.81 – 2.81	Gamma-GT 0 U/L	
Urea 4.8 mmol/L	4.28 – 15.35	T. Prot. 53 g/L	
Creat. 16 umol/L	17 – 53	Albumin 21 g/L	
Glucose 7.3 mmol/L	3.47 – 7.44	Globulin 32 g/L	
Cholest. 4.29 mmol/L	1.65 – 7.64	A:G Ratio: 0.66	
T. Bili. 1 umol/L	<17	Lipase 278 U/L	

**Note: Data adapted from Lewington JH: Ferret Husbandry, Medicine, and Surgery, 2nd ed., pp. 274-275. Elsevier Saunders, Edinburgh, New York, 2007*

Histopathologic Description: Esophagus: The muscular wall of the esophagus is circumferentially and diffusely infiltrated and expanded by dissecting infiltrates of large to very large numbers of neutrophils admixed with moderate numbers of epithelioid macrophages, occasional scattered small lymphocytes and plasma cells, and rare eosinophils and multinucleate giant cells (**fig. 1-1**). The suppurative to pyogranulomatous inflammation dissects around the circular and longitudinal layers of the muscularis externa (perifascicular myositis) and infiltrates the reticular connective tissue between individual myofibers, with disruption of the normal architecture and layering of the muscular wall. Myofibers often appear reduced in diameter (myofiber atrophy) with rare degenerative myofibers scattered within the inflamed esophageal wall. The inflammation also multifocally dissects along the connective tissues into the adjacent adventitial connective tissue and the overlying submucosal connective tissue up to the level of the muscularis mucosae, but overlying mucosal lamina propria and mucosal epithelium are spared (mural esophagitis). The small-caliber blood vessels within the inflamed wall are diffusely congested and lined by plump (reactive) endothelium.

Contributor's Morphologic Diagnosis: Esophagus: Moderate to severe, diffuse, circumferential, suppurative to pyogranulomatous mural esophagitis.

Contributor's Comment: The inflammatory myopathies are a group of acquired diseases characterized by an inflammatory infiltrate of the skeletal muscle.[1] The three major categories of idiopathic inflammatory myopathies are polymyositis (PM), dermatomyositis (DM), and inclusion body myositis (IBM).[1-5,7] PM and IBM are CD8+ cytotoxicT cell-mediated diseases whereas DM is characterized by a complement-mediated microangiopathy.[1] Other less common forms include focal myositis, infectious myositis, macrophagic myositis, and inflammatory myopathy with abundant macrophages.[7] Similar to human inflammatory myopathies, canines also are affected by a heterogenous group of disorders characterized by intramuscular inflammation. The most

common inflammatory myopathies in dogs are immune-mediated masticatory myositis, a polymyositis (similar to human polymyositis), and generalized infectious myositis.[2,3,7] Extraocular myositis is a less common canine immune-mediated myositis.[6]

Myofasciitis in domestic ferrets is an idiopathic disease characterized by suppurative to pyogranulomatous myositis and fasciitis affecting skeletal, smooth, and cardiac muscle and associated fascial connective tissues.[4] As the condition is disseminated and muscle is the predominant target tissue, the terms "polymyositis" and "disseminated idiopathic myositis" have also been used in this condition. But, as the inflammation extends into the fascia and adipose tissue around muscle bundles, myofasciitis was thought to be a more appropriate morphologic descriptor for this condition.[4]

The disease affects young adults of both sexes and is clinically characterized by rapid onset of clinical signs: weakness, muscle atrophy or lethargy, high fever, neutrophilic leukocytosis, treatment failure and death (or euthanasia). The primary presenting sign may be an ambulatory problem, primarily recognized clinically in the hindlimbs.[4] Inflammation of the alimentary smooth muscle may result in clinical presentation due to various alimentary tract problems.[4] Gross lesions seen at the time of necropsy often include atrophy of skeletal muscle, red and white mottling and dilation of the esophagus, and splenomegaly. Upon histologic examination, suppurative to pyogranulomatous inflammation in the skeletal muscle and fascia of limbs, lumbar region, body wall, head, heart, and/or esophagus is seen. The extensive suppurative to pyogranulomatous esophagitis which can be diffuse and circumferential is thought to be a unique feature of this disease. Splenic enlargement is due to myeloid hyperplasia, which can also be seen in the bone marrow.[4] In this case, suppurative to pyogranulomatous esophagitis, suppurative to pyogranulomatous hind limb myositis, suppurative to pyogranulomatous periarteritis/pericarditis and splenic myeloid hyperplasia were observed.

On CBC, a neutrophilic leukocytosis, as seen in this case, may be observed.[4] Upon evaluation of serum chemistries, no elevations of creatine kinase (CK) or aspartate aminotransferase (AST), indicators of muscle damage, have been associated with the disease and elevations of these enzyme activities were not seen in this case. This may be because the inflammation displaces and results in atrophy of the muscles rather than resulting in significant myodegeneration or myonecrosis.[4] Alanine aminotransferase (ALT) may be mildly elevated in some cases, possibly due to muscular or hepatic damage, but such an elevation was not noted in this case.

The pathogenesis of ferret myofasciitis is unclear; possibilities considered include infectious or vaccine-related mechanisms of immune mediated disease. In a recent review paper, Garner et al. (2007) investigated some possible infectious etiologies including histologic and electron microscopic evaluation for viral inclusion bodies and viral particles, immunohistochemical staining for feline and ferret coronaviral antigens, and histologic examination and immunohistochemical staining for protozoal antigens (for *Toxoplasma gondii, Neospora caninum*, and *Sarcocystis neurona*); the studies did not reveal any intralesional infectious agents.[4] However, these negative findings do not rule out the possibility of an infectious process being involved in the etiopathogenesis of this disease.

In childhood idiopathic inflammatory myopathies it has been proposed that environmental triggers in the setting of an underlying genetic susceptibility may play a role in the etiopathogenesis of the lesions.[3] With regards to genetic susceptibility, specific HLA alleles have been found to be immunogenic risk factors for juvenile dermatomyositis in humans. In dogs, the association of distinct inflammatory myopathies with certain dog breeds suggests that genetic predispositions are involved in the development of canine inflammatory myopathies.[7] Garner et al. (2007) thought that a heritable basis for myofasciitis seemed unlikely as affected ferrets are from different breeding facilities and the disease has been seen in both the USA and The Netherlands.

An adverse vaccine reaction is also a consideration as a possible cause in this disease. All of the ferrets affected have been reported to have had a least one dose of canine distemper vaccine.[4] In humans, macrophagic myositis is a recently described condition in adults and (less frequently) children which develops focally after injection of aluminum-containing vaccines.[5,6] The conspicuous macrophages within the inflammatory lesion have intensely PAS-positive cytoplasm due to intralysosomal accumulation of aluminum hydroxide, an adjuvant used in vaccines. Difficulty in clearing aluminum from the injection site and abnormal immune response to prolonged tissue retention of aluminum hydroxide is considered to be the etiology of the lesion.[6] No evidence of similar lysosomal accumulation of aluminum hydroxide was observed upon electron microscopic evaluation of domestic ferrets with myofasciitis. If a vaccine is involved, a delayed-type immune reaction to a vaccinal substance (killed or modified infectious agent, adjuvant, residual substance, or contaminant) may be involved.[4]

In conclusion, myofasciitis in domestic ferrets is an idiopathic disease characterized by suppurative to

pyogranulomatous myositis and fasciitis affecting skeletal, smooth, and cardiac muscle and associated fascia. The circumferential suppurative to pyogranulomatous esophagitis appears to be unique to this condition. The disease is unresponsive to medical treatments and appears to be uniformly fatal.

AFIP Diagnosis: Esophagus, submucosa, tunica muscularis, and serosa: Esophagitis, neutrophilic, chronic, diffuse, severe, with myofiber atrophy and adventitial and submucosal granulation tissue.

Conference Comment: The contributor provides an outstanding review of the entity. Points of discussion mentioned by the contributor and reiterated during the conference were the conspicuous absence of myocyte necrosis and degeneration, which is supported by the typical lack of elevations in CK and AST; sparing of the mucosal epithelium; and the characteristic predominance of neutrophils in the inflammatory milieu, which is unique in comparison to other inflammatory myopathies. Interestingly, while light microscopic and clinical pathology findings indicate an absence of myofiber necrosis, ultrastructural examination of affected myofibers reveals sarcoplasmic and mitochondrial swelling, disruption of myofibrils by edema, and disruption or destruction of Z bands.[4]

Contributor: Atlantic Veterinary College at University of Prince Edward Island, Department of Pathology and Microbiology, 550 University Avenue, Charlottetown, Prince Edward Island, Canada C1A 4P3
http://www.upei.ca/pathmicro/

References:

1. Briani C, Doria A, Sarzi-Puttini P, Dalakas MC: Update on idiopathic inflammatory myopathies. Autoimmunity **39:**161-70, 2006
2. Evans J, Levesque D, Shelton GD: Canine inflammatory myopathies: a clinicopathologic review of 200 cases. J Vet Intern Med **18:**679-91, 2004
3. Feldman BM, Rider LG, Reed AM, Pachman LM: Juvenile dermatomyositis and other idiopathic inflammatory myopathies of childhood. Lancet **371:**2201-12, 2008
4. Garner MM, Ramsell K, Schoemaker NJ, Sidor IF, Nordhausen RW, Bolin S, Evermann JF, Kiupel M: Myofasciitis in the domestic ferret. Vet Pathol **44:**25-38, 2007
5. Hewer E, Goebel HH: Myopathology of non-infectious inflammatory myopathies - the current status. Pathol Res Pract **204:**609-23, 2008
6. Lach B, Cupler EJ: Macrophagic myositis in children is a localized reaction to vaccination. J Child Neurol **23:**614-9, 2008
7. Shelton GD: From dog to man: the broad spectrum of inflammatory myopathies. Neuromuscul Disord **17:**663-70, 2007

CASE II: CP-08-6399-5 (AFIP 3134368).

Signalment: 4-month-old male ferret (*Mustela putorius furo*).

History: The ferret was lethargic, anorexic and had been losing weight. On physical examination the oral mucous membranes and ocular conjunctiva were yellow, indicative of jaundice.

Gross Pathology: The oral mucous membranes, ocular conjunctiva, mesentery and joints were yellow. The liver was enlarged and had a matted pattern. The gallbladder was distended and firm.

Histopathologic Description: Throughout the liver, the biliary tract is dilated and hyperplasic. In the biliary epithelium, meronts of coccidian parasites are abundant. Bile ducts are markedly dilated and contain neutrophils, cellular debris and coccidian oocytes. Portal tracts are surrounded by fibrous connective tissue with infiltrates of neutrophils, lymphocytes, plasma cells and macrophages. The gallbladder wall is markedly thickened and the epithelium is similarly affected as the bile ducts. Meronts contain at least 12 merozoites that measure about 2 microns in width and 5-6 microns in length. Oocytes are present intracellularly and in the lumen they measure approximately 10-11 microns in diameter (**figs. 2-1 and 2-2**).

Small intestine (not submitted): In the villus epithelium, meronts containing merozoites identical to those observed in the liver are abundant. Release of the merozoites into the lumen is also observed.

Contributor's Morphologic Diagnosis: Liver: Hepatobiliary coccidiosis with marked biliary hyperplasia, purulent cholangitis and portal fibrosis. Intestine: Intestinal coccidiosis.

Contributor's Comment: There is only one report in the literature of hepatic coccidiosis in ferrets.[4] In this report, the lesions were limited to the biliary tract and gallbladder with no involvement of the intestine. The organisms described in that report closely resemble those

observed in this animal. This case is unique in that the coccidian organism was also observed in the intestinal tract. The morphologic features described for this organism suggest the coccidian is of the genus *Eimeria*. The hepatic coccidian in the ferret has not been classified, but it has been suggested that it appears morphologically similar to the intestinal *E. furonis*. The ferret in this case had both intestinal coccidia and hepatic coccidia. Whether these hepatic and intestinal coccidia are the same species that infected both organs or are different coccidian species is open to speculation.

AFIP Diagnosis: 1. Liver, biliary tract: Cholangitis and pericholangitis, chronic, neutrophilic and lymphoplasmacytic, diffuse, moderate to marked, with biliary hyperplasia, and numerous intraepithelial apicomplexan schizonts and gametes, and intraluminal apicomplexan oocysts.
2. Liver: Extramedullary hematopoiesis, multifocal, marked.

Conference Comment: Conference attendees found this to be an interesting case. Participants briefly discussed the Phylum Apicomplexa and the various *Eimeria* and *Isospora* species that affect animals, summarized in the table that follows.[1,3,4]

Eimeria and _Isospora_ of Animals

Host	Coccidian	Organ(s) Affected
Cattle	*E. zuernii* *E. bovis*	Distal small intestine Distal small intestine
Sheep	*E. ovinoidalis* *E. ashata* *E. bakuensis* *E. crandallis*	Terminal ileum/ cecum and colon Distal small intestine Distal small intestine Distal small intestine
Goats	*E. ninakohlyakimovae* *E. caprina* *E. christenseni*	Cecum and colon Cecum and colon Distal small intestine
Pigs	*Isospora suis* (neonatal pigs) *E. scabra* (weaners, growers) *E. debliecki* (weaners, growers) *E. spinosa* (weaners, growers)	Distal small intestine Distal small intestine Distal small intestine Distal small intestine
Horses	*E. leuckarti*	Small intestine
Dogs	*C. canis* *C. ohioensis* complex = *(C. burrowsi, C. ohioensis, C. neorivolta)*	Distal small intestine, large intestine Distal small intestine, large intestine
Cats	*C. felis* *C. rivolta*	Small intestine, large intestine Small intestine, large intestine
Mice	*E. falciformis*	Colon
Rabbits	*E. stiedae* *E. intestinalis* *E. flavescens*	Bile ducts Ileum, cecum Ileum, cecum
Guinea pig	*E. caviae*	Large intestine
Ferret	*E. furonis*[1,4] *E. ictidea*[1,4]	Small intestine, Bile ducts Small intestine
Chickens	*E. acervulina* *E. necatrix* *E. tenella*	Small intestine Small intestine Cecum

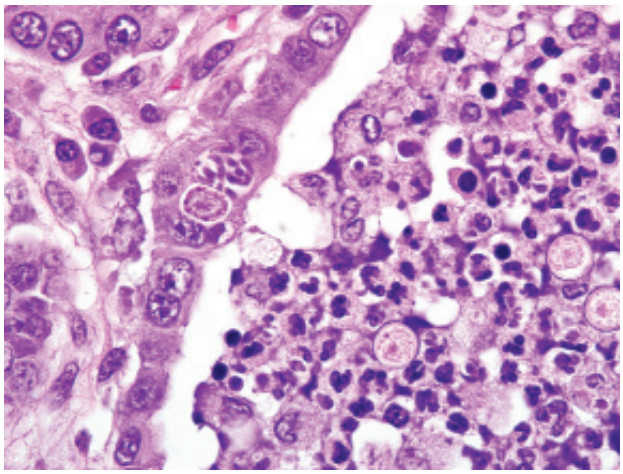

2-1. Liver, ferret. Within the biliary epithelium are many protozoal schizonts and macrogametes. Within the distended bile duct lumen there are high numbers of oocysts admixed with numerous degenerate leukocytes and sloughed epithelial cells. (HE 1000X)

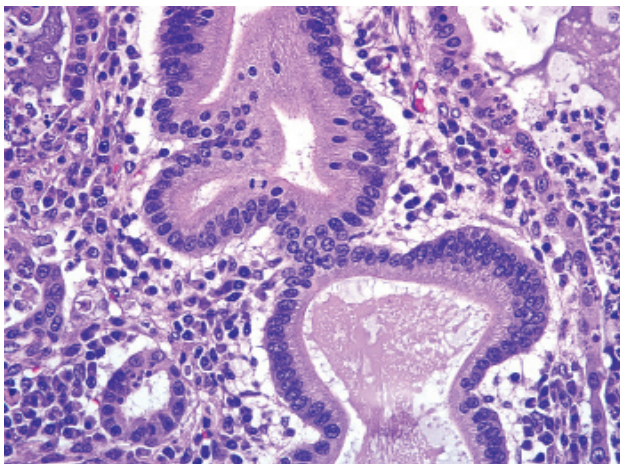

2-2. Liver, ferret. Multifocally biliary epithelium is markedly hyperplastic, piled up to 4 cell layers thick with a high mitotic rate. The interstitium surrounding bile ducts contains high numbers of lymphocytes, plasma cells, and fibroblasts. (HE 400X)

Morphologic features used to distinguish the various coccidia, such as *Cryptosporidium, Besnoitia, Sarcocystis, Toxoplasma, Eimeria,* and *Isospora* were also discussed. The primary characteristic used to differentiate the various genera of coccidia is the structure of the sporulated oocyst, particularly the number of sporocysts and sporozoites present, as summarized below.[2]

Apicomplexa Sporocyst and Sporozoite Numbers

Coccidian	Sporocysts	Sporozoites
Cryptosporidium	0	4
Besnoitia *Isospora* *Sarcocystis* *Toxplasma*	2	8
Eimeria	4	8

Additional differentiating characteristics, such as the host affected, location of the parasite within the host, and organism size and shape, were also mentioned as criteria to be considered when speciating coccidia. The moderator noted that *Eimeria* and *Isospora* may be also differentiated by their location of replication; *Eimeria* spp. replicate within the epithelium while *Isospora* spp. replicate within the lamina propria.

Attendees briefly reviewed the coccidian life cycle using *E. stiedae* as an example. In short, oocysts are shed in feces and sporulate. Sporulated oocysts contain four sporozoites that hatch within the intestine and then enter the liver via the portal vein. Sporozoites then penetrate into the bile epithelium and form trophozoites that undergo asexual nuclear division (schizogony). Schizogony results in the formation of schizonts that contain merozoites. The schizonts rupture, damaging the cell, and release merozoites which infect additional cells. Eventually, merozoites form sexual stages (i.e. male microgametes and female macrogametes) which unite to form oocysts. Oocysts are released into the bile and shed into the feces and the cycle then repeats itself.

Participants discussed the similarities and dissimilarities between the coccidian in this case and *Eimeria stiedae*. Both replicate within the hepatobiliary epithelium and cause chronic cholangiohepatitis, with marked epithelial hyperplasia, bile duct reduplication, and portal fibrosis.(3) Additionally, *E. stiedae* produces long papillary fronds within the bile duct that are not present in the case of this ferret. The moderator noted that hepatobiliary coccidiosis is rare in ferrets and has only been reported in very young animals that are generally less than four months of age. The vacuolation of hepatocytes noted in this case by attendees is a very common finding in ferrets due to inanition and fatty mobilization.

Contributor: St. Jude Children's Research Hospital, 262 Danny Thomas Place, MS 250, Memphis, TN 38105-3678
www.stjude.org

References:

1. Abe N, Tanoue T, Ohta G, Iseki M: First record of *Eimeria furonis* infection in a ferret, Japan, with notes on the usefulness of partial small subunit ribosomal RNA gene sequencing analysis for discriminating among *Eimeria* species. Parasitol Res **103:**976-970, 2008
2. Gardiner CH, Fayer R, Dubey JP: An Atlas of Protozoan Parasites in Animal Tissues, 2ne ed., p. 20, Armed Forces Institute of Pathology, Washington, DC, 1998
3. Thompson, ME: Proceedings: Department of Veterinary Pathology Wednesday Slide Conference 2006-2007. Armed Forces Institute of Pathology, Washington, D.C., 2007
4. Williams BH, Chimes MJ, Gardiner CH: Biliary coccidiosis in a ferret (*Mustela putorius furo*). Vet Pathol **33:**437-439, 1996

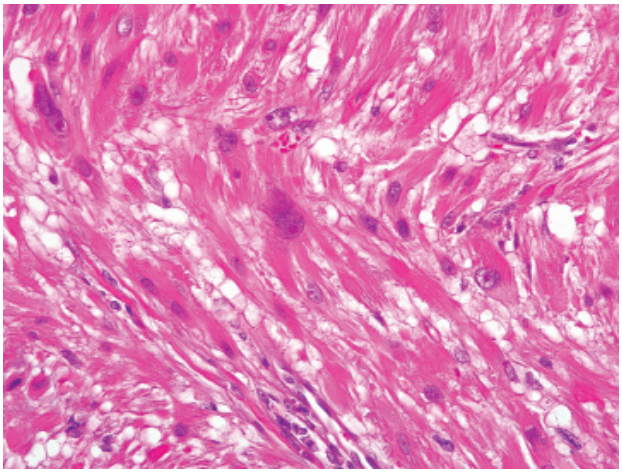

3-1. Piloleiomyosarcoma, haired skin, ferret. The malignant smooth muscle tumor is characterized by interlacing streams and bundles of neoplastic spindle cells with eosinophilic fibrillar to vacuolated cytoplasm and marked anisokaryosis and anisocytosis. (HE 400X)

CASE III: LAPV2 (AFIP 3138334).

Signalment: 2-year-old, intact male ferret (*Mustela putorius furo*).

History: This animal was presented at consultation for a slow growing nodular mass on the right side of the trunk. The animal was doing well, with no other clinical problems.

Gross Pathology: The formalin-fixed specimen was a 15 x 15 x 10 mm mass with a smooth surface. Epidermal ulceration was present. On cut section, a white irregular firm mass was present in the dermis, extending into the subjacent adipose tissue.

Histopathologic Description: The mass is ovoid, well demarcated, unencapsulated, lying between an ulcerated epidermis (not present on all sections) and the superficial muscular layer of the skin. Two or three hair follicles are embedded within the proliferation. These are spindled to strap-cells arranged in interwoven bundles. Some of them are contiguous with the arrector pili muscle cells. They have an abundant, fibrillar or vacuolated, eosinophilic cytoplasm with indistinct borders. The nucleus is large, generally ovoid or fusiform with blunt ends and a large basophilic nucleolus. Anisocaryosis is moderate to marked and anisocytosis is moderate (**fig. 3-1**). Binucleate or multinucleated cells are few. The mitotic index (1 to 2 mitoses per 10 high power fields) is low. Multiple lymphoplasmacytic inflammatory foci, with some hemosiderophages are present in and at the periphery of the mass. On some sections, a giant cell granuloma around a fragmented hair shaft is present.

Contributor's Morphologic Diagnosis: Piloleiomyosarcoma, well differentiated, dermal, ferret (*Mustela putorius furo*).

Contributor's Comment: Originating from the arrector pili muscle, this rare tumor in all animals is now well recognized in the ferret.[1,2] The histological and cytological patterns are typical. In spite of a low mitotic index (tumor with mitotic index ≥ 2 per 10 HPF is considered to be malignant) and a moderate anisocytosis, this tumor was classified as malignant because of a frank nuclear pleomorphism. However, the complete excision of this well demarcated nodule was curative and no local recurrence occured three months after surgery. These tumors are strongly vimentin, desmin and smooth muscle actin positive (not available in our unit), and negative for cytokeratin.[2]

AFIP Diagnosis: Haired skin and subcutis: Leiomyosarcoma, low-grade (piloleiomyosarcoma).

Conference Comment: Conference participants concurred with the contributor's diagnosis. Classification schemes in humans use mitotic rate to distinguish piloleiomyosarcoma from piloleiomyoma, with a mitotic rate of ≥ 2 per 10 HPF indicative of malignancy; the degree of nuclear pleomorphism does not correlate with malignancy in human classification schemes for this neoplasm.[2] In this case, the mitotic rate averages 1 per

HPF, and there is marked anisokaryosis, as noted by the contributor. Additional microscopic findings noted by participants were follicular atrophy overlying the neoplasm with many follicles in telogen, mild superficial dermal edema, mild superficial lymphoplasmacytic dermatitis, and minimal parakeratosis.

Basal cell tumors and mast cell tumors are the most commonly reported cutaneous neoplasms in ferrets. Reports of piloleiomyosarcoma in ferrets suggest that it behaves similarly to its human equivalent, i.e., it carries a good prognosis with no reports of distant metastasis and infrequent local recurrence.[1,2] This case illustrates the potential confusion that may result from classifying a neoplasm as malignant versus benign based on histologic assessment alone, particularly when histomorphology may not be predictive of a significant difference in biological behavior.

In humans, superficial leiomyosarcoma is classified by its location and origin; the dermal variety (i.e. piloleiomyosarcoma) originates from arrector pili muscles, while its subcutaneous counterpart (i.e. angioleiomyosarcoma) originates from vascular smooth muscle. The distinction between the two variants, unlike the distinction between piloleiomyoma and piloleiomyosarcoma, is clinically significant because, while piloleiomyosarcomas have only a 30% incidence of local recurrence and no reported metastasis, angioleiomyosarcomas have a 54% incidence of local recurrence and a 39% incidence of distant metastasis.[2]

Contributor: Laboratoire d'Anatomie Pathologique Vétérinaire (LAPV) d'Amboise – 6 impasse Vilvent, BP 303-37403 – Amboise Cedex (France)

References:

1. Mikaelian I, Garner MM: Solitary dermal leiomyosarcomas in 12 ferrets. J Vet Diagn Invest **14**:262-265, 2002

2. Rickman BH, Craig LE, Goldschmidt MH: Piloleiomyosarcoma in seven ferrets. Vet Pathol **38**:710-711, 2001

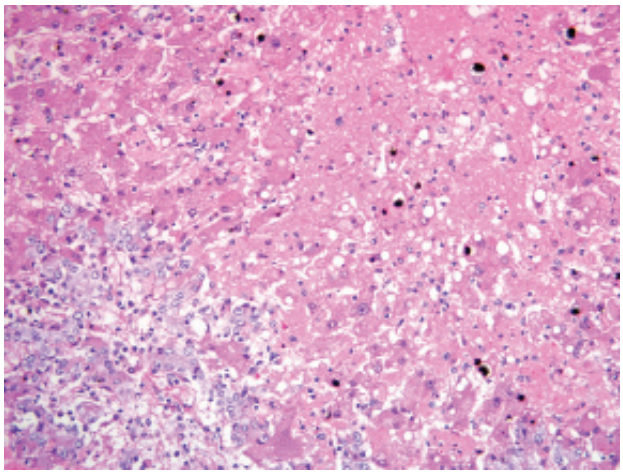

4-1. Liver, horse. There is diffuse loss of hepatic lobular architecture and replacement with necrotic cellular and karyorhectic debris. Multifocally there are increased numbers of bile duct profiles, and portal areas are closely apposed (stromal collapse). (HE 200X)

CASE IV: TAMU 01 2009 (AFIP 3139655).

Signalment: 20-year-old Arabian mare (*Equus caballus*).

History: The mare was presented obtunded and icteric with prolonged prothrombin time (PT) and partial thromboplastin time (PTT) and markedly elevated liver enzymes (GGT, AST), ammonia, bilirubin and bile acids. The animal received tetanus antitoxin soon after she foaled approximately 60 days prior to presentation. She was anorexic and had lost weight for about a month. The mare was treated with fluids, lactulose, dextrose, metronidazole, pentoxyfylline and banamine. She developed episodes of ventricular tachycardia. An ultrasound-guided liver biopsy was taken. On ultrasound, the liver appeared small. Due to the grave prognosis associated with disease progression and the results of the liver biopsy, the owner elected for humane euthanasia.

Gross Pathology: Diffusely the liver had an accentuated, lobular pattern (zonal necrosis and degeneration). The urinary bladder mucosa was uniformly red (congestion / hemorrhage). The uterus was thickened with a reddish mucosa and two, small, fluid-filled endometrial cysts measuring 1 and 0.5 cm in diameter respectively (endometrial lymphatic cysts).

Histopathologic Description: Diffusely disrupting

and collapsing the hepatic lobular architecture and distorting the hepatic cords, there is marked loss of centrilobular and midzonal hepatocytes. The remaining hepatocytes have loss of cellular detail, swollen cytoplasm with multivacuolation (degeneration) or pyknotic nuclei (necrosis). Many hepatocytes contain globular to granular, irregularly-shaped, yellow-brown material (hemosiderin / bile). The hepatic sinusoids are markedly expanded by eosinophilic, homogeneous material (edema) and erythrocytes (congestion). The parenchyma is diffusely but mildly infiltrated with macrophages, neutrophils, and rare plasma cells and lymphocytes. Many Kupffer cells are distended with intracytoplasmic, dark-brown pigment (hemosiderin) and rare erythrocytes (erythrophagocytosis). The portal areas are closely approximated (lobular collapse), often with portal-portal bridging, and are markedly expanded by proliferation of bile ducts that are lined by cuboidal to columnar cells with abundant often vacuolated cytoplasm, and a large vesicular nucleus. The cells occasionally pile up but have rare mitotic figures (biliary hyperplasia). Multifocally, the portal areas are infiltrated by fewer lymphocytes, macrophages, plasma cells, and neutrophils and rare eosinophils (**fig. 4-1**).

Contributor's Morphologic Diagnosis: Liver: Subacute hepatopathy with submassive hepatocytic degeneration and necrosis with lobular collapse, biliary hyperplasia, hemorrhage and mild, diffuse pericholangial hepatitis.

Contributor's Comment: Ever since its discovery by Theiler (thus the name Theiler's disease) in South Africa, this remains one of the most common causes of hepatic failure in horses. The onset of clinical signs is acute, and often, rapidly progresses to death. Occasionally, some horses survive.[4] The disease is also known as "serum hepatitis," "serum sickness," and "idiopathic acute hepatic failure." Theiler's disease is historically associated with injection of biologicals of equine origin such as tetanus antitoxin, *Clostridium perfringens* toxoids, equine herpesviral vaccine, pregnant mare serum and commercial plasma.[1,2,4,5,7] Clinically, the disease is manifested after an incubation period ranging from 40-90 days following an exposure to a biological. The clinical manifestations are reflective of underlying hepatic and central nervous system (CNS) disorders. These include icterus, mild circling to maniacal behavior, continuous walking, head pressing, blindness and ataxia. Although an association between the disease and use of a biological of equine origin is well accepted, sporadic cases without a history of biological make some veterinarians think there is an alternate cause, possibly a virus.[6] However, to date, no virus has been isolated. Macroscopically, the liver is flabby, either small or enlarged and dark-green to dark-brown. Microscopic changes invariably progress rapidly as in this case.

A liver biopsy taken 24 hours before euthanasia had expanded zones of hepatocytes arranged in ill-defined cords with a mild, interspersed, inflammatory infiltrate that followed the central veins and the portal units. The overall structural integrity was maintained. Thirty six hours later, the microarchitecture was obscured with massive drop out of hepatocytes, parenchymal collapse, poorly discernible central veins and portal triads that are variably expanded by proliferating biliary ductules, cellular infiltrates, and edema when the animal was euthanized. The ductular proliferation of cholangiolar or oval cells is a regenerative response to massive hepatocyte loss. The histologic progression was dramatic. Hepatic cord disruption and hepatocyte loss cause collapse of the lobular outline bringing the portal units closer. Histologic change in the CNS included Alzheimer type II astrocytes characteristic of hepatic encephalopathy.

AFIP Diagnosis: Liver: Hepatocellular degeneration and necrosis, massive, diffuse, severe, with intrahepatic cholestasis and hemorrhage, and multifocal moderate biliary hyperplasia.

Conference Comment: Participants briefly reviewed histomorphologic pattern recognition in hepatic lesions, emphasizing its utility in narrowing the differential diagnosis based on a sound understanding of the susceptibility of the parenchymal cells in each zone of the lobule to various insults. Specifically, centrilobular (i.e. zone 3, periacinar) hepatocytes are preferentially affected in many hepatopathies because of two key biologic features: 1) centrilobular hepatocytes are supplied by blood with the lowest concentration of oxygen in the liver, thereby making them exquisitely sensitive to hypoxic injury, and 2) they possess the greatest expression of biotransformation enzymes, including members of the cytochrome P450 superfamily (i.e. mixed-function oxidase system) responsible for most phase I biotransformation reactions that may yield transient reactive intermediates, rendering centrilobular hepatocytes highly susceptible to injury by toxins that are activated by cytochromes P450. By contrast, periportal (i.e. zone 1) hepatocytes, due to their close proximity to vascular inflow, are most susceptible to direct-acting toxicants. While the cause and pathogenesis of Theiler's disease remain enigmatic, the characteristic centrilobular to massive distribution of hepatocellular necrosis is helpful in making the diagnosis.[7]

Two noteworthy observations regarding this interesting condition were reiterated during the conference. First, while the majority of cases occur in horses that have received injections of equine-origin biologics, many

sporadic cases have occurred in horses that have not received such injections, leading to persistent suspicion of a serum-transmissible viral etiology, similar to hepatitis B in humans. Second, although rapid clinical progression typically culminating in death within 24 hours suggests an acute disease course, the microscopic appearance indicates some degree of chronicity, and acute hepatocellular necrosis and hemorrhage are not typical. Rather, there is centrilobular to massive loss of hepatocytes, macrovesicular fatty change with degeneration of most remaining hepatocytes, extensive deposition of bile pigments in Kupffer cells and hepatocytes, and mild portal fibroplasia with occasional ductular proliferation.[7]

Endogenous toxins associated with hepatic and, less commonly, renal failure may cause hepatic encephalopathy, as was diagnosed in the horse of this case. Horses are similar to humans, yet unique among domestic animal species, in that they characteristically develop Alzheimer type II astrogliosis attributable to hepatic encephalopathy, with myelin vacuolation being mild to absent. By contrast, in most domestic species the predominant histologic feature of hepatic encephalopathy is spongy vaculoation of myelin, particularly at the junction of cerebral gray and white matter and around the deep cerebellar nuclei, with Alzheimer type II astrogliosis being a variable finding.[3]

Contributor: Texas A&M University, College of Veterinary Medicine & Biomedical Sciences, Department of Veterinary Pathobiology, 4467 TAMU, College Station, TX 77843-4467
http://www.cvm.tamu.edu/vtpb/

References*:*

1. Aleman M, Nieto JE, Carr EA, Carlson GP: Serum hepatitis associated with commercial plasma transfusion in horses. J Vet Intern Med **19:**120-122, 2005
2. Guglick MA, McAllister CG, Ely RW, and Edwards WC: Hepatic disease associated with administration of tetanus antitoxin in eight horses. J Am Vet Med Assoc **206:**1737-1740, 1995
3. Maxie MG, Youssef S: Nervous system. *In:* Jubb, Kennedy, and Palmer's Pathology of Domestic Animals, ed. Maxie MG, 5th ed., vol. 1, pp. 386-387. Elsevier Saunders, Philadelphia, PA, 2007
4. Messer NT, and Johnson PJ: Serum hepatitis in two brood mares. J Am Vet Med Assoc **204:**1790-1792, 1994
5. Messer NT, and Johnson PJ: Idiopathic acute hepatic disease in horses: 12 cases. J Am Vet Med Assoc **204:**1934-1937, 1994
6. Smith HL, Chalmers GA, and Wedel, R: Acute hepatic failure (Theiler's disease) in a horse. Can Vet J **32:**362-364, 1991
7. Stalker MJ, Hayes MA: Liver and biliary system. *In:* Jubb, Kennedy, and Palmer's Pathology of Domestic Animals, ed. Maxie MG, 5th ed., vol. 2, pp. 298-301, 316-324, 343-344, 364-365. Elsevier Saunders, Philadelphia, PA, 2007

The Armed Forces Institute of Pathology
Department of Veterinary Pathology

Conference Coordinator:
Shannon Lacy, DVM, MPH

WEDNESDAY SLIDE CONFERENCE 2009-2010

Conference 13

27 January 2010

Conference Moderator:

Elizabeth A. Mauldin, DVM, Diplomate ACVP, Diplomate ACVD

CASE I: 5221 (AFIP 2941533).

Signalment: 11-year-old, castrated male, chinchilla longhair cat (*Felis catus*).

History: Presented with skin disease, weight loss, and polydypsia. Ultrasound revealed an abnormal pancreas, a nodular liver and congenital absence of the right kidney.

Gross Pathology: The cat was in poor condition and weighed 3.6 kg. Extensive alopecia was noted over the muzzle and periorbital areas, all four limbs, the thorax, on the ventrum and in the axillary and inguinal regions. Over the axillary and inguinal regions and plantar aspects of the carpus, metacarpus, tarsus and metatarsus, there were focally extensive erosions. Hyperpigmentation was present in the alopecic areas of the muzzle and periorbita. A paucity of subcutaneous and intra-abdominal fat was noted. Diffusely the lungs were dark, red and heavy. The cut surface was similar and 100% of the lung was involved. The pericardial sac contained 10 mL of red fluid and diffusely there was minimal nodular thickening of the left atrioventricular valve. Multifocally on the capsular and cut surface of the liver were numerous (approximately 10) raised, well-demarcated, yellow-white, soft, round nodules that were variably sized, ranging from 0.5 to 2 cm in diameter. Diffusely the pancreas was mottled dull grey-red and contained numerous raised, firm, round nodules that were up to 0.5 cm in diameter. Focally at the body of the pancreas, there was a larger, raised, poorly demarcated, yellow-white, firm, nodular mass that was 2 cm in diameter. The left kidney measured 42 x 30 x 20 mm and appeared normal. The right kidney and ureter were not present.

Laboratory Results: Bacterial culture of the liver revealed no significant growth.

Contributor's Morphologic Diagnosis: Skin: Dermatitis/cellulitis, chronic-active, diffuse, moderate with hair follicle and sebaceous gland atrophy and moderate epidermal hypoplasia and hypokeratosis.

Contributor's Comment: A diagnosis of feline paraneoplastic alopecia (FPA) was reached after postmortem diagnosis and histopathology revealed a pancreatic exocrine adenocarcinoma, which had metastasized to the liver. Changes in the hair follicles and dermis are characteristic of those reported for FPA. Feline paraneoplastic alopecia usually starts on the ventral neck, thorax or abdomen, the changes grossly apparent as a non-pruritic, progressive, symmetrical alopecia. Hairs are easily epilated and the skin is thin,

*Sponsored by the American Veterinary Medical Association, the American College of Veterinary Pathologists, and the C. L. Davis Foundation.

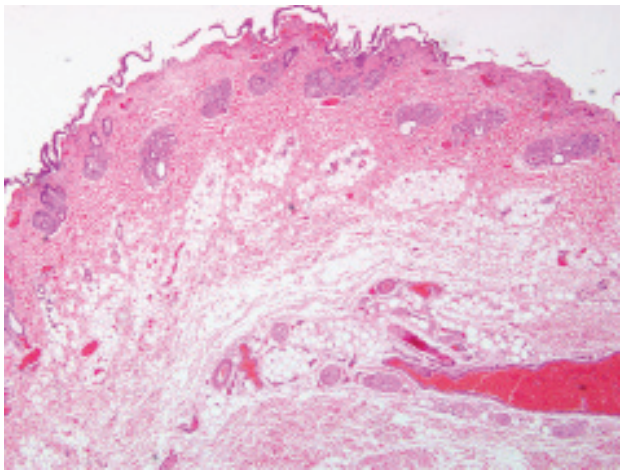

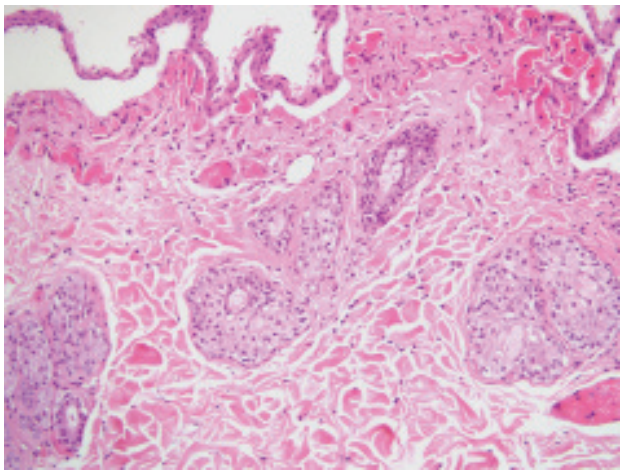

1-1, 1-2. Haired skin, cat. There is a marked paucity of hair follicles in the dermis, and the epidermis is thinned or lost, with occasional separation from the underlying superficial dermis. (HE 40X and 200X)

shiny and inelastic. Footpad involvement has also been reported, with varying presentations from dry and cracked to moist, erythematous pads. These are usually painful. The cause of the alopecia is not fully understood and it is non-responsive to corticosteroid treatment. When the carcinoma was surgically excised the condition resolved in one case, although it did recur at the time of metastasic tumour recurrence.[4] Most affected cats are reported to groom excessively, and it has been postulated that the shiny appearance of the skin arises from the resulting exfoliation of the stratum corneum.[3] Affected animals range in age from 7-16 years (median 13 years), with no apparent breed predilection.[5] Skin lesions are often accompanied by other systemic clinical signs, such as weight loss, vomiting, diarrhea, anorexia and lethargy. This disease has been reported with pancreatic carcinoma in 12 cats and biliary carcinoma in two cats.[5]

Histopathological examination of the skin consistently shows a non-scarring alopecia with characteristic marked follicular telogenization, miniaturization and atrophy, with similar adnexal atrophy. Other findings include mild epidermal acanthosis and hyperplasia with a hypo- or non-keratinized epidermis, and a mild, mixed, perivascular inflammatory infiltrate of the dermis, consisting of lymphocytes, macrophages and neutrophils.[3,4] In a recent report of feline skin biopsies complicated by *Malassezia* spp., histopathology from 7 of 15 cases was consistent with FPA. Although pancreatic carcinoma was confirmed in only four of these cats, it is possible that an indication of internal malignancy could be made when *Malassezia* spp. are detected in histopathology of cats with generalized skin disease.[2]

Neoplastic diseases of the exocrine pancreas and biliary tree are rare in the cat. The prognosis for these is generally poor since at the time of diagnosis the disease has often metastasized to distant sites, such as the liver, lymph nodes and lungs, as well as possibly local seeding to intraperitoneal sites. Twelve of the fourteen cats reported in the literature died or were euthanized within 8 weeks of onset of clinical signs.

AFIP Diagnosis: Haired skin and subcutis: Follicular atrophy, diffuse, marked, with mild, multifocal, lymphoplasmacytic and histiocytic dermatitis.

Conference Comment: The sections of haired skin from this cat contain the histologic features of FPA, including profound follicular atrophy with sparing of the sebaceous glands and acanthosis (**figs. 1-1 and 1-2**). Additionally, the presence of a pancreatic adenocarcinoma supports a diagnosis of FPA. However, the moderator and several conference participants identified other histologic features not typical of FPA, including: small areas of epidermal necrosis and/or individual cell necrosis in the epithelium in some slides; subepidermal clefting; congested small blood vessels in the superficial dermis; and ulceration in a few sections. Conference participants debated whether the subepidermal clefting was real or artifact, and suggested that additional history may be helpful in identifying other factors to explain the clefting and epithelial necrosis.

Differentiation between FPA and feline hyperglucocorticoidism (FHG) was discussed. Follicular atrophy is present in both conditions, but it is more striking in FPA and hair follicles in FHG have increased tricholemmal keratinization (bright eosinophilic core in an atrophic follicle) and follicular hyperkeratosis. Sebaceous

glands may be atrophied in FHG, but are usually normal in FPA. The most striking feature of FHG is profound dermal atrophy, whereas the dermis is normal in FPA. FPA is also characterized by acanthosis with parakeratotic hyperkeratosis.[1]

In addition to FPA, other paraneoplastic skin lesions include feline thymoma-associated exfoliative dermatitis, nodular dermatofibrosis, feminization syndrome associated with Sertoli cell tumors, superficial necrolytic dermatitis and paraneoplastic pemphigus, all of which are described in an excellent review article.[5] Nodular dermatofibrosis occurs primarily in the German Shepherd Dog and is associated with renal cystadenomas or cystadenocarcinomas and uterine leiomyomas.[5] Superficial necrolytic dermatitis occurs more commonly due to hepatopathy or diabetes mellitus, but it has also been associated with a glucagonoma.[5] Paraneoplastic pemphigus is extremely rare.

Contributor: The Royal Veterinary College, University of London, Hawkshead Lane, North Mymms, Hatfield, Herts, AL9 7TA, United Kingdom
http://www.rvc.ac.uk/

References:

1. Gross TL, Ihrke PJ, Walder EJ, Affolter VK: Skin Diseases of the Dog and Cat: Clinical and Histopathologic Diagnosis, 2nd ed., pp. 498-501. Blackwell Publishing, Ames, IA, 2005
2. Mauldin EA, Morris DO, Goldschmidt MH: Retrospective study: the presence of *Malassezia* in feline skin biopsies, a clinicopathological study. Vet Dermatol **13:**7-13, 2002
3. Pascal-Tenorio A, Olivry T, Gross TL, Atlee BA, Ihrke PJ: Paraneoplastic alopecia associated with internal malignancies in the cat. Vet Dermatol **8:**47-52, 1997
4. Tasker S, Griffon DJ, Nuttall TJ, Hill PB: Resolution of paraneoplastic alopecia following surgical removal of a pancreatic carcinoma in a cat. J Small Anim Pract **40:**16-19, 1999
5. Turek MM: Cutaneous paraneoplastic syndromes in dogs and cats: a review of the literature. Vet Dermatol **14:**279-296, 2003

CASE II: 06-26654-3 (AFIP 3134295).

Signalment: 10-year-old, castrated male, border collie cross dog (*Canis familiaris*).

History: One-month history of a mass on the ventral abdomen. The mass had doubled in size over the last few weeks. It was freely moveable within the subcutaneous layers of the skin and measured approximately 3 x 3 cm at the time of removal.

Gross Pathology: Received a 3 x 2.5 cm ellipse of haired skin containing a firm, pale 2 cm diameter subcutaneous mass.

Histopathologic Description: Haired skin: Beneath the superficial dermis is an unencapsulated, well demarcated, moderately cellular, focally infiltrative neoplastic mass. Neoplastic cells are arranged in thin streams dissecting between large thick bundles of well defined eosinophilic homogenous (hyalinized) birefringent material (collagen) within a fine fibrovascular stroma (**fig. 2-1**). In one location, neoplastic cells form interlacing bundles and streams with small embedded collagen bundles. Cells are spindloid with indistinct cell borders, a scant amount of finely fibrillar eosinophilic cytoplasm with an elongate central nucleus with finely stippled chromatin and indistinct nucleoli. There is three-fold anisocytosis and anisokaryosis. The mitotic rate is low with an average of 0.1 mitotic figures per 400x HPF. Neoplastic cells extend to one margin of the biopsy. Small areas of hemorrhage are scattered throughout the tumor and around the tumor base. Small numbers of lymphocytes and plasma cells surround small vessels around the margins of the tumor.

Contributor's Morphologic Diagnosis: Keloid fibrosarcoma.

Contributor's Comment: Keloid fibrosarcomas are an uncommon variant of fibrosarcomas, distinct from the other forms of fibrosarcoma and other collagen-rich masses due to the presence of thick bands of hyalinized collagen.[3] These bands of hyalinized collagen can also be seen in cytologic preparations.[2] Keloidal tumors are infrequently reported in dogs and have not been reported in other domestic animal species. They appear somewhat similar histologically to keloids, hypertrophic scars and keloid dermatofibromas in humans.[2] The one published retrospective study of keloidal tumors in dogs suggests that the presence of macrophages within the tumors may indicate that these tumors are reactive inflammatory lesions, rather than true neoplasms.[3]

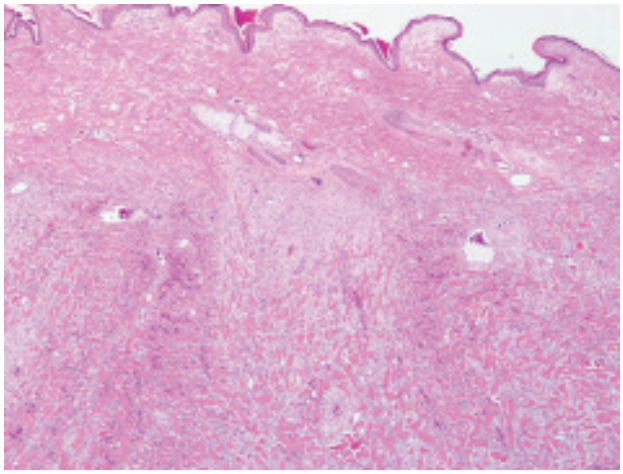

2-1. Fibrosarcoma (keloidal), haired skin and subcutis, dog. Neoplastic spindled cells are arranged in long streams within a densely collagenous matrix. (HE 200X)

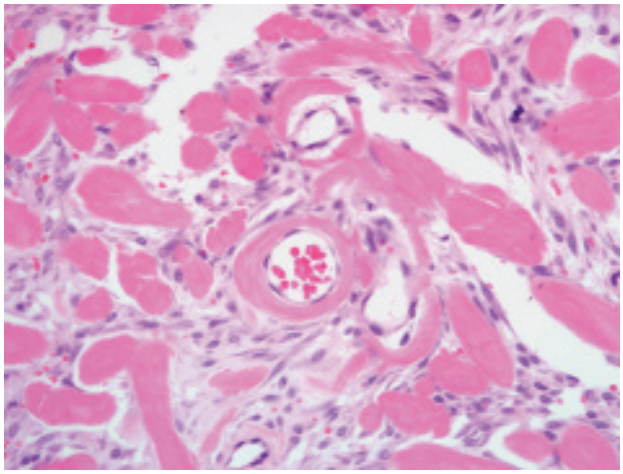

2-2. Fibrosarcoma (keloidal), haired skin and subcutis, dog. Small capilliaries occur centrally within large, hyalinized collagen fibers. (HE 400X)

Differentiation of keloid fibromasarcomas from keloidal fibromas is based on the presence of portions of the tumors that are composed largely of thickly packed neoplastic cells with only a small amount of fibrovascular stroma and small numbers of hyalinized fibers.[3] These areas are reportedly more common in the deeper margins of the tumors as is the case in this example. It was suggested that keloidal fibrosarcomas may represent a malignant transformation of keloid fibromas; however, no difference in prognosis has been demonstrated between keloid fibromas or keloid fibrosarcomas.

The neoplastic cells in keloidal tumors of dogs are vimentin positive and smooth muscle actin negative and are interpreted to be fibroblasts in contradistinction to human keloidal tumors which are comprised of myofibroblasts.[3]

AFIP Diagnosis: Haired skin and subcutis: Fibrosarcoma, low grade (keloidal).

Conference Comment: The large bundles of hyalinized collagen are a distinctive histologic feature in this case, and in dogs are generally limited to keloidal fibromas and fibrosarcomas and mast cell tumors with keloidal change.[1] Differentiation between keloidal fibromas and keloidal fibrosarcomas is based on the presence of interlacing fascicles of neoplastic cells and/or infiltration in the malignant variant. Since keloidal fibrosarcomas may arise from keloidal fibromas, the malignant characteristics may be present only in a small portion of the tumor.[3] Keloidal fibrosarcomas also may contain cellular atypia and have an increased mitotic rate.[1] The differential diagnosis includes dermatofibroma and peripheral nerve sheath tumor (PNST). In dermatofibromas, and occasionally in PNSTs, the spindle cells are separated by enlarged, but non-hyalinized, collagen bundles. Additionally, dermatofibromas usually contain inflammation and overlying epithelial hyperplasia, while PNSTs have a neural pattern, demonstrate variation in cellularity, and frequently contain a myxomatous matrix.[1]

Conference participants also noted the presence of small capillaries within the large, hyalinized collagen fibers and areas of microhemorrhage; these changes have been described previously (**fig. 2-2**).[3]

Contributor: Department of Veterinary Pathology, Western College of Veterinary Medicine, 52 Campus Drive, Saskatoon, Saskatchewan, S7N 5B4, Canada
http://www.usask.ca/wcvm/

References:

1. Gross TL, Ihrke PJ, Walder EJ, Affolter VK: Skin Diseases of the Dog and Cat: Clinical and Histopathologic Diagnosis, 2nd ed., pp. 721-722. Blackwell Publishing, Ames, IA, 2005
2. Little LK, Goldschmidt M: Cytologic appearance of a keloidal fibrosarcoma in a dog. Vet Clin Pathol **36:**364-367, 2007
3. Mikaelian I, Gross TL: Keloidal fibromas and fibrosaromas in the dog. Vet Pathol **39:**149-153, 2002

CASE III: B08-24914 (AFIP 3136050).

Signalment: 3-year-old, female spayed greyhound dog (*Canis familiaris*).

History: The dog developed two cutaneous nodules on the right and left dorsal ear pinnae two months prior to presentation.

Gross Pathology: The nodules on the right and left dorsal pinnae were alopecic, firm, focally ulcerated and measured 1 cm and 2 mm in diameter, respectively.

Histopathologic Description: Each sample has a well-demarcated, dense, nodular proliferation of inflammatory cells that expands the deep dermis and subcutis and elevates the overlying epidermis. Inflammatory cells consist predominantly of epithelioid macrophages with rare multinucleated giant cells admixed with lymphocytes, plasma cells and scattered aggregates of neutrophils (**fig. 3-1**). Discrete granuloma formation is not present. Between aggregates of inflammatory cells, there is a moderate collagenous stroma and blood vessels are lined by hypertrophied endothelial cells. Within the inflammatory lesion, there are few foci of acute hemorrhage and there are scattered melanophages. In the larger nodule, from the right pinna, there is a focal ulcer (present in some sections) covered by a fibrinocellular exudate.

Ziehl-Neelson acid fast stain: Low numbers of acid-fast-positive bacilli, measuring 1-2 um in length, are within the cytoplasm of epithelioid macrophages (**fig. 3-2**).

In the adjacent dermis, there is clumping of melanin within hair follicles with multiple melanophages in the surrounding dermis and mild periadnexal infiltrates of lymphocytes and plasma cells (**fig. 3-3**).

Contributor's Morphologic Diagnosis: 1. Haired skin (dorsal pinna): regional nodular granulomatous and lymphoplasmacytic dermatitis with focal ulcer and rare intrahistiocytic acid-fast bacilli (canine leproid granuloma syndrome).
2. Haired skin (dorsal pinna): follicular melanin clumping with dermal melanophages (possible color dilution alopecia).

Contributor's Comment: Canine leproid granuloma syndrome is a mycobacterial skin disease characterized by single or multiple, well-circumscribed, firm, variably-sized (2 mm to 5 cm diameter) nodules within the skin or subcutis, predominantly affecting the ear pinna, head and occasionally the distal extremities.[2,6] Short-coated dog breeds, particularly boxer dogs and boxer crosses, are most commonly affected.[2,6] The nodules are thought to be non-pruritic and painless, and occasionally, particularly in the larger nodules, the overlying epidermis is ulcerated or alopecic.[2,6] The nodules have been reported to spontaneously regress without treatment and in some cases surgical excision is considered curative.[2,6] Other cases with a more persistent infection may require antimicrobial therapy.[7] The lesions are confined to the skin with no involvement of lymph nodes or internal organs.[2,6]

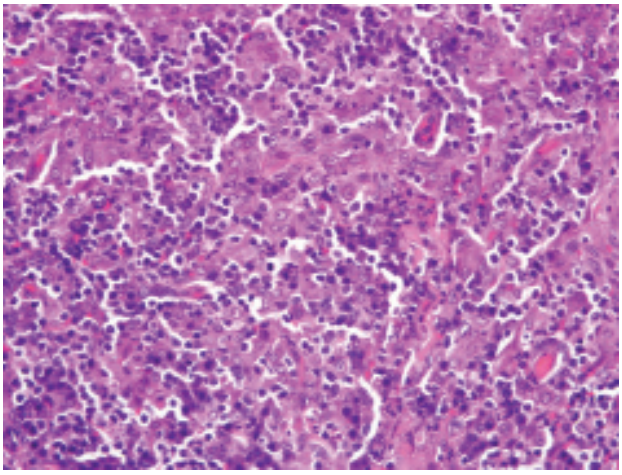

3-1. Haired skin, dog. Diffusely expanding the dermis are many epithelioid macrophages admixed with lymphocytes, plasma cells, and fewer viable and degenerate neutrophils. (HE 400X)

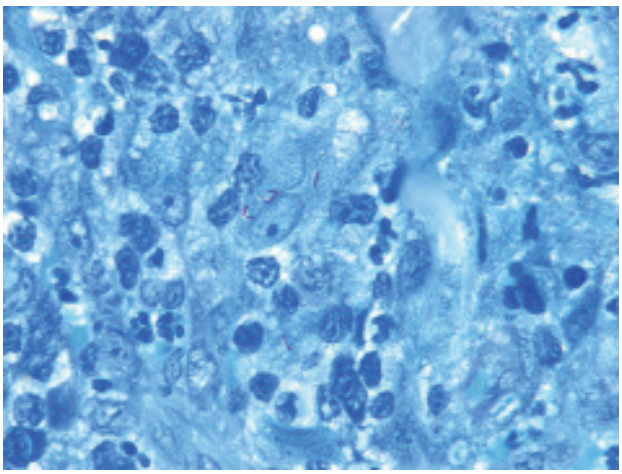

3-2. Haired skin, dog. There are few acid-fast bacilli within the cytoplasm of epithelioid macrophages (Ziehl-Neelson acid-fast stain), Photographs courtesy of Department of Pathobiology, University of Pennsylvania, School of Veterinary Medicine, Philadelphia, PA 19104

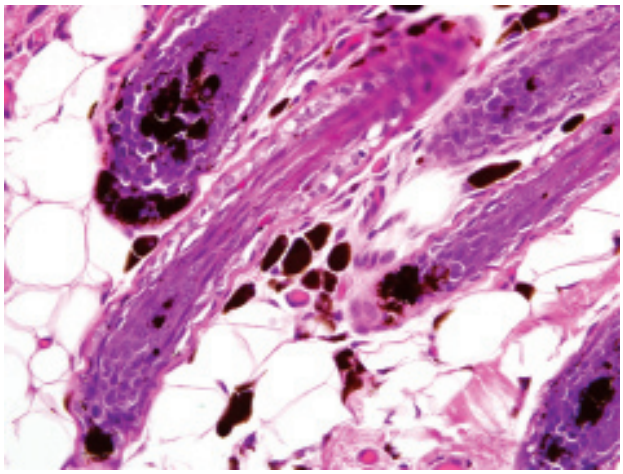

3-3. Haired skin, dog. Multifocally, there is clumping of melanin within hair follicles, and macrophages in the adjacent dermis are filled with melanin pigment (pigmentary incontinence). (HE 400X)

On cytologic evaluation of fine-needle aspirates of the nodules, there are spindle-shaped macrophages with variable numbers of lymphocytes and plasma cells with fewer neutrophils and there are few to moderate numbers of negative-staining bacilli extracellularly or within macrophages.[1] On histopathology, there is dermal and/or subcutaneous granulomatous inflammation, with or without pyogranulomatous foci, and the inflammatory lesion consists mainly of epithelioid macrophages and neutrophils with lymphocytes, plasma cells, and rare multinucleated giant cells.[1,2,6] In Ziehl-Neelson acid-fast-stained specimens, there are very low to low numbers of intracellular bacilli in the majority of cases.[1,2,6]

The cause is a saprophytic, as yet unnamed and uncultivated, species of *Mycobacterium*.[1,2,4,6] Culture is unsuccessful, but with 16s rRNA PCR-based gene analysis on fresh and formalin-fixed, paraffin-embedded tissue, a proposed novel mycobacterial sequence has been identified.[4] The closest relatives of this agent are *Mycobacterium tilburgii, M. simiae*, and *M. genavense*.[4] There are significant molecular similarities between the organisms identified in the United States and those in Australia and New Zealand.[2] The suggested mode of transmission of the etiologic agent in canine leproid granuloma syndrome is thought to be percutaneous inoculation via wounds or biting insects.[2,6]

In the present case, the follicular melanin clumping with dermal melanophages is suggestive of concurrent color dilution in this dog. Color dilution alopecia is a hereditary skin disease in dogs with "blue" or "fawn" color-diluted coats and has been reported in the greyhound.[3] This disease is typically characterized by atrophy, distortion and abnormal melanin pigmentation of hair follicles with variable alopecia. Large amounts of clumped melanin pigment are within the hair follicle and within melanophages in the dermis around the base of hair follicles.[3] Some of the features of color dilution alopecia, such as the melanin clumping, may be seen in color-dilute dogs without alopecia and are not of pathologic significance.[3]Without enough supporting clinical history in this case, the contributors cannot determine whether this dog was color-diluted or fits the criteria for color dilution alopecia.

AFIP Diagnosis: 1. Haired skin and subcutis: Dermatitis, pyogranulomatous, focally extensive, severe, with rare intrahistiocytic acid-fast bacilli.
2. Haired skin and subcutis: Follicular melanin clumping, multifocal, mild, with perifollicular pigmentary incontinence.

Conference Comment: The contributor provides an excellent review of canine leproid granuloma. Conference participants considered histiocytoma, plasmacytoma, fungal dermatitis, atypical mycobacteriosis, and sterile granuloma and pyogranuloma syndrome in the differential diagnosis. This case lacks the typical histological features of histiocytoma, including epithelial hyperplasia, superficial dermal edema, occasional reniform nuclei and a moderate mitotic rate.[3] Plasmacytomas typically have few large nuclei and binucleated cells with differential staining of the chromatin pattern, vague packeting, and more differentiated plasma cells at the tumor periphery [3]; additionally, small clusters of neutrophilic inflammation and scattered giant cells would be unusual histologic features for tumors of plasma cell origin. Opportunistic fungal infections could cause similar histologic lesions; however, fungal organisms are not observed. Atypical mycobacteriosis more commonly affects cats, and the histopathologic features consist of nodular pyogranulomatous dermatitis and panniculitis with draining tracts and rare acid-fast bacilli found within clear spaces in areas of inflammation.[2] Sterile granuloma and pygranuloma syndrome is an inflammatory condition of unknown cause that is responsive to glucocorticoid therapy; unlike leproid granuloma, lesions are more often multifocal and track hair follicles, and special stains do not reveal an etiological agent.[3] Due to the presence of epithelioid macrophages, giant cells and fibrosis, mycobacterial lesions can resemble sarcoma, and are therefore sometimes described as sarcomatoid.[5]

Contributor: Department of Pathobiology, University of Pennsylvania, School of Veterinary Medicine, Suite 4005 MJR-VHUP, 3800 Spruce Street, Philadelphia, PA

19104
http://www.vet.upenn.edu/FacultyandDepartments/Pathobiology/PathologyandToxicology/tabid/412/Default.aspx

References:

1. Charles J, Martin P, Wigney DI, Malik R, Love DN: Cytology and histopathology of canine leproid granuloma syndrome. Aust Vet J **77:**799-803, 1999
2. Foley JE, Borjesson D, Gross TL, Rand C, Needham M, Poland A: Clinical, microscopic, and molecular aspects of canine leproid granuloma in the United States. Vet Pathol **39:**234-239, 2002
3. Gross TL, Ihrke PJ, Walder EJ, Affolter VK: Skin Diseases of the Dog and Cat: Clinical and Histopathologic Diagnosis, 2nd ed., pp. 281-283, 518-522, 840-845, 866-872. Blackwell Publishing, Ames, IA, 2005
4. Hughes MS, James G, Ball N, Scally M, Malik R, Wigney DI, Martin P, Chen S, Mitchell D, Love DN: Identification by 16S rRNA gene analyses of a potential novel mycobacterial species as an etiologic agent of canine leproid granuloma syndrome. J Clin Microbiol **38:**953-959, 2000
5. Lopez A: Respiratory system. *In:* Pathologic Basis of Veterinary Disease, eds. McGavin MD, Zachary JF, 4th ed., p. 520. Mosby Elsevier, St. Louis, MO, 2007
6. Malik R, Love DN, Wigney DI, Martin P: Mycobacterial nodular granulomas affecting the subcutis and skin of dogs (canine leproid granuloma syndrome). Aust Vet J **76:**403-407, 1998
7. Malik R, Martin P, Wigney D, Swan D, Sattler PS, Cibilic D, Allen J, Mithcell DH, Chen SCA, Hughes MS, Love DN: Treatment of canine leproid granuloma syndrome: preliminary findings in seven dogs. Aust Vet J **79:**30-36, 2001

CASE IV: 22809/1 (AFIP 3138538).

Signalment: 3-year-old, female bloodhound dog (*Canis familiaris*).

History: The dog was caught in the countryside and no history was available.

Gross Pathology: Not reported.

Histopathologic Description: Haired skin and subcutis, posterior limb. Within the dermis and the hypodermis there is a nodular (approximately 1.5 cm), slightly exophytic, infiltrative, poorly demarcated, unencapsulated, densely cellular lesion that effaces the dermal collagen and displaces the adnexa (**fig. 4-1**). The population is predominantly composed by atypical discrete round cells with generally distinct cell borders and a small to moderate amount of eosinophilic cytoplasm (**fig. 4-2**). Nuclei (approximately 1.5-2 x RBC) are central irregularly round and occasionally indented, with finely stippled chromatin, and one generally indistinct nucleolus. Mitoses average 5 per high power field. The atypical cells show occasional epidermal and follicular epitheliotropism. In association there is a second cellular population composed of high numbers of disseminated protozoa-laden macrophages (**fig. 4-3**). Intrahistiocytic protozoal amastigotes are evident; they are 2-3 um in diameter with clear cytoplasmic halo, basophilic nucleus, and a smaller adjacent (perpendicular) kinetoplast (consistent with *Leishmania* spp. amastigotes) (**fig. 4-4**). In addition, numerous plasma cells and Mott cells and occasional small

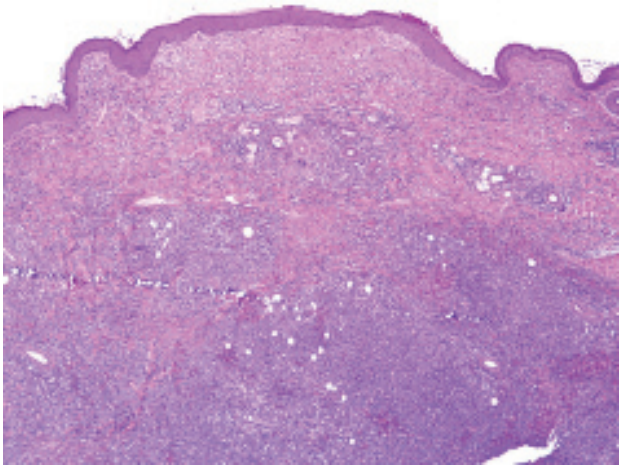

4-1. Malignant lymphoma, haired skin, dog. Neoplastic round cells infiltrate and efface the deep dermis and subcutis. (HE 40x)

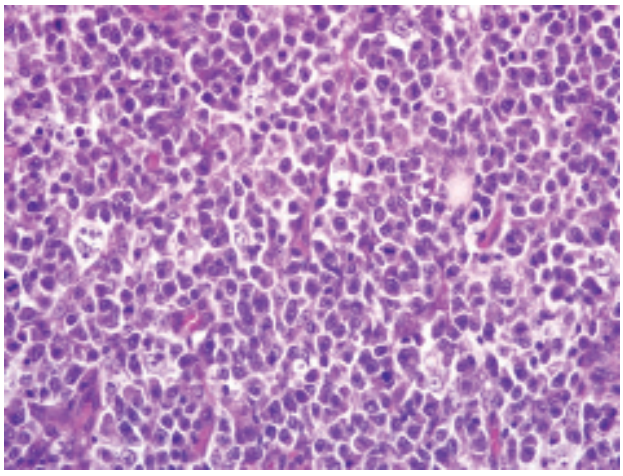

4-2. Malignant lymphoma, haired skin, dog. Neoplastic lymphoid cells have distinct borders, round central nuclei with coarsely stippled to clumped chromatin, and scant eosinophilic cytoplasm. (HE 400x)

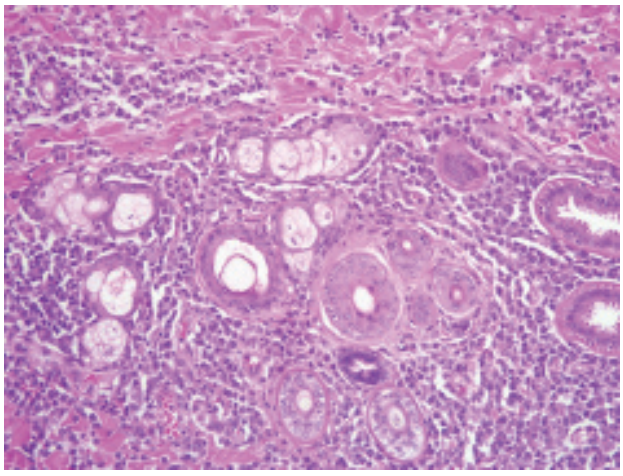

4-3. Haired skin, dog. Inflammatory cells, consisting of many macrophages and fewer lymphocytes and plasma cells, infiltrate the superficial dermis and surround adnexa. (HE 200x)

lymphocytes are also disseminated within and around the lesion, and multifocally extend into the subcutis where they are predominantly focused around blood vessels. There is also multifocal ulceration associated with degenerate and non-degenerate neutrophils, necrotic debris, and collagen lysis. There is diffuse parakeratotic hyperkeratosis. The superficial dermis is multifocally mildly expanded by edema and ectatic lymphatics.

Immunohistochemistry for CD3, CD5, CD79a, CD20 was performed (not submitted). The predominant atypical population showed a moderate diffuse cytoplasmic staining for CD3. Staining for CD5, CD20, and CD79a was negative. A nonspecific nuclear staining was detected for CD79a.

Contributor's Morphologic Diagnosis: Haired skin and subcutis, posterior limb: Epitheliotropic lymphoma associated with histiocytic and lymphoplasmacytic dermatitis, severe, diffuse with myriad intrahistiocytic protozoal amastigotes, consistent with *Leishmania* spp., *Canis familiaris*, dog.

Contributor's Comment: Canine leishmaniasis (CL) is a systemic disease caused by different species of the genus *Leishmania* that is transmitted by blood sucking phlebotomine sandflies. The majority of affected dogs present with poor body condition, immunosuppression, lymphadenomegaly and excessive skin scaling. The disease is endemic in the Mediterranean area. In the dog, the cellular immune response against *Leishmania* is still not well defined, although in affected individuals capable of overcoming the disease characteristic immune responses of type Th1 have been shown. Cutaneous epitheliotropic T-cell lymphoma in the dog is a rare neoplastic condition with unknown etiology. In dogs, epitheliotropic T-cell lymphoma pursues a progressive course of disease with several months to 2 years before death. The neoplastic population is characterized by infiltration of neoplastic T lymphocytes with a specific tropism for the epidermis and the adnexal structures.[2]

From literature, prolonged antigenic stimulation and chronic immunosuppression plays a crucial role in the etiopathogenesis of T-cell lymphoma.[1] Persistent environmental antigens act as a stimulus for chronic T-cell activation and proliferation and progression to a clonal expansion has been suggested as a possible cause of epitheliotropic lymphoma in humans.[3] To our knowledge some reports are present describing association between skin lymphoma and atopic dermatitis or chronic skin allergic disease. Our dog could further confirm that chronic antigen stimulation may be an initiator of a clonal neoplastic T-cell population in the skin. Canine epitheliotropic lymphoma has been further subtyped as a tumor predominantly of CD8-γδ-T cells. In the present case, a deeper investigation of the immunophenotype was not possible since monoclonal antibodies available for detection of CD4 and CD8 on formalin fixed tissue biopsies were not available. The cell population appeared to be CD3+ and therefore compatible with T-cell lymphoma.

AFIP Diagnosis: 1. Haired skin and subcutis: Malignant lymphoma.
2. Haired skin and subcutis: Dermatitis, histiocytic and lymphoplasmacytic, diffuse, moderate, with focal

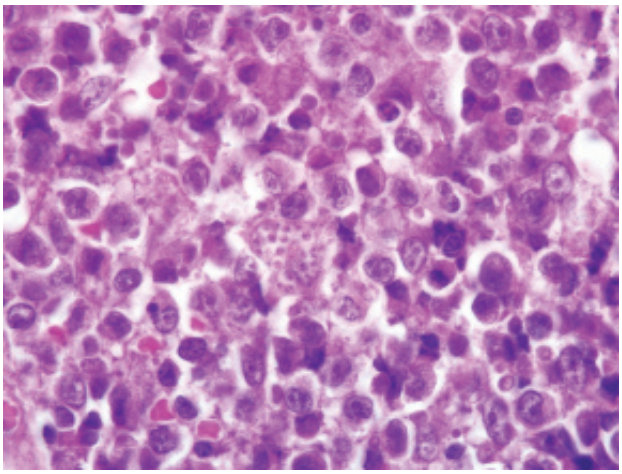

4-4. Haired skin, dog. Macrophages contain 2-3 micron protozoal amastigotes. Protozoa contain a clear cytoplasmic halo and basophilic nucleus. (HE 1000x)

ulceration and numerous intrahistiocytic protozoal amastigotes.

Conference Comment: While conference participants agreed with the histologic diagnosis of malignant lymphoma, neoplastic epitheliotropism was not observed in the slides examined during conference, suggesting this is a case of cutaneous nonepitheliotropic lymphoma. The majority of cutaneous nonepitheliotropic lymphomas in dogs and cats are of T-cell origin. Additionally, cutaneous lymphoma is more commonly epitheliotropic in dogs and nonepitheliotropic in cats.[4]

Leishmania sp. have several adaptations that allow their entry into and survival within macrophages.[5]

1. Lipophosphoglycans bind to C3b and iC3b and enhance phagocytosis, and protect organisms by scavenging oxygen free radicals and inhibiting lysosomal enzymes.
2. Gp63, a zinc-dependent proteinase, cleaves complement and some lysosomal antimicrobial enzymes.
3. Proton-transporting ATPase allows the amastigotes to survive in the phagolysosome's extremely acidic environment.

Contributor: Servizio Diagnostico di Anatomia Patologica e Patologia Veterinaria, Dipartimento di Sanità Pubblica, Patologia Comparata e Igiene Veterinaria, Facoltà di Medicina Veterinaria di Padova, Viale dell'Università, 16, 35030 Legnaro, Padova, Italy
http://www.sanitaveterinaria.unipd.it/

References:

1. Boutros N, Hawkins D, Nelson M, Lampert IA, Naresh KN: Burkitt lymphoma and leishmaniasis in the same tissue sample in an AIDS patient. Histopathology **48**:880-881, 2006
2. Fakhar M, Asgari Q, Motazedian MH, Monabati A: Mediterranean visceral leishmaniasis associated with acute lymphoblastic leukemia (ALL). Parasitol Res **103**:473-475, 2008
3. Foglia Manzillo V, Pagano A, Guglielmino R, Gradoni L, Restucci B: Extranodal γδ-T-cell lymphoma in a dog with leishmaniasis. Vet Clin Pathol **37**:298-301, 2008
4. Gross TL, Ihrke PJ, Walder EJ, Affolter VK: Skin Diseases of the Dog and Cat: Clinical and Histopathologic Diagnosis, 2nd ed., pp. 882-883. Blackwell Publishing, Ames, IA, 2005
5. McAdam AJ, Sharpe AH: Infectious Diseases. *In:* Pathological Basis of Disease, eds. Kumar V, Abbas AK, Fausto N, Aster JC, 8th ed., pp. 388-390. Saunders Elsevier, Philadelphia, PA, 2010

The Armed Forces Institute of Pathology
Department of Veterinary Pathology

Conference Coordinator:
Shannon Lacv. DVM. MPH

WEDNESDAY SLIDE CONFERENCE 2009-2010

Conference 14

3 February 2010

Conference Moderator:

Kathleen Gabrielson, DVM, PhD, Diplomate ACVP

CASE I: H-8379 (AFIP 3103222).

Signalment: 11-year-old, male owl monkey (*Aotus nancymaae*).

History: This monkey was euthanized due to cardiac and renal failure. Echocardiogram showed dilated cardiomyopathy with left ventricular hypertrophy, pericardial effusion, ascites, and abnormal kidneys.

Gross Pathology: At necropsy, the pericardial sac was filled with serosanguineous fluid; the heart was enlarged with multiple white streaks (degeneration/fibrosis) in the ventricular walls. The ascending aorta was "double-barreled," having apparently two lumina; the latter tracked into the abdominal aorta near the kidneys (**fig. 1-1**). Several linear yellow streaks (plaques) were observed in the thoracic and abdominal aorta. The kidneys were light brown with black and red speckling (nephropathy); the liver was enlarged (hepatomegaly).

Laboratory Results: Hematocrit 19.6% ↓; RBC 2.66 x 10^6/µl ↓; BUN 45 mg/dl ↑; creatinine 1.4 mg/dl ↑

Histopathologic Description: The aorta is oval-shaped and measures 4-5 mm in diameter; associated with the tunica media of the aorta is a second oval-shaped channel of slightly larger diameter that partially encircles the aorta (**fig. 1-2**). The wall of the aorta is approximately 300 µm thick versus approximately 500 µm for the second channel; the wall of the latter has an irregular endothelial lining and contains fibromuscular proliferation, degeneration/necrosis, and granulation tissue (**fig. 1-3**).

Contributor's Morphologic Diagnosis: Aorta: dissection, tunica media with fibromuscular proliferation, degeneration/necrosis, and granulation tissue.

Contributor's Comment: The aortic dissection in this owl monkey started in the ascending aorta and extended to the level of the kidneys. The dissection presented as a "double-barreled aorta" with a false channel. The false channel was partially endothelialized, suggesting it was a chronic change. Mention should be made of terminology in reference to aortic dissections. That is, while aortic aneurysm is used as a general term by many, a distinction is made by others between an aneurysm and a dissection.[3] A "true" aneurysm is considered an abnormal dilatation of a blood vessel wall that is bounded by arterial wall components. A "false" aneurysm involves an interruption in the vessel wall and the development of an extravascular

*Sponsored by the American Veterinary Medical Association, the American College of Veterinary Pathologists, and the C. L. Davis Foundation.

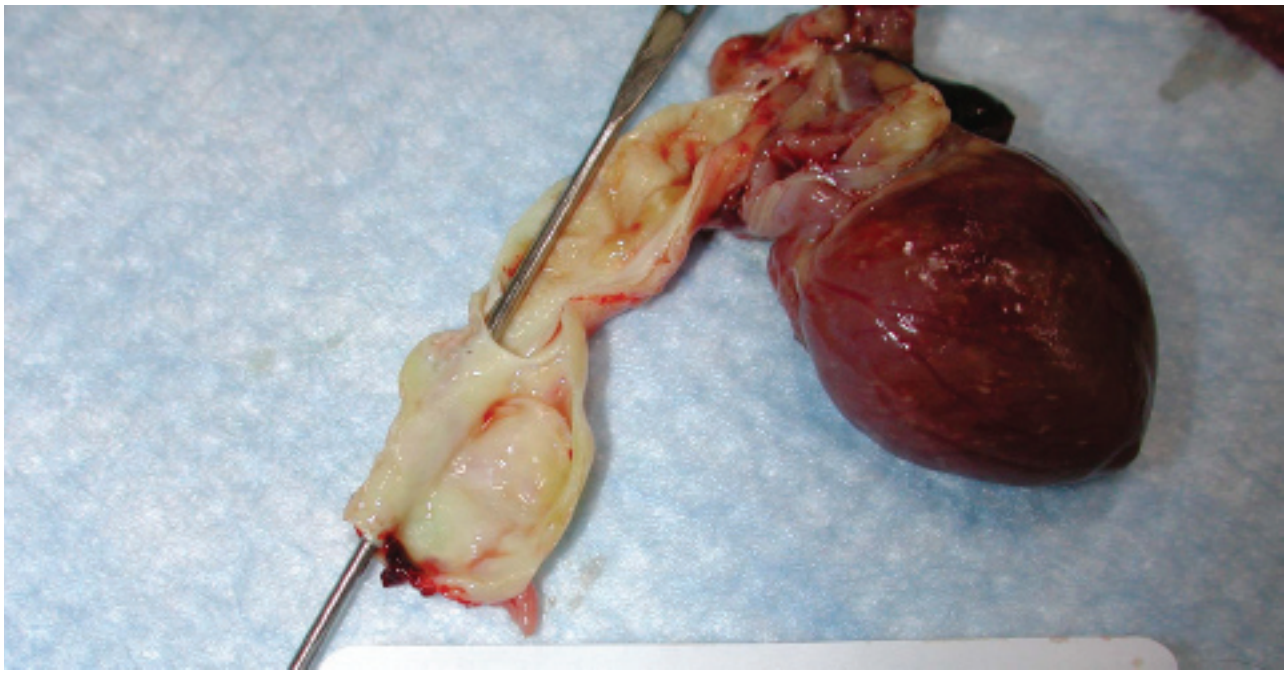

1-1. Aorta, owl monkey. The ascending aorta contains two lumina. Photographs courtesy of University of Texas M.D., Anderson Cancer Center, Keeling Center for Comparative Medicine and Research, Bastrop, Texas, 78602

hematoma that communicates with the vessel lumen. On the other hand, a dissection develops when blood enters the wall of an artery (e.g. via intimal tear), dissecting between layers, as in the aorta of this monkey. Other terms used to describe aortic dissections include dissecting hematoma and dissecting aortic aneurysm.

In general, the incidence rates for aortic aneurysms in nonhuman primates appear to be low; however, spontaneous lesions have been reported in the gorilla and squirrel, howler, capuchin, patas, spider, and owl monkeys.[1] In contrast, aortic aneurysms are not uncommon in the owl monkey, with an incidence rate of 8.6% (N=257) in one report. The majority of the aneurysms in this report were classified as dissecting with only three others termed saccular aneurysms. Aortic plaques were seen in some of these animals, as was chronic nephropathy, cardiomegaly, left ventricular hypertrophy, pericardial effusion, pleural effusion, pulmonary edema, hemothorax, hemoperitoneum, hepatomegaly, and cholelithiasis. More females than males were affected.

Hypertension is a major risk factor for aortic dissection in human males aged 40-60 years. Degenerative changes in the tunica media of the aorta may also be important. Inherited connective tissue disorders that lead to abnormal vascular structure (e.g. Marfan syndrome) fall into the latter category. Complications following arterial cannulation and pregnancy have also been associated with aortic dissection in humans. Interestingly, atherosclerosis and medial scarring due to diseases such as syphilis are not usually associated with dissections. Following the particular predisposing factor(s), an intimal tear develops with hemorrhage into the wall of the aorta.[3] Conversely, the initiating event may be a ruptured vasa vasorum with bleeding into media.[5] The pathogenesis of the aortic dissection in this monkey was not determined.

AFIP Diagnosis: Fibroelastic artery, aorta: Aortic dissection lined by endothelium, fibromuscular proliferation, cystic medial degeneration, and mucinosis.

Conference Comment: This interesting case was reviewed in consultation with the AFIP Department of Cardiovascular Pathology. During the conference, participants discussed the nomenclature pertinent to this case, with a focus on the distinction between an aneurysm and a dissection; inappropriate interchangeable use of the terms aneurysm and dissection may be culpable for undue perplexity when reviewing case reports in the literature. A true aneurysm is a localized abnormal dilation of a blood vessel or the heart, and can be further classified by its overall shape and size, with saccular (i.e. focal, bulging, asymmetrical outpouching) and fusiform (i.e. segmental to diffuse, circumferential) types being described. By contrast, a false aneurysm, also referred to

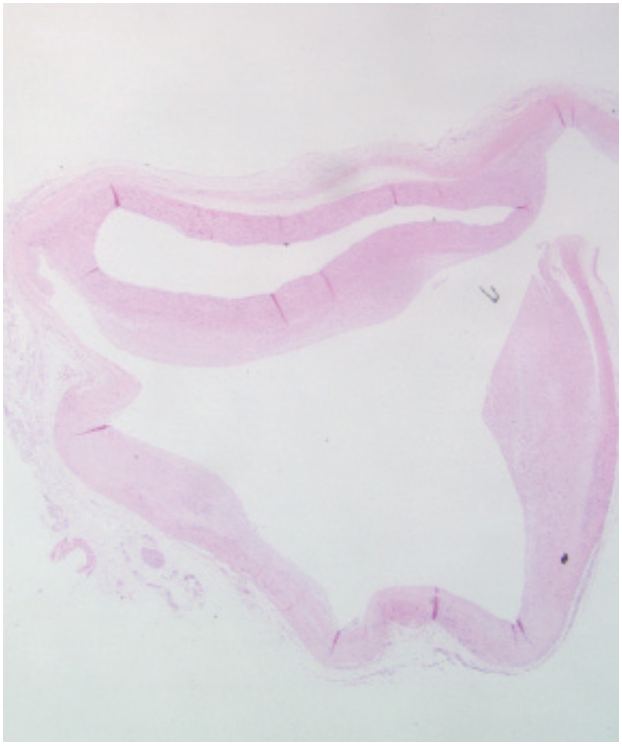

1-2. Aorta, owl monkey. Partially encircling the aorta is a second oval-shaped channel slightly larger in diameter than the adjacent aortic lumen and formed by a thick fibromuscular wall. (HE 12.50X)

as a pseudo-aneurysm, results from a vessel wall defect and extravasation of blood into a hematoma within the extravascular connective tissue that communicates freely with the vascular space (i.e. "pulsating hematoma"). Like a false aneurysm, a dissection is characterized by the extravasation of blood; however, the blood in a dissection accumulates between layers of the vessel wall, rather than in the extravascular connective tissue as occurs in a false aneurysm. Blood usually extravasates via an intimal tear, as with a false aneurysm, but a dissection may also occur by rupture of vessels of the vasa vasorum within the media. Dissections may be aneurysmal (i.e. present within a vessel that is also abnormally dilated), but are not always so; therefore, use of the term "dissecting aneurysm" may be inappropriate.[3]

The most important risk factor for aortic dissection in humans is hypertension; less commonly, aortic dissection is associated with abnormal vascular extracellular matrix (ECM) due to inherited or acquired connective tissue disorders.[3] Participants reviewed one such disorder, Marfan syndrome, an inherited defect in the extracellular glycoprotein fibrillin-1 which results from a mutation in the *FBN1* gene. Fibrillin-1 is a major component of the

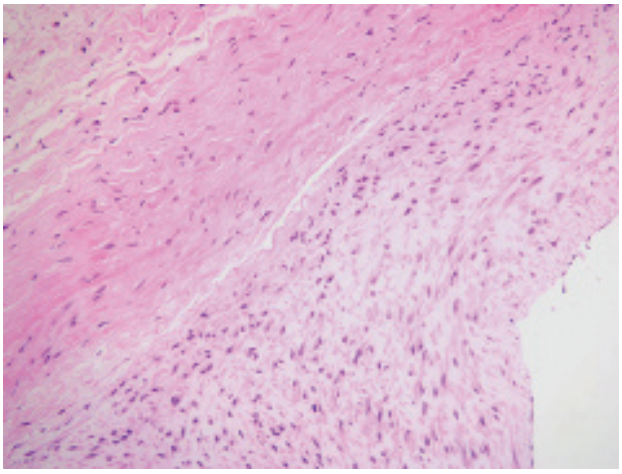

1-3. Aorta, owl monkey. The wall of the aortic dissection is composed of a fibromuscular proliferation admixed with proteoglycan material and lined by endothelium. (HE 20X)

ECM microfibrils that provide the scaffolding on which tropoelastin is deposited to form elastic fibers. Fibrillin-1 abnormalities result in defective mechanical properties of the ECM in the cardiovascular system and eyes, resulting in aortic aneurysm, aortic dissection, and lens subluxation or dislocation. Moreover, since normal microfibrils sequester transforming growth factor ß (TGF-ß) and control its bioavailability, Marfan syndrome is characterized by excessive activation of TGF-ß; this not only further contributes to the altered vascular ECM integrity, but likely accounts for other clinical manifestations of the syndrome not attributable to ECM abnormalities (e.g. bone overgrowth).[2] These observations are supported by studies in a mouse model of Marfan syndrome in which *Fbn1*$^{+/-}$ mice developed myxomatous mitral valve and aortic lesions that were prevented by the administration of TGF-ß antibodies, demonstrating the importance of TGF-ß in the pathogenesis of the lesions and indicating that elevated TGF-ß may be primarily responsible for the development of mitral valve prolapse in children with Marfan syndrome.[4]

While in most cases of aortic dissection no specific underlying pathology is identified in the aortic wall, the most frequently detected lesion is cystic medial degeneration in the absence of inflammation. In this case, some participants noted areas of cystic medial degeneration and therefore considered, in addition to Marfan syndrome, other causes of vascular ECM abnormalities, including Ehlers-Danlos syndrome, vitamin C deficiency, and defects in copper metabolism.[3] Some participants noted the presence of foam cells and rare cholesterol clefts, reminiscent of atherosclerosis; however, their subadventitial location is not consistent with atherosclerosis, and as mentioned by

the contributor, while atherosclerosis is among the most important predisposing factors for aneurysms (along with hypertension), dissections are unusual in the presence of atherosclerosis, presumably because of medial fibrosis precluding propagation of the dissection.[3] Nevertheless, the gross description of yellow plaques within the aorta is consistent with atherosclerosis and participants could not exclude it as a causal or contributory factor in this case. Finally, some participants noted striking microscopic resemblance to a stented vessel, and dissection can occur iatrogenically due to complicating arterial cannulations.[3]

Contributor: University of Texas MD Anderson Cancer Center, Michale E. Keeling Center for Comparative Medicine, 650 Cool Water Drive, Bastrop, TX 78602
www.mdanderson.org; www.kccmr.org

References*:*

1. Baer JF, Gibson SV, Weller RE, Buschbom RL, Leathers CW: Naturally occurring aortic aneurysms in owl monkeys (*Aotus* spp). Lab Anim Sci **42:**463-466, 1992
2. Kumar V, Abbas AK, Fausto N, Aster JC: Genetic disorders. *In:* Robbins and Cotran Pathologic Basis of Disease, eds. Kumar V, Abbas AK, Fausto N, Aster JC, 8th ed., pp. 144-145. Saunders Elsevier, Philadelphia, PA, 2010
3. Mitchell RN, Schoen FJ: Blood vessels. *In:* Robbins and Cotran Pathologic Basis of Disease, eds. Kumar V, Abbas AK, Fausto N, Aster JC, 8th ed., pp. 506-510. Saunders Elsevier, Philadelphia, PA, 2010
4. Ng CM, Cheng A, Myers LA, Martinez-Murillo F, Jie C, Bedja D, Gabrielson KL, Hausladen JM, Mecham RP, Judge DP, Dietz HC: TGF-beta-dependent pathogenesis of mitral valve prolapse in a mouse model of Marfan syndrome. J Clin Invest **114:**1586-1592, 2004
5. Virmani R, Burke AP: Nonatherosclerotic diseases of the aorta and miscellaneous diseases of the main pulmonary arteries and large veins. *In:* Cardiovascular Pathology, eds. Silver MD, Gotlieb AI, Schoen FJ, 3rd ed., pp. 109-117, Churchill Livingstone, New York, NY, 2001

CASE II: 47928 (AFIP 3135954).

Signalment: 13-year-old, 2.83 kg, female, spayed Persian cat (*Felis catus*)

History: This cat presented to the cardiology service with a history of collapse, pericardial effusion and chronic renal disease. Thoracic radiographs revealed cardiomegaly, and echocardiography identified a mass at the heart base and pericardial effusion. Due to the cat's declining condition, euthanasia was elected.

Gross Pathology: Based upon fat stores and muscle mass, the cat was assessed to be in fair to good body condition. At the base of the heart, between the aorta and pulmonary artery, adjacent to and compressing the right atrium, a 2.5 x 2.0 x 1.3 cm multi-nodular, pale tan to white, soft, slightly bulging mass was adhered to the epicardial surface of the right atrium. The pericardial sac contained 18 mL of non-clotted, serosanguinous effusion and 23 mL of serosanguinous effusion were noted in the pleural space. The lungs exhibited moderate to severe, diffuse congestion and pulmonary edema. Multifocally throughout the cortex and medulla of the right and left kidneys were thin walled, fluid filled cortical and medullary cysts. The liver also contained few multifocal cysts, grossly interpreted to involve the biliary tree. Additional findings included mandibular prognathism with glossal protrusion.

Laboratory Results: T4 values were normal; potassium levels were decreased at 2.55 mmol/L (3.5-5.3 mmol/L); and BUN was mildly elevated at 36 mg/dL (15-34 mg/dL).

Histopathologic Description: Examined is a section of heart that displays the left ventricular outflow tract including the left ventricle, interventricular septum, right ventricle, mitral valve, aortic valve, aorta and epicardium (visceral pericardium). At the base of the heart, adjacent to the aorta and compressing the right atrium, there is a well demarcated, expansile, densely cellular, nodular mass, composed of round to polygonal cells arranged in packets and separated by a fine fibrovascular stroma ("zelballen structures") (**figs. 2-1 and 2-2**). Neoplastic cells are mildly pleomorphic with abundant finely vacuolated eosinophilic to amphophilic cytoplasm and indistinct cell borders. Nuclei exhibit mild pleomorphism, are central to peripheral with finely stippled chromatin and a single, variably distinct nucleolus (**fig. 2-3**). Anisocytosis and anisokaryosis are mild and there are 0-1 mitotic figures per 400x field. At the periphery of the mass, small, mildly infiltrative lobules of neoplastic cells are noted adjacent to

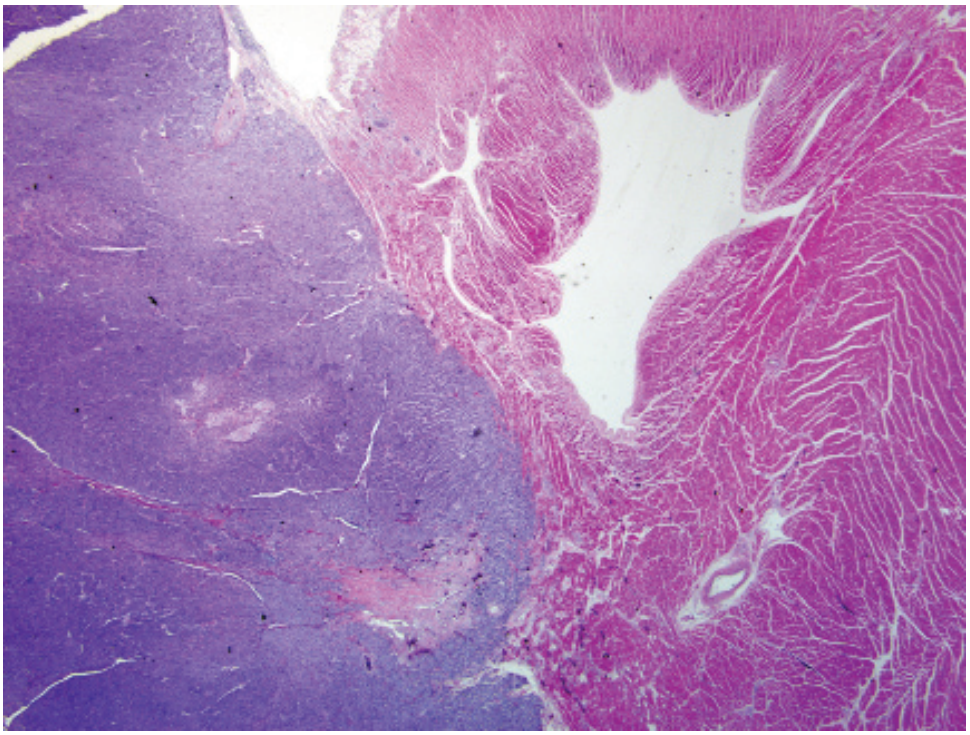

2-1. Chemodectoma, heart base, cat. Attached to and compressing the heart there is a densely cellular, lobulated neoplasm. (HE 12.50X)

ectatic vessels, but no direct vascular invasion is observed. Small numbers of lymphocytes are scattered throughout the neoplastic populations. Within the mass, there is a focal paucity of neoplastic cells in which fibrocytes are situated amongst a stroma of loosely arranged connective tissue, separated by clear space (edema) and infiltrated by scattered lymphocytes and macrophages (region of previous necrosis, presumptive).

Focally, there is a large aggregate of lymphocytes within the epicardium, and few ectatic vessels contain clusters of neoplastic cells (intracardiac metastasis, not present on every slide). Diffusely, mesothelial cells of the epicardium are enlarged (hypertrophy) and the epicardium contains moderate numbers of inflammatory cells composed of lymphocytes, macrophages, neutrophils and eosinophils, admixed with eosinophilic acellular fibrillar material (fibrin) and occasionally plump fibroblasts. Macrophages multifocally contain golden brown granular pigment (hemosiderin, confirmed with iron stain). Small numbers of inflammatory cells extend into the underlying myocardium. Diffusely, the mitral valve is moderately expanded by increased mucinous matrix and there is mild multifocal interstitial fibrosis within the interventricular septum and left ventricular myocardium. The endocardium of the left atrium is irregular and is diffusely expanded by fibrous connective tissue (endocardial fibrosis). There is also minimal to mild, multifocal myofiber disarray noted within the left ventricular myocardium. Multifocally, the tunica media of small and moderate sized arterioles is thickened by hypertrophic smooth muscle cells (arteriosclerosis).

Neoplastic cells exhibit diffuse, strong cytoplasmic staining for synaptophysin and chromogranin A, diffuse weak cytoplasmic staining for neuron specific enolase (NSE), and negative staining for thyroglobulin, cytokeratin, vimentin and calcitonin. Positive and negative controls were run and stained appropriately. Intracardiac metastatic foci stain strongly positive with synaptophysin and chromogranin A. Reticulin stains highlight the connective tissue stroma and enhance the packeted pattern of the neoplasm.

Contributor's Morphologic Diagnosis: 1. Heart (base between aorta and pulmonary artery): Focal chemodectoma with multifocal epicardial metastasis.
2. Heart: Moderate multifocal chronic ongoing lymphohistiocytic, neutrophilic, fibrinous epicarditis with mesothelial cell hypertrophy, hemosiderosis and fibroplasia.
3. Heart: Moderate diffuse mitral valve myxomatous degeneration (consistent with valvular endocardiosis) and left atrial endocardial fibrosis.
4. Heart: Moderate multifocal arteriolar tunica media hypertrophy (arteriosclerosis), mild multifocal myocardial interstitial fibrosis, and minimal to mild, multifocal ventricular myofiber disarray.

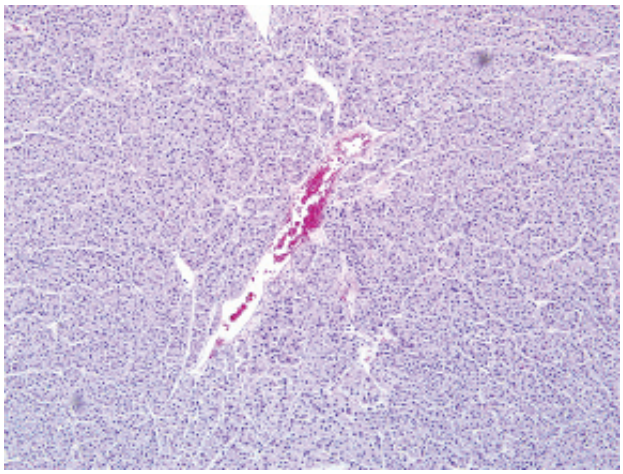

2-2. Chemodectoma, heart base, cat. Neoplastic polygonal cells are arranged in nests and packets supported by a fine fibrovascular stroma. (HE 100X)

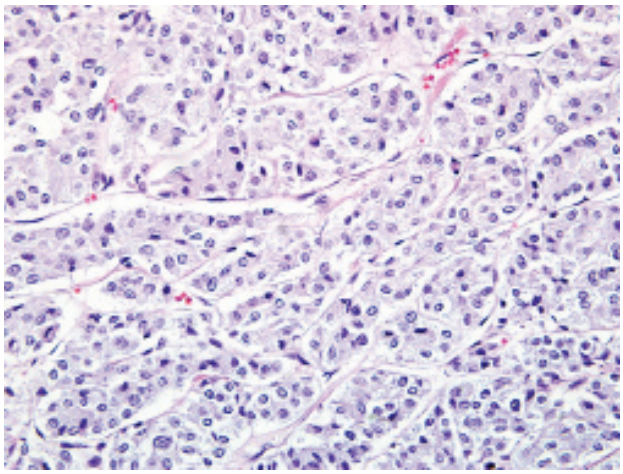

2-3. Chemodectoma, heart base, cat. Neoplastic cells have variably distinct borders and moderate amounts of finely granular pale eosinophilic to amphophilic cytoplasm. (HE 400X)

Contributor's Comment: Chemodectoma, also referred to as aortic body tumor or extra-adrenal non-chromaffin paraganglioma, is a primary neuroendocrine tumor of chemoreceptor cells in the region of the heart base.[4,5] Primary tumors of the heart and pericardium (including the great vessels) are rare in cats, with a reported incidence of 0.03%.[1,5] Chemodectomas are particularly uncommon in cats, with limited reports in the literature.

Chemoreceptor tissue is composed of parenchymal cells (chemoreceptors and glomus cells) and sustentacular cells and aids in the regulation of respiration and circulation.[2,4] Chemoreceptors are sensitive to changes in arterial partial pressure of carbon dioxide and oxygen, blood pH and temperature, and stimulation of chemoreceptors may result in adaptive modifications in respiratory rate and/or arterial blood pressure.[2,4,6] In mammals, the chemoreceptor system is part of the parasympathetic nervous system, leading to the terminology "non-chromaffin paragangliomas".[6] Neoplasms of the chemoreceptor cells most commonly arise within the aortic or carotid body and less frequently the glomus pulmonale, glandula suprarenalis or in ectopic sites.[2,4,6] Aortic body tumors are more common than carotid body tumors in animals, though carotid body tumors are more often malignant than aortic body tumors.[2] Chemodectomas typically form a single mass or multiple nodules within the pericardial sac near the base of the heart and have been reported to occur between the aorta and pulmonary artery, between the pulmonary artery and left auricular appendage, or below the aorta and right auricular appendage.[2,4-6] The mass in this cat was located at the base of the heart, adjacent to the right atrium and auricle between the aorta and pulmonary artery.

Though chemodectomas are non-functional in animals, clinical signs can be attributed to the neoplasm acting as a space occupying lesion, causing compression of multiple adjacent structures.[2,5,6] The tumors can vary greatly in size (0.5 - 12.5 cm) and are often associated with accumulation of serous, often blood tinged, fluid in the pericardial sac.[2] Pericardial effusion (as noted in this cat) can result from lymphatic invasion of neoplastic cells at the base of the heart or the compression of small pericardial veins, and may cause impairment of normal cardiac function and decompensation, depending on the speed and volume of accumulation.[2,5,6] Obstruction of the thoracic duct and/or cranial vena cava may lead to pleural effusion, pericardial effusion, ascites, and subcutaneous edema, particularly of the head, neck and forelimbs, while obstruction of blood return to the atria may manifest as systemic congestion.[2,5] Airway and esophageal compression may be clinically evident as dyspnea or coughing and vomiting, respectively.[2] Non-specific signs of systemic illness, including debilitation, anorexia and lethargy may also be noted.[2,5,6] Gross and histologic evaluation of the lungs in this case revealed moderate to severe, diffuse congestion, pulmonary edema and a moderate amount of serosanguinous pleural effusion. These findings are interpreted to be secondary to the compressive effects of the neoplasm. Pericardial effusion is likely secondary to compression, vascular invasion, and hemorrhage within the neoplasm. The associated inflammation in the epicardium of this cat is suspected to be secondary to the pericardial effusion.

Chemodectomas are typically well demarcated and comprised of round to polygonal cells with indistinct cell borders, scant cytoplasm and central round nuclei with fine chromatin and prominent nucleoli.[4] In our case, positive reticulin and trichrome staining demonstrated the small lobules delineated by fine fibrovascular stroma, which is a typical feature of this neoplasm.[4] Mitoses are rare, and occasionally there may be small amounts of scattered T-lymphocytes throughout the mass.[4,6] Lymphocytes were identified within the neoplasm in this case, but were not further characterized.

In our case, neoplastic cells exhibited diffuse, strong cytoplasmic staining for synaptophysin, chromogranin A, diffuse weak staining for neuron specific enolase (NSE), and negative staining for thyroglobulin, vimentin, cytokeratin and calcitonin, consistent with a diagnosis of chemodectoma. Chemodectomas are known to exhibit positive immunohistochemical reactivity for synaptophysin, chromogranin A and NSE.[4] Synaptophysin is considered to be a specific marker for neuroendocrine tumors because it is not detected in non-neuroendocrine cells or neoplasms.[3,4] Chromogranin positive granules are also typical of neuroendocrine tumors.[4] Occasionally, as noted in this tumor, staining of neoplastic cells for NSE may be weak, hypothesized to result from rapid autolysis of chemoreceptor cells and subsequent loss of immunoreactivity.[4] Neoplastic neuroendocrine cells also commonly exhibit argyrophilic cytoplasmic granules when stained with Churukian-Shenk or Grimelius silver stains (not performed in this case). Differential diagnoses for a heart based tumor in a cat include lymphosarcoma, ectopic thyroid adenoma/carcinoma, ectopic parathyroid chief cell adenoma, and thymoma.[2,6] Tumors of ectopic thyroid tissue may exhibit a similar histologic appearance and immunohistochemistry may be helpful in distinguishing such tumors. Ectopic thyroid tumors should stain positively for cytokeratin and thyroglobulin, while C cell tumors should stain positively for calcitonin.[4]

Because chemodectomas are so rarely identified in cats, biological behavior is essentially unknown.[5] Extrapolating from behavior in other species, aortic body tumors tend to be more benign than carotid body tumors and grow slowly by expansion.[2] Advanced lesions may be associated with neoplastic invasion of the adventitia of the great vessels, atrial myocardium, and as in this case, epicardial vessels, consistent with intracardiac metastasis.[5] Willis et al (2001) reported metastasis in 22% of canine chemodectomas and 2 of 6 (33%) of the reported feline cases.[6] In 2 of 2 cases of feline chemodectoma reported by Tilley et al (1981), tumor emboli were noted in blood vessels, with metastasis to the pericardium, epicardium and myocardium.[5] Multifocal thoracic metastatic foci, with spread to local lymph nodes (mediastinal, sternal) and/or the lungs has also been reported in the cat.[3,5] In this case, there was a site of extracardiac metastasis within tissue that was histologically most compatible with remnant thymic tissue. The highly vascularized stroma frequently associated with chemodectomas may facilitate metastasis via the bloodstream.[5] Chemodectomas may also secrete angiogenic substances, leading to the development of a collateral blood supply that can involve the local vasculature.[6] Long term prognosis is typically guarded to poor, as the tumor is often diagnosed at an advanced stage, though one cat is reported to have lived 13 months post-diagnosis.[5,6] In humans, surgical excision is the treatment of choice and is frequently associated with good success.[6] However, surgical intervention has had limited success in dogs and complete removal is rarely possible.[5,7]

This cat exhibited mandibular prognathism with glossal protrusion, consistent with brachycephalic conformation. Chronic hypoxia is likely involved in the pathogenesis of chemodectoma development, as increased prevalence of this tumor is noted in humans and cattle living at high altitudes, humans with emphysema and brachycephalic dogs.[2,4,6] However, a definitive link with chronically low oxygen tension has not been established in the cat. Ventricular myofiber disarray was minimal to mild. This finding can occur with myocardial hypertrophy, but echocardiographic evaluation revealed that wall thickness was within normal limits. In the absence of additional gross or histologic evidence of hypertrophic cardiomyopathy, the clinical significance of this lesion is not known. The cause for the left atrial endocardial fibrosis is unknown. Mitral insufficiency secondary to valvular myxomatous degeneration is a possible consideration; however, mitral valve abnormalities were not indicated on the echocardiography report.

This cat also had multiple cysts in the kidneys, which may be consistent with polycystic kidney disease, an autosomal dominant congenital disease of a variety of species and breeds of animals, including Persian cats. Mutations in PKD-1 and/or PKD-2 genes leading to altered function of related proteins polycystin-1 and polycystin-2. Polycystin-1 is involved in normal cell proliferation and apoptosis pathways and mutations allow cells either to enter a differentiation pathway that results in tubule formation or to become susceptible to apoptosis, both of which contribute to tubular cyst formation, while polycystin-2 is involved in plasma membrane calcium channels. As cysts enlarge, they compress adjacent parenchyma, leading to secondary changes (compression necrosis and fibrosis of tubules and glomeruli) and when extensive regions are polycystic and impaired, there may be clinically evident renal dysfunction. In this case,

the renal cysts are a likely contributor to the chronic renal disease noted in the history. Congenital forms of polycystic kidney disease are also often associated with cystic bile ducts and bile duct proliferation in the liver (as noted in this case) and/or pancreatic cysts (not seen in this cat). In addition, congestion and degenerative changes were noted within the centrilobular regions of the liver, likely secondary to right-sided heart insufficiency due to compression of the heart by the mass.

AFIP Diagnosis: 1. Heart, base: Chemodectoma.
2. Heart, epicardium: Epicarditis, fibrinous, diffuse, chronic, mild.
3. Heart, atrioventricular valve: Degeneration, fibromyxomatous, focally extensive, mild.

Conference Comment: The contributor provides a comprehensive review of the entity. Participants reviewed the predilection sites for chemodectoma in animals, and the moderator reiterated the point that most are nonfunctional. In contrast to many neoplasms of neuroendocrine origin, chemodectomas exert their detrimental effects on affected animals via their space occupying nature rather than a specific secretory product. In addition to the immunohistochemical stains noted by the contributor, electron microscopy is useful for distinguishing "heart base tumors" of ectopic thyroid follicular cell origin from those of aortic body chemoreceptor cell origin. While the former contain large lysosomal dense bodies, they lack the small membrane-bound secretory granules that are characteristic of aortic and carotid body chemoreceptor cells. Moreover, the number of granules may be further useful for distinguishing chemoreceptor adenomas (in which they are more numerous) from carcinomas.[2]

Contributor: The Animal Medical Center, Department of Pathology, 510 East 62nd Street, New York, NY 10065 http://www.amcny.org/

References:
1. Aupperle H, Marz I, Ellenberger C, Buschatz S, Reischauer A, Schoon HA: Primary and secondary heart tumors in dogs and cats. J Comp Path **136:**18-26, 2007
2. Capen CC: Endocrine glands. *In:* Jubb, Kennedy, and Palmer's Pathology of Domestic Animals, ed. Maxie MG, 5th ed., vol. 3, pp. 425-428. Saunders Elsevier, Philadelphia, PA, 2007
3. Davis WP, Watson GL, Koehler LK, Brown CA: Malignant cauda equina paraganglioma in a cat. Vet Pathol **34:** 243-246, 1997
4. Paltrinieri S, Riccaboni P, Rondena M, Giudice C: Pathologic and immunohistochemical findings in a feline aortic body tumor. Vet Pathol **41:**195-198, 2004
5. Tilley LP, Bond B, Patnaik AK, Liu S: Cardiovascular tumors in the cat. J Am Anim Hosp Assoc **17:**1009-1021, 1981
6. Willis R, Williams AE, Schwarz T, Paterson C, Wotton PR: Aortic body chemodectoma causing pulmonary oedema in a cat. J Small Anim Pract **42:**20-23, 2001

CASE III: 16665/9D (AFIP 3139391).

Signalment: 2-year-old, female wild boar (*Sus scrofa*).

History: An adult wild boar was caught during boar hunting.

Gross Pathology: On post mortem examination, the boar was in good body condition with adequate muscle mass and body fat stores. Within the ventricular walls and the interventricular septum there were numerous, multifocal to coalescent, well demarcated, unencapsulated, white to pale pink, from 3 mm to 2 cm, irregularly round to oval nodules that expanded and replaced the myocardial tissue and that elevated the epicardium and the endocardium, protruding within the ventricular cavities. On cut surface the nodules were homogeneous in color and diffusely firm (**fig. 3-1**).

Histopathologic Description: Heart: Within the ventricular wall there are multiple, focally extensive, well-demarcated, not infiltrating, irregularly round to oval, intramuscular and subepicardial, 3 mm to 1 cm, nodules that expand and replace the normal myocytes and composed of haphazardly disposed, irregularly shaped myocytes with markedly distended cytoplasm characterized by single or multiple, clear, up to 200 um diameter vacuoles occasionally containing a moderate amount of finely granular, eosinophilic material (**fig. 3-2**). The small amount of remaining cytoplasm and the compressed nucleus are displaced to the periphery of the cells (**fig. 3-3**). There are numerous cells characterized by a centrally located, up to 40 um in size, irregularly round nucleus, with one or two indentations, marginated chromatin and a prominent nucleolus. These cells have abundant finely granular eosinophilic cytoplasm. Minimal, diastase-labile, PAS-positive granules confirmed the presence of intracytoplasmic glycogen within many of the cells. The anisocytosis and anisokaryosis are moderate. The mitotic index is less than one. Multifocally within the nodules there are minimal inflammatory infiltrates composed of lymphocytes, macrophages and plasma cells. There is

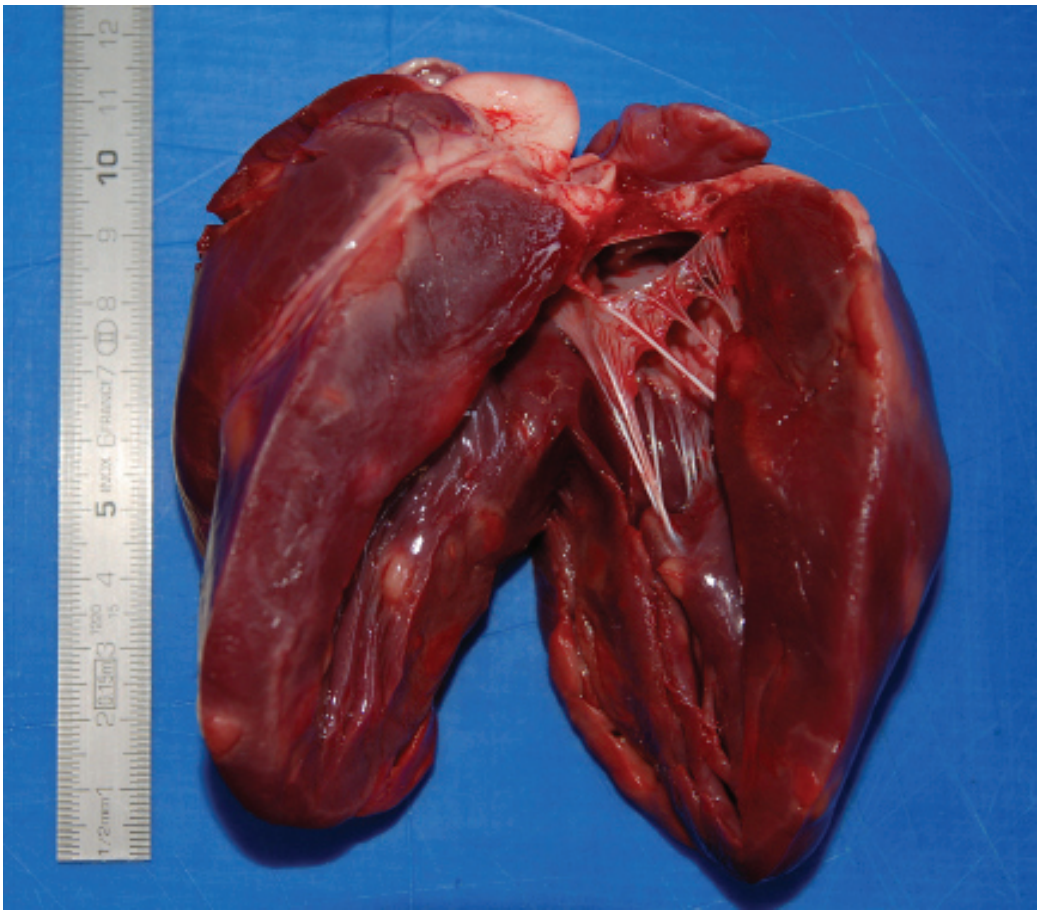

3-1. Heart, boar. Multifocal to coalescent pale nodules replace myocardial tissue. Photographs courtesy of Servizio Diagnostico di Anatomia Patologica e Patologia Veterinaria, Dipartimento di Sanità Pubblica, Patologia Comparata e Igiene Veterinaria, Legnaro Padova ITALIA

mild diffuse edema and hyperemia. At the periphery of the nodules there are multifocal hypereosinophilic myocytes with fragmented cytoplasm and pyknotic or absent nuclei (necrosis).

Contributor's Morphologic Diagnosis: Heart, myofibers: severe, multifocal myofiber vacuolar degeneration consistent with glycogen deposits, and myocyte dysplasia compatible with multiple cardiac rhabdomyoma (rhabdomyomatosis), wild boar, suid.

Contributor's Comment: Cardiac rhabdomyoma is a lesion characterized by large vacuolated myocardial cells containing glycogen, and synonymously "rhabdomyomatosis", "congenital glycogen tumor", "circumscribed glycogenic storage disease", "nodular glycogenic degeneration", "nodular glycogenosis" and nodular glycogenic infiltration are used for the lesion.[2] This kind of lesion typically occurs in children less than one year old, in pigs, and rarely in cattle, sheep, dogs and deer.[3]

In swine it is an incidental finding and occurs most commonly in the left ventricle of the heart. Some authors suggest a familial predisposition for cardiac rhabdomyomas in red wattle and red wattle-cross piglets.[4] Animals of all ages are affected and the occurrence of this lesion in animals as young as three weeks old suggests a congenital condition. The etiology and pathogenesis are not known and it is thought to be a hamartoma or malformation rather than a true neoplasm. Ultrastructural and immunohistochemical studies in swine suggest it is a congenital dysplasia of cardiac muscle and/or Purkinje cells. In fact, cardiac rhabdomyoma cells share ultrastructural features of both cardiac myofibers and Purkinje cells, creating uncertainty as to their histogenesis.[4] The relative paucity of poorly oriented myofibrils, abundant glycogen, binucleation, and desmosomal intercellular junctions in rhabdomyomas are characteristics of Purkinje cells [4], but intercalated discs, which are exclusive to cardiac myofibers, are also present in some rhabdomyoma cells.[4] This combination of ultrastructural features has led to the hypothesis that cardiac rhabdomyomas arise from either two types of fibers or a pluripotential embryonic cell.[4]

Affected animals are usually asymptomatic but in affected

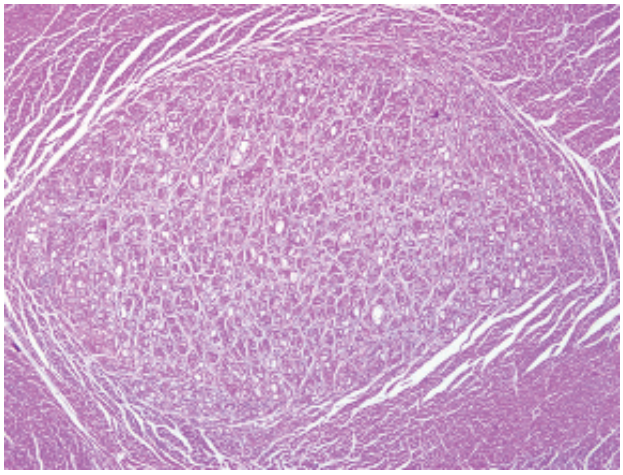

3-2. Heart, ventricular myocardium, boar. Within the myocardium, there is a well demarcated, nodular focus of cardiomyoctes that are enlarged and contain one to multiple clear vacuoles. (HE 40x)

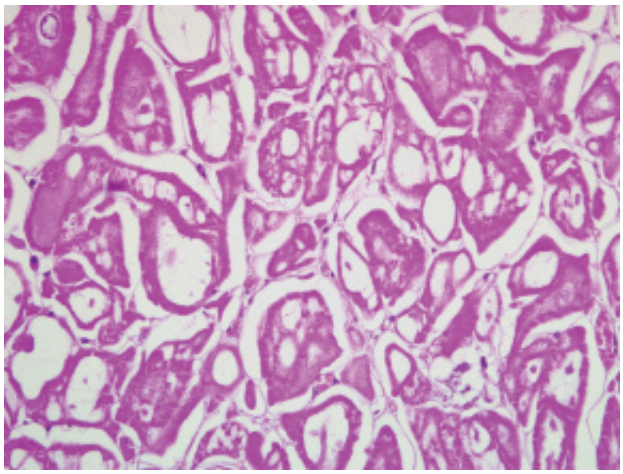

3-3. Heart, ventricular myocardium, boar. Affected cardiomyoctes are haphazardly arranged and markedly distended by one to multiple clear cytoplasmic vacuoles. (HE 400x)

dogs chylopericardium and right-sided congestive heart failure have been reported.[2] The occurrence of cardiac rhabdomyomas in stillborn and neonatal red wattle piglets in the absence of heart failure concurs with previous reports of the congenital and incidental nature of these lesions in pigs.[4] However, the absence of concurrent disease in one red wattle piglet suggests that cardiac rhabdomyomas may potentially cause sudden death, perhaps by interfering with normal myocardial conduction, as occurs in people.[4] Grossly the lesions appear as irregular, pale, white, pink or tan myocardial foci or streaks varying in diameter from barely visible to 3 cm in swine.

AFIP Diagnosis: Heart, myocardium: Cardiomyocyte swelling and glycogen-type vacuolar change, nodular, multifocal, moderate to marked (rhabdomyomatosis).

Conference Comment: In humans, cardiac rhabdomyomas occur most often in pediatric patients with tuberous sclerosis, a hereditary autosomal dominant syndrome that results from mutations in the gene *TSC1* or more commonly, *TSC2*, characterized by the development of a variety of hamartomas and benign neoplasms. The gene products, hamartin and tuberin, combine to form an inhibitor of the kinase mTOR, an important regulator of protein synthesis, anabolic metabolism, and cell size. Interestingly, the tumors associated with tuberous sclerosis (e.g. giant-cell astrocytomas and cardiac rhabdomyomas) are noted for having voluminous cytoplasm.[1]

During tissue processing, the loss of glycogen from affected cells creates a distinctive and helpful histologic artifact: "spider cells," so named because of the radial arrangement of residual sarcoplasm that extends from the nucleus.[5] Conference participants briefly discussed glycogen storage diseases in the differential diagnosis for this lesion.

In addition to the histopathologic findings described by the contributor, some sections reviewed by conference participants contained few sarcocysts.

Contributor: Servizio Diagnostico di Anatomia Patologica e Patologia Veterinaria, Dipartimento di Sanità Pubblica, Patologia Comparata e Igiene Veterinaria, Facoltà di Medicina Veterinaria di Padova, Viale dell'Università, 16, 35030 Legnaro, Padova, Italy
http://www.sanitaveterinaria.unipd.it/

References:

1. Frosch MP, Anthony DC, De Girolami U: The central nervous system. *In:* Robbins and Cotran Pathologic Basis of Disease, eds. Kumar V, Abbas AK, Fausto N, Aster JC, 8th ed., pp. 1342-1343. Saunders Elsevier, Philadelphia, PA, 2010
2. Kizawa K, Furubo S, Sanzen T, Kawamura Y, Narama I: Cardiac rhabdomyoma in a beagle dog. J Toxicol Pathol **15:**69-72, 2002
3. Kolly C, Bidaut A, Robert N: Cardiac rhabdomyoma in a juvenile fallow deer (*Dama dama*). J Wildl Dis **40:**603-606, 2004
4. McEwen BJE: Congenital cardiac rhabdomyomas in red wattle pigs. Can Vet J **35:**48-49, 1994
5. Radi ZA, Metz A: Canine cardiac rhabdomyoma. J Toxicol Pathol **37:**348-350, 2009

CASE IV: 0130/09 (AFIP 3140226).

Signalment: 2-year-old, male, castrated Maine coon cat (*Felis catus*).

History: The cat was brought to a veterinary clinic with a history of episodic dyspnea and a 2-week history of cough. On presentation, the cat had a heart rate of 180 beats per minute (tachycardia), with a gallop rhythm on auscultation. Lung sounds were difficult to evaluate. Ultrasound examination with echoradiographs showed a mild dilatation and hypertrophy of the left ventricle, and several fibrous strands between papillary muscles of the ventricle wall and the septum wall. A mild dilatation of the left atrium could also be seen. A diagnosis of restrictive cardiomyopathy of endomyocardial fibrous type was made. The cat also had moderate hydrothorax and lung edema and the owners elected euthanasia.

Gross Pathology: The heart was moderately enlarged with an elongated left ventricle, comprising a ventricular remodeling with rounded apex. Marked fibrotic structures (ventricular scar) bridged the ventricular septum (from the papillary muscle) and the free wall. The left atrium was moderately enlarged; however, the right atrium was normal and the right ventricle was only mildly hypertrophied (**figs. 4-1 and 4-2**).

Histopathologic Description: Tissue from myocardium including endocardium: A severe thickening of the endocardium with fibrotic strands is present. These fibrotic structures are comprised of fibroblasts in a dense matrix. Lobule-like structures intermingled with parallel streaks can be seen. The extracellular matrix consists of red collagen and bluish chondroid tissue. The fibroblasts are elongated to, in some areas, round (i.e. more chondrocyte-like) in appearance. In one subendocardial area, a lipid rich tissue is found. The underlying myocardium is characterized by a diffuse, moderate interstitial fibrosis (**figs. 4-3 and 4-4**).

Contributor's Morphologic Diagnosis: Endomyocardial fibrosis with myocardial interstitial fibrosis, left ventricle, eccentric hypertrophy of left ventricle, compatible with a restrictive cardiomyopathy of endomyocardial fibrous type.

Contributor's Comment: Many feline cardiomyopathies are classified as idiopathic.[2] In a retrospective study of 106 cats with cardiomyopathy, 57.5% had hypertrophic cardiomyopathy (HCM), 20.7% had restrictive cardiomyoapthy (RCM), 10.4% had dilated cardiomyopathy (DCM) and unclassified cardiomyopathy (UCM) was found in 10.4%.[2] None of the described cardiomomyopathies in that study showed the severe endomyocardial fibrosis with crossing fibrous strands in the left ventricular lumen, which characterized the heart of the Maine coon cat in this case.

Cats with RCM present with diastolic dysfunction and increased myocardial stiffness. The etiology is unknown.[3] Two basic forms of RCM in man have been reported: myocardial and endocardial RCM. These two forms are also described in the cat. The feline myocardial form, a myocardial disease with restrictive filling and severe atrial dilatation, is idiopathic. The endomyocardial form, endomyocardial fibrosis (EMF), is characterized by marked fibrosis of endocardium and

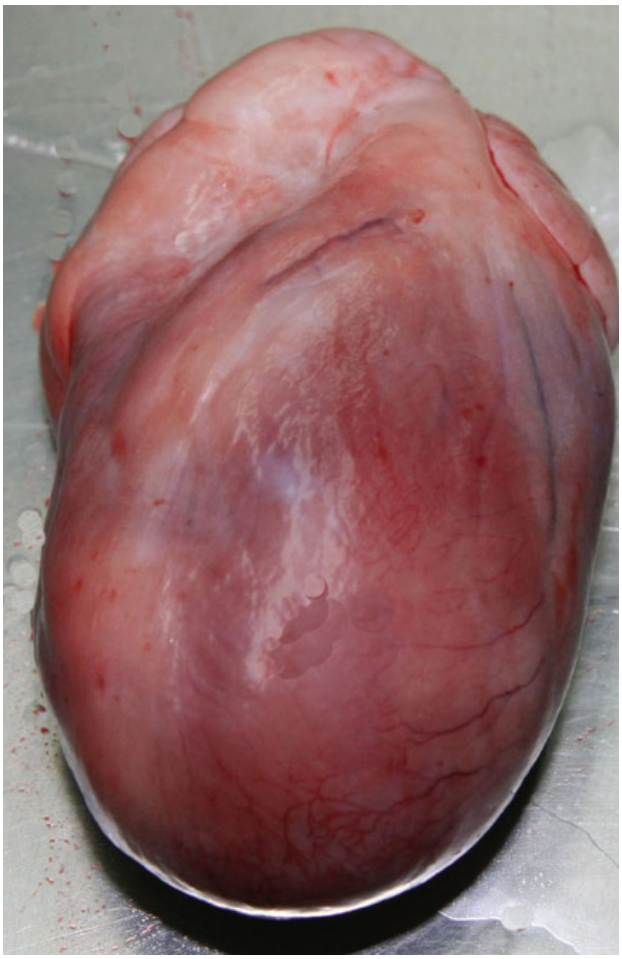

4-1. Heart, endocardium, cat. The heart is moderately enlarged with an elongate left ventricle. Photographs courtesy of Department of BVF, division of pathology, toxicology & pharmacology, Uppsala, Sweden, Stina.ekman@bvf.slu.se

4-2. Heart, endocardium, cat. Fibrotic scarring bridges the ventricular septum and the free wall. Photographs courtesy of Department of BVF, division of pathology, toxicology & pharmacology, Uppsala, Sweden, Stina. ekman@bvf.slu.se

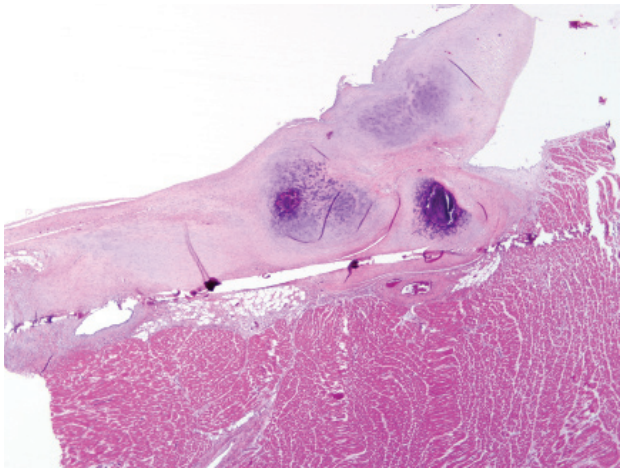

4-3. Heart, endocardium, cat: Diffusely the endocardium is markedly thickened (up to 10x normal) by dense collagen and foci of cartilage. (HE 12.50X)

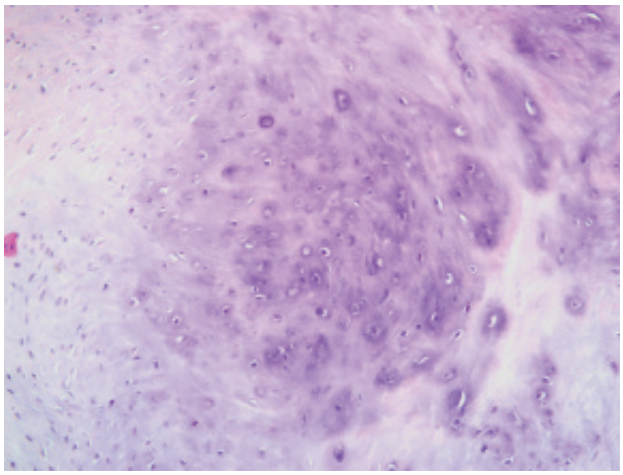

4-4. Heart, endocardium, cat. Multifocally, areas of chondroid metaplasia are present within the thickened and fibrotic endocardium. (HE 200X)

endomyocardium. The etiology of EMF is not known but different backgrounds have been discussed. In human RCM, associations with hypereosinophilic syndrome, endomyocarditis or vasculitis have been suggested.[1] Many cases of human EMF have been reported from the tropics; hence a search for infectious or nutritional causes has often been pursued.

Familial HCM has been reported in Maine coon cats.[4] However, the lack of severe concentric hypertrophy and atrial dilatation is not consistent with a diagnosis of HCM in this case. An association with endomyocarditis and left ventricular endocardial fibrosis has been reported in the cat.[6] The lack of active inflammation in the present case does not rule out a viral or immune-mediated endomyocardial injury with secondary reparative fibrous tissue formation. The ultrasonographic, macroscopic and microscopic findings in the present case are compatible with a diagnosis of restrictive cardiomyopathy of endomyocardial fibrous type. This was based on the

presence of many fibrous bands crossing between the papillary muscles and the septum wall. Secondary lung edema with hydrothorax had also developed.

AFIP Diagnosis: Heart: Endocardial fibrosis, diffuse, marked, with chondroid metaplasia, mild multifocal chronic endomyocarditis, interstitial edema, and myofiber disarray.

Conference Comment: Among the cardiomyopathies of domestic animals, the feline cardiomyopathies are probably the best characterized, and include an assortment of idiopathic cardiovascular disorders. In decreasing order of prevalence, the feline cardiomyopathies are summarized below:[5]

Feline Cardiomyopathies

Classification	Key Gross Findings	Key Microscopic Findings	Summary
Hypertrophic (HCM)	Cardiomegaly with either symmetric concentric ventricular hypertrophy or asymmetric hypertrophy of the LV and a slit-like LV lumen; LA dilation; +/- atrial thrombi, multifocal ventricular fibrosis, endocardial fibrosis in the LV outflow tract	Hypertrophied myofibers with vesicular nuclei; myofiber disarray in the LVFW and IVS; diffuse interstitial fibrosis (particularly in the inner aspect of the LFFW); focal endocardial fibrosis	Most common CM in cats; autosomal dominant inheritance in Maine coon and American shorthair cats; impaired diastolic ventricular filling (due to diminished LV lumen) with usually normal systolic function; distinct from hyperthyroidsm, which also may cause concentric myocardial hypertrophy
Restrictive (RCM)	Severe endocardial thickening; mural thrombosis; marked LA dilation +/- thrombosis; thickened LVFW with diminished LV volume	Replacement of myocardium and endocardium by granulation tissue and fibrosis; histiocytic, and/or lymphoplasmacytic endomyocarditis	Includes the myocardial form and the endomyocardial form; also termed "LV endocardial fibrosis", which may be preceded by endomyocarditis, of which *Bartonella* sp. has been suggested as a cause; occurs primarily in older cats; impaired diastolic ventricular filling with usually normal systolic function
Dilataed (DCM)	All heart chambers enlarged; ventricles dilated, flaccid, and thin-walled; atrophy of papillary muscles and trabeculae; +/- subendocardial fibrosis	Usually minor microscopic lesions; moderate myofiber hypertrophy with mild, diffuse interstitial fibrosis; +/- myofiber loss and replacement with fibrosis; usually no myofiber disarray	Distinct from and rare in comparison to taurine deficiency myocardial failure (TDMF), which causes identical gross and microscopic lesions and systolic dysfunction resulting in bilateral congestive heart failure
Excessive moderator bands (false tendons)	Numerous pink-white bands spanning the LV lumen and papillary muscles, usually connecting the cranial and caudal papillary muscles to the IVS; LV dilated or thickened	Abnormal moderator bands composed of Purkinje cells and dense collagen covered by endothelium; LV myocyte atrophy or hypertrophy; fibrosis; intramural coronary arterial intimal thickening, medial hyperplasia, perivascular fibrosis, and luminal narrowing	Occurs in mature cats but is considered a congenital defect; clinical signs of left-sided congestive heart failure

LV = left ventricle; LVFW = left ventricular free wall; IVS = interventricular septum; CM = cardiomyopathy

Cardiomyopathy is a diagnosis of exclusion and, by strict definition, should be used only to describe idiopathic primary myocardial disease. Therefore, myocardial dilation due to taurine deficiency (i.e. taurine deficiency myocardial failure [TDMF]) and concentric hypertrophy attributed to hyperthyroidism are distinct from dilated and hypertrophic cardiomyopathies, respectively. In cats with HCM, DCM, RCM, and myocarditis, the detection of feline panleukopenia virus genome by PCR suggests a possible causal role, but a definitive etiology for these conditions remains elusive.[5]

As alluded to by the contributor, this case may represent the chronic sequel of feline endomyocarditis, which can ultimately progress to left ventricular endocardial fibrosis, one of several idiopathic feline cardiovascular diseases grouped together clinically as RCM.[5,6] Some conference participants considered primary endocardial fibroelastosis (EFE) in the differential diagnosis; this congenital anomaly is exceedingly rare in domestic species, and is best documented in Burmese kittens, in which the condition results in microscopically detectable endocardial lymphedema at as early as one day of age. After 20 days of age, diffuse endocardial deposition of collagen and elastin is evident grossly; this may progress to involve Purkinje fibers, which undergo degeneration. Endocardial or myocardial inflammation are not features of EFE.[5]

The moderator emphasized the importance of echocardiography in correctly classifying feline cardiomyopathies clinically. Gross examination at necropsy is often less rewarding than antemortem echocardiography, and microscopic evaluation may be even less helpful, as evidenced by the overlap in microscopic findings between the various cardiomyopathies listed above and the usual paucity of significant microscopic lesions in feline DCM, specifically. A common sequel, observed in up to one third of affected cats, is unilateral or bilateral hindlimb ischemia due to iliac thromboembolism.[5,6]

Contributor: Department of BVF, Division of Pathology, Toxicology & Pharmacology, SLU (Swedish University of Agricultural Sciences), Box 7028, SE-750 07 Uppsala, Sweden
www.slu.se

References:

1. Bukhman G, Ziegler J, Parry E: Endomyocardial fibrosis: still a mystery after 60 years. PLoS Negl Trop Dis **2:**e97, 2008
2. Ferasin L, Sturgess CP, Cannon MJ, Caney SMA, Gruffydd-Jones TJ, Wotton PR: Feline idiopathic cardiomyopathy: a retrospective study of 106 cases (1994-2001). J Feline Med Surg **5:**151-159, 2003
3. Fox PR: Endomyocardial fibrosis and restrictive cardiomyopathy: pathologic and clinical features. J Vet Cardiol **6:**25-31, 2004
4. Kittleson MD, Meurs KM, Munro MJ, Kittleson JA, Liu SK, Pion PD, Towbin JA: Familial hypertrophic cardiomyopathy in Maine coon cats: an animal model of human disease. Circulation **99:**3172-3180, 1999
5. Maxie MG, Robinson WF: Cardiovascular system. *In:* Jubb, Kennedy, and Palmer's Pathology of Domestic Animals, ed. Maxie MG, 5th ed., vol. 3, pp. 17-18, 36, 44-47. Saunders Elsevier, Philadelphia, PA, 2007
6. Stalis IH, Bossbaly MJ, Van Winkle TJ: Feline endomyocarditis and left ventricular endocardial fibrosis. Vet Pathol **32:**122-126, 1995

The Armed Forces Institute of Pathology
Department of Veterinary Pathology

Conference Coordinator:
Shannon Lacv. DVM. MPH

WEDNESDAY SLIDE CONFERENCE 2009-2010

Conference 15

21 April 2010

Conference Moderator:

Corrie Brown, DVM, PhD, Diplomate ACVP

CASE I: A07/10654 (AFIP 3065885).

Signalment: 8-week-old, male, Holstein calf (*Bos taurus*).

History: Fifty dairy calves were purchased as neonates at a sale barn in Ohio, weaned at 5 weeks of age and in the feedlot for 3 weeks. All calves in the group reportedly developed diarrhea at 4 weeks of age with wasting, weakness and 40% mortality. One live calf was submitted for diagnostic studies.

Gross Pathology: The calf was thin (48 kg body weight) and dehydrated; the perineum was stained with liquid brown feces. The wall of the small intestine, especially the ileum, was thickened with a dark pink serosal surface. The ileal mucosa was coated by a yellow fibrinous membrane. The cecum and colon contained abundant yellow-green malodorous fluid. The wall of the gallbladder was thickened by edema; the lumen was distended by a fibrin clot. The mesenteric lymph nodes were enlarged, pale pink, and wet (**figs. 1-1, 1-2, 1-3, and 1-4**).

Laboratory Results: *Salmonella enteritidis* serotype Dublin was isolated from gallbladder, liver, spleen, small intestine and mesenteric lymph node. Fluorescent antibody tests were negative for bovine viral diarrhea virus, rotavirus, and coronavirus. Virus isolation was also negative.

Histopathologic Description: Gallbladder: The mucosa is expanded by infiltration of lymphocytes, macrophages, plasma cells and fewer neutrophils mixed with fibrin. Some capillaries and venules contain fibrin thrombi or are dilated and filled with neutrophils. Leukocytes also infiltrate the wall of some venules. The mucosal epithelium is multifocally attenuated or lost and has a few clusters of coccobacilli. A pleocellular (mostly lymphohistiocytic) inflammatory infiltrate dissects the tunica muscularis and infiltrates the edematous adventitia (**fig. 1-5**).

Small intestine: A thick layer of fibrin, neutrophils, degenerated leukocytes, and red blood cells with abundant Gram-negative bacterial coccobacilli and Gram-positive robust bacilli covers the focally denuded mucosa. Villi are blunted; goblet cells are scarce. The lamina propria is congested with numerous lymphocytes and histiocytes. Dilated crypts contain neutrophils and cellular debris. Lymphoid follicles of Peyer's patches are depleted of

*Sponsored by the American Veterinary Medical Association, the American College of Veterinary Pathologists, and the C. L. Davis Foundation.

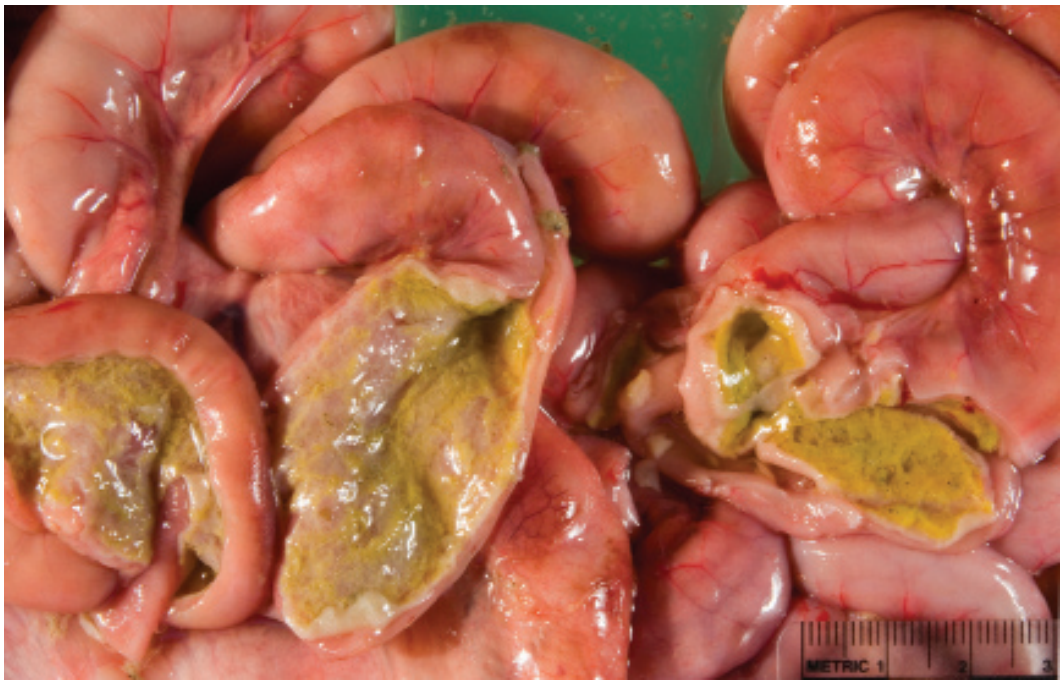

1-1., 1.2. Small intestine, calf. Multifocally, the ileal mucosa was coated by a yellow fibrinous membrane (diphtheritic membrane). Photographs courtesy of Purdue University Animal Disease Diagnostic Laboratory, 406 South University St. West Lafayette IN 47907 pegmiller@purdue.edu

lymphocytes with replacement by reticulohistiocytic cells. Vascular lesions are similar to those in the gallbladder (**fig. 1-6**).

Liver: Periportal inflammation consists of lymphocytes and macrophages with rare neutrophils. This infiltrate is particularly intense around bile ductules, some of which have attenuated epithelium and lumina distended by bile. Random foci of lytic hepatocellular necrosis are infiltrated by histiocytes, lymphocytes, and few neutrophils. Vascular lesions are similar to those in the gallbladder. There are increased numbers of sinusoidal leukocytes and hypertrophy of Kupffer cells (**fig. 1-7**).

Contributor's Morphologic Diagnosis: 1. Small intestine: Fibrinosuppurative and necrotizing enteritis.

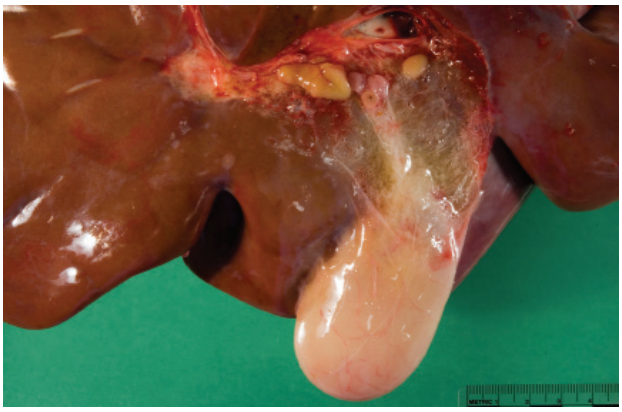

1-3., 1-4. Gallbladder, calf. Diffusely the gallbladder was expanded by edema. Photographs courtesy of Purdue University Animal Disease Diagnostic Laboratory 406 South University St., West Lafayette IN 47907 pegmiller@purdue.edu

2. Gallbladder: Ulcerative and fibrinous cholecystitis.
3. Liver: Lymphohistiocytic cholangiohepatitis and necrotizing hepatitis.

Contributor's Comment: Gross and histologic lesions in the small intestine, liver, and gallbladder are typical of those of enteric and septicemic salmonellosis. *Salmonella* Dublin and *S.* Typhimurium are the most common serovars associated with salmonellosis in calves.[1,2] In this case, *S.* Dublin was isolated from the small intestine, mesenteric lymph node, gallbladder, liver, and spleen. *S.* Dublin is considered a bovine-specific serovar and seldom infects other species of animals.[2] The Dublin serovar is also more commonly associated with septicemia than is *S.* Typhimurium due to the more common presence of plasmid-encoded *spv* genes that enhance intracellular proliferation in the former.[2] Disease usually develops in calves between 6 and 12 weeks of age and affects dairy calves much more frequently than beef calves, especially those that are purchased from sale barns.[2]

Calves with diarrhea and carrier cattle, including adult cattle, are the source for the fecal-oral route of infection.[2] *Salmonella* bacteria first colonize the distal small intestine, where pili facilitate attachment to the surface of enterocytes. The bacteria are taken up by enterocytes, macrophages and neutrophils. Production of enterotoxin results in the secretory diarrhea of enteric salmonellosis with loss of fluid and electrolytes; endotoxin production is important in septicemic salmonellosis. Some calves develop both syndromes (diarrhea and septicemia).[2]

The presence of gross lesions at necropsy examination helps to distinguish salmonellosis from enteric colibacillosis. Enteritis with yellow fibrinous exudate covering the mucosa is usually most severe in the ileum.[1] Mesenteric lymph nodes are enlarged and edematous.[1,2] The gallbladder is distended with an edematous wall and fibrinous mucosal inflammation.[2] Gray-white foci of hepatic necrosis may be observed macroscopically,[2] but were not obvious in this calf. These 'paratyphoid nodules' are easier to detect histologically as foci of lytic necrosis with infiltration by a few macrophages.[1,2] Lymphoid depletion is obvious in the mesenteric nodes and intestine; fibrin thrombi in capillaries and venules with phlebitis may be observed in the intestine, liver, gallbladder or other tissues.[1,2]

AFIP Diagnosis: 1. Small intestine: Enteritis, fibrinonecrotic, subacute, diffuse, severe, with erosions, diphtheritic membrane, and edema.
2. Gallbladder: Cholecystitis, transmural, fibrinonecrotic, diffuse, severe, with edema.
3. Liver: Cholangiohepatitis, lymphohistiocytic and neutrophilic, diffuse, mild to moderate, with multifocal, random lytic hepatic necrosis (paratyphoid nodules).

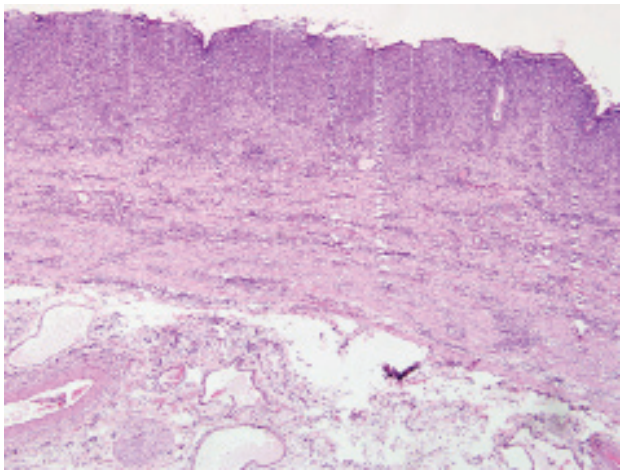

1-5. Gallbladder, calf. The gallbladder is transmurally expanded by an inflammatory cellular infiltrate, and the tunica adventitia is edematous. (HE 40x)

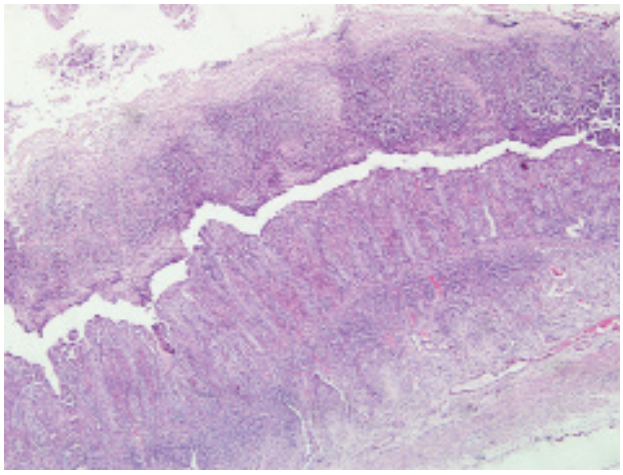

1-6. Small intestine, calf. Diffusely covering the mucosa, there is a thick layer of fibrin admixed with degenerate inflammatory cells and abundant cellular debris (diphtheritc membrane). (HE 40x)

Conference Comment: The conference moderator and participants were impressed by the strikingly similar transmural necrosis and inflammation in both the small intestine and gallbladder. Most slides lacked the fibrin thrombi in the intestinal submucosa that are typically found in cases of salmonellosis. Characteristic gross and histologic lesions of salmonellosis include a fibrinonecrotic (diphtheritic) membrane in the small intestine; the combination of hepatic and intestinal lesions; a characteristic odor of blood within intestinal contents; and paratyphoid nodules composed of mononuclear cells surrounding and infiltrating areas of coagulative necrosis with variable numbers of neutrophils.[1] Conference participants discussed the differential diagnosis for diphtheritic membranes in different species, which in the horse includes salmonellosis, colitis X (clostridial infection) and right dorsal colitis. The moderator noted that in the ox, diphtheritic membranes are highly suggestive of salmonellosis.

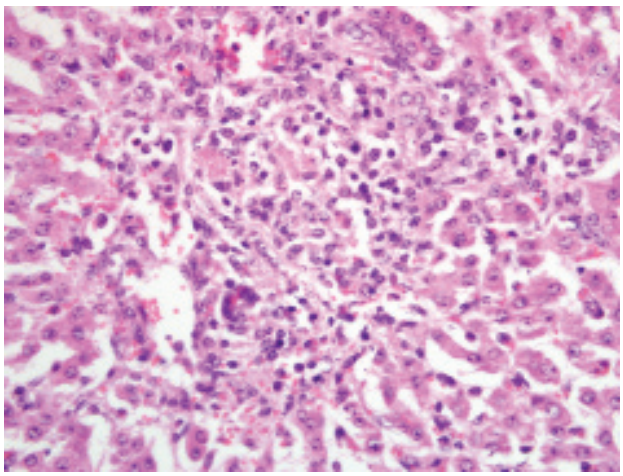

1-7. Liver, calf. Multifocally, there are random areas of lytic hepatocellular necrosis surrounded by macrophages, lymphocytes, and fewer neutrophils (paratyphoid nodules). (HE 400x)

There are now two recognized species of *Salmonella*: *S. enterica* and *S. bongori*. *S. enterica* has six subspecies: *enterica, salame, arizonae, diarizonae, indica* and *houtenae*. *S. enterica enterica* causes a majority of the cases of salmonellosis in humans and domestic animals, and contains approximately 60% of the more than 2,200 distinct serovars and serotypes of *Salmonella* that have been identified. Besides *S.* Dublin, other important serovars include *S.* Enteritidis, *S.* Pullorum-Gallinarum, *S.* Arizonae., *S.* Choleraesuis, *S.* Typhisuis, *S.* Typhi, and *S.* Typhimurium (especially the multi-drug resistant definitive phage type 104 (DT104)). *S. bongori* are primarily recognized as tropical strains.[1]

An informative review by Santos et al[3] details the fascinating mechanisms by which the non-typhoidal *Salmonella* (NTS) serotypes adapt and thrive in the milieu of the inflamed intestine. Briefly, two key abilities enable *S.* Typhimurium to incite inflammation: 1) penetration of intestinal epithelium, and 2) survival within macrophages. These traits are conferred by two type III secretion systems (T3SS): T3SS-1, the invasion-associated T3SS encoded by *Salmonella* pathogenicity island (SPI) 1; and T3SS-2, responsible for survival in macrophages, encoded by SPI2. Mucosal barrier functions against NTS dissemination are activated via the interleukin (IL)-18/interferon-γ and IL-

23/IL-17 axes, but the pathogen is adapted to survive the antimicrobial defenses of the inflamed intestininal lumen, allowing perpetuation of fecal/oral transmission.[3]

In general, three mechanisms account for the diarrhea. The first is malabsorption due to villous atrophy; there is reduced surface area for digestion and uptake of nutrients which then remain in the intestinal lumen exerting an osmotic effect which draws water. Second is secretory diarrhea due to an imbalance that results in a net excess of secretion over absorption; this is most often due to diarrheagenic enterotoxins of pathogenic bacteria, two classic examples of which are *Vibrio cholera* and *Escherichia coli*. The enterotoxins typically alter normal cellular secretory and absorptive functions of enterocytes. The final mechanism is effusive diarrhea, wherein there are changes in Starling forces or increased vascular permeability which allow fluid and solutes to move in a retrograde manner from the lateral intercellular space to the lumen. Interestingly, salmonellosis causes diarrhea via all three of these mechanisms. The secretory component is due to effector proteins, such as those encoded by SPI1 and SPI5, which block chloride channel closure or promote hypersecretion of chloride by enterocytes, respectively. Malabsorption is due to reduction of mucosal surface area and enterocyte function. Effusion of inflammatory exudates is the final component of this process.[1,2]

Contributor: Animal Disease Diagnostic Laboratory, 406 South University Street, Purdue University, West Lafayette, IN 47907
Animal Disease Diagnostic Laboratory: http://www.addl.purdue.edu/
Department of Comparative Pathobiology: http://www.vet.purdue.edu/cpb/

References:

1. Brown CC, Baker DC, Barker IK: Alimentary system. *In:* Jubb, Kennedy, and Palmer's Pathology of Domestic Animals, ed. Maxie MG, 5th ed., vol. 2, pp. 201-203. Elsevier Saunders, Philadelphia, PA, 2007
2. Fenwick SG, Collett MG: Bovine salmonellosis. *In:* Infectious Diseases of Livestock, eds. Coetzer JAW, Tustin RC, 3rd ed., vol. 3, pp. 1582-1593. Oxford University Press, Cape Town, South Africa, 2004
3. Santos RL, Raffatellu M, Bevins CL, Adams LG, Tükel Ç, Tsolis R, Bäumler AJ: Life in the inflamed intestine, *Salmonella* style. Trends Microbiol **17:**498-506, 2009

CASE II: 08-91 (AFIP 3133650).

Signalment: 148-day-old, female, Finn x Dorset lamb (*Ovis aries*).

History: This lamb was used in a medical device study.

Gross Pathology: The left lung (135 g) was pink and spongy with mild patchy atelectasis. The right lung (180 g) was pink and spongy, except for the right cranial lobe. Greater than 80% of the cranioventral right cranial lobe was pale tan-grey and firm (consolidation). On cut surface there were prominent lymphoid nodules with several mucus casts present in bronchioles (**figs. 2-1 and 2-2**).

Laboratory Results: Routine aerobic cultures from the right cranial lung lobe produced no growth. Serum obtained at necropsy was sent to the Washington Animal Disease Diagnostic Laboratory (WADDL). This animal had a serologic titer of >1:2560 to *Mycoplasma ovipneumoniae.* Immunostaining for *Mycoplasma* performed at the Michigan State University Diagnostic Center for Population and Animal Health was positive.

Histopathologic Description: In submitted sections of lung there is extensive consolidation of greater than 65% of the pulmonary parenchyma with prominent chronic "cuffing" bronchial/bronchiolar inflammation. Many bronchi/bronchioles are ectatically dilated and filled with a mixture of eosinophilic proteinaceous material, wispy basophilic mucus, and variable numbers of viable and degenerate neutrophils and sloughed epithelial cells (casts). Discrete foci of mineralization are present in the exudate in some sections. The respiratory epithelium is crowded and hyperplastic. The bronchial/bronchiolar submucosa is infiltrated and expanded by dense cuffs of moderate to large numbers of lymphocytes with frequent macrophages and fewer plasma cells, eosinophils, and neutrophils. Inflammatory cells are present within the respiratory epithelium and extend into the adjacent pulmonary interstitium and parenchyma. Lymphocytes frequently form discrete nodular aggregates, often with pale germinal centers containing large lymphoblasts and rare tingible body macrophages. Alveolar spaces are diffusely filled with variable but often large numbers of neutrophils and macrophages, the latter often containing abundant foamy cytoplasm. There are rare foreign body type multinucleate cells, with occasional lymphocytes and plasma cells. Scattered alveoli are lined by plump cuboidal epithelium (type II pneumocyte hyperplasia). There are occasional foci of squamous metaplasia (**fig. 2-3**).

2-1. Lung, lamb. Diffusely, the lung is pink with mild atelectasis. Photograph courtesy of Penn State Milton S Hershey Medical Center Penn State College of Medicine Department of Comparative Medicine H054, CG726A , 500 University Drive, PO Box 850 Hershey PA 17033-0850 tcooper@ hmc.psu.edu

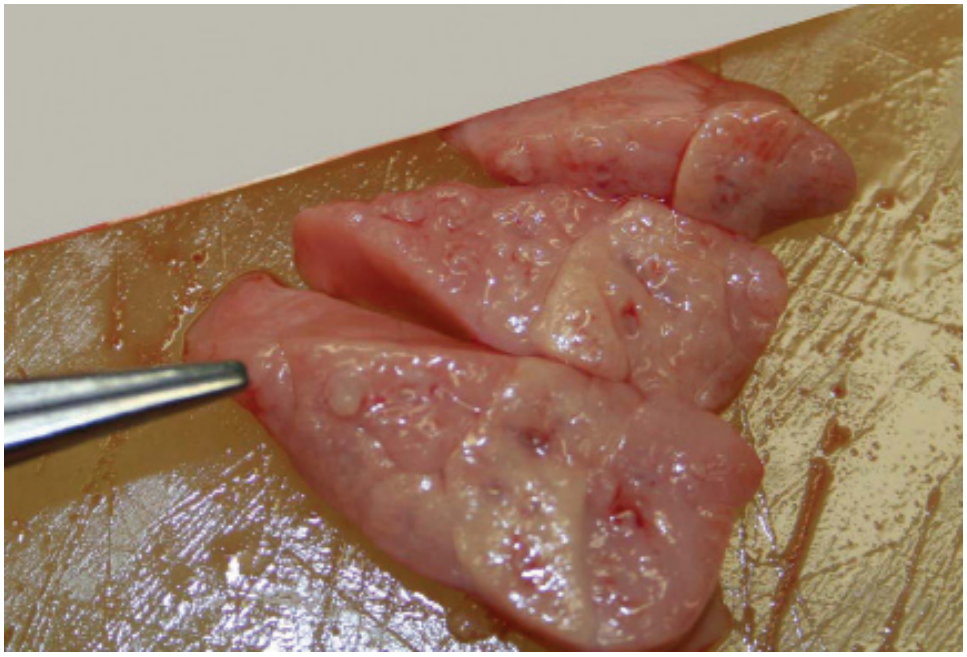

2-2. Lung, lamb. Multifocally on cut surface, there are prominent lymphoid follicles Photograph courtesy of Penn State Milton S Hershey Medical Center Penn State College of Medicine Department of Comparative Medicine H054, CG726A , 500 University Drive, PO Box 850 Hershey PA 17033-0850 tcooper@ hmc.psu.edu

Contributor's Morphologic Diagnosis: Lung, bronchitis and bronchiolitis, lymphocytic (cuffing) and proliferative, multifocal, chronic, severe, with bronchiectasis and chronic suppurative bronchopneumonia.

Contributor's Comment: Observed gross and histologic lesions are consistent with those previously reported for *Mycoplasma ovipneumoniae*.[1,11] One commonly reported histologic feature of this disease, the nodular "hyaline scar," was not observed in this case. These hyaline scars consist of polypoid masses of fibrous connective tissue protruding into the airway lumen, similar to bronchiolitis obliterans.[5]

Mycoplasma ovipneumoniae is considered the causative agent of "atypical" or "chronic, non-progressive pneumonia," a mild or subclinical respiratory disease of lambs in the first year of life.[6] Mixing of animals, high stocking density, and poor air quality are considered to be important risk factors. Concurrent or secondary infection with *Mannheimia haemolytica* is frequently reported and contributes to suppurative inflammation.[6,11]

Experimentally, *M. ovipneumoniae* adheres to luminal ciliated epithelial cells and induces ciliostasis.[4,8] In one study, infection with *M. ovipneumoniae* was correlated with the development of autoantibodies to the cilia.[7]

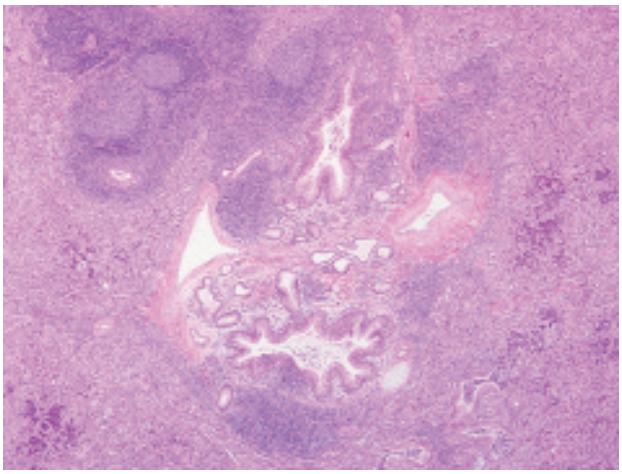

2-3. Lung, lamb. Multifocally, airways are ectatic, occasionally contain a cellular exudate, and are surrounded by discrete nodular lymphofollicular aggregates. Alveoli are filled with inflammatory cellular exudates. (HE 40x)

Additionally, *M. ovipneumoniae* has been shown to inhibit alveolar macrophage phagocytosis *in vitro*.[9] In this case, the presence of inspissated mucus casts, bronchiectasis, and mixed suppurative and histiocytic inflammation in the alveoli are strongly suggestive of impaired mucociliary clearance. Colonization of the ciliated epithelium with ciliostasis and deciliation are features of other *Mycoplasma* pneumonias.[2,5] Other virulence factors include alteration of host prostaglandin synthesis, membrane alterations, induction of apoptosis in lymphocytes and other cells, as well as the presence of superantigens in the mycoplasmal plasma membrane. This latter feature is thought to give rise to the typical "lymphocytic cuffing" that is a feature of many pulmonary mycoplasmoses.[2]

Mycoplasma ovipneumoniae has been implicated as a causative agent of enzootic and epizootic pneumonia in Rocky Mountain bighorn sheep (*Ovis canadensis canadensis*).[1] The gross and histologic lung lesions induced by *M. ovipneumoniae* are similar to that of *M. pulmonis* (and cilia-associated respiratory bacillus) in laboratory rats (and mice)[10] and *M. hyopneumoniae* in pigs,[2,5] but differ markedly from the typical appearance of *Mycoplasma bovis* pneumonia in cattle.[2,3]

AFIP Diagnosis: Lung: Bronchopneumonia, suppurative, chronic-active, diffuse, severe, with peribronchiolar nodular lymphofollicular hyperplasia, bronchiolar epithelial and type II pneumocyte hyperplasia and hypertrophy, bronchiectasis, and interlobular edema.

Conference Comment: The most striking microscopic feature of the submitted section of lung tissue is the formation of lymphoid nodules with germinal centers, which in combination with the cuffing lymphoid infiltrates and bronchiolar epithelial hyperplasia and hypertrophy, is characteristic of mycoplasmal pneumonia. Suppurative bronchopneumonia, prominent in several examined slides, is not, however, typical of mycoplasmal pneumonia, suggesting a secondary infection. In addition to *Mannheimia haemolytica* (formerly *Pasteurella haemolytica* biotype A, multiple serotypes excluding 11), common secondary infections in ovine pulmonary mycoplasmosis include *Bibersteinia trehalosi* (*Pasteurella trehalosi*, formerly *P. haemolytica* biotype T) and *Mannheimia glucosida* (formerly *P. haemolytica* biotype A, serotype 11).[5] Tissue Gram stains did not demonstrate bacteria in submitted serial unstained slides.

Conference participants reviewed and discussed the three primary respiratory tract defense mechanisms: 1) mucus and the mucociliary escalator system; 2) antibody and innate defense proteins; and 3) alveolar macrophages and recruited neutrophils. Hairs and air turbulence in the nasal passages and sinuses prevent particles larger than 10 mm in size from advancing further in the respiratory tract. Particles entrapped in mucus are cleared via the mucociliary escalator and/or coughing. The mucociliary escalator ends at the level of the terminal bronchioles, making this anatomic area in the respiratory tree the most susceptible to establishment of infection. The airway mucosa contains many non-specific antimicrobial factors, including lactoferrin, B-defensins, collectins, lysozyme, the complement membrane attack complex and lactoperoxidase, among others. Opsonizing agents in the respiratory tract include IgG, C3b from the complement system and surfactant proteins A and D. Primary defense and clearing of debris in the alveolus is accomplished by alveolar macrophages; T lymphocytes and natural killer cells assist in sampling alveolar material.[2] Conference participants discussed the importance of impaired mucociliary clearance and ciliostasis in the pathogenesis of myocoplasmal pneumonia, and noted additional causes of ciliostasis, including cilia-associated respiratory bacillus (CAR bacillus) of rodents, *Bordetella bronchiseptica*, alcohol, smoking, and primary ciliary dyskinesia.

Contributor: Department of Comparative Medicine, Penn State College of Medicine, Penn State Milton S. Hershey Medical Center, Hershey, PA 17033
http://www.pennstatehershey.org/web/comparativemedicine/home

References:

1. Besser TE, Cassirer EF, Potter KA, VanderSchalie J, Fischer A, Knowles DP, Herndon DR, Rurangirwa FR, Weiser GC, Srikumaran S: Association of *Mycoplasma*

ovipneumoniae infection with population-limiting respiratory disease in free-ranging Rocky Mountain bighorn sheep (*Ovis canadensis canadensis*). J Clin Microbiol **46:**423-430, 2008
2. Caswell JL, Williams, KJ: Respiratory System. *In:* Jubb, Kennedy, and Palmer's Pathology of Domestic Animals, ed. Maxie MG, 5th ed., pp. 579-650. Elsevier Saunders, Philadelphia, PA, 2007
3. Gagea MI, Bateman KG, Shanahan RA, van Dreumel T, McEwen BJ, Carman S, Archambault M, Caswell JL: Naturally occurring *Mycoplasma bovis*-associated pneumonia and polyarthritis in feedlot beef calves. J Vet Diagn Invest **18:**29-40, 2006
4. Jones GE, Keir WA, Gilmour JS: The pathogenicity of *Mycoplasma ovipneumoniae* and *Mycoplasma arginini* in ovine and caprine tracheal organ cultures. J Comp Pathol **95:**477-487, 1985
5. Lopez A: Respiratory System. *In:* Pathologic Basis of Veterinary Disease, ed. McGavin M, Zachary, JF, 4th ed., pp. 463-558. Mosby Elsevier, St. Louis, MO, 2007
6. Martin WB: Respiratory infections of sheep. Comp Immunol Microbiol Infect Dis **19:**171-179, 1996
7. Niang M, Rosenbusch RF, Andrews JJ, Lopez-Virella J, Kaeberle ML: Occurrence of autoantibodies to cilia in lambs with a 'coughing syndrome.' Vet Immunol Immunopathol **64:**191-205, 1998
8. Niang M, Rosenbusch RF, DeBey MC, Niyo Y, Andrews JJ, Kaeberle ML: Field isolates of *Mycoplasma ovipneumoniae* exhibit distinct cytopathic effects in ovine tracheal organ cultures. Zentralbl Veterinarmed A **45:**29-40, 1998
9. Niang M, Rosenbusch RF, Lopez-Virella J, Kaeberle ML: Expression of functions by normal sheep alveolar macrophages and their alteration by interaction with *Mycoplasma ovipneumoniae*. Vet Microbiol **58:**31-43, 1997
10. Percy D, Barthold, SW: Pathology of Laboratory Rodents and Rabbits, 3rd ed. pp. 65-67, 143-146. Blackwell Publishing, Ames, IA, 2007
11. Sheehan M, Cassidy JP, Brady J, Ball H, Doherty ML, Quinn PJ, Nicholas RA, Markey BK: An aetiopathological study of chronic bronchopneumonia in lambs in Ireland. Vet J **173:**630-637, 2007

CASE III: NCAH 2009-2 (AFIP 3134595).

Signalment: 7-week-old, specific pathogen free, White Leghorn chickens, (*Gallus gallus domesticus*).

History: The chickens were one component of an infectious bursal disease research project that included one group which had received topical ocular inoculations of infectious bursal disease virus (variant strain E) and another group of non-challenged control chickens. Four days post inoculation both groups of birds were euthanized. The challenged and control chickens were clinically normal throughout the duration of the study. Each slide contains tissues from one challenged animal and one age-matched control.

Gross Pathology: Subjectively, the bursa appeared approximately 10% smaller in the challenged group than the control group.

Histopathologic Description: Bursa of Fabricius (cloacal bursa): In the affected tissue there is marked atrophy of bursal follicles due to loss of lymphocytes in the medulla and cortex. Numerous large, foamy, macrophages containing phagocytosed cellular debris are within the collapsed follicles. The endodermal epithelium separating the medulla from the cortex is prominent due to collapse of the follicles and mild epithelial hypertrophy and hyperplasia. The interfollicular epithelium covering the surface of the bursa is also mildly hyperplastic. Diffusely, the follicular cortex and interfollicular interstitium contain increased clear space (edema), congested vessels, and multifocal areas of mild hemorrhage. Multifocally, the lamina propria, muscularis, and serosa are expanded by edema with small numbers of lymphocytes, plasma cells, and macrophages (**figs. 3-1, 3-2, and 3-3**).

Contributor's Morphologic Diagnosis: Bursa of Fabricius (cloacal bursa): Lymphoid depletion, diffuse, severe, subacute, White Leghorn (*Gallus gallus domesticus*), avian.

Contributor's Comment: Infectious bursal disease, or Gumboro disease, is an acute, highly contagious, immunosuppressive disease caused by serotype 1 infectious bursal disease virus (IBDV), a double-stranded RNA virus in the family *Birnaviridae* and genus *Avibirnavirus*.[2] Chickens are the only animals known to develop clinical disease and distinct lesions when exposed to IBDV, although other species may replicate the virus and develop neutralizing antibodies. Virtually all flocks

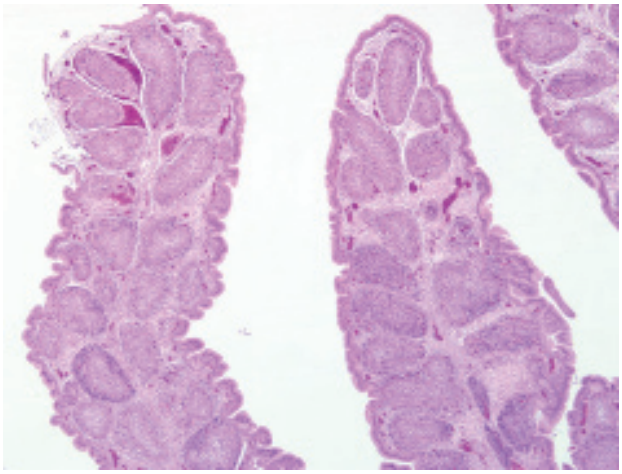

3-1. Bursa of Fabricius, chicken. There is marked atrophy of bursal follicles and depletion of lymphoid cells. (HE 12.50x)

in major poultry producing areas worldwide are exposed to the virus through natural infection or vaccination. Eliminating the virus from infected farms can be difficult, despite routine cleaning and disinfection, because the virus has been shown to survive in the environment for several months and it is relatively resistant to heat and certain disinfectants. Clinical signs of disease appear within 2-3 days after exposure and include soiled vent feathers, diarrhea, dehydration, anorexia, depression, ruffled feathers, trembling, prostration, and death. Clinical disease, although uncommon in the United States, is primarily seen in chickens 3-6 weeks old. Infection in chickens younger than 3 weeks of age is typically subclinical, but results in prolonged immunosuppression that can cause adverse economic impact to the producer due to secondary infections and poor response to routine flock vaccinations. Infected birds older than 6 weeks of age seroconvert but usually do not develop clinical signs.[2]

There are two serotypes: type 1 and type 2. The type 1 serotype is further divided into the standard (or classic) strain and variant strains. In Europe, Asia, Africa, and South America highly pathogenic serotype 1 strains have been identified and are termed very virulent infectious bursal disease (vvIBD).[2] Experimental inoculation elicits different responses depending on the strain of virus. Both the very virulent and classic strains induce typical clinical signs and gross lesions with mortality rates of 10-50% for classical strains and up to 50-100% during infections with vvIBDV.[2] Variant strains such as the type E strain used to infect this chicken typically cause bursal lesions to develop but rarely induce acute clinical signs or mortality.[5] In general, serotype 2 virus is not pathogenic and does not protect against challenge with serotype 1 viruses.[2]
Grossly the bursa initially increases in size due to edema and hyperemia, but then begins to atrophy due to lymphoid depletion and eventually decreases in size to one-third of its original weight.[1] The bursa may have necrotic foci with mild to extensive hemorrhage and the spleen may be mildly enlarged with uniform small gray foci on the surface.[2] Hemorrhages of the thigh and pectoral muscles are frequently present and severely dehydrated chickens commonly develop non-specific renal lesions.[2]

Microscopically the cloacal bursa is the most severely affected organ, but other lymphatic tissues, such as the spleen, thymus, and Harderian gland, have similar but milder lesions than the bursa.[3] Initially there is degeneration and necrosis of lymphocytes in the bursal medulla as early as 36 hours after infection.[1] As the disease progresses, heterophils, macrophages, and eventually fibroblasts accumulate in the follicular and interfollicular areas. In the spleen there may be hyperplasia of splenic reticuloendothelial cells along with lymphoid necrosis and the Harderian gland can have areas of necrosis.[1,3]

Multiple virus and host variables, including strain of virus, age and breed of chicken, and maternal immunity and vaccine status affect the development of infection/disease.[4] The pathogenesis of oral infection results in an initial viremia within five hours and a second massive viremia may occur following infection of the bursa.[2] The virus targets immature dividing B lymphocytes resulting in necrosis and apoptosis of B cells with activation of macrophages, T cells, and NK cells.[2,4] Recovery from complete immunosuppression can occur if large follicles capable of replenishing the B cell population are reconstituted from endogenous stem cells that survived the initial infection.[2,9] The long-term effect of IBD is frequently immunosuppression due to decreased humoral immunity, and to a much lesser degree, cellular immunity resulting in increased susceptibility to disease and poor immune response to vaccination.[7]

AFIP Diagnosis: Bursa of Fabricius (cloacal bursa): Lymphoid necrosis and depletion, diffuse, marked, with stromal collapse and interstitial edema.

Conference Comment: Compared to tissue from the aged-matched control, there is increased prominence of reticular cells and macrophages in the section of bursa from the infected animal. One of the focal points of discussion among conference participants was the distinction between true inflammation versus increased prominence of resident reticular cells and monocytes due to follicular collapse. Additionally, some participants' slides contained few discrete foci of heterophilic inflammation.

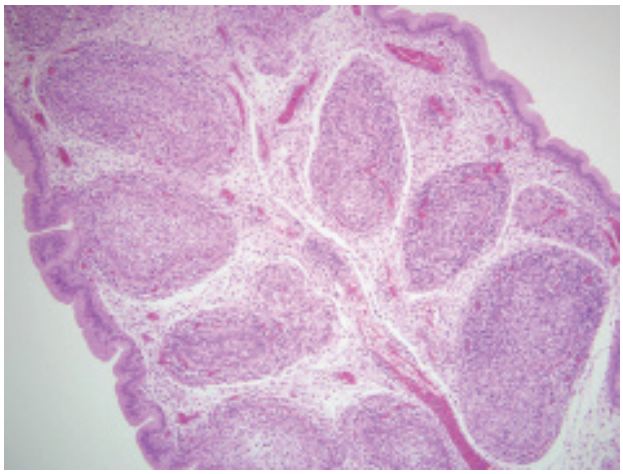

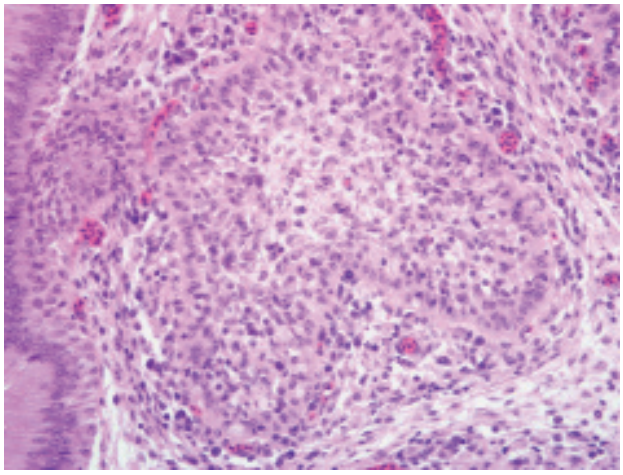

3-2, 3-3. Bursa of Fabricius, chicken. There is marked follicular atrophy and lymphocytolysis, and the lamina propria is expanded by edema and an inflammation. (HE 200x)

Based on the histomorphologic findings of lymphoid necrosis and depletion, conference participants were evenly divided between infectious bursal disease virus (IBDV) and chicken anemia virus (CAV) (Circoviridae, Gyrovirus) as the underlying etiology. Chicken anemia virus infects hemocytoblasts in the bone marrow and lymphoblasts in the cortex of the thymus, resulting in anemia with a hematocrit of 6-27% and pancytopenia. Gross lesions of CAV include thymic atrophy; bone marrow atrophy; hemorrhage in the proventricular mucosa, subcutaneous tissue, and skeletal muscle; and, less commonly, bursal atrophy. Panmyelophthisis and generalized lymphoid atrophy are commonly observed in chickens infected with CAV, with the thymus exhibiting the most severe lesions. When present, bursal lesions caused by CAV are less severe than those induced by IBDV, and include lymphofollicular atropy, few areas of necrosis, and infolding of the epithelium with hydropic degeneration and proliferation of reticular cells. In contrast, infection with IBDV frequently results in marked to severe lymphofollicular bursal atrophy, hemorrhage, edema, heterophilic inflammation, and hyperplasia of the bursal epithelium, sometimes resulting in a pseudoglandular appearance.[2,6]

The contributor discusses immunosuppression and decreased humoral immunity caused by IBDV infection, which renders infected chicks more susceptible to disease. Immunosuppression is most severe in chicks exposed to the virus within 2-3 weeks of hatch, and manifests clinically as impaired protective response to vaccination, increased incidence of secondary infections, poor feed conversion, and increased rates of carcass condemnation at processing. Interestingly, although T lymphocytes are resistant to infection with IBDV, the virus does cause thymic atrophy, thymocyte apoptosis, and impaired cell-mediated immunity, in addition to the expected impairment of humoral immunity that results from depletion of IgM+ B lymphocytes in the cloacal bursa, spleen, and cecal tonsils. Infection with IBDV is also thought to impair innate immunity, compromising the phagocytic activity of macrophages.[7] The Harderian gland is a component of the local immune system of the upper respiratory tract, and its function is also impaired by IBDV infection.[2]

The United States was considered free of the very velogenic (vvIBD) form of the disease; however, an outbreak of vvIBD was recently reported in 2009.[8] The source of the most recent disease outbreak has not been determined. Field veterinarians and diagnosticians should be aware of this report and consider vvIBD in the differential diagnosis when clinical signs, epidemiologic evidence, and diagnostic data indicate it as a potential etiology.

Contributor: National Centers for Animal Health, 2300 Dayton Avenue, Ames, IA 50010
www.nadc.ars.usda.gov/

References:

1. Cheville NF: Studies on the pathogenesis of Gumboro disease in the bursa of Fabricius, spleen, and thymus of the chicken. Am J Pathol **51:**527-551, 1967
2. Eterradossi N, Saif YM: Infectious bursal disease. *In:* Diseases of Poultry, ed. Saif YM, 12th ed., pp. 185-208. Blackwell Publishing, Ames, IA, 2008
3. Ley DH, Yamamoto R, Bickford AA: The pathogenesis of infectious bursal disease: serologic, histopathologic, and clinical chemical observations. Avian Dis **27:**1060-1085, 1983
4. Müller H, Islam MR, Raue R: Research on infectious

bursal disease-the past, the present and the future. Vet Microbiol **97:**153-165, 2003
5. Rodriguez-Chavez IR, Rosenberger JK, Cloud SS, Pope CR: Characterization of the antigenic, immunogenic, and pathogenic variation of infectious bursal disease virus due to propagation in different host systems (bursa, embryo, and cell culture). III. Pathogenicity. Avian Pathol **31:**485 - 492, 2002
6. Schat KA, van Santen VL: Chicken infectious anemia. *In:* Diseases of Poultry, ed. Saif YM, 12th ed., pp. 211-249. Blackwell Publishing, Ames, IA, 2008
7. Sharma JM, Kim I-J, Rautenschlein S, Yeh H-Y: Infectious bursal disease virus of chickens: pathogenesis and immunosuppression. Dev Comp Immunol **24:**223-235, 2000
8. Stoute ST, Jackwood DJ, Sommer-Wagner SE, Cooper GL, Anderson ML, Woolcock PR, Bickford AA, Senties-Cue CG, Charlton BR: The diagnosis of very virulent infectious bursal disease in California pullets **53:**321-326, 2009
9. Withers DR, Young JR, Davison TF: Infectious bursal disease virus-induced immunosuppression in the chick is associated with the presence of undifferentiated follicles in the recovering bursa. Viral Immunol **18:**127-137, 2005

CASE IV: 09-07233 (AFIP 3136516).

Signalment: 5-month-old, female Boer goat (*Capra hircus*).

History: This goat has a 2 week history of lethargy, anorexia, and loss of body condition.

Gross Pathology: The dependent subcutaneous tissues were wet and gelatinous. The thoracic cavity contained 600 mL of dark yellow, translucent fluid and multiple aggregates of translucent, straw colored gel. The pericardial sac was thickened and filled with multiple pockets up to 2 cm in diameter containing thick, yellow, creamy material and surrounded by a thick white capsule. Multifocally, the lungs were tightly adhered to the thoracic wall. The abdominal cavity was filled with approximately 500 mL of dark yellow translucent fluid and gel similar to that described in the thorax.

Laboratory Results: Bacterial culture yielded a heavy growth of *Corynebacterium pseudotuberculosis*.

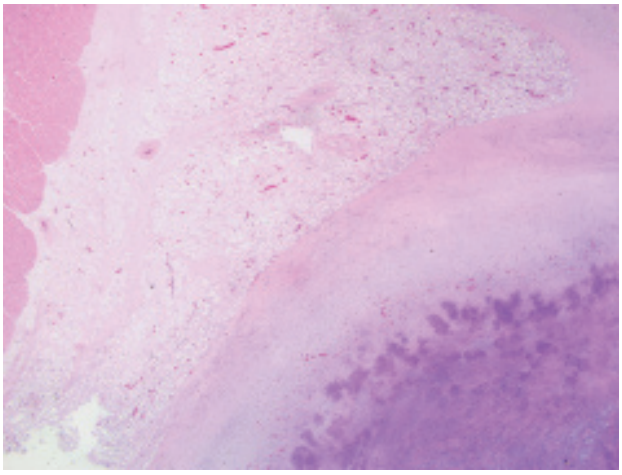

4-1. Heart, goat. The pericardium is markedly thickened by abundant fibrin, edema, degenerate inflammatory cells, mineralized necrotic debris and fibrous connective tissue. (HE 12.50x)

Histopathologic Description: The pericardium is markedly thickened and contains multifocal to coalescing abscesses characterized by a central core of necrotic cellular debris, eosinophilic proteinaceous material, neutrophils, and karyolytic and karyorrhectic cells, and dark basophilic material (mineralization). The abscesses contain many randomly scattered macrophages filled with short rod shaped, Gram-positive bacteria both intracellularly within the cytoplasm and free in the surrounding debris. The foci are surrounded by lymphocytes, plasma cells, and macrophages and are walled off with a dense band of fibrous connective tissue. The fibrous tissue has fibroblasts with closely spaced, plump, vesiculated nuclei (active fibroplasia). The epicardium is expanded with moderate amounts of edema and fibrin admixed with lymphocytes and plasma cells. The underlying myocardium contains a few randomly scattered fibers that are pale, discontinuous, and have a loss of striation pattern (**figs. 4-1 and 4-2**).

Contributor's Morphologic Diagnosis: Pericarditis, fibrosing, with multifocal abscesses and intralesional bacteria.

Contributor's Comment: A heavy growth of *Corynebacterium pseudotuberculosis* was isolated from the pericardial abscesses. *C. pseudotuberculosis* serotype I is the etiologic agent of caseous lymphadenitis (CLA) in sheep and goats. Serotype II is often isolated from buffalo and cattle. A phospholipase D exotoxin is considered to be the primary virulence factor and facilitates spread of the infection from the primary site and results in intravascular hemolysis, necrosis, pulmonary edema, and shock. Inactivation of the pld gene encoding phospholipase D

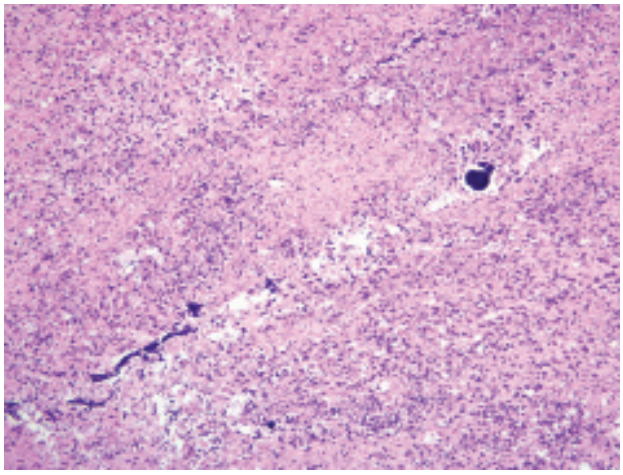

4-2. Heart, goat. The abscess is composed of a central core of necrotic cellular debris, degenerate inflammatory cells, and mineralized material. (HE 400x)

results in bacteria incapable of producing CLA.

C. pseudotuberculosis often enters the body through skin or oral wounds. The draining lymph node is then infected and subsequently the organism can spread to internal organs, typically the lungs. Treatment of animals with *C. pseudotuberculosis* often results in limited success due to the intracellular nature of the organism and the formation of abscesses leading to poor penetration of the drug. Typically, once the bacterium enters the lymph nodes, the infection is considered persistent except for the rare occasion when the node ruptures and drains through the skin to the outside of the body. A primary finding of pericarditis without lymphadenitis, as in this case, is unusual.

AFIP Diagnosis: Heart, pericardium: Pericarditis, caseonecrotic and fibrosing, chronic, diffuse, severe, with mineralization and many intrahistiocytic and extracellular small bacilli.

Conference Comment: As mentioned by the contributor, this case is unusual in that it features primary pericarditis in the absence of the lymphadenitis that typifies CLA; in fact, although participants readily identified the pathologic process in this case and considered *C. pseudotuberculosis* to be a likely etiology, many misidentified the affected tissue as lymph node.

Conference participants briefly reviewed bacteria able to survive in macrophages, including *Rhodococcus* spp., *Salmonella* spp., *Mycobacteria* spp., *Brucella* spp. and *Listeria* spp. Other less commonly encountered microbial agents in macrophages include rickettsial organisms, *Shigella* spp., *Trypanosoma* spp., *Coxiella* spp., chlamydial organisms, *Toxoplasma* spp., and *Legionella* spp.

The contributor provides a succinct synopsis of the pathogenesis of CLA in sheep; readers are referred to a comprehensive review by Baird and Fontaine[1] for more details. In addition to phospholipase D, *C. pseudotuberculosis* produces a waxy mycolic acid coat with well-described cytotoxic properties, which both contributes substantially to the organism's pathogenicity and enhances its ability to survive for extended periods in the environment. This latter attribute is common to the actinomycete family, of which the genera *Corynebacterium, Mycobacterium, Rhodococcus,* and *Nocardia* are members.[1]

In sheep, *C. pseudotuberculosis* has been hailed the "perfect parasite" because of its ability to evade the immune system, establish a chronic infection that often persists for the life of the host, and readily infect flock mates, all while only rarely producing fatal infections. Therefore, in regions where the disease is endemic, CLA may be of considerable economic importance. Visceral lesions are far less common than superficial lymphadenitis in both sheep and goats, and they occur even less frequently in goats as compared to sheep. While abscesses in sheep due to CLA are most often found in the superficial lymph nodes of the torso, in goats the lesions manifest as lymphadenitis of the superficial nodes of the head and neck.[1]

In horses, *C. pseudotuberculosis* causes three distinct disease syndromes: 1) ulcerative lymphangitis; 2) contagious folliculitis and furunculosis, which is also known as equine contagious acne, Canadian horsepox, and equine contagious pustular dermatitis; and 3) deep-seated subcutaneous abscessation, also termed pigeon fever, Wyoming strangles, and false strangles. In farmed llamas and alpacas in South America, *C. pseudotuberculosis* is a commonly identified cause of purulent lymphadenopathy. In dairy cattle in Israel, *C. pseudotuberculosis* has been implicated in several syndromes, including deep subcutaneous abscesses and mastitis. Sporadic and experimental infections have been reported in a variety of species.[1]

Contributor: University of Illinois College of Veterinary Medicine, Pathobiology Department, 2522 VMBSB, 2001 South Lincoln Avenue, Urbana, IL 61801
http://vetmed.illinois.edu/path/

References:

1. Baird GJ, Fontaine MC: *Corynebacterium pseudotuberculosis* and its role in ovine caseous lymphadenitis. J Comp Pathol **137:**179-210, 2007

2. D'Afonseca VD, Moraes PM, Corella FA, Pacheco LG, Meyer R, Portela RW, Miyoshi A, Azevedo V: A description of genes of *Corynebacterium pseudotuberculosis* useful in diagnostics and vaccine applications. Gen and Mol Res **7:**252-260, 2008
3. Valli VEO: Hematopoietic system. *In:* Jubb, Kennedy, and Palmer's Pathology of Domestic Animals, ed. Maxie MG, 5th ed., vol. 3, pp. 292-294. Elsevier Saunders, Philadelphia, PA, 2007

The Armed Forces Institute of Pathology
Department of Veterinary Pathology

Conference Coordinator:
Shannon Lacv. DVM. MPH

WEDNESDAY SLIDE CONFERENCE 2009-2010

Conference 16

24 February 2010

Conference Moderator:

Edward Stevens, DVM, Diplomate ACVP

CASE I: 2/09 (AFIP 3134519).

Signalment: 12-year-old female, mixed breed dog (*Canis familiaris*).

History: The dog was kept in a kennel and died spontaneously overnight.

Gross Pathology: Serous fluid was present around the nares and mouth. There was moderate pleural serous hemorrhagic effusion and severe consolidation of the lung lobes. Two adult filariae were noted in the right cardiac chambers. No other lesions were found in the abdominal cavity or trachea.

Laboratory Results: Adult nematodes were 18.5 and 23 cm in length and were brought to the parasitology laboratory where they were identified as *Dirofilaria immitis* adults.

Histopathologic Description: The pulmonary interstitium is expanded and partially effaced by multifocal to coalescing granulomatous foci associated with multifocal hemorrhages. The inflammatory foci are composed of macrophages, multinucleated giant cells (foreign body type), fibroblasts, lymphocytes and plasma cells, which are arranged concentrically around myriad parasitic larvae and eggs (consistent with those of *Angiostrongylus vasorum*). Larvae are elongated with a thin eosinophilic cuticle and a primitive intestinal tract. The thin-walled eggs are ovoid, 50-60 µm in diameter, and contain either a morula or larva. Numerous *A. vasorum* larvae are present in the bronchial lumina, intermixed with few histiocytes and multinucleated giant cells, sloughed epithelial cells and abundant mucus.

Focally, a pulmonary artery is severely dilated with the tunica intima thickened by moderate amount of fibrous connective tissue and few lymphocytes and plasma cells. Within the lumen there is a cross section of an adult, 0.5-1 mm in largest diameter (varies among sections and not present in all the sections), degenerate nematode with a thin eosinophilic cuticle, lateral cords, tall coelomyarian/polymyarian musculature, and a small intestine (consistent with a *Dirofilaria immitis* adult). Additionally in some sections, within this vessel and in an adjacent small artery, there are one to three tranverse sections of a smaller degenerate nematode (0.1-0.25 mm in largest diameter) characterized by a very thin coelomyarian musculature and a variably evident large strongyloid intestine; one nematode has a uterus. Intravascular nematodes are surrounded by thrombi, which focally adhere to the

*Sponsored by the American Veterinary Medical Association, the American College of Veterinary Pathologists, and the C. L. Davis Foundation.

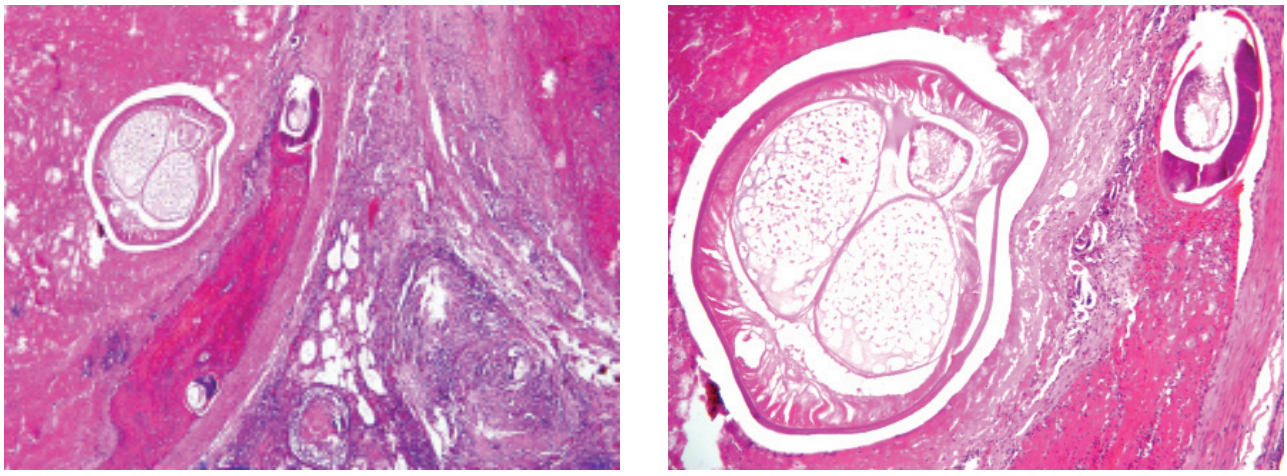

1-1., 1-2. Lung, pulmonary artery, dog. In the lumen is an adult nematode with a smooth cuticle, tall coelomyarian/ polymyarian musculature, and small diameter intestine (Dirofilaria immitis). In the same vessel there is a smaller adult nematode with low coelomyarian/ polymyarian musculature (Angiostrongylus vasorum). (HE 100x)

vessel walls. The thrombus is composed of fibrillar eosinophilic material (fibrin) that is partially organized in fibrous connective tissue containing multiple small blood-filled channels (organization and recanalization). Within the thrombi and in some vessel lumina there are occasional nematode larvae, consistent with *Dirofilaria immitis* microfilariae. The tunica media of numerous pulmonary arteries is markedly thickened (smooth muscle hypertrophy) (**figs. 1-1, 1-2, 1-3 and 1-4**).

Contributor's Morphologic Diagnosis: 1. Lung: severe, multifocal to coalescing, chronic, interstitial granulomatous pneumonia with intralesional nematode eggs and larvae.
2. Lung, pulmonary arteries: severe, focal, chronic, proliferative endarteritis with thrombus formation and an intralesional nematode adult and larvae.
Etiologies: 1. *Angiostrongylus vasorum*
2. *Dirofilaria immitis*

Contributor's Comment: Lesions were consistent with a double parasitic infection. Adult *D. immitis* and *A. vasorum* were present in the pulmonary vasculature (not in all sections) and myocardium. Most lesions of the pulmonary interstitium were attributed to *A. vasorum* laying morulated eggs in the alveoli in this case. Adults of *A. vasorum* are smaller than those of *D. immitis*. *D. immitis* adults have evenly-spaced lateral internal cuticular ridges, thicker, very well-developed coelomyarian musculature, and a smaller intestine than that of *A. vasorum*. These are the main useful morphologic features for differentiating the two parasites in dogs.[4,7] Adults of both *D. immitis* and *A. vasorum* live in the pulmonary arteries and right heart; however, *D. immitis* adult female worms are larger, are viviparous, and release microfilariae into the bloodstream.[7]

The first, second, and early third larval stages of *D. immitis* are obligate parasites of mosquitoes of the genera *Aedes*, *Culex*, and *Anopheles*. After maturation, larvae migrate into the cephalic spaces of the mosquito head and enter soft tissues of the new host when the mosquito feeds. The larvae reach the right ventricle 3-4 months after entering definitive host. Adults may live for years and microfilariae as long as 2.5 years. Clinical signs of canine dirofilariasis, such as cough and exercise intolerance, are related to cardiovascular dysfunction that may progress to congestive heart failure. The disease is seen more frequently in dogs older than 5 years, and clinical signs roughly correlate with the severity of infection. However, clinically normal dogs may harbor up to 30 worms. Adult heartworms are generally found in the pulmonary arteries and right ventricle; however, they may locate in vena cava or left ventricle in heavy infestations (i.e. 50 or more worms). The caudal lobar pulmonary arteries are generally most severely affected. Right heart failure may be caused by pulmonary hypertension due to vascular lesions.[7]

Immature and mature adult worms induce endarteritis with infiltration of eosinophils and neutrophils. Vascular lesions seem more severe in the presence of *Wolbachia*, a bacterial organism harbored by *D. immitis*.[5] The initial inflammation is followed by myointimal proliferation at sites of direct contact with worms; this reaction to chronic irritation is likely mediated by platelet-derived growth factor (PDGF). The lesions are followed by

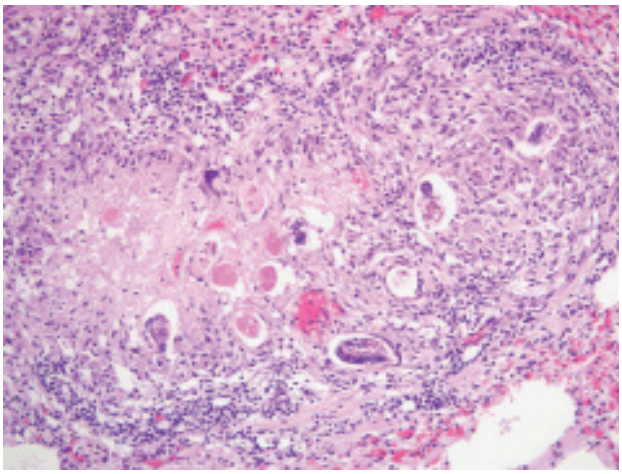

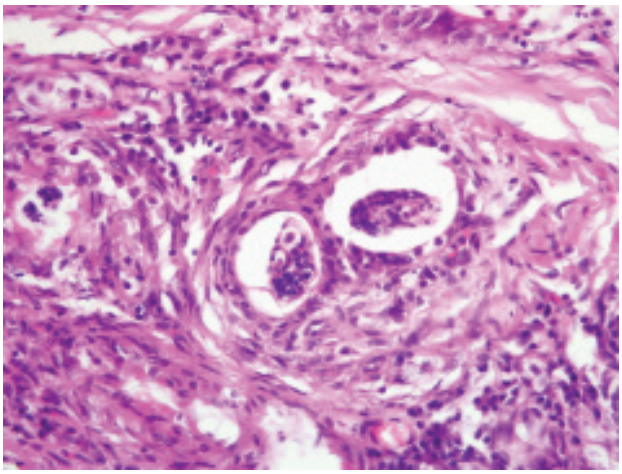

1-3., 1-4. Lung, pulmonary artery, dog. Granulomatous inflammation and fibrosis surround embryonated eggs and larvae. (HE 200x, HE 400x)

fibromuscular vascular wall hyperplasia. Pulmonary thromboembolism of viable or dead filarids (e.g. after therapy) may worsen hypertension, due to granulomatous interstitial inflammation elicited, and by occlusion of pulmonary vessels. However, pulmonary infarction seems an uncommon event.

In the pulmonary parenchyma, the most common microscopic findings associated with *D. immitis* infection are arterial thrombosis and periarterial granulomatous inflammation.[7] Additional complications of heartworm disease include progressive chronic right heart failure with chronic passive congestion of the liver and occasional ascites. The vena caval syndrome is usually seen in young dogs with large numbers of adult worms that fill the right atrium and the vena cava, most likely as a result of retrograde migration from pulmonary arteries. In these instances, dogs develop sudden weakness, anorexia, bilirubinuria, hemoglobinuria and anemia. Shock derives from venous obstruction and decreased venous return. A common renal lesion associated with *D. immitis* infection is a membranoproliferative glomerulonephritis derived from the deposition of immune complexes from the circulation or formed *in situ*. The immune response leading to immune complex formation may be elicited by adults, immature adults, and microfilariae.[10] The most frequent ultrastructural lesions observed in kidneys of affected dogs are thickening of the glomerular basement membrane zone, presence of dense deposits in the glomerular basement membrane, and effacement of foot processes. In some dogs, electron dense deposits may be seen in the mesangium with expansion of mesangial matrix.[10]

Cats may become infected with *D. immitis* and are typically microfilaremic or afilaremic due to the low number of adults (often one) and high frequency of filarial male-only infection. Cats may develop cough and dyspnea, vomiting, and neurological signs, or sudden death may be the only event. A significant decrease in pulmonary intravascular macrophage activity in cats with *D. immitis* infection has been identified.[3]

Dirofilaria sp. may occasionally infect man.[9,11,13] The infection in America is more commonly attributed to *D. immitis*, while in Europe, pulmonary dirofilariasis is most commonly attributed to aberrant migration of *D. repens*.[11] There is no clear explanation for this geographical selective distribution. The distribution of reported human cases seems to reflect the prevalence of the disease in the canine population in different areas of the United States.[13] These filarids induce a focal to multifocal pulmonary granulomatous reaction termed "coin lesions."[9,13] Coin lesions are the end-stage tissue result of the parasite's death in the vascular bed and the stimulation of a granulomatous reaction. Although the disease still seems rare in humans, serology should be performed in regions where *D. immitis* is highly enzootic. *D. immitis* coin lesions present significant differential diagnostic problems since they may resemble the lesions of tuberculosis, fungal infections, or neoplasia.[13]

Angiostrongylus vasorum can be differentiated from *D. immitis* by histopathology, as described above, or by examination of intact adults. Intact adult *A. vasorum* females have a "barber-pole" appearance due to the helically-arranged red digestive tract and white ovaries.

A. vasorum has a thin coelomyarian musculature, a large strongyloid intestine composed of few multinucleated cells, and a uterus with eggs.[2,4]

A. vasorum, termed "French heartworm" because it was reported first in France in the 1800s, is a metastrongylid nematode considered to be the most pathogenic lungworm of dogs.[1,12] Adults reside in the pulmonary artery and right heart ventricle in canids. Red foxes are the natural definitive hosts and are important reservoirs of infection for domestic dogs. Clinical signs may vary from mild coughing and exercise intolerance to fatal cardiopulmonary disease. *A. vasorum* has a worldwide distribution and the infection seems to be increasing in recent decades.[12] *A. vasorum* has an indirect life cycle in which aquatic and terrestrial snails serve as intermediate hosts.[1] Adult female nematodes shed eggs that are transported to the pulmonary parenchyma. Eggs develop and hatch, releasing first stage larvae that penetrate the alveoli. Larvae are coughed, swallowed, and excreted in the feces. Gastropods become infected with L1 larvae by eating contaminated plant material. In gastropods, L1 mature into L3 larvae. Final hosts become infected by ingestion of snails. Third stage larvae penetrate the gastrointestinal tract, migrate through visceral lymph nodes, and develop into immature adults. Juvenile worms migrate into the caudal vena cava trough the portal circulation and reach maturity in the pulmonary arteries.

A. vasorum may cause right heart failure and extensive pulmonary lesions as a consequence of egg embolization. Gross lesions consist of small, 1-2 mm diameter, red, firm, multinodular to confluent areas of hemorrhage and edema at the lung periphery. A variably severe, multifocal to coalescing, granulomatous to pyogranulomatous interstitial pneumonia with presence of eggs and larvae has been reported, often associated with prominent pulmonary arterial thrombosis. Vascular lesions are characterized by proliferative endarteritis, including thrombosis, thickening of tunica intima by fibromuscular tissue, and medial hypertrophy with infiltration of eosinophils, lymphocytes and plasma cells. Fibrosis and vascular recanalization of arterial thrombi may be seen in chronic cases. Granulomas have also been reported to occur in lymph nodes, brain, kidneys, and adrenal glands.[1,2]

The genus *Angiostrongylus* includes other important parasites, such as *A. cantonensis*, the rat lungworm. This parasite has an obligate neural migration cycle that may cause ascending paralysis and lumbar hyperalgesia in accidental hosts, such as dogs.

The differential diagnosis for pulmonary parasitic infections in dogs includes *Crenosoma vulpis, Eucoleus aerophilus* (formerly *Capillaria aerophila*), *Oslerus osleri* (formerly *Filaroides osleri*)*, Filaroides hirti and Andersonstrongylus milksi* (formerly *Filaroides milksi*).[2] *C. vulpis* infects bronchioli, bronchi and the trachea of wild canids and occasionally domestic canids, leading to chronic coughing.[2,12]

Eucoleus aerophilus is a trichurid nematode that parasitizes wild carnivores, domestic cats, and rarely dogs. The adult lungworms live embedded in the respiratory lining epithelium. Most infections are inapparent; more severe infection may result in catharral inflammation, coughing, secondary bacterial infection, and/or airway obstruction. The adult nematodes are slender, 2-3 cm long, and characterized by presence of bacillary bands (segmental thickenings of the hypodermis), a stichosome (basophilic esophageal gland), and embryonated eggs in the uterus. Eggs are oval with bipolar plugs; their morphology allows differentiation from other nematodes. Females lay eggs where larvae undergo initial development. Eggs are swallowed and are released via the feces. Animals become infected by ingesting embryonated eggs or earthworms bearing embryonated eggs. Hatched larvae migrate to the lungs, where they become adults in 3 to 6 weeks.[2,12]

Oslerus osleri is commonly reported in wild canids.[2] The infection is generally asymptomatic. The parasite induces the formation of single to multiple, 1-10 mm diameter, firm, submucosal nodules in the trachea and bronchi that are most prominent at the tracheal bifurcation. Coiled worms may be grossly visible trough the overlying mucosa. Dead worms may cause a granulomatous to pyogranulomatous reaction. Nodules are circumscribed by fibrous tissue and contain adult parasites or fifth stage larvae. Diagnosis is based on adult worm identification by histology or from crush preparations of tracheal nodules. The adults have coelomyariam musculature, an intestine composed of few multinucleated cells with indistinct microvilli, and embryonated eggs or larvae in the uterus.

Filaroides hirti has been reported in colonies of laboratory beagles with cases described in pet dogs.[2] *F. hirti* has a direct life cycle wherein infective first stage larvae are passed in the feces. Most infections are apparently acquired from the dam. Adults live in the alveoli and respiratory bronchioles. Mostly incidental findings at necropsy, lesions are 1-5 mm diameter gray-tan to black-green nodules in subpleural regions of lungs. Nodules may be white or have cystic centers. Rarely, fatal cases occur in immunosuppressed dogs; in these cases, a severe granulomatous pneumonia has been reported. Histopathology consists of minimal inflammation in response to live adult worms; however, dead parasites induce severe interstitial granulomatous and eosinophilic inflammation.

Andersonstrongylus milksi is a metastrongylid nematode. The literature regarding this parasite is confusing[2] and identification of the adult is necessary to distinguish *A. milksi* from *F. hirti*. Adults inhabit bronchioles and alveoli and the gross and histologic lesions are similar to those caused by *F. hirti*. Larvae have been reported in the brain and internal abdominal organs.

AFIP Diagnosis: 1. Lung, arteries: Endarteritis, proliferative, chronic, multifocal, marked, with organizing thrombi and few intravascular adult metastrongylid and filarid nematodes, etiology consistent with *Angiostrongylus vasorum* and *Dirofilaria immitis*.
2. Lung: Pneumonia, granulomatous, multifocal coalescing, marked, with hemorrhage, fibrosis, and many nematode larvae and eggs.

Conference Comment: This case was reviewed in consultation with Dr. Christopher Gardiner, Consulting Parasitologist for the AFIP's Department of Veterinary Pathology. Much of the discussion during the conference was devoted to the morphological features that distinguish *A. vasorum* from *D. immitis*, as described in the contributor's exceptionally complete review of the entities above. Unlike true strongyles and trichostrongyles, which have platymyarian musculature, metastrongyles, such as *A. vasorum*, have coelomyarian musculature; however, it is greatly attenuated in comparison to the robust coelomyarian musculature that typifies *D. immitis*. As compared to *A. vasorum*, *D. immitis* possesses a much thicker cuticle with distinct lateral internal cuticular ridges, and a much smaller intestine. Finally, the developing and mature larvae in the lungs are readily distinguished from microfilariae by having more developed internal structure; microfilariae, which were not noted in any conference participants' sections, lack internal structure and are therefore often described as a cuticle-bound bag of nuclei.[4]

Conference participants reviewed the classic immune response to invasive nematodes, in which a T_H2 response generally predominates. Briefly, cytokines produced by cells of the innate immune system in response to microbes activate and direct the differentiation of helper T cells in the adaptive immune system. In response to invasive nematodes, interleukin (IL)-4 initiates the differentiation of naïve T cells into T_H2 cells. This differentiation requires the lineage-specific transcription factors GATA3 and c-Maf; differentiated T_H2 cells characteristically produce IL-4, IL-5, and IL-13. Interleukin-4 acts on B cells to stimulate class-switching to IgE, which mediates the cross linking of Fc receptors on mast cells and their activation. Additionally, IL-4 further amplifies the differentiation of T_H2 cells in an autocrine loop, and inhibits the differentiation of T_H17 cells, potent recruiters of neutrophils and monocytes involved in the host defense against extracellular bacteria and fungi. Interleukin-5 activates eosinophils, and IL-13 enhances IgE production, stimulates mucus production by epithelial cells, and stimulates the synthesis of proline, an important constituent of collagen, thereby stimulating fibrosis.[6,8] Conference participants noted the paucity of eosinophils present in this case and speculated on possible explanations, such as glucocorticoid administration or immunosuppression.

Contributor: Dipartimento di Patologia Animale, Igiene e Sanità Pubblica Veterinaria, Sezione di Anatomia Patologica e Patologia Aviare, Facolta' di Medicina Veterinaria, Via Celoria 10, 20133 Milano, Italy
http://www.anapatvet.unimi.it/

References:

1. Bourque AC, Conboy G, Miller LM, Whitney H: Pathological findings in dogs naturally infected with *Angiostrongylus vasorum* in Newfoundland and Labrador, Canada. J Vet Diagn Invest **20:**11-20, 2008
2. Caswell JL, Williams KJ: Respiratory system. *In:* Jubb, Kennedy, and Palmer's Pathology of Domestic Animals, ed. Maxie MG, 5th ed., vol. 3, pp. 645-648. Saunders Elsevier, Philadelphia, PA, 2007
3. Dillon AR, Warner AE, Brawner W, Hudson J, Tillson M: Activity of pulmonary intravascular macrophages in cats and dogs with and without adult *Dirofilaria immitis*. Vet Parasitol **158:**171-176, 2008
4. Gardiner CH, Poynton SL: An Atlas of Metazoan Parasites in Animal Tissues. Armed Forces Institute of Pathology, Washington, DC, 1999
5. Kramer L, Grandi G, Leoni M, Passeri B, McCall J, Genchi C, Mortarino M, Bazzocchi C: *Wolbachia* and its influence on the pathology and immunology of *Dirofilaria immitis* infection. Vet Parasitol **158:**191-195, 2008
6. Kumar V, Abbas AK, Fausto N, Aster JC: Diseases of the immune system. *In*: Robbins and Cotran Pathologic Basis of Disease, eds. Kumar V, Abbas AK, Fausto N, Aster JC, 8th ed., pp. 183-201. Saunders Elsevier, Philadelphia, PA, 2010
7. Maxie MG, Robinson WF: Cardiovascular system. *In:* Jubb, Kennedy, and Palmer's Pathology of Domestic Animals, ed. Maxie MG, 5th ed., vol. 3, pp. 88-89. Saunders Elsevier, Philadelphia, PA, 2007
8. Miossec P, Korn T, Kuchroo VK: Interleukin-17 and type 17 helper T cells. N Engl J Med **361:**888-898, 2009
9. Narine K, Brennan B, Gilfillan I, HIdge A: Pulmonary presentation of *Dirofilaria immitis* (canine heartworm) in man. Eur J Cardiothor Surg **16:**475-477, 1999
10. Paes-de-Almeida EC, Ferreira AMR, Labarthe NV,

Cladas MLR, McCall JW: Kidney ultrastructural lesions in dogs experimentally infected with *Dirofilaria immitis* (Leidy, 1856). Vet Parasitol **113:**157-168, 2003
11. Pampiglione S, Rivasi F, Gustinelli A: Dirofilarial human cases in the Old World, attributed to *Dirofilaria immitis*: a critical analysis. Histopathology **54:**192-204, 2009
12. Taubert A, Pantchev N, Globokar Vrhovec M, Bauer C, Hermosilla C: Lungworm infections (*Angiostrongylus vasorum*, *Crenosoma vulpis*, *Aelurostrogylus abstrusus*) in dogs and cats in Germany and Denmark in 2003-2007. Vet Parasitol **159:**175-180, 2009
13. Theis JH: Public health aspects of dirofilariasis in the United States. Vet Parasitol **133:**157-180, 2005
14. Traversa D, Di Cesare A, Milillo P, Iorio R, Otranto D. Infection by *Eucoleus aerophilus* in dogs and cats: is another extra-intestinal parasitic nematode of pets emerging in Italy? Res Vet Sci **87:**270-272, 2009

CASE II: 09-11870-9 (AFIP 3135619).

Signalment: 5-year-old male, castrated domestic shorthair cat (*Felis catus*).

History: This cat had a history of fever and clinical signs consistent with acute liver failure.

Gross Pathology: Not provided.

Histopathologic Description: Duodenum with pancreatic duct: Diffusely, the villi are short, clubbed, regionally fused, and lined by non-ciliated attenuated epithelium. There is a segmental loss of crypts and the lamina propria within these attenuated areas is collapsed and contains karyolytic and karyorrhectic nuclear debris admixed with small numbers of lymphocytes, plasma cells, and rare macrophages and neutrophils. Crypts are occasionally collapsed and their lumina contain sloughed epithelium admixed with necrotic cellular debris (crypt abscess). Occasionally the crypts are dilated and are lined by attenuated to disorganized hyperplastic epithelium characterized by 2-3 layers of nuclear piling and increased numbers of mitotic figures. Often macrophages contain multiple, intracellular 2-4 um, round basophilic, intracytoplasmic protozoal zoites. Similar individualized tachyzoites are present free within the lamina propria. The underlying submucosa is similarly infiltrated by moderate numbers of lymphocytes, plasma cells, and macrophages (**figs. 2-1 and 2-2**).

Pancreas: Rarely the endocrine islets are effaced and the cells are individualized by a homogenous, pale, eosinophilic material (amyloid).

Immunohistochemistry for parvovirus was positive in the duodenum (**fig. 2-3**). Immunohistochemistry for *Toxoplasma gondii* was positive in the duodenum, lung, liver, spleen, and mesenteric lymph nodes. The liver, spleen, and mesenteric lymph nodes are not submitted.

Contributor's Morphologic Diagnosis: 1. Duodenum: duodenitis, lymphohistiocytic, diffuse, with crypt necrosis and crypt abscesses, epithelial loss and regeneration, collapse of lamina propria, and protozoal tachyzoites.
2. Pancreas: amyloidosis, islet, mild.

Etiologies: Feline panleukopenia virus and *Toxoplasma gondii*

Contributor's Comment: The histologic findings and positive IHC within the duodenum are consistent with feline panleukopenia virus (FPV) and concurrent infection with *Toxoplasma gondii*. Parvoviruses are single stranded DNA viruses. Unlike papillomaviruses, which are double stranded DNA viruses and possess DNA polymerase and genes for inducing mitosis, parvoviruses do not possess DNA polymerase and other genes for inducing mitosis; therefore, parvovirus infects only actively dividing cells, particularly in the S (synthetic) phase of cell division. The enteric, lymphoid, and hematopoietic systems are predominantly affected. Large intranuclear inclusions can sometimes be seen within infected cells.

The mode of FPV exposure is typically oronasal, allowing the virus to infect the tonsillar epithelium. Free virus released into the lymph as well as dissemination of infected lymphocytes results in infection of other lymphoid organs, such as the thymus, spleen, Peyer's patches, and bone marrow. Lymphocytolysis results in lymphopenia as well as viremia. The enteric system and bone marrow are infected following viremia and by circulating infected lymphocytes. Destruction of crypt cells results in villus atrophy and mucosal erosion or ulceration. Infection of the bone marrow causes depletion of myeloid and erythroid precursors. The lymphopenia and secondary bone marrow destruction can result in significant immunosuppression, allowing the animal to become susceptible to normally harmless infectious agents.

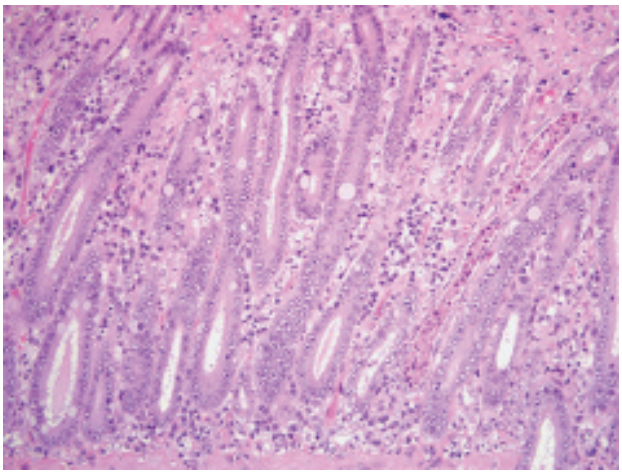

2-1. Duodenum, cat. Many regenerative and ectatic crypts are surrounded by a mild inflammatory cellular infiltrate in the lamina propria. (HE 200x)

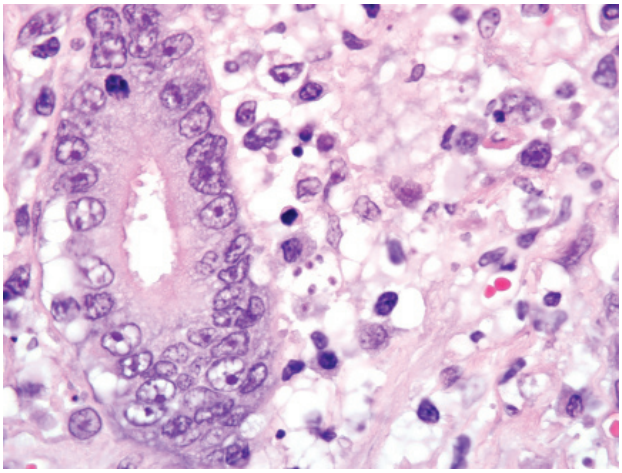

2-2. Duodenum, cat. Multifocally in the lamina propria, macrophages contain 2 – 4um, round, basophilic intracytoplasmic protozoal tachyzoites. The adjacent crypt epithelium is regenerative. (HE 1000x)

Although infection with *Toxoplasma gondii* typically results in seroconversion without clinical disease, immunosuppression due to concurrent FPV infection can allow the protozoa to disseminate systemically, resulting in necrotizing lesions in a multitude of organs, such as the liver, heart, spleen, eye, or brain. Cats are easily infected by ingestion of tissues containing the latent asexual stage (bradyzoite) in latently infected prey animals. Another possible but more difficult route of infection of cats is by direct transmission from ingestion of oocysts passed in the feces of another cat (after exposure to oxygen and time for sporulation).

Once *Toxoplasma* organisms penetrate the intestinal mucosa, the protozoa can spread via lymphocytes to regional lymph nodes, lymph, and the bloodstream, or from the intestine they may pass directly into the portal circulation, allowing dissemination to a variety of organs. Tachyzoites invade (or are phagocytosed by) host cells, proliferate and spread to neighboring cells, causing lysis of host cells upon egress.

AFIP Diagnosis: 1. Small intestine, duodenum: Enteritis, necrotizing, diffuse, moderate, with crypt regeneration, few crypt abscesses, and many intracellular and extracellular protozoal tachyzoites.
2. Pancreas, endocrine: Islet amyloidosis, focal, mild.

Conference Comment: There is substantial slide variation with respect to the severity of islet amyloidosis in this case. As noted by the contributor, the presence of disseminated toxoplasmosis in an adult cat should trigger an investigation for a cause of immunosuppression. In this case, most conference participants appropriately suspected underlying immunosuppression, and considered feline panleukopenia virus (FPV) and feline leukemia virus (FeLV) as the most likely etiologies. During the conference, attendees discussed the histomorphologic features used to distinguish these entities.

This case is unique in that FPV classically affects younger animals after maternal antibodies have waned. Gross lesions of FPV are most consistently discovered in the thymus (e.g. marked involution and reduced mass in young kittens) and intestines (e.g. dry, nonreflective serosa; mucosal, submucosal, and/or muscular petechiae; and segemental dilation and/or increased turgidity). Because the gross intestinal lesions may be subtle, histopathology is indispensable to achieve a definitive diagnosis of FPV enteritis. Microscopic lesions are most consistently found in the intestines, bone marrow, and lymphoid organs. As noted by the contributor, the rapidly dividing crypt epithelial cells are chiefly affected, and early in the course of infection may contain intranuclear inclusion bodies, particularly within cells sloughed into crypt lumina. The likelihood of visualizing inclusions is increased if tissues are fixed in Bouin's solution rather than formalin.[1] Villar enterocytes, which are not actively dividing, are not affected; in the present case, necrosis of villar epithelium is attributed to toxoplasmosis, and crypt regeneration is attributed to FPV.

Because FeLV can cause crypt necrosis in some cats, distinguishing it from FPV depends on examination of the lymphoid and hematopoietic tissues. In early FPV, lymphocytolysis is characteristic in lymphoid organs such

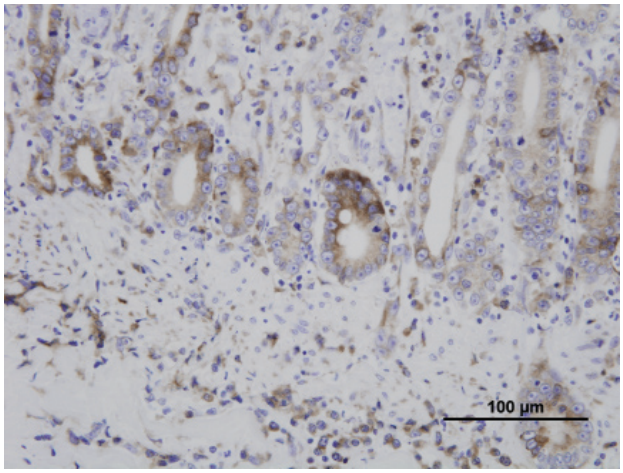

2-3. Duodenum, cat. Immunohistochemistry for feline panleukopenia virus demonstrating positive immunoreactivity. Photographs courtesy of University of Illinois College of Veterinary Medicine pathobiology Department 2522 VMBSB 2001 South Lincoln Ave Urbana IL 61801 mawallig@illinois.edu

as the thymus, lymph nodes, and Peyer's patches; by 7-8 days post-infection, regenerative lymphoid hyperplasia may instead be found. Similarly, early bone marrow lesions include marked depletion of all cell line precursors; this results first in neutropenia, because of the relatively short circulating half-life of neutrophils, followed next by lymphopenia, then finally thrombocytopenia. Bone marrow changes later progress to marked stem cell hyperplasia. In FeLV, by contrast, lymphoid hyperplasia, rather than lymphocytolysis, is typical of early disease. Additionally, enteric FeLV is characterized by associated mononuclear cell inflammation in the mucosa, whereas the enteric lesions of FPV infection contain a paucity of inflammatory cells. Antemortem hematology may also be helpful in distinguishing FPV from FeLV; the former elicits panleukopenia, as suggested by its name and as described above, while the latter results in a nonregenerative anemia. Finally, the detection of viral antigen by immunohistochemistry, as employed in this case, is also useful for distinguishing enteric FeLV from FPV.[1]

Conference participants briefly reviewed several other parvoviruses of importance in veterinary medicine, including canine parvovirus (CPV)-2; canine minute virus (CPV-1); mink enteritis virus; Aleutian mink disease virus; bovine parvovirus; porcine parvovirus; and the parvoviruses of rats, mice, and Syrian hamsters. Receptor binding to the transferrin receptor TfR determines the host ranges of FPV and CPV infection.[1]

In most domestic animal species, with the possible exception of placentitis and abortion in sheep and goats, infection with *Toxoplasma gondii* only rarely causes overt disease. In immunocompetent hosts, cell-mediated immunity, dominated by a T_H1 response, is sufficient to maintain the organism as quiescent tissue cysts, which are non-pathogenic. Systemic toxoplasmosis is generally only seen in neonates or immunocompromised hosts, such as the cat in this case. Specifically, decreased levels of interferon-γ, and resultant impaired ability to activate macrophages, are associated with increased susceptibility to systemic disease.[1] During the conference, the moderator drew parallels between this case and canine toxoplasmosis secondary to canine distemper virus infection. For another example of toxoplasmosis and more detailed review of the entity, readers are referred to WSC 2008-2009, Conference 1, case I.

Contributor: University of Illinois College of Veterinary Medicine, Pathobiology Department, 2522 VMBSB, 2001 South Lincoln Avenue, Urbana, IL 61801
http://vetmed.illinois.edu/path/

References:

1. Brown CC, Baker DC, Barker IK: Alimentary system. *In:* Jubb, Kennedy, and Palmer's Pathology of Domestic Animals, ed. Maxie MG, 5th ed., vol. 2, pp. 134-135, 176-183, 270-272. Saunders Elsevier, Philadelphia, PA, 2007

CASE III: 08 B 14569 10 (AFIP 3138188).

Signalment: 10-month-old, Angus-cross steer (*Bos taurus*).

History: These calves were purchased as stocker calves between 6 and 9 months of age. The calves were being fed a ration composed of millet hay, wet beet pulp, and whole corn, with access to protein blocks containing monensin. At 10 months of age, seven calves demonstrated abrupt onset of neurological signs, including behavioral changes (apprehension and aggression), staggering, muscle twitching/fasciculation, recumbency, and opisthotonos, followed shortly by death. Several calves were treated with broad-spectrum antibiotics, thiamine, calcium gluconate, and a variety of corticosteroids with no response. Three calves were examined postmortem by the referring veterinarian and samples were collected on two calves for histopathology and associated testing.

Gross Pathology: Per the submitting veterinarian, all three calves demonstrated some combination of the following: subcutaneous edema, mild subcutaneous hemorrhages, visceral congestion, ascites, pulmonary edema and emphysema, and hepatomegaly, with enlarged congested livers having a prominent "mottled" or lobular pattern on surface and section.

Laboratory Results: Fresh tissues were received from two calves. Bacterial culture attempts did not yield growth of any significant aerobic or anaerobic pathogens from the lung, liver, or small intestine. Fluorescent antibody tests for a variety of viral pathogens (i.e. infectious bovine rhinotracheitis, parainfluenza-3, and bovine respiratory syncytial virus) were negative and virus isolation attempts on pooled tissue homogenates were negative (bovine embryonic testis cells). A serum chemistry panel and complete blood count performed on one calf revealed the following abnormalities: elevated ALP, AST, CK, GGT and LDH; evidence of mild dehydration (elevated PCV and hemoglobin); and a mild leukocytosis with neutrophilia. Tissue (liver) levels of lead, arsenic, mercury, copper, selenium, and several other metals were within normal limits. A developmental (not commercially available) thin-layer chromatography assay detected a "significant" (not quantified) level of carboxyatractyloside in rumen contents from both calves tested.

Histopathologic Description: Striking lesions are confined to the liver for both calves, and include diffuse acute hepatocellular necrosis most severe in centrilobular, and to a lesser extent, midzonal areas (zones 3 and 2), generally sparing periportal (zone 1) hepatocytes. In some sections there also is patchy sinusoidal congestion and pooling of blood, mild vacuolar change of remaining hepatocytes in zone 1, and variable, but light infiltrates of inflammatory cells (predominantly neutrophils) in sinusoids and attending necrotic hepatocytes (**figs. 3-1 and 3-2**). Other changes observed microscopically include diffuse pulmonary congestion and edema with multifocal emphysematous bullae and subtle changes suggestive of cerebral edema.

Contributor's Morphologic Diagnosis: Hepatocellular necrosis, marked, acute, diffuse, centrilobular and midzonal (zones 3 and 2), with multifocal congestion/hemorrhage and multifocal mild hepatocellular vacuolar change.

Contributor's Comment: Zone 3 (periacinar or centrilobular) necrosis is the most common form of zonal hepatocellular necrosis observed in domestic animals, including cattle, and is a relatively stereotyped response/lesion that may be caused by a variety of infectious, inflammatory, metabolic, and toxic insults.[4] Given the clinical history and microscopic findings in this case, a toxic etiology was suspected, particularly a toxic plant incorporated into the millet hay. Other etiologies, such as cyanobacteria (blue-green algae) and molybdenum toxicosis, were considered less likely given the controlled diet, season (winter), and location (western Nebraska). Examination of rumen contents from two affected calves and of the millet hay incorporated into the feed ration revealed abundant mature burs or fruits of the common cocklebur plant (*Xanthium strumarium*), and thin-layer chromatography analysis of rumen contents from both calves demonstrated a "significant" amount of the cocklebur toxic principle, the diterpenoid glycoside carboxyatractyloside.[4,5]

Carboxyatractyloside and other atractylosides are inhibitors of cellular oxidative phosphorylation, and act specifically by binding to and inhibiting ADP/ATP carriers, leading to ATP depletion and subsequent mitochondrial dysfunction, ion pump failure, lipid peroxidation, and glutathione depletion resulting in cellular apoptosis and/or necrosis.[4,5] All members of the *Xanthium* genus seem to produce carboxyatractyloside, and other plants in the families Asteraceae and Compositae may produce the same or similar glycosides causing similar clinical syndromes in susceptible species, including cattle, sheep, swine, and humans.[2,3,5-8]

The common cocklebur, a coarse herbaceous annual, is common throughout much of the United States; it grows

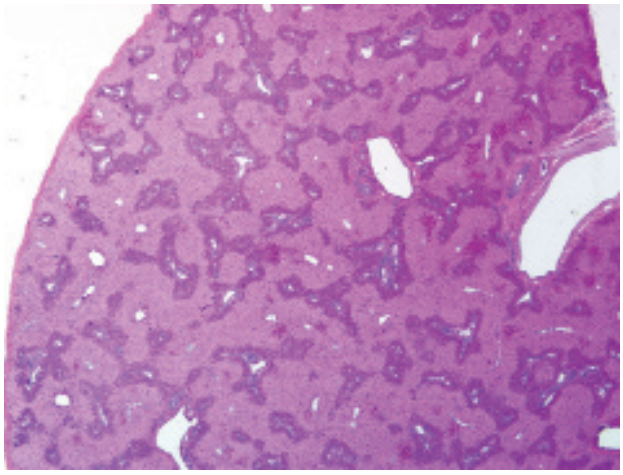

3-1. Liver, calf. There is diffuse centrilobular to midzonal hepatocellular necrosis, with sparing of a thin rim of periportal hepatocytes. (HE 12.50x)

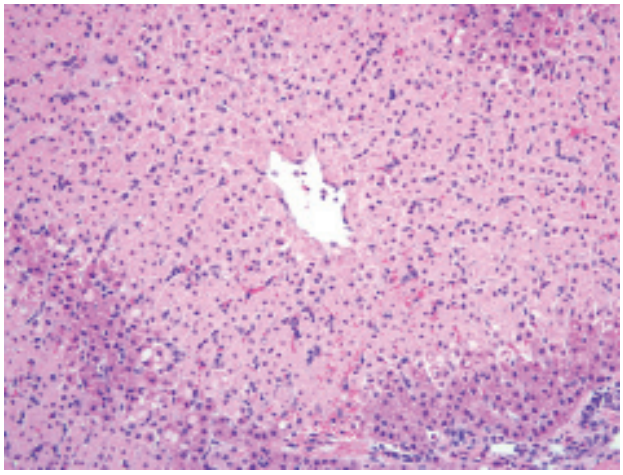

3-2. Liver, calf. Centrilobular and midzonal hepatocytes are pale, swollen, with pyknotic nuclei (coagulative necrosis). (HE 200x)

to a mature height of 2-5 feet, with an erect, often angled stem, and alternate, triangular or heart-shaped rough leaves. The plant produces hard, prickly, oval fruits or burs approximately 0.75 inches long containing two seeds; these can be found entangled in the coats of livestock and long-haired dogs. The plants are invasive and are often found growing in pastures and meadows (especially those with a history of previous or seasonal flooding), along fencerows, in roadside ditches, along stream and pond banks, in dried out ponds or stock reservoirs, and occasionally in disturbed areas in feedlots.[7]

Cocklebur poisoning is most common in the spring or early summer, associated with the ingestion of germinated seeds and palatable young dicotyledon seedling plants that are high in the toxic principle, carboxyatractyloside; adult plants contain relatively little toxin, other than in seeds or burs. Most poisonings seem to occur in pigs foraging naturally, but the plant is toxic to a wide range of animals, including ruminants, horses, dogs, rats, and humans; most cases of toxicity in these species are caused by incorporation of seedlings or mature plants with seeds into feed rations (hay, haylage, silage, or grain rations).[2,3,6,8] As with the submitted case, there are several reports of poisoning in cattle associated with the presence of mature cocklebur plants and seeds (burs) in hay.[8]

Common clinical signs observed with cocklebur poisoning include anorexia, depression or other behavioral changes including apprehension or excitability, blindness, ataxia, twitching progressing to spasmodic muscle contractions or convulsions, recumbency, opisthotonos, and rapid progression to death. Clinical signs may follow ingestion of the plant by as short a period as several hours in monogastric animals and may be delayed for a day or so in ruminants. Characteristic gross lesions of cocklebur poisoning are not specific, but can include ascites and various effusions, hemorrhages (associated with consumption of clotting factors), hepatic swelling, congestion and mottling, fibrin tags on serosal surfaces of viscera, renal congestion, and gastrointestinal congestion.[2,4,8] Microscopic lesions generally are confined to the liver, with characteristic centrilobular/periacinar (zone 3) to midzonal (zone 2) or rarely panzonal hepatocellular degeneration, necrosis, and apoptosis with congestion and/or hemorrhage; however, lesions also may be observed in the kidney (e.g. tubular epithelial degeneration and necrosis) and brain (e.g. neuronal degeneration/necrosis and cerebral edema) on occasion.[2,4,5,8] Diagnosis of cocklebur poisoning generally requires some combination of the following: 1) evidence of ingestion of cotyledonary seedlings or seeds/burs, 2) appropriate history and clinical signs, 3) characteristic clinical pathology findings, and 4) consistent gross and microscopic lesions. Diagnostic assays that detect the toxic principle in tissues or other biological samples have been or are being developed, but none are routinely or widely available to veterinary diagnosticians.

Treatment of affected animals is generally unrewarding once clinical signs have progressed to the neurological stage, and there is no antidote for the toxic principle; supportive care and therapy aimed at increasing gastrointestinal clearance of ingested plants, decreasing gastrointestinal absorption of the toxin, and treating metabolic and neuromuscular complications all have been shown to be effective on occasion. Prevention of poisoning is more effective than treatment of clinical cases, and can be achieved by elimination of plant populations (e.g.

mowing before seed production begins, use of herbicides, limiting access to contaminated pastures and meadows, manual removal of plants from hay fields, etc.).

AFIP Diagnosis: Liver: Hepatocellular necrosis, coagulative, centrilobular and midzonal (submassive), acute, diffuse.

Conference Comment: In WSC 2009-2010, Conference 12, case IV, we discussed the reasons why centrilobular hepatocytes are particularly susceptible to hypoxic injury and to indirect-acting toxins that undergo biotransformation through cytochromes P450. This superb example of centrilobular to midzonal hepatocellular necrosis due to cocklebur ingestion provides a timely reminder of the importance of pattern recognition in the evaluation of hepatic lesions. We thank the contributor for a concise overview of the entity.

The bulk of the discussion during the conference was focused on toxic plants that cause centrilobular to midzonal hepatocellular necrosis. Several of these are summarized in the table below:[1]

Hepatotoxic Plants Causing Centrilobular Necrosis

Plant Family	Plants	Species Affected	Toxic Principle
Compositae	*Xanthium* spp.	Pigs, cattle	Carboxyatractyloside
Myoporaceae	*Myoporum* spp.	Pigs, cattle, sheep, horses	Furanosesquiterpenoid oils (ngaione)
Leguminosae	*Cassia* spp.	Cattle	Unknown
Ulmaceae	*Trema aspera*	Cattle, sheep, goats	Trematoxin
Solanaceae	*Cestrum parqui*	Cattle, sheep	Saponins
Zamiaceae Cycadaceae Strangeriaceae		Cattle, sheep, goats, dogs	Methoxymethanol
Fabaceae	*Indigofera linnaei*	Cattle, dogs	Indospicine
Cyanophyceae	*Microcystis* spp. *Aphanizomenon* spp.	Cattle, sheep, goats, horses, dogs	Microcystins, others

As mentioned by the contributor and well-illustrated by this case, the investigation of a suspected plant intoxication often involves linking a number of pieces of evidence, including clinical signs, pathological and clinical pathological findings, examination of the feed and/or environment for the offending plant(s), and ancillary diagnostics, when available. In this case, the use of an investigational assay to detect carboxyatractyloside in rumen contents proved helpful in substantiating the diagnosis.

Contributor: Wyoming State Veterinary Laboratory, University of Wyoming, 1174 Snowy Range Road, Laramie, WY 82070
http://uwadmnweb.uwyo.edu/vetsci/
http://wyovet.uwyo.edu/

References:

1. Cullen JM: Liver, biliary system, and exocrine pancreas. *In:* Pathologic Basis of Veterinary Disease, eds. McGavin MD, Zachary JF, 4th ed., p. 441. Mosby Elsevier, St. Louis, MO, 2007
2. Martin T, Stair EL, Dawson L: Cocklebur poisoning in cattle. J Am Vet Med Assoc **189:**562-563, 1986
3. Mendez, MC, dos Santos RC, Riet-Correa F: Intoxication by *Xanthium cavanillesii* in cattle and sheep in southern Brazil. Vet Human Toxicol **40:**144-147, 1998
4. Stalker MJ, Hayes MA: Liver and biliary system: toxic hepatic disease. *In:* Jubb, Kennedy, and Palmer's Pathology of Domestic Animals, ed. Maxie MG, 5th ed., vol. 2, pp. 368-369. Saunders Elsevier, Philadelphia, PA, 2007
5. Stuart, BP, Cole RJ, Gosser HS: Cocklebur (*Xanthium*

strumarium, L. var. *strumarium*) intoxication in swine: review and redefinition of the toxic principle. Vet Pathol **18:**368-383, 1981
6. Turgut M, Alhan CC, Gurgoze M, Kurt A, Dogan Y, Tekatli M, Akpolat N, Aygun D: Carboxyatractyloside poisoning in humans. Ann Tropical Paediatr **25:**125-134, 2005
7. Whitson TD, Burrill LC, Dewey SA, Cudney DW, Nelson BE, Lee RD, Parker R, Ball DA, Cudney D, Dewey SA, Elmore CL, Lym RG, Morishita DW, Swan DG, Zollinger RK: Common cocklebur. *In:* Weeds of the West, ed. Whitson TD, 9th ed., pp. 194-195. Western Society of Weed Science/Western United States Land Grant Universities Cooperative Extension Service/University of Wyoming, Laramie, WY, 2001
8. Witte ST, Osweiler GD, Stahr HM, Mobley G: Cocklebur toxicosis in cattle associated with the consumption of mature *Xanthium strumarium*. J Vet Diagn Invest **2:**263-267, 1990

CASE IV: V08-28214 (AFIP 3141624).

Signalment: 1-year-old, female, spayed, Labrador retriever dog (*Canis familiaris*).

History: The dog, which lived in Kansas for a period, presented to the referring veterinarian in respiratory distress and was sent to the emergency clinic. The dog deteriorated significantly and was supplemented with nasal oxygen. The dog died later and was submitted for necropsy examination.

Gross Pathology: The dog was in normal body condition with mild postmortem autolysis. There was a linear midline incision on the ventral abdomen. The lungs were dark red and firm with a granular texture, and did not collapse when the thoracic cavity was opened. The hilar lymph nodes were moderately enlarged, congested and "wet" on cut surface.

Laboratory Results: Bacterial culture from the lung, liver and blood was negative. *Blastomyces dermatitidis* and *Penicillium* sp. were isolated by fungal culture.

Histopathologic Description: Lung: In multifocal to coalescing areas, the alveoli contain moderate to large numbers of intact and degenerate neutrophils and macrophages, fewer foreign body type multinucleated giant cells, lymphocytes, plasma cells, fibrin, edema fluid and eosinophilic cellular and karyorrhectic debris (necrosis). The inflammatory infiltrate surrounds large numbers of round to oval, 8-25 µm yeasts with a thick, double-contoured wall, basophilic central zone and broad-based budding. A few macrophages and/or multinucleated giant cells contain organisms within their cytoplasm. Multifocally alveolar septa are thickened and infiltrated by inflammatory infiltrate similar to that described previously. The pulmonary capillaries and larger blood vessels are congested and there are multiple hemorrhages scattered throughout some sections. Multifocally, perivascular and peribronchiolar spaces are distended by edema. Although the organisms are readily visible in H&E staining, PAS and GMS stains more selectively demonstrate the outer wall (**figs. 4-1 and 4-2**).

Contributor's Morphologic Diagnosis: Lung: Pneumonia, pyogranulomatous and necrotizing, multifocal to coalescing, severe with intra- and extracellular budding yeasts, etiology consistent with *Blastomyces dermatitidis*, Labrador retriever, canine.

Contributor's Comment: North American blastomycosis is a systemic disease caused by *Blastomyces dermatitidis*, a dimorphic fungus that mainly affects dogs and humans. The disease in humans was first described in 1894; since then it has been documented in many species of vertebrate animals such as cats and horses, as well as captive non-domestic animals such as sea lions, wolves, ferrets, polar bears, tigers, cheetahs and snow leopards.[6] More recently blastomycosis was identified in a rhesus monkey.[9]

Geographically, the disease mainly occurs in North America, with occasional infections in Africa, Europe, Asia and Central America. In North America, the Mississippi, Ohio and St. Lawrence river basins; northern Ontario; the Mid-Atlantic states; and the Canadian provinces of Quebec and Manitoba have had endemic infections.[1] Sporadic cases have been described in New York. The prevalence of blastomycosis is 10 times higher in dogs than in humans, with occasional simultaneous infections; therefore, dogs are considered sentinels for human disease.[2]

Blastomyces dermatitidis is thought to originate from the soil; however, the organism is not commonly recovered at the suspected exposure sites. In the environment it grows as mycelia, requiring sandy, acidic soil and proximity to water; it causes disease to animals by inhalation of the

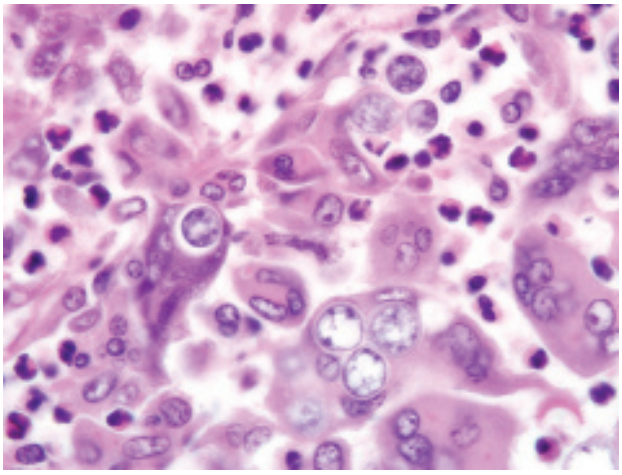

4-1. Lung, dog. Alveoli contain many degenerate neutrophils, lymphocytes, plasma cells, epithelioid macrophages, and fewer multinucleated giant cells that often contain round yeasts with a thick, double-contoured wall and basophilic central zone; yeasts occasionally demonstrate broad-based budding. (HE 1000x)

spores.[1] The mycelial form converts to the yeast form in the terminal bronchioles of the lung, then disseminates to other preferred sites in the body via the blood and lymphatic vessels. In dogs these include the skin, eyes, bones, lymph nodes, subcutaneous tissues, external nares, brain and testes. Less commonly the mouth, nasal passages, prostate, liver, mammary gland, vulva and heart also might be affected. Skin lesions may be caused by local inoculation. Intestinal lesions are uncommon in dogs with systemic disease. Subclinically infected dogs are very rare. Experimentally infected dogs develop mild lesions, but with much higher frequency than for other systemic mycoses. However, the disease in experimentally infected dogs is mostly mild and the animals recover without treatment.[4] Lung lesions may resolve by the time other organs present with signs of infection. The lesions normally present as either granulomas with many epithelioid and giant cells, or pyogranulomatous foci that consist of necrotic neutrophils and macrophages.[6]

The virulence factors of *B. dermatitidis* remain mostly unknown and naturally infected animals may have a suppressed immune response, the mechanism of which is not clear. Moreover, it has not yet been determined whether dissemination of the disease depends upon a compromised immune system.[1] An effective immune response requires T lymphocytes targeting a surface adhesion virulence factor *Blastomyces* adhesion 1 (BAD-1) immunodominant antigen (formerly called Wisconsin 1 (WI-1)), a molecule that mediates attachment to the host cells and blocks tumor necrosis factor (TNF)-α production. Antibody responses to BAD-1, although associated with reduced disease severity, were not able to entirely protect against the infection. Moreover, the cell wall polysaccharide α-glucan was also shown to be associated with virulence and to inhibit elimination by macrophages.[6]

Cytologic or histologic evaluation can be used to identify the organism. Usually, the diagnosis is made by demonstrating the yeast bodies in tissue sections or cytologic preparations. Safety measures must be taken because laboratory personnel can become infected by the cultured mycelia.[1,6] Serologic tests are also available but commonly produce false negative results. Measurement of *Blastomyces* antigen in urine or serum by antigen enzyme immunoassay (EIA) is more sensitive than measurement of anti-*Blastomyces* antibodies for the diagnosis of blastomycosis in dogs.[8]

Hypercalcemia has been associated with blastomycosis, and is likely caused by abnormal vitamin D metabolism. The kidneys provide the site of hydroxylation of 25-hydroxy-cholecalciferol to produce active 1,25-dehydroxy- cholecalciferol. Studies suggest, however, that granulomas composed primarily of monocyte derived phagocytes can metabolize 25-hydroxyl-cholecalciferol to calcitriol *in vitro*, providing the extrarenal source for hypercalcemia associated with blastomycosis. The production of calcitriol by the granulomas seems to be de-regulated or mediated differently than by the kidneys.[3]

Multinodular lesions in the lung and other organs must be differentiated from those of other systemic mycoses and metastatic neoplasia that can be distinguished by examination of impression smears or histologic sections. Neoplastic nodules tend to be larger and more variable in size. Other fungi are normally differentiated from *Blastomyces* based on morphologic features. *Blastomyces* cells are yeast-like, multinucleated, spherical, 8-20 µm in diameter, possess thick double walls, and produce single, broad-based buds. *Histoplasma capsulatum* is much smaller (2-4 µm) and found in the cytoplasm of macrophages. *Cryptococcus neoformans* has a thick capsule and cause a mild inflammatory response. Mutant forms of *Cyptococcus* lacking the typical thick capsule might resemble *Blastomyces* and induce a similar granulomatous response, but this fungus displays narrow-based budding. *Coccidioides immitis* is much larger (20-200 µm) and contains endospores. *Blastomyces*, *Cryptococcus* and *Histoplasma* can be differentiated in culture by the presence and morphology of mycelia, conidia, and yeast, respectively.[1] *Histoplasma capsulatum* var. *duboisii* (African histoplasmosis) has narrow-based buds and is not multinucleated. *Aspergillus* organisms

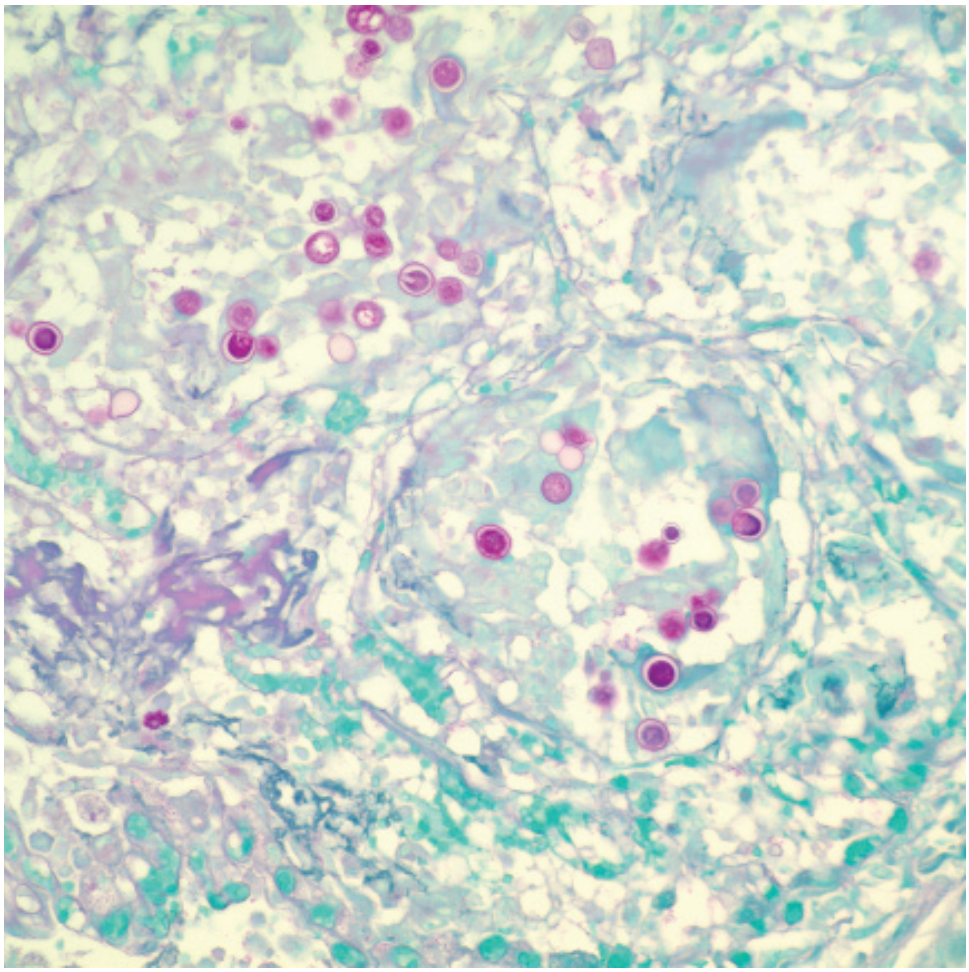

4-2. Lung, dog. The organisms outer is highlighted with PAS staining (PAS). Photographs courtesy of NMDA-Veterinary Diagnostic Services, PO Box 4700, Albuquerque NM, 87196-4700 ftalyor@nmda.nmsu.edu

are septate, thin, and parallel walled with acute-angle dichotomous branching. *Paracoccidioides braziliensis* causes South American blastomycosis and reproduces in tissues by multiple budding.[4]

AFIP Diagnosis: Lung: Pneumonia, pyogranulomatous, diffuse, severe, with edema, hemorrhage, many Langhans and foreign body type giant cells, and myriad intrahistiocytic and extracellular broad-based budding yeasts, etiology consistent with *Blastomyces dermatitidis*.

Conference Comment: The contributor provides an excellent overview of blastomycosis and most of the other etiologies that conference participants considered in the differential diagnosis. Other, less likely considerations mentioned during the conference included protothecosis, chlorellosis, zygomycosis, pythiosis, sporothricosis, mycobacteriosis, and neoplasia (e.g. histiocytic origin or metastatic carcinoma).

Careful consideration of the molecular basis for histomorphologic changes is often useful in their proper interpretation. Both the T_H1 and T_H2 responses are important in cell-mediated immunity to invasive fungi; however, they result in dissimilar histomorphologic changes. The former is typified by the formation of discrete granulomas with the hallmark being epithelioid macrophages, while in the latter neutrophils and activated monocytes and macrophages predominate.[5,7] Conference participants reviewed the mechanisms responsible for T_H1 and T_H17 responses in detail.

In response to intracellular bacteria and fungi, dendritic cells present fungal antigen to naïve T cells and secrete interleukin (IL)-12 which, along with interferon (IFN)-γ, initiates the differentiation of naïve T cells into T_H1 cells. This differentiation requires the lineage-specific transcription factor T-bet; differentiated T_H1 cells characteristically produce IFN-γ and IL-12. Interferon-γ further amplifies the differentiation of T_H1 cells in an autocrine loop, and inhibits the differentiation of T_H17 cells, potent recruiters of neutrophils and monocytes involved in

the host defense against extracellular bacteria and fungi. Interferon-γ induces isotype switching in B cells to favor IgG production, and causes a number of functional and morphological alterations in macrophages, resulting in their activation, e.g. enhanced phagocytosis and killing ability; increased class II major histocompatibility complex expression; and increased production of TNF-α, IL-12, and other proinflammatory cytokines. Interleukin-12, acting synergistically with IL-18, further amplifies the T_H1 response. Tumor necrosis factor-α is an important cytokine in phagocyte-mediated killing of yeast; thus, as mentioned by the contributor, its depressed production in the presence of the BAD-1 antigen impairs the cell-mediated immunity that is vital to the host defense against *Blastomyces dermatitidis*.[5,7]

In response to extracellular bacteria and fungi, naïve T cells under the control of transforming growth factor (TGF)-β plus IL-6 and IL-1, or TGF-β plus IL-21 followed by IL-23, undergo differentiation into T_H17 cells. Transforming growth factor-β, classically characterized as an immunosuppressive cytokine, induces the expression of forkhead box P3 (Foxp3) in naïve T cells, driving the induction of regulatory T cells that suppress inflammation. Interleukin-6 is a potent inhibitor of this pathway, and in combination with TGF-β and IL-1, drives the expression of IL-17 by naïve T cells, committing them to the T_H17 lineage. Activation of the transcription factor ROR-γt in cells committed to the T_H17 lineage causes expression of the receptor for IL-23. Interleukin-23 exposure to these developing TH17 cells enhances IL-17 expression, induces IL-22 expression, and suppresses the expression of IL-10 and IFN-γ, thus stabilizing the T_H17 phenotype. Unlike the signature cytokines produced by cells of the T_H1 and T_H2 pathways (i.e. IFN-γ and IL-4, respectively), IL-17 produced by T_H17 cells does not amplify T_H17 responses in an autocrine loop; rather, IL-21, produced by mature T_H17 cells, in combination with TGF-β, amplifies T_H17 differentiation. Notably, the differentiation of T_H17 cells is inhibited by IFN-γ (T_H1 pathway) and IL-4 (T_H2 pathway).[5,7]

Contributor: NMDA-Veterinary Diagnostic Services, 700 Camino de Salud NE, Albuquerque, NM 87106-4700 http://www.nmda.nmsu.edu/animal-and-plant-protection/veterinary-diagnostic-services

References:

1. Caswell J: Respiratory system. *In:* Jubb, Kennedy, and Palmer's Pathology of Domestic Animals, ed. Maxie MG, 5th ed., vol. 2, pp. 641-642. Saunders Elsevier, Philadelphia, PA, 2007
2. Cote E, Barr SC, Allen C, Eaglefeather E: Blastomycosis in six dogs in New York state. J Am Vet Med Assoc **210:**502-504, 1997
3. Dow SW, Legendre AM, Stiff M, Greene C: Hypercalcemia associated with blastomycosis in dogs. J Am Vet Med Assoc **188:**706-709, 1986
4. Jones TC, Hunt RD, King NW: Veterinary Pathology, 6th ed., pp. 508-510. Williams and Wilkins, Baltimore, MD, 1997
5. Kumar V, Abbas AK, Fausto N, Aster JC: Diseases of the immune system. *In*: Robbins and Cotran Pathologic Basis of Disease, eds. Kumar V, Abbas AK, Fausto N, Aster JC, 8th ed., pp. 183-201. Saunders Elsevier, Philadelphia, PA, 2010
6. Legendre A: Blastomycosis. *In:* Infectious Diseases of the Dog and Cat, ed. Greene CE, 3rd ed., pp. 569-576. Saunders, St. Louis, MO, 2006
7. Miossec P, Korn T, Kuchroo VK: Interleukin-17 and type 17 helper T cells. N Engl J Med **361:**888-898, 2009
8. Spector D, Legendre AM, Wheat J, Bemis D, Rohrbach B, Taboada J, Durkin M: Antigen and antibody testing for the diagnosis of blastomycosis in dogs. J Vet Intern Med **22:**839-843, 2008
9. Wilkinson LM, Wallace JM, Cline JM: Disseminated blastomycosis in a rhesus monkey (*Macaca mulatta*). Vet Pathol **36:**460-462, 1997

The Armed Forces Institute of Pathology
Department of Veterinary Pathology

Conference Coordinator:
Shannon Lacv. DVM. MPH

WEDNESDAY SLIDE CONFERENCE 2009-2010

Conference 17

3 March 2010

Conference Moderator:

Dana P. Scott, DVM, MSS, Diplomate ACVP

CASE I: H-8401 (AFIP 3107575).

Signalment: 24-year-old female chimpanzee (*Pan troglodytes*).

History: Six days prior to death the chimpanzee was stiff, hesitant to move its neck and held its head down. The differential diagnosis included trauma or a neurologic disease. A complete blood count and clinical chemistry panel on the day following presentation revealed a mild leukocytosis and moderate hypokalemia. Radiographs of the cervical region were noncontributory, although physical examination of the area elicited a pain reaction even under anesthesia. Antibiotic and anti-inflammatory therapies were instituted with waxing and waning of results over the next six days and a relatively rapid decline culminating in death.

Gross Pathology: Numerous light brown foci (5-11 mm) were present on the surface (dorsal and ventral) and extending into the neuropil of the brain. Since this animal was housed in an outdoor corral, cross sections of the brainstem and a portion of the hippocampus were submitted for rabies diagnosis (negative) (**fig. 1-1**).

Laboratory Results:

Day 1: Leukocytosis (16.3 k/µl); neutrophilia (13.3 k/µl); and hypokalemia (2.6 mEq/L).
Day 3: Leukocytosis (35.5 k/µl); neutrophilia (31.2 k/µl); and hypokalemia (2.5 mEq/L).
Day 4: Leukocytosis (28.7 k/µl); neutrophilia (22.4 k/µl); and hypokalemia (2.8 mEq/L).
Day 5: Leukocytosis (28.0 k/µl); neutrophilia (22.2 k/µl); and hypokalemia (2.7 mEq/L).

Histopathologic Description: The brain contains a large area of hemorrhage and necrosis with admixtures of neutrophils, mononuclear cells and multinucleated giant cells; cellular debris; fibrinoid necrosis of blood vessels; astrocytosis; and protozoal organisms consistent with *Balamuthia mandrillaris*. Trophozoites measure 30-60 µm. Also observed is a diffuse mild infiltration of mononuclear cells in the meninges and perivascular spaces (**figs. 1-2 and 1-3**).

Contributor's Morphologic Diagnosis: Brain: Multifocal, marked, necrohemorrhagic and pyogranulomatous meningoencephalitis with fibrinoid vasculitis and protozoal organisms consistent with *Balamuthia mandrillaris*.

Contributor's Comment: Balamuthiasis is an

*Sponsored by the American Veterinary Medical Association, the American College of Veterinary Pathologists, and the C. L. Davis Foundation.

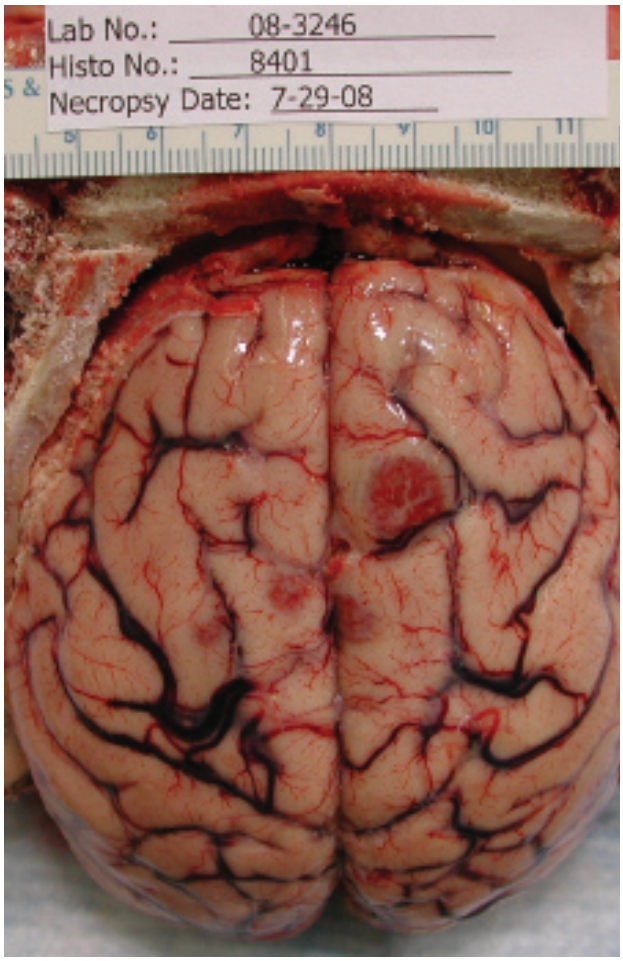

1-1. Cerebrum, chimpanzee. There are multifocal cerebral hemorrhages. Photographs courtesy of The University of Texas M.D. Anderson Cancer Center Michale E. Keeling Center for Comaprative Medicine and Research 650 Cool Water Drive Bastrop, Texas 78602 Wbaze@mdanderson.org

emerging disease of humans and animals with fatal consequences.[4] Originally isolated and identified from a fatal case of meningoencephalitis in a pregnant mandrill (*Papio sphinx*), *Balamuthia mandrillaris* is a free-living amoeba; however, it was not recovered from the environment until 2003.[1,2,5] Encephalitis caused by free-living amoeba (e.g. *Acanthamoeba* and *Balamuthia*) is primarily a problem of immunocompromised patients, although immunocompetent patients are affected by both *Balamuthia* and *Naegleria*.[6] Granulomatous amoebic encephalitis associated with Acanthomeba and Balamuthia is typically slow in developing and insidious, and a hematogenous route of entry has been hypothesized but not proven for these disease agents.[6] By contrast, the rapidly fatal primary amoebic encephalitis associated with *Naegleria* is associated with exposure to freshwater lakes and swimming or water skiing with entry through the olfactory neuroepithelium.[6] The fact that this animal had a ruptured eardrum leads to somewhat of a quandary as to how the agent entered. Lesions in the brain appeared to represent a hematogenous spread; however, no parasitic lesions were observed outside of the central nervous system, and the presence of an open eardrum would appear to provide an open portal of entry.

AFIP Diagnosis: Brain: Meningoencephalitis, necrohemorrhagic, histiocytic and neutrophilic, focally extensive, severe, with vasculitis, fibrin thrombi, and many amoebae.

Conference Comment: In a diagnostic setting, it is often important, but sometimes difficult, to determine whether vascular inflammatory lesions represent true vasculitis or are simply "innocent bystander" vessels caught within foci of inflammation. The conference moderator emphasized the importance of evaluating vessels distant from the most severely affected areas when making this histologic assessment. In this case, conference participants noted striking endothelial hypertrophy, inflammatory cells transmigrating and occasionally disrupting vessel walls, and perivascular accumulations of gitter cells both in severely and less affected areas of the section, and therefore agreed with the contributor's diagnosis of vasculitis.

This case was reviewed in consultation with Dr. Christopher Gardiner, Consulting Parasitologist for the AFIP's Department of Veterinary Pathology; he noted that the large size of the *Balamuthia mandrillaris* trophozoites is helpful in distinguishing it from those of *Naegleria fowleri* and *Acanthomoeba* sp., the two other free-living amoebae most commonly implicated in human and animal disease. Only one case of amebic encephalitis has been attributed to a fourth free-living amoeba, *Sappinia diploidea*. During the conference, participants reviewed the free-living amoebae, emphasizing the important distinguishing morphologic features. *Acanthamoeba* sp. and *B. mandrillaris* are closely related to one another phylogenetically, but are distant from *N. fowleri* and *S. diploidea*. While most *B. mandrillaris* trophozoites are uninucleate, binucleate forms may be seen, and the presence of multiple nucleoli may be useful in differentiating *B. mandrillaris* from *Acanthamoeba* sp. Although trophozoites are more numerous than cysts, the presence of cysts in brain tissue is useful in excluding *N. fowleri*, as only *B. mandrillaris* and *Acanthamoeba* sp. form cysts in the brain. However, the absence of cysts does not exclude a diagnosis of BAE, as cyst formation is not consistent, as the present case illustrates. When present, the cyst

wall of *B. mandrillaris* is unique in that it is three-layered (i.e. composed of an outer ectocyst, inner endocyst, and intervening mesocyst) and lacks pores, whereas the cyst walls of *Acanthamoeba* sp. and *N. fowleri* are two-layered with pores.[3,4]

As mentioned by the contributor, differences in epidemiology and pathophysiology are also useful in differentiating the diseases caused by free-living amoebae. *Acanthamoeba* sp. generally only produces encephalitis in immunocompromised patients, whereas *Balamuthia* amebic encephalitis (BAE) is reported in both the immunocompetent and immunocompromised. By contrast, *N. fowleri* causes primary amebic meningoencephalitis (PAM) in immunocompetent children and young adults, classically within days of exposure to warm fresh waters. Primary amebic meningoencephalitis due to *N. fowleri* has also been reported naturally in bovids and a tapir (see WSC 2007-2008, Conference 22, case IV) and experimentally in a number of mammalian species. Of note, most humans with BAE present with characteristic skin lesions that predate central nervous system signs; such lesions are not characteristic of PAM produced by *N. fowleri*. Intriguingly, individuals of Hispanic origin are overrepresented among human BAE cases in the United States; unique environmental exposures and genetic predispositions have been proposed, but an explanation for this disparity has not been definitively proven. Among animals, BAE is most common in nonhuman primates, but has also been diagnosed in dogs, a sheep, and a horse.[3,4]

The major features that characterize and distinguish the pathogenic free-living amoebae are summarized in the following table, adapted from Schuster and Visvesvara:[3]

Pathogenic Free-living Amoebae

Feature	***Balamuthia mandrillaris***	***Acanthamoeba* sp.**	***Naegleria fowleri***
Diseases	Balamuthia amebic encephalitis (BAE); cutaneous and sinus infections	Amebic encephalitis; cutaneous and sinus infections*	Primary amebic meningoencephalitis (PAM)
Risk factors	Immunocompromised status (also occurs in immuno-competent); breaks in skin contaminated with soil	Immunocompromised status	Activity in warm fresh waters; diving; not associated with immunocompromised status
Incubation period	Weeks to years	Weeks to months	Days
Trophozoite stage	12-60 um	15-30 um	15-30 um
Flagellate stage	Not found	Not found	Flagellate stage with 2 flagella
Cyst stage	3-layered wall lacking pores; 10-30 um diameter; cysts form in brain tissue	2-layered wall with pores; 10-15 um diameter; cysts form in brain tissue	2-layered wall with pores; 7-15 um diameter; cysts do not form in brain tissue

**Acanthamoeba* sp. also is associated with amebic keratitis in immunocompetent humans; risk factors include soft contact lens wear and wearing contact lenses while swimming; incubation period is days (versus weeks to months in systemic infections).

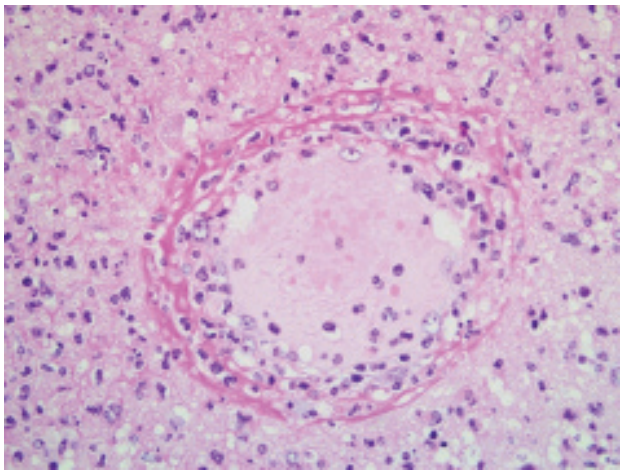

1-2. Cerebrum, chimpanzee. Vessel walls are expanded and disrupted by viable and degenerate neutrophils and macrophages, admixed with necrotic debris (vasculitis); the endothelium is hypertrophied. There is necrosis of the surrounding neuropil. (HE 400x)

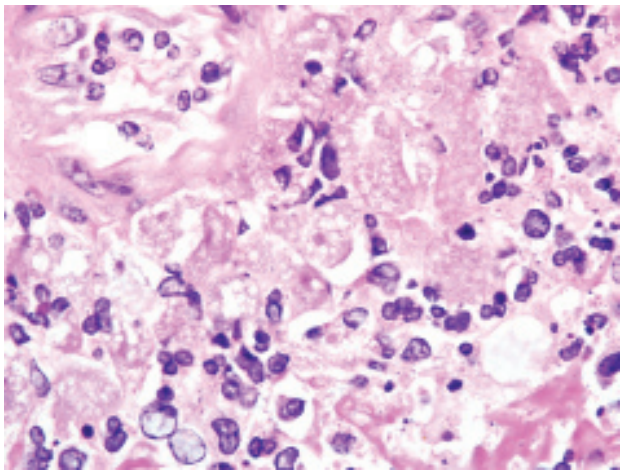

1-3. Cerebrum, chimpanzee. Foci of necrosis contain viable and degenerate neutrophils and macrophages admixed with large (up to 40um) amoebae with vacuolated cytoplasm and a prominent eosinophilic karyosome. (HE 400x)

Contributor: University of Texas MD Anderson Cancer Center, Michale E. Keeling Center for Comparative Medicine, 650 Cool Water Drive, Bastrop, TX 78602
www.mdanderson.org; www.kccmr.org

References:

1. Rideout BA, Gardiner CH, Stalis IH, Zuba JR, Hadfield T, Visvesvara GS: Fatal Infections with *Balamuthia mandrillaris* (a free-living amoeba) in gorillas and other old world primates. Vet Pathol **34:**15-33, 1997
2. Schuster FL, Dunnebacke TH, Booton GC, Yagi S, Kohlmeier CK, Glaser C, Vugia D, Bakardjiev A, Azimi P, Maddux-Gonzalez M, Martinez AJ, Visvesvara GS: Environmental isolation of *Balamuthia mandrillaris* associated with a case of amebic encephalitis. J Clin Microbiol **41:**3175-3180, 2003
3. Schuster FL, Visvesvara GS: Free-living amoebae as opportunistic and non-opportunistic pathogens of humans and animals. Int J Parasitol **34:**1001-1027, 2004
4. Siddiqui R, Khan NA: *Balamuthia* amoebic encephalitis: an emerging disease with fatal consequences. Microb Pathog **44:**89-97, 2008
5. Visvesvara GS, Martinez AJ, Schuster FL, Leitch GJ, Wallace SV, Sawyer TK, Anderson M: Leptomyxid ameba, a new agent of amebic meningoencephalitis in humans and animals. J Clin Microbiol **28:**2750-2756, 1990
6. Visvesvara GS, Moura H, Schuster FL: Pathogenic and opportunistic free-living amoebae: *Acanthamoeba* spp., *Balamuthia mandrillaris, Naegleria fowleri*, and *Sappinia diploidea*. FEMS Immunol Med Microbiol **50:**1-26, 2007

CASE II: A098567 (AFIP 3136043).

Signalment: 5-month-old, female, mixed-breed dog (*Canis familiaris*).

History: This puppy, purchased in Texas, but living in Indiana at presentation, was evaluated for chronic respiratory distress (present since purchase at 8 weeks of age) and a 2-month history of progressive neurologic dysfunction. Littermates had responded to antibiotic therapy for *Bordetella* infection, but this puppy's respiratory condition had not improved. Serum titers were positive for canine distemper virus. Radiographically, the lungs had a diffuse interstitial pattern. A cerebral mass was detected in the frontal/parietal lobes by magnetic resonance imaging. Histologic evaluation of a biopsy specimen of the cerebral mass resulted in a diagnosis of granulomatous amebic encephalitis. The dog died about 36 hours after the cerebral biopsy procedure and was presented for necropsy examination.

Gross Pathology: Gross lesions were found in the brain and thoracic cavity. A friable, dark-brown to tan, 1.3 cm in diameter, roughly spherical mass extended from the dorsal aspect of the right frontal lobe of the cerebrum into the thalamus. The thymus was atrophied. Both lungs were over-expanded, firm, and mottled tan to red-brown. Indistinct, pale gray to tan, coalescing nodules, 1 to 3 mm in diameter, were evident in cross-section (**fig. 2-1**).

Laboratory Results: Frozen lung specimens were submitted to Dr. Visvesvara at the Centers for Disease Control and Prevention (CDC) for identification of the amoebae. The lung was positive by immunofluorescence and real-time PCR for *Acanthamoeba* spp., and negative by both tests for *Balamuthia mandrillaris* and for *Naegleria fowleri*.

Pseudomonas aeruginosa and *Escherichia coli* were isolated from the lung by bacterial culture. The lung and spleen were positive by immunofluorescence for canine distemper virus, and negative for canine adenovirus, herpesvirus, and parvovirus. No virus was isolated from the lung, spleen or brain.

Histopathologic Description: The submitted sections of lung are representative of the pulmonary lesions. Individual and coalescing, poorly demarcated nodules (up to 2 mm in diameter) of granulomatous inflammation were scattered through the pulmonary parenchyma. The centers of the nodules had undergone amorphous to fibrinoid necrosis with scanty hemorrhage.

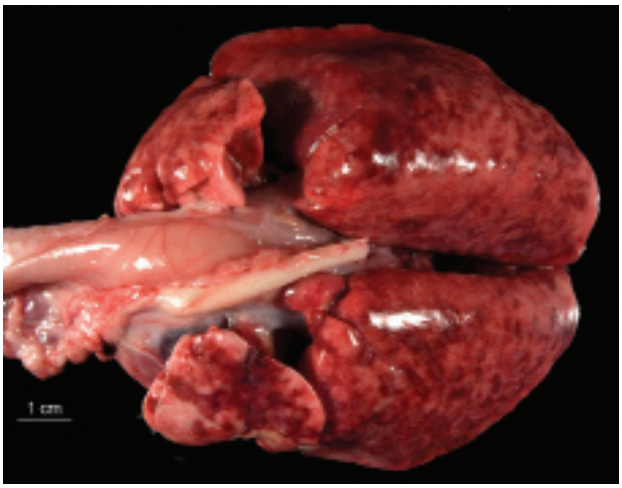

2-1. Lung, canine. Multifocally, there is extensive mottling of the lungs. Photographs courtesy of Animal Disease Diagnostic Laboratory, 406 S. University Street Purdue University, West Lafayette, IN 47907 pegmiller@purdue.edu

Alveolar spaces in necrotic (central) and viable peripheral zones of the nodules were partially filled with neutrophils, macrophages, fibrin, and numerous amoebic trophozoites with fewer cysts. Trophozoites were spherical to ovoid, ranged from 7 to 19 µm in maximal dimension (mean, 14 µm), and had a large nucleus with a prominent karyosome and abundant vacuolated cytoplasm. Encysted amoebae had amphophilic cyst walls, 1-2 µm in thickness, with space between the exocyst and endocyst (**fig. 2-2**).

Where granulomatous inflammation extended to the visceral pleura, overlying mesothelial cells were hypertrophied. Between nodules of granulomatous inflammation, the lung was congested and edematous with increased numbers of alveolar macrophages. Eosinophilic inclusions were observed in the cytoplasm (and less commonly in the nucleus) of bronchiolar epithelial cells and alveolar macrophages; these were labeled immunohistochemically with antibody to canine distemper virus. In other sections (not a feature in the submitted section), sloughed bronchiolar epithelial cells had large amphophilic intranuclear inclusions that were labeled immunohistochemically with antibody to canine adenovirus.

Contributor's Morphologic Diagnosis:
1. Multifocal granulomatous pneumonia with intralesional amebic trophozoites and cysts.
2. Histiocytic alveolitis with eosinophilic cytoplasmic and intranuclear inclusions.

Contributor's Comment: Canine distemper viral

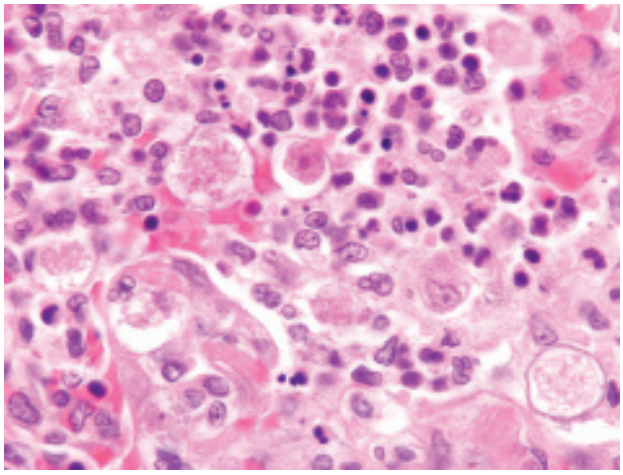

2-2. Lung, canine. Alveoli contain many macrophages, degenerate neutrophils, hemorrhage, and necrotic debris admixed with amoebic cysts and trophozoites. Trophozoites are spherical to ovoid, have a large nucleus with a prominent karyosome (center of field). Cysts have amphophilic cyst walls, 1-2 um in thickness, with a space between the exocyst and endocyst (center and bottom right fields). (HE 1000x)

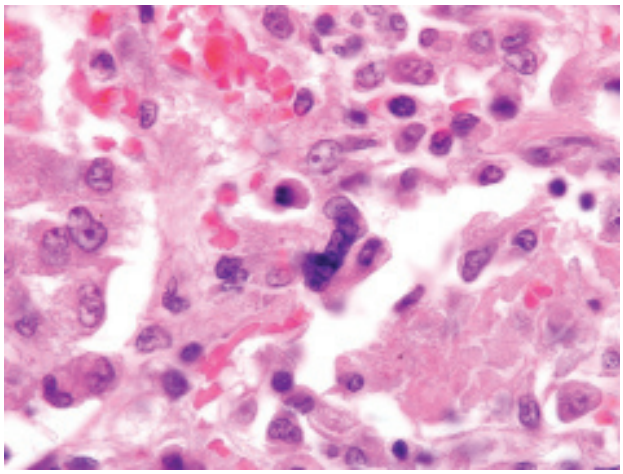

2-3. Lung, canine. Multifocally, alveolar septae contain syncytial cells. (HE 1000x)

infection may have resulted in immunosuppression that predisposed this puppy to other infections. Acanthamoebiasis was considered the most important of these and the cause for granulomatous encephalitis and pneumonia. Amoebae were not detected in tissues other than brain and lung. However, the puppy also had histologic evidence of pulmonary infection with canine adenovirus and oral candidiasis.

Acanthamoeba, Balamuthia, and *Naegleria* species are the free-living amoebae that have been associated with encephalitis and disseminated infection in dogs and humans.[2] In histologic sections, recognition of nuclear features, such as the prominent karyosome and lack of peripheral chromatin, is useful in distinguishing amebic trophozoites from macrophages. In this case, the presence of cysts in addition to trophozoites in infected tissues tended to eliminate *Naegleria* from the differential diagnosis, but definitive diagnosis of *Acanthamoeba* infection was based on immunofluorescence and PCR results (performed on lung specimens). Some reported canine cases of acanthamoebiasis have had granulomatous encephalitis and pneumonia [1], and it has been proposed that pulmonary infection is the result of inhalation or aspiration of the organism from water with hematogenous extension to the brain. However, amebic encephalitis has also been recognized in a dog with widely disseminated acanthamoebiasis in which no organisms were detected in the lungs.[2]

AFIP Diagnosis: 1. Lung: Pneumonia, pyogranulomatous, multifocal, severe, with necrosis and many amebic trophozoites and few amebic cysts.
2. Lung: Pneumonia, bronchointerstitial, diffuse, moderate, with alveolar histiocytosis, type II pneumocyte hyperplasia, viral syncytia, and few bronchiolar and histiocytic intranuclear and intracytoplasmic viral inclusion bodies.

Conference Comment: Like several others evaluated in recent WSC sessions, this case demonstrates the importance of searching for an underlying cause of immunosuppression upon the identification of an opportunistic pathogen. In this case, the extensive pyogranulomatous nodules in the lung were clearly evident to conference participants as the predominant lesion. Following description of the most striking lesions, the conference moderator encouraged participants to carefully examine the remainder of the lung; closer examination, beyond cursory subgross perusal, reveals diffuse bronchointerstitial pneumonia attributed to canine distemper virus infection (**fig 2-3**). Slide variation is present, and the characteristic intranuclear and intracytoplasmic eosinophilic viral inclusions are rare in some sections, underscoring the utility of molecular diagnostics (e.g. immunohistochemistry) as employed in this case. Additional microscopic findings noted by conference participants include multifocal hypertrophy of the pleural mesothelium, and in some sections, small aggregates of extracellular and intrahistiocytic coccobacilli (consistent with the bacterial culture results reported by

the contributor).

Conference attendees compared and contrasted cases I and II of this conference, and continued the discussion of pathogenic free-living amoebae, as summarized in the conference comment for case I. This case differs from case I by the presence of numerous cyst forms, the walls of which are Periodic Acid-Schiff (PAS)-positive. Additionally, systemic acanthamoebiasis is associated almost exclusively with immunosuppression, as noted above, whereas balamuthiasis occurs in both immunocompromised and immunocompetent hosts. Primary amebic encephalitis caused by *Naegleria fowleri* is not associated with immunocompromise. Interestingly, *Acanthamoeba* keratitis is a disease of immunocompetent humans associated with corneal trauma or improper contact lens hygiene, and carries a far better prognosis than does *Acanthamoeba* encephalitis.[3]

We thank Dr. Christopher Gardiner, Consulting Parasitologist for the AFIP's Department of Veterinary Pathology, for reviewing this case.

Contributor: Animal Disease Diagnostic Laboratory, 406 South University Street, Purdue University, West Lafayette, IN 47907
Animal Disease Diagnostic Laboratory: http://www.addl.purdue.edu/
Department of Comparative Pathobiology: http://www.vet.purdue.edu/cpb/

References:

1. Bauer RW, Harrison LR, Watson CW, Styer EL, Chapman WL: Isolation of *Acanthamoeba* sp. from a greyhound with pneumonia and granulomatous amebic encephalitis. J Vet Diagn Invest **5:**386-391, 1993
2. Dubey JP, Benson JE, Blakely KT, Booton GC, Visvesvara GS: Disseminated *Acanthamoeba* sp. infection in a dog. Vet Parasitol **128:**183-187, 2005
3. Schuster FL, Visvesvara GS: Free-living amoebae as opportunistic and non-opportunistic pathogens of humans and animals. Int J Parasitol **34:**1001-1027, 2004

CASE III: T09-1217 (AFIP 3149412).

Signalment: 8-year-old, captive-bred, male rhesus macaque (*Macaca mulatta*).

History: This rhesus macaque was on a pharmacology protocol with indwelling vascular catheters and ports. The catheter and port had to be moved several times due to loss of catheter patency and infection. The animal was placed on long term antibiotics and found down in its cage. Bacterial culture of the port area was positive for coagulase-positive *Staphylococcus* spp. resistant to all fluoroquinolones. The animal was febrile with a holosystolic heart murmur. Clinical pathology revealed mild anemia, leukocytosis and neutrophilia with a left shift (see below). The animal was given fluids and cefazolin but it died overnight.

Gross Pathology: Externally, there was a 1 cm diameter ulcerated cutaneous lesion on the right thigh adjacent to the tunneled area for the vascular line and the point of entry into the femoral vessel. The lungs were diffusely congested and edematous with blood tinged froth in the trachea and nares. The stomach contained red tinged mucus. Multifocal areas of the liver were firm and paler than adjacent tissue. The kidneys were bilaterally enlarged with multifocal yellow-white foci throughout. There were "chicken fat" clots in both ventricles of the heart. The right atrioventricular valve had an adherent vegetative lesion and a fibrotic valve leaflet. The vena cava contained a large thrombus. The spleen was firm and meaty. There was moderate acute hemorrhage within the meninges.

Laboratory Results: CBC and clinical chemistry: PCV 30%, WBC 16 k/µl (PMN 90% with 5% bands), BUN 28 mg/dL, creatinine 0.9 mg/dL, ALT 131 U/L, total protein 6.7 g/dL; Microbiology of port area: *Staphylococcus* spp., coagulase positive, enrofloxacin resistant.

Histopathologic Description: Kidney: Diffusely, the renal cortex demonstrates numerous prominent, large glomeruli and a focal area of infarction with inflammatory effacement of the parenchyma. The infarcted area is composed of several enlarged and obliterated glomerular capsules filled with primarily neutrophils that efface the glomerular tufts and extend into the surrounding tubules. Bacterial (coccoid) colonies can sometimes be seen in these abscessed glomeruli. There is multifocal hemorrhage and coagulative necrosis of adjacent tubules characterized by bright eosinophilic cytoplasmic staining, loss of nuclei and retention of tubular shape. Diffusely

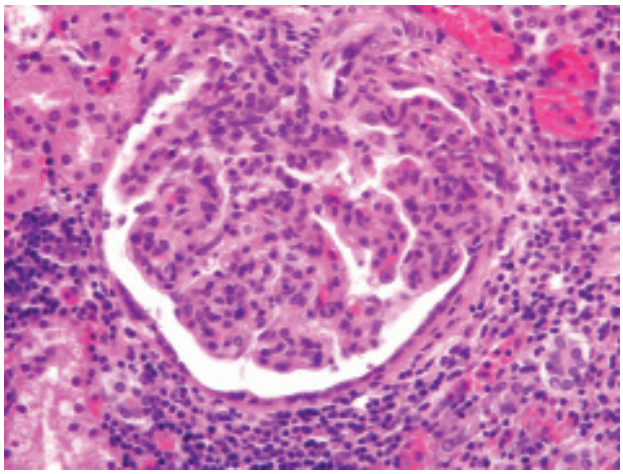

3-1. Kidney, rhesus macaque. The expanding the periglomerular interstitium are numerous lymphocytes, macrophages, and plasma cells. The glomerular tufts are hypercellular, and there is parietal and visceral epithelial hypertrophy and hyperplasia with synechiae. (HE 200x)

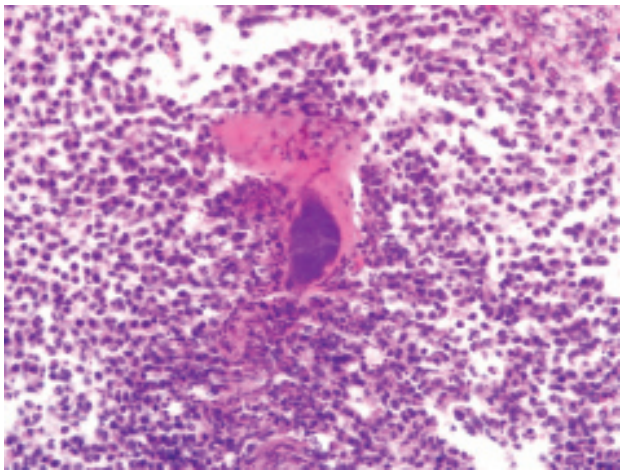

3-2. Kidney, rhesus macaque. Multifocally within the cortex there are large colonies of bacteria surrounded by many viable and degenerate neutrophils and necrotic cellular debris. (HE 200x)

the glomeruli are enlarged, with increased numbers of glomerular tufts; capillaries and occasional glomeruli also demonstrate increased eosinophilic matrix. Some glomeruli demonstrate increased periglomerular fibrosis and synechiae. Multifocally there are aggregates of lymphocytes in the interstitium and random increases of interstitial fibrous connective tissue. An arcuate vessel is occluded by eosinophilic fibrillar material and surrounded by subacute inflammation (**figs. 3-1 and 3-2**).

Contributor's Morphologic Diagnosis: Kidney, bilateral:

1. Infarction and abscessation, multifocal, subacute, severe with coagulative tubular necrosis and bacterial (cocci) colonies.
2. Glomerulopathy, membranoproliferative and mesangioproliferative, diffuse, severe with mild sclerosis.
3. Nephritis, interstitial, lymphoplasmacytic, chronic diffuse, mild.
4. Thrombosis, arcuate artery, focal.

Contributor's Comment: The acute pulmonary edema was likely the cause of death in this animal, interpreted to be caused by zealous fluid administration with impaired kidney clearance, endocarditis and pulmonary thrombi. The cardiovascular lesions were the direct result of chronic indwelling catheterization with subsequent infection. There was disseminated thrombosis involving multiple organs including the liver, heart, cerebrum, and mesentery. The renal lesions were likely the result of both vascular disease and chronic inflammation.

Indwelling catheters are convenient tools for the administration of compounds tested for pharmaceutical safety and effectiveness research. Cynomolgus monkeys, rhesus monkeys and baboons are commonly used in these studies, often involving psychoactive compounds with subsequent behavioral testing paradigms. Catheters may be tolerated successfully for years if appropriate care is taken to prevent infection. The use of vascular access ports has reduced the numbers of infections due to the closure and healing of the skin, preventing casual exposure. However, ports or extravasated materials into the port pocket may cause focal necrosis with ulceration and exposure of the apparatus.

The formation of infarcts associated with thrombosis and embolization is not as difficult a concept as the pathogenesis of immune complex glomerulonephritis. Several texts have covered this subject extensively, and participants are encouraged to review the mechanisms of membranous, membranoproliferative, and mesangioproliferative glomerular changes.

Several studies of indwelling catheters in baboons have revealed infarcts, septic embolic nephritis and mesangioproliferative glomerulonephritis. Bacteria isolated were *Aciteobacter* (*Herella*) sp., *Streptococcus* sp., *Klebsiella* sp., *Staphylococcus* sp., and *Providencia* sp. Immunofluorescence studies in six animals on frozen sections revealed granular deposits of IgG (6/6), IgM (5/6), C3 (4/6), and IgA and C4 (2/6) in glomerular lesions. Additionally the IgG deposits correlated with the severity of the lesions. Bacterial antigens were seen in three of six cases, strongly suggesting immunological mediation.[3]

Baboons in a second study demonstrated renal and hepatic impairment related to long-term catheterization. The renal lesion in that study was described as membranoproliferative glomerulonephritis with dense deposits noted ultrastructurally in a variety of locations, with mesangial cell interpositioning and foot process fusion. These alterations were found in conjunction with the isolation of *Staphylococcus aureus* from the blood and catheters.[4] Sheep have been used to study renal infarcts and chronic indwelling catheters. Bacterial species isolated differed from those found in primates and humans, but membranoproliferative glomerulonephritis and mesangial immune complex deposition were present in clinically asymptomatic sheep.[6]

In a retrospective study of renal tissue from 62 humans with confirmed infective endocarditis, common renal lesions noted were localized infarcts in 31%, and acute glomerulonephritis in 26%. The most common type of glomerulonephritis was vasculitic, without deposition of immunoproteins in glomeruli. Of the renal infarcts, over half were due to septic emboli, mostly in patients infected with *Staphylococcus aureus.* Acute interstitial nephritis was found in 10% but was more common in biopsy material and seemed attributable to antibiotics. Renal cortical necrosis was found in 10%.[5] In a recent study of long term venous access devices (n=102), it was determined that cultures taken from the inflamed pocket surrounding the implanted port were as reliable as cultures from the catheter tip on removal. The major organisms cultured were coagulase negative *Staphylococcus* sp., *Candida*, and *Staphylococcus aureus*.[2]

AFIP Diagnosis: 1. Kidney: Nephritis, cortical, suppurative, acute, multifocal, moderate to severe, with focally extensive coagulative necrosis (infarction), fibrin thrombi and few Gram positive cocci.
2. Kidney: Glomerulonephritis, membranoproliferative, global, multifocal, moderate, with synechiae, glomerular senescence, chronic interstitial nephritis and fibrosis.
3. Ureter: Ureteritis, chronic, diffuse, mild.

Conference Comment: This case, which illustrates an important complication associated with the use of vascular ports, provided conference participants with the opportunity to describe a challenging slide featuring concomitant chronic and acute processes. The conference moderator encouraged participants, who were not provided with the full signalment and history, to develop and propose a logical pathogenesis to explain the lesions. Primary learning points included: 1) recognizing that the acute cortical nephritis was of hematogenous origin, which in a diagnostic setting should prompt a search for the primary nidus of infection (e.g. in the heart valves or a vascular port) and disseminated lesions in other capillary beds (e.g. in the lung, spleen, and liver); and 2) identifying membranoproliferative glomerulonephritis (MPGN) and properly interpreting it as a chronic lesion, which should also prompt an investigation into the underlying cause. The moderator and conference participants interpreted the tubular lesions, described by the contributor, as most likely secondary to the glomerular lesions.

Numerous specific human glomerular diseases have been characterized in exquisite detail, and an exhaustive review is beyond the scope of these proceedings. In general, glomerular diseases are classified into three broad categories: primary glomerulopathies, systemic diseases with glomerular involvement (i.e. secondary glomerulopathies, e.g. systemic lupus erythematosis [SLE], diabetes mellitus, amyloidosis, bacterial endocarditis, vasculitis), and hereditary disorders (e.g. Alport syndrome, thin basement membrane disease, Fabry disease). Primary glomerulopathies include, among many others, postinfectious glomerulonephritis, rapidly-progressive (crescentic) glomerulonephritis, membranous glomerulopathy, and minimal-change disease.[1] A superb example of crescentic glomerulonephritis was recently examined in WSC 2009-2010, Conference 3, case IV.

Immune mechanisms, including both cell-mediated and antibody-associated, are thought to underlie most primary and many secondary glomerulopathies. The two best-characterized antibody-associated mechanisms of glomerular injury are: 1) antibodies reacting to antigens within the glomerulus; and 2) deposition of circulating antigen-antibody complexes in the glomerulus. In the former, antigens may be intrinsic to the glomerular basement membrane (GBM) proper, or "planted" in the glomerulus from the circulation. For example, in Goodpasture syndrome, the noncollagenous domain (NC1) of the $\alpha 3$ chain of type IV collagen, intrinsic to the GBM, is the antigen responsible for classic anti-GBM antibody-induced glomerulonephritis. By contrast, myriad antigens, including bacterial products, aggregated immunoglobulins, and nuclear proteins, may be "planted" in the GBM; antibodies then bind to these antigens, resulting in the formation of immune complexes *in situ*. Circulating immune complex glomerulonephritis differs from anti-GBM glomerulonephritis in that the immune complexes lack immunological specificity for the glomerulus; rather, they form outside of and localize in the glomerulus due to a variety of physiochemical and hemodynamic factors. The culpable antigens that initiate immune complex formation may be exogenous (e.g. products of infectious agents) or endogenous (e.g. SLE).[1]

Morphologically, glomerulopathies are often evaluated

using immunofluorescence microscopy and electron microscopy. Two patterns of immune complex deposition are noted using immunofluorescence: 1) granular, which is characteristic of both circulating immune complex deposition and immune complexes formed in situ against "planted" antigens; and 2) linear, which is characteristic of classic anti-GBM glomerulonephritis. An understanding of the structures comprising the glomerular capillary wall is essential to properly interpreting the ultrastructure of immune complex glomerulonephritis. The glomerular capillary lumen is bounded by fenestrated endothelial cells, which is further subtended by the GBM, which is composed primarily of type IV collagen, laminin, heparin sulfate, and several other glycoproteins. The GBM has a thick, electron-dense, central lamina densa, and inner and outer, thinner, electron-lucent peripheral layers, the lamina rara interna and lamina rara externa, respectively. The GBM is surrounded by visceral epithelial cells, also known as podocytes, which have foot processes (pedicels) that abut the basement membrane and are separated by 20-30 nm wide filtration slits, each bridged by a thin diaphragm. Finally, mesangial cells, which are contractile, phagocytic cells of mesenchymal origin, are interposed between the glomerular capillaries and support the glomerular tuft. Ultrastructurally, immune complexes are electron-dense deposits which can be localized specifically to one or more of the following sites: subendothelial (i.e. between the fenestrated glomerular capillary endothelium and the GBM), intramembranous (i.e. within the basement membrane), subepithelial (i.e. between the pedicel and GBM), epimembranous (i.e. upon the GBM interposed between adjacent pedicels), or mesangial (i.e. within the mesangial matrix). Localization of immune complex deposition ultrastructually is useful diagnostically, because many glomerulopathies are characterized by immune complex deposition specifically in one or more of these locations.[1]

Membranoproliferative glomerulonephritis, also known as mesangiocapillary glomerulonephritis, may be secondary to other systemic disorders (i.e. secondary MPGN) or idiopathic (i.e. primary MPGN), and is further divided into types I and II based on ultrastructural, immunofluorescent, and pathologic findings. In humans, the majority of MPGN cases are type I, characterized by discrete subendothelial electron-dense deposits ultrastructurally, and C3 deposition in a granular pattern by immunofluorescence. The pathogenesis of type I MPGN involves activation of both the classical and alternative complement pathways; IgG, C1q, and C4 are also often present. In the less common type II MPGN, also known as dense deposit disease, the lamina densa of the GBM contains an irregular, ribbon-like, extremely electron-dense material. Immunofluorescence demonstrates C3 in an irregular granular or linear pattern on either side of the lamina densa within the GBM, but not within the dense deposits. The pathogenesis is thought to involve activation of the alternative pathway; IgG, C1q, and C4 are usually absent.[1]

Contributor: Air Force Research Laboratory, 711th Human Performance Wing/RHDV, 2509 Kennedy Circle, Brooks City-Base, TX 78235

References:

1. Alpers CE: The kidney. *In:* Robbins and Cotran Pathologic Basis of Disease, eds. Kumar V, Abbas AK, Fausto N, Aster JC, 8th ed., pp. 907-938, Saunders Elsevier, Philadelphia, PA, 2010
2. Brouns F, Schuermans A, Verhaegen J, De Wever I, Stas M: Infection assessment of totally implanted long-term venous access devices. J Vasc Access **7:**24-28, 2006 (abstract only)
3. Heidel JR, Giddens WE Jr., Boyce JT: Renal pathology of catheterized baboons (*Papio cynocephalus*). Vet Pathol **18:**59-69, 1981 (abstract only)
4. Leary SL, Sheffield WD, Strandberg JD: Immune complex glomerulonephritis in baboons (*Papio cynocephalus*) with indwelling intravascular catheters. Lab Anim Sci **31:**416-420, 1981
5. Majumdar A, Chowdhary S, Ferreira MA, Hammond LA, Howie AJ, Lipkin GW, Littler WA: Renal pathological findings in infective endocarditis. Nephrol Dial Transplant **15:**1782-1787, 2000
6. Rao VP, Poutahidis T, Marini RP, Holcombe H, Rogers AB, Fox JG: Renal infarction and immune-mediated glomerulonephritis in sheep (*Ovis aries*) chronically implanted with indwelling catheters. J Am Assoc Lab Anim Sci **45:**14-19, 2006

CASE IV: S 34/05 (AFIP 3135084).

Signalment: 4-day-old, male, crossbred, domestic pig (*Sus scrofa domestica*).

History: This piglet was part of a study and was experimentally infected with a recombinant porcine coronavirus (rTGEV). At 24 hours post-infection, the animal was bright and alert and was humanely destroyed.

Gross Pathology: At necropsy, there was diffuse mesenteric edema in the colon. No further gross lesions were observed and reported.

Laboratory Results: CBC: WBC 11.1 k/µl (↑), neutrophils 8.87 k/µl (80.2 %), lymphocytes 1.48 k/µl (13.4 %), monocytes 0.623 k/µl (5.63 %), eosinophils 0.002 k/µl (0.014 %), basophils 0.086 k/µl (0.779 %), RBC 4.56 M/µl, hemoglobin 10.2 g/dl(↓), HCT 30.7% (↓), MCV 67.3 fl (↓), MCH 22.4 pg (↓), MCHC 33.3 g/dl, RDW 26.9 % (↑), platelets 884.0 k/µl (↑↑), MPV 12.2 fl; mild leukocytosis; mild anemia.

Bacteriology: Lungs: *S. aureus* +, *S. intermedius* +; kidney: *E. coli* ++; liver: *E. coli* +; spleen: negative; duodenum: *Bacteroides* spp. +; jejunum: *Bacteroides* spp. +, *Streptococcus* spp. (+); ileum: *Streptococcus* spp. (+); colon: *E. coli* +, *Streptococcus* spp. +, *Bacteroides* spp. ++.

Fluorescent antibody test (FAT): Direct immunofluorescence on cryosections of the small intestine was negative for coronavirus, but positive for rotavirus antigens.

Virology: By RT-PCR a 433 bp long fragment of genome segment 6 of group A rotavirus was amplified in RNA obtained from a jejunum sample.[6]

Electron Micrograph Description: Small intestine, mid-jejunum, fixed in glutaraldehyde, transmission electron micrograph, 11,800X: The image is composed of at least six intestinal absorptive epithelial cells which are characterized by numerous, even, long, plush microvilli along their luminal borders. The terminal web, especially of the two most lateral absorptive cells, shows immediately beneath the microvilli, few electron-dense filamentous structures extending into the cores of the microvilli. Within the cytoplasm there are numerous mitochondria, abundant rough endoplasmic reticulum (RER), occasional lysosomes and few spherical electron-dense vesicles. Three nuclei are present. The lateral cellular borders of the slightly interdigitating enterocytes show apical junctional complexes. Between two absorptive cells there is one goblet cell liberally endowed with characteristic electron-lucent mucous granules. In the center of the image there are two absorptive cells with more electron-lucent and brightened cytoplasm and a disorganized terminal web. Most strikingly is the severe dilation of the RER which has almost completely lost the ribosomes (ribosomal detachment). Within the dilated cisternae of

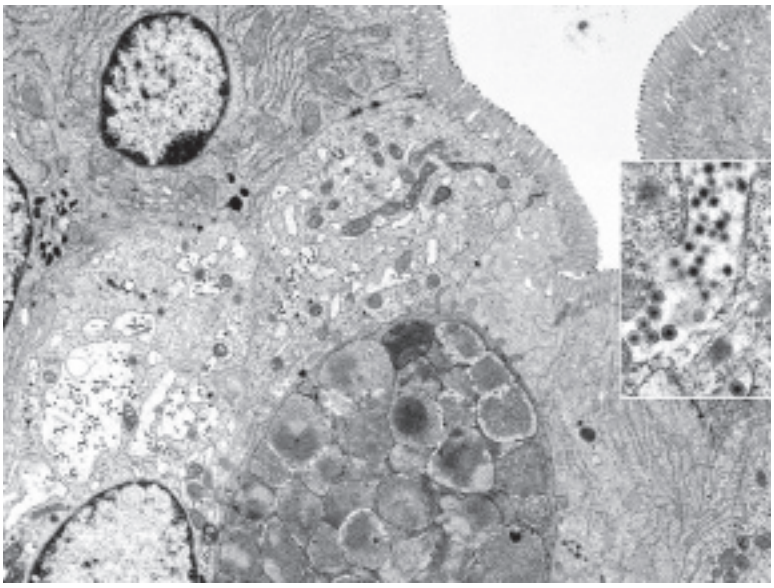

4-1. Small intestine, pig. Multiple intestinal epithelial cells with plush, even microvillar surface, prominent apical tight junctions, desmosomes, lysosomes, mitochondria, and basally located heterochromatic nuclei with peripheralized chromatin. The endoplasmic reticulum within an absorptive epithelial cell is dilated and contains many round virions. (TEM) Courtesy of Friedrich-Loeffler-Institut, Federal Research Institute for Animal Health, 17493 Greifswald-Insel Riems, Germany www.fli.bund.de

RER there are numerous electron dense viral particles. The microvilli of these cells appear to be less dense and slightly out of register; mitochondria show lysis of cristae and a moderately condensed matrix (**fig. 4-1**).

Inset: Within the dilated cisternae of the RER numerous virus particles with envelope and mature virions after loss of the envelope, with a diameter of 60-80 nm, are present with ultrastructural features identical with those of rotaviruses (47,000X).

Contributor's Morphologic Diagnosis: Jejunum: Absorptive cell, cytoplasmic brightening, dilation of RER with abundant rotavirus particles.

Contributor's Comment: Rotaviruses belong to the family Reoviridae and are clustered in the genus Rotavirus. Infectious rotaviruses are large, nonenveloped, nearly spherical particles with up to three concentric capsid layers. The shells surround a central protein core which contains the viral genome. Most rotaviral preparations contain both intact, complete particles resembling wheels (Latin: rota), and particles which have lost the outer capsid layer. The diameter of intact particles is 65-68 nm; particles with only the inner capsid layer have a diameter of approximately 60 nm. The diameter of the core is approximately 38 nm.[2]

Rotaviruses are the causative agents of severe gastroenteritis in animals and humans and also have the potential to be transmitted between species. They are one of the most important infectious agents of severe diarrhea of infants and are associated with approximately 870,000 deaths per year in children under three years of age in developing countries.[2] Rotaviruses infect differentiated epithelial cells of the villi in the jejunum of a multitude of species including calves, piglets, foals, lambs, and avian species. The results are destruction of enterocytes at the apices of the villi of the small intestine, atrophy of the infected villi, restricted absorption, and increased secretion after neurogenic stimulation with a massive loss of liquid and electrolytes. The main clinical signs are diarrhea ("white scours"), weakness and anorexia. Young animals may die as a result of dehydration or secondary bacterial infection.[7]

Infections with rotaviruses are economically important, especially in younger animals one to eight weeks of age. In calves and pigs, lethal infections are seen during the first months of age. In contrast, infections of human newborns are usually relatively mild and asymptomatic. In humans, an increase in the incidence of infections and the severity of the clinical signs with fever and anorexia is seen not before several months of age. Most of the rotavirus infections with gastroenteritis in children are seen between the ages of six months and two years.[2]

Rotavirus is a nonenveloped virus; therefore, its stability and infectivity at temperatures of 18-20 °C is very high. Rotaviruses are also relatively resistant to treatment with formaldehyde, ether or detergents. Viral particles may remain infectious in the environment for several years.[2] The genome of rotaviruses consists of double stranded, segmented RNA. The entire genome has 11 segments and in general a molecular weight of 11-12 x 106. Differences in the migration pattern of the single genome segments after elecrophoresis can be used for classification. Four groups (I-IV) of these electropherotypes can be differentiated. A distinct feature of rotavirus morphogenesis is that subviral particles, which assemble in the cytoplasmic viroplasms, bud through the membrane of the RER, and maturing particles are transiently enveloped. This is one of the most interesting aspects of rotavirus replication.[2,3]

Serologically, rotaviruses are divided into seven distinct groups (A-G). There is no correlation between the electropherotype and the serotype or group specificity of rotaviruses. Within the genus Rotavirus most of the characterized rotavirus isolates harbor a common group antigen. They are classified as group A. Isolates with similar replication characteristics, but which lack the group specific antigen are classified in additional groups (e.g. B, C, D, and E). Due to numerous additional characteristics of isolates belonging to one of the five groups, rotaviruses are subdivided into several subtypes. Rotavirus infections in cattle most often belong to group A. In humans infections are caused by viruses of group A or B. Rotavirus infections in pigs are often caused by viruses belonging to group B, C, or E. Infections in birds belong mainly to group D. Due to the large variety of rotavirus serotypes and subtypes present in the different species, animals and humans can be infected within a short time period with different serotypes.[4]

AFIP Diagnosis: Small intestine, absorptive epithelial cells: Degeneration, with dilated endoplasmic reticulum and intracytoplasmic round virions.

Conference Comment: The contributor provides a useful appraisal of the entity, and readers may find it helpful to compare the pathogenesis of rotaviral infection with that of parvoviral infection, reviewed in WSC 2009-2010, Conference 16, case II. The diarrhea that results from rotaviral infection is attributed to three mechanisms: 1) malabsorption due to enterocyte necrosis and villus atrophy; 2) villus ischemia and activation of the enteric nervous system by a vasoactive agent released from infected enterocytes; and 3) rotaviral production of nonstructural

protein 4 (NSP4), which acts as a secretory enterotoxin.[1] Therefore, both malabsorption and hypersecretion of fluid and electrolytes likely contribute to diarrhea and dehydration seen in rotaviral enteritis.

In addition to "three week scours" or "white scours" in pigs, there are several other distinct syndromes in animals attributed to rotaviral infection, including infectious diarrhea of infant rats (IDIR), enzootic diarrhea of infant mice (EDIM), and diarrhea in young rabbits, calves, lambs, foals, puppies, kittens and poultry. Among these syndromes, rotaviral infection is generally characterized by several consistent themes, including a propensity to cause clinical disease in only young animals, a tendency to cause mild disease, and a predilection for infection of enterocytes at the villar tips.[1,5] That said, several intricacies regarding rotaviral infection in certain species warrant elaboration. In rats and mice respectively, IDIR and EDIM are both characterized by diarrhea in neonates less than two weeks old, with only subclinical infection in older animals. Infectious diarrhea of infant rats is caused by an atypical (i.e. non-Group A) rotavirus that is likely of human origin. In addition to intestinal villus attenuation and enterocyte necrosis that is typical of other rotaviral infections, IDIR is characterized by epithelial syncytia that are considered pathognomonic and may contain eosinophilic intracytoplasmic viral inclusions. In both wild and laboratory mice, EDIM is caused by a single, highly contagious strain of Group A rotavirus and results in transient diarrhea that may or may not be clinically significant.[5] In both lambs and rabbits, rotaviral infection is often seen in combination with bacterial co-pathogens (e.g. *E. coli*); lambs are unique in that viral infection of the colon may occur in this species, whereas in other species the small intestine is affected, with the specific site (i.e. duodenum, jejunum, or ileum) varying by species.[1,5]

Most conference participants considered coronaviral enteritis (i.e. transmissible gastroenteritis [TGE]) in the differential diagnosis for this case. The signalment and clinical signs of coronaviral and rotaviral infections are analogous, although the latter is generally less severe and less frequently characterized by vomiting. The gross and histopathologic findings are also comparable between the two entities, and both cause lesions whose severity is inversely proportional to age in piglets. Similarly, the microscopic lesions in the small intestine of calves with rotaviral enteritis are identical to those of calves with coronaviral enteritis; however, the former does not cause colonic lesions. Coronaviruses have a single-stranded RNA genome, are enveloped, and measure slightly larger than rotaviruses, ranging from 70-200 nm in diameter and averaging 100-130 nm in diameter. The characteristic "corona" of peplomers for which coronaviruses are named is best visualized ultrastructurally in negatively stained preparations.[1]

Contributor: Friedrich-Loeffler-Institut, Federal Research Institute for Animal Health, 17493 Greifswald-Insel Riems, Germany
www.fli.bund.de

References:

1. Brown CC, Baker DC, Barker IK: Alimentary system. *In:* Jubb, Kennedy, and Palmer's Pathology of Domestic Animals, ed. Maxie MG, 5th ed., vol. 2, pp. 169-176. Elsevier Saunders, Philadelphia, PA, 2007
2. Estes MK, Kapikian AZ: Rotaviruses. *In:* Fields Virology, eds. Knipe DM, Howley PM, 5th ed., pp. 1917-1974, Lippincott Williams & Wilkins, Philadelphia, PA, 2007
3. Granzow H, Schirrmeier H, Beyer J, Lange E: Morphologische Studien bei Virusinfektionen des Darmtraktes – Virusreplikation und Zytopathologie in Zellkulturen und Enterozyten beim Ferkel, 1. Mitteilung: Ultrastruktur des nichtinfizierten Darmepithels und bei Rotavirusinfektionen. [Morphologic studies of virus infection of the intestinal tract--virus replication and cytopathology in cell cultures and enterocytes in piglets. 1. Ultrastructure of intestinal epithelium without viral infiltration and in rotavirus infection]. Arch Exper Vet Med **42:**558-70, 1988
4. Matthijnssens J, Ciarlet M, Rahman M, Attoui H, Bányai K, Estes MK, Gentsch JR, Iturriza-Gómara M, Kirkwood CD, Martella V, Mertens PP, Nakagomi O, Patton JT, Ruggeri FM, Saif LJ, Santos N, Steyer A, Taniguchi K, Desselberger U, Van Ranst M: Recommendations for the classification of group A rotaviruses using all 11 genomic RNA segments. Arch Virol **153:**1621-1629, 2008
5. Percy DH, Barthold SW: Pathology of Laboratory Rodents and Rabbits, 3rd ed., pp. 42-43, 135-136, 261-262. Blackwell Publishing, Ames, IA, 2007
6. Schwarz BA, Bange R, Vahlenkamp TW, Johne R, Müller H: Detection and quantitation of group A rotaviruses by competitive and real-time reverse transcription-polymerase chain reaction. J Virol Methods **105:**277-285, 2002
7. Yuan L, Stevenson GW, Saif LJ: Rotavirus and reovirus. *In:* Diseases of Swine, eds. Straw BE, Zimmermann JJ, D'Allaire S, Taylor D, 9th ed., pp. 435-454, Blackwell, Ames, IA, 2006

The Armed Forces Institute of Pathology
Department of Veterinary Pathology

Conference Coordinator:
Shannon Lacy, DVM, MPH

WEDNESDAY SLIDE CONFERENCE 2009-2010

Conference 18

10 March 2010

Conference Moderator:

Thomas J. Van Winkle, VMD, Diplomate ACVP

CASE I: 09/256 (AFIP 3148215).

Signalment: 16-year-old pony breed mare (*Equus caballus*).

History: The pony became ataxic one week before presenting at the clinic. The referring veterinarian found neurological signs affecting the tail and hindlimbs. At the Norwegian School of Veterinary Science clinic, neurological examination indicated that facial nerves (V and VII) were affected. Muscle tone in the tail and anus was reduced. Hindquarter skin had areas of hypersensitivity and areas of reduced sensitivity. Severe ataxia was found.

Gross Pathology: In the gluteal region there was edema and hemorrhages centered on nerves. The lumbosacral spinal cord (L5-S1) was firm and slightly irregular in thickness. There was hemorrhage in the epidural and subdural spaces and dark hemorrhagic foci in the spinal cord (**fig. 1-1**).

Histopathologic Description: Cauda equina: Nerves, extradural and intradural, are moderately to severely infiltrated by lymphocytes, plasma cells, epithelioid macrophages and fewer multinucleated giant cells. There is axonal degeneration and loss within the affected nerves. The nerve fibers are embedded in a collagen rich fibrous tissue (fibrosis) with a moderate lymphoplasmacytic infiltrate and focally extensive hemorrhages. Fibroplasia is also seen within nerves. Dorsal root ganglia (not present in all sections) have a moderate to severe lymphoplasmacytic infiltration and show axonal degeneration and loss as well as rare hypereosinophilic shrunken neurons (neuronal necrosis) (**figs. 1-2 and 1-3**).

Several cranial nerves and nerves associated with hemorrhages in the gluteal region had moderate lymphoplasmacytic infiltrates (tissue not submitted).

Contributor's Morphologic Diagnosis: Cauda equina: Neuritis and perineuritis, granulomatous, multifocal to diffuse with epineurial and perineurial fibrosis.

Contributor's Comment: Neuritis of the cauda equina, or polyneuritis equi, is a nonsuppurative inflammation mainly affecting the nerve trunks of the cauda equina in horses.[2] Clinically the disease is characterized by paralysis of the tail, reduced muscle tone of the anus and rectum, paralysis of the bladder (sometimes with urinary incontinence), paresthesia or anesthesia of the tail and perineum, and incoordination of the hindlimbs.

*Sponsored by the American Veterinary Medical Association, the American College of Veterinary Pathologists, and the C. L. Davis Foundation.

1-1. Spinal cord, horse. Multifocally there is subdural and epidural hemorrhage. Photographs courtesy of Norwegian School of Veterinary Science, Departments of Basic Sciences and Aquatic Medicine, PO Box 8146 Dep, N-0033 Oslo, Norway; kailie@veths.no

There may also be involvement of cranial nerves.[2] Lesions are reported to be most severe in the sacral and coccygeal nerves, and are characterized by granulomatous inflammation, hemorrhage and fibrosis causing irregular thickening and discoloration of the nerve roots. The inflammation is usually more severe in the extradural parts of the nerves compared to the intradural nerve segments. Although more mildly, nerves outside the cauda equina, including cranial nerves, are commonly also affected.[2] In the present case, nerve associated hemorrhagic lesions were grossly visible in the gluteal region. A recent case report described biopsy of tail musculature as an aid in the antemortem diagnosis of polyneuritis equi.[1] The cause is unknown, but the morphology of the lesion suggests that it is an immune-mediated disorder.[2]

AFIP Diagnosis: Spinal cord, cauda equina: Polyradiculoneuritis, granulomatous, multifocally extensive, marked, with perineural and epineural fibrosis and nerve fiber loss.

Conference Comment: The contributor provides a succinct overview of this perplexing entity. Many favor the term *polyneuritis equi* (PNE) over n*euritis of the cauda equina* or *cauda equina syndrome* because it more accurately reflects the typical widespread distribution of inflammation affecting not only the cauda equina, but often spinal roots and cranial nerves as well.[3] As alluded to by the contributor, while the pathogenesis of the lesion remains obscure, Adenovirus I has been isolated from horses with PNE, and it is hypothesized that a viral infection may incite an autoimmune polyradiculoneuritis in horses with this condition.[3] *Halicephalobus gingivalus* has been reported as a cause in one case of PNE.[2]

Whatever the inciting etiology, an immune-mediated mechanism is suggested by similarities with Guillain-Barre syndrome (GBS) in humans and experimental allergic neuritis (EAN) in laboratory animals. Specifically, PNE, GBS and EAN are all characterized by demyelination in the proximal roots with invading mononuclear cells and macrophages stripping away segments of the myelin sheath. Furthermore, circulating antibodies to the P2 myelin protein, the antigen that upon injection into laboratory animals produces EAN, have been demonstrated in horses with PNE. Nevertheless, the role of these antibodies in the pathogenesis of PNE is unknown; they may be causal or arise secondary to demyelination and inflammation.[3]

As mentioned by the contributor, a recent case report describes biopsy of the sacrocaudalis dorsalis lateralis muscle, the innervation of which arises in the cauda equina, for the antemortem diagnosis of PNE. In frozen biopsy specimens, intense lymphohistiocytic inflammation infiltrated and effaced terminal intramuscular nerve branches while sparing the myofibers, which exhibited angular atrophy of both muscle fiber types (neurogenic atrophy) and occasional hypertrophic or split fibers.[1]

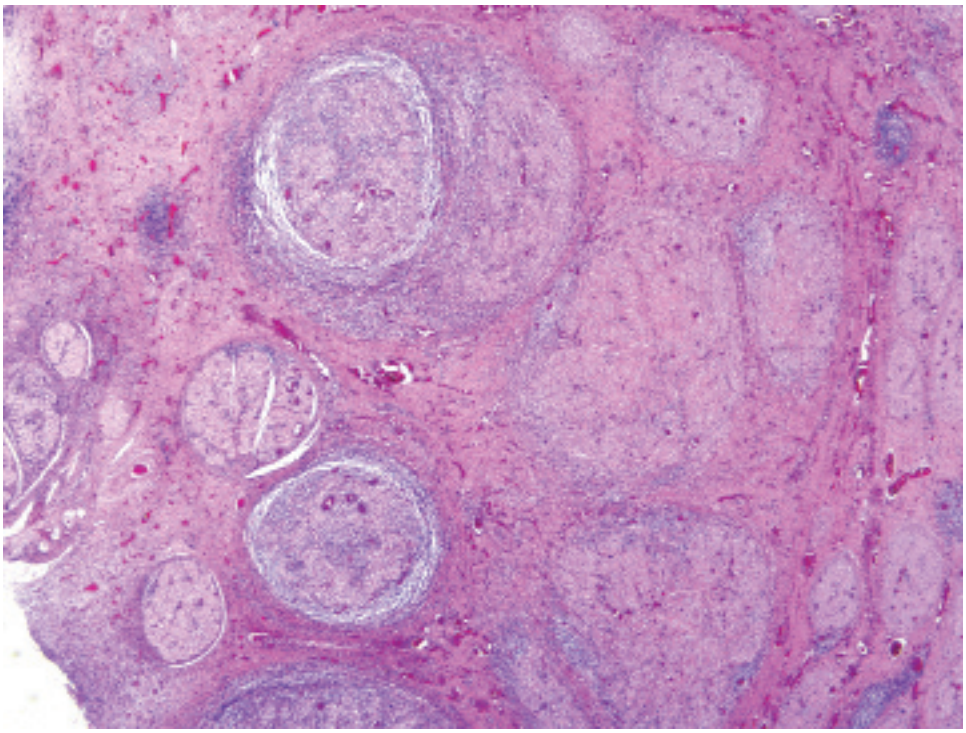

1-2. Cauda equina, horse. Extradural and intradural nerves are separated by abundant fibrosis and surrounded and infiltrated by many inflammatory cells. (HE 200x)

Contributor: Norwegian School of Veterinary Science, Departments of Basic Sciences and Aquatic Medicine, POB 8146 Dep, N-0033 Oslo, Norway
http://www.nvh.no

References:

1. Aleman M, Katzman SA, Vaughan B, Hodges J, Crabbs TA, Christopher MM, Shelton GD, Higgins RJ: Antemortem diagnosis of polyneuritis equi. J Vet Intern Med **23:**665-668, 2009
2. Maxie MG, Youssef S: Nervous system. *In:* Jubb, Kennedy, and Palmer's Pathology of Domestic Animals, ed. Maxie MG, 5th ed., vol. 3, p. 444. Elsevier Saunders, Philadelphia, PA, 2007
3. Summers BA, Cummings JF, De Lahunta A: Veterinary Neuropathology, pp. 433-434. Mosby, St. Louis, MO, 1995

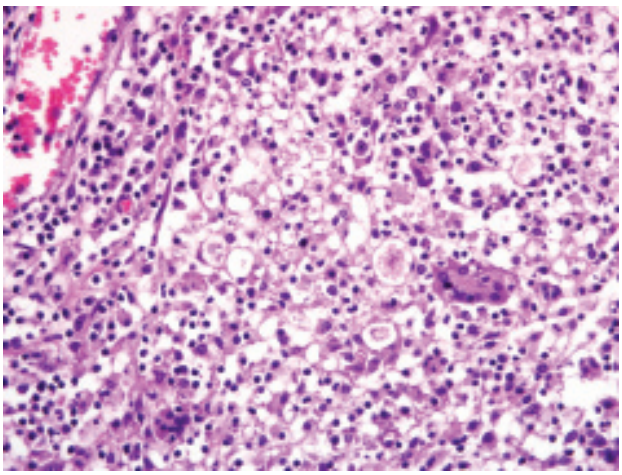

1-3. Cauda equina, horse. Inflammatory cells, composed of many lymphocytes, plasma cells, epithelioid macrophages, and fewer multinucleated giant cells, separate and replace myelinated axons. The few remaining axons are swollen and degenerate. (HE 400x)

CASE II: 126998 (AFIP 3149866).

Signalment: 7-year-old, Thoroughbred cross mare (*Equus caballus*).

History: The horse presented with a sudden onset of anorexia, dysphagia and severe colic with no discernible gut sounds. Tachycardia (80 beats per minute), dehydration, patchy sweating and muscle tremors were also noted. On rectal examination the mucosa was dry and tacky and the content was dry with mucosal casts. Euthanasia was elected.

Gross Pathology: At necropsy, the stomach was distended with green fluid. Multiple linear red erosions were noted in the distal third of the esophagus. The small intestine was dilated with green fluid and gas, with pale red mucosal and serosal surfaces. The large and small colons were filled with large dry balls of fecal material coated with a black viscous substance (blood). There was multifocal reddening of the colonic mucosa (**figs. 2-1 and 2-2**).

Histopathologic Description: Many neurons in the coeliaco-mesenteric ganglion have a swollen, hypereosinophilic, finely vacuolated cell body with significant reduction in or absence of Nissl granules and either a pyknotic nucleus or absence of nuclear detail. Others have a deeply eosinophilic, rounded cell body with absence of Nissl substance and a paracentral or peripheral pyknotic nucleus. Smaller numbers of neurons show margination of the Nissl granules with central deeply eosinophilic cytoplasm (central chromatolysis). There are numerous perineuronal axonal spheroids of various sizes. Many neurons contain small amounts of clumped, granular golden-brown pigment (lipofuscin) (**fig. 2-3**).

Contributor's Morphologic Diagnosis: Coeliaco-mesenteric ganglion: Neuronal degeneration and necrosis, acute, multifocal, severe.

Contributor's Comment: These gross and histological lesions are considered diagnostic for equine dysautonomia, or "grass sickness," a disease that largely occurs in horses at pasture (of a wide variety of breeds) in the United Kingdom, western parts of continental Europe, and South America. The risk is highest for young horses (2 to 7 years of age). The greatest number of cases in the UK occurs in the spring. A similar syndrome has been described in cats in the same areas, in a few dogs, and in wild hares. Acute, subacute or chronic cases may be seen with typical clinical signs in horses including muscle tremors, abnormal sweating patterns, dysphagia, reflux of gastric contents, distended small intestinal loops, absence of gut sounds and absence of or abnormal (dry) feces. Megaesophagus occurs in more than 90% of feline and canine cases. Many horses die or are euthanized within the first two weeks but small numbers of animals have survived long-term. Chronic cases present with a more insidious onset of clinical signs.

In acute cases, which are more common, at post-mortem examination there is typically distension of the stomach, and there may be evidence of gastro-esophageal reflux, i.e. distal esophageal ulceration. The large colon is usually filled with firm fecal balls that have a black coating of blood products. Histological lesions are classically described as being found in postganglionic sympathetic and parasympathetic neurons; typically at post-mortem the coeliaco-mesenteric and cranial cervical ganglia are sampled in addition to intestinal tract specimens. Normal neuronal numbers in these sites have been published.[6] Lesions are also found in parasympathetic terminal cardiac ganglia and have been associated with a functional reduction in cardiac autonomic control.[5] Cytoplasmic vacuolation, chromatolysis and necrosis of neurons is noted, and numbers of neurons are reduced significantly.[1] More chromatolytic neurons are noted in acute than in chronic cases. However, lesions have also been reported in general somatic efferent and general visceral efferent lower motor neurons in the brainstem and spinal cord including chromatolysis of lower motor neurons of the general visceral efferent nucleus of cranial nerves III and X, and the general somatic efferent nuclei of cranial nerves III, V, VII and XII.[2] For antemortem diagnosis it is typical to submit a full-thickness biopsy specimen from the ileum as pathology in the intestinal tract is seen most consistently and severely in that segment, particularly in the submucosal plexuses.[1]

The cause is not known, but the most popular current theory being, with some circumstantial evidence, that this is a form of botulism (*Clostridium botulinum* type C).[4]

AFIP Diagnosis: Ganglion, celiaco-mesenteric (per contributor): Neuronal degeneration and necrosis, acute, diffuse, with satellite cell hypertrophy and proliferation, and minimal multifocal lymphocytic ganglioneuritis.

Conference Comment: During the conference, participants reviewed the key diagnostic features of this perplexing entity, as expertly synthesized in the contributor's comments. This condition highlights the importance of carefully considering the clinical history and presenting signs when collecting tissues at necropsy;

2-1. Esophagus, horse. There are multiple linear erosions on the distal esophagus. Photograph courtesy of Faculty of Veterinary Medicine, University of Glasgow, Bearsden Road, Glasgow G61 1QH, United Kingdom j.patterson-kane@

vet.gla.ac.uk
2-2. Colon, horse. The colon is filled with large dry fecal balls which are coated with a black viscous substance. Additionally, there is multifocal reddening of the colonic mucosa. Photograph courtesy of Faculty of Veterinary Medicine, University of Glasgow, Bearsden Road, Glascow G61 1QH, United Kingdom j.patterson-kane@ vet.gla.ac.uk

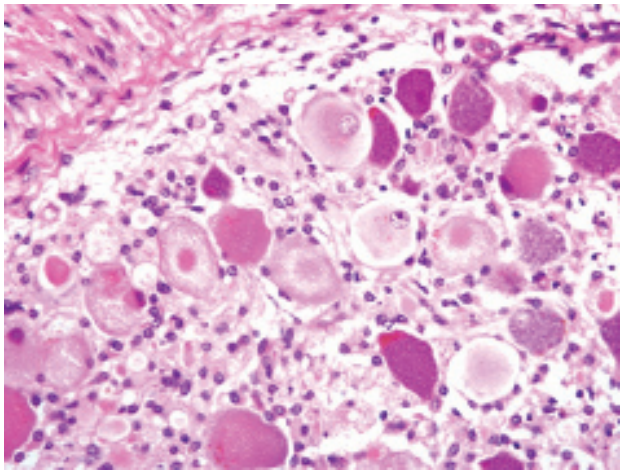

2-3. Celiaco-mesenteric ganglion (per contributor), horse. Multifocally, numerous neurons are swollen and hypereosinophilic, with fewer neurons showing margination of Nissl granules with central deeply eosinophilic cytoplasm. (HE 400x)

an elevated index of suspicion for grass sickness should prompt the astute diagnostician to examine the celiaco-mesenteric ganglion. The conference moderator reminded participants to be cautious when evaluating autonomic ganglia microscopically, specifically to avoid misinterpreting the hypertrophic and hyperplastic satellite cells as lymphocytes. In this case, there is minimal lymphocytic ganglioneuritis, which is not always present in horses with grass sickness; more prominent are the numerous proliferating satellite cells, which can sometimes be mistaken for lymphocytes.

Conference participants based a discussion of chromatolysis on the example provided here. Chromatolysis is a histologically appreciable change in the soma resulting from dispersal of Nissl granules, which are composed of rough endoplasmic reticulum; chromatolysis may be classified as central or peripheral based on its location within the soma and is best demonstrated with special stains, such as cresyl violet. Cells undergoing central chromatolysis are usually swollen with a distinctly eccentric nucleus, while peripheral chromatolysis is more commonly associated with cell shrinkange. Chromatolysis is always considered to be a lesion; however, correctly identifying and interpreting it is predicated on knowing the normal distribution of Nissl granules at a given location.[3] In the autonomic ganglia, for instance, Nissl granules are normally concentrated at the periphery of the soma, so chromatolysis results in intense central eosinophilia, often with multiple fine clear vacuoles at the periphery of the soma, as is superbly demonstrated in this case.[7]

Chromatolysis is a nonspecific reaction that essentially represents a metabolic adaptation to change. For instance, in cases of axonal injury, chromatolysis is evidence of the anabolic response required for regeneration, and has in this context been referred to as the *axon reaction.* When axonal regeneration is complete, the chromatolytic soma may pass through a densely basophilic phase before returning to normal. Alternatively, chromatolysis may precede cell death, the likelihood of which increases with increasing proximity of the axonal lesion to the cell body. Chromatolysis is also a characteristic feature of numerous motor neurodegenerative conditions and perinatal copper deficiency in sheep and goats.[3]

The dysautonomias of horses, cats, dogs, and hares share not only compelling epidemiological and geographical commonalities, but also a similar distribution of central neuropathology, lending further credence to the suggestion of a common etiology.[2]

Contributor: Faculty of Veterinary Medicine, University of Glasgow, Bearsden Road, Glasgow G61 1QH, United Kingdom
http://www.gla.ac.uk/vet/

References:

1. Doxey DL, Milne EM, Woodman MP, Gilmour JS, Chisholm HK: Small intestine and small colon neuropathy in equine dysautonomia (grass sickness). Vet Res Commun **19:**529-543, 1995
2. Hahn CN, Mayhew IG, de Lahunta A: Central neuropathology of equine grass sickness. Acta Neuropathol **102:**153-159, 2001
3. Maxie MG, Youssef S: Nervous system. *In:* Jubb, Kennedy, and Palmer's Pathology of Domestic Animals, ed. Maxie MG, 5th ed., vol. 3, p. 444. Elsevier Saunders, Philadelphia, PA, 2007
4. Newton JR, Hedderson EJ, Adams VJ, McGorum BC, Proudman CJ, Wood JLN: An epidemiological study of risk factors associated with the recurrence of grass sickness (dysautonomia) on previously affected premises. Equine Vet J **36:**105-112, 2004
5. Perkins JD, Bowen IM, Else RW, Marr CM, Mayhew IG: Functional and histopathological evidence of cardiac parasympathetic dysautonomia in equine grass sickness. Vet Rec **146:**246-250, 2000
6. Pogson DM, Doxey DL, Gilmour JS, Milne EM, Chisholm HK: Autonomic neurone degeneration in equine dysautonomia (grass sickness). J Comp Pathol **107:**271-283, 1992
7. Summers BA, Cummings JF, De Lahunta A: Veterinary Neuropathology, pp. 433-434. Mosby, St. Louis, MO, 1995

CASE III: 07-5486029 (AFIP 3141621).

Signalment: 18-month-old, female Merino sheep (*Ovis aries*).

History: For each of the past five years, several male and female Merino sheep in the 12-18 months age range developed hindlimb incoordination. When the flock was driven, these sheep lagged behind and eventually collapsed; after a short time, they regained their feet. Over the next three months, they gradually lost hindlimb function and could only move using the forelimbs. They eventually became permanently recumbent and would have perished if not euthanized. Wasting was not a feature until late in the course of the disease when affected sheep were unable to obtain feed. Central nervous system (CNS) tissues from two of these sheep were examined, and a wide range of other tissues examined from the second sheep.

Gross Pathology: There were no obvious gross findings in either of the sheep.

Laboratory Results: A complete blood count and biochemistry was normal in the second sheep (not done on first sheep). Brain and liver tissue was subjected to PCR using primers to highly conserved regions of exon 1-9 from the gene for glial fibrillary acidic protein (GFAP). Numerous homozygous nucleotide variations in both the affected and control sheep were found, when compared to the published bovine sequence (no ovine sequences available), but these were considered to represent interspecies variations (see later discussion).

Histopathologic Description: In sheep #1 (forwarded here), there were large numbers of Rosenthal fibers (RF) in the brain and spinal cord, particularly in perivascular astrocytic end-feet, and in subpial and subependymal locations where astrocytes normally form a dense meshwork of processes. They often formed perpendicular arrays. Rosenthal fibers were found at all levels of the brain and spinal cord, although they were more numerous in white than gray matter and much more plentiful in the spinal cord and medulla than in the rostral brainstem and cerebellum. Rosenthal fibers were irregularly shaped, elongated or round, deeply eosinophilic intraastrocytic aggregates that varied in diameter from 4 to 20 μm. Hypertrophied astrocyte cell bodies accompanied and paralleled in density the number of RF and were thus more numerous in subpial and perivascular locations in the caudal brainstem and spinal cord. These astrocytes sometimes attained a diameter of 60 μm and contained large nuclei with prominent nucleoli and pale-staining, hyaline cytoplasm. They were occasionally multi- (bi- or tri-) nucleated and rare nuclei contained large eosinophilic intranuclear inclusions consistent with cytoplasmic invaginations (**figs. 3-1 and 3-2**).

Within the cerebral cortex, RF were present in subpial locations. They were attended by low numbers of hypertrophied, and occasionally multinucleated astrocytes with stout fibrillar extensions into the pial membrane. Subcortical and central white matter did not contain RF, although there were a few hypertrophied astrocytes. However, RF density was high in the periventricular and subependymal regions around the third ventricle, and of lesser degree in the subependymal region of the temporal horns. The white matter of the hippocampus and corpus callosum contained occasional RF and mild astrocytic reaction. Perivascular RF were observed in the central gray matter.

The molecular layer of the cerebellum showed small numbers of subpial RF which, as in the cerebral gray matter, were attended by a few hypertrophied astrocytes. The granular layer, and more particularly the folial and deeper white matter, contained abundant RF and associated hypertrophied astrocytes.

In the pons and medulla, there were prominent subpial, subependymal and perivascular RF aggregates, accompanied by numerous hypertrophied astrocytes, with lesser numbers in the white matter. Ependymal cells were hypertrophied. αB -crystallin immunostaining showed positive cytoplasmic expression in many glia, including a subset of astrocytes with a ring-like perinuclear pattern of staining. Many RF were immunonegative, except for a thin rim of positive staining. Many of the αB -crystallin-positive astrocytes were GFAP-negative.

Rosenthal fibers reacted strongly with ubiquitin, but were vimentin-negative. GFAP gradually replaces vimentin in astrocytic IF during brain development, although both may be coexpressed in reactive astrocytes and some astrocytic subpopulations. Rosenthal fiber HSP70 expression resembled that for αB-crystallin but normal astrocytic perikarya, unlike the latter, did not stain for HSP70.

Within the spinal cord, RF formation was florid, generally being greatest in perivascular and subependymal locations. However, in some areas, gray matter contained nearly as many RF as white matter. There were also moderate to large numbers of hypertrophied astrocytes, small numbers of axonal spheroids, and minimal Wallerian degeneration.

All neuronal populations in the brain and spinal cord,

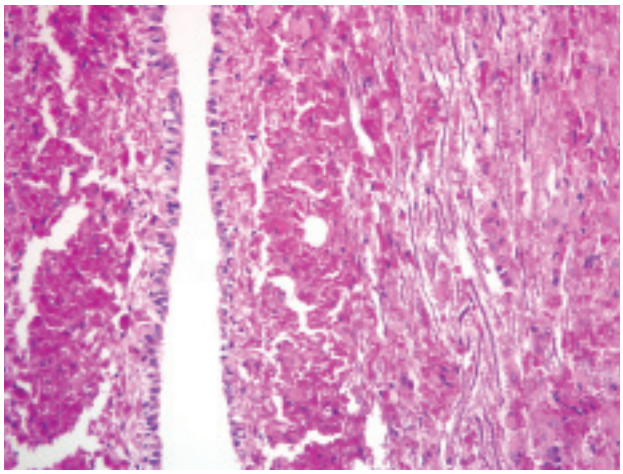

3-1. Brain stem, cerebellum and medulla, sheep. There are numerous Rosenthal fibers within the subependymal area. (HE 400x)

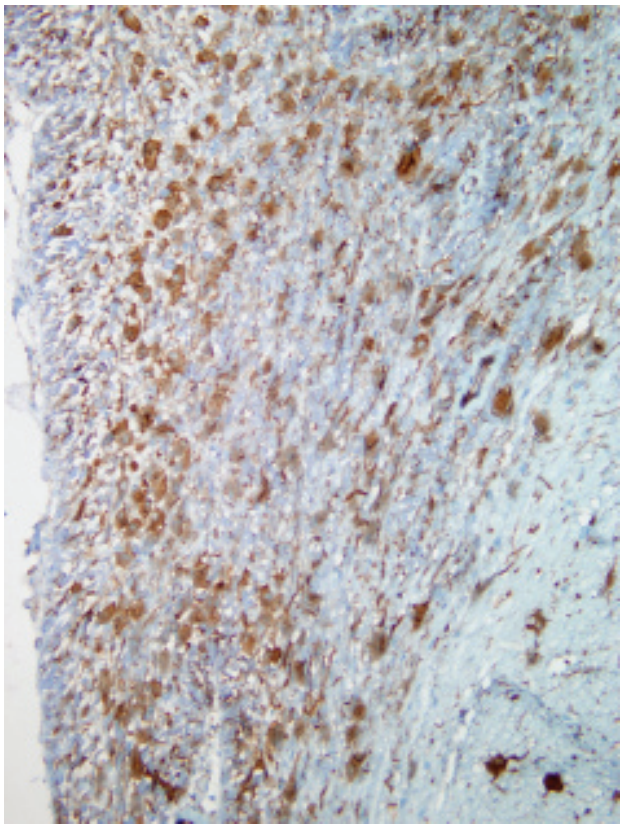

3-2. Brain stem, cerebellum, and medulla, sheep: Numerous Rosenthal fibers within the subependymal area are immunopositive for glial fibrillary acidic protein. (GFAP 200x)

including those in cortical, central, brainstem and spinal gray matter, as well as the pyramidal and granule cells of the hippocampus and cerebellar Purkinje and granule cells, were of normal morphology. Oligodendroglial nuclei also appeared normal.

In sheep #2, the neuroanatomical distribution of RF was similar to sheep #1, but they were greater in number and density. There was mild, Wallerian degeneration in the spinal cord, with ellipsoids (digestion chambers) containing axon fragments, and sometimes macrophages. Myelin ellipsoids were found in all funiculi, but were sometimes more prominent in, or largely restricted to, the ventral funiculi.

Electron Microscopy Results: At the ultrastructural level, within astrocytes, RF were electron-dense, rounded or elongated, coarsely granular structures of variable size with irregular contours. They were surrounded by densely aggregated sheaths of IF, some of which appeared to be continuous with the central osmiophilic mass.

Contributor's Morphologic Diagnosis: Brainstem (medulla or rostral colliculi): Moderate, multifocal (primarily perivascular/subpial/periependymal) Rosenthal fiber deposition, accompanied by moderate astrocytic hypertrophy.

Contributor's Comment: Alexander's disease (AD) is a rare (approximately 450 cases worldwide) and frequently fatal human neurological disorder. Diagnosis of AD can only be confirmed histologically and the signature lesion is the presence of large numbers of hypereosinophilic, intraastrocytic inclusions termed Rosenthal fibres (RF) that contain the heat shock proteins, αB crystallin and HSP27, as well as ubiquitin.[1] The swollen processes and perikarya of astrocytes containing these fibers are more numerous in perivascular, subpial and subependymal sites, often disposed in dense, perpendicular arrays. Alexander's disease is the only documented primary astrocytic disorder, and in approximately 90% of those cases examined at the molecular level various mutations in the glial fibrillary acidic protein (GFAP) gene, which encodes the major intermediate filament protein in these glia, have been found.[2] The phenotypic expression of AD depends on the age of onset and three forms (i.e. infantile, juvenile and adult) are recognized. Spontaneous encephalopathies resembling human AD have been reported in six juvenile dogs (onset at 9 weeks to 6 months of age) of both sexes and different breeds (two Labrador retrievers, two Bernese mountain dogs, one Scottish terrier, and one miniature poodle) and one adult (4-year-old), female, White Alpine sheep.[1,3,4,7] In none of these cases was the GFAP region of the genome examined for mutations.

The histopathological, immunohistochemical and ultrastructural features of the RF encephalomyelopathy described in these two sheep resembled those found in human AD cases and the AD-like encephalopathies previously reported in several dog breeds and one sheep. The age of the present sheep, neuroanatomical distribution of RF, and paucity of myelin loss was similar to adult-onset AD in humans and the only other AD-like neuropathy reported in sheep, while canine cases resembled the human juvenile form of AD. However, this is the first case of an AD-like encephalopathy in domestic animals to be subjected to molecular pathological analysis. In almost all humans with AD, a heterozygous mutation has been identified in exons 1 to 8 of the GFAP gene, and since the sheep GFAP gene has not been sequenced, fragments corresponding to the highly conserved regions of exons 1 to 9 of the bovine GFAP gene were amplified. Polymerase chain reaction results revealed numerous homozygous nucleotide variations in both the affected and control sheep when compared to the published bovine sequence, but these were considered to represent interspecies variations.

It is hoped that further cases of ovine AD from this property will become available for molecular and pathological evaluation so that the strongly suspected genetic basis for the disease may be confirmed and characterized.

AFIP Diagnosis: Brain, cerebellum and medulla: Encephalopathy, bilaterally symmetrical, characterized by perivascular, subpial, and periependymal hypereosinophilic filament accumulation, astrocytosis, marked astrocytic hypertrophy, and multinucleated astrocytes (Rosenthal fiber encephalopathy).

Conference Comment: The contributor provides a very useful review of AD and a thorough description of the microscopic lesions and immunohistochemical findings in the sheep examined in this interesting case, which provides a dramatic example of striking astrocytosis. The conference moderator used this case to emphasize the importance of lesion distribution and pattern. Recognition of RF accumulation alone is insufficient for making a specific diagnosis, because a number of conditions (e.g. reactive astrocytosis, some astrocytomas) may feature RF formation; accurately characterizing RF distribution is therefore of paramount importance in making the correct diagnosis.[5] In this case, RF accumulation is noted in both the gray and white matter in a distinctly symmetrical pattern. The conference moderator emphasized that symmetry is often helpful in identifying lesions with a toxic, metabolic, nutritional, or degenerative etiology.

In humans, the infantile form of AD is characterized not only by RF accumulation, but by severe myelin changes in the frontal lobes, resulting in the characterization of AD as a leukodystrophy; this may be attributable to oligodendrocyte dysfunction secondary to the primary astrocytopathy. However, demyelination may or may not be present in the juvenile and adult forms, and pathology is primarily confined to the brainstem; thus, characterization as a leukodystrophy may not be appropriate in all cases.[3] As noted by the contributor, the lack of demyelination in the present case is reminiscent of the juvenile and adult forms of AD in humans.

Contributor: Gribbles Veterinary Pathology, 1868 Dandenong Road, Clayton, Melbourne, Victoria, Australia, 3168

References*:*

1. Aleman N, Marcaccini A, Espino L, Bermudez R, Nieto JM, Lopez-Pena M: Rosenthal fiber encephalopathy in a dog resembling Alexander disease in humans. Vet Pathol **43:**1025-1028, 2006
2. Brenner M, Johnson AB, Boespflug-Tanguy O: Mutations in GFAP, encoding glial fibrillary acidic protein, are associated with Alexander disease. Nat Genet **27:**117-120, 2001
3. Cox NR, Kwapien RP, Sorjonen DC, Braund KG: Myeloencephalopathy resembling Alexander's disease in a Scottish terrier dog. Acta Neuropathol (Berl) **71:**163-166, 1986
4. Fankhuaser R, Fatzer R, Bestetti G, Derauz JP, Perentes E: Encephalopathy with Rosenthal fiber formation in a sheep. Acta Neuropathol (Berl) **50:**57-60, 1980
5. Summers BA, Cummings JF, De Lahunta A: Veterinary Neuropathology, pp. 281-283. Mosby, St. Louis, MO, 1995
6. Tomokane N, Iwaki T, Tateishi J, Iwaki QA, Glodman JE: Rosenthal fibres share epitopes with αB-crystallin, glial fibrillary acidic protein, and ubiquitin, but not with vimentin. Immunoelectron microscopy with colloidal gold. Am J Pathol **138:**875-885, 1991
7. Weissenbock H, Obermaier G, Dahme E: Alexander's disease in a Bernese mountain dog. Acta Neuropathol (Berl) **91:**200-204, 1996

CASE IV: 08-2005 (AFIP 3133949).

Signalment: 5-month-old, female Maltese dog (*Canis familiaris*).

History: The dog failed to gain weight since obtained two months previously. Neurologic signs of circling, trembling, and loss of hearing and vision developed one month ago.

Gross Pathology: None reported.

Histopathologic Description: The cerebral cortex has severe, diffuse perivascular inflammation composed of lymphocytes and plasma cells, prominent astrocytosis (including many gemistocytic astrocytes), microgliosis, neuronal necrosis, and edema. Clusters of organisms, 1-3 µm in diameter, are present within blood vessels; these organisms are gram positive and consistent with *Encephalitozoon* (**fig. 4-1**).

The kidney has diffuse interstitial inflammation composed of lymphocytes and plasma cells within the cortex and similar, but milder inflammation, within the medulla. Extensive cortical tubular necrosis is present and occasional necrosis of medullary tubules is seen. Occasional clusters of organisms are present within cortical tubular epithelial cells and vascular lumina.

Contributor's Morphologic Diagnosis: 1. Encephalitis and meningitis, lymphoplasmacytic, diffuse, severe with intralesional protozoa consistent with *Encephalitozoon*.
2. Interstitial nephritis, lymphoplasmacytic, diffuse, severe with intralesional protozoa consistent with *Encephalitozoon*.

Contributor's Comment: *Encephalitozoon* is a microsporidian in the phylum Microspora and is considered to be a protozoan, although the organism has some features common to fungi. It is an obligate intracellular parasite with a wide host range, but disease is seen most commonly in rabbits and canids, particularly dogs and foxes. Spores are excreted in urine and feces and are resistant to environmental influences. Transmission is by ingestion, inhalation or transplacental. There are several species of *Encephalitozoon* but only *E. cuniculi* is reported in dogs.

Encephalitozoonosis is a systemic disease of neonatal dogs that tends to localize in the kidney and brain. Clinical signs are neurologic in origin. Gross lesions are often absent but radial streaks may be seen in the kidneys. Histopathology reveals a lymphoplasmacytic interstitial nephritis and meningoencephalitis. Spores may be visible in the lesions with hematoxylin and eosin (H&E) staining, but are few and difficult to see. The spores are rod-shaped, 1-3 µm in diameter, and form aggregates within a parasitophorous vacuole. They are located predominantly within endothelial cells but can be found in epithelial cells and macrophages. Spores are gram-positive and are easily visualized with a Gram's stain.

AFIP Diagnosis: 1. Brain, cerebrum and hippocampus: Meningoencephalitis, lymphoplasmacytic and histiocytic, multifocal, moderate, with neuronal necrosis, gliosis, and intraendothelial anisotropic microsporidia.
2. Kidney: Nephritis, interstitial, lymphoplasmacytic and histiocytic, multifocal to coalescing, moderate to marked, with pyelitis, tubular degeneration and necrosis, and few anisotropic microsporidia.

Conference Comment: We thank Dr. Christopher Gardiner, Consulting Parasitologist for the AFIP's Department of Veterinary Pathology, for reviewing this case. Conference participants discussed several potential causes of nonsuppurative encephalitis in dogs, including numerous viruses (e.g. canine distemper virus, canine and suid herpesviruses, rabies virus, avian influenza virus, West Nile virus, other arboviruses) and protozoa (e.g. *Toxoplasma gondii, Neospora caninum, Sarcocystis neurona*). There is some slide variation in the number of microsporidian organisms present in this case, and in many slides they are difficult to observe with routine H&E staining. Tissue gram staining reveals numerous gram positive organisms in both the brain and kidney, underscoring the utility of special histochemical stains for the detection of pathogens in a diagnostic setting.

Discussion during the conference was primarily devoted to the comparative pathology of mammalian microsporidiosis in general, and encephalitozoonosis in particular. Microsporidia have an obligate intracellular life stage, and exist as environmentally resistant spores outside the host. The polar filament, the defining morphologic feature of the microsporidia, is a unique organelle that remains coiled within the spore until stimulated by some poorly-defined environmental signal to extrude. Upon extrusion, the polar filament penetrates a host cell and injects infectious sporoplasm, which then divides to form meronts, which further differentiate into sporoblasts, sporonts, and spores; these may be contained within a parasitophorous vacuole, as in the case of *Encephalitozoon* spp., or may remain free in the cytoplasm, as in the case of *Enterocytozoon bieneusi*. Other typical microsporidian

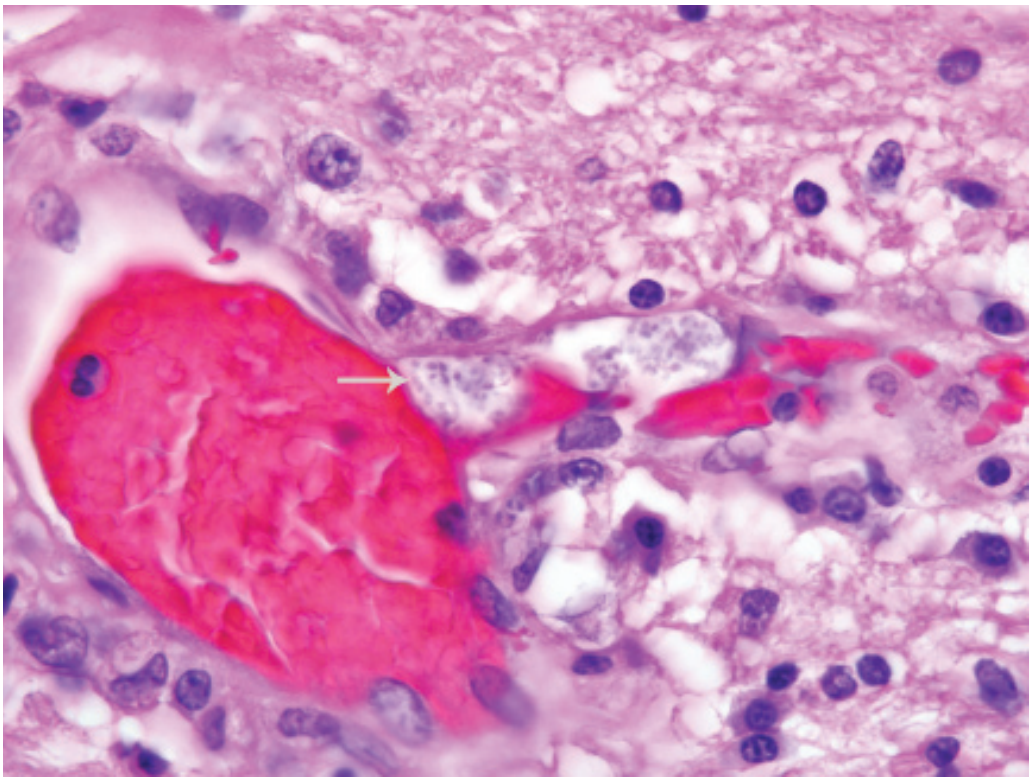

4-1. Brain, cerebrum, and hippocampus, dog. The vascular endothelium occasionally contains 1 – 3 µm microsporidia (arrows) (HE 1000x)

features include a proteinaceous exospore; a chitinous endospore; an anchoring disc at the anterior pole; an electron-lucent posterior vacuole; and a distinct lack of mitochondria, peroxisomes, and stacked Golgi membranes at all developmental stages. In addition to polar filament extrusion, phagocytosis of spores by host cells may also produce intracellular infection.[2]

Best characterized in rabbits, the species in which it was first identified, spontaneous encephalitozoonosis has also been described in numerous other species, including guinea pigs, mice, rats, hamsters, muskrats, ground shrews, goats, sheep, pigs, horses, dogs, foxes, cats, exotic carnivores, humans, and nonhuman primates. Generally, infection in immunocompetent rabbits, guinea pigs, mice, and squirrel monkeys is subclinical, whereas infection in domestic dogs, farm-raised blue foxes, and immunocompromised mice and humans results in clinical disease. As noted by the contributor and illustrated by this case, infection in carnivores often results in fulminating disease. In particular, domestic dogs in South Africa and the United States, and farm-raised blue fox kits in Scandinavian countries have been affected in outbreaks. Gross lesions include pale streaks extending from the renal cortex to the renal pelvis; edematous meninges; and thickened, tortuous, medium-sized to small arteries in the heart, intestines, and central nervous system, reminiscent of polyarteritis nodosa. Microscopic lesions include lymphoplasmacytic meningoencephalitis, lymphoplasmacytic nephritis, micro-granulomatous hepatitis, and interstitial pneumonia.[2]

In rabbits, *E. cuniculi* is shed in the urine and the ingestion of infective urine is the primary route of infection. The brain and kidney are the organs primarily affected, and usually do not exhibit any gross abnormalities, although multifocal irregularly-shaped depressions in the renal cortex are sometimes present. Microscopic lesions in the brain include multifocal nonsuppurative meningoencephalitis, astrogliosis, and perivascular lymphocytic inflammation; lymphoplasmacytic interstitial nephritis is the typical renal lesion. The microsporidian organisms are primarily identified within epithelial cells, endothelial cells, and/or macrophages of affected tissues, but also are commonly found in the lens, lung, liver, and/or heart.[2]

In guinea pigs, as in rabbits, encephalitozoonosis is usually subclinical, but may result in multifocal necrotizing and granulomatous encephalitis and interstitial nephritis. In mice, *E. cuniculi* results in mononuclear inflammatory foci in the liver, lungs, and brain; the differential diagnosis includes *Clostridium piliforme, Corynebacterium kutscheri, Pseudomonas aeruginosa, Salmonella* species, mouse hepatitis virus (coronavirus), and ectromelia virus (mousepox). Infection in squirrel monkeys is also

typically subclinical, but has been implicated in cases of granulomatous encephalitis, nonsuppurative meningitis, and vasculitis in immunosuppressed and neonatal animals; in utero infection is suspected in the latter. Interestingly, microsporidiosis in psittacines is reported with increasing frequency, and many cases are caused by *Encephalitozoon hellem*. Microsporidiosis is an emerging human disease, largely attributed to growing populations of immunocompromised hosts; *E. bieneusi* is the most frequently diagnosed microsporidian pathogen in humans, but disease is also attributed to *E. cuniculi, E. hellem*, and *Encephalitozoon intestinalis*.[2]

Contributor: College of Veterinary Medicine, Virginia Tech, Blacksburg, VA 24061
http://www.vetmed.vt.edu

References*:*

1. Maxie MG, Youssef S: Nervous system. *In:* Jubb, Kennedy, and Palmer's Pathology of Domestic Animals, ed. Maxie MG, 5th ed., vol. 3, pp. 433-434. Elsevier Saunders, Philadelphia, PA, 2007
2. Wasson K, Peper RL: Mammalian microsporidiosis. Vet Pathol **37:**113-118, 2000

The Armed Forces Institute of Pathology
Department of Veterinary Pathology

Conference Coordinator:
Shannon Lacy, DVM, MPH

WEDNESDAY SLIDE CONFERENCE 2009-2010

Conference 19

17 March 2010

Conference Moderator:

Michael A. Eckhaus, VMD, Diplomate ACVP

CASE I: YN08-443 (AFIP 3134620).

Signalment: 15-year-old, female sooty mangabey (*Cercocebus atys*).

History: This adult female sooty mangabey was born at the Field Station of the Yerkes National Primate Research Center. She was found in her social group recumbent, hypothermic and pale with a tense abdomen. Laboratory analysis revealed a moderately elevated blood urea nitrogen, moderate anemia and hyperglycemia. Abdominal ultrasound revealed a large amount of fluid in the abdomen. Fluid collected by abdominocentesis appeared dark brown/red. Due to the poor prognosis, the animal was euthanized.

Gross Pathology: This animal weighed 8.18 kilograms at necropsy. The lung parenchyma had multiple pinpoint red nodules (2-5 mm diameter). Approximately 200 ml unclotted blood, intermixed with extensive adhesions between the mesentery and serosa of the intestines and uterus, was observed in the abdominal cavity. The uterus was enlarged to approximately five times its normal size. When opened, the endometrium was hemorrhagic and thrown into folds. Clotted blood was present in the uterine lumen.

Laboratory Results: No significant pathogen was isolated from the blood, liver or contents of the colon.

Histopathologic Description: The lung parenchyma has 1-2 foci consisting of glands and periglandular stroma. These foci resemble the glands and stroma in the uterine endometrium. In other sections, disseminated endometriosis is seen in the mesentery and serosa of gastrointestinal tract, urinary bladder and uterus (**figs. 1-1 and 1-2**).

Contributor's Morphologic Diagnosis: Lung, endometriosis.

Contributor's Comment: Endometriosis is defined as the appearance of endometrial tissue outside the uterine cavity.[5] Theories about its etiology include shedding of viable endometrial cells through retrograde menstruation and implanting onto the peritoneal surface, or decreased immunological clearance of shed endometrial cells within the peritoneal cavity.[6] Endometriosis is an important cause of reproductive failure in both rhesus and cynomolgus macaques due to blocked fallopian tubes or scarred ovaries.[5] Pelvic adhesions and serosal 'chocolate cysts' are a part of gross appearance of endometriosis.[4] To histologically diagnose endometriosis two of the following three are required: endometrial glands, endometrial stroma,

*Sponsored by the American Veterinary Medical Association, the American College of Veterinary Pathologists, and the C. L. Davis Foundation.

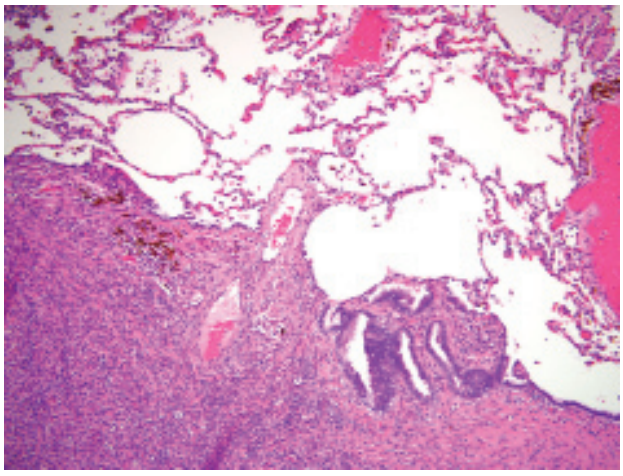

1-1. Lung, sooty mangabey. Multifocally expanding and replacing the lung are densely cellular areas of endometrial stroma and few endometrial glands admixed with hemosiderin-laden macrophages . (HE 200x)

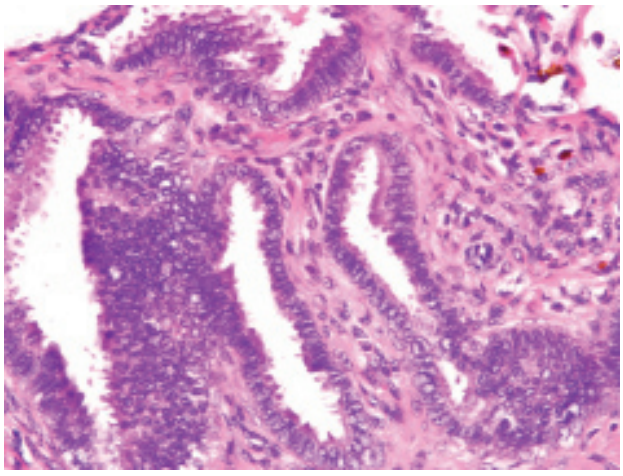

1-2. Lung, sooty mangabey. Endometrial stroma contains scattered endometrial glands and hemosiderin-laden macrophages. (HE 400x)

and hemosiderin-laden macrophages.[1] Older lesions may have only hemosiderin deposits and no glands.

Spontaneous endometriosis has been studied in rhesus macaques, cynomolgus macaques and baboons, although the disease has also been reported in other captive and wild species.[3] Risk factors examined for the development of spontaneous endometriosis in nonhuman primates include maternal age, parity, captivity and experimental procedures such as laparoscopies, hysterectomies, and treatment with estradiol implants.[3] Nonprimates (e.g. rats, syngenic mice, nude mice, hamsters and rabbits) do not develop spontaneous disease, but the disease has been experimentally induced in them.[6]

In the present case, metastasis of endometrial cells by lymphatic and/or hematogenous routes could have disseminated the endometriosis to the thorax. To the authors' knowledge, endometriosis has not been reported in sooty mangabeys, and only one case of endometriosis in lung has been reported in a rhesus macaque.[5]

AFIP Diagnosis: Lung: Endometriosis, with uterine stroma, few endometrial glands, and hemosiderin-laden macrophages.

Conference Comment: We thank the contributor for providing this captivating example of a classic condition in an unusual anatomical location. In women, endometriosis occurs more commonly in the following sites, in descending order of frequency: 1) ovaries; 2) uterine ligaments; 3) rectovaginal septum; 4) cul du sac; 5) pelvic peritoneum; 6) large and small bowel and appendix; 7) mucosa of the cervix, vagina, and fallopian tubes; and 8) laparotomy scars.[2]

Because foci of endometriosis respond to hormonal stimulation with periodic bleeding, the diagnosis is not always straightforward, as mentioned by the contributor. In some cases, lesions consist only of endometrial stroma and areas of hemorrhage or hemosiderin; longstanding lesions may be obscured by secondary fibrosis.[2] A rather atypical example with decidualized stromal cells from a rhesus macaque on a therapeutic course of Depo-Provera® (medroxyprogesterone acetate) was reviewed in WSC 2007-2008, Conference 10, case III. In cases lacking the distinctive features of endometriosis described by the contributor, the differential diagnosis may include retroperitoneal fibromatosis and neoplasia of mesenchymal origin. In such cases, immunohistochemistry may be useful; endometriotic stromal cells exhibit markedly upregulated estrogen production due largely to high levels of the aromatase enzyme, which is absent in normal endometrial stroma. Interestingly, high levels of such proinflammatory cytokines as prostaglandin E_2, interleukin (IL)-1ß, IL-6, and tumor necrosis factor are also noted in endometriosis. Prostaglandin E_2 stimulates local estrogen synthesis, and endometriotic tissue is resistant to the antiestrogenic effect of progesterone; therefore, the overall inflammatory and endocrine milieu in endometriotic tissue is characterized by the overproduction of estrogen and prostaglandin and resistance to progesterone.[2]

Conference participants discussed the two predominant theories for the development of endometriosis, i.e. the metastatic theory and the metaplastic theory. The former postulates that endometrial tissue is physically transplanted to extrauterine locations through: retrograde

menstruation, with subsequent spread to the peritoneum; surgical procedures, with subsequent spread to the cervix, vagina, and laparotomy scars; or metastasis via blood and lymphatic vessels. The metaplastic theory suggests that endometrial tissue arises directly from cell rests in the mesothelium, from which the Müllerian ducts arise during embryogenesis.[2] The mechanism by which endometriosis developed in the lung of the sooty mangabey in this case is unclear. Participants considered hematogenous dissemination, but based on the generally peripheral distribution of the lesions in the sections examined, many speculated that direct extension from the abdominal cavity through the esophageal hiatus, aortic hiatus, or caval opening could have occurred.

In addition to the microscopic features described by the contributor, conference participants noted individualized round cells scattered throughout the endometrial stroma characterized by round, hyperchromatic nuclei and small amounts of cytoplasm containing brightly eosinophilic globules. The round cells are interpreted as endometrial stromal granulocytes, which are likely large granular lymphocytes that reach peak numbers during the secretory phase, the onset of which is marked by ovulation.[7]

Contributor: Division of Pathology, Yerkes National Primate Research Center, Emory University, 954 Gatewood Road, Atlanta, GA 30329
http://www.yerkes.emory.edu/

References:

1. Clement PB: The pathology of endometriosis: a survey of the many faces of a common disease emphasizing diagnostic pitfalls and unusual and newly appreciated aspects. Adv Anat Pathol **14:**241-260, 2007
2. Ellenson LH, Pirog EC: The female genital tract. *In:* Robbins and Cotran Pathologic Basis of Disease, eds. Kumar V, Abbas AK, Fausto N, Aster JC, 8th ed., pp. 1028-1029. Saunders Elsevier, Philadelphia, PA, 2010
3. Hadfield RM, Yudkin PL, Coe CL, Scheffler J, Uno H, Barlow DH, Kemnitz JW, Kennedy SH: Risk factors for endometriosis in the rhesus monkey (*Macaca mulatta*): a case-control study. Hum Reprod Update **3**:109-115, 1997
4. Lowestine LJ: A primer of primate pathology: lesions and nonlesions. Toxicol Pathol **31:**92-102, 2003
5. McClure HM, Graham CE, Guilloud NB: Widespread endometriosis in a rhesus monkey (*Macaca mulatta*). Proc 2nd Int Congr Primatol **3**:155-161, 1969
6. Story L, Kennedy S: Animal studies in endometriosis: a review. ILAR J **45:**132-138, 2004
7. Young B, Lowe JS, Stevens A, Heath JW: Wheater's Functional Histology: A Text and Colour Guide, 5th ed., p. 373. Elsevier Limited, Philadelphia, PA, 2006

CASE II: 07-A-266 (AFIP 3138297).

Signalment: 16-year-old, female rhesus macaque (*Macaca mulatta*).

History: Two days prior to necropsy, the animal was lethargic and dehydrated with loss of appetite. Physical examination revealed an abdominal mass. Humane euthanasia was elected due to a poor response to supportive therapy.

Gross Pathology: The animal was dehydrated and in emaciated body condition. Multiple thrombi were present within the mesenteric vasculature, distal thoracic aorta, distal abdominal aorta and right iliac artery. An irregular multilobulated tan mass with distinct margins that measured up to 4 cm in greatest dimension was present involving the lateral aspect of the spleen. The liver was diffusely congested and the margins were rounded. Two firm round tan nodules, approximately 0.1 cm in diameter, were present near the margin of the left hepatic lobe. A large thrombus and associated hemorrhage were present in a large vessel within the pancreas. A vessel within the peripancreatic fat was thrombosed. Segments of the jejunum were black with sharply demarcated full-thickness necrosis. Necrosis of the cecal mucosa was present segmentally. The mesenteric vessels supplying necrotic intestinal segments were thrombosed. The contour of the renal cortex was mildly distorted with few depressed foci in the cortex.

Histopathologic Description: Pancreas: The walls of the small and medium sized arteries are circumferentially thickened up to five times normal with fibroblasts, fragmented collagen bundles, a mixed inflammatory infiltrate, extensive, often transmural foci of necrosis, and cellular and karyorrhectic debris (necrotizing vasculitis). The tunica intima and media are disrupted and the endothelium is denuded and necrotic with loss of the internal and external elastic laminae (**fig. 2-1**). The walls are multifocally replaced by bands of amorphous to flocculent, brightly eosinophilic material (fibrinoid necrosis). Transmurally, moderate numbers of lymphocytes, plasma cells, macrophages, and variable numbers of neutrophils are present. Lumina are stenotic and are partially or completely occluded with organized or organizing fibrin thrombi. Vasa vasorum of medium sized arteries are similarly affected. There are multifocal areas of hemorrhage and moderate numbers of hemosiderin-laden macrophages present in and around the walls of affected vessels. Multifocally, the lobules adjacent to the affected vessels are edematous with loss of acini and ducts

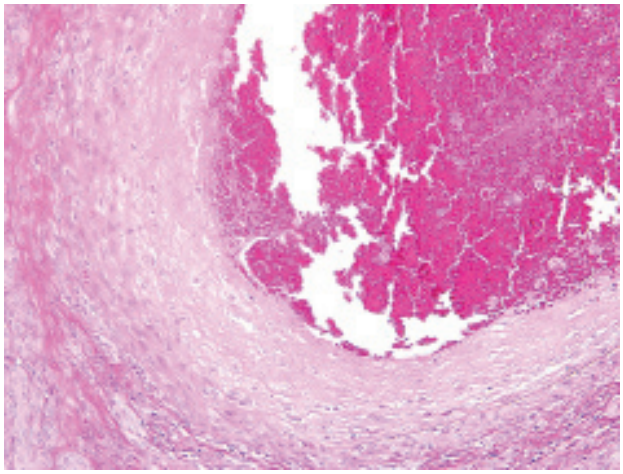

2-1 . Pancreas, artery, rhesus macaque. Diffusely, the vascular wall is markedly thickened up to 5x normal and the smooth muscle of the tunica media is replaced by dense fibrous connective tissue and reactive fibroblasts. Lumina are completely or partially occluded with organized fibrin thrombi. (HE 200x)

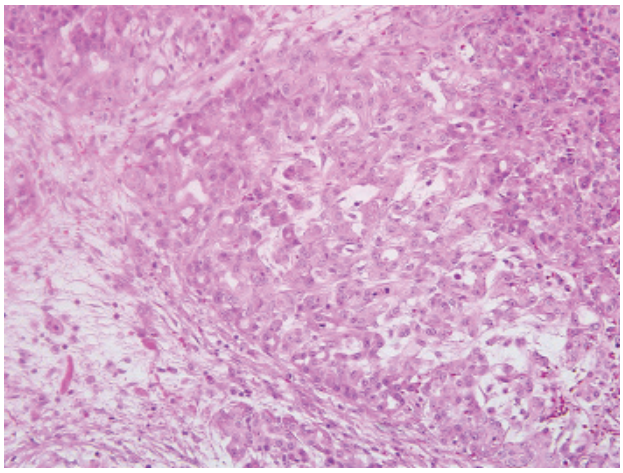

2-2. Pancreas, artery, rhesus macaque. Multifocally there is pancreatic acinar atrophy with loss of zymogen granules in the cytoplasm of epithelial cells. (HE 200x)

(**fig. 2-2**). Diffusely, within the affected areas, acini are dilated and there is zymogen granule depletion. Moderate numbers of fibroblasts within a basophilic matrix are also present. There is variation in the severity, chronicity and degree of inflammation of the lesion among the slides submitted. Within vessel lumina in some slides there is a population of round cells with distinct cell borders, small to moderate amounts of cytoplasm, and round to indented, centrally to eccentrically placed nucleus. Anisokaryosis is marked. There are generally one but up to three prominent nucleoli. Up to seven mitotic figures are present per high power field. Apoptotic cells are numerous.

Contributor's Morphologic Diagnosis:
1. Pancreas: Arteritis, chronic-active, proliferative, necrotizing, circumferential, transmural, severe with fibrinoid necrosis, luminal stenosis and thrombosis and multifocal pancreatic necrosis with atrophy and ectasia of acini.
2. Liver (not submitted): Arteritis, chronic-active, segmental to circumferential, transmural, severe with fibrinoid necrosis, luminal thrombosis, narrowing or obliteration of the vascular lumen, sclerosis and thickening of the arterial wall, perivascular accumulation of hemosiderin-laden macrophages, multifocal hepatic necrosis and loss of hepatic parenchyma rimmed by a lymphohistiocytic plasmacytic inflammatory infiltrate.
3. Kidney (not submitted): Arteritis, interlobular and arcuate arteries, chronic-active, circumferential, segmental, transmural, severe with fibrinoid necrosis, sclerosis and thickening of the arterial wall, hemorrhage, chronic-active, lymphoplasmacytic, tubulointerstitial nephritis, tubular dilatation, distortion, degeneration and regeneration, proteinaceous casts, neutrophilic casts, periglomerular, interstitial fibrosis and loss of nephrons.

Contributor's Comment: The primary finding in this case was severe, multisystemic arteritis with consequent ischemic change and loss of tissue elements in the kidneys, liver, spleen, pancreas, jejunum and cecum. Thrombi were observed grossly in the mesenteric arteries and the right iliac arteries. The gross and microscopic vascular lesions have features of polyarteritis nodosa (PAN).

Polyarteritis nodosa is a commonly occurring entity in humans. It is sporadically reported in many domestic species of animals and is characterized by necrotizing inflammation of small and medium sized arteries and most commonly involves arteries of the tongue, pancreas, heart, kidneys, mesentery, urinary bladder, testes, head and gastrointestinal tract. Impaired perfusion may result leading to hemorrhage, ulceration, infarction, and atrophy of affected tissues. The etiology is not clear; however, deposits of immune complexes have been localized in the affected arteries.[5] Microscopically, acute lesions are characterized by segmental or circumferential necrosis and fibrous thickening of the walls of arteries with varying degrees of inflammation and fibrinoid necrosis. Thrombosis of vessels may lead to infarction and hemorrhage. In chronic lesions, typically the walls may be completely fibrosed. Affected vessels may show lesions of all stages of development and both acute and

chronic lesions may be present in the same vessel.[4]

Polyarteritis nodosa is commonly reported in MRL and NZB mice that are prone to autoimmune diseases.[5] In rats with experimentally induced hypertension, the occurrence of PAN is related to amount of sodium chloride in the diet.[7] Also, experimentally, it has been induced with streptozotocin, nicotinamide and several other agents.[1] In dogs, PAN is associated with rheumatoid arthritis, systemic lupus erythematosus, and "beagle pain syndrome."[8] In blue foxes, it has been reported in association with *Encephalitozoon cuniculi* infection. Polyarteritis nodosa has been described in the brains of sows with reproductive disorders[3] and is reported to be associated with Border disease in sheep.[4] A single case of PAN has been reported in a cynomolgus monkey.[6]

The intravascular round cell population in this case was an unexpected finding. These cells were present only in areas supplied by lesioned vessels and were not present in the bone marrow. Nuclear pleomorphism, prominent and multiple nucleoli and high mitotic activity of the intravascular round cell population support malignancy; however, given the distribution it may be a response to the severe inflammation and ischemia present. The tan masses noted grossly within the spleen and liver corresponded to foci of necrosis and replacement fibrosis as a consequence of necrotizing arteritis and thrombosis. No neoplastic mass lesions were present.

AFIP Diagnosis: Pancreas: Arteritis, transmural, proliferative and necrotizing, chronic-active, multifocally extensive, marked, with luminal stenosis and multifocal pancreatic lobular atrophy and necrosis.

Conference Comment: As noted by the contributor, there is marked slide variation, and not all participants' slides featured the atypical proliferation of intravascular round cells described above. This case was reviewed in consultation with pathologists in AFIP's Department of Hematopathology, who concluded that the cells of interest most likely represent either malignant round cell neoplasia (i.e. lymphoma) or extramedullary hematopoiesis. Using additional materials kindly submitted by the contributor, immunohistochemical stains were performed on several serial tissue sections in an attempt to identify the cell of origin for the atypical intravascular round cells. Most of the atypical round cells exhibit positive cytoplasmic immunoreactivity for CD3, consistent with T-cell lymphoid origin; admixed with the CD3-positive atypical round cells are scattered B-cells that stain positively for CD79a and CD20. The atypical round cells are immunonegative for myeloperoxidase, hemoglobin, CD34, and CD117 (c-kit). The histologic and immunohistochemistry findings suggest an atypical lymphoid proliferation of T-cell origin, but we are uncertain whether the finding reflects hematopoiesis or neoplasia; the absence of neoplasia in other organs, as reported by the contributor, argues against a neoplastic process.

The contributor provides a succinct overview of PAN. Conference participants noted histopathologic similarities between the blood vessels in this case and those examined in the hearts of dogs with drug-induced vascular injury due to the administration of a phosphodiesterase inhibitor (see WSC 2009-2010, Conference 2, case III). Indeed, PAN is best regarded as a heterogenous group of arteritides, as evidenced by the assorted list of conditions that have been reported in association with the entity and summarized by the contributor. In humans, PAN is a vasculitis confined to small and medium-caliber arteries, with a predilection for branching points; arterioles, capillaries, and venules are spared, as is the pulmonary circulation. Many of the conditions that have been categorized as PAN in the veterinary literature adhere only loosely to the classic definition of PAN, and would more appropriately be referred to as systemic necrotizing vasculitides.[4]

As alluded to by the contributor, many cases of polyarteritis nodosa are thought to be caused by immune complex-mediated (type III) hypersensitivity, the pathogenesis of which is divided into three phases: 1) immune complex formation, 2) immune complex deposition, and 3) immune complex-mediated inflammation and tissue injury. Phase I, i.e. immune complex formation, occurs when antibody combines with antigen in the circulation (forming circulating immune complexes) or antigen that has been previously deposited in extravascular sites (forming in situ immune complexes). As described in the recent case of membranoproliferative glomerulonephritis (WSC 2009-2010, Conference 17, case III), the inciting antigens may be of either exogenous or endogenous origin. Hepatitis B virus antigens, for example, are incriminated as the inciting cause of a subset of human cases of PAN. Phase II, i.e. immune complex deposition, remains incompletely understood; however, it appears that medium-sized immune complexes formed in slight antigen excess are the most pathogenic. The distribution of immune complex deposition in part determines the distribution of resulting lesions. For example, systemic immune complex-mediated diseases result from immune complex deposition in many organs, while localized disease (e.g. glomerulonephritis, arthritis, or the Arthus reaction) results from deposition confined to specific tissues. Phase III is inflammation and tissue injury. Complement-fixing antibodies, i.e. IgG and IgM, activate complement via the classical pathway, yielding C3b and C4b as by-products; neutrophils and macrophages with receptors for these opsonins contribute

to inflammation and tissue injury. The importance of this pathway in tissue injury is underscored by the observation of decreased serum levels of C3, presumably due to consumption of complement, in humans in the active phase of a systemic type III hypersensitivity reaction. Additionally, some subclasses of IgG bind to leukocyte Fc receptors, exacerbating the inflammatory response to immune complex deposition.[2]

Contributor: Pathology Services Unit, Department of Animal Resources, Oregon National Primate Research Center, 505 NW 185th Avenue, Beaverton, Oregon 97006 http://onprc.ohsu.edu

References:

1. Baczako K, Dolderer M: Polyarteritis nodosa-like inflammatory vascular changes in the pancreas and mesentery of rats treated with streptozotocin and nicotinamide. J Comp Pathol **116**:171-180, 1997
2. Kumar V, Abbas AK, Fausto N, Aster JC: Diseases of the immune system. *In:* Robbins and Cotran Pathologic Basis of Disease, eds. Kumar V, Abbas AK, Fausto N, Aster JC, 8th ed., pp. 201-205. Saunders Elsevier, Philadelphia, PA, 2010
3. Liu CH, Yan-Han Chiang Y-H, Chu RM, Pang VF, Lee: High incidence of polyarteritis nodosa in the brains of culled sows. J Vet Med Sci **67**:125-127, 2005
4. Maxie MG, Robinson WF: Cardiovascular system. *In:* Jubb, Kennedy, and Palmer's Pathology of Domestic Animals, ed. Maxie MG, 5th ed., vol. 3, pp. 72-73. Saunders Elsevier, Philadelphia, PA, 2007
5. Percy DH, Barthold SW: Pathology of Laboratory Rodents and Rabbits, 2nd ed., p. 153. Iowa State University Press, Ames, IA, 2001
6. Porter BF, Frost P, Hubbard GB: Polyarteritis nodosa in a cynomolgus macaque. Vet Pathol **40**:570-573, 2003
7. Race GJ, Peschel E: Pathogensesis of polyarteritis nodosa in hypertensive rats. Circ Res **11**:483-487, 1954
8. Son WC: Idiopathic canine polyarteritis in control beagle dogs from toxicity studies. J Vet Sci **5**:147-150, 2004

CASE III: 09-A-270 (AFIP 3138303).

Signalment: 11.5-year-old, female rhesus macaque (*Macaca mulatta*) infected with SIVmac251.

History: This animal had been sedated for research related bronchoalveolar lavage several times during a study. The animal had persistent thrombocytopenia and leukopenia for four months before necropsy.

Gross Pathology: The animal was in good body condition. The right cranial lung lobe was soft, enlarged, edematous, and hemorrhagic. The caudal two thirds of the lobe were more severely affected and the caudal margin was overlain with a gray-white fibrinous exudate. The caudal half of the right middle lung lobe was partially demarcated by a serpiginous pale margin with hemorrhage and was depressed, dense, firm and tan. The pulmonary vessels in these lobes contained elongate mottled pale red and gray occlusive thrombi. There was mild, multifocal hemorrhage in the remaining right lung lobes and minimal hemorrhage in the left caudal lung lobe. The left lung lobes exhibited a fine black stippling.

Laboratory Results:

	Test and Value	Reference Range
RBC	5.26 x 10^6/mm^3	5.0 - 6.5 x 10^6/mm^3
WBC	2.0 x 10^3/mm^3	6.0 - 15.0 x 10^3/mm^3
Lymphocytes	56.1%	25.0 - 60.0%
Monocytes	20.5%	0.0 - 8.0%
Eosinophils	0.5%	0.0 - 5.0%
Platelets	66 x 10^3/mm^3	330 - 650 x 10^3/mm^3

Histopathologic Description: Within the section of lung is a focally extensive area of coagulative necrosis, hemorrhage, fibrin accumulation, edema and karyorrhectic and cellular debris (infarct) affecting almost 40% of the tissue. The infarct is rimmed by high numbers of fibroblasts and newly formed blood vessels (granulation tissue). Edema, fibrin and hemorrhage fill the alveolar spaces adjacent to the infarct. The rest of the lung is hyperemic and edematous. Moderate numbers of hemosiderin-laden macrophages, foamy macrophages, fewer neutrophils and occasional lymphocytes fill many alveoli. Multifocally, alveoli are lined by cuboidal epithelium (type II pneumocyte hyperplasia) and the septa are expanded with a small amount of collagen. Multifocally, the tunica intima of medium sized arteries is severely and circumferentially thickened with occlusion of the lumen. The tunica media is also thickened. The pleura is thickened with fibrous connective tissue, hemorrhage,

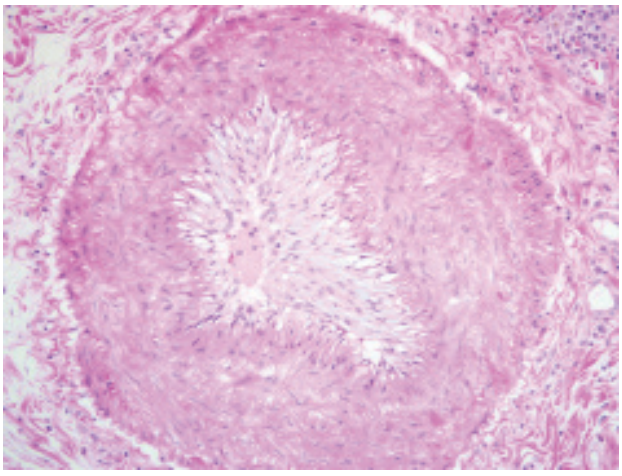

3-1. Lung, rhesus macaque. The tunica media of medium sized arteries is circumferentially thickened by fibroblasts, with almost complete occlusion of the lumen (HE 200x)

edema, fibrin and an inflammatory infiltrate composed of moderate numbers of neutrophils and few lymphocytes (**figs. 3-1 and 3-2**).

Contributor's Morphologic Diagnosis: Lung: Arteriopathy, proliferative, intimal and medial, multifocal, marked with hemorrhagic infarction.

Contributor's Comment: This animal had persistent thrombocytopenia, and grossly a thrombus was identified in a major vessel of one of the affected lung lobes. The three principal causes of thrombosis are endothelial injury, disruption in regular blood flow, and hypercoagulability.[2] As in this case, thrombi may cause infarction of the region downstream from the occluded vessel. Microscopic lesions in the lung included intimal and medial proliferation of the muscular arteries. The intimal proliferation resulted in luminal obstruction, reduced blood flow and consequent ischemic injury. It also served as a platform for clot formation within vessels. Proliferative arteriopathy characterized by endothelial cell activation and proliferation is associated with human immunodeficiency virus (HIV)[8] and simian immunodeficiency virus (SIV)[10,11] infections. Thrombosis of the pulmonary artery and vena cava has been reported in rhesus macaques infected with SIV.[3]

Thrombocytopenia usually results from either impaired production or enhanced destruction of platelets. In most cases it is due to immune mediated destruction of platelets or megakaryocytes or increased utilization of platelets as in disseminated intravascular coagulation. Thrombocytopenia is a common complication in HIV patients and SIV-infected macaques.[7] Although several factors attributable to thrombocytopenia have been identified, the precise mechanism of thrombocytopenia is unclear. Autoantibodies against platelet GPIIIa protein induces a hypercoagulable state by interacting with phospholipids and other clotting factors, thus causing platelet aggregation in HIV patients.[7] In SIV-infected rhesus macaques, synthesis of platelet autoantibodies results in increased phagocytosis of platelets.[1] Also, megakaryocytes express CD4 molecules and are productively infected by HIV/SIV resulting in decreased production of platelets. In addition, SIV-infected macaques develop cold agglutinins resulting in thrombocytopenia.[4]

In this animal, the endothelial cell activation, intimal proliferation, altered hemodynamics and blood hypercoagulability predisposed to clot formation. Vascular obstruction resulted in pulmonary infarction. The cause of thrombocytopenia in this case is most likely multifactorial and may be attributed to destruction of megakaryocytes by replicating virus, production of autoantibodies against platelet autoantigens and/or increased aggregation and removal of platelets.

Infectious diseases associated with thrombocytopenia in animals are provided in the table below:[2,9]

Species	*Etiology*
Cat	Feline immunodeficiency virus Feline leukemia virus Feline panleukopenia virus
Dog	Canine distemper virus *Ehrlichia canis*
Horse	Equine infectious anemia virus Equine arteritis virus African horse sickness virus
Cattle	Bovine viral diarrhea virus *Theileria parva* *Trypanosoma congolense* *Trypanosoma vivax*
Pig	African swine fever virus Hog cholera virus

AFIP Diagnosis: 1. Lung: Arteriopathy, proliferative, intimal and medial, multifocal, marked, with luminal occulusion, multifocal hemorrhagic coagulative necrosis with peripheral fibrosis (infarcts), and pleural fibrosis.
2. Lung: Alveolar histiocytosis and hemosiderosis, diffuse, mild to moderate, with type II pneumocyte hypertrophy and hyperplasia.

Conference Comment: This conference year we have reviewed several cases representing a variety of complications of SIV infection in rhesus macaques. The contributor's thoughtful comments outline a plausible

pathogenesis for this lesion while illuminating the otherwise rather inconspicuous link between thrombocytopenia and thrombosis. The contributor alluded to Virchow's triad of primary abnormalities that lead to thrombus formation, the components of which merit further discussion here.

Endothelial injury resulting in denudation of the endothelium exposes the subendothelial extracellular matrix, allowing platelet adhesion, release of tissue factor, and local depletion of antithrombotic prostaglandin (PG) I_2 and plasminogen activators. More inclusively, this vertex of Virchow's triad might be termed *endothelial dysfunction,* since any disturbance in the balance of pro- and antithrombotic activities may lead to thrombosis. Specifically, dysfunctional endothelium is characterized by relatively increased production of procoagulant factors (e.g. tissue factor, platelet adhesion molecules, plasminogen activator inhibitors) and decreased production of anticoagulant factors (e.g. thrombomodulin, PGI_2, tissue plasminogen activator); insults that lead to this type of endothelial dysfunction are varied and include, among others, turbulent blood flow, hypertension, endotoxins, and hypercholesterolemia.[5]

Altered blood flow, or turbulence, not only causes endothelial dysfunction as described above, but also causes the formation of pockets of stasis. Normal blood flow is laminar, which maintains platelets in the center of the vessel lumen; areas of stasis lack laminar flow, bringing platelets into contact with the endothelium and thus promoting thrombosis. Moreover, blood in areas of stasis becomes stagnant; activated clotting factors are not readily diluted and washed away from these areas; and clotting factor inhibitors do not flow into them.[5]

Hypercoagulability, also referred to as thrombophilia, is the third vertex of Virchow's triad. While a number of hereditary causes of hypercoagulability are described in human medicine, acquired hypercoagulability is more commonly encountered in veterinary medicine, and is often multifactorial. For instance, coagulation factor I may be elevated due to inflammation, stress, tissue necrosis, while factors I and VIII may be elevated due to trauma or hyperthyroidism. Conversely, depletion of antibrombin III, a common complication of the nephrotic syndrome, leads to hypercoagulability via loss of thrombin inhibition.[5,6]

The conference moderator noted that anatomic location is of critical importance in determining the consequences of thrombosis. While thrombosis in the heart or brain is likely to cause catastrophic infarction, organs like the liver and lung, which have collateral circulation, are less prone to clinically significant infarction.

Selected causes of thrombosis, categorized by their respective vertices of Virchow's triad, are summarized below:[6]

Causes of Thrombosis

Mechanism	Examples
Endothelial Injury / Dysfunction	Nematodiasis (*Strongylus vulgaris* larvae, dirofilariasis, angiostrongylosis, spirocercosis) Bacterial infection (salmonellosis, mannheimiosis, erysipelas, histophilosis) Viral infection (arterivirus, morbillivirus, herpesvirus, orbivirus, pestivirus) Fungal infection (aspergillosis, zygomycosis) Disseminated intravascular coagulation (DIC) Vitamin E / selenium deficiency Immune-mediated vasculitis Endotoxin
Altered Blood Flow	Gastric dilation and volvulus Intestinal torsion or volvulus Cardiomyopathy Hypovolemia Aneurysm
Hypercoagulability	Increased clotting factor activation (neoplasia, DIC) Antithrombin III deficiency (nephrotic syndrome, DIC, liver disease) Increased platelet activity (diabetes mellitus, neoplasia, dirofilariasis, uremia) Metabolic abnormalities (hyperthyroidism, hyperadrenocorticism)

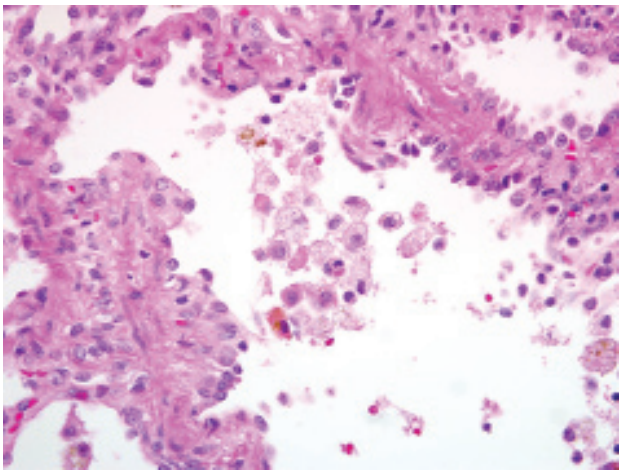

3-2. Lung, rhesus macaque. Multifocally, alveoli are lined by hypertrophied and hyperplastic type II pneumocytes and contain vacuolated and hemosiderin-laden macrophages. (HE 400x)

Contributor: Pathology Services Unit, Department of Animal Resources, Oregon National Primate Research Center, 505 NW 185th Avenue, Beaverton, Oregon 97006 http://onprc.ohsu.edu

References:

1. Dittmer U, Coulibaly C, Sauermann U, Stahl-Hennig C, Petry H, Hunsmann G, Kaup FJ: Autoantibody-mediated platelet phagocytosis in SIV-infected macaques. AIDS **8:**1509, 1994
2. Jones TC, Hunt RD, King NW: Veterinary Pathology, 6th ed., p. 161. Williams & Wilkins, Baltimore, MD 1997
3. Kuwata T, Nishimura Y, Whitted S, Ourmanov I, Brown CR, Dang Q, Buckler-White A, Iyengar R, Brenchley JM, Hirsch VM: Association of progressive CD4(+) T cell decline in SIV infection with the induction of autoreactive antibodies. PLoS Pathog **5**:e1000372. Epub 2009
4. Mandell CP, Spinner A: Cold agglutinins in rhesus macaques infected with simian immunodeficiency virus. Compara Haem Inter **7:**238-242, 1997
5. Mitchell RN: Hemodynamic disorders, thromboembolic disease, and shock. *In:* Robbins and Cotran Pathologic Basis of Disease, eds. Kumar V, Abbas AK, Fausto N, Aster JC, 8th ed., pp. 121-126. Saunders Elsevier, Philadelphia, PA, 2010
6. Mosier DA: Vascular disorders and thrombosis. *In:* Pathologic Basis of Veterinary Disease, eds. McGavin MD, Zachary JF, 4th ed., pp. 86-91. Mosby Elsevier, St. Louis, MO, 2007
7. Onlamoon N, Pattanapanyasat K, Ansari A: Human and nonhuman lentiviral infection and autoimmunity. Ann NY Acad Sci **1050:**397-409, 2005
8. Perez-Atayde AR, Kearney DI, Bricker JT, Colan SD, Easley KA, Kaplan S, Lai WW, Lipshultz SE, Moodie DS, Sopko G, Starc TJ, P2C2 HIV Study Group: Cardiac, aortic, and pulmonary arteriopathy in HIV-infected children: the prospective P2C2 HIV multicenter study. Pediatr Dev Pathol **7:**61-70, 2004
9. Russell KE, Grindem CB: Secondary thrombocytopenia. *In:* Schalm's Veterinary Hematology, eds. Feldman BF, Zinkl JG, Jain NC, 5th ed., pp. 487-495. Lippincott Williams & Wilkins, Baltimore, MD, 2000
10. Shannon RP, Simon MA, Mathier MA, Geng YJ, Mankad S, Lackner AA: Dilated cardiomyopathy associated with simian AIDS in nonhuman primates. Circulation **101:**185-193, 2000
11. Yanai T, Lackner AA, Sakai H, Masegi T, Simon MA: Systemic arteriopathy in SIV-infected rhesus macaques (*Macaca mulatta*). J Med Primatol **35:**106-112, 2006

CASE IV: 09-22 1 (AFIP 3139388).

Signalment: 23-year-old, male rhesus macaque (*Macaca mulatta*).

History: The animal was part of a long term visual-based cognition study. Cephalic implants and circumferential scleral search coils had been surgically placed. Euthanasia was performed due to a history of chronic weight loss and failure to thrive.

Gross Pathology: Overall, the animal was in fair body condition with petechiae on the skin of the inguinal region bilaterally, as well as multifocally on the abdomen. The liver and spleen were both enlarged with diffuse pallor. There was a 3 mm deep, focal surface depression of the cortex of the left kidney, and on cut section the cortex also contained a focal, 1 cm diameter cyst. Marked degenerative changes were also seen in both stifles, with the left medial condyle in particular being irregular and roughened.

Histopathologic Description: Splenic architecture is diffusely effaced by marked deposits of amorphous, smudgy to finely fibrillar, extracellular eosinophilic substance (amyloid). This material fills and expands the parenchyma, and especially replaces the microanatomic regions of white pulp and also imparts a nodular pattern to its deposition. There is associated compression of the

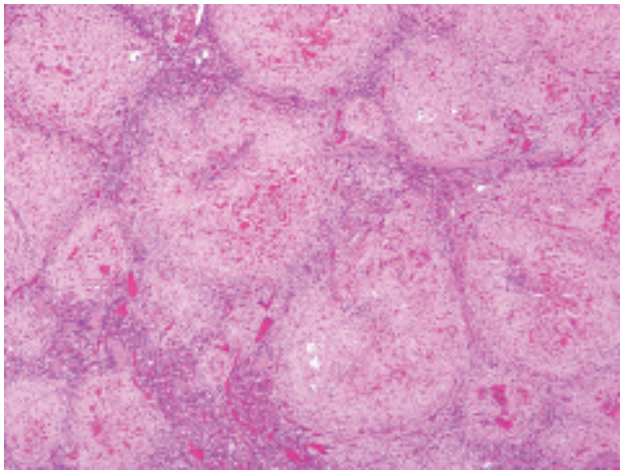

4-1. Spleen, dog. Diffusely filling splenic sinuses in the red pulp and replacing lymphocytes in the white pulp is abundant extracellular amorphous, eosinophilic, hyaline proteinaceous material (amyloid). (HE 100x)

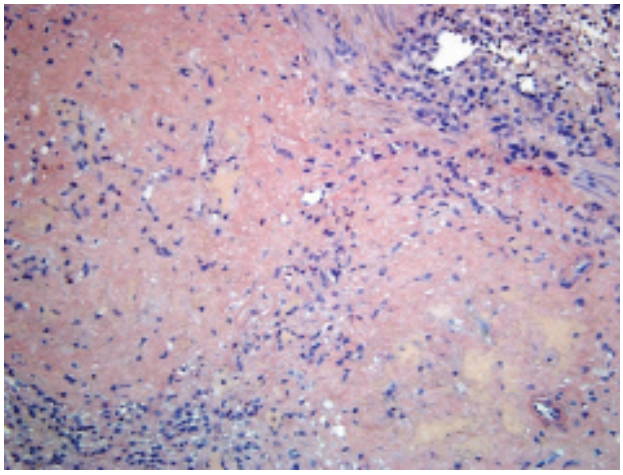

4-2. Spleen,dog. The eosinophilic, waxy, plaque-like material is diffusely congophilic. (Congo Red 200x)

adjacent red pulp regions, although many of the blood vessels are distended and congested. Foci of hemorrhage are also seen within the nodular amyloid deposits (**figs. 4-1 and 4-2**).

Contributor's Morphologic Diagnosis: Diffuse splenic amyloidosis.

Contributor's Comment: Amyloidosis is a disease caused by extracellular deposition of insoluble abnormal fibrils, derived from aggregation of misfolded, normally soluble, protein. The name amyloid originates from results of early crude iodine-staining techniques that led to the mistaken identification of the protein material as starch. Serum amyloid A (SAA) proteins comprise a family of vertebrate proteins that associate predominantly with high density lipoproteins (HDL). All amyloid fibrils share a common cross-ß-pleated sheet core structure, with the polypeptide chains running perpendicular to the fibril long axis, regardless of the particular protein from which they are formed. Fibrils are usually about 10 nm in diameter, and are straight, rigid, and nonbranching. Numerous biochemically distinct amyloid proteins have been characterized in humans and animals, but the three most common types are as follows: 1) AA (amyloid-associated) (a unique non-immunoglobulin protein synthesized by the liver); 2) AL (derived from plasma cells and contains immunoglobulin light chains); and 3) Aß (ß-amyloid protein found in cerebral lesions of Alzheimer disease).

Amyloidosis may be primary or secondary. Primary amyloidosis arises due to overproduction of the immunoglobulin light chain and may be neoplastic or genetic in origin. Secondary, or reactive systemic amyloidosis is a complication of chronic infections and inflammatory conditions and is characterized by a sustained acute phase response. Although the pathogenesis of reactive systemic amyloidosis is poorly understood, it is associated with persistently increased production of SAA (thus making SAA a major acute phase reactant). Although its major physiological function remains unclear, SAA is produced under the control of numerous cytokines, including interleukin-1, interleukin-6 and tumor necrosis factor-α released during inflammation. Increased levels of SAA are common in chronic inflammation, but amyloid deposition usually does not occur. In individuals that do develop amyloidosis, there is limited or defective SAA proteolysis with formation and deposition of insoluble AA protein. Proposed underlying mechanisms include failure of degradation due to excess levels of SAA relative to enzyme; an intrinsic proteolytic enzyme defect; or a structural defect in the SAA molecule that makes it resistant to degradation. The end result, however, is that accumulated amyloid deposits cause pressure atrophy of surrounding tissues, thus impairing normal body function and resulting in organ failure and ultimately death.

Reactive systemic amyloidosis is not uncommon in rhesus macaques, and has additionally been reported in other nonhuman primates (including common marmosets, squirrel monkeys, pigtail macaques, Celebes macaques, cynomolgus macaques, a stumptailed macaque, baboons, a mangabey and chimpanzees). The condition has been associated with chronic vascular catheterization, as well as underlying conditions such as rheumatoid arthritis, retroviral infection, parasitism, and enterocolitis. Amyloid deposition is most frequently seen in the space of Disse in the liver, the lamina propria of the gastrointestinal tract, the corticomedullary

junction of the adrenal gland, either the red or white pulp of the spleen, and the renal medullary interstitium. The small intestine is the region of the gastrointestinal tract most often and most severely affected. Renal glomerular involvement is rare, except in marmosets.

Clinical signs are related to the affected site as well as the amount of amyloid deposited, but include weight loss, diarrhea, and hepatosplenomegaly. Protein losing enteropathy may accompany enteric amyloidosis. Laboratory findings may include elevated levels of SAA, hypoproteinemia, hypoalbuminemia, hypergammaglobulinemia, and elevated liver enzymes with hepatic involvement. There is, however, no reliable diagnostic assay, preventive measure or treatment for secondary amyloidosis. Although gross postmortem lesions are often absent, the liver and/or spleen may be massively enlarged, pale, waxy and firm. Prominent splenic nodules may be seen cut section, and the intestinal mucosa may be thickened. With the light microscope and hematoxylin and eosin staining, amyloid appears as an amorphous, eosinophilic, extracellular substance. Its differentiation from other similar appearing materials, like fibrin and collagen, depends on the pathognomonic, red-green birefringence observed when preparations correctly stained with Congo red are viewed in intense unidirectional polarized light. This optical effect is produced by alignment of the dye molecules along the protein fibrils.

AFIP Diagnosis: Spleen, white pulp: Amyloidosis, nodular, diffuse, marked, with lymphoid depletion and loss.

Conference Comment: The contributor provides an exemplary review of amyloidosis, and the fairly classic example provided herein features the typical pattern of amyloid deposition in the spleen, with the white pulp being primarily affected and compressing the adjacent red pulp. The following table, adapted from Snyder summarizes the most commonly encountered amyloidoses in veterinary medicine:[10]

Amyloidosis

Category	Associated Diseases	Major Fibril Protein	Precursor Protein
Systemic			
Primary amyloidosis (immunocyte dyscrasias)	Multiple myeloma Monoclonal B cell proliferations	AL	Immunoglobulin light chains
Secondary amyloidosis (reactive systemic amyloidosis)	Chronic inflammation	AA	SAA
Familial amyloidosis (may be systemic and/or localized)	Amyloidosis in Shar-Pei dogs (renal medullary interstitium), Abyssinian cats (renal glomeruli), and Siamese cats (liver)	AA	SAA
Localized			
Amyloid of aging	Senile plaques Cerebral amyloid angiopathy Neurodegenerative disease	Aß	APP
Endocrine tumors	Thyroid C cell tumors	A Cal	Calcitonin, polypeptide hormones and/ or prohormones
Islets of Langerhans	Diabetes mellitus	IAPP	IAPP
Isolated amyloid of pulmonary vasculature		Apolipoprotein A-1	Apolipoprotein A-1
Prion diseases	Transmissible spongiform encephalopathies	Misfolded prion protein (PrP^{sc})	Normal prion protein (PrP)

AL = amyloid light chain; AA = amyloid associated; SAA = serum amyloid A; APP = amyloid precursor protein; A Cal = amyloid of hormone origin; IAPP = islet amyloid polypeptide

Contributor: Division of Comparative Medicine, Massachusetts Institute of Technology, 77 Massachusetts Avenue, Cambridge, MA 02139
http://web.mit.edu/comp-med/

References:

1. Abbas AK: Diseases of immunity: amyloidosis. *In:* Robbins and Cotran Pathologic Basis of Disease, eds. Kumar V, Abbas AK, Fausto N, 7th ed., pp. 258-264. Elsevier, Philadelphia, PA, 2005
2. Blanchard JL: Generalized amyloidosis, nonhuman primates. *In:* Monographs on Pathology of Laboratory Animals: Nonhuman Primates I, eds. Jones TC, Mohr U, Hunt RD, pp. 194-197. Springer-Verlag, Berlin Heidelberg, Germany, 1994
3. Cohen AS: General introduction and a brief history of the amyloid fibril. *In:* Amyloidosis, eds. Marrink J, Van Rijswijk MH, pp. 3-19. Nijhoff, Dordrecht, The Netherlands, 1986
4. Hukkanen RR, Liggitt HD, Anderson DM, Kelley ST: Detection of systemic amyloidosis in the pig-tailed macaque (*Macaca nemestrina*). Comp Med **56:**119-127, 2006
5. Jakob W: Spontaneous amyloidosis of mammals. Vet Pathol **8:**292-306, 1971
6. Ludlage E, Murphy CL, Davern SM, Solomon A, Weiss DT, Glenn-Smith D, Dworkin S, Mansfield KG: Systemic AA amyloidosis in the common marmoset. Vet Pathol **42:**117-124, 2005
7. MacGuire JG, Christe KL, Yee JL, Kalman-Bowlus AL, Lerche NW: Serologic evaluation of clinical and subclinical secondary hepatic amyloidosis in rhesus macaques (*Macaca mulatta*). Comp Med **59:**168-172, 2009
8. Pepys MB: Amyloidosis. Ann Rev Med **57:**223-241, 2006
9. Puchtler H, Sweat F, Levine M: On the binding of Congo red by amyloid. J Histochem Cytochem **10:**355–64, 1962
10. Snyder PW: Diseases of immunity. *In:* Pathologic Basis of Veterinary Disease, eds. McGavin MD, Zachary JF, 4th ed., p. 248. Mosby Elsevier, St. Louis, MO, 2007

The Armed Forces Institute of Pathology
Department of Veterinary Pathology

Conference Coordinator:
Shannon Lacv. DVM. MPH

WEDNESDAY SLIDE CONFERENCE 2009-2010

Conference 20

7 April 2010

Conference Moderator:

Donald H. Schlafer DVM, MS, PhD, Diplomate ACVP, Diplomate ACVM,

CASE I: AFIP Case 2 (AFIP 3066307).

Signalment: 12-year-old, female, Quarterhorse mare (*Equus caballus*); placental tissues retrieved at 310 days of gestation.

History: Placental tissues submitted were from a 12-year-old, multiparous, Quarterhorse mare. The mare produced a live foal in 2006. The mare was pregnant in 2007 with a thickened placenta detected by ultrasound at 290 days of gestation. The animal was treated medically for placentitis and delivered a live foal naturally at 310 days of gestation. The placenta was submitted for laboratory analysis.

Gross Pathology: Gross examination revealed a large region of placentitis on the dorsal chorionic surface near the cervical star. The placentitis was characterized by a markedly thickened placenta that was discolored brown and covered with a "mucoid-type" film. Gross morphologic diagnosis: Placentitis, cervical star region of the body.

Laboratory Results: Aerobic bacterial culture: Trace numbers of *Delftia acidovorans, Acinetobacter lwoffi* and *Staphylococcus epidermidis*. Fungal culture: *Bipolaris* sp.

Histopathologic Description: Histopathology revealed focally severe inflammation (suppurative and pyogranulomatous) along the chorionic surface with small bacterial rods, fungal hyphae and cellular debris. On H&E stains, the fungi (depending on the section) are inconspicuous. Of those present, few are pigmented. On GMS, the numbers and morphology of fungi are evident. The fungi are characterized by hyphae exhibiting non-parallel walls, 3-7 µm in width with occasional septa and branching. Branching occurs at both right and acute angles (**figs. 1-1 and 1-2**).

Contributor's Morphologic Diagnosis:
1. Placenta: Marked pyogranulomatous placentitis, chronic with necrosis and squamous metaplasia.
2. Amnion: Membrane hyperplasia with moderate funisitis.

Contributor's Comment: Placentitis is an important cause of equine reproductive loss with some variations in etiologies based upon the geographic distribution of the mares. *Streptococcus zooepidemicus, Escherichia coli, Pseudomonas aeruginosa, S. equisimilis, Enterobacter* sp. and *Klebsiella pneumonia* are bacterial agents most frequently isolated.[1] The distribution of the placentitis has important implications for the etiopathogenesis.[1,2] A diffusely distributed placentitis is more often found

***Sponsored by the American Veterinary Medical Association, the American College of Veterinary Pathologists, and the C. L. Davis Foundation.**

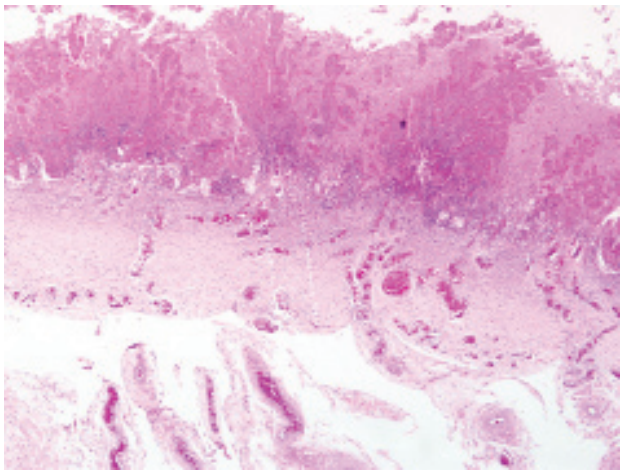

1-1. Placenta, chorioallantois, horse. Diffusely, the chorionic epithelium is disrupted and replaced by inflammatory cells and necrotic cellular debris, and the wall of the placenta is edematous and congested. (HE 40x)

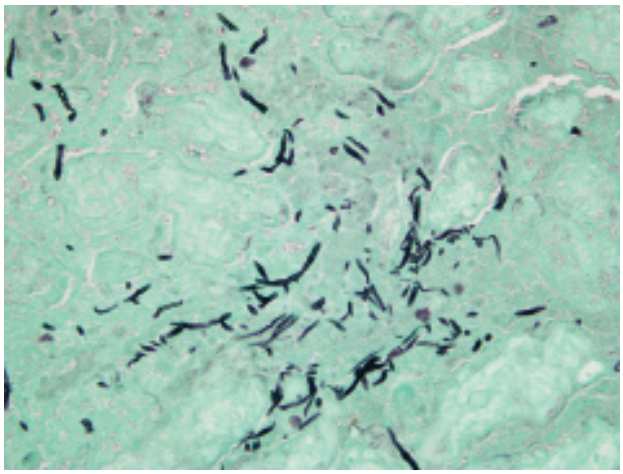

1-2. Placenta, chorioallantois, horse. There are numerous fungal hyphae measuring 3-7 um in width, characterized by non-parallel cell walls, occasional septae, and acute and right angle branching (GMS 200x)

in early reproductive losses (mid-gestation or earlier), whereas focal placentitis, particularly at/or near the cervical star, is most frequently found in late gestational losses. Diffuse placentitis is the result of hematogenous infection; focal placentitis is associated with an ascending infection through the cervix.

Though recognized less often than bacterial placentitis, mycotic placentitis is still an important cause of reproductive loss. Mycotic placental infections are typically characterized by brown, thickened "leathery" lesions at the cervical star that indicates (as above) an ascending route of infection. Ascending mycotic infections can result in lesions restricted to the placenta only. Historically, this was hypothesized to be the reason for the delay in recognizing the importance of fungal abortions as well as the reason for the plea to submit fetal membranes along with the fetus for an accurate diagnostic work-up.[3] Certainly, the mycotic lesions can spread to the amnion and the fetus as well.

This horse was part of a group of horses that was under continual gestational monitoring and the placentitis was recognized and treated. The mare entered an uncomplicated parturition and the foal was born alive and healthy and as of this writing (4 months later) remains healthy. Unfortunate outcomes include fetal loss due to separation of the placenta or placental insufficiency or perinatal loss as an extension of either placental insufficiency (hypoxia) or infection of the fetus with the microorganisms causing the placentitis. In this case, there were trace numbers of bacteria and a dematiaceous fungus (*Bipolaris* sp.) isolated from the fetal membranes. Teeming numbers of fungi were seen associated with the placental lesion on GMS stains; however, on H&E stains, only a minority of the fungal hyphae seen was pigmented. As *Bipolaris* sp. exhibits rapid "take-over" growth in vitro, it is possible that a second fungal isolate was obscured. Otherwise, the inconspicuous nature of the pigmentation seen on H&E may be related to the age of the fungal growth within the lesion (intensity of pigmentation increases with time).

AFIP Diagnosis: Chorioallantois: Placentitis, fibrinonecrotizing, diffuse, marked, with fibrin thrombi, edema, reactive allantoic epithelial hypertrophy, and fungal hyphae.

Conference Comment: We thank the contributor for generously providing the additional GMS-stained slides for distribution to all WSC participants. There is considerable slide variation in the H&E-stained slides and in the conspicuousness of the fungal hyphae. The GMS method reveals myriad fungal hyphae, underscoring the utility of special histochemical stains for inflammatory lesions of suspected mycotic etiology.

In addition to the microscopic lesions described by the contributor, participants noted that the allantoic epithelium is diffusely cuboidal to columnar (i.e. reactive), in contrast to the squamous epithelium typical of the normal equine allantoic membrane. The histologic finding of reactive allantoic epithelium may be of particular diagnostic utility in cases with suboptimal sampling of the affected chorion, such as in cases with only focal or multifocal placentitis where inflammation is not present in the microscopic sections, because it usually occurs as a diffuse change and

suggests inflammation somewhere in the placenta. The large size of the equine allantois as a proportion of the entire fetal membranes renders the finding of reactive allantoic epithelium a useful microscopic "sentinel" for inflammation elsewhere in the placenta. This is well-illustrated by the finding in this case that both severely and minimally affected areas of chorion are present in most sections, but the allantoic epithelium is diffusely reactive. Additionally, participants noted foci of coagulative necrosis in the chorion; these are interpreted as areas of ischemia secondary to thrombosis, as substantiated by the presence of variable numbers of vascular thrombi in the section.

In both mares and cows with mycotic placentitis, *Aspergillus fumigatus* is the most frequent isolate; however, significant species differences in distribution reflect a fundamental disparity in pathogenesis. In mares, fungi usually ascend through a patent cervix, resulting in a chronic, focally extensive placentitis in the region of the cervical star. In cattle, by contrast, lesions initially develop in placentomes, reflecting hematogenous arrival from rumen or pulmonary infections.[4]

Prior to the conference, the moderator reviewed comparative placentation with conference participants, emphasizing equine placentation and placental pathology. As discussed by the contributor, lesion distribution is of tremendous diagnostic significance for elucidating the etiopathogenesis of equine placentitis. As described above, many infectious agents ascend through the cervix to cause a focally extensive placentitis that originates near the cervical star. One exception is *Leptospira* spp., which characteristically produce a diffuse placentitis with numerous spirochetes demonstrated with special silver stains, particularly in the stroma.[1] A second exception is nocardiaform placentitis, caused by several genera of gram-positive, branching, filamentous actinomycetes (i.e. *Crossiella equi, Streptomycin* sp., *Amycolatopsis* sp.), which is typically localized to the cranial uterine body and entrance to the uterine horns and does not communicate with the cervical star.[4]

Finally, the conference moderator noted that syncytia and focal areas of mineralization are normal findings in the equine chorioallantois, but may increase in pathologic conditions. Other normal components of the equine placenta that may be confused with lesions were reviewed, including amniotic plaques, hippomanes, chorioallantoic pouches, allantoic pouches, and the yolk sac remnant.

Contributor: Department of Veterinary Pathobiology and Oklahoma Animal Disease Diagnostic Laboratory, College of Veterinary Medicine, Oklahoma State University, Stillwater, OK 74074
http://www.cvm.okstate.edu

References:

1. Hong CB, Donahue JM, Giles Jr. RC, Petrites-Murphy MB, Poonacha KB, Roberts AW, Smith BJ, Tramontin RR, Tuttle PA, Swerczek TW: Etiology and pathology of equine placentitis. J Vet Diagn Invest **5:**56-63, 1993
2. Hong CB, Donahue JM, Giles Jr. RC, Petrites-Murphy MB, Poonacha KB, Roberts AW, Smith BJ, Tramontin RR, Tuttle PA, Swerczek TW: Equine abortion and stillbirth in central Kentucky during 1988 and 1989 foaling seasons. J Vet Diagn Invest **5:**560-566, 1993
3. Mahaffey LW and Adam NM: Abortions associated with mycotic lesions of the placenta in mares. J Am Vet Med Assoc **144:**24-32, 1964
4. Schlafer DH, Miller RB: Female genital system. *In:* Jubb, Kennedy, and Palmer's Pathology of Domestic Animals, ed. Maxie MG, 5th ed., vol. 3, pp. 507-509. Saunders Elsevier, Philadelphia, PA, 2007

CASE II: 09-30175 (AFIP 3139936).

Signalment: 3-month-old, male, Clydesdale horse (*Equus caballus*).

History: Not reported.

Gross Pathology: The parenchyma of both testes is diffusely dark brown to black. Within one testis is an approximately 1 cm diameter, well circumscribed, white to tan, firm mass.

Histopathologic Description: Within the testis and compressing the adjacent parenchyma is an approximately 2 x 1.5 cm expansile, unencapsulated mass composed of large nodules of cartilage surrounded by a mix of adipose tissue, neural tissue, often lined by ependymal epithelium, myxomatous mesenchymal tissue, mature connective tissue with occasional glandular structures lined by cuboidal to columnar epithelial cells, and small foci of smooth muscle and skeletal muscle (**figs. 2-1 and 2-2**). The seminiferous tubules are small and hypocellular and present within an abundant, mesenchymal matrix. A large number of polygonal cells containing abundant, globular,

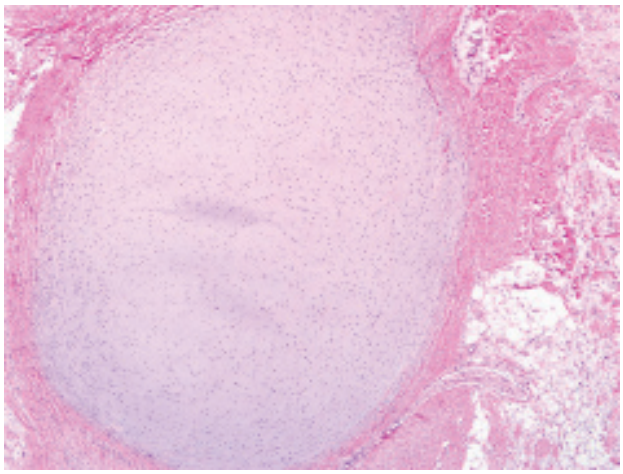

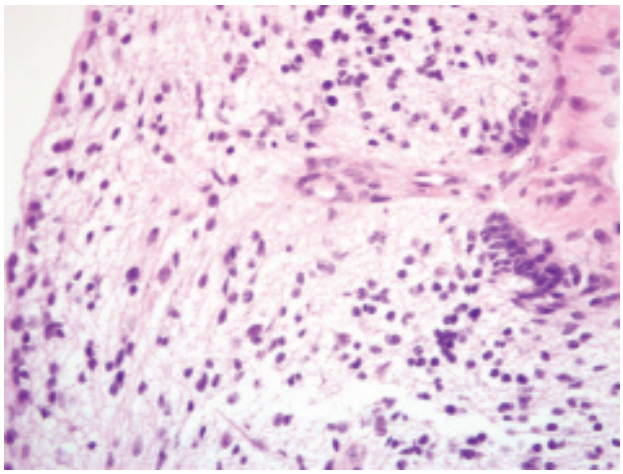

2-1 and 2-2. Teratoma, testis, horse. Multifocally within the neoplasm are large areas of cartilage, adipose tissue (2-1), and neuropil (2-2). (HE 40x, HE 200x)

intracytoplasmic, golden-brown pigment (lipochrome) are present within the interstitium surrounding most of the seminiferous tubules (**fig. 2-3**). A similar smaller mass is present within the contralateral testis. Note that not all sections of teratoma show all the features listed above.

Contributor's Morphologic Diagnosis: Testes: Bilateral teratomas.

Contributor's Comment: A teratoma is a benign germ cell tumor in which the cells have undergone somatic differentiation, producing mature but disorganized tissues of two or more embryonic layers.[1] They are thought to be parthenogenic tumors derived from a single germ cell that has completed its first meiotic division, but not its second.[6] This case was unusual in that the teratomas occurred in such a young, non-cryptorchid foal, and that they were bilateral.

Teratomas of the testis are the most frequently reported testicular tumor in young horses and are more commonly found in cryptorchid testes.[1] To the contributor's knowledge, there are two published reports in horses less than a year old, one in a cryptorchid, neonatal 3 day old foal[5] and the other a cryptorchid 4-day-old foal,[4] in which the spermatic cord entrapped the small colon resulting in signs of abdominal pain. It is thought that testicular teratomas may be congenital[4] and that their presence in a fetal testis may prevent normal descent,[1,4] although this may depend on the size of the tumor relative to the size of the inguinal canal at the time of testicular descent.[4] There have been no reports, to the contributor's knowledge, of bilateral testicular teratomas in horses.

Grossly, teratomas may be single or multiple and often have a cystic or multilobular structure. Hair and mucoid or sebaceous-like secretions are often seen on cut section (and these are sometimes referred to as "dermoid cysts") as well as yellow-white masses with fibrous, adipose, cartilaginous, and bony tissue.[1] Histologically, teratomas are composed of structures derived from all embryonic germ layers, including ectodermal, neuroectodermal, endodermal, or mesodermal.[1] The presence of nervous and adipose tissue is very common.

The remainder of the testicular parenchyma in this foal is normal for the age of the horse. The seminiferous tubules are immature, as spermatogenesis is not initiated until approximately 2 years of age.[2] From a fetal gestational age of 155 days to 1 year old, the seminiferous epithelium consists of gonocytes and Sertoli cells. Another interesting feature of these testes was the dark-brown discoloration grossly, and the abundant pigmented interstitial cells present around immature seminiferous tubules histologically. This is also a normal feature for testes from a foal of this age (3 months). These pigmented cells are not present between fetal gestational ages 155 days to 248 days, but are present in large numbers in the neonatal 3-day-old testis. They increase to reach a maximum number at 2 months of age, and then gradually diminish and disappear by 3 years of age.[2] A morphologic study on these pigmented cells of the horse testis found that ultrastructurally, they were characterized by the presence of abundant residual bodies consisting of secondary lysosomes, having variable internal structures, and an eccentrically located nucleus.[3] In combination with histochemical staining, it was suggested that the pigmented granules found within the pigmented cells have some characteristics of ceroid.

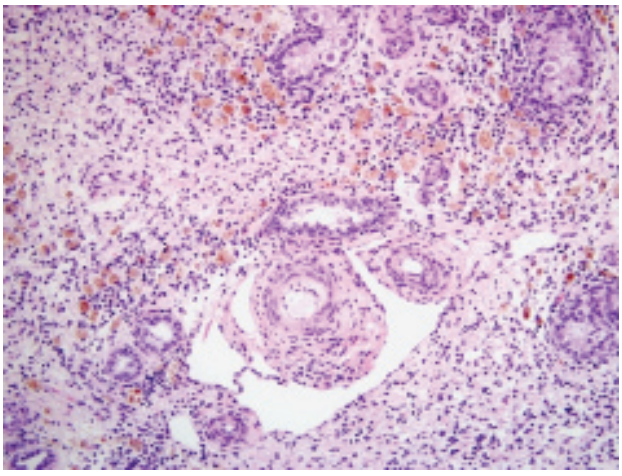

2-3. Teratoma, testis, horse. Polygonal cells containing abundant, globular, intracytoplasmic, golden-brown pigment (lipochrome) are present in the interstitium surrounding small, hypoplastic seminiferous tubules. (HE 200x)

It is hypothesized that these pigmented cells may be derived from macrophages which are phagocytizing the degenerating fetal type of interstitial cells, and that they gradually increase in volume by storing digested materials as ceroid-like pigment.[2,3]

AFIP Diagnosis: Testis: Teratoma.

Conference Comment: As mentioned by the contributor, there is substantial slide variation in this case. On the surface, this is an apparently undemanding example of a teratoma of the young horse. However, several findings in this case are particularly intriguing. Foremost is the highly unusual bilateral occurrence. Furthermore, the neoplasm is more common in cryptorchid testes, in which it may prevent testicular descent. Finally, the conference moderator noted that the absence of skin and hair in equine teratoma is fairly atypical.

While gonadal teratomas are uncommon, still rarer are the extragonadal teratomas, the most common form of which is the dentigerous cyst, usually found at the base of the ear in horses. Extragonadal teratomas are well-documented in humans, and sporadically reported in other domestic, wild, and laboratory species. Specifically, adrenal teratomas have been reported in humans, ferrets, an ox, and a rat. Interestingly, extragonadal teratomas are thought to arise from diploid pluripotent progentior cells that escape embryonal organizers during maturation, in divergence from the histogenesis of gonadal teratomas described by the contributor.[7]

Of equal or perhaps greater interest are the pigmented interstitial cells, which garnered the bulk of the discussion during the conference, and remain fairly enigmatic. What little is known about these cells is well-summarized by the contributor; from a diagnostic standpoint, it is important to recognize them as normal structures in the neonatal foal testis.

Contributor: Cornell University, College of Veterinary Medicine, Department of Biomedical Sciences, S2-121 Schurman Hall, Ithaca, NY 14850
http://www.vet.cornell.edu/

References:

1. Foster RA, Ladds PW: Male genital system. *In:* Jubb, Kennedy, and Palmer's Pathology of Domestic Animals, ed. Maxie MG, 5th ed., vol. 3, pp. 598-600. Saunders Elsevier, Philadelphia, PA, 2007
2. Hondo E, Murabayashi H, Hoshiba H, Kitamura N, Yamanouchi K, Nambo Y, Kobayashi T, Kurohmaru M, Yamada J: Morphological studies on testicular development in the horse. J Reprod Dev **44:**377-383, 1998
3. Murabayashi H, Hondo E, Kitamura N, Furuoka H, Taguchi K, Nambo Y, Yamada J: Morphological study on pigmented cells in the horse testis. J Vet Med Sci **61:**1183-1186, 1999
4. Parks AH, Wyn-Jones G, Cox JE, Newsholme BJ: Partial obstruction of the small colon associated with an abdominal testicular teratoma in a foal. Equine Vet J **18:**342-343, 1986
5. Pollock PJ, Prendergast M, Callanan JJ, Skelly C: Testicular teratoma in a three-day-old foal. Vet Rec **150:**348-350, 2002
6. Schlafer DH, Miller RB: Female genital system. *In:* Jubb, Kennedy, and Palmer's Pathology of Domestic Animals, ed. Maxie MG, 5th ed., vol. 3, pp. 453-454. Saunders Elsevier, Philadelphia, PA, 2007
7. Williams BH, Yantis LD, Craig SL, Geske RS, Li X, Nye R: Adrenal teratoma in four domestic ferrets (*Mustela putorius furo*). Vet Pathol **38:**328-331, 2001

CASE III: W9332754 (AFIP 3134193).

Signalment: 8-year-old, intact, female Great Dane (*Canis familiaris*).

History: This dog had intermittent abdominal pain for the last 4 weeks. An exploratory laparotomy revealed the presence of a 9 cm diameter mass coming from the left ovary.

Gross Pathology: Not reported.

Histopathologic Description: Ovary: Sections are largely effaced by sheets of neoplastic round cells that exhibit mild to moderate anisocytosis and anisokaryosis. Rarely, these sheets are separated by a fine stroma. Neoplastic cells completely efface the architecture and have round euchromatic nuclei with single prominent nucleoli. Mitotic figures are present in moderate numbers (2-4 per 40x HPF). Neoplastic cells (17-25 µm) have moderate amounts of amphophilic cytoplasm and large round nuclei (12-17 µm) with 1-2 prominent nucleoli (**figs. 3-1 and 3-2**). Rare aggregates of 2-5 small lymphocytes are present amid the neoplastic cells. Immunohistochemistry: Approximately 50% of the neoplastic cells stain positively for vimentin and negatively for CD18, synaptophysin and pancytokeratin.

Contributor's Morphologic Diagnosis: Ovary: Dysgerminoma.

Contributor's Comment: The primary ovarian neoplasms are classified into 3 categories according to their histogenic origin: tumors of the surface coelomic epithelium, tumors of the gonadal stroma, and tumors of germ cells. Germ cell neoplasms of the ovary include dysgerminomas and teratomas.[2,4] Dysgerminomas are rare neoplasms that are considered to be the counterpart of the more common seminoma of the testicle in gross and microscopic features. They are extremely rare in all species but most cases have been reported in the bitch and mare.[1,2] They are usually unilateral and have a low potential for local and distant metastasis. The neoplastic cells stain positively for vimentin and alkaline phosphatase and negatively for cytokeratin.[1] The differential diagnosis in the current case included lymphoma, neuroendocrine carcinoma, pheochromocytoma and histiocytic sarcoma. The diagnosis of dysgerminoma was confirmed using immunohistochemsitry, wherein, the neoplastic cells stained positively for vimentin and stained negatively for CD18, pancytokeratin, and synaptophysin.

AFIP Diagnosis: Ovary: Dysgerminoma.

Conference Comment: In addition to the morphologic features described by the contributor, conference participants noted frequent individual cell necrosis among the neoplastic cells. Moreover, many sections contain abundant hemorrhage; in the absence of evidence for chronicity (e.g. hemosiderin-laden macrophages), participants interpreted the finding as likely representing acute, surgical induced hemorrhage associated with ovariectomy. The moderator also

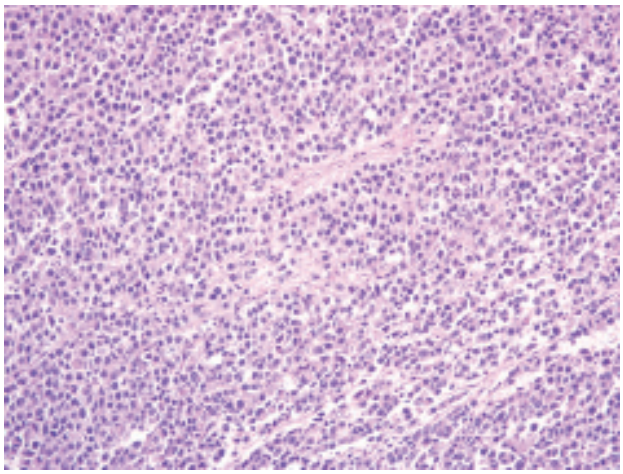

3-1. Dysgerminoma, ovary, dog. Neoplastic round cells are arranged in sheets and nests supported by a fine fibrovascular stroma. (HE 200x)

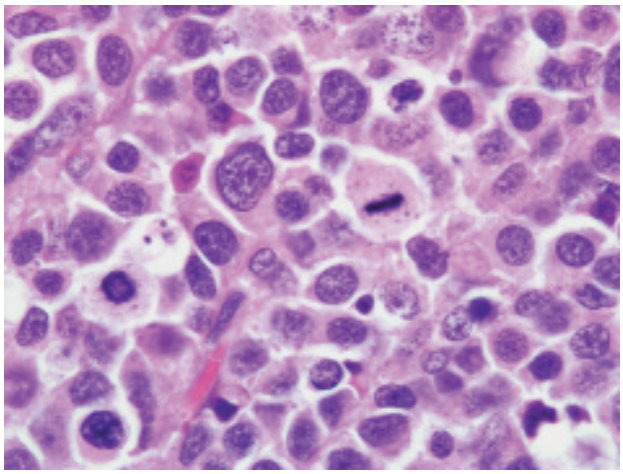

3-2. Dysgerminoma, ovary, dog. Neoplastic round cells have distinct cell borders, moderate amounts of pale eosinophilic cytoplasm, finely to coarsely stippled chromatin, and 1–2 prominent nucleoli; there is mild to moderate anisoytosis and aniskaryosis. Mitoses average 2–4 per 40x HPF. (HE 1000x)

commented that reproductive tissues are very sensitive to surgical manipulation and susceptible to hemorrhage. The conference moderator further reminded participants that it is not uncommon to find two or more different neoplasms in a single gonad.

Conference participants reviewed the primary ovarian tumors of domestic species, among which the dysgerminoma is rare. As classified by the World Health Organization, these are summarized below:[3,4]

Primary Ovarian Tumors of Domestic Animals

Category	Neoplasm	Notes
Tumors of the surface coelomic epithelium	Papillary adenoma; papillary cystadenoma	Common only in the bitch; arise from the coelomic mesothelium forming surface epithelium or subsurface epithelial structures (SES); form papillary projections covered by ciliated cuboidal to columnar cells, with or without glandular or cystic cavity formation
	Papillary adenocarcinoma	Common only in the bitch; malignant counterpart of papillary adenomas; larger and extends through ovarian bursa; fronds may dislodge and cause metastatic implantations (carcinomatosis) and ascites
	Rete adenoma	Rare; reported only in the bitch; arise from the tubular network of rete; differentiate from papillary adenomas by location in the tubal extremity of the ovarian medulla (vs. surface epithelium for the latter)
Mesenchymal tumors	Hemangioma	Most common ovarian tumor of the sow; rare in the cow, mare, and bitch
	Leiomyoma	Rare; reported in the bitch, queen, and sow; arise from smooth muscle of the mesovarium
Sex cord-stromal (gonadostromal) tumors	Granulosa (granulosa-theca) cell tumor; thecoma (theca cell tumor); interstitial cell tumor (luteoma, lipid cell tumor, steroid cell tumor)	Most common ovarian tumor of the cow and mare; slightly less common than epithelial tumors of the ovary in the bitch; infrequent in the queen; arise from granulosa and theca interna cells (and their luteinized counterparts); may produce estrogens or androgens; produce inhibin in the mare with contralateral ovarian atrophy; rarely metastasize; distinctive Call-Exner bodies are present histologically
Germ cell tumors	Dysgerminoma	Uncommon; arise from germ cells before differentiation; may metastasize or spread locally but biological behavior largely unknown due to low incidence in domestic species; histologically indistinguishable from the much more common testicular seminoma
	Teratoma	Rare; arise from totipotential germ cells that have undergone somatic differentiation; consist of two or more of the three embryonic layers (i.e. endoderm, mesoderm, ectoderm); usually well-differentiated and benign
	Embryonal carcinoma	Arise from embryonic multipotential cells capable of further differentiation; variable histologic pattern

Contributor: Department of Veterinary Pathology, Egyptian Society of Comparative and Clinical Pathology, Faculty of Veterinary Medicine, Alexandria University, Edfina, Rashid, Behira Province, Egypt
http://www.vetmedalex.org/

References:

1. Chandra AMS, Woodard JC, Merritt AM: Dysgerminoma in an Arabian filly. Vet Pathol **35:**308-311, 1998

2. Jackson ML, Mills JHL, Fowler JD: Ovarian dysgerminoma in a bitch. Can Vet J **26:**285-287, 1985

3. Kennedy PC, Cullen JM, Edwards JF, Goldschmidt MH, Larsen S, Munson L, Nielsen S: Histological Classification of Tumors of the Genital System of Domestic Animals, 2nd series, vol. IV, ed. Schulman YF, pp. 24-28. Armed Forces Institute of Pathology (in cooperation with the ARP and the WHO Collaborating Center for Worldwide Reference on Comparative Oncology), Washington, DC, 1998

4. Schlafer DH, Miller RB: Female genital system. *In:* Jubb, Kennedy, and Palmer's Pathology of Domestic Animals, ed. Maxie MG, 5th ed., vol. 3, pp. 450-454. Saunders Elsevier, Philadelphia, PA, 2007

CASE IV: 09030 WFUHS (AFIP 3134304).

Signalment: 31-year-old, female, rhesus macaque (*Macaca mulatta*).

History: This rhesus macaque developed vaginal bleeding 13 months prior to euthanasia. Pap smear revealed atypical epithelial cells with large, irregularly shaped, vesicular nuclei. Colposcopic examination was suggestive of cervical intraepithelial neoplasia at the cervico-vaginal junction. Surgical removal of the cervix was performed 1.5 months later, and a 2.0 x 1.5 x 0.6 cm, multilobular, unencapsulated, bright red, fleshy, mass was found at the external cervical os near the cervico-vaginal junction. Histological examination was consistent with cervical adenocarcinoma. Nearly a year later the animal became anorexic and constipated, and was euthanized.

Gross Pathology: At necropsy the distal colon was constricted and adhered to the urinary bladder, and a 7 x 5 x 5 mm, unencapsulated, reddish-brown mass infiltrated the vaginal mucosa adjacent to the cervical stump (**fig 4-1**). Multifocal to coalescing, tan to milky white plaques were present on the serosa of the urinary bladder and colon. Gross morphologic diagnoses: Cervical adenocarcinoma with serosal metastasis to the colon and urinary bladder.

Laboratory Results: A PCR on Pap smear tissue using a rhesus papillomavirus D sequence was positive.

Histopathologic Description: Extensively infiltrating and replacing the vaginal wall is part of an unencapsulated, poorly demarcated, densely cellular epithelial neoplasm. The neoplastic cells are arranged in solid sheets, acini, and nests supported by a fine fibrovascular stroma. The cells are often irregularly multilayered, range from oval to polygonal or columnar, have indistinct cell borders, moderate to abundant pale eosinophilic, homogenous or finely vacuolated cytoplasm, and vesicular, oval nuclei with 1-2 basophilic nucleoli. Anisokaryosis and anisocytosis are moderate to marked, and mitoses range from 3-8 per 40x HPF (**figs. 4-2, 4-3 and 4-4**). Invasion of the lymphatics, colonic serosa, muscularis and submucosa is present multifocally, although it is not present in all sections. The surface of the neoplasm is variably covered by a 2 mm thick sheet of fibrin and necrotic debris admixed with degenerate neutrophils and small basophilic bacterial colonies.

Contributor's Morphologic Diagnosis: Cervical adenocarcinoma with vaginal and colonic invasion.

Contributor's Comment: Papillomaviruses are a diverse group of epitheliotropic double-stranded DNA viruses, of which more than 75 have been identified in 20

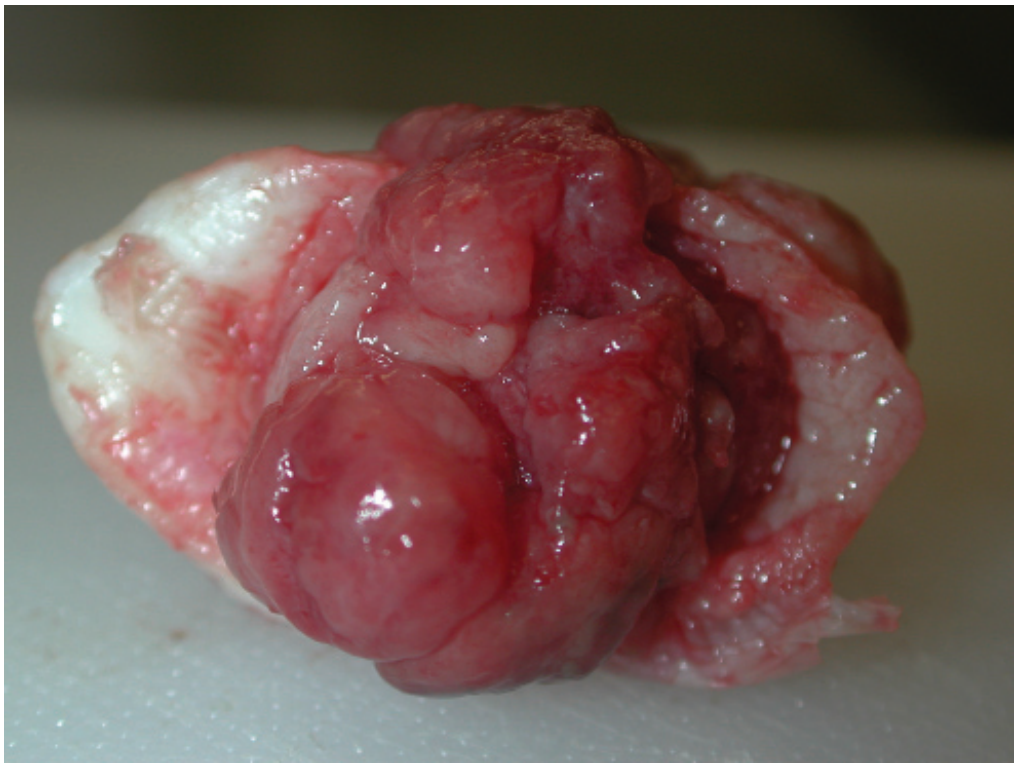

4-1. Cervical adenocarcinoma, cervicovaginal junction, rhesus macaque. Multilobular fleshy mass at the external cervical os near the cervico-vaginal junction. Photographs courtesy of Animal Resources Program Wake Forest University Health Sciences Medical center Blvd., Winston Salem, NC 27103 nkock@wfubmc.edu

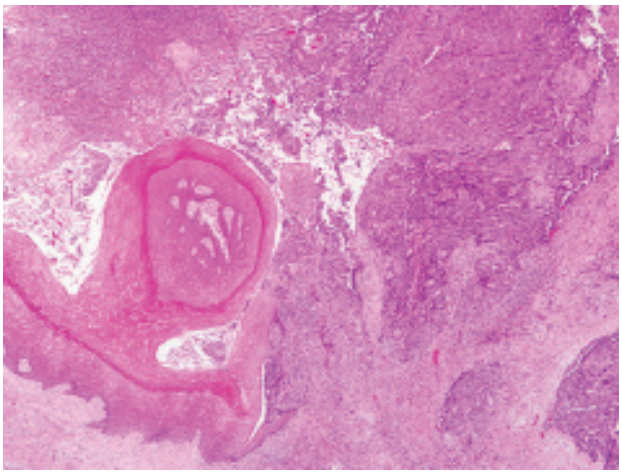

4-2. Cervical adenocarcinoma, cervicovaginal junction, rhesus macaque. Infiltrating and expanding the vaginal wall is an unencapsulated, poorly circumscribed malignant epithelial neoplasm. (HE 12.50x)

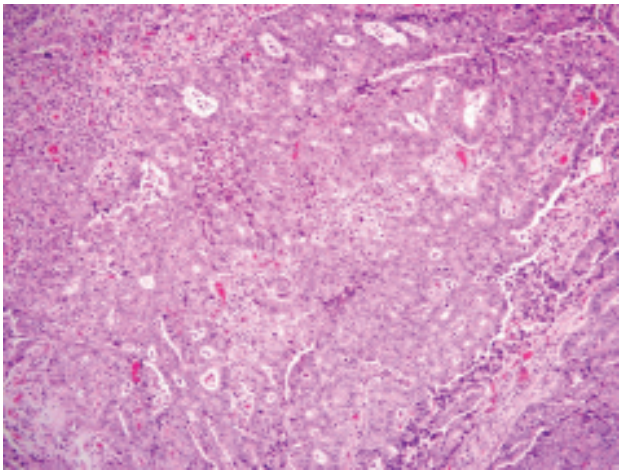

4-3. Cervical adenocarcinoma, cervicovaginal junction, rhesus macaque. Neoplastic cells are arranged in nests, acini, and solidly cellular areas supported by a fine to moderate fibrovascular stroma. (HE 100x)

species. The rhesus papillomavirus type D (RhPV-d) is the most common isolate associated with genital infections in macaques, and was associated with 60% of genital lesions diagnosed in rhesus macaques,[7] which include vaginal papillomas, varying stages of intraepithelial dysplasia, and invasive cervical carcinoma.[6] Infection requires the availability of epidermal or mucosal epithelial cells still able to proliferate (basal cells).[9] Histological characteristics include koilocytosis, epithelial atypia and loss of basal cell maturation.

Cervical adenocarcinoma associated with genital papillomaviruses has been well described in human medical literature and recently in macaques.[6-8] The normal cervix has two distinct epithelial zones, an ectocervix covered by squamous epithelium, and an endocervix lined by simple glandular epithelium. During adolescence, the endocervical epithelium undergoes squamous metaplasia and is replaced by immature squamous epithelial cells which later undergo maturation. This metaplastic region is called the transformation zone and is the most common site for the development of cervical cancer.[3] High grade lesions often occur at the squamo-columnar junction. In humans, nearly 80 percent of the population is infected by genital papillomaviruses, which are considered the most prevalent sexually transmitted ongocenic pathogens. Only rarely does infection lead to invasive cervical carcinoma which is characterized as squamous cell carcinoma (SCC) or adenocarcinoma (AC). Human papillomavirus (HPV) 16 is the most frequent isolate in SCC, while HPV 18 is detected more frequently in AC. In many human cases, the cervical lesions harbor multiple HPV types.[8]

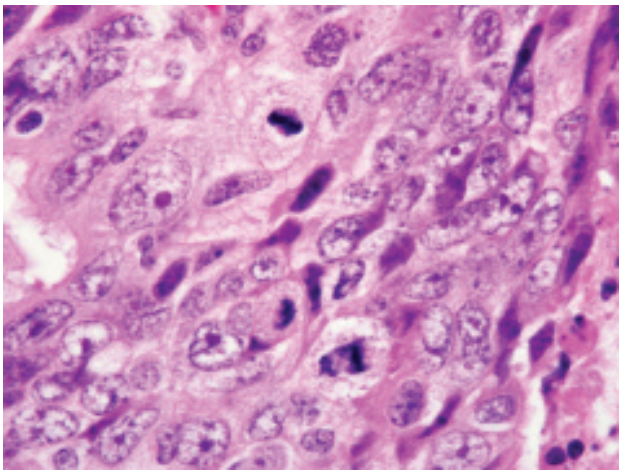

4-4. Cervical adenocarcinoma, cervicovaginal junction, rhesus macaque. Neoplastic epithelial cells are irregularly multilayered and contain moderate to abundant vacuolated eosinophilic cytoplasm and stippled to vesiculate nuclei. Anisocytosis is moderate, and mitoses range from 3 – 8 per 40x HPF. (HE 1000x)

Human papillomavirus integration into the genome leads to inactivation of the p53 and retinoblastoma (Rb) pathways by the action of primary papillomaviral oncoproteins E6 and E7. Viral E6 protein binds to and degrades p53, and viral E7 protein causes functional inactivation of the Rb protein. High-risk HPV infections are associated with increased expression of E6 and E7 genes in precancerous lesions.[2] E5 is another gene important in the early course of infection as it stimulates cell growth by binding the epidermal growth factor receptor, the platelet-derived growth factor-ß receptor, and the colony-stimulating

factor-1 receptor. Recently, E5 has also been shown to prevent apoptosis following DNA damage.[9]

AFIP Diagnosis: Cervicovaginal junction: Cervical adenocarcinoma.

Conference Comment: As one of very few suitable animal models for one of the leading causes of cancer mortality in women worldwide, this entity is extremely relevant and timely. Furthermore, the contributor provides a superb synopsis of its pathogenesis. Readers may recall a recent discussion of the role of oncoproteins E5, E6, and E7 in neoplastic transformation in bovine enzootic hematuria associated with bovine papillomaviruses 2 and 4 and bracken fern (see WSC 2009-2010, Conference 10, case IV). Not surprisingly, oncoproteins E5 and E7 are expressed in and have been implicated in the pathogenesis of equine sarcoid, a condition of which bovine papillomaviruses 1 and 2 are the suspected etiologies. The E5 oncoprotein binds the platelet-derived growth factor –beta receptor, which is also expressed in equine sarcoids.[1] In general, papillomaviruses characteristically exhibit marked species specificity, and equine sarcoid is one of the rare exceptions to this tendency. Recently, feline sarcoid-associated papillomavirus DNA sequences have been amplified from bovine skin, suggesting that cattle may be the reservoir host of this papillomavirus.[4] Finally, RhPV-d and RhPV-a, previously found only in rhesus macaques, recently were isolated from the genital tracts of female cynomolgus macaques.[6,7]

Contributor: Animal Resources Program, Wake Forest University Health Sciences, Medical Center Blvd., Winston-Salem, NC 27103
http://www1.wfubmc.edu/pathology/training/index.htm

References:

1. Borzacchiello G, Russo V, Della Salda L, Roperto S, Roperto F: Expression of platelet-derived growth factor-beta receptor and bovine papillomavirus E5 and E7 oncoproteins in equine sarcoid. J Comp Pathol **139**:231-237, 2008
2. Dray M, Russell P, Dalrymple C, Wallman N, Angus G, Leong A, Carter J, Cheerala B: P16(INK4a) as a complementary marker of high-grade intraepithelial lesions of the uterine cervix. I: Experience with squamous lesions in 189 consecutive cervical biopsies. Pathology **37**:112-124, 2005
3. Jenkins D: Histopathology and cytopathology of cervical cancer. Dis Markers **23**:199-212, 2007
4. Munday JS, Knight CG: Amplification of feline sarcoid-associated papillomavirus DNA sequences from bovine skin. Vet Dermatol [Epub ahead of print], 2010 Mar 29
5. Ogura K, Ishi K, Matsumoto T, Kina K, Nojima M, Suda K: Human papillomavirus localization in cervical adenocarcinoma and adenosquamous carcinoma using in situ polymerase chain reaction: Review of the literature of human papillomavirus detection in these carcinomas. Pathol Int **56**:301-308, 2006
6. Wood CE, Borgerink H, Register TC, Scott L, Cline JM: Cervical and vaginal epithelial neoplasms in cynomolgus monkeys. Vet Pathol **41**:108-115, 2004
7. Wood CE, Chen ZG, Cline JM, Miller BE, Burk RD: Characterization and experimental transmission of an oncogenic papillomavirus in female macaques. J Virol **81**:6339-6345, 2007
8. Zuna RE, Allen RA, Moore WE, Mattu R, Dunn ST: Comparison of human papillomavirus genotypes in high-grade squamous intraepithelial lesions and invasive cervical carcinoma: evidence for differences in biologic potential of precursor lesions. Mod Pathol **17**:1314-1322, 2004
9. zur Hausen H: Papillomaviruses and cancer: From basic studies to clinical application. Nat Rev Cancer **2**:342-350, 2002

The Armed Forces Institute of Pathology
Department of Veterinary Pathology

Conference Coordinator:
Shannon Lacv. DVM. MPH

WEDNESDAY SLIDE CONFERENCE 2009-2010

Conference 21

14 April 2010

Conference Moderator:

F. Yvonne Schulman, DVM, Diplomate ACVP

CASE I: 59688 (AFIP 3134335).

Signalment: Multiple adult long-tailed finches (*Poephila acuticauda*).

History: Tissues submitted were from multiple individuals that were among 12 captive Australian finches in the same exhibit that presented with feather loss, dehydration, weight loss, lethargy, and/or respiratory distress. Most birds died or were euthanized shortly after presentation (1-2 days). On physical exam, these birds were very thin and dehydrated, and had feather loss on their heads and necks. Many were treated with fluids, enrofloxacin, and injectable calcium with little clinical response. Other affected species included the diamond firetail finch (*Emblema guttata*), star finch (*Neochmia ruficauda*), black-throated finch (*Poephila cincta*), double-barred finch (*Poephila bichenovi*), red-browed finch (*Neochmia temporalis*), masked finch (*Poephila personata*), and blue-faced parrot finch (*Erythrura trichroa*). The birds ranged from 7 months to 3 years and 8 months of age, and most were acquired from an outside source.

Gross Pathology: The finches presented emaciated with prominent keels and missing feathers on the head and neck. Multiple birds had enlarged gizzards and undigested millet seed throughout the intestines. Gastrointestinal squash preps occasionally revealed mixed bacteria. There were no other significant gross findings.

Histopathologic Description: Ventriculus: The koilin is multifocally disrupted by numerous nematode parasites, parasite eggs, bacterial colonies and mixed inflammatory cells (heterophils and lymphocytes) with associated necrosis. There are multiple cross and longitudinal sections of nematode parasites, the majority of which are sexually mature, gravid females with larvated eggs. The parasites are 200 um in diameter and have a 7-10 um thick, smooth cuticle with 8 um thick transverse striations, polymyarian-coelomyarian musculature, and indistinct lateral cords. The intestine is lined by few, multinucleate enterocytes with a distinct brush border. Eggs are ovoid, non-operculate, and measure an average of 23 x 35 um with a 2-3 um thick refractile shell. Eggs contain either an ovoid embryo or a folded larva (**figs. 1-1 and 1-2**). There are multifocal cystic spaces within the koilin (parasite tracts), some of which contain cellular debris, coccoid bacteria and heterophils. There is also multifocal mild lymphoplasmacytic and heterophilic inflammation that expands the lamina propria. Some sections also include proventriculus, with multifocal mild interstitial

*Sponsored by the American Veterinary Medical Association, the American College of Veterinary Pathologists, and the C. L. Davis Foundation.

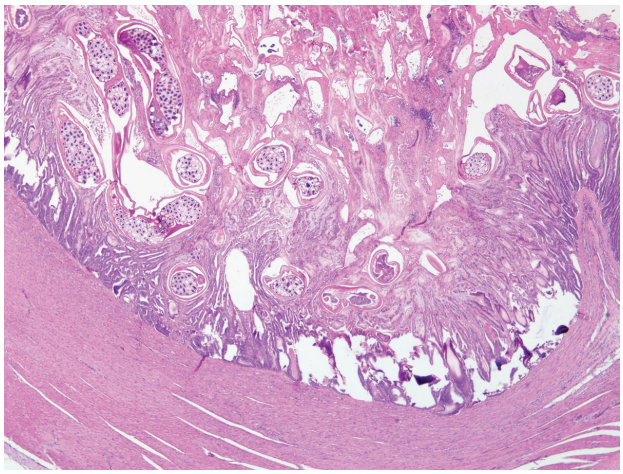

1-1. Ventriculus, long tailed finch. Multifocally, the koilin layer is disrupted by numerous adult nematodes (HE 40x)

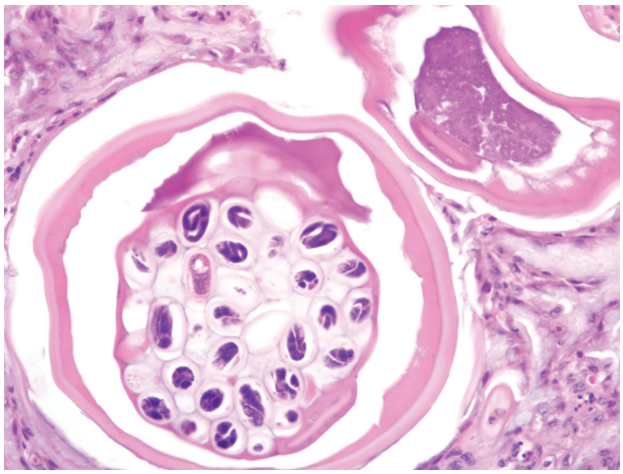

1-2. Ventriculus, long tailed finch. Adult spirurid nematodes contain a thick cuticle, polymyarian-coelomyarian musculature, and indistinct lateral cords, whose morphology is consistent with Acuaria species. Female nematodes contain thick shelled eggs in the uterus. Both an adult female and male are present. (HE 400x)

lymphoplasmacytic inflammation and, variably, clusters of elongate (5 x 20-90 um) eosinophilic yeast within glands or along the mucosal surface at the ventriculus-proventriculus junction (*Macrorhabdus ornithogaster*) (**fig. 1-3**). Also, within the proventricular glands of some sections, there are many 3 – 6 µm amphophilic protozoal organisms along the apical surface of mucosal epithelial cells (*Cryptosporidium* sp.) (**fig. 1-4**). Few sections contain normal small intestine.

Contributor's Morphologic Diagnosis:
1. Ventriculus, ventriculitis, heterophilic and lymphocytic, multifocal, severe with koilin disruption and intralesional nematodes, bacteria and yeasts (some sections).
2. Proventriculus, proventriculitis, lymphocytic, multifocal, mild with intralesional yeasts (some sections) and apical protozoa (some sections).

Contributor's Comment: Ventricular nematodiasis in finches has been reported to be caused by various genera of parasites, including *Acuaria*, *Dispharynx, Tetrameres, Contracecum* and *Echinura*. The morphologic characteristics of these worms in tissue sections and the species affected were consistent with two nematode species: *Acuaria skrjabini* and *Dispharynx nasuta*. Examination of whole fixed parasites ultimately confirmed these nematodes to be most consistent with *Acuaria skrjabini*, a spiruroid.

Acuaria spp. have been reported in cases of finches with a history of diarrhea, lethargy and inappetence.[6] Spiruroids are active parasites of many finch species, especially the ground dwelling species of finch like long-tailed finches, and can be a significant source of mortality.[6] In addition to finches, *A. skrjabini* has been reported to infect and cause severe disease in sparrows from multiple regions of the world.[8] Fatal *A. skrjabini* infections with severe ventricular lesions have been reported in aviary finches in Australia and New Zealand.[8] In one population of aviary finches infected with *A. skrjabini*, there was a reported 66% mortality rate with severe gizzard lesions.[3] Other findings associated with *Acuaria* spp. include no gross lesions, embryonated eggs in intestinal smears, poor body condition, whole seeds in the intestinal tract, tapeworms in the intestine, and degeneration of the koilin with foci of bacteria.[3,4,8] In this population of finches, small nematodes rarely could be seen at necropsy beneath the koilin layer of the ventriculus.

Acuaria spp. have a two-host life cycle that requires an arthropod intermediate host, which may include beetles, sandhoppers and grasshoppers.[6] Treatment with oral levamisole or fenbendazole has been reported to reduce morbidity and mortality in affected birds,[6] providing supportive evidence that the disruption caused by these spiruroid gizzard worms is the primary cause of this disease syndrome.

Speciation of *Acuaria* nematodes is difficult, although there are some features to distinguish *A. skrjabini*. Adult *A. skrjabini* parasites have seven pairs of postanal papillae in the male, and male cordons reach to and usually beyond

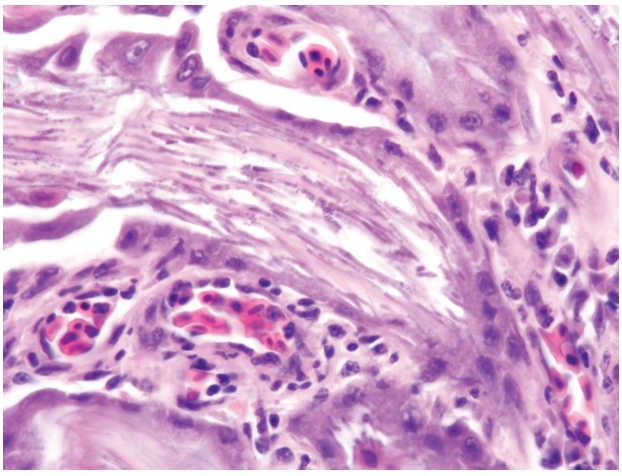

1-3. Proventriculus, long tailed finch. Numerous ascomycetous yeasts fill the proventricular glands; the yeast morphology is consistent with Macrorhabdus ornithogaster. (HE 1000x)

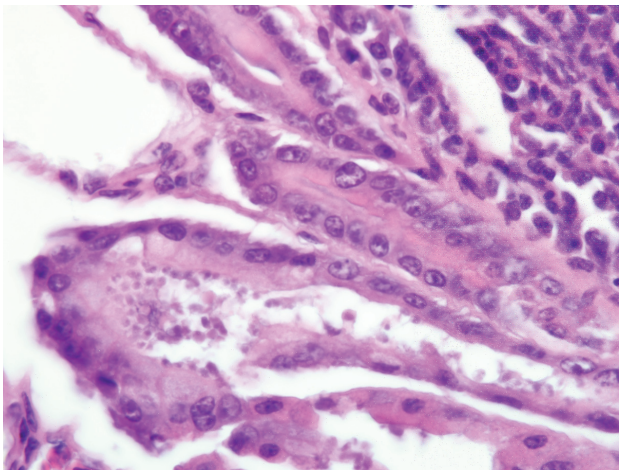

1-4. Proventriculus, long tailed finch. Numerous round cryptosporidian protozoa line the mucosal epithelium. (HE 1000x)

the excretory pore.[5] The caudal alae of the male are wider anteriorly.[5] Females are characterized by thick shelled eggs approximately 40-43 x 23-24 um in the common trunk of uterus.[5] There are also distinguishing features between male and female worms; for example, female worms are about four times as long as the males, and transverse striations at mid body are at about 4 um intervals in the male while they are at 8 um intervals in the female.[5]

Yeast forms consistent with *Macrorhabdus ornithogaster* were also found in the proventriculus of five of the affected birds in this population. *M. ornithogaster* is a Gram positive, ascomycetous yeast which was originally classified as a bacterium. This organism has been reported in a variety of avian species, including finches, budgerigars and cockatiels. The yeasts are often found at the isthmus between the ventriculus and proventriculus, along the mucosal surface or within proventricular glands. Organisms isolated from chickens are infectious to young chicks, causing reduced weight gain and heterophilic inflammation of the isthmus of the proventriculus.[2]

Cryptosporidia are apicomplexan parasites that infect a wide range of hosts. Cryptosporidia occupy a unique intracellular but extracytoplasmic location on the apical surface of mucosal epithelial cells. Avian crytopsporidiosis can affect the epithelia of the respiratory tract, genitourinary tract, gastrointestinal tract or bursa of Fabricius. In birds, cryptosporidiosis has been reported in chickens, turkeys, quail, pheasants, peafowl, junglefowl, ducks, geese, parrots, finches, lovebirds, and budgerigars. *Cryptosporidium meleagridis* and *C. baileyi* are the species that infect turkeys and chickens, respectively. Two novel species, infecting black ducks and finches, have also been described.[7]

AFIP Diagnosis: 1. Ventriculus: Ventriculitis, heterophilic and lymphocytic, multifocal, severe, with intramucosal spirurid eggs, larvae, and adults and numerous yeasts, etiology consistent with *Acuaria* species and *Macrorhabdus ornithogaster*, respectively.
2. Proventriculus: Proventriculitis, lymphocytic, multifocal, mild to moderate, with yeasts and many surface epithelial-associated protozoa, etiology consistent with *Macrorhabdus ornithogaster* and *Cryptosporidium* species, respectively.

Conference Comment: This interesting case features several infections occurring simultaneously, presenting conference participants with a formidable descriptive challenge. The contributor has masterfully summarized the etiologies involved above. There is substantial slide variation, and not all conference slides include a section of proventriculus.

During the conference, attendees first discussed the differential diagnosis for proventricular and ventricular nematodiasis, and like the contributor, narrowed the list to *Acuaria* sp. and *Synhimatus* (*Dispharynx*) sp. based on the histomorphology of the nematodes and favored *Acuaria* sp. because of the location. An example of the *Synhimatus* (*Dispharynx*) sp. in the proventriculus of a Northern bobwhite quail was reviewed in WSC 2008-2009, Conference 18, case II.

This case was reviewed in consultation with Dr. Christopher

Gardiner, Consulting Parasitologist for the AFIP's Department of Veterinary Pathology, who emphasized that the presence of many small, thick-shelled, embryonated eggs is the most obvious indicator of a spirurid infection. However, the absence of characteristic spirurid eggs is not always sufficient to exclude a spirurid infection, because several spirurids (e.g. *Draschia* and *Thalazia* spp.) produce embryos lacking shells. Although there is substantial morphological variety among the spirurids, other features typically observed in members of the group include coelomyarian musculature, large intestines lined by uninucleate cuboidal to columnar cells that often have a brush border, large lateral chords that are often vacuolated, and eosinophilic fluid within the pseudocoelom.[1]

Particularly intriguing is the fact that both in this case and in reports in the literature [3,6,8] infection with *Acuaria skrjabini* manifests as an outbreak, despite its requirement for an intermediate host. In one aviary outbreak, a ceramic heat lamp attracted an infestation of cockroaches and earwigs, which were implicated as possible intermediate hosts. The authors noted that while finches of the Estrildidae family normally feed primarily on grass seeds, they transition to a greater dietary intake of insects during the breeding season, which may account for the nearly simultaneous onset of disease in a number of birds. Death of affected birds was attributed to starvation due to maldigestion caused by ventricular dysfunction.[3]

The contributor alluded to the original misclassification of *M. ornithogaster* as a bacterium (based on Gram staining characteristics), giving rise to the misnomer "megabacterium," by which it was formerly known. *M. ornithogaster* survives only in a microaerophilic environment in a narrow pH range of 3-4, consistent with its peculiar environmental niche at the isthmus of the proventriculus and ventriculus of birds.[2] Although many birds appear asymptomatically infected, the yeast has been implicated in three specific avian disease syndromes: 1) chronic wasting disease in budgerigars, canaries, and finches; 2) acute hemorrhagic gastritis in budgerigars and parrotlets; and 3) reduced feed conversion in experimentally-infected chickens.[2] The clinical significance of the organism in the present case is unclear, but most conference participants interpreted it as an incidental finding, and certainly less important than the spirurids discussed above. By contrast, because they are so numerous and associated with areas of proventricular inflammation, the cryptosporidia in this case are considered clinically significant.

Contributor: Department of Molecular and Comparative Pathobiology, Johns Hopkins University School of Medicine, Baltimore, MD 21205

http://www.hopkinsmedicine.org/mcp/

References:

1. Gardiner CH, Poynton SL: An Atlas of Metazoan Parasites in Animal Tissues, 2nd ed., p. 30. Armed Forces Institute of Pathology, Washington, DC, 1999
2. Hannafusa Y, Bradley A, Tomaszewski EE, Libal MC, Phalen DN: Growth and metabolic characterization of *Macrorhabdus ornithogaster*. J Vet Diagn Invest **19:**256-265, 2007
3. Hindmarsh M, Ward K: Mortality of finches (family Estrildidae) caused by *Acuaria skrjabini*. Aust Vet J **70:**451-452, 1993
4. Mason PC, Hodgkinson NL, McAllum HJ: *Acuaria skrjabini* Ozerska, 1926 in a caged finch. N Z Vet J **26:**131-132, 1978
5. Mawson PM: The genus *Acuaria* Bremser (Nematoda: Spirurida) in Australia. Trans R Soc S Aust **96:**139-147, 1972
6. McOrist S, Barton NJ, Black DJ: *Acuaris skrjabini* infection of the gizzard of finches. Avian Dis **26:**957-960, 1982
7. Morgan UM, Monis PT, Xiao L, Limor J, Sulaiman I, Raidal S, O'Donoghue P, Gasser R, Murray A, Fayer R, Blagburn BL, Lal AA, Thompson RC: Molecular and phylogenetic characterisation of *Cryptosporidium* from birds. Int J Parasitol **31:**289-296, 2001
8. Sato H, Osanai A, Kamiya H, Une Y: Gizzard spirurid nematode *Acuaria skrjabini* in Japanese tree sparrows and a gray starling from Tokyo. J Vet Med Sci **67:**607-609, 2005

CASE II: 13738-09 (AFIP 3138207).

Signalment: 12-year-old, male, castrated, West Highland white terrier dog (*Canis familiaris*).

History: A palpable intestinal mass was found on routine examination. Exploratory laparatomy and intestinal resection and anastamosis were performed. The mass was fixed in 10% formalin and submitted for histologic examination.

Gross Pathology: Examination of the fixed tissue revealed large, cystic structures expanding the intestinal wall. The cysts were filled with gelatinous, clear material (mucus) (**fig. 2-1**).

Histopathologic Description: In sections of jejunum

2-1. Adenocarcinoma, mucinous type, jejunum, dog. Multifocally, the intestinal wall is expanded by cystic structures. Photograph courtesy of Veterinary Diagnostic center, University of Nebraska, 1900 North 42nd Street, Lincoln, NE 68583-0907 bbroderson1@unl.edu

examined, a sparsely cellular mass infiltrates the base of the mucosa, is present in the lamina muscularis, extends to the tunica muscularis and forms expansile mucus-filled, cysts. They diffusely distort the lamina muscularis and submucosa (**fig. 2-2**). In some sections, aggregates of mineralized debris are seen in the center of the mucus-filled cysts. Neoplastic cells are columnar to cuboidal or flattened, form small nests or line cyst walls, and are supported by fine to moderately abundant fibrous stroma (**fig. 2-3**). Cell layers 1-6 cells thick surround lakes of mucus that at times contain small clusters of cells. Cytoplasm is eosinophilic and faintly granular. Nuclei are round and contain reticular chromatin and one to three distinct nucleoli. Frequently, cells are rounded with abundant foamy amphophilic cytoplasm that peripheralizes the nucleus (signet ring cells). Mitoses (sometimes bizarre) are rare. Neoplastic cells are present in the most terminal sections of the resected segment of intestine examined. In some sections, the surface epithelium is eroded, hemorrhagic and contains rod-shaped bacteria mixed with fibrin. The lamina propria is defined by moderate numbers of neutrophils, few lymphocytes and plasma cells, rare eosinophils and mildly congested blood vessels. Immunohistochemical staining for cytokeratin positively stains enterocytes and neoplastic cells.

Contributor's Morphologic Diagnosis:

1. Intestine, jejunum: Mucinous adenocarcinoma.
2. Intestine, jejunum: Moderate, sub-acute, multifocal, fibrinosuppurative, erosive enteritis with bacterial rods.

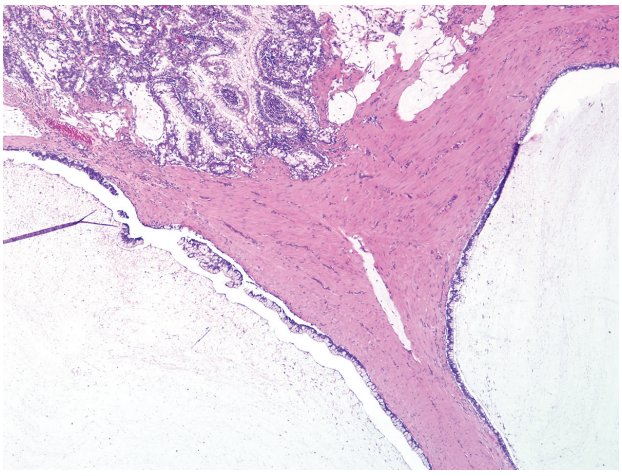

2-2. Adenocarcinoma, mucinous type, jejunum, dog. The jejunum is infiltrated and expanded by malignant epithelial neoplasm arranged in tubuloacinar structures and large, mucous filled cysts supported by a thick fibrous stroma. (HE 4x)

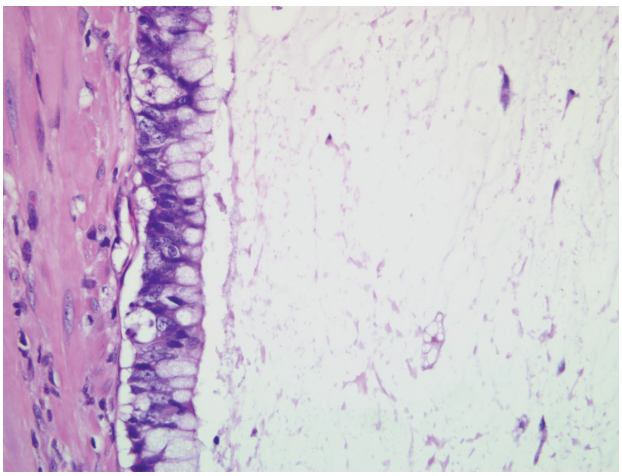

2-3. Adenocarcinoma, mucinous type, jejunum, dog. Neoplastic epithelial cells are vacuolated, cuboidal to columnar, and often line mucus filled cysts. (HE 400x)

Contributor's Comment: Intestinal neoplasms in the dog are rare, with primary intestinal neoplasms being more common than metastatic disease.[2,4,6] Primary intestinal neoplasms may arise from the following tissues: epithelium, neuroendocrine cells, mesenchyme (vascular, connective tissue, adipose, or peripheral nerve sheath tumors), lymphoid tissues, extramedullary plasma cells, mast cells, smooth muscle, or serosa.[4] Colonic masses are more frequently encountered, with papillomatous lesions making up the majority of colon tumors.[6] Most are reported to be scirrhous and mucus producing.[2] Other gross lesions can appear as mural thickening, areas of ulceration, white and fibrous tissue, or serosal plaque-like masses.

Transmural invasion is a differentiating feature between adenomatous hyperplasia and neoplasia.[2] Histologic patterns reported include acinar, papillary, solid, carcinoid, and mucinous (including signet-ring cell carcinoma).[6] Signet-ring cells are cells filled with copious mucin that perpheralizes the nucleus. No prognostic behavior has been attributed to the difference in histological pattern.

Intestinal adenocarcinomas metastasize widely via lymphatics, and, at times, via direct serosal implantation.[2] Serosal implantation can cause lymphatic blockage, leading to ascites.[2] Rare manifestations of metastasis include cutaneous masses and pseudomyxoma peritonei.[1,5] Cutaneous lesions in a dog with duodenal adenocarcinoma and masses in numerous organs consisted of undifferentiated, non-cohesive islands of round to polygonal cells.[5] In this case, definitive diagnosis of the undifferentiated mass was supported by identification of a primary intestinal lesion and positive staining of metastases by pancytokeratin, periodic acid Schiff, and Alcian blue. A single case of pseudomyxoma peritonei describing mucin accumulation in the peritoneum and peritoneal cavity was reported in 2003.[1] Mucin was trapped in fibrous reticulin mesh in tissue from the peritoneum and mesenteric fat and in fibrous septa in tissue from the diaphragm. To date, no pathologic basis for mucin accumulation has been identified in this patient or in humans affected by a similar condition.

AFIP Diagnosis: Small intestine: Adenocarcinoma, mucinous type.

Conference Comment: The contributor provides a fairly straightforward case of mucinous adenocarcinoma in the jejunum of a dog, pairing it with a succinct synopsis of the entity. The conference moderator cautioned participants to carefully consider adenocarcinoma, which in dogs is more common than intestinal adenoma, whenever glands are present in the submucosa, tunica muscularis or serosa, even in cases with a predominance of histologically bland neoplastic cells; tumor cells in intestinal adenocarcinoma can be well-differentiated, a finding that may vary regionally within a given malignant neoplasm. This case is typical in that intestinal neoplasms of epithelial origin are more commonly found in males than females, whereas the opposite is true for nonepithelial intestinal tumors. Of note, adenocarcinomas in dogs are more common in the large intestine than in the small intestine.[3]

The following summary of the World Health Organization classification of intestinal adenocarcinoma is provided with the caveats that a given tumor often exhibits more than one growth pattern, and as mentioned by the contributor, growth pattern is not correlated with prognosis:[3]

Classification of Intestinal Adenocarcinoma in Domestic Animals	
Type	Microscopic Features
Acinar (tubular)	Acini and tubules replace the intestinal mucosa
Papillary (polypoid, cribriform)	Multiple layers of anaplastic columnar cells line papillary projections
Mucinous (colloid, mucoid)	Acinopapillary growth with at least 50% of the tumor replaced by extracellular mucin
Signet ring cell (goblet cell, intracellular mucinous)	At least 50% of the neoplasm is composed of signet-ring cells with intracytoplasmic mucin that peripheralizes crescentic nuclei; lacks gland formation; severe desmoplasia
Undifferentiated	Solid sheets of anaplastic or pleomorphic cells without squamous or glandular differentiation
Adenosquamous (adenoacanthoma, adenocarcinoma with squamous differentiation)	Gland-forming adenocarcinoma with areas of squamous differentiation and variable keratinization

Contributor: Veterinary Diagnostic Center, University of Nebraska, 1900 North 42nd Street, Lincoln, NE 68583 http://nvdls.unl.edu/

References:

1. Bertazzolo W, Roccabianca P, Crippa L, Caniatti M: Clinicopathological evidence of pseudomyxoma peritonei in a dog with intestinal mucinous adenocarcinoma. J Am Anim Hosp Assoc **39:**72-75, 2003

2. Brown CC, Baker DC, Barker IK: Alimentary system. *In:* Jubb, Kennedy, and Palmer's Pathology of Domestic Animals, ed. Maxie MG, 5th ed., vol. 2, pp. 117-120.

Saunders Elsevier, Philadelphia, PA, 2007
3. Head KW, Cullen JM, Dubielzig RR, Else RW, Misdorp W, Patnaik AK, Tateyama S, van der Gaag I: Histological Classification of Tumors of the Alimentary System of Domestic Animals, 2nd series, vol. X, ed. Schulman YF, pp. 89-94. Armed Forces Institute of Pathology (in cooperation with the ARP and the WHO Collaborating Center for Worldwide Reference on Comparative Oncology), Washington, DC, 2003
4. Head KW, Else RW, Dubielzig RR: Tumors of the intestines. *In:* Tumors in Domestic Animals, ed. Meuten DJ, 4th ed., pp. 461-468. Iowa State Press, Ames, IA, 2002
5. Juopperi TA, Cesta M, Tomlinson L, Grindem CB: Extensive cutaneous metastases in a dog with duodenal adenocarcinoma. Vet Clin Pathol **32:**88-91, 2003
6. Patnaik AK, Hurvitz, AI, Johnson GF: Canine intestinal adenocarcinoma and carcinoid. Vet Pathol **17:**149-163, 1980

CASE III: 12303-08 (AFIP 3134626).

Signalment: 5-year-old, female, spayed, domestic shorthair cat (*Felis catus*).

History: The cat had neurologic signs that ended in torticollis and vocalization.

Gross Pathology: There were no gross lesions in the viscera, brain, or spinal cord.

Laboratory Results: Rabies fluorescent antibody test: Negative. West Nile Virus PCR: Negative. Bacterial culture: Brainstem, anterior cervical spinal cord = 2+ *Listeria monocytogenes*; liver = no growth.

Histopathologic Description: A diffuse and severe influx of neutrophils was present throughout the brainstem. Only slight lymphocytic perivascular cuffing with a few neutrophils was in the adjacent cerebellar white matter and focally in the posterior cerebral white matter and midbrain. Mostly neutrophils with some lymphocytes and histiocytes surrounded the vessels and infiltrated and thickened their walls with mostly neutrophils within the brain parenchyma (**figs. 3-1 and 3-2**). Occasionally, the cytoplasm of degenerating neurons was filled with neutrophils (neurophagia). The trigeminal ganglia (not on slide) were collected from the refrigerated body about three days later, and one also had mild lymphocytic inflammation, a few neutrophils, and multiple colonies of short gram-positive bacilli, compatible with *Listeria* ("cold enrichment"). Inflammation was absent in the meninges except for occasional perivascular inflammation in the subarachnoid spaces of the brainstem.

Contributor's Morphologic Diagnosis: Diffuse, suppurative brainstem encephalitis.

Contributor's Comment: This is neurologic listeriosis as would be expected in a ruminant. In ruminants, infection is generally associated with feeding silage. The bacteria can live if the silage pH is above 5.5. In Arkansas, we see sporadic cases in cattle and goats on pasture and eating round bales of hay that may be spoiling on the ground side. Infection gains entry to a mouth lesion and the bacteria travel up axons of the trigeminal nerve to

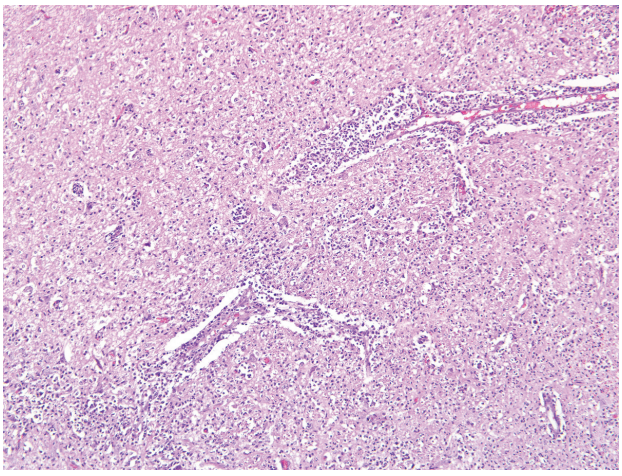

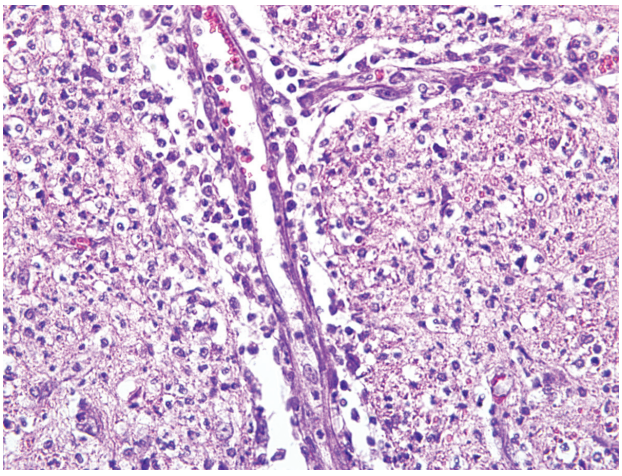

3-1., 3-2. Brain stem and cerebellum, cat: Multifocally, Virchow-Robin spaces are filled with many viable and degenerate neutrophils, fewer lymphocytes and macrophages, and necrotic cellular debris. Inflammatory cells extend into and disrupt the adjacent neurophil and there is moderate diffuse gliosis. (HE 100x, HE 400x)

the trigeminal ganglion and brainstem. The characteristic lesion is brainstem microabscesses or glial nodules that eventually fill with neutrophils, and lymphocytic perivascular cuffing and local brain parenchymal edema and rarefaction. Mild meningitis of the cerebellum and anterior spinal cord is common. Encephalitic cases are rare in dogs[2] and no report was found of neurologic listeriosis in a cat and few septicemic cases.[3] Listeriosis typically has one of three separate entities: encephalitis, septicemia, or metritis/abortion.[3] The lesions in this cat are much more suppurative than we usually see in ruminants.

AFIP Diagnosis: Brainstem and cerebellum: Encephalitis, suppurative, multifocal to coalescing, marked.

Conference Comment: In addition to the lesions described by the contributor, conference participants noted reactive astrocytosis and rare foci of neutrophilic inflammation within the cerebellar white matter on some slides. Several conference participants considered feline infectious peritonitis (FIP) in the differential diagnosis. However, several histologic findings argue against a diagnosis of FIP: 1) inflammation elicited in FIP is classically pyogranulomatous, whereas the inflammation in this case is predominantly neutrophilic; 2) neutrophils in the pyogranulomatous inflammation of FIP are classically nondegenerate, whereas the neutrophils in this case are mostly degenerate; and 3) inflammation in FIP is generally centered on blood vessels, ventricles, and choroid plexus, whereas in this case, foci of inflammation are scattered randomly throughout the neuropil of the brainstem. The tissue Gram stain demonstrates numerous gram-positive short bacilli, and in congruence with the reported bacterial culture results, solidifies the diagnosis of encephalitic listeriosis.

In humans and animals, *L. monocytogenes* is credited with producing three distinct syndromes, each of which is thought to develop by a unique pathogenesis. The first, as demonstrated by this case, is encephalitis, which occurs almost exclusively in ruminants and is associated with feeding incompletely fermented silage where the bacterium readily multiplies, as described by the contributor. Interestingly, although *L. monocytogenes* has been shown experimentally to breach the blood-brain barrier, the distribution of lesions in naturally-occurring cases of listerial encephalitis suggests direct invasion through the oral mucosa, ascension through the trigeminal nerves, and centripetal travel via axons to the brain, rather than hematogenous infection. Preferentially affected are the medulla and pons, with less severe infection in the thalamus and cervical spinal cord. Classically, clinical signs consist of depression, head-pressing, and circling, often with unilateral paralysis of the seventh cranial nerve and resultant facial drooping and/or unilateral purulent endophthalmitis, which may be confused with malignant catarrhal fever.[2]

The second syndrome is abortion, which is thought to result from hematogenous infection of the pregnant uterus following an asymptomatic bacteremic phase. In cattle and sheep, abortions occur in the third trimester of pregnancy, often without clinical illness in the dam, followed typically by retention of the placenta. Infection in the early part of the third trimester results in expulsion of an autolyzed fetus. Late third trimester infections produce the third listeriosis syndrome, septicemia, characterized by miliary yellow foci of necrosis and bacteria that are grossly evident in the liver, and microscopically also found in the lung, heart, kidney, spleen, and brain. Both the cotylendonary and intercotyledonary regions of the placenta are affected by a robust necrotizing placentitis. Interestingly, it is uncommon for the encephalitis and abortion syndromes to occur together in a herd or flock.[4]

In addition to the remarkable ability of this ubiquitous saprophyte to survive and grow in the environment, *L. monocytogenes* persists indefinitely in macrophages, thereby escaping the humoral immune system. The bacterium induces phagocytosis via a cell surface protein called internalin; inside the cell it escapes phagosome-mediated killing via such virulence factors as listeriolysin O and phospholipases. Then, in a most impressive display of stealth, *L. monocytogenes* manipulates host cell contractile actin to facilitate movement from cell to cell without exposure to antibodies.[1,2]

Contributor: Arkansas Livestock and Poultry Commission, #1 Natural Resources Drive, Little Rock, AR 72205

References:

1. Greene CE: Listeriosis. *In:* Infectious Diseases of the Dog and Cat, ed. Greene CE, 3rd ed., pp. 311-312. Saunders Elsevier, St. Louis, MO, 2006
2. Maxie MG, Youssef S: Nervous system. *In:* Jubb, Kennedy, and Palmer's Pathology of Domestic Animals, ed. Maxie MG, 5th ed., vol. 1, pp. 405-408. Elsevier Saunders, Philadelphia, PA, 2007
3. Rogers JJ: Listeriosis in a young cat. J Am Vet Med Assoc **168:**1025, 1976
4. Schlafer DH, Miller RB: Female genital system. *In:* Jubb, Kennedy, and Palmer's Pathology of Domestic Animals, ed. Maxie MG, 5th ed., vol. 3, pp. 492-493. Saunders Elsevier, Philadelphia, PA, 2007

CASE IV: 07-21444 (AFIP 3152276).

Signalment: 10-year-old male Labrador retriever dog (*Canis familiaris*).

History: This dog had a clinical history of "CNS signs." The dog was a stray, and because it was acting "odd" according to the property owner, the dog was submitted to the laboratory for rabies testing. The brain was removed and the rest of the body was not examined.

Gross Pathology: The cerebrum was distorted by an approximately 2 x 2.5 cm spherical, pale yellow-tan soft friable mass. The mass was not encapsulated and was not connected to the meninges.

Laboratory Results: Direct FA for rabies virus antigen was negative. An aerobic culture of the brain was positive for *Pasteurella* sp.

Histopathologic Description: The meninges and adjacent neuropil have been infiltrated by numerous variable-sized nests of plump, round neoplastic cells. Individual nests are separated by a delicate fibrovascular stroma. The neoplastic cells have finely granular eosinophilic cytoplasm, a central or eccentric, small, finely stippled nucleus with one or two nucleoli (**figs. 4-1, 4-2, and 4-3**). Mitotic figures are rare (not visible on all slides) and in some slides there are microfocal lymphocytic perivascular cuffs within the tumor or the adjacent unaffected neuropil.

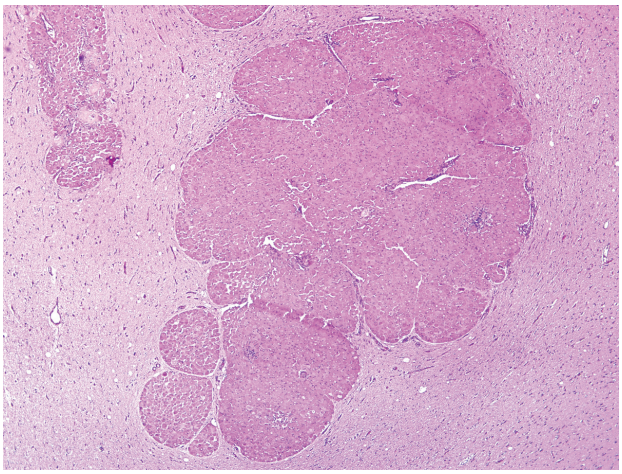

4-1. Granular cell tumor, cerebrum, dog. Infiltrating and compressing the neuropil is a multilobulated neoplasm composed of nests of brightly eosinophilic round cells. (HE 12.5x)

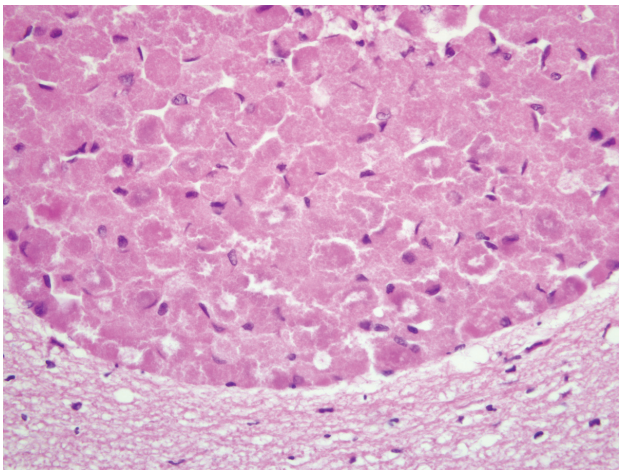

4-2. Granular cell tumor, cerebrum, dog. Neoplastic round cells are plump, round, with abundant granular eosinophilic cytoplasm (HE 400x)

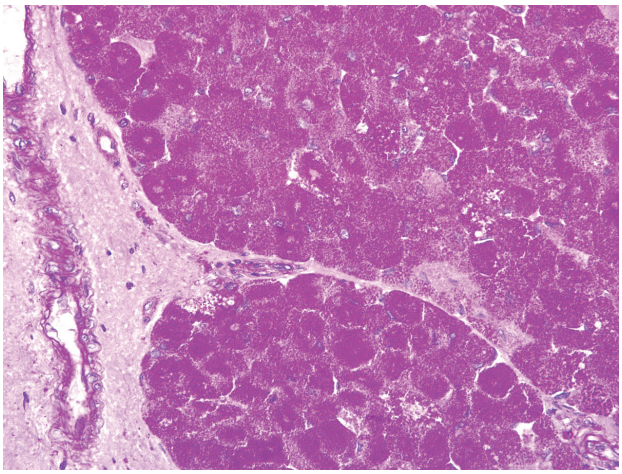

4-3. Granular cell tumor, cerebrum, dog. Neoplastic cells contain diastase- resistant PAS –positive cytoplasmic granules (PASD 200x)

Contributor's Morphologic Diagnosis:
Intracerebral granular cell tumor.

Contributor's Comment: In rats, granular cell tumors are the most common intracranial tumor.[5] In horses, this type of tumor has only been reported in the lungs, where it may be an incidental finding.[4] In dogs, granular cell tumors are most commonly located in the oral cavity.[2] Other, less frequently reported sites in dogs include the heart, skin and brain.[1] Other species with reported granular cell tumors include cats[6] and ferrets.[5] Granular cell tumors arising in the peripheral soft tissues of non-human animals are generally believed to originate from Schwann cells.[1,4] The tumor cells usually contain diastase-resistant PAS-positive cytoplasmic granules.[1,3] A definitive origin for granular cell tumors in the CNS of

non-human animals has not been determined.

In humans, these tumors are histogenetically heterogeneous and occur both within the nervous system and in extra-neural locations.[3] The tumors in the CNS are believed to arise from astrocytes or pituicytes and tumors in extra-neural sites are believed to be of peripheral nerve origin (usually Schwann cells).[6]

In previously reported cases of intracranial granular cell tumors, the clinical signs have included blindness (when the tumor entraps the optic nerves), seizures, ataxia, weakness, nystagmus, opistotonus, and proprioceptive deficits.[1,3,5,6] Unfortunately, the history in this particular case was limited to "CNS signs" and "acting odd."

In this case, small perivascular cuffs of lymphocytes and less frequently neutrophils were present in the non-involved cerebrum and hippocampus (not included in most slides). In the cerebellum and hippocampus the endothelial cells lining most blood vessels were plump and hypertrophic (reactive endothelial cells). Perivascular cuffing associated with this type of tumor has been reported previously[1], and in this case we assume that the lymphocytic perivascular cuffing is associated with the tumor while the neutrophils and reactive endothelium may be in response to the presence of a *Pasteurella* sp., believed to be an acute infection.

AFIP Diagnosis: Cerebrum: Granular cell tumor.

Conference Comment: This case was reviewed in consultation with the AFIP Department of Neuropathology. It is perplexing that while the gross description indicates that the neoplasm was not attached to the meninges, microscopic evaluation reveals that the neoplasm, indeed, expands the meninges, often obliterating Virchow-Robin space, and infiltrates the adjacent neuropil. As indicated by the contributor's comments, the diverse list of examples of granular cell tumors in various species suggests that the granular cell phenotype may develop in tumors that have different cells of origin. While the histogenesis of granular cell tumors from various anatomic locations in several animal species is known, the cell of origin of the cerebral granular cell tumor remains enigmatic.

Conference participants briefly discussed oncocytoma and laryngeal rhabdomyoma in the dog; these neoplasms share histological similarities with granular cell tumors. Electron microscopy indicates that the prominent cytoplasmic granules in granular cell tumors are lysosomes and autophagosomes.[1,3] In oncocytomas and laryngeal rhabdomyoma, the cytoplasm is packed with mitochondria, accounting for the granules seen on H&E.[7]

Contributor: Animal Disease Research and Diagnostic Laboratory, South Dakota State University, Veterinary Science Department North Campus Drive, Brookings, SD 57007
http://vetsci.sdstate.edu

References*:*

1. Barnhart KF, Edwards JF, Storts RW: Symptomatic granular cell tumor involving the pituitary gland in a dog: a case report and review of the literature. Vet Pathol **38:**332-336, 2001
2. Head KW, Else RW, Dubielzig RR: Tumors of the intestines. *In:* Tumors in Domestic Animals, ed. Meuten DJ, 4th ed., p. 433. Iowa State Press, Ames, IA, 2002
3. Higgins RJ, LeCouteur RA, Vernau KM, Sturges BK, Obradovich JE, Bollen AW: Granular cell tumor of the canine central nervous system: two cases. Vet Pathol **38:**620-627, 2001
4. Kelley LC, Hill JE, Hafner S, Wortham KJ: Spontaneous equine pulmonary granular cell tumors: morphologic, histochemical, and immunohistochemical characterization. Vet Pathol **32:**101-106, 1995
5. Liu CH, Liu CI, Liang SL, Cheng CH, Huang SC, Lee CC, Hsu WC, Lin YC: Intracranial granular cell tumor in a dog. J Vet Med Sci **66:**77-79, 2004
6. Mandara MT, Ricci G, Sforna M: A cerebral granular cell tumor in a cat. Vet Pathol **43:**797-800, 2001
7. Wilson DW, Dungworth DL: Tumors of the respiratory tract. *In:* Tumors in Domestic Animals, ed. Meuten DJ, 4th ed., pp. 378-379. Iowa State Press, Ames, IA, 2002

The Armed Forces Institute of Pathology
Department of Veterinary Pathology

Conference Coordinator:
Shannon Lacv. DVM. MPH

WEDNESDAY SLIDE CONFERENCE 2009-2010

Conference 22

28 April 2010

Conference Moderator:

Steven E. Weisbrode, DVM, PhD, Diplomate ACVP

CASE I: AFIP 3147900.

Signalment: 17-year-old chestnut Hanoverian mare (*Equus caballus*).

History: This mare presented approximately seven years prior to euthanasia with lameness which progressed to swelling over the splint bones of the left forelimb. A bone scan showed intramedullary sclerosis of the left distal humerus occupying approximately one third of the bone and a suspected lesion of the glenoid cavity of the left scapula. The mare was treated with non-steroidal anti-inflammatory drugs (NSAIDs) and stall rest. No follow-up examination was recorded with reference to the lesions in the humerus and scapula.

Nearly two years prior to euthanasia, the mare presented with an approximately 10 cm diameter, rounded, boney tumor on the caudal aspect of the left mandible. The mandible was thickened in the horizontal plane, with a craterous depression immediately caudal to the mass. Radiographs revealed an "altered trabecular pattern of bone" extending dorsally into the mandibular cheek tooth roots.

Previous clinical history included a left-sided ethmoid hematoma diagnosed approximately eight years prior to euthanasia, which was treated with serial surgeries and formalin injection. Following complete recovery, the mare later developed a chronic, low-volume, bilateral, mucoid nasal discharge due to a mucocele, which resolved in response to 10% formalin injection. No further mucoid discharge or endoscopic changes to the ethmoid turbinates were observed following treatment. The reason for eventual euthanasia was not specified by the case contributor.

Gross Pathology: Necropsy examination was performed by the attending clinician, who reported boney masses in the left mandible and left scapula; the masses effaced pre-existing bone and contained coalescing pockets of soft, white material. The clinican's working diagnosis included osteosarcoma and fibrosarcoma.

Histopathologic Description: Bone, mandible and scapula: Extending to the margins of the submitted tissue, expanding the medulla, separating and surrounding regularly-spaced, irregularly-shaped trabeculae of woven bone, and invading and effacing overlying cortical bone is an unencapsulated, infiltrative, well-demarcated moderately cellular neoplasm composed of spindle to stellate mesenchymal cells arranged in haphazard streams on a moderately edematous fibromyxomatous

*Sponsored by the American Veterinary Medical Association, the American College of Veterinary Pathologists, and the C. L. Davis Foundation.

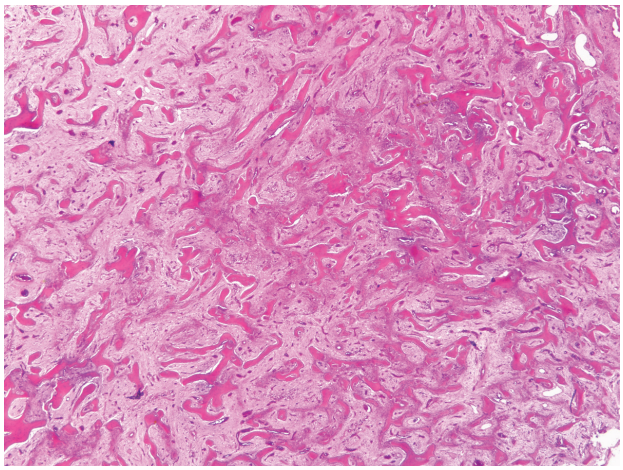

1-1. Ossifying fibroma, mandible and scapula, mare. In the medullary cavity there is an unencapsulated neoplasm composed of spindle cells arranged in short haphazard streams within a fibro-osseous matrix that contains irregular spicules and trabeculae of bone. (HE 20x)

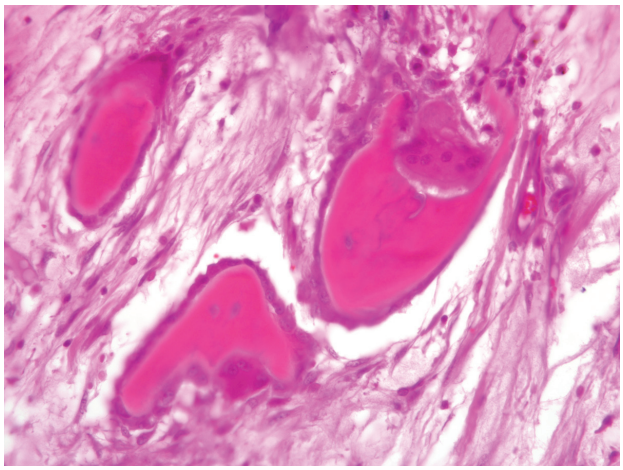

1-2. Ossifying fibroma, mandible and scapula, mare. Trabeculae of bone are lined by hypertrophied osteoblasts, and there are few multinucleate osteoclasts within Howships lacunae. Additionally there are scattered lymphocytes and plasma cells. (HE 400x)

matrix. Trabeculae are lined by a single layer of plump, hypertrophied, active osteoblasts, and frequently, one or more osteoclasts within Howship's lacunae (osteoclastic osteolysis) (**figs. 1-1 and 1-2**). Proliferating mesenchymal cells have indistinct cell borders, scant eosinophilic cytoplasm, and one oval to elongate nucleus with finely-stippled chromatin and 1-2 generally indistinct nucleoli. Mitoses are rare (less than 1 per ten 40X HPF). Scattered throughout the connective tissue are moderate numbers of osteoclasts, few aggregates of hematopoietic precursors (marrow elements), few perivascular foci of lymphocytes and plasma cells, and rare hemosiderin-laden macrophages. Multifocally, the spindle cells invade and replace the overlying woven or compact cortical bone, which also undergoes osteoclastic osteolysis. In some slides, there are aggregates of lymphocytes and plasma cells in the overlying fascia, and attached skeletal muscle myocytes exhibit sarcoplasmic pallor, swelling, vacuolation, with formation of contraction bands (degeneration) or are shrunken, angulated, fragmented, and have hypereosinophilic sarcoplasm with loss of cross striations and pyknosis (necrosis).

Contributor's Morphologic Diagnosis: Bone, mandible and scapula: Ossifying fibroma.

Contributor's Comment: The lesions in the submitted section of mandible and scapula are essentially identical. Ossifying fibroma is a benign, but invasive, lytic, and expansile fibro-osseous proliferation that is most commonly reported in the mandible in horses less than one year of age, where it is classified as equine juvenile mandibular ossifying fibroma. The lesion is less frequently seen in cats, dogs, and sheep, has been reported in greater kudus, a llama, a goat, and a rabbit, and has not been reported to undergo malignant transformation or metastasize.[4,6,8]

This case is unusual in that the affected mare was much older than is typical, and scapular involvement is uncharacteristic of this tumor, which classically presents as a well-demarcated, expansile, non-painful mass protruding from the rostral mandible.[4,6,8] However, ossifying fibroma has been reported in sites other than the mandible, including the maxilla, and the os penis of a dog.[5] Like the most commonly affected bones of the skull, the proximal scapula develops by intramembranous ossification, so its involvement in this case is not completely unexpected. Moreover, the lesion has been reported in tubular bones in humans and cats.[2]

AFIP Diagnosis: Bone, mandible and scapula: Ossifying fibroma.

Conference Comment: During the conference, participants discussed the differential diagnosis for this case in detail. Without the benefit of knowing the clinical history and radiographic findings, most conference participants diagnosed fibrous osteodystrophy (FOD), a fairly common metabolic bone disease caused by persistent primary or secondary hyperparathyoridism. Primary hyperparathyroidism results from a functional parathyroid gland adenoma, and is far less common than secondary hyperparathyroidism in all domestic species. Secondary

hyperparathyroidism can result from renal disease or a nutritional deficiency or imbalance (i.e. simple dietary calcium deficiency, dietary phosphorus excess, or vitamin D deficiency). Nutritional secondary hyperparathyroidism is most common in horses, a species exquisitely sensitive to the effects of high dietary phosphorus. Horses fed a diet containing a calcium to phosphorus ratio of 1:3 or wider are highly susceptible to FOD; this most commonly occurs in horses fed a diet consisting primarily of grain, giving rise to the colloquial term "bran disease" for the condition. The disease is also reported in horses grazing pastures high in oxalate, even when calcium and phosphorus are normal. Disease prevalence is highest in young growing horses, and the characteristic clinical presentation is bilateral swelling of the mandibles and maxillae, prompting another colloquial term, "big head." Serum PTH concentrations and urinary fractional clearance of phosphorus are increased in affected horses, and are more useful for antemortem diagnosis than are serum calcium and phosphate concentrations.[7]

Microscopically, FOD is characterized by the triad of increased osteoclastic bone resorption, fibroplasia, and increased osteoblastic activity with the formation of trabeculae of woven bone; all three features are also seen in normal bone remodeling and certain stages of fracture repair, and are present in this case as well.[7] Therefore, the diagnosis requires correlation with the clinical and radiographic findings, and examination of sections of bone distant from sites of bone remodeling or fracture repair. The numerous osteoclasts present in this case compelled some participants to discount ossifying fibroma entirely in favor of a diagnosis of FOD; however, the conference moderator cautioned participants to remember that any mesenchymal cell can secrete RANK-L, resulting in osteoclast differentiation and activation. In this case, fibrous osteodystrophy can be excluded only in light of the clinical history and radiographic findings.

The foci of inflammation within marrow spaces seen in this case are unusual, and are not typical of FOD or ossifying fibroma, urging some participants to consider osteomyelitis in the differential diagnosis. While inflammation in the marrow spaces and reactive new bone growth may result from chronic, productive osteomyelitis, the conference moderator and participants noted several features that argue against osteomyelitis in this case: 1) inflammation in osteomyelitis would be expected to occur in larger pockets, whereas in this case the foci of inflammatory cells are small and generally confined to perivascular areas; 2) the reactive trabecular bone in osteomyelitis would generally exhibit a distinct orientation around pockets of inflammation, whereas in the examined slides the new bone is arranged haphazardly; and 3) productive osteomyelitis generally yields reactive periosteal new bone growth that is oriented perpendicular to the cortex initially (though it may orient parallel to the cortex after remodeling), and would not typically produce the degree of cortical osteoclasis seen in this case.

Microscopically, ossifying fibroma is often described as intermediate between fibrous dysplasia and osteoma, two other benign bone-forming tumors considered by conference attendees and discussed during the conference. Fibrous dysplasia has been ascribed to a mesenchymal developmental abnormality, hamartomatous anomaly, or neoplastic process. While relatively common in humans, it has been only rarely reported in the horse, including once in the accessory carpal bone causing sudden-onset lameness,[2] and once in the nasal cavity causing epistaxis.[3] Fibrous dysplasia closely resembles ossifying fibroma in all respects except one: while spicules of bone in ossifying fibroma are lined by a single layer of plump osteoblasts which apparently arise from the proliferating mesenchymal cells that separate them, spicules of bone in fibrous dysplasia form directly from mesenchymal cells and are not lined by osteoblasts.[2-4,6-8] At the other end of the spectrum, osteomas are composed primarily of dense trabeculae of woven bone that, as in ossifying fibroma, are lined by a layer of plump osteoblasts; however, osteomas generally project from the surface of the bone, and their bony trabeculae are more separated by smaller spaces with more loosely-arranged mesenchymal tissue than is present in ossifying fibroma.[4,6,8]

Because reports of fibrous dysplasia, ossifying fibroma, and osteoma in horses remain sparse, differences in prognosis among these benign fibro-osseous proliferations are not yet apparent, and the more practically important duty of the veterinary histopathologist is distinction between these proliferative lesions and malignant neoplasia. Affirming this, the submitting clinician's working diagnosis, based on the gross and radiographic findings, included osteosarcoma and fibrosarcoma. Osteosarcoma, while less common than ossifying fibroma in horses, is occasionally reported in the bones of the face and jaw and shares with ossifying fibroma the tendency to replace alveolar and cortical bone, causing tooth loosening and increased susceptibility to pathological fracture. Osteosarcoma is excluded in this case by the presence of regularly-spaced, irregularly-shaped spicules of well-differentiated woven bone, a feature characteristic of ossifying fibroma but not osteosarcoma. Moreover, the spicules of bone are lined by plump osteoblasts that are clearly distinct from the proliferating mesenchymal cells that separate the bone trabeculae. In contrast to the usually overtly malignant neoplastic cells of osteosarcoma, the proliferating mesenchymal cells in this case are microscopically bland, with a low mitotic

rate, minimal anisocytosis and anisokaryosis, and absence of osteoid.[4,5,7,8] Similarly, fibrosarcoma is excluded based on the bland microscopic features of the proliferating mesenchymal cells and the gradual transition between the proliferative cell population and adjacent tissue.

Finally, though not associated with the degree of cortical lysis present in this case, idiopathic enostosis-like lesions have been reported in the long bones of horses[1] and should be considered when a proliferation of woven bone is encountered in a diagnostic setting. An example from the right distal humerus of a Swedish Warmblood riding horse was reviewed in WSC 2008-2009, Conference 21, case IV.

Contributor: Department of Veterinary Pathology, Armed Forces Institute of Pathology, Washington, DC 20306

References*:*

1. Bassage LH, Ross MW: Enostosis-like lesions in the long bones of 10 horses: scintigraphic and radiographic features. Equine Vet J **30:**35-42, 1998
2. Jones NY, Patterson-Kane JC: Fibrous dysplasia in the accessory carpal bones of a horse. Equine Vet J **36:**93-95, 2004
3. Livesey MA, Keane DP, Sarmiento J: Epistaxis in a standardbred weanling caused by fibrous dysplasia. Equine Vet J **16:**144-146, 1984
4. Miller MA, Towle HAM, Heng HG, Greenberg CB, Pool RR: Mandibular ossifying fibroma in a dog. Vet Pathol **45:**203-206, 2008
5. Mirkovic TK, Shmon CL, Allen AL: Urinary obstruction secondary to an ossifying fibroma of the os penis in a dog. J Am Anim Hosp Assoc **40:**152-156, 2004
6. Speltz MC, Pool RR, Hayden DW: Pathology in practice: ossifying fibroma of the right mandible. J Am Vet Med Assoc **235:**1283-1285, 2009
7. Thompson K: Bones and joints. *In:* Jubb, Kennedy, and Palmer's Pathology of Domestic Animals, ed. Maxie MG, 5th ed., vol. 1, pp. 82-88, 110-124. Elsevier Saunders, Philadelphia, PA, 2007
8. Thompson KG, Pool RR: Tumors of bones. *In:* Tumors in Domestic Animals, ed. Meuten DJ, 4th ed., pp. 248-255, Iowa State Univ. Press, Ames, IA, 2002

CASE II: 04-2259 (AFIP 2988004).

Signalment: 6-month-old, male, domestic shorthair cat (*Felis catus*).

History: This cat presented with lameness in right rear and left front legs. Radiographs revealed multiple old and new fractures in several bones. The animal was maintained on a diet of Hill's Science Diet® for 1.5 months and then became lame again with a new fracture.

Gross Pathology: All bones are brittle and fracture easily. Bone callus is present on several ribs, the left distal femur and the left distal ulna. The right distal tibia has a fresh oblique fracture.

Histopathologic Description: The radius and ulna are submitted. Both have a normal growth plate. The primary spongiosa lack osteoid and are mostly cartilage. Cartilage is retained in the secondary spongiosa and the metaphyseal bone. No osteoclast activity is seen. The radius has a healing fracture with a mixture of cartilage, bone and fibrous tissue.

Contributor's Morphologic Diagnosis:
Osteogenesis imperfecta, probable.

Contributor's Comment: The bones in this cat are failing to produce osteoid. The growth plate is normal and no remodeling of bone by osteoclasts is seen. These features support a bone formation problem as the most likely disease. Osteogenesis imperfecta is the most likely cause for the changes in this bone. Confirmation of the disease as the cause would require examination of the teeth, which was not done in this case. The histologic appearance does not support other metabolic bone diseases as causes, including rickets and osteodystrophy fibrosa. Osteodystrophy fibrosa is characterized by bone resorption and fibrosis. Rickets has thick, abnormal growth plates and widened osteoid seams in the primary spongiosa.

Osteogenesis imperfecta is an inherited disease caused by a genetic defect of the COL1A1 or COL1A2 genes, which encode the procollagen molecules of collagen type 1. This results in quantitative and qualitative abnormalities in type 1 collagen. Bone and teeth are affected, but other type 1 collagen-rich tissues, such as skin, are not affected. Osteogenesis imperfecta has been reported in dogs, cats, cattle, sheep, mice and tigers. Defects in the COL1A1 and COL1A2 genes have been found in the Golden retriever dog and mice.

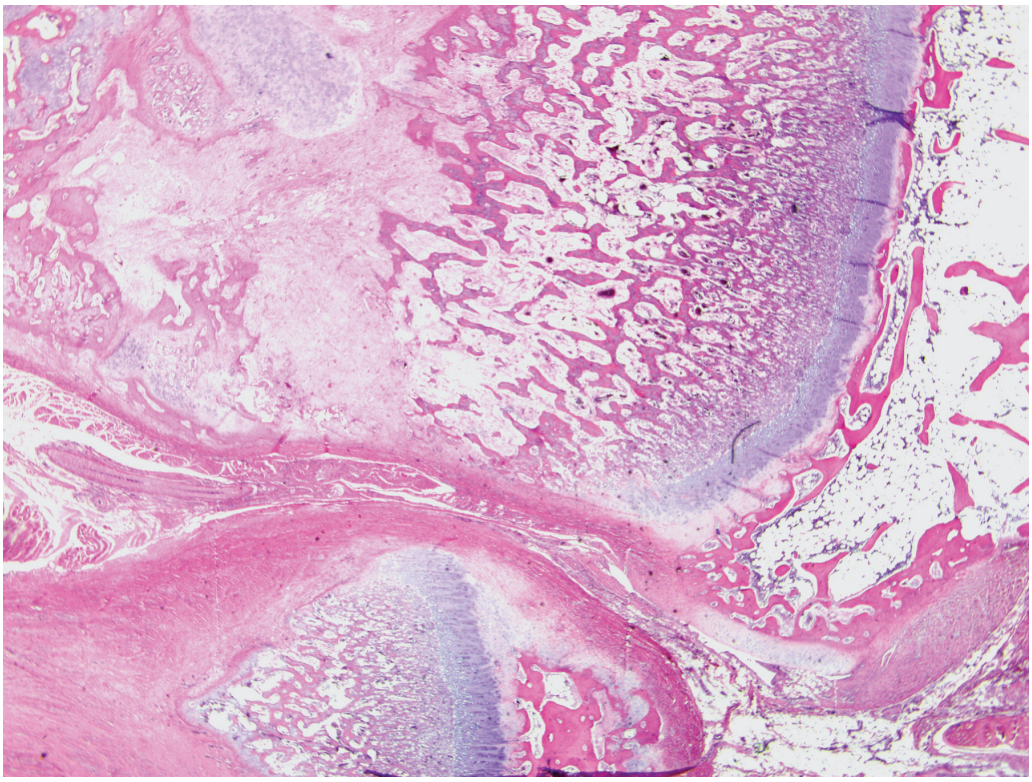

2-1. Distal radius and ulna, cat. Multifocally within the metaphyses, there is retention of cartilage within the primary spongiosa. Within the overlying epiphysis there is osteopenia. (HE 12.5x)

AFIP Diagnosis: 1. Bone, distal radius and ulna: Osteopenia, epiphyseal, focally extensive, marked, with metaphyseal reactive woven bone formation (fracture callus), synoviocyte hyperplasia, and pannus.
2. Bone, proximal humerus: Osteosclerosis, epiphyseal and metaphyseal, focally extensive, marked, with growth retardation lattices, mild trabecular woven bone formation, mild marrow fibrosis and myxomatous metaplasia, and focally extensive periosteal granulation tissue.

Conference Comment: In the distal radius and ulna, conference participants noted several changes in addition to those described by the contributor, including proteoglycan loss in the articular cartilage with empty chondrocyte lacunae (chondrocyte necrosis), synoviocyte hyperplasia, and proliferation of a layer of synoviocytes covering the articular cartilage (pannus) (**figs. 2-1 and 2-2**) . The relationship of the additional observed changes to the underlying condition in this kitten is unclear, but conference participants speculated that the radial fracture may have accounted for both the osteopenia in the radial epiphysis (i.e. due to disuse) and secondary degenerative lesions in the joint (i.e. due to instability). Joint laxity is a characteristic feature of osteogenesis imperfecta (OI), along with bone and tooth fragility and blue sclerae, and therefore may also have contributed to secondary joint lesions in this animal.

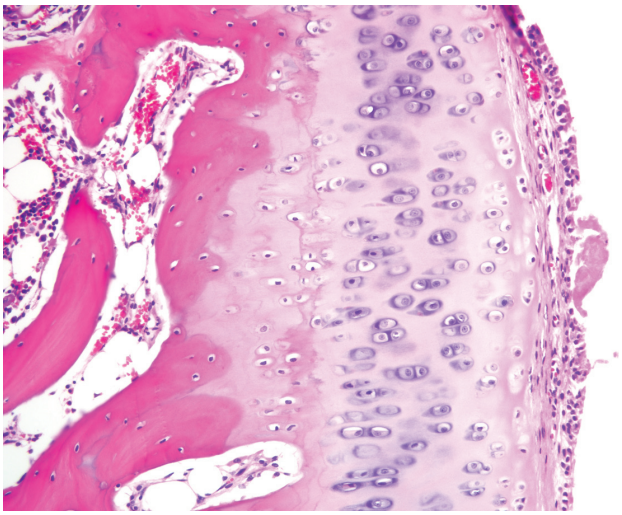

2-2. Humerus, cat. There is proliferation of a layer of synoviocytes covering the articular cartilage (pannus). In the immediate subjacent articular cartilage, there is proteoglycan loss with empty chondrocyte lacunae (chondrocyte necrosis) and syniovocyte hypertrophy and hyperplasia in the deeper layers of cartilage. (HE 100x)

Additionally, many conference participants received a section of bone interpreted as proximal humerus instead of the distal radius and ulna described by the contributor. In contrast to the epiphyseal osteopenia noted in the radius, the primary lesion in the proximal humerus is osteosclerosis attributed to the persistence of primary spongiosa with increased cross connections between cartilage spicules resulting from decreased osteoclasis (growth retardation lattices). Throughout the metaphysis, there are scattered trabeculae of woven bone, and within the metaphyseal bone marrow there is mild fibrosis and/or myxomatous metaplasia. In the adjacent periosteum, there is focally extensive granulation tissue.

Osteogenesis imperfecta, though well-described in humans, remains a rare diagnosis in animals. As mentioned by the contributor, most cases of OI stem from mutations in COL1A1 and/or COL1A2 genes that encode the α1 and α2 chains of type I collagen, respectively. Collagen in bone, dentin, ligaments, tendons, and the sclera is primarily type I, resulting in the characteristic confinement of lesions to these anatomic locations.[1-6] While type I collagen also predominates in the skin, OI usually does not produce cutaneous lesions,[6] although skin fragility has been reported in affected newborn New Zealand Romney lambs.[1]

Noteworthy, OI represents a heterogenous group of diseases, and defects in glycosaminoglycan and proteoglycan metabolism[2] or deficient osteonectin synthesis[6] may also account for some cases. This observation, combined with evidence that a wide variety of mutations in COL1A1 and/or COL1A2 have been demonstrated in humans with OI, explains the substantial phenotypic variation seen in the disease.[1] The conference moderator emphasized this point and noted that because mutations that produce OI can cause qualitative and/or quantitative collagen defects, the bone fragility that results is not necessarily related to bone mass, and thus a uniform set of pathognomonic microscopic findings cannot be relied upon for the diagnosis of OI. As a result, the definitive diagnosis of OI based solely on the tissues provided for histologic examination in this case is not possible, although the clinical history in combination with the gross and microscopic findings is certainly suggestive of the disease. As described by the contributor, the growth plates in this case are microscopically normal, an expected finding in OI since the collagen found in cartilage is primarily type II.[6]

The osteosclerotic lesions in the proximal humeral metaphysis and epiphysis led some participants to consider osteopetrosis in the differential diagnosis, and the conference moderator noted that osteopetrosis, like OI, may manifest as brittle bones prone to fracture. Osteopetrosis in cats has been associated with feline leukemia virus (FeLV) infection and chronic vitamin D toxicosis.[5] However, osteopetrosis classically results in a more severe failure of bone modeling than is present in this case. Additionally, although trabecular bone in OI is often described as microscopically normal or osteopenic, some cases, particularly those seen in lethal OI with skin fragility in New Zealand Romney lambs, result in persistent trabeculae of calcified cartilage that extend into long bone diaphyses and fill marrow cavities, accompanied by a paucity of osteoclasts, similar to osteopetrosis.[1,5]

Of note, some of the earliest cases of "OI" in dogs and cats were later shown to represent misdiagnoses of fibrous osteodystrophy (FOD) due to nutritional secondary hyperparathyroidism, with apparent familial susceptibility actually derived from exposure to common nutritional deficiencies.[2] The paucity of osteoclasts in this case argues against a diagnosis of FOD. Other considerations briefly discussed during conference included osteopenia secondary to protein calorie malnutrition and lack of osteoclasts due to inconsistent exposure to such anti-osteoclastic agents as lead or bisphosphonates. In addition, the lesion in the distal metaphyses of the radius and ulna is somewhat reminiscent of the scorbutic lattice of vitamin C deficiency (scurvy). However, conference participants uniformly agreed that there is more osteoid deposition on the primary spongiosa than would be expected in scurvy. Furthermore, the growth retardation lattice noted in the proximal humeral metaphysis is not expected in scurvy, and this case lacks other classic findings of scurvy, such as microfractures or infractions with associated hemorrhage and fibrin.[5,6]

Contributor: College of Veterinary Medicine, Virginia Tech, Blacksburg, VA 24061
http://www.vetmed.vt.edu

References:

1. Arthur DG, Thompson KG, Swarbrick P: Lethal osteogenesis imperfecta and skin fragility in newborn New Zealand Romney lambs. NZ Vet J **40:**112-116, 1992
2. Denholm LJ, Cole WG: Heritable bone fragility, joint laxity and dysplastic dentin in Fresian calves: a bovine syndrome of osteogenesis imperfecta. Aust Vet J **60:**9-17, 1983
3. Leeb F, Peters M, Brugmann M, Fehr M, Hewicker-Trautwein M: Osteogenesis imperfecta in two litters of dachshunds. Vet Pathol **40:**530-539, 2003
4. Seeliger F, Leeb T, Peters M, Brugmann M, Fehr M, Hewicker-Trautwein M: Osteogenesis imperfecta in two litters of Dachshunds. Vet Pathol **40:**530-539, 2003
5. Thompson K: Bones and joints. *In:* Jubb, Kennedy, and Palmer's Pathology of Domestic Animals, ed. Maxie MG,

5th ed., vol. 1, pp. 33-38. Saunders Elsevier, Philadelphia, PA, 2007
6. Weisbrode SE: Bones and joints. *In:* Pathologic Basis of Veterinary Disease, eds. McGavin MD, Zachary JF, 4th ed., pp. 1065-1066. Mosby Inc., St. Louis, MO, 2007

CASE III: 0801631 (AFIP 3122074).

Signalment: Mouse (*Mus musculus*), heterozygous F1 *p53*(+/-) transgenic (C3H/HeNTac female inbred x C57BL/6-Tr*p53*tml Brd het N12 male inbred F1), approximately 45 weeks of age, both sexes affected.

History: Several untreated and treated mice developed hindlimb paresis or paralysis and were euthanized.

Gross Pathology: In some mice there were masses involving the vertebral column (size ranged from only 1-2 mm raised above the rest of the vertebra to >1 cm masses attached to the vertebra); however, in some cases gross lesions were not noted.

Histopathologic Description: The vertebral body is expanded by numerous disorganized trabeculae of eosinophilic to amphophilic matrix (osteoid) which largely fills the marrow cavity, extends into the spinal canal, and extends slightly out from the external (periosteal) surface (**fig. 3-1**). Osteoblasts (tumor cells) are oriented at random with respect to the bone surfaces. They are plump and irregular-shaped, except where they are piled up into sheets extending into the spinal canal or in layers extending out from the periosteum, where they are more spindle-shaped. Cell boundaries are indistinct. The cytoplasm is faintly eosinophilic and often vacuolated. Nuclei are large and round, and occasionally there is a single prominent nucleolus. Mitotic figures are uncommon (1-2 per 0.238 mm^2 high power field) (**fig. 3-2**). The spinal cord within the canal is misshapen; numerous vacuoles are present within the white matter (grey matter is rarely present in the sections provided). Where osteoid abuts muscle cells they occasionally are smaller than normal, with amphophilic to basophilic cytoplasm and centrally-located nuclei.

Contributor's Morphologic Diagnosis: Vertebral osteosarcoma with leukomalacia of the spinal cord and lumbar muscle degeneration and regeneration.

Contributor's Comment: Although it seems obvious that a mass need be only small in this location to cause clinical signs, osteosarcomas are not something one generally thinks of as a cause of paresis/paralysis when gross lesions are absent. The smaller tumors in these cases remind us that such a clinical observation requires very close examination of the spinal column, and in some cases tumors may best be detected by microscopic examination of the relevant (i.e. thoracic to lumbar) sections of spinal column.

This is a typical osteoblastic osteosarcoma with

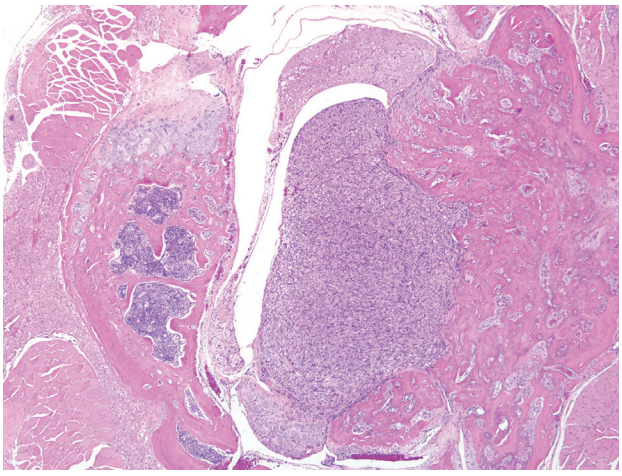

3-1. Vertebral osteosarcoma, bone, vertebral arch, mouse. Expanding and infiltrating the vertebral body and compressing the adjacent spinal cord is an unencapsulated neoplasm composed of spindle cells arranged in short haphazard streams. (HE 40x, HE 200x)

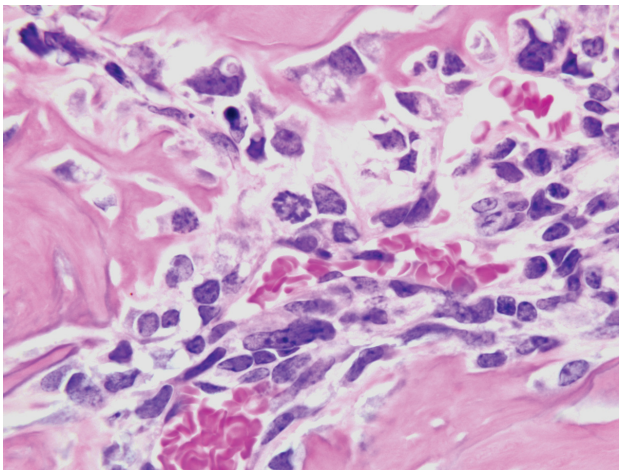

3-2. Vertebral osteosarcoma, bone, vertebral arch, mouse. Neoplastic spindle and polygonal cells are separated by variable amounts of osteoid, and contain moderate amounts of lightly eosinophilic vacuolated cytoplasm, large round nuclei, and occasionally prominent nucleoli. Mitotic figures are uncommon (1-2/10 HPFs). (HE 1000x)

abundant osteoid production making diagnosis fairly simple. Osteosarcomas in mice can be osteoplastic, chondroblastic, osteoclastic, anaplastic, osteoblastic, fibroblastic, telangiectatic (vascular), or compound.[3] The National Toxicology Program records an overall incidence of osteosarcomas in 9-month-old *p53* transgenic mice of 2.0% in males and 7.3% in females.[2] In the study in question, the maxilla was the most common site of osteosarcomas, with the vertebrae second most common; osteosarcomas were also recorded in the femur, tibia, and rib. In a mouse model of osteosarcoma development, wherein one or both *p53* alleles were inactivated with or without inactivation of one or both Rb alleles, the most common sites of osteosarcoma development were the jaw (mandible followed by maxilla), followed by the hind leg/hip, and ribs and vertebrae.[6] Metastases were present (largely in the lungs and liver) in 9% of mice, and rarely in those animals presenting with tumors on the jaws (presumably because they had a significantly decreased lifespan due to the primary tumor). It was noted in that study also that many tumors were microscopic.[6]

The incidences of several tumors, predominantly osteosarcomas and soft tissue sarcomas, are increased in *p53* transgenic mice.[1] This observation, together with the observations that a high percentage of osteogenic sarcomas have rearrangements or deletions of the *p53* gene and that bone tumors occur as part of a syndrome of germline mutations of *p53* (the Li-Fraumeni family syndrome), supports the hypothesis that inactivation of *p53* is an important step in development of bone tumors.[1]

AFIP Diagnosis: Bone, vertebral arch: Osteosarcoma, osteoblastic and fibroblastic, with spinal cord compression atrophy.

Conference Comment: The contributor provides a succinct overview of osteosarcoma in this transgenic mouse model, and readers may wish to review the conference proceedings for WSC 2009-2010, Conference 11, case III for a general discussion of osteosarcoma. Put simply, neoplasia results from the clonal expansion of a single precursor cell that has incurred nonlethal genetic damage. Specifically, four classes of normal regulatory genes comprise the primary targets of genetic damage: 1) growth-promoting proto-oncogenes, 2) growth-inhibiting tumor suppressor genes, 3) genes that regulate apoptosis, and 4) genes involved in DNA repair.[5] This case is the second neoplasm reviewed during this conference year from a mouse model with increased susceptibility to neoplasia; WSC 2009-2010, Conference 1, case II is a mandibular ameloblastic odontogenic tumor in a Tg.AC hemizygous mouse attributed to the expression of the *ras* oncogene, exemplifying the first of the classes of targets of genetic damage in carcinogenesis listed above. By contrast, neoplasia in the present case, as described by the contributor, is attributed to germline mutations of the *p53* gene, and thus illustrates the second of these classes of targets.

As indicated by its distinction as the "guardian of the genome" and "molecular policeman," *p53* is among the most influential and best characterized tumor suppressor genes known, and is the most common target for genetic damage in human neoplasia; *p53* mutations are identified in over 50% of human tumors. The *p53* gene encodes the *p53* protein, a transcription factor whose role is essentially to prevent the propagation of cells with genetic damage, a function it accomplishes via three mechanisms: 1) temporary cell cycle arrest (i.e. quiescence), 2) permanent cell cycle arrest (i.e. senescence), and/or 3) apoptosis. Cell cycle arrest conferred by *p53* is largely mediated by *p53*-dependent transcription of the CDK inhibitor p21, which inhibits cyclin-CDK complexes and phosphorylation (i.e. inactivation) of the retinoblastoma (RB) protein; the inhibition prevents cell cycle progression from the late G_1 phase to the S phase (i.e. the "point of no return") at the G_1/S checkpoint, providing an opportunity for repair of DNA damage. Apoptosis, on the other hand, is induced by *p53* in the face of irreversible DNA damage, and results from *p53*-directed transcription of such pro-apoptotic genes as *BAX* and *PUMA*.[5]

The contributor alluded to the germline *p53* mutation in this transgenic mouse as analogous to the Li-Fraumeni syndrome of humans, discussion of which is best preceded by a cursory review of the "two-hit" hypothesis of oncogenesis. This hypothesis applies to a number of genes, but best illustrated by the *RB* tumor suppressor gene. Basically, the "two-hit" hypothesis states that oncogenesis depends on the presence of two mutations (i.e. "hits") involving both alleles of a given tumor suppressor gene. As applied to the *RB* gene, retinoblastoma occurs only in the presence of two mutations – one in each allele. Children with familial retinoblastoma inherit one defective copy of the *RB*gene as the result of a germline mutation (i.e. the first "hit"), and the second (i.e. somatic) mutation occurs sporadically. In sporadic cases, a single retinoblast must suffer two separate somatic mutations in the *RB* gene – one in each allele – to result in retinoblastoma. Therefore, children who inherit a germline *RB* mutation are at increased risk for developing retinoblastoma, because only one additional "hit" is required to confer complete loss of RB function. A germline mutation in *p53* is the basis of the Li-Fraumeni syndrome, which is directly analogous to germline *RB* mutations in familial retinoblastoma. Affected humans with the Li-Fraumeni syndrome have a 25-fold higher chance of developing malignant neoplasia

by age 50 than the general population.[5]

Wide histomorphological variation within a given tumor and between individual cases is typical of osteosarcoma, which may complicate tumor classification.[4] Accordingly, the neoplasm in this case exhibits substantial intratumoral histomorphologic variation, ranging from an expansile highly productive zone at the periphery, to an invasive lytic internal zone. Based upon this finding, the conference moderator encouraged participants to consider and discuss alternative diagnoses, including osteosarcoma arising in osteoma, or even a collision tumor. Close examination of the interface between the neoplasm and surrounding muscle is helpful in excluding these possibilities; in osteoma and reactive bone, as alluded to in case I above, a gradual transition between a dense fibrous layer and a well-differentiated layer of osteoblasts lining trabeculae is expected, whereas no such transition is present in this case and atypical ovoid neoplastic cells are present throughout the neoplasm.

Contributor: Toxicology Battelle Columbus, 505 King Avenue, Columbus, OH 43201
www.battelle.org

References:

1. Hung J, Anderson R: *p53*: functions, mutations and sarcomas. Acta Orthop Scand Suppl **273:**68-73, 1997
2. Kissling GE: Historical control rates for NTP Tg.AC *p53* mice. National Toxicology Program (available at http://ntp.niehs.nih.gov/?objectid=522CD99F-F1F6-975E-74484178722ECB7C), 2008
3. Long PH, Leininger JR: Bones, joints, and synovia. *In:* Pathology of the Mouse, ed. Maronpot RR, pp. 665-671. Cache River Press, Vienna, IL, 1999
4. Slayter MV, Boosinger TR, Inskeep W, Pool RR, Dämmrich K, Larsen S: Histological Classification of Bone and Joint Tumors of Domestic Animals, 2nd series, vol. I, ed. Schulman FY, pp. 9-11. Armed Forces Institute of Pathology (in cooperation with the CL Davis DVM Foundation and The World Health Organization Collaborating Center for Comparative Oncology), Washington, DC, 1994
5. Stricker TP, Kumar V: Neoplasia. *In:* Robbins and Cotran Pathologic Basis of Disease, eds. Kumar V, Abbas AK, Fausto N, Aster JC, 8th ed., pp. 273-292. Saunders Elsevier, Philadelphia, PA, 2010
6. Walkley CR, Qudsi R, Sankaran VG, Perry JA, Gostissa M, Roth SI, Rodda SJ, Snay E, Dunning P, Fahey FH, Alt FW, McMahon AP, Orkin SH: Conditional mouse osteosarcoma, dependent on *p53* loss and potentiated by loss of Rb, mimics the human disease. Genes Dev **22:**1662-1676, 2008

CASE IV: AFIP 08001 (AFIP 3148218).

Signalment: Rats (*Rattus norvegicus*) (Crl:CD®[SD]), 6 weeks old (± 1 week), males, 218-236 grams.

History: Rats received an aerosolized, inhaled, dry powder formulation of corticosteroid for 45 minutes, once daily for 14 days. Scheduled sacrifice was performed at the termination of the study. This study was conducted in an Association for Assessment and Accreditation of Laboratory Animal Care (AAALAC) accredited facility in accordance with the National Research Council (NRC) Guide for the Care and Use of Laboratory Animals, and the Animal Welfare Act.

Gross Pathology: None.

Histopathologic Description: Bone (stifle joint; tibia): In comparison to untreated control animals, there is a diffuse, mild to moderate thinning of the tibial physeal growth plate cartilage with retention of normal architecture, as well as elongation of the zone of the tibial primary spongiosa. Subjectively, the growth plate-to-spongiosa ratio varies from 1:2 to 1:6 (compared to approximately 1:1 in control animals). Within the region of the primary spongiosa there is minimal to mild thinning of trabecular bone, with widening of the intervening spaces and multifocal dilation of the intervening vasculature. There is a mild to moderate, diffuse hypocellularity of bone marrow hematopoietic elements with a corresponding increase in marrow lipocytes.

Contributor's Morphologic Diagnosis: Proximal tibia: Osteochondrodysplasia, mild to moderate, with minimal to mild trabecular osteopenia and moderate elongation of the primary spongiosa.

Contributor's Comment: These findings are attributed to systemic corticosteroid exposure following repeated inhalation at high doses. Other changes in these rats included mild decreases in lymphocyte counts, minimal increases in neutrophil counts, as well as slight hypertriglyceridemia and elevated gamma glutamyl transferase (GGT). In addition, other findings seen histologically included thymic lymphocyte depletion (increased apoptosis with tingible body macrophages), adrenocortical atrophy and depletion of peripheral lymphoid tissue (splenic white pulp and lymph nodes). These changes are all commonly recognized effects of exogenous systemic corticosteroid exposure.

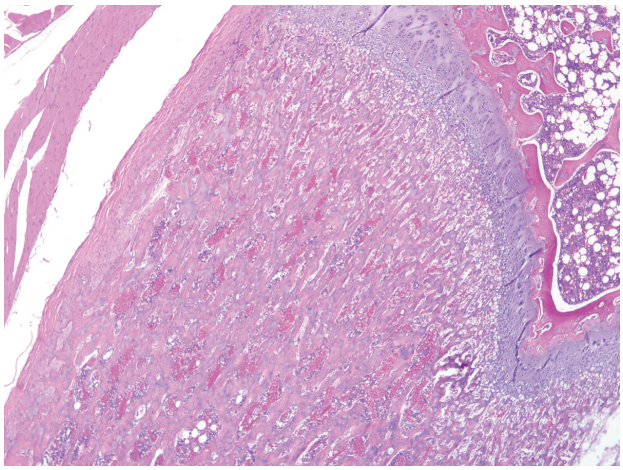

4-1., Bone, proximal tibia, rat. Diffusely within the metaphyses, there is moderate elongation of the primary spongiosa and there is mild to moderate thinning of the tibial physeal growth plate. (HE 40x)

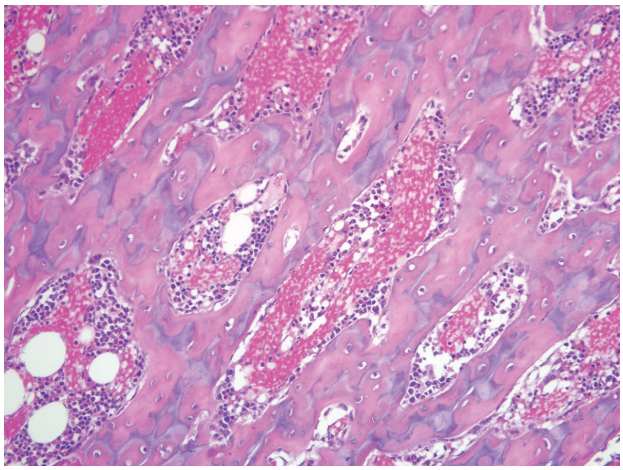

4-2. Bone, proximal tibia, rat. Multifocally within the metaphyses there is retention of unmodeled primary bony trabeculae. (HE 400x)

Normal longitudinal bone growth occurs as a result of endochondral ossification, a highly coordinated process whereby the production of a cartilaginous scaffold at the growth plate is replaced by bone. Many factors have been identified as playing a role in this process; hormones such as estrogens, thyroid and growth hormone, leptin, sex hormones and glucocorticoids, as well as growth factors such as insulin-like growth factor, Indian hedgehog, PTH-rp, fibroblast growth factor, bone morphogenetic proteins, vascular endothelial growth factor (VEGF) and vitamin D have all been implicated.[2,6]

Glucocorticoids exert their effect via the ubiquitous glucocorticoid receptor or the less widely distributed mineralocorticoid receptor. The glucocorticoid receptor is a cytoplasmic receptor which, upon ligand binding, forms a multi-component complex, translocates to the nucleus and functions as a transcription factor, binding to promoter regions of glucocorticoid responsive genes. This activity may promote or repress transcription depending on the gene involved. As well, the glucocorticoid-bound receptor complex may exert an indirect effect, by interfering with the normal function of other transcription factors (nuclear factor-κB or smad-3 for example). The result is a myriad of effects, both desired and unwanted, across multiple systems.[4]

Glucocorticoids are generally considered inhibitory to endochondral ossification and have been associated with a number of adverse skeletal affects, including delayed or reduced growth and osteopenia. Glucocorticoids exert a direct effect on growth plate chondrocytes, which express the glucocorticoid receptor, by decreasing the rate of chondrocyte proliferation as well as increasing the rate of chondrocyte apoptosis at the zone of hypertrophy.[2] Glucocorticoids also interact with other mediators of bone growth. Insulin-like growth factor-1 (IGF-1) is considered a key mediator of bone growth, and its expression at the growth plate is determined by the relative influence of locally acting glucocorticoids, thyroid and growth hormones. In this regard, glucocorticoids have been shown to modulate both IGF-1 production and growth hormone receptor expression at the growth plate.[2] Other cell populations responsible for growth and remodeling are also impacted by glucorticoid exposure; osteoblast activity is typically inhibited, with decreased matrix/osteoid production whilst osteclastic activity is often increased, resulting in an uncoupling of the tightly controlled interplay between these two populations.[4]

Angiogenesis is an important part of the endochondral ossification process. In piglets treated with short term prednisolone, there was a decrease in VEGF mRNA expression by hypertrophic chondrocytes, with diminished capillary ingrowth and loss of parallel organization in the metaphysis.[5] Interestingly, trabecular bone length in the primary spongiosa was also diminished, in contrast to the case presented here. Elongation of the primary spongiosa, as was seen in our case, appears not to be specifically referenced within the literature; it seems reasonable to hypothesize that the net outcome of glucorticoid exposure seen here results from the balance of relative dose or exposure both systemically and at the growth plate, acting in concert at multiple levels in young, actively growing rats under the conditions of this study.

This case also demonstrates marrow hematopoietic hypocellularity with a corresponding increase in marrow

lipocytes. This is also a recognized effect of glucocorticoid therapy and has been implicated in the pathogenesis of steroid-induced osteonecrosis. Rather than unmasking existent adipocytes due to loss of hematopoietic elements, a shift in differentiation of pluripotential marrow stem cells has been proposed to occur under the influence of glucocorticoids.[1]

AFIP Diagnosis: Bone, proximal tibia: Metaphyseal osteosclerosis, focally extensive, marked, with retention of unmodeled primary trabeculae.

Conference Comment: The slide submitted for this case prompted a brief discussion of the benefits and drawbacks of the sagittal and frontal planes of section. The preferred plane of section depends on which structures are of greatest interest in a given study, and must be carefully considered. Studies in which the cruciate ligaments, articular cartilage, and joint space are of primary interest are generally best supported by frontal sectioning of the stifle, whereas assessment of the growth plate of the distal femur, of particular interest in this case, is best accomplished by sagittal sectioning.

As in the section of proximal humerus discussed in case II of this conference, metaphyseal osteosclerosis in this case is the result of retention of unmodeled primary trabeculae. The contributor's other assessments, including thinning of the physeal cartilage, increased growth plate-to-spongiosa ratio, and bone marrow hypocellularity are substantiated by the microscopic images supplied from unaffected control animals; without the benefit of the control images for reference, conference participants were unable to confidently make the same interpretations (**figs. 4-1 and 4-2**). Regardless, the conference moderator emphasized that the presence of retained unmodeled primary trabeculae is far more reliable evidence of deficient osteoclasis than is the subjective determination that osteoclast numbers are reduced, particularly when a section from an age-matched control is not available for evaluation. As in case II, this finding prompts the consideration of other anti-osteoclast agents, including lead and bisphosphonates. Participants noted the apparent lack of similar lesions in the epiphysis, and speculated that this unexpected finding may have resulted from a different growth rate or plane of section.

The finding of osteosclerosis in this case is counterintuitive; due to their well-known catabolic properties, glucocorticoids would be expected to result in increased osteoclast lifespan and osteopenia. The contributor offers several plausible explanations for this irony. Conference participants discussed the important roles that dosage route and frequency may have on the net effect of a given drug, using as a corollary the paradox of parathyroid hormone. As alluded to in the discussion of fibrous osteodystrophy in case I of this conference, persistent hyperparathyroidism is known to increase bone resorption. Less obviously, parathyroid hormone (PTH) can also stimulate bone formation and increased bone mass, depending on the route and frequency of administration. Specifically, while continuous infusions of PTH cause bone resorption, intermittent injections of the same hormone cause increased bone formation and bone mineral density. This is the therapeutic basis for teriparatide (Forteo™), a recombinant drug composed of the first 34 amino acids of PTH, which exerts its main biologic effects and is clinically shown to decrease the risk of fractures and increase bone mineral density in postmenopausal women with osteoporosis when administered as a daily subcutaneous injection.[2]

Contributor: Schering-Plough Research Institute, 556 Morris Avenue, S12-2, Summit, NJ 07901

References*:*

1. Cui, Q, Wang GJ, Balain G: Steroid-induced adipogenesis in a pluripotential cell line from bone marrow. J Bone Joint Surg Am **79:**1054-1063, 1997
2. Neer RM, Arnaud CD, Zanchetta JR, Prince R, Gaich GA, Reginster JY, Hodsman AB, Eriksen EF, Ish-Shalom S, Genant HK, Wang O, Mitlak BH: Effect of parathyroid hormone (1-34) on fractures and bone mineral density in postmenopausal women with osteoporosis. N Engl J Med **344:**1434-1441, 2001
3. Nilsson O, Marino R, De Luca F, Phillip M, Baron J: Endocrine regulation of the growth plate. Horm Res **64:**157-165, 2005
4. Schäcke H, Döcke WD, Asadullah K: Mechanisms involved in the side effects of glucocorticoids. Pharmacol Ther **96:**23-43, 2002
5. Smink JJ, Bucholz IM, Hamers N, van Tilburg CM, Christis C, Sakkers RJ, de Meer K, van Bull-Offers SC, Koedam JA: Short-term glucocorticoid treatment of piglets causes changes in growth plate morphology and angiogenesis. Osteoarthritis Cartilage **12:**864-871, 2003
6. van der Eerden BC, Karperien M, Wit JM: Systemic and local regulation of the growth plate. Endocr Rev **24:**782-801, 2003

The Armed Forces Institute of Pathology
Department of Veterinary Pathology

Conference Coordinator:
Shannon Lacv. DVM. MPH

WEDNESDAY SLIDE CONFERENCE 2009-2010

Conference 23

5 May 2010

Conference Moderator:

Thomas P. Lipscomb, DVM, Diplomate ACVP

CASE I: 09021035 (AFIP 3136277).

Signalment: 3.5-week-old, female, Angus calf (*Bos taurus*).

History (per referral): This calf was born on 2 February 2009 with no known complications. The patient was lethargic post partum and was administered synthetic colostrum, florfenicol (6 mL), and ceftiofur hydrochloride. The patient never improved and was transported to the referring veterinarian. The referring veterinarian felt there was a liver abnormality based upon severe icterus and treated the calf with antimicrobials and vitamin injections. The patient did not improve and was referred to Oklahoma State University. Physical exam at OSU revealed severe icterus. Ultrasound revealed hepatomegaly and hyperechoic liver parenchyma, and the gallbladder could not be located. A congenital biliary anomaly was suspected.

Gross Pathology: The patient was in good body condition. The mucous membranes and sclerae were dark yellow. Internally, the subcutaneous fat, retroperitoneal and pelvic canal fat, intra-abdominal fat, joint fluid, and cerebrospinal fluid were deep yellow. The liver was enlarged with rounded margins and the capsular surface was mottled red and yellow. The hepatic parenchyma was diffusely and markedly firm. The gallbladder was not present, and while the duodenal papilla was present, a discernible bile duct was not observed to communicate with the papilla. A 2.5 cm diameter focus of gelatinous yellow tissue was present in the region where the gallbladder was expected to be located (**fig. 1-1**).

1-1. Gallbladder, calf. Gallbladder aplasia. Photograph courtesy of Department of Veterinary Pathobiology, Oklahoma State University, Room 250, McElroy Hall, Stillwater, OK, 74078, www.cvm.okstate.edu

*Sponsored by the American Veterinary Medical Association, the American College of Veterinary Pathologists, and the C. L. Davis Foundation.

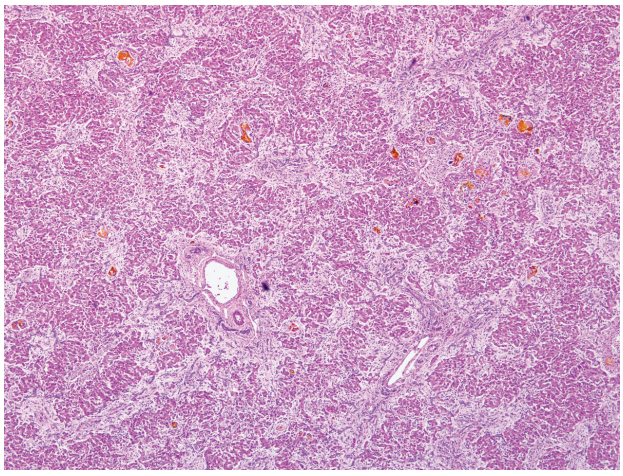

1-2. Liver, calf. Diffusely there is bridging portal fibrosis and the hepatic lobular architecture is disrupted by immature fibrous connective tissue. Multifocally there are small lakes of bright orange bile pigment. (HE 40x)

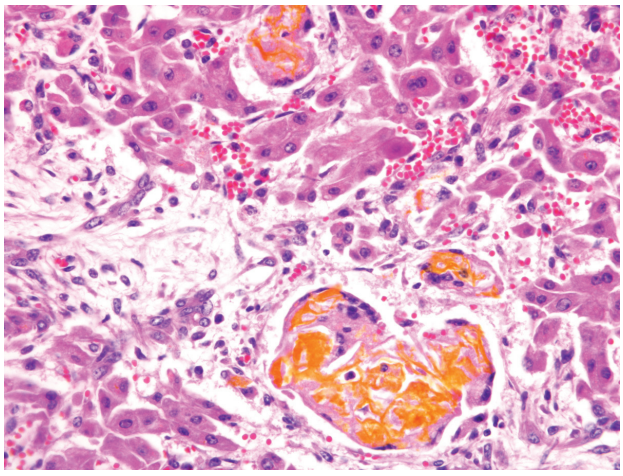

1-3. Liver, calf: Diffusely there marked hepatocellular loss, increase in reactive fibroblasts, and canilicular cholestasis. (HE 400x)

Histopathologic Description: The normal lobular architecture of the liver is disrupted by tracts of proliferative, branching and anastomosing, hyperplastic bile ducts surrounded by moderate to marked amounts of fibrous connective tissue (confirmed with trichrome stain). These tracts extend between adjacent portal triads and often to the central veins. Hepatocellular cords are separated into small islands by the bands of fibrous connective tissue and hyperplastic bile ducts. Golden bile pigment (confirmed with Hall's special stain) forms multiple lakes that often replace hepatocytes and are scattered throughout the hepatic parenchyma. Bile pigment is also often present within multinucleated giant cells (**figs. 1-2 and 1-3**).

The small tissue specimen from the region of the gallbladder is composed largely of fibrous connective tissue that contains few bile duct profiles nested together peripheral to a larger, central, epithelial-lined ductal or aplastic bladder-like structure. Scattered at the borders of the tissue are small amounts of smooth muscle.

Contributor's Morphologic Diagnosis:
1. Liver: Severe intrahepatic bile duct hyperplasia and periportal fibrosis with marked hepatocellular loss and severe, multifocal cholestasis with bile lake formation.
2. Gallbladder and duct: Gallbladder aplasia with extrahepatic biliary atresia.

Contributor's Comment: Congenital biliary atresia is discontinuity or obstruction of the biliary tree (extrahepatic or intrahepatic) that results in severe icterus and liver damage in young patients. The disease is rare, though well-described in people, and the defect occurs alone or in combination with other congenital defects. The condition has been reported in several veterinary species including foals, lambs, calves, cats and dogs.[1,4-6] Whether or not gallbladder agenesis/aplasia is included or encompassed within the diagnosis of biliary atresia is variable between reports. Since it is well documented that biliary atresia can be intrahepatic or extrahepatic (or both) and occurs with or without gallbladder lesions, it is probably best that the two conditions remain separate morphological diagnoses.

In reports from people and animals, livers have been described as macroscopically large or shrunken. The histological lesion in the liver is more similar across species and characterized predominantly by portal and bridging fibrosis with either an absence of bile ducts (intrahepatic atresia) or marked proliferation of bile ducts (in extrahepatic atresia). There is marked cholestasis. The hepatic histological lesion is similar to that of calves with congenital hepatic fibrosis syndrome; therefore, evaluation/verification of the gallbladder and bile duct is important in the delineation of these syndromes.

The etiology of biliary atresia in man and animals is debatable. Most follow two pathways of either congenital defects in morphogenesis or post-formation destruction (whether prenatal or postnatal), usually blamed on infection/inflammation.[1,2] Defects in morphogenesis are suspected to be either inherited or secondary to gestational toxin exposure.[2,5] Post-formation inflammatory destruction of the biliary tree has been blamed on viral infections and immune-mediated destruction in people and severe biliary ascarid invasion with subsequent inflammation and

blockage in the dog.[2,6]

AFIP Diagnosis: Liver: Bridging fibrosis, diffuse, marked, with biliary hyperplasia, hepatocellular loss, canalicular cholestasis and bile granulomas.

Conference Comment: We are grateful to the contributor for furnishing this very instructive case. As is customary at the AFIP, conference participants were denied prior access to the submitted history, necropsy findings, and gross image; while creating a rather artificial handicap, the method provides for a rich educational opportunity, primarily by reducing bias and thus stimulating discussion. Uniformly, conference participants strongly suspected a toxic etiology in this case based upon the diffuse distribution of the lesions. More specifically, participants interpreted the prominent bridging fibrosis and loss of hepatocytes as consistent with chronic hepatointoxication. The striking lesions attributable to cholestasis (i.e. bile lakes and granulomas; ectatic, albeit usually empty, bile canaliculi; and biliary hyperplasia) led many participants to precisely implicate toxins that target the biliary epithelium, such as the mycotoxin sporidesmin and the plant *Tribulus terrestris*, which causes a toxicosis known as "geeldikkop" in sheep. Careful examination of the specimen, however, reveals compelling evidence against both of these toxins, such as the paucity of inflammation, besides that which is associated with bile lakes (bile granulomas). Sporidesmin, produced by the fungus *Pithomyces chartarum*, concentrates in the bile, directly irritating the connective tissues of the portal tracts and bile ducts, and at high concentrations, causes biliary epithelial necrosis; the result is acute cholangitis or cholangiohepatitis. Although generally mild, the inflammation in sporidesmin toxicosis is typically more severe than that present in this case. Moreover, sporidesmin causes extensive necrosis of bile duct epithelium with sloughing of necrotic debris into the lumen, features lacking in this case. Saponins of the plant *Tribulus terrestris* are likely responsible for geeldikkop ("yellow bighead") in sheep, which is distinguished grossly by the presence of white, semifluid, crystalline material in the cystic and larger intrahepatic bile ducts. Histologically, hepatocyte vacuolation and Kupffer cell hyperplasia are characteristic of the acute toxicosis, whereas crystalline material within the bile ducts and hepatocytes is more obvious in chronic intoxication; none of these is a feature of the present case.[7]

This exercise underscores the value of resisting the temptation to commit to just one category of etiology (e.g., toxic, infectious, congenital, degenerative, neoplastic, etc.) without first giving due deliberation to the other potential categories that may produce a similar constellation of microscopic lesions. The clinical history and gross findings substantially amplify the index of suspicion for a congenital abnormality in this case. That said, the cause of biliary atresia remains enigmatic, and indeed the condition may represent a common phenotypic result of a number of different causes, including inherited defects and/or in utero intoxication targeting the biliary epithelium. In support of the latter, the pyrrolizidine alkaloid-containing plant, *Senecio* sp., has been implicated as the cause of *in utero* liver damage in calves whose dams ingested the plant during pregnancy.[3] Intriguingly, a 1988 outbreak of congenital biliary atresia in lambs and calves in New South Wales, Australia, occurred at the same site as a similar outbreak in lambs in 1964. Epidemiologic evidence, including the simultaneous occurrence in both calves and lambs in the second outbreak, argued against an inherited defect, and signified that the lesion may have stemmed from a toxic or infectious insult to the developing fetuses that produced choledysgenesis and biliary atresia *in utero*; although several suspect weeds were investigated, a specific etiology was not confirmed.[5]

This case was reviewed in consultation with the AFIP Department of Hepatic Pathology, which noted remarkable histomorphological similarities with cases of biliary atresia in human neonates. Although only rarely reported in other species, biliary atresia in humans is the most common cause of neonatal cholestasis and the most common indication for pediatric liver transplantation; yet, its cause remains obscure, with evidence put forth in support of five possible mechanisms: 1) viral infection, 2) environmental toxin exposure, 3) immunologic/inflammatory dysregulation, 4) defective biliary tract morphogenesis, and 5) defective fetal/prenatal circulation.[2]

Contributor: Department of Veterinary Pathobiology, College of Veterinary Medicine, Oklahoma State University, Stillwater, OK 74074
http://www.cvm.okstate.edu

References:

1. Bastianello SS, Nesbit JW: The pathology of a case of biliary atresia in a foal. J S Afr Vet Assoc **58:**89-92, 1987
2. Bezerra JA: Potential etiologies of biliary atresia. Pediatr Transplantation **9:**646-651, 2005
3. Fowler ME: Pyrrolizidine alkaloid poisoning in calves. J Am Vet Med Assoc **152:**1131-1137, 1968
4. Hampson ECGM, Filippich LJ, Kelly WR, Evans K: Congenital biliary atresia in a cat: a case report. J Small Anim Pract **28:**39-48, 1987
5. Harper P, Plant JW, Unger DB: Congential biliary atresia and jaundice in lambs and calves. Aust Vet J **67:**18-22, 1990
6. Schulze C, Rothuizen J, van Sluijs FJ, Hazewinkel HA, van den Ingh TSGAM: Extrahepatic biliary atresia in

a border collie. J Small Anim Pract **41:**27-30, 2000
7. Stalker MJ, Hayes MA: Liver and biliary system: toxic hepatic disease. *In:* Jubb, Kennedy, and Palmer's Pathology of Domestic Animals, ed. Maxie MG, 5th ed., vol. 2, pp. 372-378. Saunders Elsevier, Philadelphia, PA, 2007

CASE II: 6860-09; 8358-08 (AFIP 3149858).

Signalment: Juvenile, female herring gull (*Larus argentatus*).

History: Several juvenile herring gulls were found dead.

Gross Pathology: All examined gulls were in very poor nutritional condition. The air sacs contained numerous greenish plaques and the lungs were full of disseminated yellow nodules typical of aspergillosis. The spleen was enlarged. The bursa of Fabricius contained few *Ichthyocotylurus platycephalus* trematodes.

Laboratory Results: *Aspergillus fumigatus* was isolated from the lungs and air sacs, and *Salmonella* Typhimurium phage type 41 from the intestines and liver. Avian influenza virus (not H5 or H7) was shown with RT-PCR from tissue samples.

Histopathologic Description: Bursa of Fabricius: There is diffuse severe lymphoid depletion in the cortex and medulla of bursal follicles (**figs. 2-1 and 2-2**). Numerous large basophilic intracytoplasmic inclusion bodies, often in clusters (botryoid), are seen both in the cortex and medulla, in the cytoplasm of macrophages or vacuolated reticular cells (**fig. 2-3**). Some follicles have cystic lumina with pseudostratified epithelium. Trematode eggs can be seen in some sections in the bursal lumen.

Contributor's Morphologic Diagnosis: Bursa of Fabricius: Lymphoid depletion, subacute, severe, with numerous intrahistiocytic intracytoplasmic inclusions, consistent with avian circovirus infection.

Contributor's Comment: Botryoid bursal inclusion bodies are considered pathognomonic for avian circovirus infection.[1] Circovirus-like disease has been reported in several countries in die-offs of young gulls since 1999.[1] Birds have typically been severely emaciated, and often affected with secondary aspergillosis and/or salmonellosis, as in this case.[1,2] Large intracytoplasmic basophilic/amphophilic inclusion bodies have been detected in macrophages and in lymphocytes in atrophic bursal follicles and in the spleens of these birds.[1] Circovirus-like virions have been demonstrated in these lesions with electron microscopy.[1] Recently, *in situ* hybridization with a pigeon circovirus probe was used to demonstrate circovirus in gulls from Sweden and New Zealand.[2] Avian circovirus has not been isolated in cell cultures thus far. The epidemiology of this disease in wild birds is largely unknown.

Circoviridae are small, nonenveloped viruses with a circular, single-stranded DNA genome. Infections caused by circoviruses are often subclinical or cause immunosuppression. Virions are highly stable in the environment. The family Circoviridae consists of two

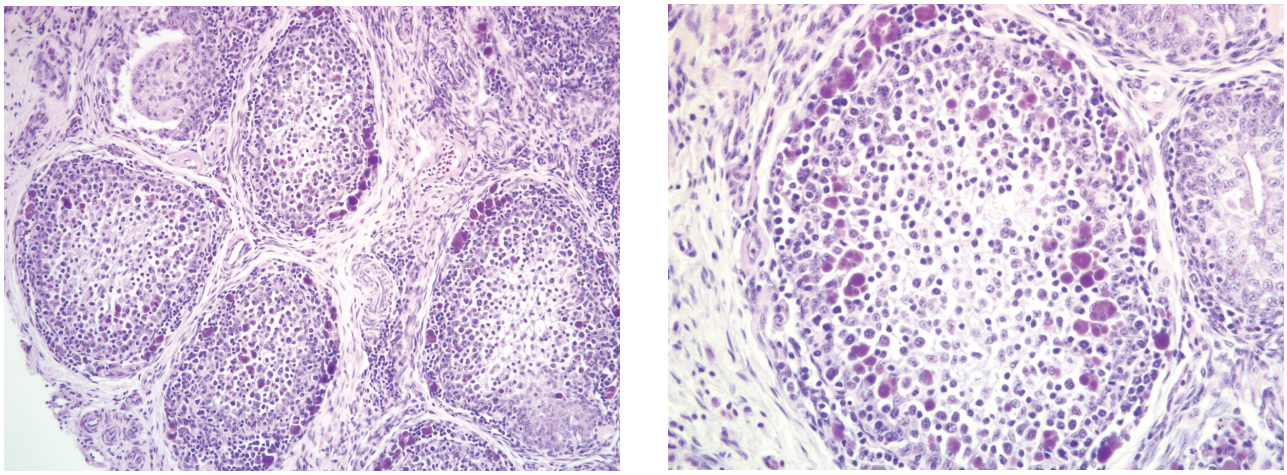

2-1, 2-2. Bursa of fabricius, herring gull. Lymphoid follicles are atrophied, and there is diffuse lymphoid depletion. (HE 40x and 100x)

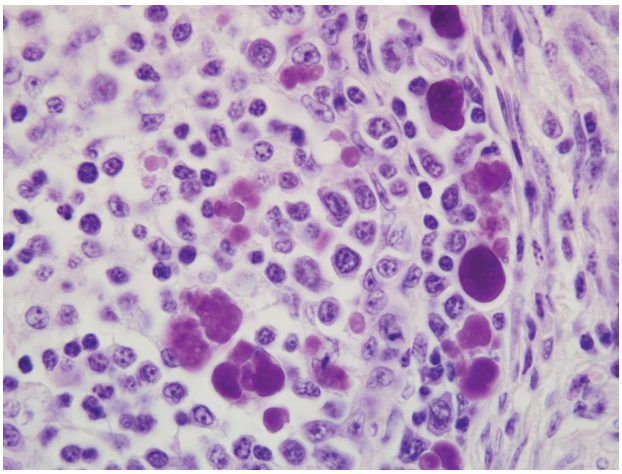

2-3. Bursa of fabricius, herring gull. Within macrophages in lymphoid follicles, there are numerous large, basophilic, botryoid, intracytoplasmic inclusion bodies. (HE 200x, HE 400x)

genera: Circovirus and Gyrovirus.[3] Chicken anemia virus, which is the best known of the circoviruses, belongs to Gyrovirus. It causes chicken infectious anemia (CIA), and has not been detected in species other than the chicken.[3] It causes atrophy of bone marrow hemocytoblasts and T-cells in lymphoid tissue with consequent aplastic anemia and immunosuppression in 1-3 week old chicks.[3] Histologically, lymphoid and bone marrow atrophy is detected.

Porcine circovirus (PCV) 1 and 2, psittacine beak and feather disease (PBFD) virus, and avian circoviruses are members of the genus Circovirus.[3] These viruses cause a rather similar disease in different species.[3] PCV2 is the cause of post-weaning wasting syndrome in pigs. Weight loss, secondary infections and lymphadenopathy are seen mainly in approximately 6-week-old pigs. Granulomatous inflammation with severe lymphoid depletion, histiocytosis, giant cells and large basophilic botryoid intracytoplasmic inclusion bodies are seen in macrophages in several tissues.

Psittacine beak and feather disease virus infects the basal layer of the epidermis and the monocyte-macrophage system of young (under 3 years old) psittacines and causes immune suppression, beak and feather deformities and baldness.[1] The disease can be also acute or peracute in neonates or very young birds. Basophilic intracytoplasmic or intranuclear, often large, botryoid inclusion bodies are seen in feather follicle epidermis or in macrophages in the bursa of Fabricius or thymus.

Other avian circoviruses have been discovered from several species (e.g. gulls, pigeons, goose, ducks, canaries, finches, ostriches).[1,2] It seems likely that the infection is much more prevalent than the disease; virus can be found in clinically normal birds.[3] The disease seen in pigeons and geese resembles that detected in gulls, with immunosuppression, lymphoid depletion and secondary infections.

Virus replication takes place in actively dividing cells, like the basal epithelial cells in PBFD. Inclusions in macrophages are likely to be phagocytosed material.[3] Lymphoid depletion has been speculated to be induced by cytokines, not due to direct viral infection of the lymphocytes.[3]

AFIP Diagnosis: 1. Bursa of Fabricius (cloacal bursa): Lymphoid depletion, diffuse, marked, with numerous intrahistiocytic intracytoplasmic botryoid inclusion bodies, etiology consistent with circovirus.
2. Bursa of Fabricius (cloacal bursa): Intraluminal trematode eggs.

Conference Comment: The contributor provides a succinct discussion of this interesting entity, and the notes on salient comparative pathology findings are especially relevant. Accordingly, conference participants readily attributed the distinctive intrahistiocytic intracytoplasmic botryoid inclusion bodies in the submitted sections of cloacal bursa to circoviral infection, noting their conspicuous resemblance to those characteristically encountered in the lymph nodes of pigs with post-weaning multisystemic wasting syndrome (PMWS). Readers are urged to review WSC 2009-2010, Conference 3, case IV for additional details regarding circoviruses in general, and in particular, the contentious role of PCV2 in porcine dermatitis and nephropathy syndrome (PDNS). Attendees briefly reviewed the histology and function of the cloacal bursa by examining the section from a normal chicken submitted with WSC 2009-2010, Conference 15, case III. In addition to the microscopic lesions described by the contributor, some participants' slides featured small foci of fat atrophy at the periphery of the section, a finding consistent with the reported gross lesions.

Contributor: Finnish Food Safety Authority Evira, Fish and Wildlife Health Research Department, P.O. Box 517, FI-90101 Oulu, Finland
http://www.evira.fi

References:
1. Pare JA, Robert N: Circovirus. *In:* Infectious Diseases of Wild Birds, eds. Thomas NJ, Hunter DB, Atkinson CT, pp.195-205. Blackwell Publishing, Ames, IA, 2007
2. Smyth JA, Todd D, Scott A, Beckett A, Twentyman

CM, Bröjer C, Uhlhorn H, Gavier-Widen D: Identification of circovirus infection in three species of gull. Vet Rec **159:**212-214, 2006
3. Todd D: Avian circovirus diseases: lessons for the study of PMWS. Vet Microbiol **98:**169-174, 2004

CASE III: N06-358-9 (AFIP 3036133).

Signalment: 29-year-old, 16.27 kg, female Baboon (*Papio* sp.).

History: This baboon was selected for euthanasia due to dark loose stools and senescence.

Gross Pathology: On external examination the animal was found in good body condition and adequately hydrated. Gross findings included multiple, pale tan to white, irregularly shaped, firm nodules, up to 5 cm in diameter, multifocally distributed in the hepatic parenchyma (**figs. 3-1 and 3-2**).

Histopathologic Description: On light microscopy the liver architecture was multifocally effaced and replaced by a well demarcated, unencapsulated, infiltrative, highly cellular neoplasm composed of nests, packets, and cords of epithelial cells often forming glandular structures (rosettes and pseudorosettes), supported by a fine to moderate fibrovascular stroma. The neoplastic cells were cuboidal to columnar with variably distinct cell borders and a moderate amount of eosinophilic, finely granular cytoplasm. The nuclei were central to basilar, round to oval, with coarsely stippled chromatin. Mitoses were rare (less than 1 per 10 HPF, 400X magnification) (**figs. 3-3 and 3-4**). Additional features included scattered central areas of necrosis and hemorrhage, and variable amounts of homogeneous, eosinophilic material filling the central lacunae of the rosette formations. The adjacent portions of the non-affected liver parenchyma showed mild to moderate atrophy from neoplastic compression.

By immunohistochemistry the neoplastic cells were positive for pancytokeratin, chromogranin A, NSE and synaptophysin and were negative for vimentin, S100 protein, glucagon and insulin (**fig. 3-5**).

Contributor's Morphologic Diagnosis: Liver: Carcinoma, neuroendocrine, Baboon, *Papio* sp.

Contributor's Comment: The morphologic features, along with the positive staining for the neuroendocrine markers described above, led to the classification of this neoplasm as a neuroendocrine carcinoma.[1] No similar neoplastic changes were observed in all the other tissues examined; therefore the liver was considered as the primary site of origin of the tumor.[1] This case represents the first known primary neuroendocrine carcinoma of the liver to be reported in a non-human primate.[1-3] There are rare reports of primary hepatic neuroendocrine carcinomas in humans and domestic animals in the literature. As in this case, neuroendocrine carcinomas in humans are consistently immunopositive for chromogranin A, NSE, and synaptophysin.[6] This is contrary to what has been observed in dogs and cats, where the expression of chromogranin A is inconsistent, and NSE and synaptophysin are considered better indicators.[6] The oval cell is considered to be the progeny of the hepatic stem cells and is bipotential in nature, giving rise to both

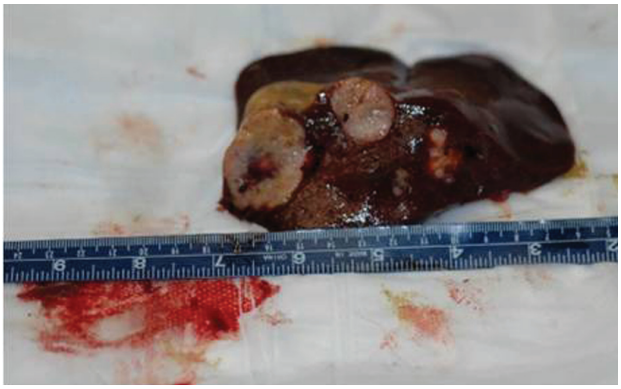

3-1, 3-2. Neuroendocrine carcinoma, low grade (carcinoid), liver, baboon. There is a multifocal tan-white nodule that measures up to 5 cm in diameter. Photograph courtesy of Veterinary Science Branch, 2509 Kennedy Circle, Bldg 125, Brooks City- Base, Texas 78235

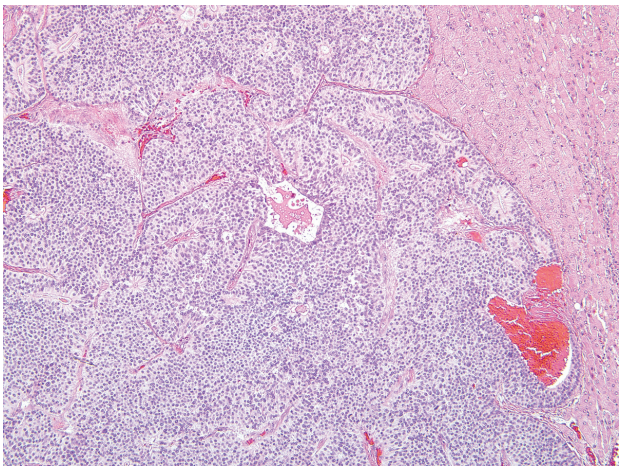

3-3. Neuroendocrine carcinoma, low grade (carcinoid), liver, baboon. Multifocally effacing and compressing the hepatic parenchyma is an unencapsulated, infiltrative, lobulated neoplasm composed of polygonal cells arranged in nests, packets, and rosettes and pseudorosettes. (HE 40x)

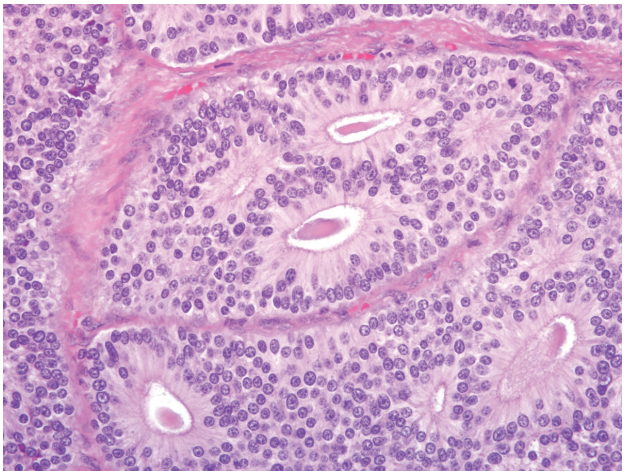

3-4. Neuroendocrine carcinoma, low grade (carcinoid), liver, baboon. Neoplastic cells palisade along a fine to moderate fibrovascular stroma, contain a moderate amount of eosinophilic granular cytoplasm, and round to oval nuclei. (HE 200x)

hepatocytes and bile duct cells.[4] These cells are located in the terminal biliary ductules and canal of Hering, which represent the terminal branches of the biliary tree that connects the interhepatocytic bile canaliculi with the biliary ducts in the portal tracts. They express markers of both immature hepatocytes (e.g. α-fetoprotein) and bile ducts cells (e.g. bile duct type cytokeratin).[7] In addition, the hepatic progenitor cell (HPC) compartment has neuro/neuroendocrine features such as the expression of chromogranin A, neural cell adhesion molecule (NCAM), neurotrophin 4/5, neurotrophin receptor tyrosine kinase B and parathyroid hormone related peptide.[4] Roskams *et al.* showed that during the early stages of regeneration, bile duct epithelium displays neuroendocrine features including cytoplasmic, dense core neurosecretory granules and chromogranin-A expression while reactive bile ductules have been shown to express NSE.[7]

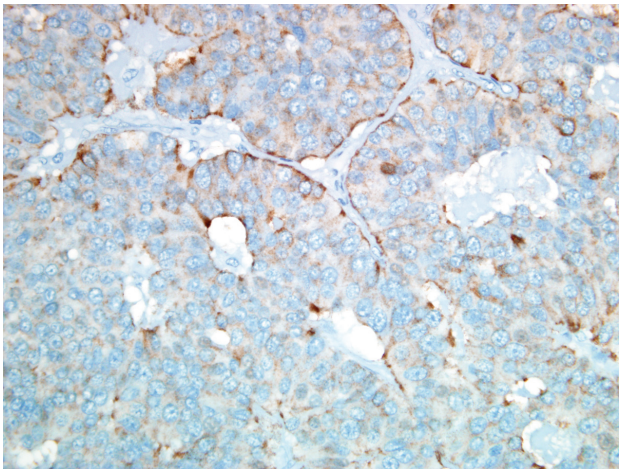

3-5. Neuroendocrine carcinoma, low grade (carcinoid), liver, baboon. Diffusely, the cytoplasm of neoplastic neuroendocrine cells is immunopositive for chromogranin. (Chromogranin A 200x)

AFIP Diagnosis: Liver: Neuroendocrine carcinoma, low grade (carcinoid).

Conference Comment: The contributor has provided an excellent example, accompanied by an informative overview, of a rare entity. Conference participants contemplated a diagnosis of adenocarcinoma based on the formation of cystic and tubular structures by neoplastic cells, but uniformly favored the contributor's diagnosis because of the prominent rosette-like glandular structures that have basally-situated nuclei and finely granular cytoplasm, characteristic of neuroendocrine carcinoma. Because of potential prognostic implications, correctly distinguishing hepatic neuroendocrine carcinoma from biliary adenocarcinoma or hepatocellular carcinoma is of paramount importance. For instance, in one study, dogs with hepatic neuroendocrine carcinoma experienced a significantly shorter survival/euthanasia interval than did those with biliary adenocarcinoma or hepatocellular carcinoma. In dogs and cats, cytokeratin AE1/AE3 immunostaining is reportedly positive in adenocarcinoma and negative in hepatic neuroendocrine carcinoma, testifying to the utility of immunohistochemistry in making the distinction.[6] In the present case, results of the immunohistochemical stains listed by the contributor

and repeated at the AFIP confirmed the diagnosis of neuroendocrine carcinoma.

Conference attendees briefly reviewed the term "carcinoid," which is well-ensconced in the texts, where it is sometimes used interchangeably with neuroendocrine carcinoma. Although the term is used less frequently in the recent literature, it facilitates professional communication, because unlike "neuroendocrine carcinoma," it requires no further modification to connote low-grade malignancy. In humans, carcinoids are most frequently identified in the gastrointestinal tract, followed by the tracheobronchial tree and lungs. Among gastrointestinal carcinoids, those of the jejunum and ileum are most common, followed by those of the colorectum and appendix; those of the stomach, proximal duodenum, and esophagus are least common. Gastrointestinal carcinoids arise from cells that release peptide and nonpeptide hormones to coordinate gastrointestinal function; these cells, formerly referred to as amine precursor uptake and decarboxylation (APUD) cells, comprise the diffuse endocrine system of the gastrointestinal tract. In humans, carcinoid syndrome is a rare clinical manifestation of the neoplasm characterized by cutaneous flushing, sweating, bronchospasm, abdominal pain, diarrhea, and fibrosis of right-sided heart valves. The syndrome results from the secretion and systemic release of vasoactive substances by the tumor, and is strongly associated with metastatic disease.[8] While carcinoid syndrome has not been reported in animals, conference attendees discussed neuroendocrine tumor-related paraneoplastic syndromes documented in veterinary medicine, such as Zollinger-Ellison syndrome due to functional gastrin-secreting tumors, and superficial necrolytic dermatitis, which is sometimes associated with glucagonomas.

This case was reviewed in consultation with the Departments of Hepatic and Soft Tissue Pathology at the AFIP, both of which concurred with the above diagnosis, while emphasizing the importance of excluding the possibility of hepatic metastasis from a primary gastrointestinal carcinoid because of the extreme rarity of primary hepatic neuroendocrine carcinoma.

Contributor: Air Force Research Laboratory, Veterinary Sciences Branch, 711th Human Performance Wing/RHDV, 2509 Kennedy Circle, Brooks City-Base, TX 78235

References*:*

1. Aloisio F, Dick EJ Jr, Hubbard GB: Primary hepatic neuroendocrine carcinoma in a baboon (*Papio* sp.). J Med Primatol **38:**23-26, 2009
2. Cianciolo RE, Butler SD, Eggers JS, Dick EJ, Leland M, de la Garza M, Brasky KM, Cummins LB, Hubbard GB: Spontaneous neoplasia in the baboon (*Papio* spp.). J Med Primatol **36:**61-79, 2007
3. Cianciolo RE, Hubbard GB: A review of spontaneous neoplasia in baboons (*Papio* spp.). J Med Primatol **34:**51-66, 2005
4. Libbrecht L, Roskams T: Hepatic progenitor cells in human liver diseases. Semin Cell Dev Biol **13:**389-396, 2002
5. Patnaik AK, Lieberman PH, Erlandson RA, Antonescu C: Hepatobiliary neuroendocrine carcinoma in cats: a clinicopathologic, immunohistochemical, and ultrastructural study of 17 cases. Vet Pathol **42:**331-337, 2005
6. Patnaik AK, Newman SJ, Scase T, Erlandson RA, Antonescu C, Craft D, Bergman PJ: Canine hepatic neuroendocrine carcinoma: an immunohistochemical and electron microscopic study. Vet Pathol **42:**140-146, 2005
7. Roskams T, Cassiman D, De Vos R, Libbrecht L: Neuroregulation of the neuroendocrine compartment of the liver. Anat Rec A Discov Mol Cell Evol Biol **280:**910-23, 2004
8. Turner JR: The gastrointestinal tract. *In:* Robbins and Cotran Pathologic Basis of Disease, eds. Kumar V, Abbas AK, Fausto N, Aster JC, 8th ed., pp. 787-789. Saunders Elsevier, Philadelphia, PA, 2010

CASE IV: D0810008 (AFIP 3149417).

Signalment: 1.5 year-old, female, Angus cow (*Bos taurus*).

History: This heifer was one of 200 head of Angus beef cattle that were rotated through a new pasture for 2 days then moved back to previous pasture. Initially, 3 were found dead, and 3 sick cows, presenting weak and anorexic, were hospitalized. The number of sick cows increased to 30, and 15 of these were reported dead within 3 days. Two cows survived at the hospital and became icteric, with elevated liver enzymes.

Gross Pathology: At necropsy, the heifer was in good muscular condition. The liver was uniformly swollen and pale, and on cut sections an enhanced reticular pattern was evident, somewhat resembling a nutmeg liver. Numerous petechiae were noted within the epicardium and endocardium, but the hemorrhages did not extend into

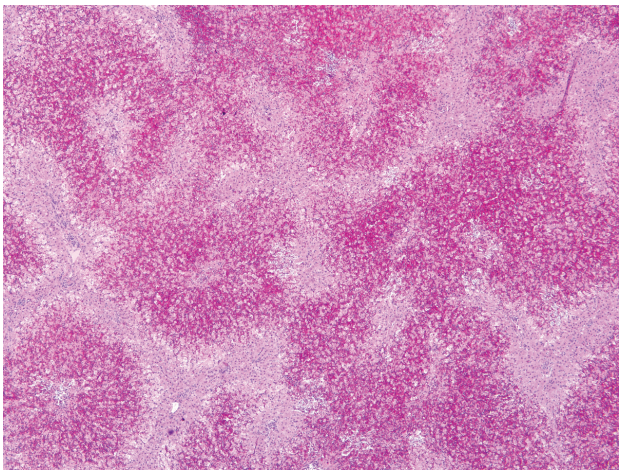

4-1. Liver, cow. Diffusely within hepatic parenchyma, there is an accentuated zonal pattern characterized by centrilobular to midzonal hemorrhage. (HE 40x)

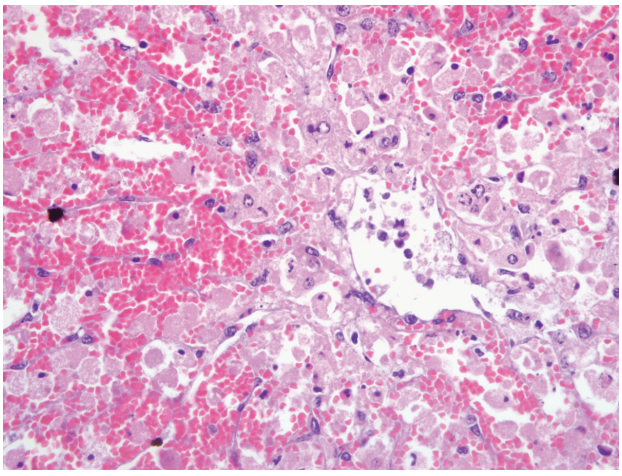

4-2. Liver, cow. Centriloular to midzonal hemorrhage and lytic necrosis characterized by disassociated hepatocytes admixed with eosinophilic cellular and karryorrhectic debris. (HE 400x)

the subjacent myocardium.

Laboratory Results: Microcystin LR was detected in the rumen and cecal contents by liquid chromatography-mass spectrometry.

Histopathologic Description: Liver: There is severe periacinar to massive hepatic necrosis. Periportal hepatocytes are often spared, and form a bridging border around the necrotic foci. The hepatocytes are disassociated from their neighboring hepatocytes, and have rounded up. There is moderate sinusoidal hemorrhage within the fields of the disassociated hepatocytes. Sloughed cells admixed with necrotic debris and inflammatory cells accumulate within the central vein lumens (**figs. 4-1 and 4-2**).

Contributor's Morphologic Diagnosis: Liver: Hepatitis, periacinar to massive, acute, necrotizing, with hepatocytic dissociation and sinusoidal hemorrhage.

Contributor's Comment: Microcystin LR (MCLR) is a microcyclic heptapeptide hepatotoxin, a secondary metabolite that is produced during excessive growth and bloom of cyanobacterium (blue-green algae) in water sources. Cyanobacterial bloom occurs most often in water that contains high concentrations of mineral nutrients, especially phosphorus, and during times of sustained sun exposure with calm wind conditions.[3] After production, cyanotoxins are often blown to the shallow regions and margins of the water source, effectively concentrating their levels.

After ingestion of water contaminated with MCLR, the toxin is rapidly taken up in hepatocytes by carrier-mediated transport. Within the hepatocytes, MCLR inhibits protein phosphorylases 1 and 2A, which regulate cellular structural proteins. Inhibition of phosphorylases 1 and 2A promotes hyperphosphorylation of cytoskeletal proteins. Hepatocyte and endothelial cytoskeletal actin filaments distort and collapse, causing cellular structure alteration, detachment from adjoining hepatocytes and membrane instability.[1,2]

In early stages, periacinar to massive hepatic necrosis is represented by the detachment and rounding up of the altered hepatocytes and endothelial cells, extrusion of blood into the disrupted sinuses, with blood and necrotic, fully detached hepatocytes flowing into the central venous network. Hypovolemic shock due to hepatic hemorrhage usually causes death, although hypoglycemia and hyperkalemia from fulminant cessation of hepatic function can also be terminal events.[3] In cumulative low doses, liver failure, chronic inflammation and bilirubinemia can result in mortality.[3] If the animal survives the initial episode of hepatic damage, leukocytic inflammation within the periacinar necrosis proceeds to postnecrotic scarring, periacinar fibrosis, and irregular areas of parenchymal regeneration.[4]

Microcystin LR was detected in the rumen contents from this heifer, and additional heifers that died following exposure. Acute hepatic necrosis with hemorrhage was featured in the early cases that were submitted, and heifers that survived and later died exhibited subacute microscopic lesions. This incident occurred during late summer in Northern California, and site visits to the pasture where the affected heifers were housed found one water source that was a shallow, warm pond with brackish water and

blue-green algae growth.

AFIP Diagnosis: Liver: Necrosis, centrilobular to midzonal, diffuse, with hepatocellular dissociation, hemorrhage and biliary hyperplasia.

Conference Comment: Participants were approximately evenly divided between morphologic diagnoses of necrotizing hepatitis and hepatocellular necrosis, and debated the merits of each during the conference session, ultimately favoring the latter because of the absence of inflammation in the sections available for examination. Massive hepatic necrosis indicates necrosis of entire acini and is present in some areas of the examined sections. Submassive necrosis, with sparing of periportal hepatocytes, is prevalent. Using the acinar approach to hepatic histology, the findings could be summarized as submassive necrosis involving acinar zones 2 and 3.

This case was also studied in consultation with the AFIP Department of Hepatic Pathology; their differential diagnosis for the histologic lesions was broad, and included viral infection, severe ischemia, metabolic disease, and acute autoimmune hepatitis, but a toxic etiology was favored. As detailed in the conference proceedings for WSC 2009-2010, Conference 16, case III, numerous plant toxins – some of which are summarized in a table therein – preferentially target centrilobular hepatocytes because of the extraordinary vulnerability of this cell population to hypoxia and their relatively high concentration of cytochromes P450. Therefore, the recognition of a centrilobular to midzonal distribution of hepatocellular necrosis, while essential to the development of an inclusive differential diagnosis, is not sufficient to definitively implicate a particular plant toxin. Additional evidence is required, and in this case, prominent hepatocellular dissociation is a key clue to prompt further investigation of MCLR as a possible etiology. Reiterating the importance of ancillary diagnostic tests, particularly in cases of suspected toxicosis, the detection of MCLR in ruminal and cecal contents by liquid chromatography-mass spectrometry solidifies the diagnosis in this case. The contributor provides an edifying review of the entity.

Contributor: California Animal Health and Food Safety Laboratory, University of California, Davis, San Bernardino Branch, 105 West Central Avenue, San Bernardino, CA 92408
http://www.cahfs.ucdavis.edu/

References:
1. Batista T, deSousa G, Suput JS, Rahmani R, Suput D: Microcystin-LR causes the collapse of actin filaments in primary human hepatocytes. Aquat Toxicol **65:**85-91, 2003
2. Billiam M, Mukhi S, Tang L, Gao W, Wang JS: Toxic response indicators of microcystin-LR in F344 rats following a single-dose treatment. Toxicon **51:**1068-1080, 2008
3. Briand JF, Jacquet S, Bernard C, Humbert JF: Health hazards for terrestrial vertebrates from toxic cyanobacteria in surface water ecosystems. Vet Res **34:**361-377, 2003
4. Stalker MJ, Hayes MA: Liver and biliary system. *In:* Jubb, Kennedy, and Palmer's Pathology of Domestic Animals, ed. Maxie MG, 5th ed., vol. 2, p. 327. Saunders Elsevier, Philadelphia, PA, 2007

The Armed Forces Institute of Pathology
Department of Veterinary Pathology

Conference Coordinator:
Shannon Lacv. DVM. MPH

WEDNESDAY SLIDE CONFERENCE 2009-2010

Conference 24

12 May 2010

Conference Moderator:

Donald Nichols, DVM, Diplomate ACVP

CASE I: 072188-03 (AFIP 3153650).

Signalment: Adult, male cynomolgus macaque (*Macaca fascicularis*).

History: This animal was part of a research colony of macaques at the U.S. Army Research Institute of Infectious Diseases (USAMRIID). This macaque was administered an experimental vaccine against ebolavirus. Twenty-eight days after vaccination, it was challenged with ebolavirus and it survived the viral challenge. This monkey was euthanized at the end of the study and then it was submitted for a complete necropsy.

Note: The viral challenge study and necropsy were performed under biosafety level 4 (BSL-4) conditions. The research was conducted under an Institutional Animal Care and Use Committee approved protocol in compliance with the Animal Welfare Act and other federal statutes and regulations relating to animals and experiments involving animals and adheres to principles stated in the *Guide for the Care and Use of Laboratory Animals*, National Research Council, 1996. The facility where this research was conducted is fully accredited by the Association for Assessment and Accreditation of Laboratory Animal Care International.

Gross Pathology: No lesions were noted grossly.

Histopathologic Description: There are two sections of tissue on the slide: 1) nasal vestibule (including haired skin and nasal mucosa) and 2) lip (including haired skin, oral mucosa, and mucocutaneous junction). Each of these tissues is described separately below.

Nasal vestibule: There are multifocal and coalescing infiltrates of moderate numbers of lymphocytes, plasma cells, and fewer eosinophils and macrophages within the lamina propria and the submucosa. These inflammatory cell infiltrates usually have a perivascular orientation and often extend into and disrupt the vessel walls. The deep dermis adjacent to the submucosa also has multifocal perivascular infiltrates of similar, but fewer, inflammatory cells. There is multifocal moderate orthokeratotic hyperkeratosis of the mucosal epithelium accompanied by aggregates of keratinized debris and numerous coccoid and bacillary bacteria along the luminal surface of the epithelium. Multifocally, infiltration of the epithelium by low numbers of neutrophils is also present.

Lip: There are multifocal infiltrates of low to moderate numbers of lymphocytes and fewer plasma cells within the submucosal labial glands, often accompanied by atrophy and loss of glandular cells.

*Sponsored by the American Veterinary Medical Association, the American College of Veterinary Pathologists, and the C. L. Davis Foundation.

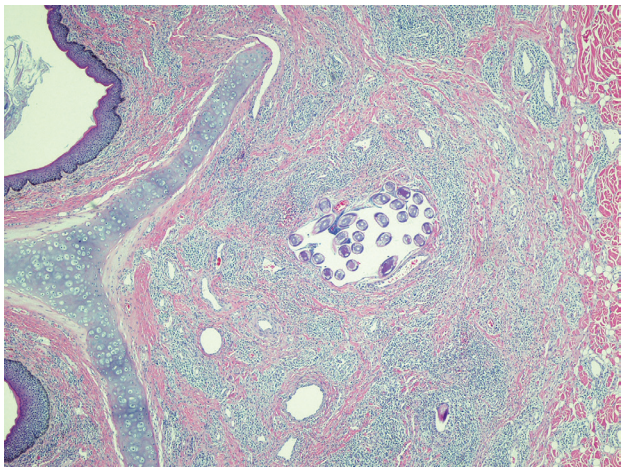

1- 1. Haired skin and subcutis, nasal vestibule, cynomolgus macaque: Within a submucosal vessel there are sections of nematodes. Photographs courtesy of US Army Research Institute of Infectious Diseases, Fort Detrick, Maryland 21702-5011 (HE 4x)

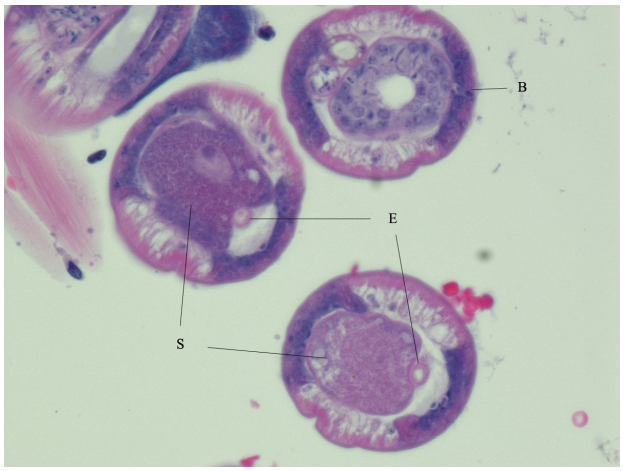

1-2. Haired skin and subcutis, nasal vestibule, cynomolgus macaque. Nematodes have a small esophagus (E) partially surrounded by a stichocyte (S). Each section has two bacillary bands (B). Photographs courtesy of US Army Research Institute of Infectious Diseases, Fort Detrick, Maryland 21702-5011 (HE 20x)

Contributor's Morphologic Diagnosis:
1. Nasal vestibule: Multifocal and coalescing lymphoplasmacytic and eosinophilic rhinitis, moderate to marked, with mucosal hyperkeratosis and perivascular dermatitis.
2. Lip: Multifocal lymphocytic labial gland adenitis, mild.

Contributor's Comment: The location and nature of the lesions present in the nasal vestibule are consistent with those that can occur in cynomolgus and rhesus macaques infected with nematode parasites in the genus *Anatrichosoma*. In some of the histology slides from this case, sections of nematodes are present in the submucosa of the nasal vestibule. Most of these are located within the lumen of a dilated venule (or perhaps lymphatic vessel); however, one section appears to be in fibrous connective tissue and is surrounded by inflammatory cells. In some of the sections of the worm (or worms) in the vessel lumen, a stichocyte is adjacent to and partially surrounds the esophagus;[2,4] the presence of a stichosome esophagus is a distinguishing feature of trichenelloid nematodes, which include species in the genera *Trichinella, Trichuris,*

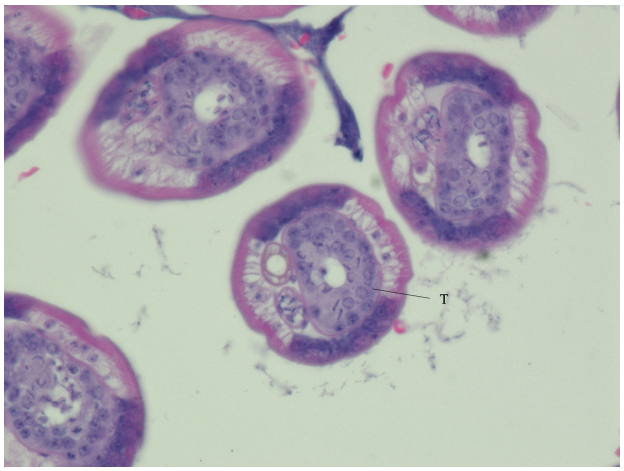

1-3. Haired skin and subcutis, nasal vestibule, cynomolgus macaque. Nematodes in this field contain a testis (T) with developing spermatocytes. Photographs courtesy of US Army Research Institute of Infectious Diseases, Fort Detrick, Maryland 21702-5011 (HE 60x)

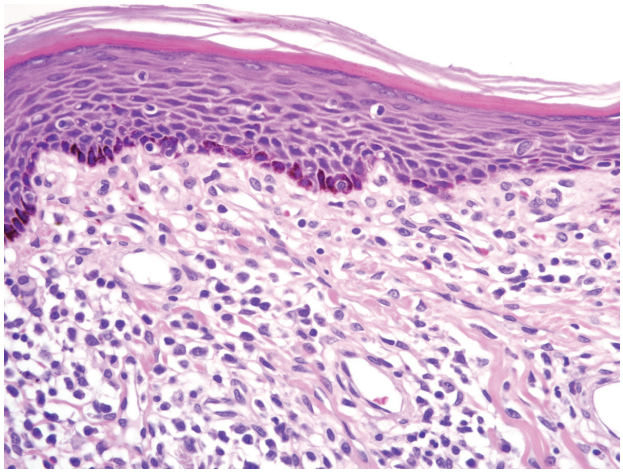

1-4. Haired skin and subcutis, nasal vestibule, cynomolgus macaque. Multifocally within the subepithelial connective tissue there are moderate numbers of lymphocytes, plasma cells, and fewer eosinophils, and there is overlying epithelial hyperplasia and hyperkeratosis. (HE 40x)

Capillaria, Trichosomoides, and *Anatrichosoma*.[2] Another feature of this group of nematodes is the presence of one or more hypodermal bands;[2,4] the parasites in this monkey have two such bands, which is consistent with *Anatrichosoma* spp.[2] In some of the intravascular worm sections, a testis containing developing spermatocytes is present (**figs. 1-1, 1-2, 1-3, and 1-4**).

Two species of *Anatrichosoma* have been described in macaques, *A. cynamolgi* and *A. cutaneum,* and each species can infect both cynomolgus and rhesus macaques.[1,3,8,10] The first of these parasite species discovered, *A. cutaneum*, was initially described in association with significant inflammatory lesions in the skin and subcutis of the hands and feet of rhesus macaques. However, these were apparently aberrant locations for the parasites;[1] the mucosa and submucosa of the nasal vestibule is the normal site of parasitism for both species of worms,[1,3] and infections in this location have not been associated with clinical signs or gross lesions. Differentiation of the two *Anatrichosoma* species is most reliably accomplished by examination of unfixed eggs and/or intact worms.[3,10]

Surveys of wild-caught macaques have indicated that the prevalence of infection in some free-ranging populations can range as high as 48%.[5] In one report concerning an experimental inhalation toxicity study, the parasites and/or nasal inflammation consistent with *Anatrichosoma* sp. infection were detected in 27 of 32 (84%) juvenile rhesus macaques.[6]

The full life cycle of these parasites is unknown. Mature female worms are located within the stratified squamous epithelium of the nasal vestibule where they are associated with epithelial hyperplasia and hyperkeratosis and varying degrees of inflammation of the epithelium and underlying tissues.[1,6,7] The female worms and released eggs are often present within intra-epithelial "tunnels" made by the worms. Immature parasites and mature males are usually located in the lamina propria and submucosa and are often intravascular (as in this case).[1,3,7,10] It is postulated that the male worms migrate up to the epithelial layer for mating and then return to the deeper tissues afterwards.[7] Eggs may be released directly by the females into the nasal vestibular lumen or reach the lumen from the intra-epithelial tunnels during epithelial desquamation.

There have been limited and unsuccessful attempts to experimentally infect macaques by direct transmission of the eggs.[10] This has led to speculation that one or more intermediate hosts are required.[9]

Although fecal samples from *Anatrichosoma*-infected monkeys may contain the parasite eggs, examination of nasal swabs for presence of eggs has been shown to be a more reliable method for ante mortem detection of parasitized individuals.[5]

The inflammation present in the labial glands of this case is mild; this is a common, incidental finding in macaques and is unlikely to be associated with the ebolavirus challenge or the nematode parasitism. At our institution, we routinely include a section of lip in the histology block with the nasal vestibule.

Note: Opinions, interpretations, conclusions, and recommendations above are those of the author and are not necessarily endorsed by the U.S. Army or Department of Defense.

AFIP Diagnosis: 1. Haired skin and nasal vestibule: Rhinitis, lymphoplasmacytic, histiocytic, and eosinophilic, multifocal to coalescing, moderate, with epithelial hyperplasia, orthokeratotic and parakeratotic hyperkeratosis, spongiosis, and perivasculitis.
2. Mucocutaneous junction, lip, minor salivary gland: Sialoadenitis, interstitial, lymphoplasmacytic and histiocytic, chronic, multifocal, mild.

Conference Comment: Unfortunately, of the 195 slides produced for this WSC submission, only one contained sections of the nematode. The contributor, who also moderated this conference, remarked that this case accurately reflects reality, i.e. the nematodes are often scarce in histologic section, and the diagnosis must often be made presumptively based on telltale inflammation in the nasal vestibule. In the absence of a nematode in the submitted sections, conference participants considered a hypersensitivity reaction most likely, and suggested a number of potential etiologies, including an inhaled environmental allergen, arthropod bite, or intranasal vaccine. The contributor provides a detailed review of anatrichosomiasis.

Contributor: U.S. Army Medical Research Institute of Infectious Diseases, Fort Detrick, MD 21702
http://www.usamriid.army.mil/

References:
1. Allen AM: Occurence of the nematode, *Anatrichosoma* cutaneum, in the nasal mucosa of *Macaca mulatta* monkeys. Am J Vet Res **21:**389-392, 1960
2. Bowman DD, Lynn RC, Eberhard ML, Alcaraz A: Georgis' Parasitology for Veterinarians, 8th ed., pp. 225-230, 391-393. Saunders, St. Louis, MO, 2003
3. Chitwood MB, Smith WN: A redescription of *Anatrichosoma cynamolgi* Smith and Chitwood, 1954. Proc Helmin Soc Wash **25:**112-117, 1958

4. Gardiner CH, Poynton SL: An Atlas of Metazoan Parasites in Animal Tissues, pp. 40-42. Armed Forces Institute of Pathology, Washington, DC, 1999
5. Karr SL, Henrickson RV, Else JG: A survey for *Anatrichosoma* (Nematoda:Trichonellida) in wild-caught *Macaca mulatta*. Lab An Sci **29:**789-790, 1979
6. Klonne DR, Ulrich CE, Riley MG, Hamm TE, Morgan KT, Barrow CS: One-year inhalation toxicity study of chlorine in rhesus macaques (*Macaca mulatta*). Fundamen Appl Toxicol **9:**557-572, 1987
7. Little MD, Orihel TC: The mating behavior of *Anatrichosoma* (Nematoda: Trichuroidea). J Parasit **58:**1019-1020, 1972
8. Reardon LV, Rininger BF: A survey of parasites in laboratory primates. Lab An Care **18:**577-580, 1968
9. Ulrich CP, Henrickson RV, Karr S: An epidemiological survey of wild caught and domestic born rhesus monkeys (*Macaca mulatta*) for *Anatrichosoma* (Nematoda: Trichinellida). Lab An Sci **31:**726-727, 1981
10. Wong MM, Conrad HD: Prevalence of metazoan parasite infections in five species of Asian macaques. Lab An Sci **28:**412-416, 1978

CASE II: R04-43 (AFIP 2948651).

Signalment: Adult, female crocodile (*Crocodylus niloticus*).

History: This crocodile was kept in a local zoo for over 2 years and was listless and anorexic for 5 weeks.

Gross Pathology: All lung lobes contained multiple, 0.5-1.0 cm diameter, irregularly-shaped, well-defined, firm, homogenous white to yellow nodules. Several firm, large nodules, 2.0-2.5 cm in diameter, white to yellowish in color, surrounded by dark red foci, were found in some part of the lungs. Visceral surfaces in the lung and pleural surfaces appeared dull and rough with a yellowish fibrous appearance. The liver and spleen were enlarged and cut surfaces revealed several gray to pale nodules.

Laboratory Results: *Escherichia coli* and *Aeromonas* sp. were isolated from the lungs and liver.

Histopathologic Description: Microscopic examination of the lung consists of a hemorrhagic, necrotizing bronchopneumonia with massive aerial mycelial growth within the airways. These affected airways are filled with numerous degenerated heterophils admixed with macrophages, necrotic debris, and bacillary colonies. The fungal organisms contain 3-5 µm chains of conidia, 4-7 µm dichotomous-branching, septate fungal hyphae. Airways are markedly dilated and the mucosal epithelium is extensively ulcerative with hemorrhage, many heterophils and macrophages are invading into the adjacent lung parenchyma. In these pneumonic areas, inflammation is associated with the appearance of numerous birefringent crystals with radiating spokes; the morphology of these crystals is suggestive of calcium oxalate. Histochemistry reveals many PAS-positive fungal hyphae scattered throughout the necrotic foci of lungs, liver, and spleen, primarily along the margins of the necrotic lesion (**figs. 2-1 and 2-2**).

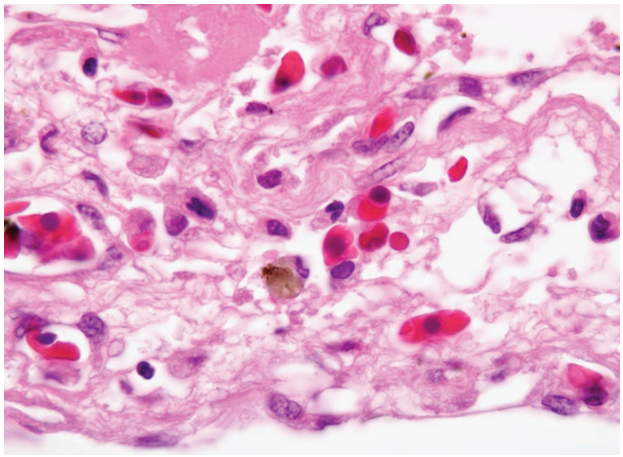

2-1. Lung, crocodile. In the pulmonary interstitium associated with pneumonic areas of lung there are numerous pale brown, birefringent, radiating crystals (oxalate crystals). (HE 1000x)

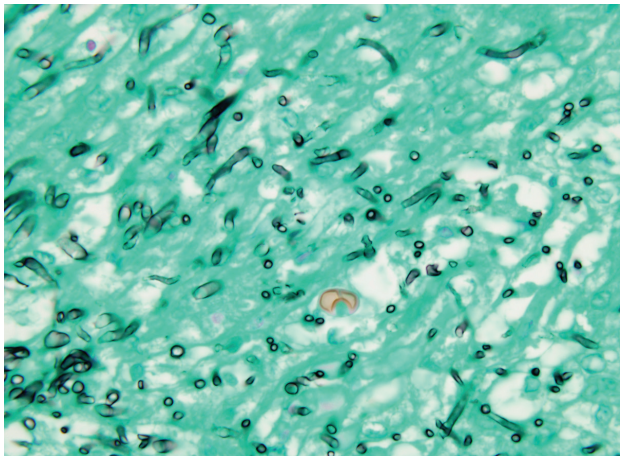

2-2. Lung, crocodile. Pulmonary airways contain numerous septate fungal hyphae and conidia that demonstrate dichotomous branching. (GMS 1000x)

Contributor's Morphologic Diagnosis:
Lung: Bronchopneumonia, necrogranulomatous and hemorrhagic, severe, subacute to chronic, multiple, with intralesional fungal hyphae, oxalate crystals, necrotic vasculitis, and pleuritis, crocodile (*Crocodylus niloticus*), reptile.

Contributor's Comment: Clinically, oxalate is produced by a variety of fungi, including saprophytic (e.g. *Aspergillus niger* and *A. flavus*) and phytopathogenic species, and other sources including methoxyflurane, ethylene glycol, large doses of ascorbic acid (vitamin C), primary hyperoxaluria (humans, cats, and tibetan spaniels), pyridoxine (vitamin B_6) deficiency, and plants (e.g. *Halogeton glomeratus, Sarcobatus vermiculatus, Rheum rhaponticum, Oxalis cernua, Rumex* sp., Russian vine, etc.). Several pathways have been described for oxalic acid production, but the mechanism of oxalate crystal production is not known. In *Aspergillus niger*, the organism apparently possesses oxaloacetate acetylhydrolase (OAH), one of the enzymes of the tricarboxylic acid cycle, and degrades oxaloacetate to oxalate by this route (i.e. oxaloacetate + H2O → oxalate + acetate). In humans, similar morphological findings have been reported, with often localized deposition of calcium oxalate crystals around a pulmonary *A. niger* fungal ball.[1-3,5,6]

Aspergillus, a ubiquitous environmental organism, is an opportunistic pathogen in mammals and birds. *Aspergillus fumigatus* is the most commonly reported cause of aspergillosis in animals, whereas *A. flavus, A. terreus, A. nidulans*, and *A. niger* are incriminated less frequently. In animals, localized deposition of massive numbers of calcium oxalate crystals in tissues has been reported in association with *Aspergillus* infections.[5,7-9] This is the first report of pulmonary oxalosis in a crocodile.

AFIP Diagnosis: Lung: Pneumonia, necrohemorrhagic, multifocal to coalescing, severe, with pleuritis, myriad fungal hyphae, and abundant anisotropic crystalline material (oxalate crystals).

Conference Comment: The GMS method highlights the fungal conidia and is helpful in demonstrating the other hyphal characteristics described by the contributor; while these features, in combination with oxalate crystal formation, are certainly suggestive of aspergillosis, the results of confirmatory testing (e.g. fungal culture) would be particularly valuable for solidifying the specific etiologic diagnosis. Furthermore, while the morphology of the prismatic crystalline material is consistent with oxalate crystals, histochemical stains (e.g. Yasue's silver nitrate-rubeanic acid), though not performed, may be employed to definitively identify oxalate crystals.[5]

In domestic species, oxalate crystals are more commonly encountered in the renal tubules due to ethylene glycol toxicosis in cats and dogs, or intoxication with one of the oxalate-containing plants listed above in sheep and cattle. Interestingly, the rumen microflora have some capacity to degrade oxalate to bicarbonate and carbonates, conferring sheep and cattle with a degree, albeit limited, of resistance to oxalosis; yet, remarkably, horses are far more resistant to oxalate-induced nephrosis. Because oxalate chelates calcium, hypocalcemia is a characteristic finding in both ethylene glycol toxicosis and oxalate toxicosis.[4]

Contributor: Division of Animal Medicine, Animal Technology Institute Taiwan, P.O. Box 23, Chunan, Miaoli, Taiwan 350

References:
1. Blackmon JA: *Aspergillus niger*. Am J Clin Pathol **76:**506, 1981
2. Kauffman CA, Wilson KH, Schwartz DB: Necrotizing pulmonary aspergillosis with oxalosis. Mykosen **27:**535-538, 1984
3. Kurrein F, Green GH, Rowles SL: Localized deposition of calcium oxalate around a pulmonary *Aspergillus niger* fungus ball. Am J Clin Pathol **64:**556-563, 1975
4. Maxie MG, Newman SJ: Urinary system. *In:* Jubb, Kennedy, and Palmer's Pathology of Domestic Animals, ed. Maxie MG, 5th ed., vol. 2, pp. 470-472. Elsevier Saunders, Philadelphia, PA, 2007
5. Muntz FH: Oxalate-producing pulmonary aspergillosis in an alpaca. Vet Pathol **36:**631-632, 1999
6. Severo LC, Londero AT, Geyer GR, Picon PD: Oxalosis associated with an *Aspergillus niger* fungus ball: report of a case. Mycopathologia **73:**29-31, 1981
7. Tham VL, Purcell DA: Fungal nephritis in a grey-headed albatross. J Wildl Dis **10:**306-309, 1974
8. Wobeser G, Saunders JR: Pulmonary oxalosis in association with *Aspergillus niger* infection in a great horned owl (*Bubo virginianus*). Avian Dis **19:**388-392, 1975
9. Wyand DS, Langheinrich K, Helmboldt CF: Aspergillosis and renal oxalosis in a white-tailed deer. J Wildl Dis **7:**52-56, 1971

CASE III: 0408061 (AFIP 2940154).

Signalment: Mature female red-tailed boa constrictor (*Boa constrictor*).

History: This snake became listless, inappetant, and died approximately one month after birthing. It had regurgitated recently. One other snake (also a red-tailed boa) also died recently.

Gross Pathology: This boa was in good nutritional condition and had ample internal body fat stores. No gross lesions were seen.

Contributor's Morphologic Diagnosis: Inclusion body disease of boids, with widespread intracytoplasmic inclusion bodies in epithelial cells of liver hepatocytes and biliary epithelial cells and hepatocellular degeneration and necrosis.

Contributor's Comment: Inclusion body disease of boid snakes has been recognized for the past 30 years, and is named for the characteristic intracytoplasmic inclusion bodies seen in a variety of epithelial cells. These include epithelial cells of the pancreas, renal tubules, gastrointestinal tract, respiratory tract, hepatocytes, biliary epithelium, thyroid follicular cells, and neurons of brain and spinal cord.[4] All tissues involved are reported to have varying degrees of degenerative changes, including vacuolation, cellular collapse and necrosis. Meningoencephalitis has been reported in both boas and pythons; however, the severity of both the neural histopathologic changes and clinical signs is much higher in Burmese pythons than in boa constrictors.[4]

Workers at the University of Florida found this disease to be caused by a retrovirus through the use of transmission electron microscopy. Further characterization efforts conducted demonstrated reverse transcriptase activity. Western blot analysis of viruses from different snakes was also done; these different isolates from different snakes were found to be similar.[1]

Clinical signs are quite variable. Regurgitation and signs of central nervous system (CNS) disease are commonly seen in boa constrictors. Stomatitis, pneumonia, undifferentiated cutaneous sarcomas, and lymphoproliferative disorders have all been seen. Burmese pythons generally show signs of CNS disease without manifesting any other clinical signs; regurgitation is not seen in Burmese pythons.[4]

This snake was one of several in this household that died with similar clinical presentations and pathologic findings. There is no treatment, and the disease is highly contagious and always fatal. As the disease seems to be occurring with increasing incidence, it is imperative that all new boids brought into a collection be quarantined from acquisition for at least 3-6 months, and that appropriate precautions be taken when visiting other collections, pet stores, expositions, and swap events.

Although slides submitted from this snake for the conference were all from the liver, similar inclusion bodies were also seen in most of the tissues cited above.

AFIP Diagnosis: 1. Liver: Hepatocellular degeneration, diffuse, moderate, with scattered single hepatocellular necrosis, and many hepatocellular and biliary epithelial intracytoplasmic eosinophilic inclusion bodies.
2. Liver: Hepatitis, necrotizing, random, acute, multifocal, moderate, with colonies of coccobacilli.

Conference Comment: Conference participants noted the characteristic eosinophilic intracytoplasmic inclusion bodies both in hepatocytes and biliary epithelial cells. Additionally, scattered randomly throughout the liver are foci of lytic necrosis with colonies of coccobacilli, which participants ascribed to embolic showering resulting from terminal sepsis, thus accounting for the lack of associated inflammation (**fig. 3-1**).

Despite an abundance of research on this important entity, fulfillment of Koch's postulates remains elusive, and the cause of inclusion body disease (IBD) is still enigmatic.

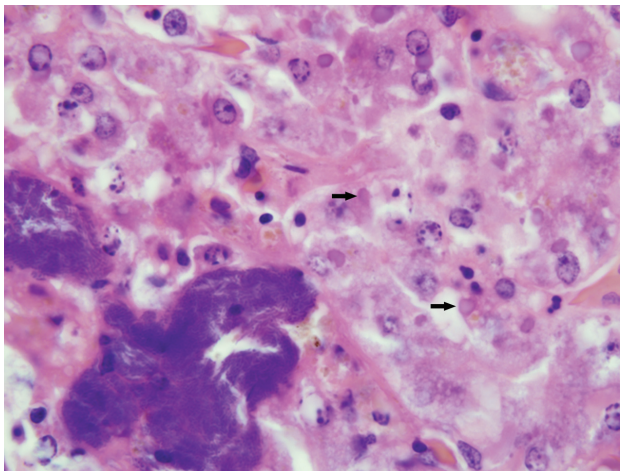

3-1. Liver, boa constrictor. Eosinophilic intracytoplasmic inclusion bodies occur within degenerate hepatocytes (arrows). Additionally, there are areas of acute hepatic necrosis associated with large colonies of coccobacilli. (HE 1000x)

As noted by the contributor, a retroviral etiology has been strongly suspected, and clinicopathologic evidence (e.g. stomatitis, lymphoproliferative disorders, etc.) supports this conclusion. Moreover, retroviruses have been isolated from various species of snakes with IBD; however, a causal role has not been established, and it remains possible that retroviruses play only an incidental role in IBD. Similarly, reoviruses and adenoviruses have also been isolated from snakes with IBD, and may play causal and/or incidental roles in the disease. Notably, electron microscopy demonstrates that IBD inclusions are nonviral, and consist of radio-dense round particles that accumulate at the periphery of the inclusion; particles are composed of a 68-KDa protein deposited by polyribosomes.[2]

As noted by the contributor, epidemiologic evidence suggests that IBD is indeed contagious, and quarantine measures are therefore warranted. Antemortem diagnosis is achieved by biopsy examination of the liver or kidney, or the esophageal tonsil, in which inclusions are generally present in the overlying epithelial cells.[2] In a recent study, investigators readily identified inclusions in the leukocytes of boas with IBD using concentrated buffy coat examinations, and hence recommended the screening technique as a less invasive alternative to biopsy; however, the technique may not be applicable in pythons, in which the distribution of inclusions is often limited to the central nervous system.[3]

Contributor: NMDA-Veterinary Diagnostic Services, 700 Camino de Salud NE, Albuquerque, NM 87106-4700 http://www.nmda.nmsu.edu/animal-and-plant-protection/veterinary-diagnostic-services

References:

1. Jacobson ER, Orós J, Tucker SJ, Pollock DP, Kelley KL, Munn RJ, Lock BA, Mergia A, Yamamoto JK: Partial characterization of retroviruses from boid snakes with inclusion body disease. Am J Vet Res **62:**217-224, 2001
2. Jacobson ER: Viruses and viral diseases of reptiles. *In:* Infectious Diseases and Pathology of Reptiles, ed. Jacobson ER, pp. 410-412. CRC Press, Boca Raton, FL, 2007
3. Pees M, Schmidt V, Marschang RE, Heckers KO, Krautwald-Junghanns M-E: Prevalence of viral infections in captive collections of boid snakes in Germany. Vet Rec **166:**422-425, 2010
4. Schumacher J, Jacobson ER, Homer BL, Gaskin JM: Inclusion body disease in boid snakes. J Zoo Wildl Med **25:**511-524, 1994

CASE IV: 60848 (AFIP 3134333).

Signalment: Adult, female, wild-caught Giant Pacific octopus (*Octopus (Enteroctopus) dofleini*).

History: Three Giant Pacific octopuses, *Octopus (Enteroctopus) dofleini*, wild-caught in Alaska and held in captivity, died or were euthanized following periods of decreased appetite and lethargy, despite treatments for possible septicemia and heavy metal exposure. This particular wild-caught female came in October 2006 and spawned 20 April 2008. She continued to eat, interact with the environment, and behave normally until found moribund 4 December 2008, requiring euthanasia. Lesions were similar in all three giant octopus submissions.

Gross Pathology: Multiple gill biopsies were submitted in formalin and 95% ethanol.

Histopathologic Description: Gills: There are abundant piriform structures lining up along the apical surface of columnar gill epithelium. The parasites extend slender structures connecting them to apical aspects of the epithelium. The submucosa is diffusely and variably expanded by numerous degenerate and viable hemocytes with abundant granular eosinophilic cytoplasm and reniform-to-bilobed nuclei. Within the inflammatory hemocytes, and often extracellularly, is variably-sized spherical, amphophilic, pink-to-olive brown, refractile material. Individual inflammatory cells are observed transmigrating through the crowded tall columnar pseudostratified epithelial cells and occasionally coalescing into small aggregates of exudated hemocytes. There is some epithelial loss with parasites adhered to areas of disruption; adjacent degenerate to necrotic epithelial cells are vacuolated or collapsed with nuclear pyknosis. There are multifocal areas of increased clear space between haphazardly arranged bundles and individual connective tissue fibers of the submucosa (edema) (**figs. 4-1, 4-2, and 4-3**).

Contributor's Morphologic Diagnosis: Gills: Inflammation, subacute, hemocytic, diffuse, severe with epithelial necrosis (branchitis).

Etiologic Diagnosis: Necrotizing branchitis with intralesional apical piriform protozoa consistent with *Ichthyobodo*.

Contributor's Comment: Histopathological findings showed extensive gill degeneration and necrosis and hemocytic inflammation associated with a heavy infection of *Ichthyobodo*-like flagellates. The gills had a large

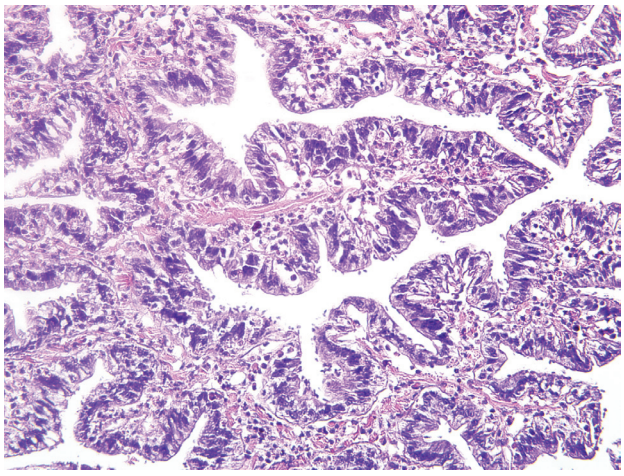

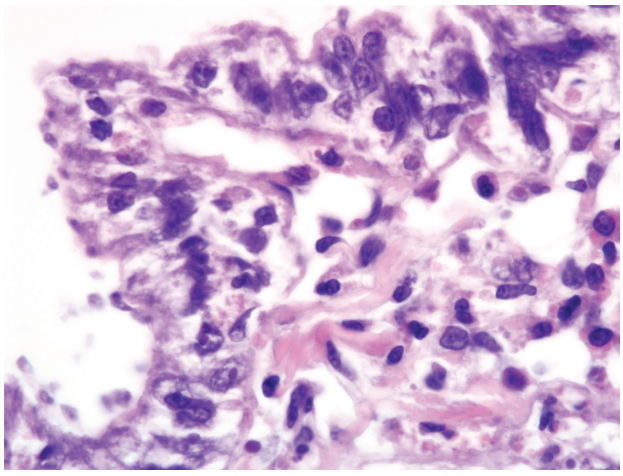

4-1, 4-2. Gill, octopus. The gill interstitium is infiltrated hemocytes that have granular eosinophilic cytoplasm and reniform to bi-lobed nuclei. (HE 40x)

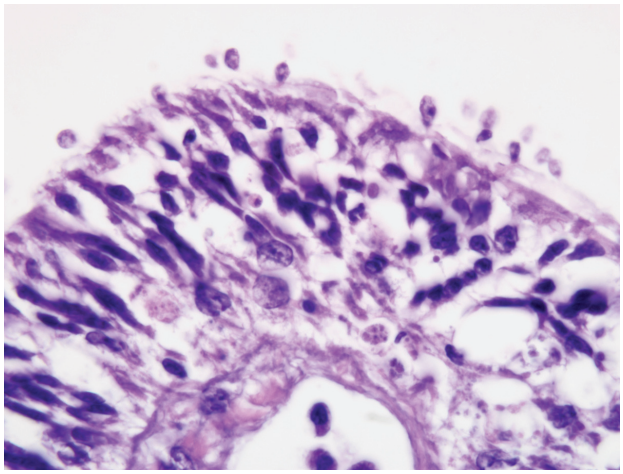

4-3. Gill, octopus. Numerous piriform flagellated protozoa attach and line the apical surface of the gill epithelium. (HE 1000x)

number of the piriform protozoal structures queued up along the apical margin of the gill epithelium, and attended by variable submucosal hemocytic inflammation.

Samples of gills tissues were processed for genomic DNA extraction, PCR amplification, and cloning and sequencing of the rRNA genes; phylogenetic analysis was conducted on the SSU, D1-D3 and D8-D10 LSU rDNA sequences. Gene sequences were deposited in GenBank. Phylogenetic analysis indicated that the *Ichthyobodo* species identified in this study was most closely related to those from freshwater fish.

Ultrastructural features were similarly characteristic of *Ichthyobodo* species. Scanning electron microscopy showed that the flagellates were flattened pyriform to trapezoidal, approximately 6-10 µm long and 3-6 µm wide. In some regions the infection was so dense that the gill surfaces were completely covered with the flagellates. Flagellates were attached to the host cell's cytoplasm by a narrow cytostome via a crateriform puncture through the smooth mucous covering of the gill epithelium. Transmission electron microscopy revealed two unequal-width flagella lying in a U-shaped flagellar pocket, microtubules and striated fibers surrounding the flagellar pocket, and radiating fibres lying in a semi-circle around the cytostome primordial. The spherical nucleus had a large central nucleolus and peripheral chromatin, and the cytoplasm also contained rough endoplasmic reticulum, and mitochondria. There was an attachment plate anchoring the flagellate to the epithelial cell, and the cytostome process, reinforced with fibrillar structures, passed though the plate into the cytoplasm of the host cell.

Bodonid flagellates, of the genus *Ichthyobodo*, have long been recognized as significant ectoparasitic pathogens of freshwater and marine fish in aquaculture, and have been the subject of extensive research. The parasite can be found both free-swimming in the water column and attached to epithelial surfaces such as gills and skin.[6,13] The free-swimming form moves in a spiral motion with the aid of flagella. *Ichthyobodo* attaches to epithelial cells via a long, slender organelle that facilitates the ingestion of host cellular contents.[6,13] Ichthyobodiasis can impede osmoregulation and predispose to secondary infection; alternatively, *Ichthyobodo* infections are often found in association with stressful circumstances in freshwater

fish.[6,13] In contrast, there are only intermittent reports of bodonids and "*Ichthyobodo*-like" flagellates from cephalopods, and their host-parasite interaction and identity have not been reported in detail.

Invertebrates, including mollusks, rely on innate immunity to combat disease, with no evidence of acquired immunity.[9] Members of the phylum Mollusca, which includes the class Cephalopoda (squids, cuttlefish, octopus and nautilus), have both cellular and humoral mechanisms of defense. Hemagluttins are the best studied and understood component of molluscan "humoral" immunity. These soluble factors, named after the agglutination of erythrocytes from other species, is thought to play a role in the recognition and opsonization of foreign material, although cell-free hemolymph is reported to have limited ability to agglutinate bacterial isolates in vitro.[3] The hemocyte is the primary component of cephalopod cellular immunity and develops from stem cells found in the white body, a multilobed leukopoietic organ located in the retrobulbar areas.[4] The role of octopus hemocytes in wound healing is well documented; a progression from skin wound infiltration, transformation of hemocytes to fibroblastic morphology and establishment of a "dermal plug" with subsequent contraction culminates in wound repair.[2] A multi-function cell with oxygen-carrying and nutrient transport capacities, the octopus hemocyte also performs phagocytosis, producing reactive oxygen species and lysozyme to destroy pathogens.[8,11] Stress and low temperature have been shown to alter the phagocytic function of hemocytes in vivo.[7] In addition to phagocytosis, hemocyte encapsulation serves as defense mechanism against foreign substances. Resident hemocytes are described in gill tissues of octopus, complicating the evaluation and characterization of potential gill pathogens.[12]

The reproductive physiology of cephalopods is interesting and enigmatic. In cephalopods including Giant Pacific octopus, endocrine secretions from the paired optic glands direct the development of senescence, characterized by loss of appetite, change in feeding behavior, loss of condition and behavioral changes that culminate in death. Hence these species of octopus have a brief lifespan of only about 3 years and inevitably die after spawning.[1] In the captive octopus of this report, it is unclear whether there is any association of senescence and enhanced susceptibility to the *Ichthyobodo* infections. Removal of the optic glands is reported to reduce senescence-associated behavior and greatly extends the lifespan of cephalopods.[14]

These observations demonstrate that *Ichthyobodo* sp. can be a significant ectoparasitic pathogen of captive cephalopods. The host-parasite interaction and parasite ultrastructure are essentially similar to those of the better known *Ichthyobodo* sp. affecting teleosts. Molecular phylogeny showed that the *Ichthyobodo* sp. from these wild-caught captive Giant Pacific octopuses was most closely related to flagellates from several species of freshwater teleosts.

AFIP Diagnosis: Gill: Branchitis, hemocytic, multifocal, moderate, with many surface epithelial-associated flagellated protozoa.

Conference Comment: The contributor provides an excellent synopsis of the entity in this mysterious species. Conference participants discussed the challenge of estimating a lesion's chronicity based solely on microscopic examination in invertebrate species. In contrast to most vertebrates, in which the composition of inflammatory infiltrates correlates fairly reliably with chronicity, to the best of our knowledge, the composition of the inflammatory infiltrate has not been reported relative to lesion chronicity in the octopus, in which the hemocyte is the primary inflammatory cell. Accordingly, participants debated the merits of including the modifier "hemocytic" in the morphologic diagnosis, with some favoring its omission on the basis of redundancy, though most agreed with the contributor that its inclusion is an appropriate enhancement to the morphologic diagnosis, most precisely reflecting the pathologic processes involved.

Because *Ichthyobodo* infection is commonly associated with stress in freshwater fish, participants speculated that senescence-associated immunosuppression may have rendered this octopus particularly vulnerable to parasitism by *Ichthyobodo*-like flagellates. Curiously, some species of *Ichthyobodo* are capable of survival both in saltwater and freshwater; for instance, *I. necator*, which survives and causes disease over a wide range of temperatures, can survive in saltwater and cause mortality in marine-adapted salmonids. Other *Ichthyobodo*-like flagellates exclusively infect marine fish.[10] *Ichthyobodo*-like flagellate infection was reported in a laboratory cultured population of California mud-flat octopus (*Octopus bimaculoides*) and two related species (*O. maya* and *O. digueti*), in which the organism was initially found on the gill, then spread over the course of the disease to involve the internal surface of the mantle cavity and the body surface, leading the authors to conclude that the gill was the initial site of infection. Gross lesions included small white foci on the dorsal surfaces of the arms and mantle; however, these may have been partly attributed to co-infection with an ancistrocomid ciliate.[5]

Contributor: Department of Molecular and Comparative Pathobiology, Johns Hopkins University

School of Medicine, Baltimore, MD 21205
http://www.hopkinsmedicine.org/mcp/

References:

1. Anderson RC, Wood JB, Byrne RA: Octopus senescence: the beginning of the end. J Appl Anim Welf Sci **5:**275-83, 2002
2. Bullock AM, Polglase JL, Phillips SE: The wound healing and haemocyte response in the skin of the lesser octopus *Eledone cirrhosa* (Mollusca: Cephalopoda) in the presence of *Vibrio tubiashii*. J Zool **201:**185-204, 1986
3. Fisher WS, DiNuzzo AR: Agglutination of bacteria and erythrocytes by serum from six species of marine molluscs. J Invertebr Pathol **57:**380-94, 1991
4. Ford LA: Host defense mechanisms of cephalopods. Annual Rev of Fish Diseases **2:**25-41, 1992
5. Forsythe JW, Hanlon RT, Bullis RA, Noga EJ: *Octopus bimaculoides*: a marine invertebrate host for ectoparasitic protozoans. J Fish Dis **14:**431-442, 1991
6. Gratzek JB: Parasites associated with freshwater tropical fishes. *In:* Fish Medicine, ed. Stoskopf MK, pp. 576-577. W.B. Saunders, Philadelphia, PA, 1993
7. Malham SK, Lacost A, Gelebart F, Cueff A, Poulet AS: A first insight into stress-induced neuroendocrine and immune changes in the octopus *Eledone cirrhosa*. Aquat Living Resource **15:**187-192, 2002
8. Malham SK, Runham N, Secombes C: Lysozyme and antiprotease activity in the lesser octopus *Eledone cirrhosa* (Cephalopoda): developmental and comparative immunology. Immunology **22:**22-37
9. Mydlarz LD, Jones LE, Harvell CD: Innate immunity, environmental drivers, and disease ecology of marine and freshwater invertebrates. Annu Rev Ecol Evol Syst **37:**251-288, 2006
10. Noga EJ: Fish Disease: Diagnosis and Treatment, pp. 108-110. Iowa State University Press, Ames, IA, 2000
11. Rodriguez-Dominguez H, Soto-Bua M, Iglesias-Blance R, Crespo-Gonzalez C, Arias-Fernandez C, Garcia-Estevez J: Preliminary study on the phagocytic ability of *Octopus vulgaris* Cuvier, 1797 (Mollusca: Cephalopoda) haemocytes in vitro. Aquaculture **254:**563-570, 2006
12. Schipp R, Mollenhauer S, von Boletzky S: Electron microscopical and histochemical studies of differentiation and function of the cephalopod gill (*Sepia officinalis* L.) Zoomorphology **93:**193-207, 1979
13. Thune RL: Parasites of catfishes. *In:* Fish Medicine, ed. Stoskopf MK, pp. 528-529. W.B. Saunders, Philadelphia, PA, 1993
14. Wodinsky J: Hormonal inhibition of feeding and death in octopus: control by optic gland secretion. Science **198:**948-951, 1977

The Armed Forces Institute of Pathology
Department of Veterinary Pathology

Conference Coordinator:
Shannon Lacy, DVM, MPH

WEDNESDAY SLIDE CONFERENCE 2009-2010

Conference 25

19 May 2010

Conference Moderator:

Jo Lynne Raymond, DVM, Diplomate ACVP

CASE I: 089-65832 (AFIP 3134358).

Signalment: Adult male striped skunk (*Mephitis mephitis*).

History: An adult male striped skunk was submitted to the Colorado State University Diagnostic Laboratory with a history of being found dead and suspected poisoning. No other history was provided.

Gross Pathology: The skunk was in fair body condition, with minimal autolysis. Gross findings included nasal and ocular discharge, diarrhea staining of the perineum, thickened and alopecic skin over the shoulders, neck, and head, and a moderate load of subcutaneous nematodes grossly consistent with *Dracunculus insignis* over the lower limbs, thorax, and abdomen. The right ventricle contained a single, pale focus 2 mm in diameter with indistinct borders, consistent with focal myocardial necrosis (**fig. 1-1**).

Laboratory Results: Fluorescent antibody testing of the brain for canine distemper virus was positive. Fluorescent antibody testing of the brain for rabies virus was negative.

Histopathologic Description: Haired Skin: Diffusely, there is marked orthokeratotic hyperkeratosis of the skin surface and mild to moderate acanthosis of the epidermis. Within the cells of the stratum spinosum, there is frequent cytoplasmic vacuolar degeneration, and occasional single cell necrosis characterized by shrunken

1-1. Haired skin, skunk. Thickened alopecic skin overlying the head, neck, and shoulders. Photographs courtesy of Department of Microbiology, Immunology, and Pathology, Colorado State University, Fort Collins, Colorado 80525, karen.fox@colostate.edu

***Sponsored by the American Veterinary Medical Association, the American College of Veterinary Pathologists, and the C. L. Davis Foundation.**

cells with hypereosinophilic cytoplasm and nuclear pyknosis. Cells of the stratum spinosum also frequently contain one or more variably-sized, intracytoplasmic, glassy eosinophilic inclusions. Similar inclusions are occasionally present within nuclei of the stratum spinosum. The changes affecting the epidermis and skin surface extend to involve hair follicles. The superficial dermis is moderately expanded by fibroblasts, with mild infiltration by lymphocytes, plasma cells, and neutrophils. Some sections submitted also contain multifocal serocellular crusting of the skin surface with multiple intralesional cross sections of thick-shelled, embryonated eggs approximately 30 µm in diameter.

Contributor's Morphologic Diagnosis:
1. Haired skin: Hyperkeratosis, orthokeratotic, marked, with acanthosis and intracytoplasmic and intranuclear inclusions consistent with canine distemper virus infection.
2. Haired skin: Multifocal serocellular crusting of the skin surface with intralesional nematode embryonated eggs consistent with *Dracunculus insignis* (only in some slides).

Contributor's Comment: Canine distemper virus (CDV), of the genus *Morbillivirus* and family *Paramyxoviridae*, is a common and important pathogen encountered in a wide range of wild carnivores including, but not limited to coyotes, raccoons, skunks, wolves, foxes, black-footed ferrets, bears, and javelin.[8] Clinical signs of CDV are variable and reflect tropism of the virus for epithelial tissues and brain. Clinical signs include respiratory disease, enteric disease, and neurologic disease that can ultimately be fatal.[2]

Histologic lesions of CDV include lymphoid atrophy and necrosis, bronchointerstitial pneumonia, non-suppurative encephalomyelitis, demyelination of white matter tracts, enamel hypoplasia, conjunctivitis, keratitis, retinitis, optic neuritis, hyperkeratosis, persistence of primary spongiosa of bones, and myocardial necrosis. Viral inclusions are most prominent in the brain and epithelial tissues. Intracytoplasmic inclusions tend to be more common in epithelial cells, while intranuclear inclusions are more common in the brain.[2]

Skin lesions of CDV are most commonly found on the foot pads, nose, eyelids, lips, and anus,[8] although the haired skin can also be affected.[2,5] Histologic findings in the epidermis of haired or non-haired skin include hyperkeratosis and/or parakeratosis, acanthosis, rete ridge formation, epidermal syncytial cells, cytoplasmic and nuclear inclusions, pustular dermatitis secondary to hyperkeratosis, and periadnexal and perivascular mononuclear inflammation.[2] Immunohistochemistry and viral inclusions visible on H&E-stained slides demonstrate that viral particles are primarily located within the stratum spinosum and stratum granulosum.[5] The pathogenesis of hyperkeratosis in CDV is suggested to be due to defective differentiation of infected keratinocytes.[5]

In the case presented here, the infected skunk demonstrated multiple gross and histologic features of systemic infection by CDV, including oculonasal discharge, interstitial pneumonia, evidence of diarrhea, focal myocardial necrosis, and the submitted lesion of hyperkeratosis of the haired skin overlying the shoulders, neck, and head. Interestingly, the epidermis of the foot pads was not noticeably thickened in this case. Fluorescent antibody testing of the brain confirmed infection with CDV.

The additional finding in some slides of multifocal serocellular crusting of the skin surface with intralesional cross sections of nematode eggs is consistent with the gross finding of subcutaneous nematodes suggestive of *Dracunculus insignis* infection. Definitive identification of the parasite was pending at the time of case submission. *Dracunculus insignis* is a member of the spirurid group of nematodes and is commonly found in wild mammals (predominantly raccoons), but can also be transmitted to domestic mammals including dogs and cats.[1] For this parasite to reproduce, the female uterus is prolapsed through an ulcer in the skin to release larvae. The larvae are then ingested by *Cyclops* spp. (an aquatic copepod) where they develop to infective third stage larvae. The copepod is ingested either directly by the definitive host, or can be ingested first by a paratenic host such as a frog. Once ingested by the definitive host, the copepod dies, the infective stage is released, and the larvae penetrate the host's stomach and intestinal wall to mature and reproduce. Once fertilized, the female parasites migrate to the subcutaneous tissues, typically of the lower limbs, to expel ova.[1]

AFIP Diagnosis: 1. Haired skin and subcutis: Epidermal hyperplasia, diffuse, marked, with epidermal and follicular orthokeratotic hyperkeratosis, intracorneal pustules, and few embryonated filarid nematode eggs, etiology consistent with *Filaria taxideae*.
2. Haired skin and subcutis, epidermis, hair follicles, and apocrine glands: Epithelial degeneration, multifocal, mild, with rare intracellular edema and numerous intracellular eosinophilic viral inclusion bodies, etiology consistent with canine distemper virus.

Conference Comment: This case was studied in consultation with Dr. Christopher Gardiner, Consulting Parasitologist to the AFIP Department of Veterinary

Pathology; he opined that because adult females of the genus *Dracunculus* expel intact larvae as detailed by the contributor, the thick-shelled, embryonated eggs in the serocellular crust in this case are unlikely to be those of *Dracunculus* species (**figs. 1-2 and 1-3**).[1] Rather, the eggs are interpreted as being most consistent morphologically with those of the primitive filarial nematode *Filaria taxidae*, which has been reported as a cause of filarial dermatitis in the American badger (*Taxidea taxus*)[4,6], striped skunk (*Mephitis mephitis*)[7], and lesser panda (*Ailurus fulgens*).[3] A high prevalence of infection has also been reported in raccoons (*Procyon lotor*) in Texas, but without associated lesions. The life cycle of *F. taxideae* is incompletely described; tabanid flies have been suggested as possible intermediate hosts.[6]

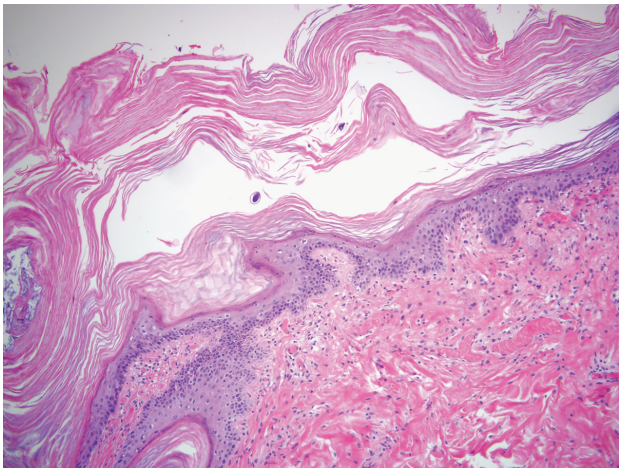

1-2. Haired skin, skunk. There is diffuse orthokeratotic hyperkeratosis and epidermal hyperplasia. Within the hyperkeratotic stratum corneum there are few nematode eggs. (HE 100x)

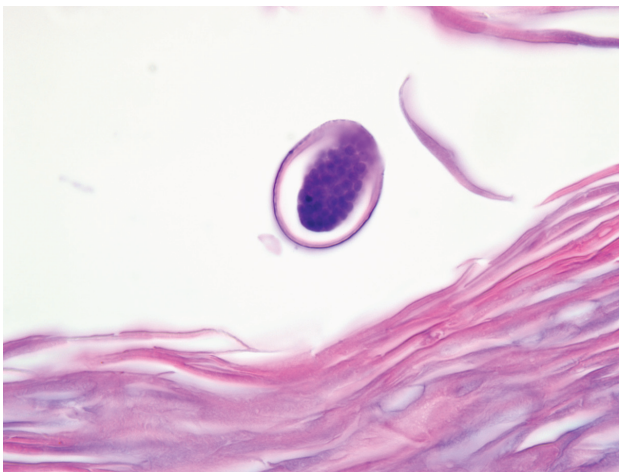

1-3. Haired skin, skunk. Embryonated nematode eggs measure approximately 30um in diameter and have a thick shell. (HE 1000x)

Two surveys of badgers in Wyoming found *F. taxideae* in 81%[6] and 39%[4] of badgers examined, respectively, and an apparent seasonal occurrence of associated dermatitis, with active lesions peaking during the summer. In badgers, gross lesions are most pronounced in the inguinal area, proximal thigh, and ventral abdomen and are characterized by blood-tinged fluid-filled vesicles and/or areas of serocellular crusting and ulceration.[6] In the single published report of filarial dermatitis attributed to *F. taxideae* in a striped skunk, the lesions consisted of large confluent areas of alopecia and marked thickening of the skin overlying the head, thoracolumbar region, and tail base; the description of the lesions in the case report bear striking resemblance to those depicted in the image submitted by the contributor for this case.[7]

Adult filarids are white, often tightly coiled, nematodes ranging from 122-131 mm (males) to 285-420 mm (females) in length; they are readily visualized in the subcutis and fascia, where they elicit little inflammatory response. Lesions result when gravid females deposit eggs in the upper dermis or between the epidermis and cutaneous basement membrane. Early microscopic findings in badgers consist of subepidermal vesiculobullous dermatitis extending into follicular infundibulae, with numerous embryonated filarid eggs occupying vesicles; lesions progress to ulceration and dermatitis, with orthokeratotic hyperkeratosis and acanthosis in the adjacent epidermis.[6] In skunks, reported lesions include marked epidermal hyperplasia with orthokeratotic hyperkeratosis, and numerous dermoepidermal pustules containing larvated eggs.[7]

Conference participants attributed much of the acanthosis and hyperkeratosis observed in the submitted case to filarial dermatitis, rather than CDV infection, but acknowledged that the CDV inclusions in the epidermis, follicular epithelium, and apocrine glands are numerous and prominent (**fig. 1-4**). Infection with CDV may have predisposed this skunk to nematode infection; in addition to the microscopic lesions described by the contributor, several participants' slides contained few pigmented fungal hyphae in the superficial layers of the epidermis, interpreted as opportunistic dematiaceous fungi.

The contributor provides a useful synopsis of CDV infection, which participants reviewed in conference. Attendees briefly reviewed other noteworthy morbilliviruses of importance in veterinary medicine, including measles virus, rinderpest virus, peste-des-petits-ruminants virus, phocine distemper virus, and cetacean morbillivirus.

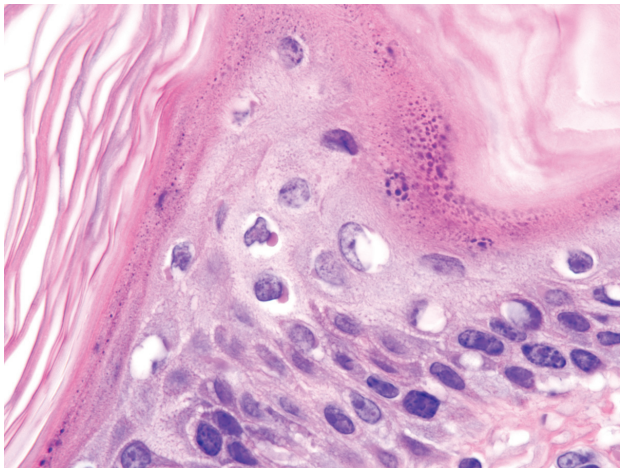

1-4. Haired skin, skunk. Within the hyperplastic epidermis there are variably-sized eosinophilic intracytoplasmic inclusion bodies. (HE 1000x)

Contributor: Colorado State University, College of Veterinary Medicine and Biomedical Sciences, Department of Microbiology, Immunology and Pathology, 1619 Campus Delivery, Fort Collins, CO 80523
http://www.cvmbs.colostate.edu/mip/

References:

1. Beyer TA, Pinckney RD, Cooley AJ: Massive *Dracunculus insignis* infection in a dog. J Am Vet Med Assoc **214:**366-367, 1999
2. Caswell JL, Williams KJ: Respiratory system. *In:* Jubb, Kennedy, and Palmer's Pathology of Domestic Animals, ed. Maxie MG, 5th ed., vol. 2, pp. 635-638. Elsevier Saunders, Philadelphia, PA, 2007
3. Gardiner CH, Loomis MR, Britt JO Jr., Montali RJ: Dermatitis caused by *Filaria taxideae* in a lesser panda. J Am Vet Med Assoc **183:**1285-1287, 1983
4. Keppner EJ: The pathology of *Filaria taxideae* (Filarioidea: Filariidae) infection in the badger, J Wildl Dis **7:**317-232, 1971
5. Koutinas AF, Baumgärtner W, Tontis D, Polizopoulou Z, Saridomichelakis MN, Lekkas S: Histopathology and immunohistochemistry of canine distemper virus-induced footpad hyperkeratosis (hard pad disease) in dogs with natural canine distemper. Vet Pathol **41:**2-9, 2004
6. O'Toole D, Williams ES, Welch V, Nunamaker CE, Lynn C: Subepidermal vesiculobullous filarial dermatitis in free-ranging American badgers (*Taxidea taxus*). Vet Pathol **30:**343-351, 1993
7. Saito EK, Little SE: Filarial dermatitis in a striped skunk. J Wildl Dis **33:**873-876, 1997
8. Williams ES: Canine distemper. *In:* Infectious Diseases of Wild Mammals, eds. Williams ESW, Barker IK, 3rd ed., pp. 50-55. Iowa State University Press, Ames, IA, 2001

CASE II: SP-08-8399 (AFIP 3134511).

Signalment: 12-year-old, female, spayed Toy Poodle dog (*Canis familiaris*).

History: The history provided by the referring veterinarian indicated that the right eye suddenly proptosed and ruptured. The dog had a history of cataracts. In the last few weeks, the dog had developed a purulent discharge from the right eye and had been rubbing its eye.

Gross Pathology: The received sample consisted of a globe with intact inferior and superior palpebrae and third eyelid. The base of the third eyelid was expanded by a well circumscribed, 1.0x1.3x1.0 cm, firm, pale white mass that had central areas of necrosis and hemorrhage. The cornea of the eye adjacent to this mass was indented and the anterior chamber of the globe was moderately collapsed. There were anterior and posterior synechiae between the iris and posterior cornea and the iris and anterior aspect of the lens, respectively.

Histopathologic Description: Sections of globe and periorbital tissue including superior and inferior palpebrae and third eyelid are submitted. The posterior aspect of the base of the third eyelid is expanded by a highly cellular, fairly circumscribed, partially encapsulated, slightly lobulated mass that replaces portions of the gland of the third eyelid. This mass is composed of varying populations of neoplastic epithelial cells and myoepithelial cells. Neoplastic epithelial cells are arranged in tubules, acini, nests, and sheets. Tubules and acini are generally lined by a single densely packed layer of neoplastic epithelial cells. Lumens of these structures often contain variable amounts of blood, eosinophilic to amphophilic secretory product, and few macrophages and/or neutrophils. Neoplastic epithelial cells are cuboidal to attenuated with mild to moderate amounts of eosinophilic cytoplasm and indistinct cell borders. In some portions of the mass, the cytoplasm of neoplastic cells is obliterated by few sharply defined, open vacuoles. Nuclei are round to ovoid, finely stippled to vesiculated, and generally contain a single prominent nucleolus. Anisokaryosis is moderate. Mitotic figures are uncommon with 4-5 observed per ten high power fields. Neoplastic epithelial cells are supported by variable amounts of fibrovascular stroma containing myoepithelial cells. In some areas, this stroma is characterized by a fine fibrovascular meshwork separating the neoplastic tubules and nests. In other areas, the supporting stroma is composed of moderate bands of dense fibrous tissue. Significant proportions of some lobules are composed of highly cellular populations of spindle shaped myoepithelial

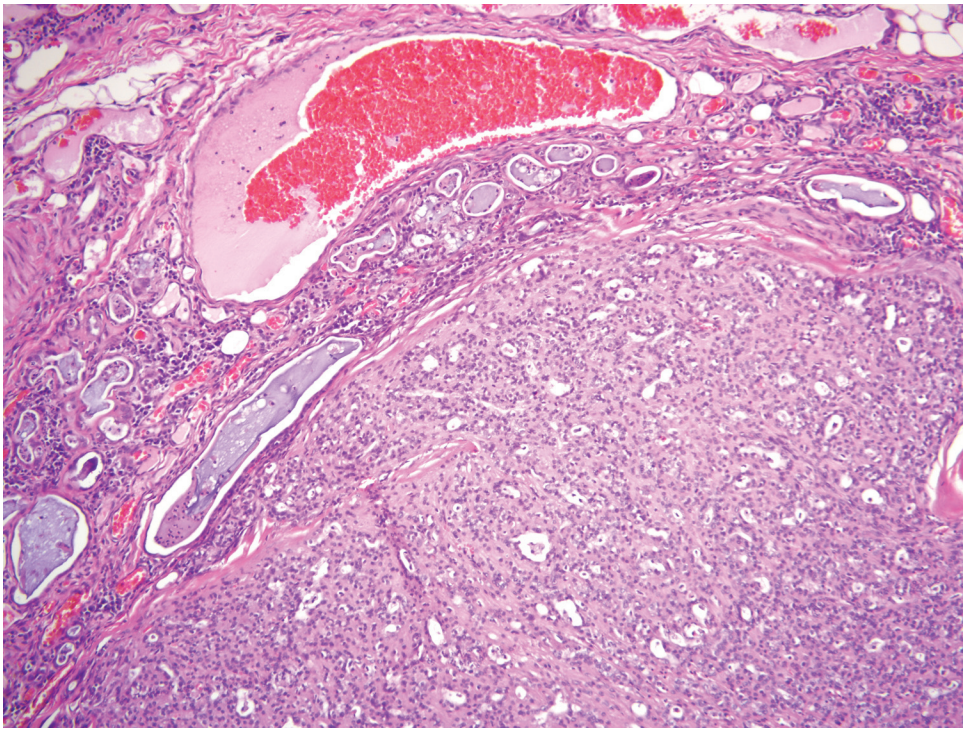

2-1. Epithelial-myoepithelial carcinoma, eye, lacrimal gland, canine. The third eyelid is expanded by an epithelial neoplasm arranged in tubules, acini, nests, and solidly cellular areas on a variable fibrovascular stroma; the tumor compresses the adjacent preexisting structures of the third eyelid. (HE 20x)

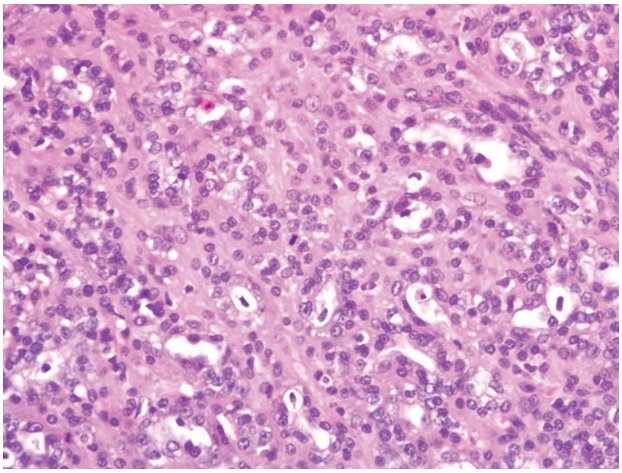

2-2. Epithelial-myoepithelial carcinoma, eye, lacrimal gland, canine. Neoplastic epithelial cells have variably distinct borders, scant to moderate amount of eosinophilic cytoplasm, and round to oval nuclei with finely stippled chromatin. (HE 200x)

cells that are surrounded by dense haphazardly arranged collagenous stroma. Myoepithelial cells have scant to mild amounts of eosinophilic cytoplasm, indistinct cell borders, and round to ovoid, finely stippled nuclei (**figs. 2-1 and 2-2**). Vast central areas of the mass are replaced by pools of hemorrhage, organizing mats of fibrin, and amorphous to flocculent proteinaceous fluid containing moderate numbers of hemosiderin and hematoidin laden macrophages and few neutrophils. Such central pools are bordered by dense bands of fibrosis that are often covered by a thin layer of neoplastic epithelial cells. There are few small aggregates of hemosiderin laden macrophages also within the stroma of the mass surrounding central areas of hemorrhage.

The remaining portions of the gland of the third eyelid located adjacent to the mass are compressed and markedly infiltrated by varying numbers and combinations of lymphocytes, plasma cells, histiocytes, hemosiderin laden macrophages, and neutrophils. Lymphocytes form dense sheets and few lymphofollicular aggregates that separate glandular structures. Glandular structures are often tortuous and are occasionally hyperplastic, with hypertrophied plump cuboidal epithelium lining. Glandular structures are variably distended by variable amounts of eosinophilic to amphophilic proteinaceous fluid and occasional neutrophils. Severely distended glandular structures are lined by markedly attenuated epithelium. Occasionally, glandular tubules are surrounded by thin rings of fibrosis. Blood vessels within the gland and the surrounding stroma are prominently congested.

The conjunctival epithelium overlying the mass is variably eroded and ulcerated. There is prominent exocytosis of neutrophils through areas of intact epithelium. In areas of severe erosion, the epithelium is reduced to a thin layer of attenuated cells. In areas of ulceration, there is mild hemorrhage and prominent exudation of fibrin and

neutrophils into the conjunctival sac. There is segmental squamous metaplasia of the mucosal epithelium lining the remainder of the conjunctiva, with focal erosion and ulceration. The normal pseudostratified columnar conjunctival epithelium in this area is variably replaced by thick nonkeratinizing squamous epithelium. Goblet cells are rare. In many areas, the superficial surface of the squamous epithelium is eroded and tattered. There is prominent exocytosis of neutrophils through the epithelium, with neutrophils rarely forming small aggregates in the superficial epithelial layers. A variably thick band of primarily lymphocytes and plasma cells, and fewer neutrophils and histiocytes parallels the junction of the mucosal epithelium and the underlying substantia propria of the third eyelid, the palpebrae, and the globe. Blood vessels in the superficial substantia propria of the entire conjunctiva are prominently congested.

The corneal epithelium of the globe is diffusely hyperplastic. The basal border of the epithelium is irregularly undulated with the epithelium rarely forming short thick rete pegs that extend into the underlying stroma. Rare basal epithelial cells contain finely granular, intracytoplasmic, dark brown pigment consistent with melanin. Exocytosis of neutrophils and, to a lesser degree, lymphocytes through the corneal epithelium is focally prominent. The corneal stroma contains small blood vessels lined by plump endothelial cells that are often surrounded by infiltrates of lymphocytes and neutrophils. Ingrowth of blood vessels is most prominent in the superficial corneal stroma, but is also present in the mid and deep stroma. The normal regularly arranged, pale staining corneal stroma is superficially replaced by dense, more haphazardly arranged collagenous stroma. Blood vessels at the limbus are surrounded by aggregates of lymphocytes and plasma cells.

The anterior chamber of the globe is moderately collapsed and contains scant amounts of fibrin and proteinaceous flocculent material. There is widespread synechiation between the axial posterior cornea, the iris, the ciliary body and the lens. In this region, there is focally extensive loss of the corneal endothelium, and the pupillary margins of the iris and the anterior capsule of the lens are adhered to Descemet's membrane by a thick band of fibrosis containing occasional melanin-containing round to spindle cells. This band of fibrosis is continuous with a thin periridal fibrovascular membrane composed of fibroblasts, small blood vessels, and scant collagenous stroma. In some sections, a dense retrocorneal band of fibrosis extends from areas of synechiation over the inferior portions of Descemet's membrane. The pupillary margins of the iris are reflected into the posterior chamber of the anterior compartment by bands of fibrovascular stroma that extend onto the posterior aspect of the iris creating entropion uveae. The pigmented epithelium that normally lines the posterior iris is widely lost and there are numerous loosely arranged fibrous adhesions between the posterior iris, the pars plicata of the ciliary body, and the lens capsule. The superior aspect of the iris is bowed into the anterior chamber (iris bombé) and the associated ciliary cleft is collapsed. The anterior uvea (iris and ciliary body) is moderately infiltrated by lymphocytes, plasma cells and fewer histiocytes that aggregate around blood vessels. The stroma of the pars plicata of the ciliary body is expanded by edematous, myxomatous matrix containing melanin-laden round cells. A band of dense fibrovascular stroma extending from the ciliary body lines the posterior lens capsule. Within this cyclitic membrane, there are few variably sized, spherical, dull gray bodies consistent with asteroid hyalosis, and many melanin-laden cells.

There is severe cataractous change of the lens. Lens epithelial cells are widely lost. There is marked liquefaction of cortical lens material. Amorphous, eosinophilic pools of liquefied lens material contain numerous granular foci of dense mineralization. There are occasional granular to globular foci of mineralization distributed throughout the remaining lens fibers. The posterior lens capsule is focally wrinkled. There is marked plasmoid degeneration of the vitreous characterized by replacement of normal vitreous with pale eosinophilic flocculent material admixed with dependent aggregates of neutrophils, scant hemorrhage, and occasional pigment-laden cells.

The tapetal (superior) retina is widely detached. Peripheral portions of the tapetal retina are markedly atrophied showing marked loss of neurons throughout all layers, vesiculation of plexiform layers, blending of the inner and outer nuclear layers, and loss of photoreceptors. More centrally within this portion of retina, ganglion cells and inner nuclear layer neurons remain intact, but many neurons in the outer nuclear layer and nearly all photoreceptors are lost. There are rare foci of interretinal hemorrhage. The subretinal space contains mild accumulation of flocculent basophilic material and scant hemorrhage. Retinal pigmented epithelial cells in the superior fundus are markedly hypertrophied, creating rounding and tombstoning of the apical border of these cells. The nontapetal (inferior) retina is nondetached, but is severely atrophied. Atrophy within this portion of the retina is often diffuse, but is generally most severe within the inner most retinal layers. In the most severely affected areas, the retina is reduced to a thin layer of glial cells that contains occasional round to spindle shaped pigmented cells. In segmental areas of the nontapetal fundus, there is loss of retinal pigmented epithelial cells with adherence of the atrophied retina to Bruch's membrane. In one area, the nontapetal

retina is torn and the anterior portion of the torn retina is detached (not present in all sections). The free end of the torn retina is rounded while the end that remains adherent to the RPE is attenuated. There is mild accumulation of hemorrhage in the subretinal space. Vessels in the choroid and retina are lined by plump endothelial cells and often contain prominent numbers of neutrophils. The neuropil of the optic nerve is mildly vesiculated.

Contributor's Morphologic Diagnosis:

1. Third eyelid:
   - Complex adenocarcinoma of the gland of the third eyelid
   - Chronic lymphoplasmacytic adenitis of the gland of the third eyelid
2. Third eyelid and palpebrae: Severe chronic lymphoplasmacytic and suppurative conjunctivitis with squamous metaplasia and multifocal ulceration
3. Eye:
   - Severe chronic superficial keratitis with corneal epidermalization
   - Retrocorneal fibrous membrane
   - Preiridal fibrovascular membrane
   - Anterior and posterior synechiae, lenticular-corneal synechia, and iridocyclitic synechia
   - Retrolenticular cyclitic membrane
   - Entropion uveae and mild iris bombé
   - Moderate chronic lymphoplasmacytic anterior uveitis
   - Mature cataract (loss of lens epithelium, lens fiber liquefaction, and mineralization)
   - Plasmoid degeneration of the vitreous and asteroid hyalosis
   - Chronic diffuse tapetal retinal detachment with moderate outer retinal atrophy
   - Severe diffuse nontapetal inner retinal atrophy with focal retinal tear and detachment

Contributor's Comment: While this case may not be a diagnostic challenge, as there is an obvious glandular epithelial neoplasm in the region of the gland of the third eyelid, it does present a challenge from a descriptive standpoint, as there are numerous other changes within the adjacent globe and periorbital tissue.

A diagnosis of adenocarcinoma rather than adenoma was based on the moderate cellular atypia of neoplastic epithelial cells and the focal infiltration of neoplastic cells into the partial capsule. Carcinomas of the gland of the third eyelid may be locally invasive, but metastasis is generally considered rare. In a report by Wilcock and Peiffer, local recurrence occurred in three of four dogs in which a carcinoma of the gland of the third eyelid was excised.[4]

In our case, the neoplastic mass was diagnosed as a complex adenocarcinoma based on the prominence of myoepithelial cells within the mass. On immunohistochemistry, the prominent spindle cell populations within some areas of the mass were immunoreactive for muscle specific actin and a pancytokeratin marker (MNF116), but were not labeled for vimentin. This pattern of immunoreactivity supports the designation of these cells as myoepithelial cells. To our knowledge, complex adenocarcinoma of the gland of the third eyelid has not previously been reported. In the report by Wilcock and Peiffer, spindle-cell and squamous metaplasia was described in a proportion of the tumors.[3] It is possible that the spindle-cell metaplasia described by Wilcock and Peiffer actually represented myoepithelium, but was not addressed as such in their report.

There was marked inflammation within the remaining portion of the gland of the third eyelid and throughout the conjunctiva. Such inflammation may be secondary to the mass itself and local irritation, but a secondary bacterial infection cannot be ruled out. The changes within the globe are numerous, and all are likely secondary to the presence of the mass in the third eyelid and associated trauma.

Corneal epidermalization (cutaneous metaplasia) is an adaptive change to chronic superficial irritation/trauma. Such change in this case was characterized by epithelial hyperplasia with mild rete peg formation, rare epithelial pigmentation, and superficial stromal fibrosis and vascularization. Keratinization of the corneal epithelium is another feature that is commonly seen with corneal epidermalization, but it was not prominent in this case.

Chronic uveitis likely led to the formation of a preiridal fibrovascular membrane, a retrocorneal fibrous membrane, a retrocorneal cyclitic membrane, and multiple synechiae between the cornea, iris, lens and ciliary body. The widespread synechiae between the iris, lens, and cornea resulted in obstruction of the pupil and glaucoma. Changes consistent with glaucoma are most prominent in the nontapetal retina. There is some degree of sparing of the detached tapetal retina in terms of atrophy in comparison to other segments of the retina. Such differences between the degree of atrophy between the tapetal and nontapetal retina and between detached and nondetached portions of the retina are common. The pathophysiology explaining the differences in susceptibility between various segments of the retina is unclear. The cataractous changes within the lens may have occurred secondary to uveitis and the proliferation of fibrovascular stroma surrounding the lens or may be a degenerative age related change as cataracts were reported in both eyes of this dog. Clear evidence of the reported prolapse of the eye and rupture was not

observed in the examined sections.

AFIP Diagnosis: 1. Eye, lacrimal gland: Epithelial-myoepithelial carcinoma of lacrimal gland (low-grade complex adenocarcinoma of the lacrimal gland).
2. Eye, conjunctiva, third eyelid and palpebrae: Conjunctivitis, lymphoplasmacytic and neutrophilic, chronic, diffuse, severe, with squamous metaplasia.
3. Eye, cornea: Keratitis, superficial, diffuse, chronic, severe, with epidermalization.
4. Eye, uvea: Anterior uveitis, lymphoplasmacytic, moderate, diffuse, with anterior and posterior synechiae, lenticular-corneal synechia, iridocyclitic synechia, and preiridal fibrovascular membrane formation.
5. Eye, lens: Lens fiber degeneration and liquefaction, diffuse, severe, with mineralization (mature cataract) and retrolenticular cyclitic membrane formation.
6. Eye, retina: Detachment, focally extensive, with marked atrophy.

Conference Comment: The submitted section of globe and periorbital tissues, studied in the context of the contributor's detailed, logical morphologic description, provides an eloquent tour through numerous microscopic lesions unique to ocular pathology. Conference participants appreciated the challenge of identifying, describing, and interpreting the numerous ancillary changes present, and in well-constructed comments, the contributor adeptly elaborates on the complex relationships among these lesions and with the neoplasm.

Histologically, the neoplasm resembles epithelial-myoepithelial carcinoma of salivary gland, i.e., well-circumscribed, partially encapsulated tumor of both luminal epithelium and myoepithelium, in which the myoepithelium predominantes and myoepithelial cells are multifocally polygonal with clear cytoplasm. Using the unstained serial histologic sections submitted with this case, immunohistochemistry was performed for cytokeratin AE1/AE3, vimentin, smooth muscle actin, and the myoepithelial markers calponin and p63. Most neoplastic cells display strong cytoplasmic immunoreactivity for cytokeratin, and many – particularly the spindled neoplastic cells – are strongly immunoreactive for smooth muscle actin. Rare vimentin-positive cells are scattered throughout the tumor; these are interpreted as non-neoplastic supporting stromal cells. While neoplastic cells are negative for calponin by immunohistochemistry performed at the AFIP, over 80% of the neoplastic cells exhibit positive, specific nuclear immunohistochemical staining for p63, which is a sensitive and specific marker for myoepithelium in canine tissue (**fig. 2-3**).[2]

The immunohistochemistry results generally agree with

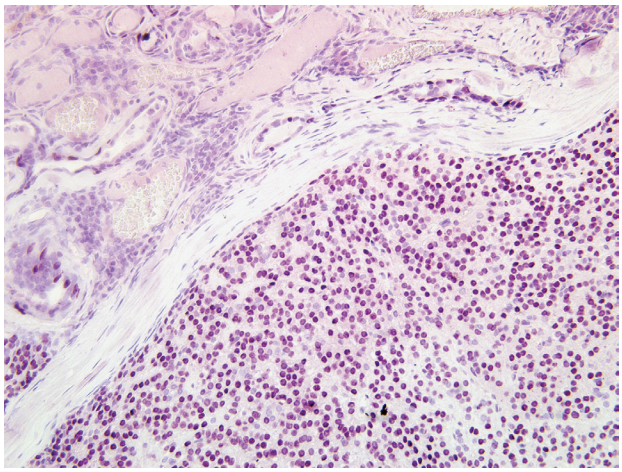

2-3. Epithelial-myoepithelial carcinoma, eye, lacrimal gland, canine. Diffusely, many neoplastic myoepithelial cells exhibit positive nuclear immunohistochemical staining for p63. Multifocally, adjacent pre-existent myoepithelial cells in the lacrimal gland demonstrate positive nuclear staining for p63. (p63- 200x)

those reported by the contributor, and support the presence of myoepithelial proliferation; and although not officially recognized in the current World Health Organization classification scheme, participants agreed with the contributor's diagnosis of complex adenocarcinoma. This case was also studied in consultation with the AFIP Department of Ophthalmic Pathology, which concurred with the diagnosis. Dubielzig and coworkers at the Comparative Ocular Pathology Laboratory of Wisconsin reportedly have collected 109 cases of epithelial tumors of the gland of the third eyelid in dogs, which includes adenocarcinoma, adenoma, and complex and mixed tumors that collectively represent 1.9% of canine tumor submissions to that laboratory.[1]

Conference participants briefly reviewed neoplasia in the nictitating membrane among animals, a rarity in the dog, a species more prone to the development of protrusion of the gland of the third eyelid ("cherry eye"). Squamous cell carcinoma is the most common neoplasm in domestic animal species, particularly in cattle and horses; its prevalence is correlated with high altitude and sunlight exposure. Conjunctival squamous cell carcinoma (SCC) develops via progression from precancerous changes to malignancy, akin to those described for cutaneous SCC: squamous plaque, squamous papilloma, squamous cell carcinoma in situ, and invasive SCC. Less common tumors of the nictitans include vascular tumors (e.g. hemangioma, hemangiosarcoma, and angiokeratoma), lymphoma, melanoma, and mast cell tumor.[3]

Contributor: Diagnostic Center for Population and

Animal Health, Michigan State University, 4125 Beaumont Road, Lansing, MI 48910
http://www.animalhealth.msu.edu

References:

1. Dubielzig RR, Ketring KL, McLellan GJ, Albert DM: Veterinary Ocular Pathology: A Comparative Review, p. 188. Saunders Elsevier, Philadelphia, PA, 2010
2. Gama A, Alves A, Gartner F, Schmitt F: p63: a novel myoepithelial cell marker in canine mammary tissues. Vet Pathol **40:**412-420, 2003
3. Wilcock B, Dubielzig RR, Render JA: Histological Classification of Ocular and Otic Tumors of Domestic Animals, 2nd series, vol. IX, ed. Schulman FY, pp. 18-22. Armed Forces Institute of Pathology (in cooperation with the American Registry of Pathology and the World Health Organization Collaborating Center for Worldwide Reference on Comparative Oncology), Washington, DC, 2002
4. Wilcock B, Peiffer R Jr. Adenocarcinoma of the third eyelid in seven dogs. J Am Vet Med Assoc **193:**1549-1550, 1988

CASE III: D-09-7312(18) (AFIP 3149836).

Signalment: 63-day-old, unknown gender, White Leghorn chicken (*Gallus gallus domesticus*).

History: This white leghorn chicken was hatched from specific-pathogen-free (SPF) eggs and grown up in a clean and non-infectious environment. It was part of a vaccination trial which was recently conducted by this laboratory. The birds were challenged intranasally with a highly pathogenic avian influenza H5N1 virus.

On day two post challenge, this vaccinated chicken was found to be quiet. It was lethargic and anorexic on day three post inoculation and dead on day four. Virus was isolated at day two, three and four days post inoculation from both upper respiratory and cloacal swabs. Post mortem examination was performed and organs submitted for histopathological examination.

Gross Pathology: At post mortem examination, the head region was swollen with an edematous cervicocephalic air sac. The lungs were mildly congested.

Histopathologic Description: Brain: Multifocally, the meninges are massively expanded by an infiltrate of large numbers of heterophils, macrophages, fewer lymphocytes along with abundant fibrin, proteinaceous fluid (edema) and necrotic cellular and karyorrhectic debris. The necrosis and inflammation extends multifocally into the underlying neuropil. Occasionally neuron cell bodies are hypereosinophilic and shrunken with pyknotic nuclei (neuronal necrosis). Neuronophagia is also evident rarely. There is a mild diffuse gliosis. Blood vessels diffusely in the meninges, grey matter, and white matter are lined by reactive endothelial cells and many are undergoing fibrinoid necrosis. Fibrin thrombi are seen multifocally. Perivascular cuffs are prominent and comprised of macrophages and lymphocytes (**figs. 3-1 and 3-2**).

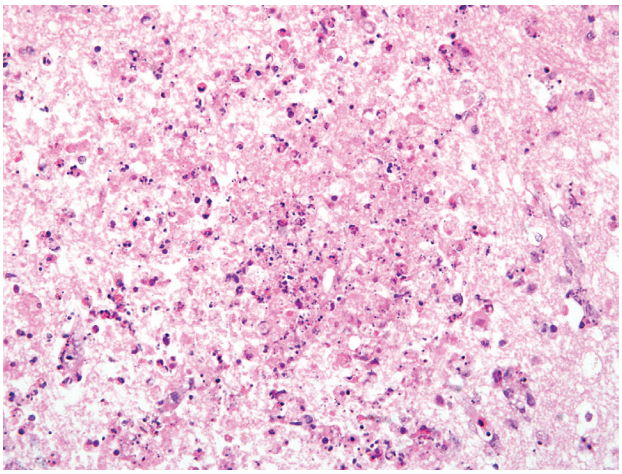

3-1. Brain, chicken. Multifocally, the neuropil is infiltrated by heterophilic inflammation and replaced by areas of lytic necrosis. (HE 100x)

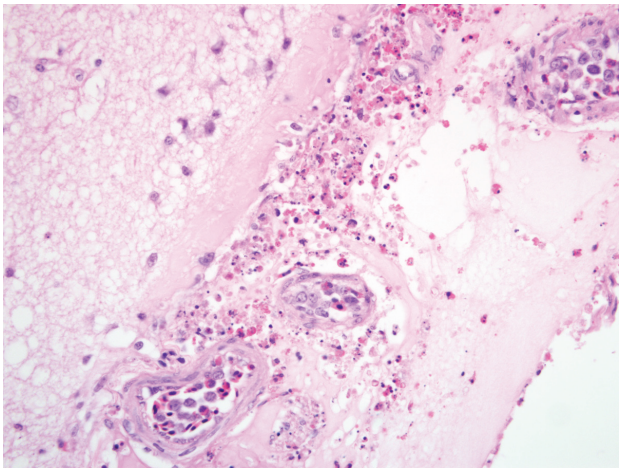

3-2. Brain, meninges, chicken. Multifocally, the meninges are expanded by many heterophils, macrophages, fewer lymphocytes, fibrin, edema, hemorrhage, and necrotic cellular debris. The vascular endothelium is hypertrophied. (100x)

Contributor's Morphologic Diagnosis: Brain: Meningoencephalitis, diffuse, severe, fibrinous, heterophilic and lymphohistiocytic with fibrinoid necrosis, vasculitis and thrombosis, white leghorn chicken, avian.

Contributor's Comment: Highly pathogenic avian influenza (HPAI) is caused by infection with influenza A viruses of the family Orthomyxoviridae.[5] The viral genome is composed of eight segments of single-stranded, negative-sense RNA that code for ten proteins.[6] Two of these proteins are hemagglutinin (HA) and neuraminidase (NA). All 16 HA and 9 NA influenza A subtypes have been isolated from avian species but HPAI viruses have been restricted to subtypes H5 and H7.[5]

The HA gene is the primary determinant of high pathogenicity in chickens, but a proper constellation of all eight gene segments is required for the maximal expression of virulence potential. The cleavage of the HA into the HA1 and HA2 proteins is essential for the virus to be infectious and produce multiple replication cycles. In moderately pathogenic AI viruses, trypsin-like proteases found in restricted anatomical sites, such as respiratory and intestinal epithelial cells or within secretions of the respiratory lumen, are required to cleave the HA and thereby produce infectious virus. However, in HPAI viruses the HA is cleaved by ubiquitous furin proteases present in many cells of numerous visceral organs, the nervous system and the cardiovascular system. Trypsin-like proteases will also cleave the HA of HPAI viruses.

An issue separate from HA cleavability is receptor binding between the receptor-binding site of the HA and the receptor on the host cells. This is a poorly understood phenomenon but impacts both host specificity (host-adaptation) and cell or tissue tropism within the host. This may restrict virus replication to specific cells, tissues and organs. Changes in the receptor-binding site of the HA have been shown to change the host range of an influenza virus. Both the virus and the host impact receptor binding.

Avian influenza viruses exert pathological effects on avian cells by two mechanisms: necrosis and apoptosis. Necrosis has been associated with intense virus replication and demonstration of abundant AI viral nucleoprotein in the nucleus and cytoplasm. Apoptotic cell death has been demonstrated in various cell culture systems. In chicken embryos, apoptosis and necrosis may share similar biochemical features and their differentiation is neither always easy nor clear.

Typically, histological lesions consist of multi-organ necrosis and/or inflammation. The most consistently and severely affected tissues are the brain, heart, lung, pancreas and primary and secondary lymphoid organs. Lymphocytic meningoencephalitis with focal gliosis, neuronal necrosis and neuronophagia are common, but edema and hemorrhage may be seen. Lesions in the

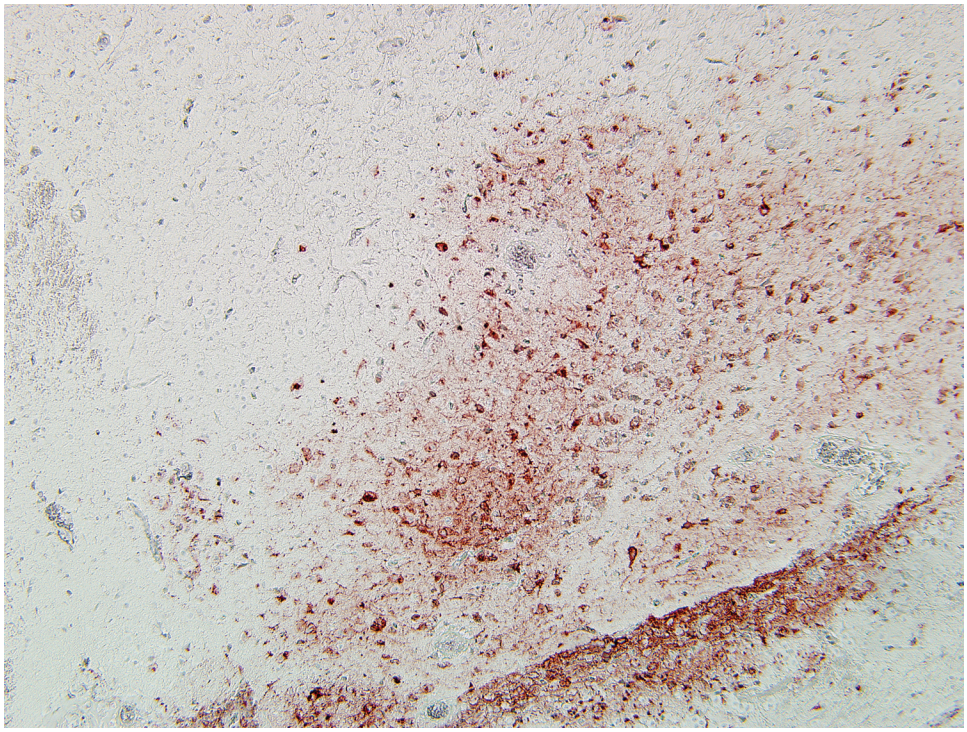

3-3. Brain, chicken. Multifocally, there is positive immunoreactivity to HPAI proteins. (IPXH5 100x)

brain have abundant associated influenza virus proteins in neurons.[6] In our case, immunoperoxidase staining revealed antigen in a variety of cells in the brain including endothelial cells, neurons, perivascular cuffs, ependymal cells as well as inflammatory cells in the meninges (**fig. 3-3**). Lesions were present in most organs including the lung, heart, kidney, spleen, ventriculus, small and large intestines, and pancreas.

In most cases involving chickens, HPAI is fulminating with some birds being found dead prior to observance of any clinical signs. If the disease is less fulminating and birds survive for 3-7 days, as in our case, individual birds may exhibit nervous disorders such as tremors of the head and neck, inability to stand, torticollis, opisthotonos and other unusual positions of head and appendages. Respiratory signs are less prominent than with less pathogenic AI viruses, but can include rales, sneezing and coughing.

The virus is transmitted by direct contact between infected and susceptible birds or indirect contact through aerosol droplets or exposure to virus-contaminated fomites. Aerosol generation from the respiratory tract is a significant mode of transmission because of high virus concentrations in the respiratory tract, but the large volume of lower concentration AI virus in infected feces makes fomites a major mode of transport.[6]

The importance of the human health implications of AI infections were revealed during the 1997 Hong Kong outbreak, in which the H5N1 virus was shown to have infected 18 people, six of whom died.[1] This virus, which is panzootic in poultry, continues to spread and pose a major challenge to animal and human health. While the H5N1 virus transmits zoonotically from infected poultry to humans, often with fatal consequences, such transmission remains inefficient. Although the virus replicates efficiently in diseased humans, it has not yet adapted to efficient human-to-human transmission. The H5N1 virus therefore continues to challenge our understanding of interspecies transmission of influenza viruses.[4]

AFIP Diagnosis: Brain: Meningoencephalitis, necrotizing, acute, diffuse, severe, with multifocal neuronal necrosis, gliosis and vasculitis.

Conference Comment: We thank the contributor for the timely provision of this relevant case, which features an etiology with tremendous global economic and public health implications. Without having the elevated index of suspicion afforded by knowing the history or age of this chicken, most conference participants considered several other etiologies much more likely than HPAI (fowl plague) in the differential diagnosis, including nutritional encephalomalacia (e.g. vitamin E deficiency), fungal encephalitis, or bacterial infection with septicemia, among others.

Vitamin E deficiency affects chicks, causing encephalomalacia, exudative diathesis, and nutritional myopathy. Encephalomalacia usually manifests clinically between days 15 and 30 of life as ataxia or paresis, and grossly, hemorrhages are often noted on the cerebellar surface. Microscopic lesions include ischemic necrosis, demyelination, and neuronal degeneration, most prominently in the cerebellum, striatal hemispheres, medulla oblongata, and mesencephalon.[3] The submitted case is characterized by more severe inflammation than would be expected in nutritional encephalomalacia.

Fungal encephalitis of young chickens, turkey poults, and quail chicks is caused by the dematiaceous thermophilic fungus *Ochroconis gallopavum* (*Dactylaria constricta* var. *gallopava*). Gross lesions may involve both the cerebellum and cerebrum, and range from hard, gray, well-circumscribed foci to focally extensive areas of red discoloration. Histologic lesions include infiltration by numerous heterophils, macrophages, and multinucleated giant cells centering on areas of necrosis with numerous readily-apparent dematiaceous fungal hyphae, which are conspicuously absent in this case.[2]

The contributor provides a succinct review of AI in general, and H5N1 HPAI specifically, which since 2003 has produced natural infection in a number of species, including humans, domestic pigs, dogs, cats, tigers, leopards, stone martins, and civets. Migratory aquatic birds, particularly those belonging to the orders Anseriformes and Charadriiformes, are the reservoirs of all AI viruses, and typically do not develop disease due to infection. In poultry, as described by the contributor, clinical signs and pathology depend not only on the pathotype of AI virus (i.e. low pathogenicity [LP] or high pathogenicity [HP]), but also on host species, age, sex, immune status and environmental factors, among others. The gross and histologic lesions of HPAI listed by the contributor are nonspecific, and the differential diagnosis includes velogenic Newcastle disease virus, septicemic fowl cholera (Pasteurella multocida), heat exhaustion, water deprivation, and several toxins. For LPAI, which affects the respiratory tract and causes reduced egg production, the differential diagnosis is long, and includes lentogenic Newcastle disease virus, avian pneumovirus and other paramyxoviruses, infectious laryngotracheitis (gallid herpesvirus 1), infectious bronchitis (avian coronavirus), chlamydiosis and mycoplasmosis, among others. As such, the diagnosis of AI infection requires the employment of virologic and serologic methods.[5]

Conference participants briefly discussed several salient properties of influenza viruses in general. Ultrastructurally, virions are spherical to pleomorphic and range from 80 to 120 nm in diameter, although filamentous forms may be much longer.[5] Germane to any review of influenza virus epidemiology is mention of the two mechanisms by which new variants of the virus emerge, forcing the continual need for vaccine reformulation to maintain population immunity: antigenic drift, accomplished through point mutations; and antigenic shift, resulting from genomic segment reassortment when two influenza viruses infect the same cell. Notably, both human and avian influenza viruses have established stable infections in pigs, which is attributed to the presence of receptors for both types of viruses on porcine epithelium; accordingly, pigs are regarded as a potential "mixing vessel" for the generation of pandemic influenza virus through reassortment.[4]

Contributor: Agriculture, Fisheries and Conservation Department, Tai Lung Veterinary Laboratory, Sheung Shui, New Territories, Hong Kong Special Administrative Region
http://www.afcd.gov.hk

References:

1. Capua I, Alexander DJ: The challenge of avian influenza to the veterinary community. Avian Pathol **35:**189-205, 2006
2. Charlton BR, Chin RP, Barnes HJ: Fungal infections. *In:* Diseases of Poultry, ed. Saif YM, 12th ed., pp. 1005-1006. Blackwell Publishing, Ames, IA, 2008
3. Klasing KC: Nutritional diseases. *In:* Diseases of Poultry, ed. Saif YM, 12th ed., pp. 1128-1130. Blackwell Publishing, Ames, IA, 2008
4. Peiris JSM, de Jong MD, Guan Y: Avian influenza virus (H5N1): a threat to human health. Clin Microbiol Rev **20:**243-267, 2007
5. Swayne DE, Halvorson DA: Influenza. *In:* Diseases of Poultry, ed. Saif YM, 12th ed., pp. 153-184. Blackwell Publishing, Ames, IA, 2008
6. Tanimura N, Tsukamoto K, Okamatsu M, Mase M, Imada T, Nakamura K, Kubo M, Yamaguchi S, Irishio W, Hayashi M, Nakai T, Yamauchi A, Nishimura M, Imai K: Pathology of fatal highly pathogenic H5N1 avian influenza virus infection in large-billed crows (*Corvus macrorhynchos*) during the 2004 outbreak in Japan. Vet Pathol **43:**500-509, 2006

CASE IV: C9775-08 (AFIP 3149913).

Signalment: 2.5-year-old, male American pit bull terrier (*Canis familiaris*).

History: A young pit bull dog presented to a veterinary clinic with a 5-day history of lethargy and vomiting. Initial blood work revealed the following: BUN 76 mg/dl (7-25), creatinine 5.3 mg/dl (0.5-1.4), phosphorus 10 mg/dl (9-10.8), calcium 9 mg/dl (9-10.8), total protein 8.1 g/dl (5.4-7.1), albumin 2.4 g/dl (2.5-3.6), globulin 5.7 g/dl (2.4-3.6) and amylase 1,056 U/L (510-1,864); other values were within normal limits. The owner's initial concern was that the dog had been poisoned and the veterinarian's presumptive diagnosis was ethylene glycol toxicity. Some treatment was attempted, but the dog was euthanized shortly after presentation.

Gross Pathology: The dog was in good body condition. Mucous membranes were pale with occasional random petechiae. The kidneys were bilaterally swollen and had prominent hyperemia of capsular vasculature. The subcapsular surface of the kidney and the corresponding cut surface of the cortex were pale tan and had numerous, disseminated, slightly raised, tan to white, pinpoint to 0.2 cm foci. A raised, fairly well-delineated, irregular, 0.2-0.5 cm band of similar coalescing nodular foci followed the corticomedullary junction; occasional sometimes discontinuous similar bands were in the adjacent outer medulla. A wider dark reddish purple medullary band that was up to 1.2 cm wide extended from the renal crest into

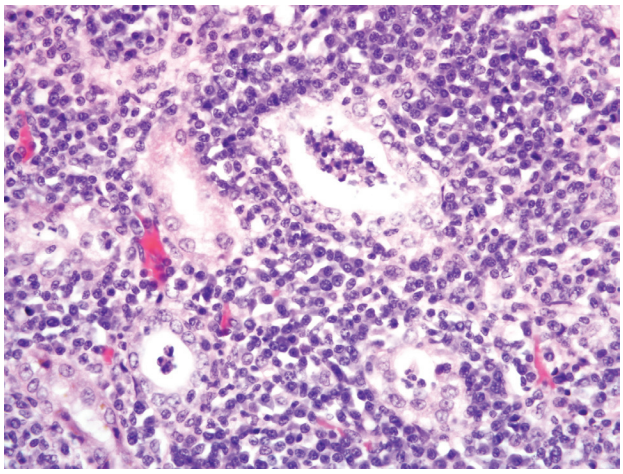

4-1. Kidney, canine. Multifocally, the interstitium in the renal cortex and outer medulla is infiltrated by many lymphocytes, macrophages and plasma cells that separate and surround degenerate and necrotic tubules. Some ectatic tubules contain degenerate neutrophils and necrotic cellular debris. (HE 400x)

the medulla. The renal pelvis was dilated. Some pale tan streaks radiated from the capsular surface into the medulla. The urinary bladder was distended with pale yellow urine. The lungs were red and some frothy fluid was present on the cut surface.

Laboratory Results: Serology (Texas VMDL) revealed the following titers:

L. pomona	12,800
L. grippotyphosa	12,800
L. bratislava	12,800
L. hardjo	3,200
L. icterohaemorrhagiae	3,200
L. canicola	3,200

PCR of kidney and urine for *Leptospira* sp. (Texas VMDL) was positive.

Histopathologic Description: An intense predominantly mononuclear interstitial inflammatory infiltrate was within the cortex and outer medulla, although similar filtrates occurred in the inner medulla. Lymphocytes, plasma cells and macrophages predominated, although neutrophils were intermingled in multiple foci. These infiltrates often separated and effaced tubules within the cortex. Intermittent tubules had attenuation or irregularity of the tubular epithelial lining and luminal necrotic debris (**fig. 4-1**). The inner medulla along the renal crest had extensive necrosis and hemorrhage. Warthin Starry stain revealed clumps of black argyrophilic material within tubular lumina and in the apical cytoplasm of tubular epithelial cells. No discrete leptospires were identified. However, the argyrophilic material corresponded with discrete positive staining by immunohistochemistry (Purdue ADDL). The staining could be identified both within proximal convoluted tubules and collecting ducts.

Contributor's Morphologic Diagnosis: Tubulointerstitial nephritis, lymphoplasmacytic, with necrosis, subacute, diffuse, severe. Etiology: *Leptospira* sp.

Contributor's Comment: Leptospirosis is a ubiquitous and important bacterial infection resulting in significant disease in food animals, dogs and humans. Part of the enigma and mystery of leptospirosis is a consequence of cycling of infection in wildlife species resulting in sporadic spillover into domestic animals and humans. Although lately the presumed reemergence of leptospirosis has fallen into the opportunism of blaming global warming, a more likely explanation of the increased awareness is improved methods of detection. The organism has unique niche requirements and does not multiply outside of a host species, although it can survive quite well in wet soil, and, particularly, stagnant surface water. Transmission is typically by direct contact with infected urine or discharges subsequent to abortion; such contact may occur indirectly from water contaminated with the urine of wildlife carriers.

Classically, hosts for leptospirosis have been subdivided into primary versus incidental or accidental. Therefore, dogs are regarded as the primary host for *Leptospira canicola* and accidental hosts for *Leptospira icterohaemorrhagiae* (primary host, rat). In the last 12 years or so, multiple outbreaks of leptospirosis have been attributed to non-canine serovars such as *Leptospira grippotyphosa* (primary host, vole), *Leptospira pomona* (primary host, cattle and pig) and *Leptospira bratislava* (primary reservoir, pig and horse). The dog in the case submitted had high serologic titers to all of the atypical canine serovars. Although it is fun to speculate that *Leptospira grippotyphosa* is the primary infection and that the other serovars are cross reactions, this is always arrogant speculation and not evidence-based science.

The *Leptospira* microscopic agglutination test (MAT) is ideally performed on paired sera 3-4 weeks apart, looking for a fourfold rise in antibody titer. This is likely more important with *Leptospira canicola*, particularly if a dog was previously vaccinated. The high levels seen in this case are more typical of an accidental host with a non-canine serovar. Antibodies are typically first detected 7-10 days after infection. Several other diagnostic techniques were pursued to confirm the diagnosis. PCR of kidney and urine was positive for *Leptospira* DNA (Texas VMDL). This is a genus-specific result only. Warthin-Starry silver staining was attempted to demonstrate leptospires in tubules and was unsuccessful. Immunohistochemistry was performed (Purdue ADDL) revealing convincing clumped *Leptospira* antigen in tubular epithelial cells and tubular lumina. This disparity was interpreted as a consequence of lack of viability of the leptospires due to the prolonged postmortem interval. Similarly, dark field microscopy of urine was inconclusive; this test also requires fresh urine to observe normal leptospires. Fluorescent anybody testing of centrifuged urine sediment also has the advantage of not requiring leptospires to be viable. Researchers at Mississippi State University have identified transcriptional regulator genes that are present in pathogenic *Leptospira* strains and absent in non-pathogenic strains. PCR primers have been developed that conceivably can easily separate pathogenic from nonpathogenic *Leptospira*.[4]

The stratified appearance of an intense white band in the inner cortex and zones of hemorrhage and necrosis in the medulla are a classic pattern of acute leptospirosis culminating in acute renal failure in dogs. A series of these cases was studied retrospectively and prospectively

and determined to have a unique ultrasonographic pattern strongly suggestive of acute leptospirosis by Lisa Forrest and colleagues at the University of Wisconsin.[1] When dogs are presented in acute renal failure to veterinarians, initiation of appropriate antibiotic therapy requires timely decisions, and ultrasonography was determined to be a strongly suggestive finding for identifying leptospirosis due to atypical serovars. Otherwise, many of these dogs are euthanized with the presumption of chronic renal failure.

The classification of Leptospira has recently been changed.[3] Previously, one pathogenic species (Leptospira interrogans) and one nonpathogenic species (Leptospira biflexa) were recognized. These two species were subdivided into serovars—200 in *Leptospira interrogans* and around 60 in *Leptospira biflexa*. Based on DNA hybridization *Leptospira* has been reclassified into 13 genomospecies. Since both pathogenic and nonpathogenic species may occur in a single genomospecies, the utility of this scheme for veterinarians, microbiologists, pathologists and others dealing with the disease has not been clarified. Therefore, serovars and serogroups will likely persist in diagnostic reports.

AFIP Diagnosis: Kidney: Nephritis, tubulointerstitial, lymphoplasmacytic and neutrophilic, diffuse, severe, with tubular degeneration and necrosis and focally extensive medullary hemorrhage.

Conference Comment: The contributor provides an instructive example of this entity, the importance of which in both veterinary and human medicine is apparently ever-growing. In general, leptospirosis is characterized by any combination of septicemia, hepatitis, nephritis, and meningitis in humans and animals, and abortion and stillbirth in livestock. In maintenance hosts, which serve as the natural reservoir for the spirochete, the organism persists in the renal proximal convoluted tubules, and in some cases, the genital tract. As the contributor notes, recent taxonomic revisions have introduced tremendous complexity into the classification of *Leptospira* spp. Fortunately the serovar, which correlates most reasonably with epidemiology and disease, persists in the current nomenclature, and many circumvent the new taxonomy altogether by simply abbreviating to genus and serovar names, as in the contributor's comments. The bulk of the discussion during conference was devoted to comparative pathology of leptospirosis, as outlined in the table that follows:[2,5-9]

Leptospira Serovars, Maintenance Hosts, and Disease		
Serovar	**Maintenance host(s)**	**Significant Disease**
canicola	Dog	Dog: primarily renal disease; now rare due to vaccination
grippotyphosa	Raccoon, skunk, rodent	Dog: renal and hepatic disease; increasingly important
		Horse: abortion, premature foaling
icterohemorrhagiae	Rat	Dog: primarily hepatic disease; hyperacute disease in puppies; now rare due to vaccination
bratislava	Pig, horse, +/- dog	Dog: nephritis and abortion
		Pig: abortion, small litters of weak piglets
		Horse: abortion, premature foaling
pomona type kennewicki	Pig	Dog: renal and hepatic disease; increasingly important
		Pig: abortion, small litters of weak piglets
		Cattle: • Acute form (calves): hemoglobinuria, hematuria, fever, anemia, icterus, dyspnea, +/- meningitis • Acute form (adults): agalactia, abortion of decomposed fetus • Chronic form (adults): abortion, stillbirth, or premature weak calves
		Horse: • Chronic form: recurrent uveitis ("periodic ophthalmia"), abortion, premature foaling • Acute form (rare): fever, icterus
		Pinnipeds: abortions, hemorrhagic syndromes in fetuses and neonates, interstitial nephritis and glomerulonephritis, hepatic necrosis
autumnalis	Rodents	Dog: renal and hepatic disease; increasingly important
		Pig: infertility syndrome ("repeat breeder")
hardjo type hardjo-bovis (North America)	Cattle, sheep	Cattle: chronic form; abortion, stillbirth, or premature weak calves
		Sheep: • Lambs: acute form; similar to *pomona* in calves • Ewes: late-term abortion, stillbirth, weak lambs, agalactia
hardjo type hardjoprajitno (Europe)	Cattle	Cattle: • Subacute form: "milk drop syndrome," "flabby udder mastitis" • Chronic form: abortion, stillbirth, or premature weak calves
		Sheep: • Lambs: acute form; similar to *pomona* in calves • Ewes: late-term abortion, stillbirth, weak lambs, agalactia
ballum	Mouse	Hamster: severe hemolysis, icterus, hemoglobinuria, nephritis, hepatitis

Contributor: Mississippi State University, College of Veterinary Medicine, P.O. Box 6100, Mississippi State, MS 39762
http://www.cvm.msstate.edu

References*:*

1. Forrest LJ, O'Brien RT, Tremelling MS, Steinberg HS, Cooley AJ, Kerlin RL: Sonographic renal findings in 20 dogs with leptospirosis. Vet Radiol Ultrasound **39:**337-340, 1998
2. Greene CE, Sykes JE, Brown CA, Hartmann K: Leptospirosis. *In:* Infectious Diseases of the Dog and Cat, ed. Greene CE, 3rd ed., pp. 402-417. Saunders Elsevier, St. Louis, MO, 2006
3. Levett PN: Leptospirosis. Clin Microbiol Rev **14:**296-326, 2001
4. Liu D, Lawrence ML, Austin FW, Ainsworth AJ, Pace LW. PCR detection of pathogenic *Leptospira* genomospecies targeting putative transcriptional regulator genes. Can J Microbiol **52:**272-277, 2006
5. Newman SJ, Confer AW, Panciera RJ: Urinary system. *In:* Pathologic Basis of Veterinary Disease, ed. McGavin MD, Zachary JF, 4th ed., pp. 658-662. Mosby Elsevier, St. Louis, MO, 2007
6. Percy DH, Barthold SW: Pathology of Laboratory Rodents and Rabbits, 3rd ed., pp. 65, 152, 192, 211. Blackwell, Ames, IA, 2007
7. Prescot JF: Leptospirosis. *In:* Jubb, Kennedy, and Palmer's Pathology of Domestic Animals, ed. Maxie MG, 5th ed., vol. 2, pp. 481-490. Elsevier Saunders, Philadelphia, PA, 2007
8. Radostits OM, Gay CC, Blood DC, Hinchcliff KW: Diseases caused by *Leptospira* spp. *In:* Veterinary Medicine: A textbook of the Diseases of Cattle, Sheep, Pigs, Goats and Horses, eds. Radostits OM, Gay CC, Blood DC, Hinchcliff KW, 9th ed., pp. 971-982. W.B. Saunders, London, England, 2000
9. Szeredi L, Haake DA. Immunohistochemical identification and pathologic findings in natural cases of equine abortion caused by leptospiral infection. Vet Pathol **43:**755-761, 2006